SEDIMENTOLOGICAL, MINERALOGICAL AND GEOCHEMICAL STUDIES OF HOLOCENE COASTAL SEDIMENTS, SOUTH-WESTERN SCOTLAND

by

LIFTAA SELMAN KADEM, B.Sc., M.Sc.

A thesis submitted for the degree of Doctor of Philosophy

at

The University of Glasgow

Department of Geology & Applied Geology

University of Glasgow

February 1990

To my:

FATHER

All thanks and respect

CONTENTS

LIST OF FIGURES
(Abbreviated titles)

LIST OF TABLES
(Abbreviated titles)

LIST OF PLATES

ACKNOWLEDGEMENTS

Firstly, I would like to thank Dr. W. G. Jardine, who supervised this study, for all his help, considerable interest and constant advice, especially towards improvement of the text of this thesis.

I wish to give my sincerest thanks to Professor B. E. Leake for his helpful support by supervising the part of the study dealing with clay mineralogy and geochemistry, and in providing the facilities that enabled the work to be done.

I thank Professor B. J. Bluck and Dr. M. C. Keen for their scientific suggestions at the beginning of the work, and I am very grateful to Dr. P. D. W. Haughton for his fruitful discussions and suggestions and for reading part of the thesis.

Dr. C. M. Farrow is thanked for his instruction and help in the use of computing facilities, and Dr. C. J. Burton for his help in the field course at Malvern in 1986.

I would like to thank my good friend Abdussalam Sghair for his help in tracing some of the Figures.

I would like to express my special thanks to Mr. R. Morrison for supplying me with the materials etc. that I required, and my thanks to Mr. D. Maclean for reproducing Figures and Plates at short notice, and to G. Bruce, J. Gallagher, R.McDonald and P. Ainsworth for their help during the practical part of the work.

I wish to thank the Iraqian Government for providing a grant towards the financing of the research.

I wish to express my undying gratitude to my father and my brothers for their continual support and encouragement.

Finally, I would like to express my thanks to my wife, Amera, and my children, Tariek and Sadik, who have been the reason behind this work and whose mere presence beside me was the help I needed.

SUMMARY

Holocene raised coastal sediments of the Dalbeattie, Kirkcudbright and New Abbey areas in Galloway, and the area of the former Lochar Gulf in Dumfriesshire, together with present-day intertidal surface sediments from the first three of these areas, were studied. In Part I, the nature of the research project and previous related work is considered. A summary of the geological setting of the field areas is also given.

The first half of Part II is concerned with the methods used in data-recording and sample collection in the field and with stratigraphical correlation of the Holocene raised coastal sediments within the Dalbeattie, Kirkcudbright and New Abbey areas on the basis of exposed vertical sections and auger-drilled boreholes. Correlation of the sedimentary sequences recorded in these sections and boreholes suggests that several sedimentary facies can be distinguished in the three areas studied in this way. Four sedimentary facies are also recognised within the present-day intertidal deposits of the same areas. Following a discussion of the concept of sedimentary facies, previous recognition of such facies in SW Scotland and the criteria on which sedimentary facies were distinguished in the course of the research project, descriptions of the present-day and Holocene facies are given. The four sedimentary facies recognised within the present-day intertidal deposits are: tidal-flat; tidal-creek; salt marsh; sand-barrier. The seven sedimentary facies recognised within the Holocene sediments are: A, complex of fine-grained sediments; B, inter-laminated fine sand and silt; C, coarse sand with pebbles; D, fine sand, rich in microfaunal remains; E, clays, rich in plant debris; F, coastal gravel and sand; G, peat.

In Part III, data on the shapes, sphericity, roundness and lithological compositions of Pleistocene glaciofluvial and Holocene storm-beach gravel deposits in

the Dalbeattie area are presented and compared. Pleistocene clasts are mainly discs, Holocene clasts mainly blades; sphericity ranges between 0.5 and 0.9 in both cases, but the degree of roundness is greater in the Holocene clasts than in the Pleistocene. Greywacke is the commonest rock type in both. The Pleistocene gravels probably were derived mainly from the NW and west, the Holocene gravels partly from the Criffell-Dalbeattie granodioritic pluton and partly from Pleistocene glaciofluvial deposits. The results of orientation studies of (mainly) Holocene gravel clasts in the Dalbeattie and New Abbey areas are also given. They suggest deposition by SE-NW water flow. Detailed grain-size analysis indicates that most of the Holocene sediments in the Dalbeattie area and in the upper part of the successions in the Kirkcudbright and New Abbey areas (sediments of facies A) are of silt grade and bimodal or polymodal in grain-size distribution, whereas sand-grade and unimodal grain-size distribution predominate in the Holocene sediments (of facies D) in the area of the former Lochar Gulf and in the lower part of the succession in the Kirkcudbright and New Abbey areas. The present-day intertidal sediments of the Dalbeattie, Kirkcudbright and New Abbey areas are mainly of fine-sand grade and unimodal in grain-size distribution. In descending order of abundance, illite (mainly with the composition of biotite and muscovite), chlorite (mainly Fe-chlorite), kaolinite and vermiculite are the main clay minerals present in both the present-day intertidal and Holocene raised coastal sediments in the areas studied. Both detrital and authigenic illite, chlorite and kaolinite are present; detrital material greatly predominates over authigenic material in the cases of chlorite and kaolinite. Vermiculite is more abundant in the uppermost facies, A, than in the various underlying facies. Mixed-layer clays and montmorillonite are present in minor amounts in the Holocene sediments. Geochemical analysis of bulk samples and samples of the clay fraction of both the Holocene and

present-day sediments indicates that the SiO_2 content, which is inversely related to the content of Al_2O_3, total iron, TiO_2, MgO and K_2O, is higher in the Holocene sediments of the Lochar Gulf area than in the sediments of the same age in the three other areas studied. The CaO content in Holocene sedimentary facies D, which is approximately equal to that in the present-day sediments and higher than in the other Holocene sediments, may have been derived from fossil shell and other organic carbonate fragments in facies D. The trace elements Y, Sr, Rb, Th, Pb, Zn, Ni, Co, Ce, Cr, Ba and La are associated with the clay minerals present in the sediments.

Environments of deposition and possible provenances of the Holocene sediments are discussed in Part IV. The environments of deposition recognised, and their corresponding sedimentary facies or sub-facies, were: intermediate to low tidal-flat, facies D; intermediate to high tidal-flat, facies B; high tidal-flat, sub-facies Ab; *very* high tidal-flat or supra-tidal (salt marsh), sub-facies Ac; salt-marsh, sub-facies Aa; lake or marsh, facies E; storm-beach, facies F. A minor, additional, environment recognised in the New Abbey area only, was that of the fluvial channel-filling (facies C). Determination of provenance of the Holocene sediments on the basis of clay mineralogical and geochemical content must be regarded as very tentative.

DECLARATION

The material presented in this thesis is the result of independent research by the author, undertaken between January 1986 and November 1989, at the Department of Geology & Applied Geology, University of Glasgow. Any published or unpublished results of other works have been given full acknowledgement in the text.

Liftaa S. Kadem

PART I

THE RESEARCH PROJECT AND ITS GEOLOGICAL SETTING

CHAPTER 1

INTRODUCTION TO THE RESEARCH PROJECT

1.1 Introduction

Sedimentological, stratigraphical and geomorphological evidence demonstrates that in the early part of post-glacial (Holocene) times (i.e. from c. 10,000 to 5,000 years B.P.) a major marine transgression, followed by regression, occurred in south-western Scotland. The marine events were marked by the deposition of coastal sediments that vary in facies, composition, grain size and textural properties, and that represent a variety of depositional environments and sub-environments.

The Holocene marine sediments occur now at altitudes of a few metres above British Ordnance Datum (Newlyn), either as raised sand and gravel bodies or as areas of fine-grained deposits known locally as 'carse lands', and they rest on tills or glaciofluvial deposits of the Devensian glaciation. Identification of the surface of contact between the inorganic Holocene and Devensian deposits is based partly on the presence, in places, of a thin layer of organic (peaty) debris, and partly on the distinctly different nature of the Holocene sediments and the Pleistocene glacial and glaciofluvial deposits.

As discussed below, prior to 1986 the coastal sediments had been studied at several locations along the northern shore of the Solway Firth. Research, however, had been devoted mainly to stratigraphical and geomorphological aspects; only limited sedimentological studies had been undertaken (Griffiths 1988), and mineralogical and geochemical studies had been almost totally neglected. It was considered useful, therefore, to undertake a research project that would concentrate on sedimentological, mineralogical and geochemical aspects of the Holocene raised coastal sediments. The

geographical areas chosen for study were the New Abbey and Lochar Gulf areas, which already had been the subject of stratigraphical and geomorphological research (Jardine 1975; 1980), and areas in the vicinity of the towns of Dalbeattie and Kirkcudbright, which previously had received little attention (Fig. 1.1).

1.2 Previous work

The Holocene sediments of the Dumfriesshire and Kirkcudbrightshire shore of the Solway Firth were first mapped by the Geological Survey prior to 1879. Brief reference to the extent and nature of the deposits was made by Horne et al. (1896, 36-39). Investigations of the inorganic coastal sediments and associated organic deposits by Wallace (1918), Donner (1959; 1963) and Marshall (1962a; 1962b) were mainly geomorphological in emphasis. Botanical and palynological studies of Lochar Moss, which overlies Holocene coastal deposits of the former Lochar Gulf, were made by Erdtman (1928, 175) and Nichols (1967), and brief reference to the same Moss was made by Godwin (1943, 227-228) in a general survey of British coastal peats.

The environmental history of Lateglacial and early Flandrian (Holocene) times in south-western Scotland was interpreted by Bishop & Coope (1977, 61-67) from detailed local stratigraphical investigations at several localities between the Solway Firth and the Clyde Estuary. Stratigraphical and faunal evidence and radiocarbon dates were discussed. Of particular interest is the dating of woody peat (with a pollen spectrum dominated by pine, birch and hazel) from the foreshore of Brighouse Bay (NX 634 452), which provided evidence that sea level in the Kirkcudbright area was below Ordnance Datum (O.D.) at c. 9,640 ±180 years B.P. (Godwin & Willis 1962; see also Bishop & Coope 1977, 68).

Other early work regarding changes of sea level within the Solway Firth area was undertaken by Donner (1963). He recorded evidence for the Holocene marine transgression at seven sites along the northern shore of the Firth and discussed the results in terms of the so-called 'Late-glacial 100-foot beach' and 'Post-glacial 25-foot beach'. More recent research on the sediments and events of the Holocene transgression along the northern shore of the Solway Firth is described in a series of papers by Jardine (1964; 1967; 1971; 1975; 1977; 1980; 1981a; 1982). The chronology of Holocene marine transgression and regression and the archaeological significance of the Holocene coastal deposits of the same area are discussed by Jardine & Morrison (1976).

Studies with a sedimentological emphasis are those of Bridges & Leeder (1976), who examined intertidal mudflat channels near Carsethorn (south of New Abbey), and of Griffiths (1988), who recorded, analysed and re-appraised sedimentary facies and sub-environments of deposition both in Holocene times and at present in the estuaries of the River Cree and Water of Fleet, western Galloway.

1.3 Geographical areas studied

The areas studied in the course of the research project are located on the northern side of the Solway Firth (Fig. 1.1). In the **Dalbeattie area**, the Holocene raised coastal sediments that were examined occur on both sides of the Urr Water at, and south of, the town of Dalbeattie, and in the adjacent low, flat areas bordering Auchencairn Bay, Orchardton Bay and Rough Firth. The **Kirkcudbright** area consists mainly of the flat ground adjacent to the western side of the River Dee to the west, and for a few km to the north, of the town of Kirkcudbright. Sediments on either side of New Abbey Pow (i.e. burn or stream) downstream from the village of the same

name are the deposits that were studied in the **New Abbey area.** The former **Lochar Gulf** occurs to the south-east of the town of Dumfries.

1.4 Aims of the research project

As explained above (Chapter 1.1), no detailed account has been given, as yet, of the sedimentological, mineralogical and geochemical characteristics and conditions of accumulation of the Holocene raised coastal sediments of the Dalbeattie, Kirkcudbright, New Abbey and Lochar Gulf areas. In addition, the extent and distribution of these sediments in the Dalbeattie and Kirkcudbright areas have not been mapped in detail. The main aims of the project therefore may be stated as follows:

Aim1 Mapping of the extent and distribution of the various facies of Holocene coastal sediments in the Dalbeattie and Kirkcudbright areas, (a) to determine the position of the shoreline at the maximum of the Holocene marine transgression, and (b) to investigate the nature and, if possible, successive positions of the shoreline during the period of marine regression.

Aim 2 Detailed study, both laterally and vertically, of the various sedimentary facies that occur in the Holocene sediments of the Dalbeattie, Kirkcudbright and New Abbey areas, and to a lesser extent of the former Lochar Gulf. Such a study should lead to identification of the various environments and sub-environments of deposition in which the Holocene sediments accumulated in these areas.

Aim 3 (a) Field recording of sedimentary structures (where observed) and shapes of Holocene sedimentary bodies, and their relationships to depositional events that occurred in the course of the Holocene marine transgression and regression. (b) Determination of the shape, sphericity and roundness, and of the orientation of the long axes, of clasts contained in natural and artificial exposures of Holocene beach gravels and adjacent Pleistocene glaciofluvial gravels, with a view to determining, (1) criteria for distinction between these two types of gravel deposit, and (2) current flow directions during deposition of these sediments.

Aim 4 Grain-size analysis of the various facies of the Holocene coastal sediments and of present-day intertidal deposits, with a view to determining, (a) the textural characteristics of the Holocene sediments and present-day intertidal sediments, (b) grain-size variation within the Holocene sediments from one area to another, (c) vertical variation in grain size within the Holocene sediments, (d) criteria for distinction between the present-day intertidal sediments and the Holocene sediments, and (e) modes of transportation and deposition of the Holocene sediments in the various environments and sub-environments of deposition.

Aim 5 Laboratory analysis to determine the clay mineral content of the Holocene sediments, with a view to determining, (a) the sources of the sediments and, (b) any differences in clay mineralogy from one facies or sub-facies to another that may be attributable to changes in environmental conditions.

Aim 6 Major and trace element geochemical analysis of bulk samples of the fine-grained Holocene and present-day intertidal sediments and of the clay fraction of both these groups of sediments, with a view to determining the provenances of these deposits.

1.5 Organisation of the thesis

The text of the thesis is divided into four Parts. The first two chapters, comprising Part I, explain the nature of the research project, outline previous related work and give a summary of the geological setting of the field areas that were studied.

Part II is concerned with the methods used in data-recording and sample collection in the field, stratigraphical correlation of the Holocene raised coastal sediments within the Dalbeattie, Kirkcudbright and New Abbey areas, and definition and description of the various sedimentary facies and sub-facies that were recognised in the Holocene sediments and present-day intertidal sediments.

Part III presents field and laboratory data on the sedimentological characteristics of Pleistocene and Holocene gravel deposits, and the results of grain-size, clay mineralogical and geochemical laboratory analyses of selected samples of the Holocene raised coastal deposits and present-day intertidal surface sediments.

In Part IV, the environments in which the Holocene raised coastal sediments accumulated and the provenances of these sediments are considered. A final chapter is devoted to a summary of the results of the research project, conclusions reached and suggestions for further study of the Holocene coastal sediments in the areas to which the study was directed.

1.6 Nomenclature and terminology

1.6.1 Nomenclature

The project is concerned mainly with the study and interpretation of sediments deposited during the Flandrian (Holocene) marine transgression and regression in south-western Scotland.

The beginning of the time interval involved is shortly before the time boundary between the Late Devensian Sub-Age and the Flandrian Age (or Holocene Epoch) (Table 1.1). The 'Windermere Interstadial', spanning the time interval c. 13,000 years B.P. to 11,000 years B.P. and with stratotype at Lake Windermere, NW England, is as defined by Coope & Pennington (1977). The term 'Loch Lomond Stadial' is used as equivalent to the Younger Dryas Chronozone of NW Europe (Mangerud et al. 1974), and is correlative with stratigraphical units described elsewhere by several authors (e.g. Jardine & Peacock 1973; Lowe & Gray 1980; Jardine 1981b). The end of the Loch Lomond Stadial is taken as 10,000 radiocarbon years B.P., the date selected by the INQUA Holocene Commission as the beginning of the Holocene Epoch and, therefore, the Flandrian Age (cf. Bowen 1978, 106). In Britain, the boundary between the Loch Lomond Stadial and the Flandrian 'Interglacial' appears to represent a moderately synchronous major environmental change (Coope & Pennington 1977).

The Late Devensian glacial episode spans the interval between c. 26,000 years B.P. and 10,000 years B.P. (Shotton 1973), and the term 'late Late Devensian' is used informally to denote the combined climatostratigraphical units of the Windermere Interstadial and Loch Lomond Stadial.

1.6.2 Terminology

Several terms and abbreviations used in the thesis are defined below:

Holocene raised coastal sediments

These include the products of several individual sedimentary environments, each of which existed in the neighbourhood of the northern coast of the Solway Firth during part or all of the Holocene Epoch.

Estuarine sediments

These form extensive relatively-flat, low-lying tracts in the lower parts of river valleys and at the heads of bays. They are dominantly medium- or fine-grained sediments (cf. Jardine 1975, 174-175).

Salt marsh deposits

These are present-day sediments, locally called 'merse deposits', forming the low areas adjacent to but landward of the limit of present mean high water spring tides (MHWS). They are flooded occasionally by tidal waters, and they extend inland for variable distances up to c.100m. They are colonised by halophytic plants and are traversed by a ramifying system of shallow creeks or gullies.

Present-day intertidal deposits

These are sediments that are deposited between present-day mean low water (MLW) and mean high water (MHW) and are separated from the adjacent salt marsh deposits by very low cliffs. The areas in which these deposits accumulate are covered by water at times of high tide.

Altitude or elevation

This value is given as above Ordnance Datum (AOD) or below Ordnance Datum (BOD), Ordnance Datum being Mean Sea Level at Newlyn, Cornwall.

Positions of the surface of the sea

Several positions of the surface of the sea are denoted by the abbreviations used in Figure 1.2.

Units of measurement

The units of length used in the determination and recording of distances, thicknesses, size grades etc. are the metre (m), kilometre (km, equivalent to 10^3m), millimetre (mm, equivalent to 10^{-3} m), micron (μm, equivalent to 10^{-6}m). The units of mass used are the gramme (g) and kilogramme (Kg, equivalent to 10^3g).

Locations and directions

Reference to specific locations is given by use of the British National Grid Reference system, e.g. NX 9828 6581. Directions are abbreviated in some cases to NE, SSW, etc. National Grid References of all boreholes and natural sections from which samples of Holocene sediments were collected are given in Table 1.2.

Changes of sea level

All references to changes of sea level are to **relative** rather than absolute (eustatic) changes.

Size grades

The terms used to describe the size grades in mechanical analysis of the sediments (Chapter 7) are those of the Udden-Wentworth scheme (after Pettijohn et al. 1972). In the field, size grades were estimated. Field descriptions are of the form, for example, 'silty sand with clay', denoting a sediment predominantly of sand grade, with a lesser amount of silt grade and minor amount of clay grade.

Clay fraction

The size fraction finer in grade than 2 μm or >8.0 Ø is the fraction that was separated in the laboratory by the sedimentation method based on Stokes's Law.

Sample code numbers

Each sample collected in the field and analysed in the laboratory has a unique

code number, e.g. D2 0.70, NM 1.50 or Np 3-1, which is used in reference to that sample in the Tables included in the thesis.

In the first example given above, the initial capital letter and number, D2, refers to the geographical area and the number of the borehole or natural section in that area: D denotes the Dalbeattie area, K the Kirkcudbright area and N the New Abbey area. In the case of samples collected in the Lochar Gulf area, the relevant section or borehole is denoted by two capital letters. For example, NM denotes the Newmains borehole. The full list of abbreviations is as follows:

BB Bankend Bridge section	NM Newmains borehole
HH Horseholm borehole	NP Northpark borehole
HM Highlandman's Pool section	PH Powhillon borehole
MT Midtown borehole	SK South Kirkblain section

In the case of samples of Holocene sediments the depth, in metres, at which the sample was taken below the ground surface is indicated. For example, 0.55 following the initial code letter and number denotes a sample taken at 0.55m below the ground surface.

In the case of samples of present-day intertidal surface sediments, the initial capital letter D, K or N is followed by the letter p (present-day). The number of the line of traverse within the relevant area and the number of the sample along that traverse are also given. For example, Dp 2-3 denotes present-day sample number 3 along traverse 2 in the Dalbeattie area.

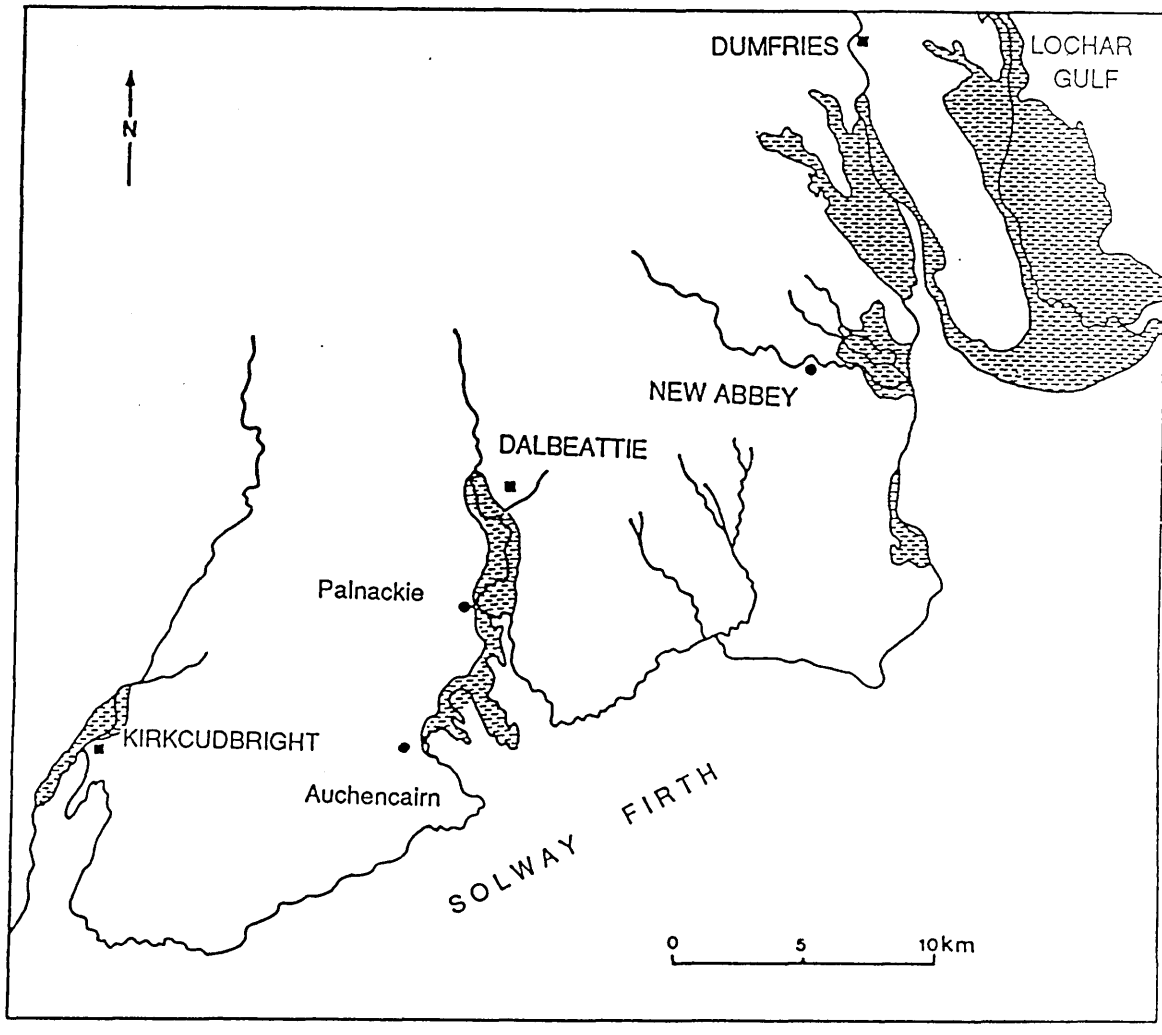

Figure 1.1 Map of part of Dumfriesshire and Galloway, showing the locations of the Dalbeattie, Kirkcudbright, New Abbey and Lochar Gulf areas, which were studied in the course of the research project. Two other areas of Holocene raised coastal sediments, between Dumfries and New Abbey, and south of New Abbey, were not included in the study.

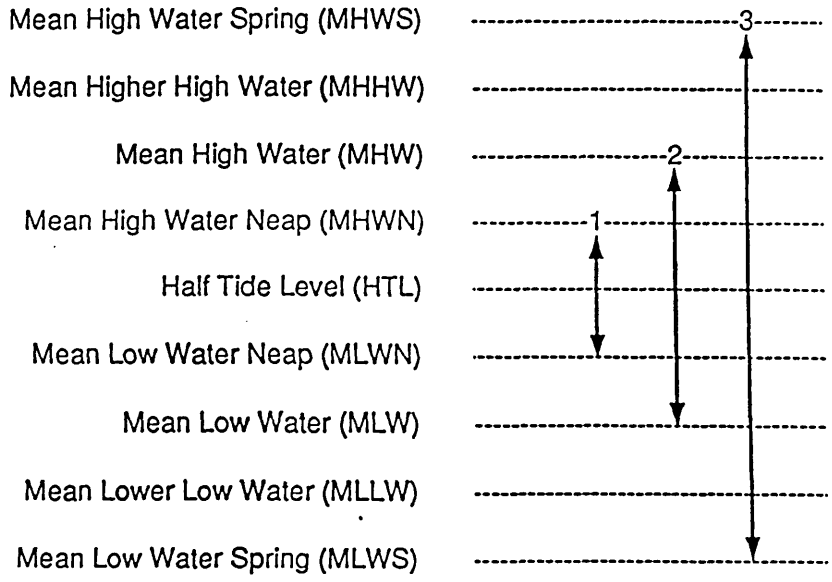

Figure 1.2 Diagrammatic representation of the surface of the sea (after Weimer et al., 1982, Fig. 2).

1. Mean Neap Range
2. Mean Range
3. Mean Spring Range

Table 1.1 Nomenclature of climatostratigraphic and geologic units used in the thesis (modified from Mangerud et al., 1974).

Radiocarbon Years (B.P.)	Climatostratigraphic Units	Equivalent Geological Time Units	
	Flandrian 'Interglacial' (Holocene)	Flandrian Age (Holocene Epoch)	
10,000			
	Loch Lomond Stadial (Younger Dryas Chronozone)	Loch Lomond Sub-Age	Late Devensian Sub-Age
11,000			
	Windermere Interstadial	Windermere Sub-Age	
13,000			

Table 1.2 Locations of boreholes and natural sections from which samples of Holocene sediments were collected and/or analysed in the course of the research project.

Dalbeattie area

Borehole or section	National Grid Reference		
D1	NX	8302	5915
D2	NX	8210	5717
D3	NX	8271	5797
D4	NX	8265	5760
D5	NX	8224	5897
D6	NX	8253	6097
D7	NX	8294	6034
D8	NX	8234	5865
D9	NX	8025	5479
D10	NX	8060	5282

Kirkcudbright area

Borehole or section	National Grid Reference		
K1	NX	6871	5212
K2	NX	6862	5223
K3	NX	6846	5239
K4	NX	6780	5159

New Abbey area

Borehole or section	National Grid Reference		
N1	NX	9868	6550
N2	NX	9870	6563
N3	NX	9858	6571
N4	NX	9809	6575
N5	NX	9802	6572
N6	NX	9798	6586

continued

Table1.2 continued

Lochar Gulf area

Borehole or section	National Grid Reference		
Bankend Bridge (BB)	NY	0291	6847
Horseholm (HH)	NY	0313	7062
Highlandman's pool (HM)	NY	0447	6692
Midtown (MT)	NY	1189	6577
Newmains (NM)	NY	0403	6663
Northpark (NP)	NY	0372	6685
Powhillon (PH)	NY	0572	6750
South Kirkblain (SK)	NY	0269	6956

CHAPTER 2

GEOLOGICAL SETTING OF THE RESEARCH AREAS

In this chapter the geological setting of the research areas is discussed briefly in terms of the origin and distribution of the underlying solid rocks, Pleistocene deposits and Holocene sediments.

2.1 Solid rocks

The four geographical areas chosen for study (Chapter 1.1 and 1.3) are located on the southern margin of the Southern Uplands of Scotland, a region of strongly-deformed sedimentary rocks of Ordovician and Silurian age, intruded in places by acid igneous plutons (Fig. 2.1). The deformed strata, striking approximately SW-NE, are traversed by a number of strike-oriented faults, which are thought to be rotated reverse faults (Weir 1974; McKerrow et al. 1977; Cook & Weir 1979). Sediments preserved in the Solway basin, to the south of the Southern Uplands, suggest that the basin was initiated as a SW-NE trending feature in late Devonian or early Dinantian times (Ord et al. 1988). Basin formation has been attributed to back-arc stretching similar to that operative in the present Aegean Sea area (Leeder 1976; 1982a) and to dextral shear movements (Dewey 1982).

The predominant types of solid rock in the Southern Uplands are these:

Igneous intrusions

The largest of the igneous intrusions are the granites and granodiorites of The Cheviot, in the east, and, in the west, Cairnsmore of Fleet, Criffell and Loch Doon -

Loch Dee (immediately east of Merrick, Fig. 2.1). They were emplaced during and after formation of the Lower Palaeozoic sedimentary rocks, but prior to folding and (minor) metamorphism of these rocks (Greig 1971). The granitic bodies have been studied by a number of workers, e.g. Gardiner & Reynolds (1932; 1937), Macgregor (1937; 1938), Phillips (1956), Parslow (1968; 1971), Leeder (1971) and Cook (1976).

Upper Ordovician and Silurian rocks

The sedimentary rocks of the greater part of the Southern Uplands consist of greywackes and shales, together with thin slivers of basic igneous rocks associated with black shales (Hall 1970; Dewey 1971; Bluck 1980; Hall et al. 1984; Bluck 1985). The Late Ordovician and Silurian history of sedimentation in the Southern Uplands trough can be understood in terms of several facies within the greywacke succession (Walton 1963). According to Adesanya (1982, 4a), the greywacke rocks may be divided broadly into two groups, fine-grained and coarse-grained. The latter are poorly sorted, with grain sizes ranging from <0.1mm to c. 3.0mm. Large-sized grains are typically shale (and occasionally other rock) fragments. In the fine-grained greywackes, grain sizes average c. 0.01mm to 0.04mm. Fractured quartz is predominant. The cementing medium is typically calcite in the coarse-grained variety and clay in the fine-grained variety. Clay minerals, however, constitute about 10% or less of the composition of the greywackes.

Lower Palaeozoic greywackes and shales, together with the western part of the large granodioritic pluton of Criffell, underlie most of the Dalbeattie area, and Permian and Silurian sedimentary rocks underlie the former Lochar Gulf area. Ordovician and Silurian sedimentary rocks, together with the eastern margin of the

Criffell granodioritic intrusion, are the bedrocks of the New Abbey area. The Kirkcudbright area is underlain mainly by Silurian greywackes (cf. Fig. 2.2).

2.2 Pleistocene deposits

During cold intervals of the Quaternary period, the Scottish uplands nourished valley glaciers that coalesced on the adjacent lowlands to form piedmont glaciers and, ultimately, ice sheets. The western part of the Southern Uplands has many corries, several rock basins and much ice-scraped bare rock, all these features being evidence of the former presence of glacier ice in that region. The influence of glacial meltwater is particularly obvious in SW Scotland, kames, kettles and outwash deposits being common (cf. Charlesworth 1926a & 1926b; Jardine 1956, 180-212; Holden 1977; May 1981; Cornish 1981).

2.2.1 Dalbeattie and Kirkcudbright areas

In the Dalbeattie and Kirkcudbright areas, the Pleistocene deposits range from massive, unstratified and unsorted till to well-bedded and sorted gravel, sand and silt deposits. The till is mainly compact, but locally is sandy, and contains abundant striated cobbles and pebbles. In colour it ranges from dark grey to reddish brown, depending on the type and composition of the underlying bedrock. Ablation of the ice sheets released large quantities of meltwater, which in turn deposited sand and gravel in the hollows and flat areas around and between the decaying ice masses. In the Dalbeattie area, undulating spreads of kame mounds and esker ridges were formed, whereas in the Kirkcudbright area the glaciofluvial deposits form wide, flat-topped mounds of well-stratified sand and gravel. In both areas, the meltwater deposits have been incised by later river erosion and (nearer the Solway Firth) by marine

incursion, to leave terraces above and adjacent to flat tracts that are largely composed of Holocene deposits (cf. Horne et al.1896; Greig 1971; Brown 1980; 1981; see also Figs. 2.3 and 2.4).

2.2.2 New Abbey and Lochar Gulf areas

During the last major glaciation of southern Scotland these areas were scoured by ice that moved in a generally easterly or south-easterly direction. The glaciers carried many boulders of granodiorite from the Criffell massif and these are now distributed widely as distinctive erratics on the low ground adjacent to the inlets that existed later (during the early part of the Holocene Epoch) at New Abbey and as the Lochar Gulf (cf. Greig 1971). The distribution of the tills and glaciofluvial deposits in these areas is shown in maps of the British Geological Survey (Brown 1981; 1983a; 1983b) and of Jardine (1971; 1980).

2.3 Holocene deposits

The Holocene deposits of the four geographical areas chosen for study are the sediments with which the research project is mainly concerned. There is little need, therefore, to describe or discuss the nature and origin of these deposits here. Their distribution and geographical limits, however, are of relevance in relation to the geological setting of the project, so these aspects of the deposits are discussed briefly in this section.

2.3.1 Holocene deposits of the Dalbeattie area

In the northern, western and eastern parts of this area, the inland limit of the sediments deposited by the Flandrian marine transgression and regression is marked

by small cliffs on either side of the valley of the Urr Water. The cliffs separate the Holocene deposits from higher areas that consist of Pleistocene deposits and solid rocks (e.g. at NX 8220 6108). In the south, the limit of the Holocene sediments is marked by a line of very low 'cliffs', located at present highest tide position. The 'cliffs' are cut in the Holocene raised coastal sediments. Seawards of them, and at a lower level, present-day salt marsh sediments occur. The width of the area of Holocene sediments varies from one place to another within the Dalbeattie area, being up to a maximum of c. 2km in the south. From the present distribution of these deposits, it may be deduced that the maximum northern extent of the shoreline during the Holocene marine transgression was c. 12km landwards of the position of the present shoreline (Fig. 2.3).

2.3.2 Holocene deposits of the Kirkcudbright area

The Holocene deposits of this area, forming a tract of variable width between the River Dee and mounds of Pleistocene sand and gravel, are exposed in parts of the banks of the river by the action of high spring tides. The Holocene deposits extend northwards from the town of Kirkcudbright to Tongland Bridge (NX 6921 5334), the position of the maximum landward extent of the sea in this area during the Holocene marine transgression. The position of the former shoreline is marked by either a small 'cliff' or a facies change or a break in slope of the ground surface. A few discontinuous remnant 'cliffs' of Holocene sediments are present to the west of Kirkcudbright Bridge (NX 6841 5125) on the western bank of the River Dee (Fig. 2.4).

2.3.3 Holocene deposits of the New Abbey area

Holocene raised coastal sediments extend on both sides of New Abbey Pow and Drumillan Pow north-westwards from the mouth of New Abbey Pow (Pow Foot, Fig. 2.5). The sediments are typically developed in south-bank meander scars of New Abbey Pow at NX 9858 6571, NX 9809 6575 and NX 9802 6572 . The shoreline that existed during the main Flandrian transgression was located about 3km inland from the present shoreline, the maximum landward extent of the Holocene raised coastal sediments along the course of New Abbey Pow being c. 400m to 500m west of the village of New Abbey.

2.3.4 Holocene coastal deposits of the former Lochar Gulf

Much of the large tract of Holocene coastal sediments that extends northwards on either side of the Lochar Water from the Solway Firth to the vicinity of the village of Locharbriggs is covered by thick deposits of peat, so natural exposures of the former marine sediments are few (Jardine 1980, 25). Locations of relevance to the present research project are those where boreholes were sunk or sections exposed at NY 1189 6577 (Midtown), NY 0372 6685 (Northpark), NY 0403 6663 (Newmains), NY 0447 6692 (Highlandman's Pool), NY 0572 6750 (Powhillon) and NY 0313 7062 (Horseholm) . In the course of the present project, sections at NY 0269 6956 (South Kirkblain) and NY 0291 6874 (Bankend Bridge) were sampled.

At the time of the main Holocene marine transgression, the area that is now located c. 5km to the east of Dumfries was a large embayment (the so-called **Lochar Gulf**, Jardine 1975) with narrow inlets at its northern extremity. The inlet in which the upper reaches of the Lochar Water are now sited was by far the largest

extension of the gulf. The site of the village of Locharbriggs, which was on the shoreline at the time of the maximum of the Holocene transgression, is sited now c. 15km from the coast (Fig. 2.6).

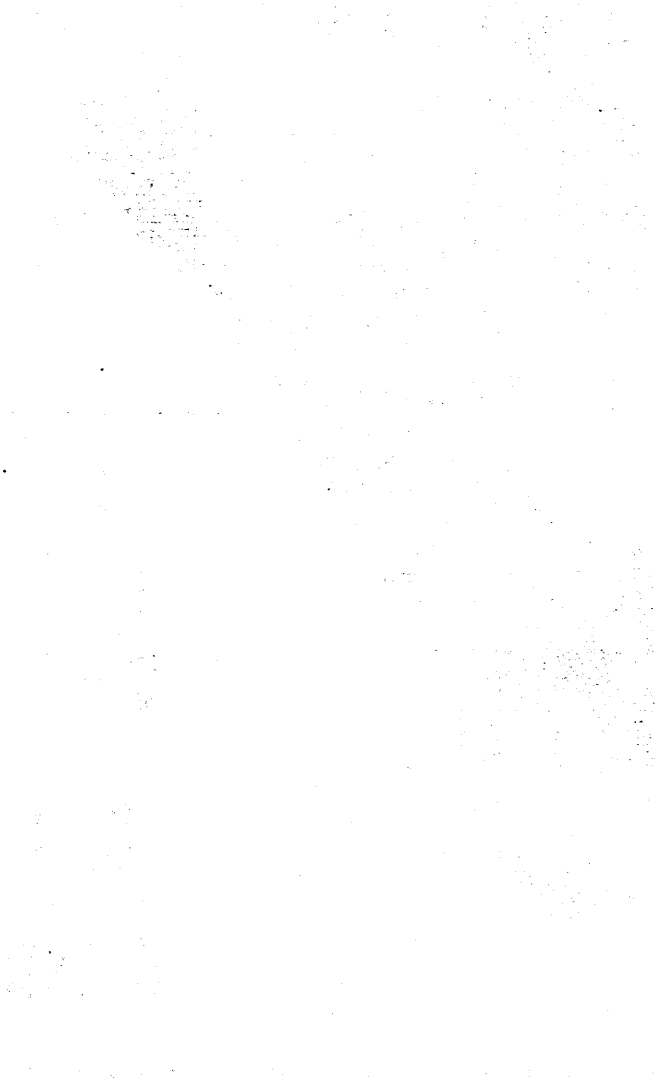

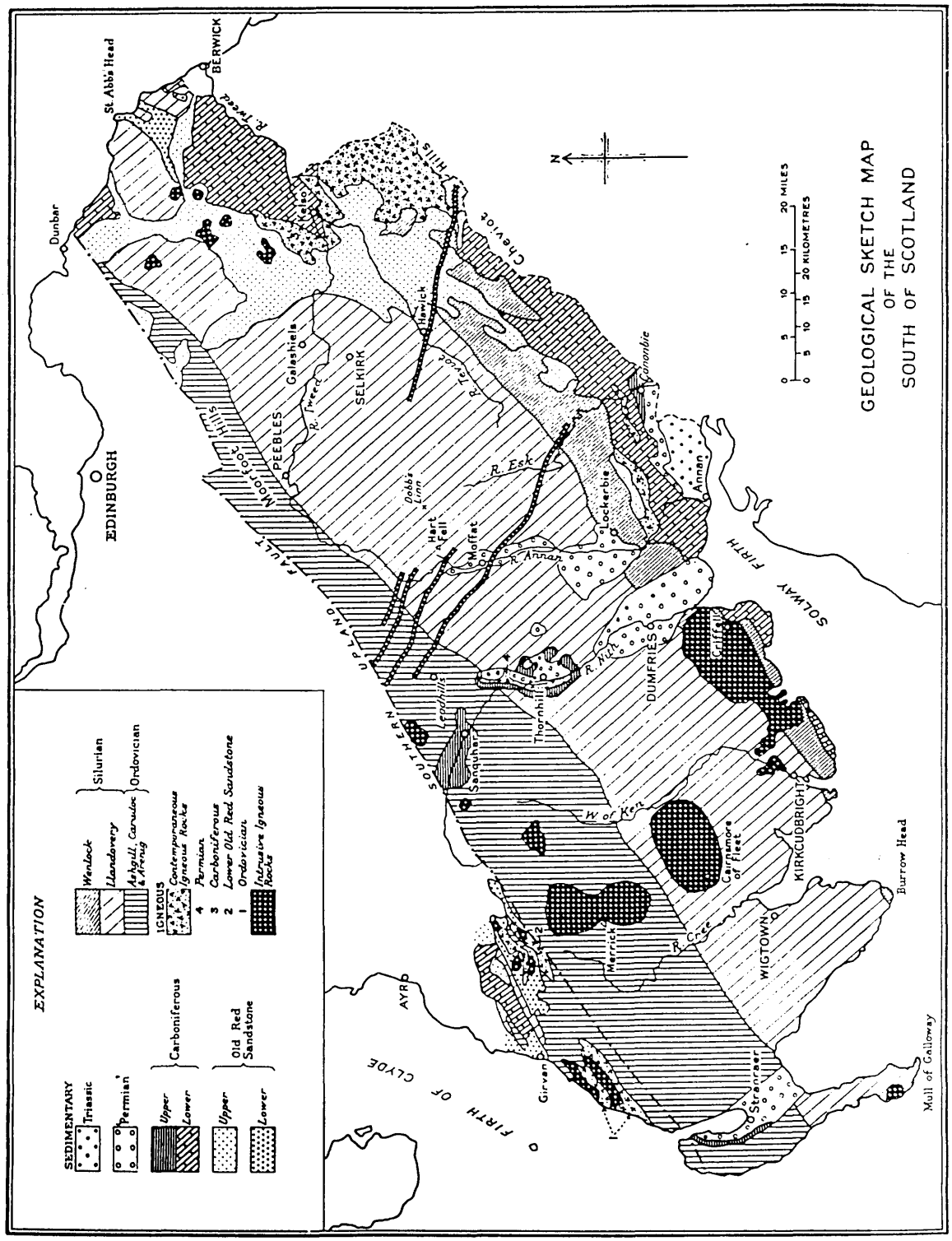

Figure 2.1 Map of the solid rocks of the Southern Uplands of Scotland (Greig, 1971, Plate XIII)

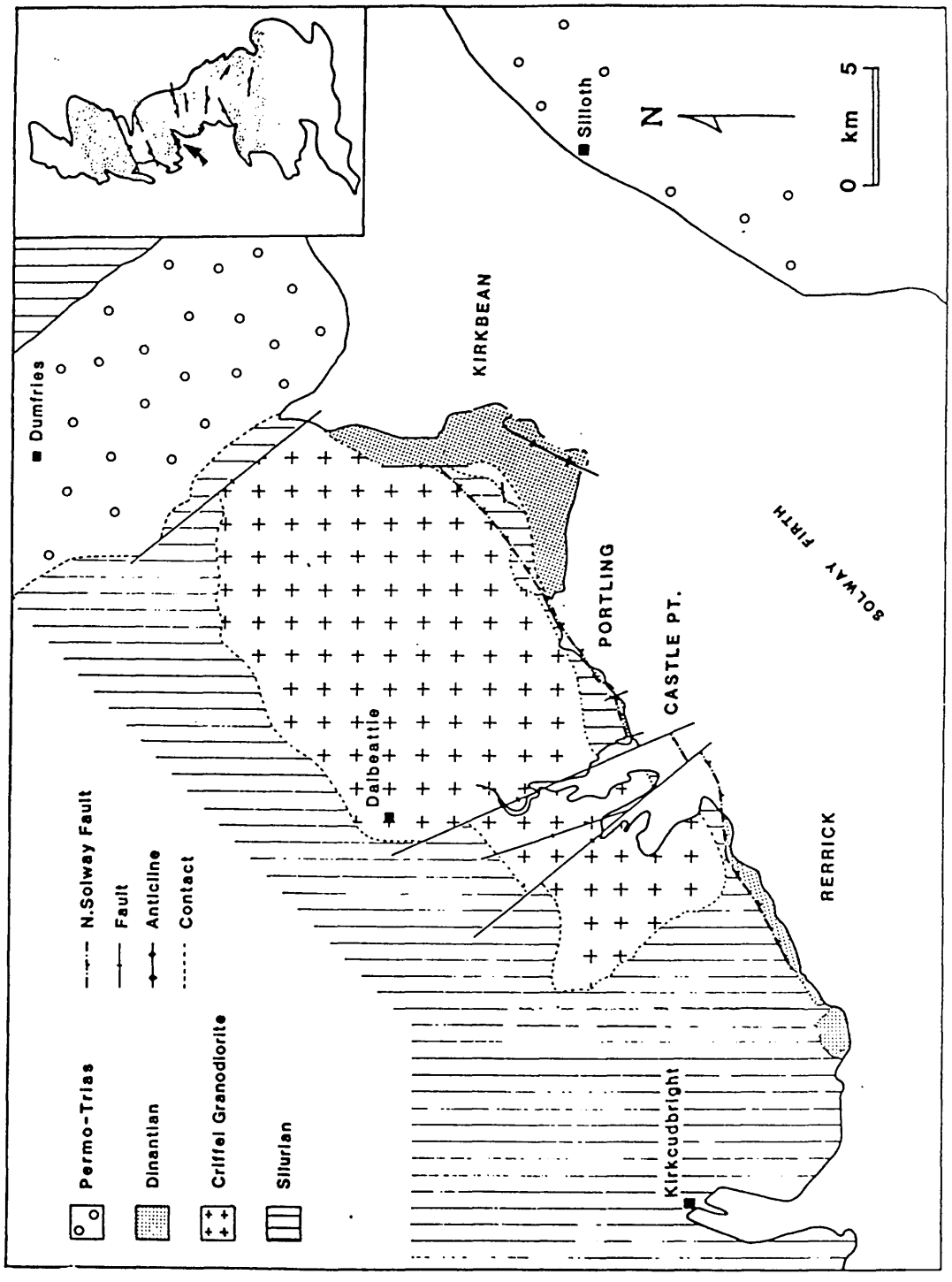

Figure 2.2 Map of the solid rocks of the research area (Ord et al. 1988, fig.1)

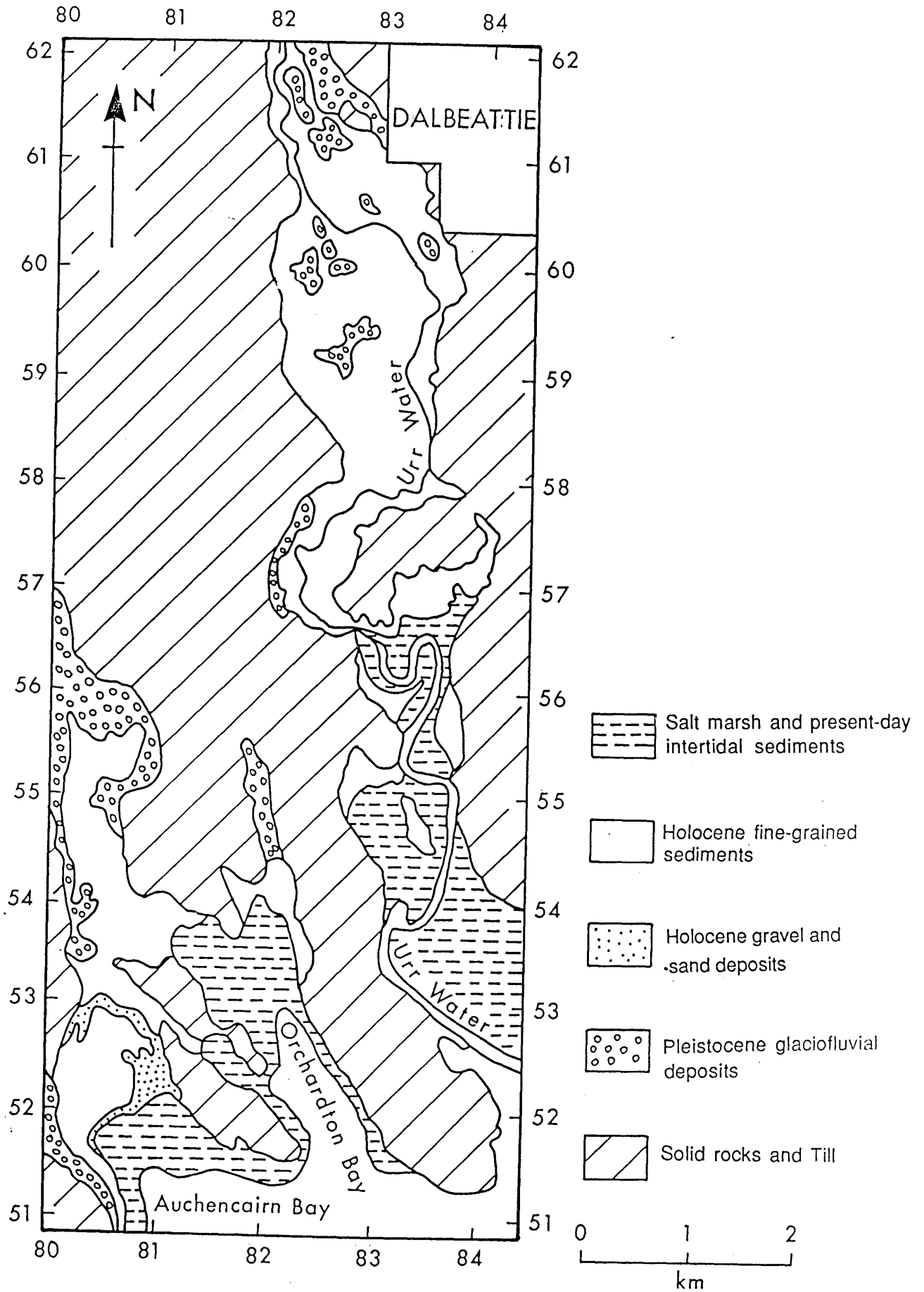

Figure 2.3 Map of the Dalbeattie area, showing the distribution of Pleistocene, Holocene and present-day sediments (based on field mapping).

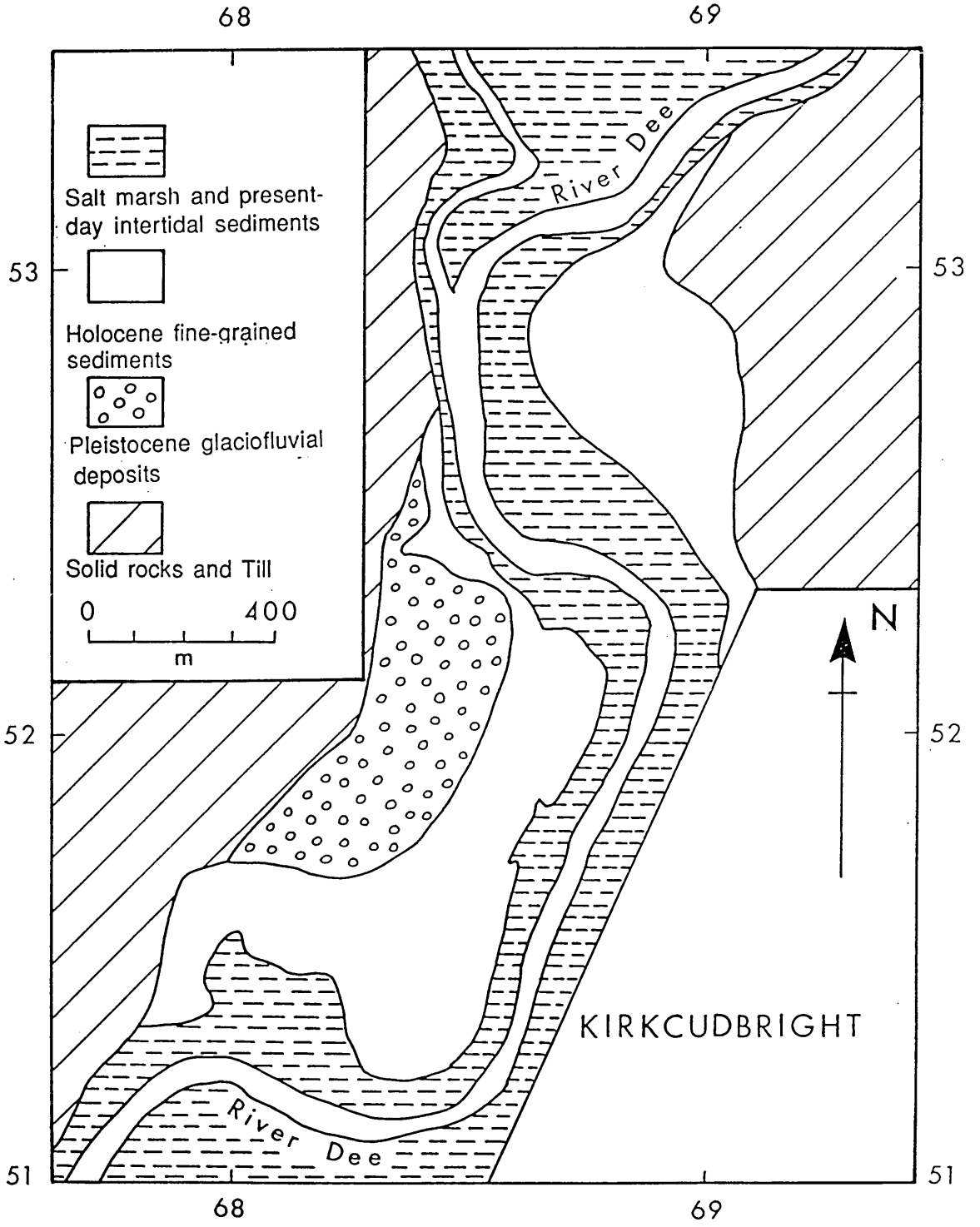

Figure 2.4 Map of the Kirkcudbright area, showing the distribution of Pleistocene, Holocene and present-day sediments (based on field mapping).

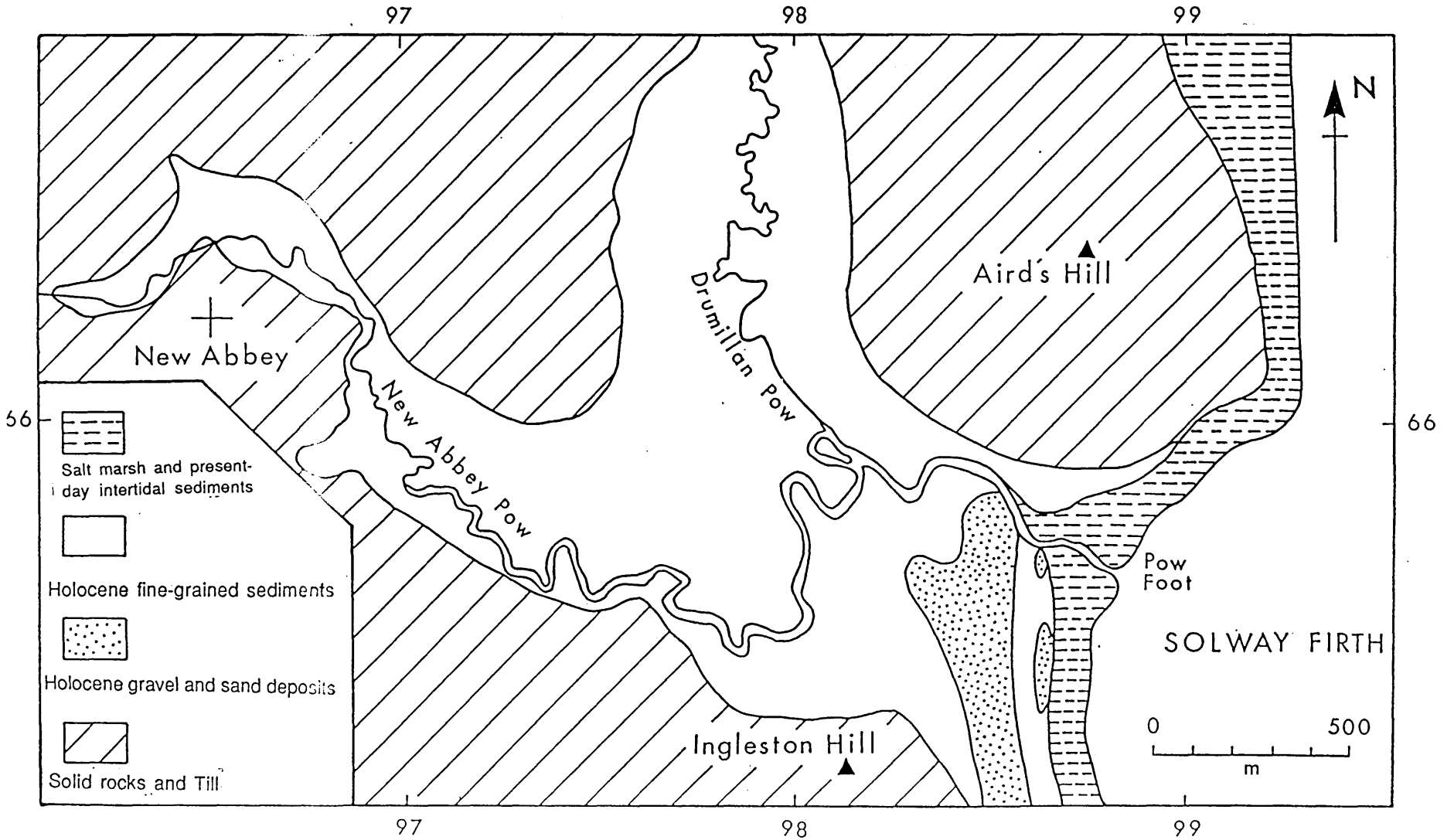

Figure 2.5 Map of the New Abbey area, showing the distribution of Holocene and present-day sediments (after Jardine 1980, fig. 8).

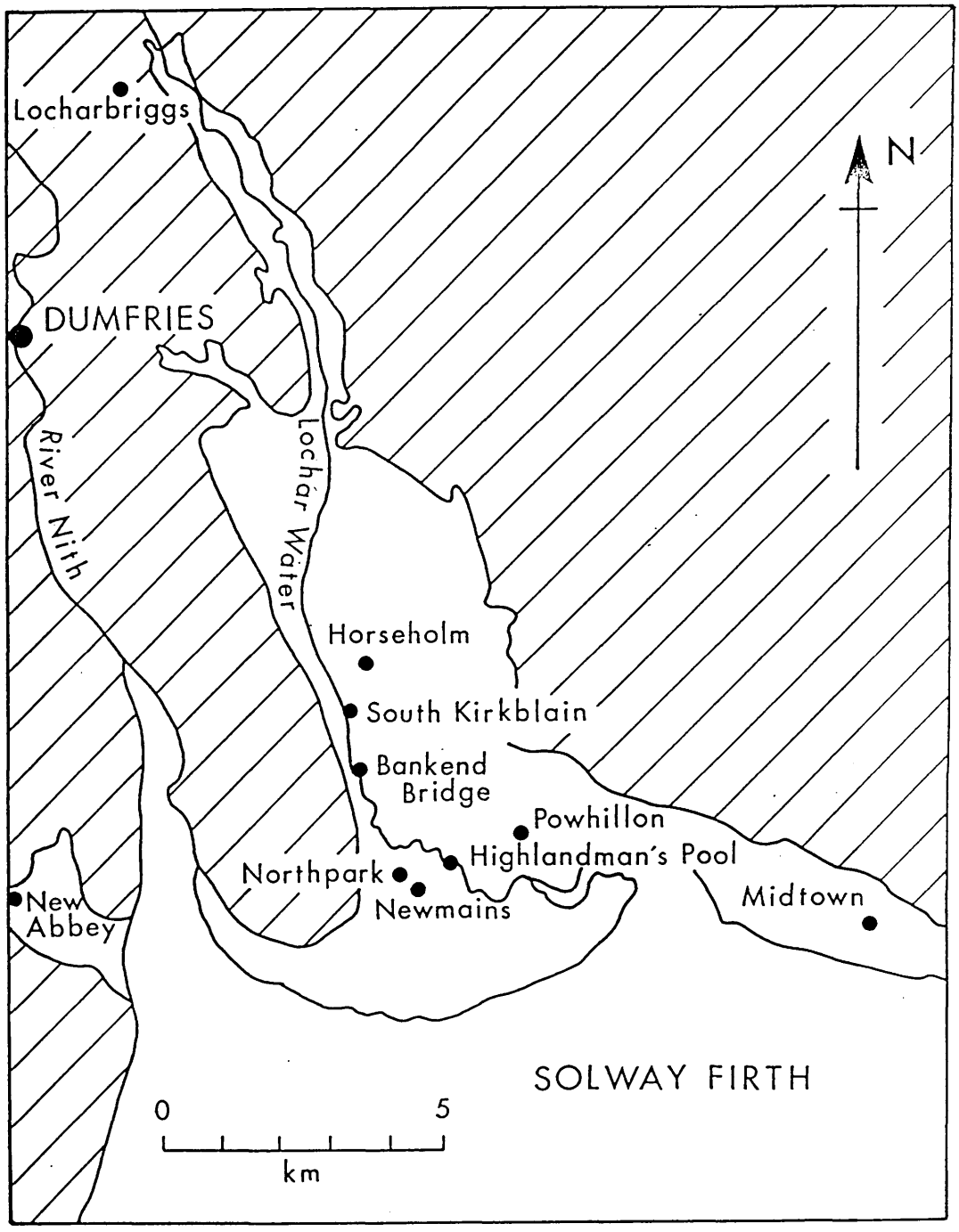

Figure 2.6 Map of the Lochar Gulf area, showing the distribution of Holocene sediments (unshaded) in relation to surrounding areas of solid rocks and Pleistocene deposits (shaded).

PART II

FIELD DATA RECORDING, STRATIGRAPHICAL CORRELATION AND FACIES DESCRIPTION

CHAPTER 3

DATA-RECORDING AND SAMPLING IN THE FIELD

Fieldwork in the course of the research project was concentrated on examination and sampling of sediments rather than recording of geomorphological features. Recognition of such features, however, was used as an aid in the mapping of the extent of the various sedimentary units.

3.1 Mapping and vertical logging of Holocene raised coastal deposits

The lateral extent and, in lesser degree, the thicknesses of the various units of the Holocene raised coastal deposits are controlled by the morphology and distribution of the Pleistocene tills and glaciofluvial sand and gravel bodies that are adjacent to and underlie the Holocene sediments. The lateral extent and thicknesses of the Holocene sediments also depend on the topography of the local bedrocks and their structures, the latter of which affect the width of the valley floors and the orientation and slope of the valley sides.

The main aim of the mapping of the raised coastal sediments was to determine, as accurately as possible, the position of the shoreline at the maximum of the Flandrian marine transgression, in order to compare the former shoreline with the present shoreline.

Vertical logging of profiles through the Holocene sediments was carried out at selected locations, with a view to recording the characteristics of the sediments that are typical of the various facies and sub-facies that exist in the areas studied.

Two different types of profile were recorded by vertical logging. In the first

type, the sediments were exposed in natural, (approximately) vertical sections, mainly along river banks and streams. In such cases, each log was measured and recorded downwards from an arbitrary 'zero recording point' at a measured altitude, above Ordnance Datum, determined by instrumental levelling of the profile to an established Ordnance Survey bench mark. This allowed precise inter-section correlation to known altitudes above or below Ordnance Datum (AOD/BOD). In some cases, to enable a continuous vertical profile to be constructed, a series of steps had to be cut down the stream bank. Also, in a few cases, information concerning the lower part of a logged succession was obtained by augering below the lowest exposed part of the river or stream bank.

In the second type of profile recorded, a hand-operated 75mm diameter bucket-auger, with extension rods, was used to core through the Holocene sediments from the ground surface to maximum depths of about 3.75m. In such cases, the 'bucket' of the auger was emptied at successive depths equal to the length of the bucket. By this method, the vertical positions of changes in the sedimentary succession could be recorded accurately as the work progressed. The altitude of the ground surface at each location where an auger profile was recorded was determined by instrumental levelling to established Ordnance Survey bench marks. This allowed auger-hole profiles and profiles recorded as natural vertical sections to be correlated with each other, both within the individual geographical areas studied, and from one area to another.

Ground-level heights of recorded sections and boreholes are given in Table 3.1.

3.1.1 Mapping in the Dalbeattie and Kirkcudbright areas

The methods used in determination of former shoreline positions in the Dalbeattie and Kirkcudbright areas were recognition of geomorphological features of the

former shoreline, e.g. small cliffs and breaks in slopes, and changes in lithology at boundaries between Holocene coastal sediments and adjacent Pleistocene deposits. In the latter case, it was noted that in places the Holocene and Pleistocene sediments are separated by a thin layer of organic debris, which may contain angular pebble-sized clasts of inorganic material.

The Dalbeattie and Kirkcudbright areas were mapped on a scale of 1 : 10,560. Mapping was based on the nature of the sediment exposed at the ground surface, except where the surface soil layer was thick. In such cases, small pits were dug to examine the nature of the sediments immediately beneath the soil, and to determine changes in sedimentary facies.

In the Dalbeattie area, the upper surface of the fine-grained Holocene sediments was found to be generally at c. 9.0m AOD, whilst in the Kirkcudbright area the highest recorded surface elevation of the fine-grained Holocene sediments was 6.16m AOD.

3.1.2 Mapping in the New Abbey and Lochar Gulf areas

In the present project, no mapping of the distribution of Holocene sediments or of former shoreline positions in these areas was carried out since both these objectives had been achieved already by Jardine (1975; 1980). Maps from these publications have been used in the course of the parts of the present project that are concerned with the New Abbey and Lochar Gulf areas.

In the New Abbey area, the upper surface of the fine-grained Holocene sediments was found to be generally at c. 7.5m AOD, whilst in the Lochar Gulf area the surface elevation of the fine-grained Holocene sediments was generally at c. 9.0m AOD.

3.2 Sample collection

Sampling of sediments was carried out in four ways:

1) Core sampling

A hand-operated 75mm diameter bucket-auger was used in the sampling of Holocene coastal sediments underlying extensive tracts of flat ground in the Dalbeattie area, no natural exposures being present in these areas. Eight auger holes were sunk at selected locations, and samples taken of the various sedimentary units that could be distinguished in the course of the augering (Fig. 3.1). The depth of the auger holes varied between 2.95m and 3.65m, and it should be noted that some of the auger-hole profiles represent a complete Holocene sedimentary succession, whilst others represent only part of the Holocene sequence.

Samples collected from certain parts of the Lochar Gulf area by power and hand augering in the 1970s were provided by Dr. W. G. Jardine for laboratory analysis in the course of the research project discussed in this thesis (Fig. 2.6).

2) Sampling of exposed natural sections

Sampling was carried out at selected exposed sections on stream and river banks (Figs. 3.1, 3.2, 3.3 and 2.6). In addition, coring by hand auger at the base of exposed sections was used to augment or complete sampling of sections as far as possible.

3) Sampling of gravel deposits

In the Dalbeattie area, samples of gravel-sized clasts were collected from two abandoned gravel pits in Pleistocene glaciofluvial deposits, at Chapelcroft (NX 804 550) and Broomisle (NX 823 592) (Fig. 3.1). Samples of gravel-sized clasts were

also collected from natural exposures and by digging small pits in an upper ridge (NX 804 531 to NX 808 529) and a lower ridge (NX 808 521 to NX 810 522) of Holocene beach deposits at Torr.

4) **Sampling of present-day intertidal areas**

Samples of present-day intertidal sediments were collected from the surface layers of these sediments. The collection of samples of these sediments was carried out, at times of low tide, either along the direction of gentle slope of the intertidal zone (Kirkcudbright area) or transverse to the direction of stream flow at the heads of bays (Auchencairn Bay, Dalbeattie area, and New Abbey Pow, New Abbey area).

3.3 Recording of sedimentary structures and of pebble orientation

Sedimentary structures were difficult to recognise in the areas studied, but the present work included recording of sedimentary structures that were preserved and of pebble orientation in relevant facies of the sediments studied.

The following structures were identified:

1) Small-scale cross-bedding was recorded in pits in Pleistocene glaciofluvial gravel deposits in the Dalbeattie area (at Chapelcroft and Broomisle; see Chapter 6). Also, a few cross-strata were recorded in the lower part of the Holocene coastal sediments in naturally-exposed sections in the banks of New Abbey Pow.

2) Inter-lamination of clay, silt and fine sand was recorded in sections of Holocene sediments in the Kirkcudbright and New Abbey areas.

3) Bioturbation of fine-grained sediments, which occasionally causes destruction of pre-existing sedimentary structures, was recorded.

4) Layers that include lenses of pebbles and sand were recorded in small cliffs in

salt marsh deposits, mainly in the New Abbey area.

5) Current-ripple structures were recorded in present-day intertidal sediments. Such structures are common on the floors of channels that cut these sediments.

In the Dalbeattie area, dip-direction readings were taken in imbricated gravel deposits exposed in Potterland Lane (see Chapter 6.8.1), and in two units of Holocene beach gravels at Torr, where there are occasional exposures at the bottom, and in the banks, of a few streams (see Chapter 6.8.2). Dip-direction readings were also taken in Holocene beach gravel ridges in the New Abbey area, at NX 985 657 and NX 986 653 (see Chapter 6.8.2). The purpose of these readings was to determine the flow directions of currents that deposited these gravels.

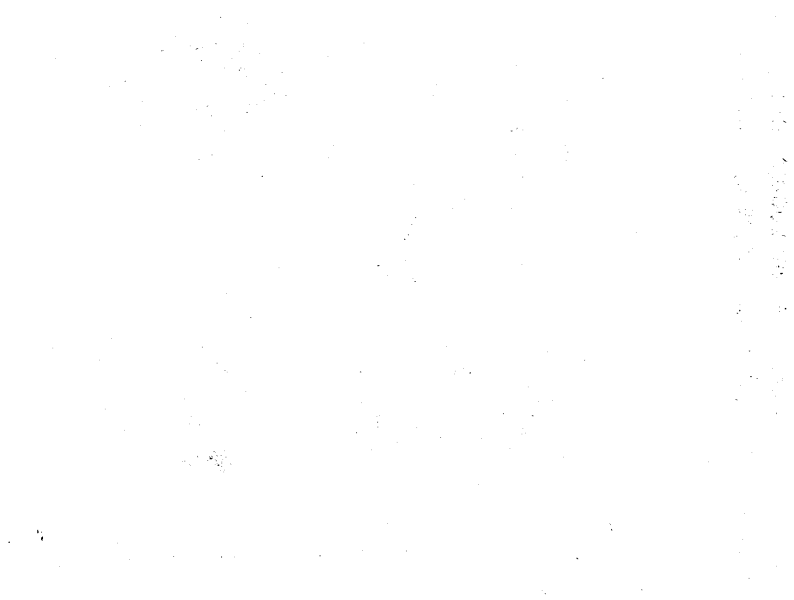

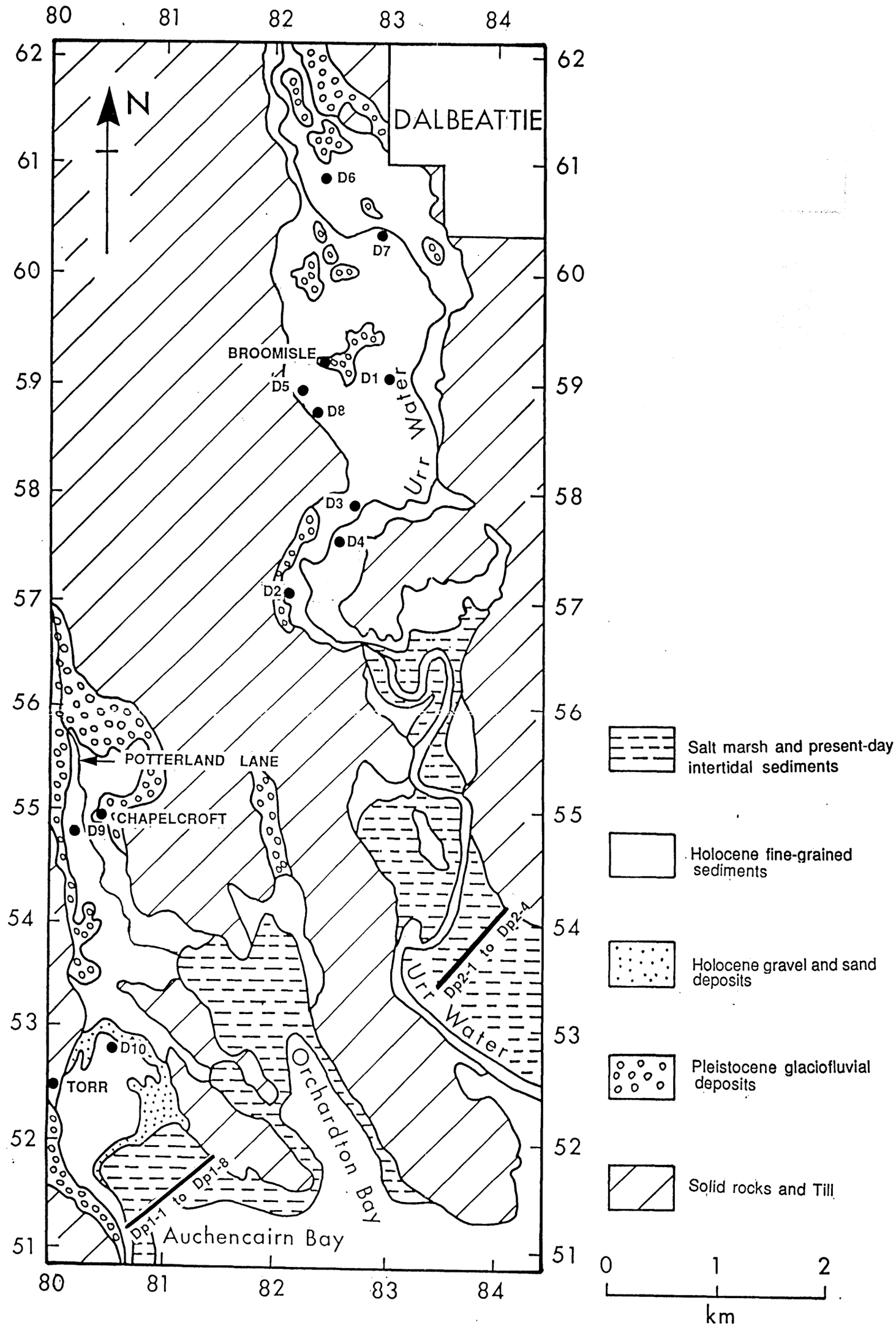

Figure 3.1 Map of the Dalbeattie area, showing positions of sites (D1, D2 etc.) where samples of Holocene sediments and traverses (Dp1-1 to Dp1-8 and Dp2-1 to Dp2-4) where samples of the present-day intertidal sediments were collected. The positions of sites where Pleistocene and Holocene gravel deposits were sampled and/or pebble orientation was recorded are also shown.

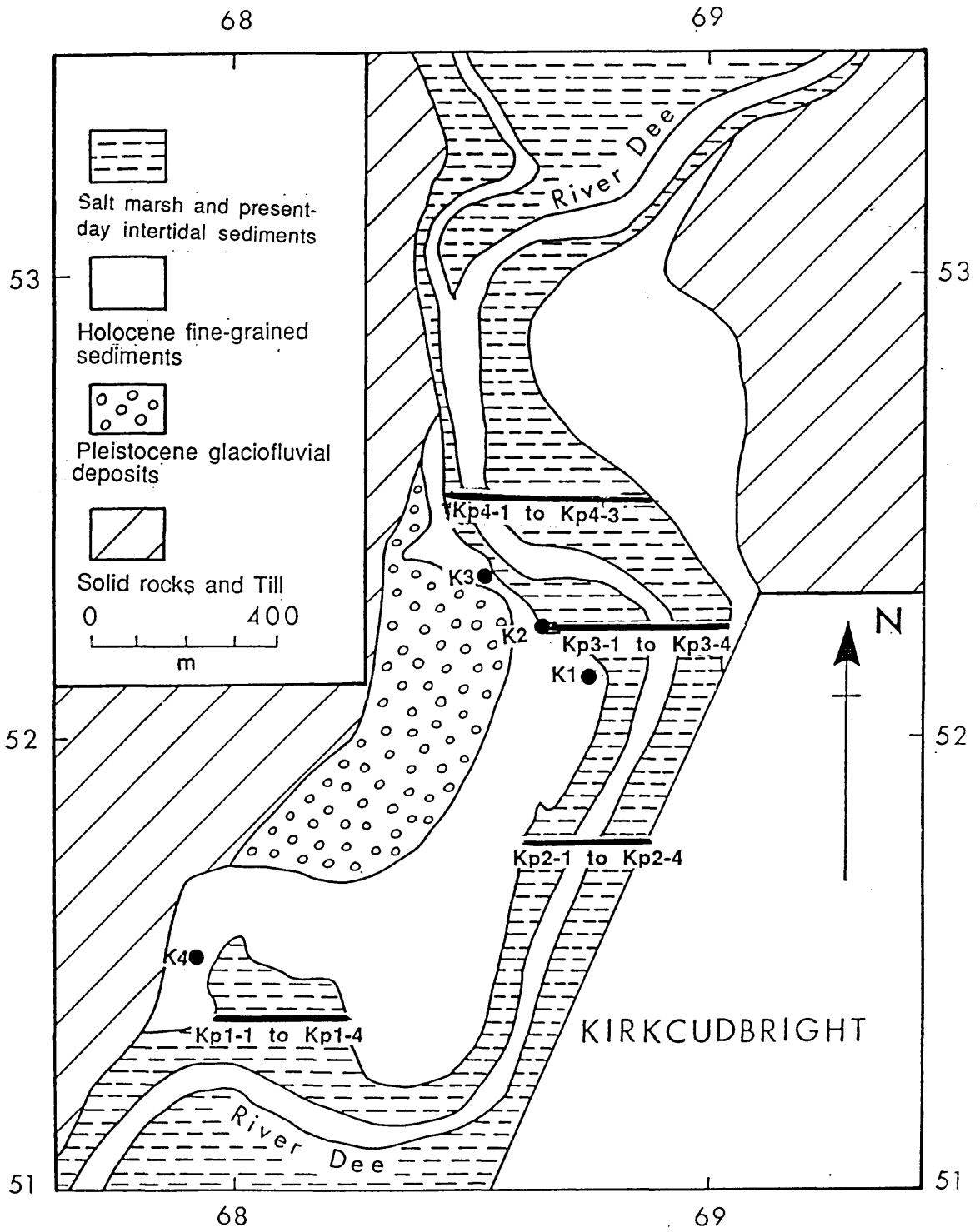

Figure 3.2 Map of the Kirkcudbright area, showing positions of sites (K1, K2, K3 and K4) where samples of Holocene sediments and traverses (Kp1-1 to Kp1-4, Kp2-1 to Kp2-4, Kp3-1 to Kp3-4 and Kp4-1 to Kp4-3) where samples of the present-day intertidal sediments were collected.

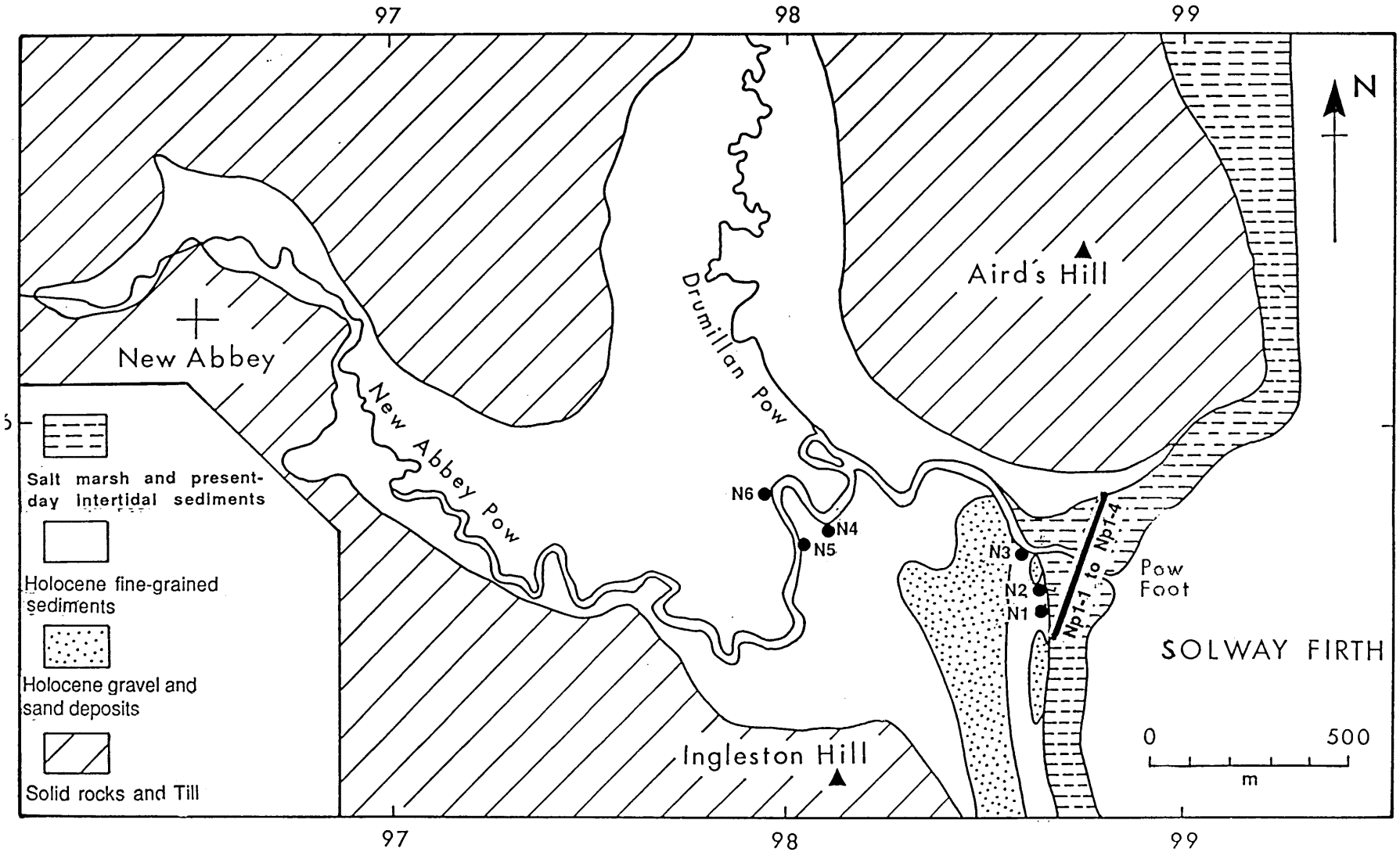

Figure 3.3 Map of the New Abbey area, showing positions of sites (N1,N2 etc.) where samples of Holocene sediments and traverse (Np1-1 to 1-4) where samples of the present-day intertidal sediments were collected.

Table 3.1 Ground-level heights of sampled sections and boreholes in Holocene sediments in the four areas studied

1. Dalbeattie

Section or borehole	Height in metres AOD
D1	9.385
D2	7.550
D3	9.158
D4	9.070
D5	9.005
D6	9.500
D7	8.870
D8	9.215
D9	8.940
D10	7.642

2. Kirkcudbright

Section	Height in metres AOD
K1	5.305
K2	4.180
K3	6.160
K4	4.410

3. New Abbey

Section	Height in metres AOD
N1	Not measured
N2	Not measured
N3	7.550
N4	7.700
N5	7.180
N6	7.255

4. Lochar Gulf

Section or borehole	Height in metres AOD
BB	Not measured
HH	9.910
HM	9.340
MT	9.330
NM	9.020
NP	10.045
PH	8.120
SK	Not measured

CHAPTER 4

STRATIGRAPHICAL CORRELATION OF THE HOLOCENE RAISED COASTAL SEDIMENTS

4.1 Introduction

Logging of natural and artificial vertical profiles through the Holocene raised coastal sediments in the four areas of study gives an indication of changes in lithology through Holocene time at each of the individual locations where profiles were recorded. When individual profiles are represented together diagrammatically, as in Figures 4.2, 4.3, 4.5 and 4.7 for the Dalbeattie, Kirkcudbright and New Abbey areas, a more useful picture of changes in lithology in time and space is obtained. The main aims in constructing correlated vertical lithological columns, therefore, were to determine the equivalence and lateral extent of each of the distinctive sedimentary units it was possible to distinguish in the field at individual locations. A subsidiary aim was to determine the relationships between the Holocene raised coastal sediments and the adjacent Pleistocene till and glaciofluvial deposits in the areas studied.

4.2 Dalbeattie area

4.2.1 North-South section

A correlation diagram along an approximately North-South line (Fig. 4.1) was constructed from seven recorded borehole or naturally-exposed sections in the Dalbeattie area. The diagram (Fig. 4.2) extends from section D6 at the town of Dalbeattie in the north, near the farthest 'inland' extent of the shoreline during the Holocene marine transgression, to section D10 in the south, near the head of Auchencairn Bay. The diagram shows vertical variations in the sedimentary succession

and the lateral continuity of the various sedimentary units. In places, e.g. at locations D2 and D6, the complete succession of Holocene sediments may be present in the recorded section. At other locations, perhaps only the upper part of the Holocene sedimentary sequence is present.

From the diagram it may be inferred that, in places, a thin layer of organic (plant) debris and reworked gravel clasts is present at the contact between the Holocene sediments and the underlying Pleistocene deposits in this area. The organic-rich layer is succeeded upwards by a layer of pale grey clayey silt that varies in thickness over the Dalbeattie area. This layer in turn is overlain by clayey silt with fine sand. A layer of brown or grey clayey silt, rich in plant matter and variable in thickness, forms the uppermost stratum of the Holocene sediments throughout the length of the diagrammatic section. In section D10, the uppermost layer of clayey silt is interrupted by a thin unit of pebbly sand, which may have been deposited in a local channel. In section D9, a layer of grey fine sand and coarse silt, rich in plant debris, ostracods and foraminifers, was encountered at the base of the auger hole drilled at this location. This unit resembles the present-day intertidal sediments of the same area in terms of its general appearance and size grade. In terms of its microfossil content it resembles the deposits found in many of the boreholes sunk in the Lochar Gulf area by Jardine (1980, 29-31) and in the lower part of sections recorded in parts of the Kirkcudbright and New Abbey areas (see Chapter 4.3 and 4.4 below).

4.2.2 NNW - SSE section

Three boreholes, D5, D3 and D4, sunk in the area between the town of Dalbeattie and the village of Palnackie (Fig. 4.1), and represented in an approximately

NNW to SSE diagrammatic section (Fig. 4.3), show a marked variation in the Holocene sedimentary sequence between the NNW and SSE ends of the diagram. In the NNW, adjacent to a former cliff-line in solid rocks, borehole D5 penetrated Holocene sediments that appear to have been separated at least partially from the contemporaneous sea by a higher area of Pleistocene glaciofluvial deposits. The area where borehole D5 was sunk is thought to have been occupied at the maximum of the Holocene marine transgression by brackish water, or to have been a marsh environment in which there accumulated clayey silt and large amounts of plant debris, including pieces of wood. In contrast, to the SSE near Urr Water, where section D3 is common to both Figures 4.2 and 4.3, and borehole D4 penetrated deposits similar to many of those represented in Figure 4.2, the Holocene sediments are composed of pale grey clayey silt at the base, overlain by clayey silt with fine sand and occasional pieces of plant matter. The uppermost deposit of the sequence is the layer of brown silty clay that also tops the sequence in the North-South section of the Dalbeattie area (Fig. 4.2).

4.3 Kirkcudbright area

Figure 4.5 is a roughly North-South section, aligned approximately parallel to the course of the River Dee west of the town of Kirkcudbright (Fig. 4.4). It shows the relationships of the sedimentary units identified in four recorded sections. In K4, the contact zone between the Holocene coastal sediments (above) and Pleistocene glaciofluvial gravels (below) consists of a layer of compacted plant debris ('peat') overlain by a layer of reworked pebble-sized clasts. In the other three sections (K1, K2 and K3), the lowermost recorded Holocene sedimentary unit comprises grey fine sand and silt, rich in mica flakes and also in foraminifers, ostracods and fragments of

bivalve shells. The fossiliferous sediments are overlain in sections K1 and K2 by a layer, consisting of alternating laminae of fine sand and silt, that is absent in section K3. This may be due to the deposition in K3 of reworked pebbles, embedded in sand (Fig. 4.5), derived from adjacent Pleistocene gravels, which are exposed at present in nearby low cliffs. The uppermost layer of Holocene sediments, occurring in all four sections but thicker in K1, K2 and K3 than in K4, is of clayey silt with a variable content of clay and fine sand. It changes gradually in colour from grey at the base to brown nearer the ground surface, where it also is richer in organic (plant) matter.

4.4 New Abbey area

The Holocene sediments of the New Abbey area are represented by four recorded sections, at N3, N4, N5 and N6 (Fig. 4.6), shown in correlated vertical successions in Figure 4.7. The lowermost recorded sedimentary unit common to all four sections consists of grey fine sand with silt, rich in mica flakes and also in foraminifers, ostracods and fragments of bivalve shells. In section N3, a layer of pebbles and sand, possibly due to local deposition in an intertidal channel, was recorded below the layer of grey fine sand with silt. In sections N5 and N6 the fossiliferous fine sand layer was overlain by a brown-coloured layer of pebbles and sand that was seen in the banks of New Abbey Pow to extend laterally for a distance of several metres. The pebbly sand, rich in plant debris but devoid of marine faunal remains, may be the product of local deposition in a fluvial channel. This is suggested by the sharpness of the contact of the pebble layer with both the underlying and overlying sediments, and by evidence of channel-cutting into the underlying layer of fossiliferous fine sand with silt.

The pebbly sand layer of N5 and N6 and the fossiliferous fine sand with silt layer of N3 and N4 are overlain by a laterally-continuous layer of clayey silt with fine

sand. The layer is of a characteristic pale grey colour and contains rare remains of marine microfossils. It is succeeded upwards by a layer consisting of alternating laminae of fine sand and silt. Both these layers vary markedly in thickness (Fig. 4.7).

In all four recorded sections in the New Abbey area, the uppermost layer of Holocene sediments consists of clayey silt with a variable amount of sand. The colour varies from grey or pale grey at the base to brown near the ground surface. The thickness is variable (Fig. 4.7).

4.5 Lochar Gulf area

Correlation diagrams were not constructed for the Lochar Gulf area because distinct laterally-continuous units within the Holocene inorganic sediments of that area are not readily distinguishable. The Holocene inorganic sediments of the former Lochar Gulf appear to consist largely of fine sand with silt, rich in foraminifers, ostracods and fragments of marine bivalve shells, together with minute fragments of dark-coloured matter that may be organic in nature (cf. Jardine 1980, 25-31).

4.6 Conclusions

Comparison of the diagrammatic vertical sections for the Dalbeattie, Kirkcudbright and New Abbey areas (Figs. 4.2, 4.3, 4.5 and 4.7) suggests that the Holocene sedimentary units listed below can be recognised in at least one or in all of these areas:

Unit consisting of clayey silt, or of clayey silt with fine sand

Unit consisting of laminated fine sand and silt

Unit consisting of coarse sand with pebbles

Unit consisting of fine sand, rich in microfaunal remains

Unit consisting of clayey silts with plant debris.

These sedimentary units, together with two others, a peat unit and a coastal gravel-and-sand unit, are considered to represent seven sedimentary **facies** of the Holocene deposits of SW Scotland. The characteristics of these facies in the Dalbeattie, Kirkcudbright, New Abbey and Lochar Gulf areas, and the characteristics of four facies recognised within the present-day intertidal sediments of the Dalbeattie, Kirkcudbright and New Abbey areas are discussed and described in detail in Chapter 5.

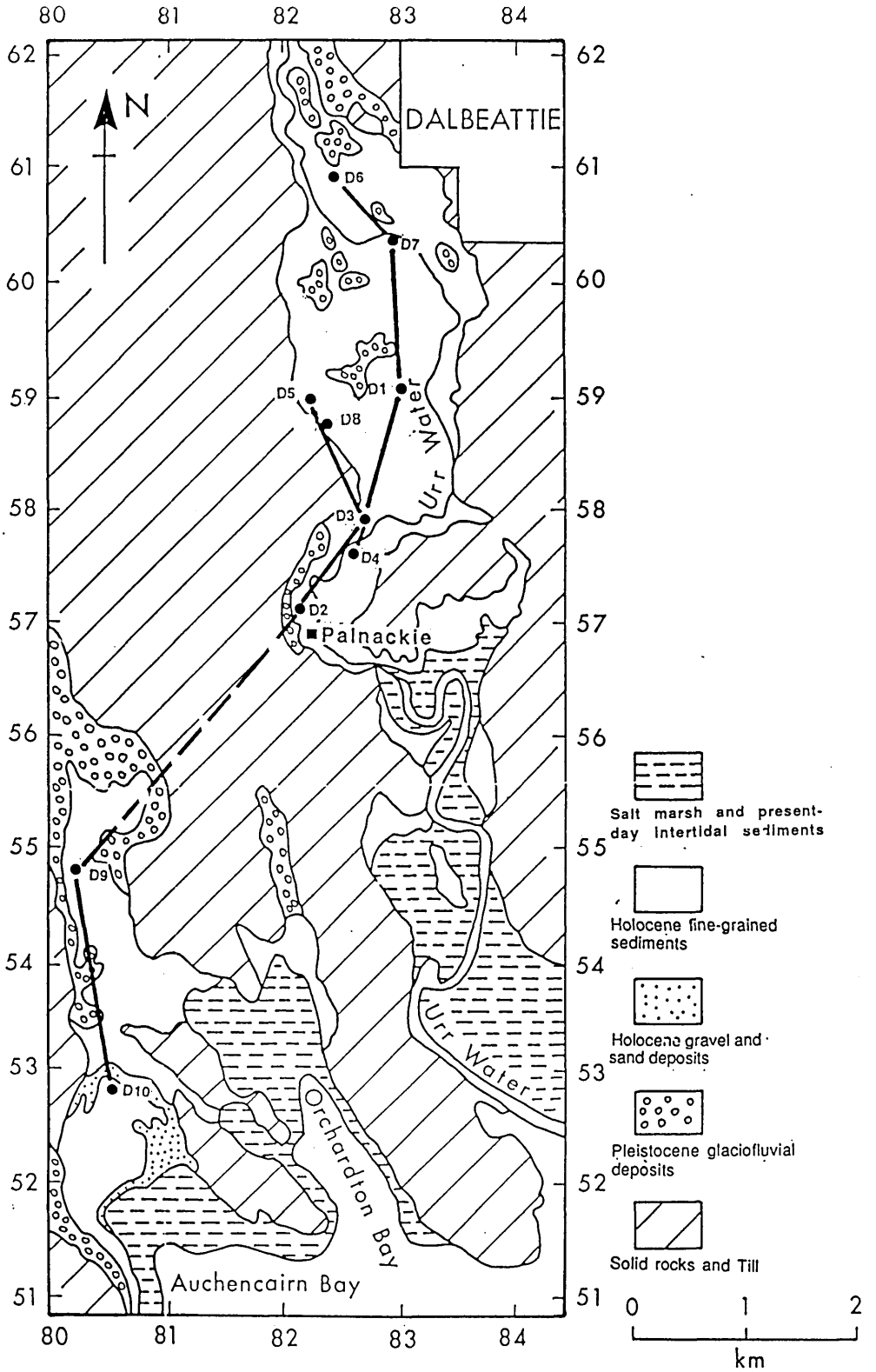

Figure 4.1 Map of the Dalbeattie area, showing positions of vertical profiles (D1, D2 etc.) through the Holocene sediments, and the North-South and NNW-SSE correlation lines of these profiles.

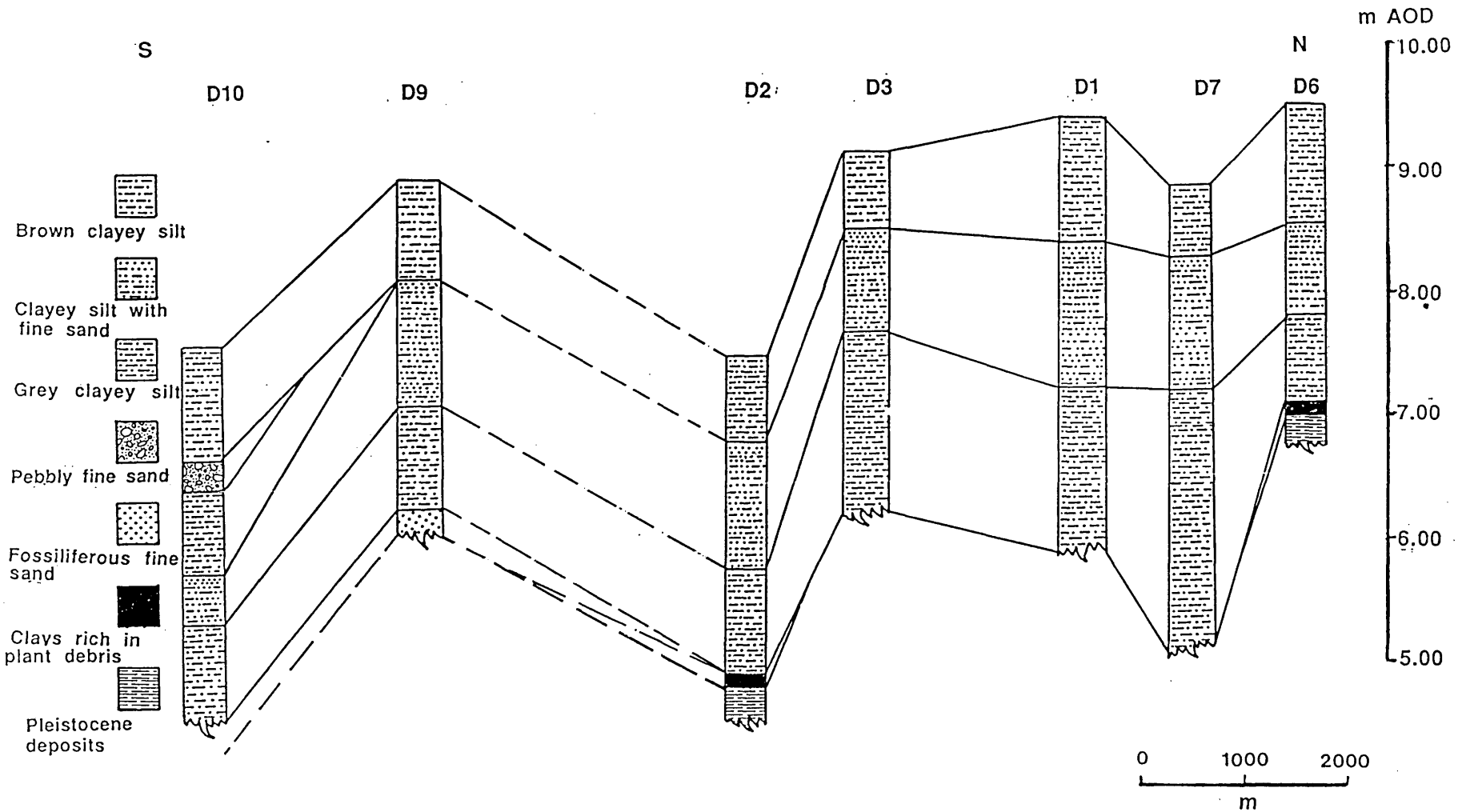

Figure 4.2 Correlated vertical profiles in Dalbeattie area, along the North-South line shown in Figure 4.1.

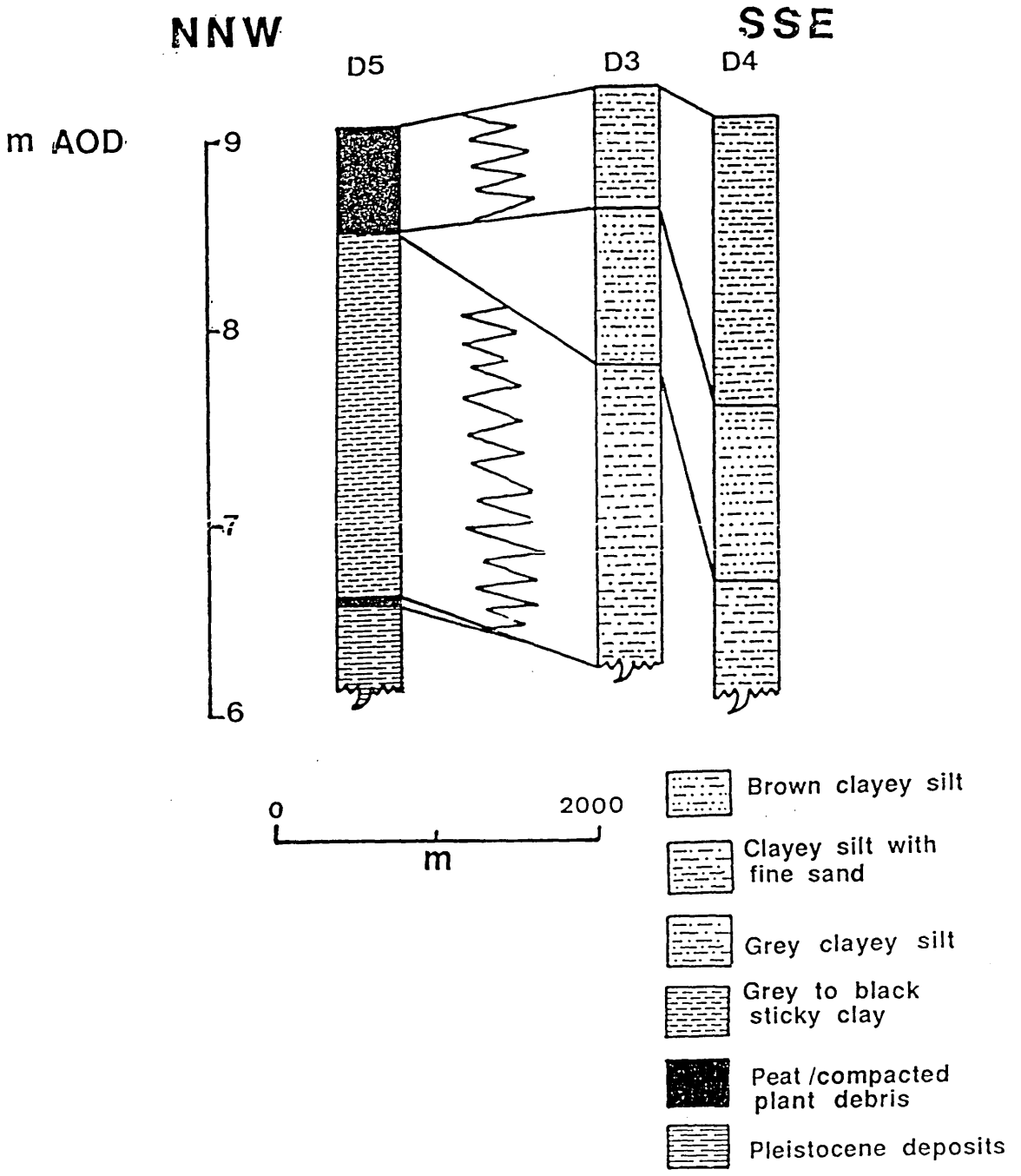

Figure 4.3 Correlated vertical profiles in Dalbeattie area, along the NNW-SSE line shown in Figure 4.1.

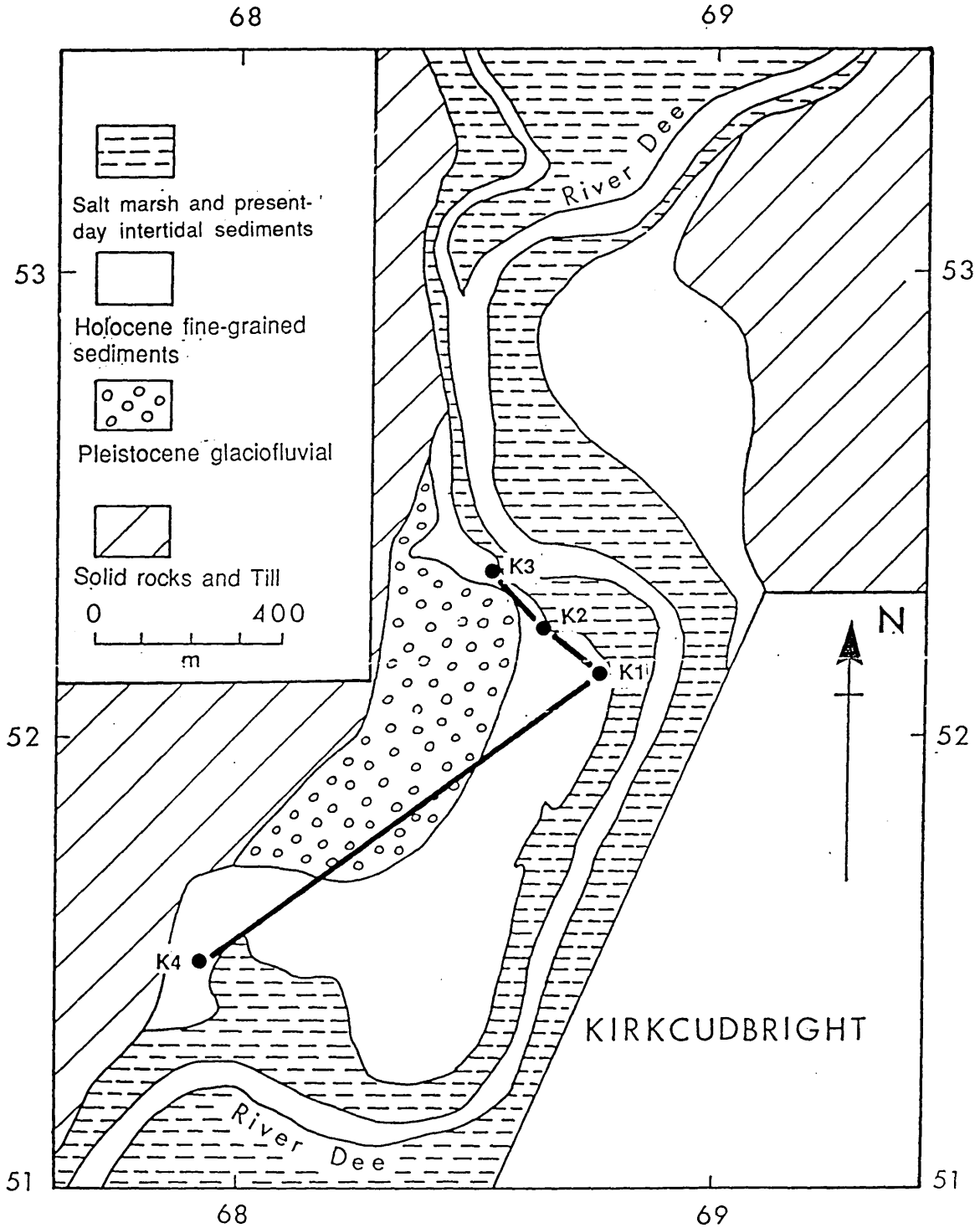

Figure 4.4 Map of the Kirkcudbright area, showing positions of vertical profiles (K1, K2 etc.) through the Holocene sediments, and the approximately North-South correlation line of these profiles.

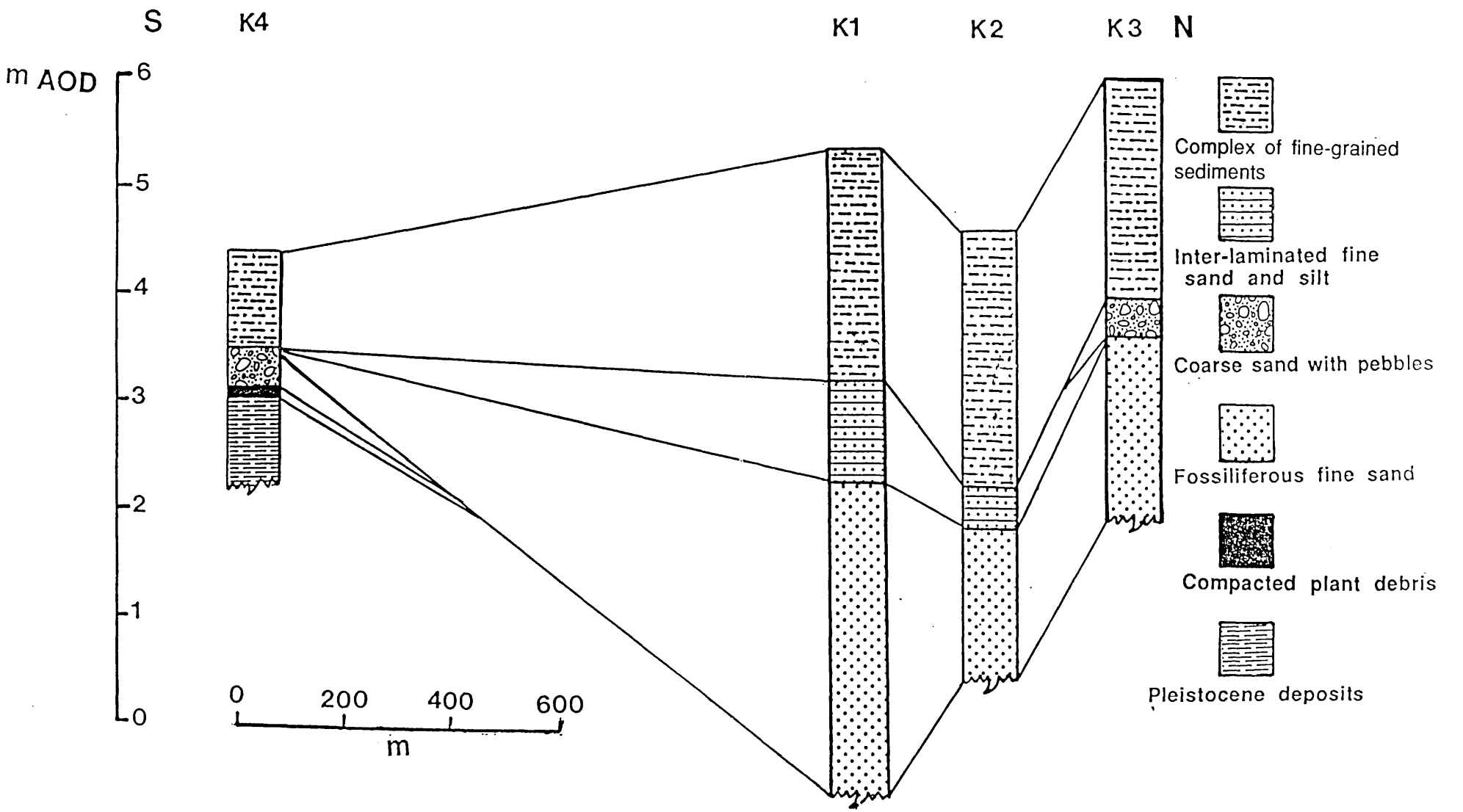

Figure 4.5 Correlated vertical profiles in the Kirkcudbright area, along the approximately North-South line shown in Figure 4.4.

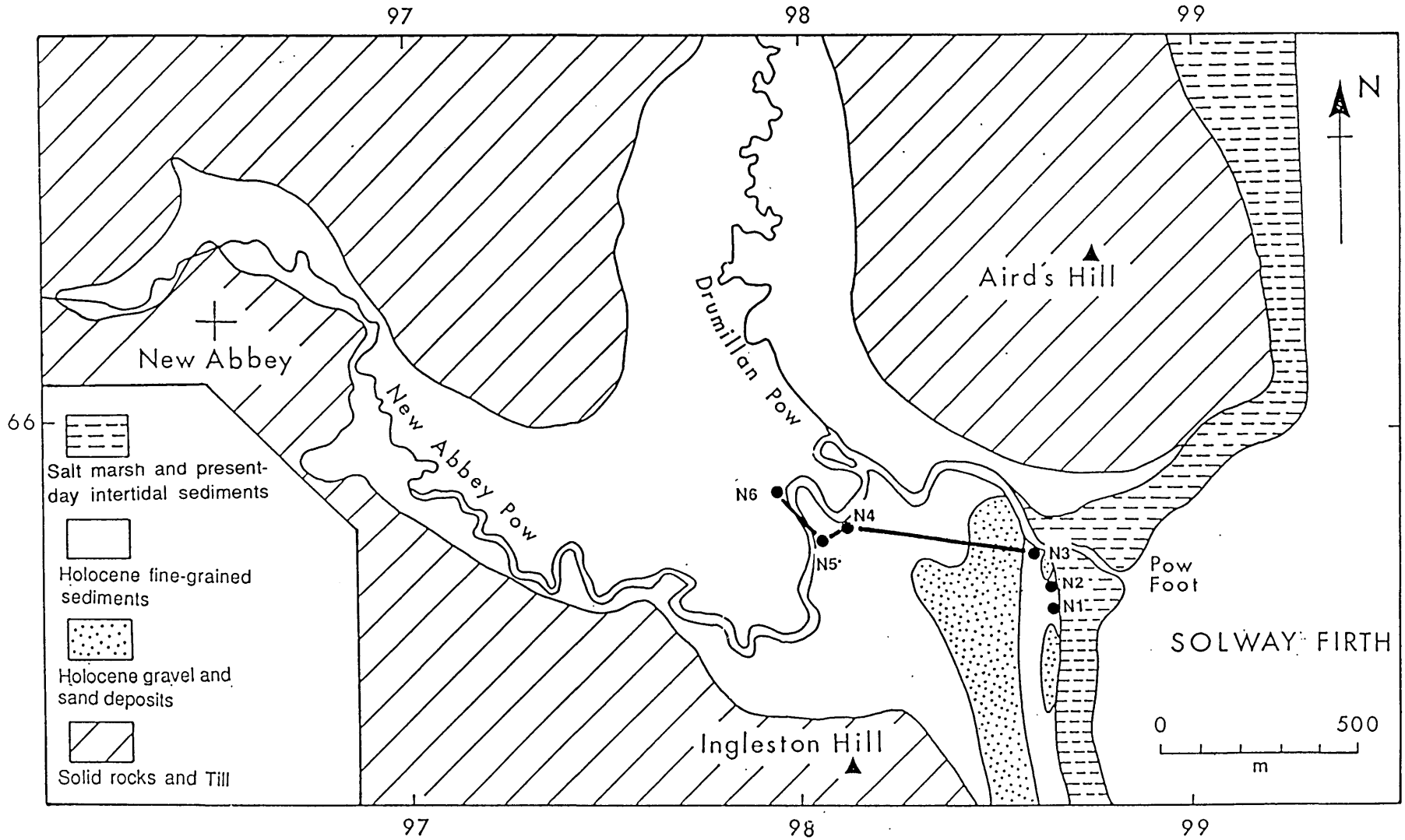

Figure 4.6 Map of the New Abbey area, showing positions of vertical profiles (N1, N2 etc.) through the Holocene sediments, and the approximately East-West correlation line of these profiles.

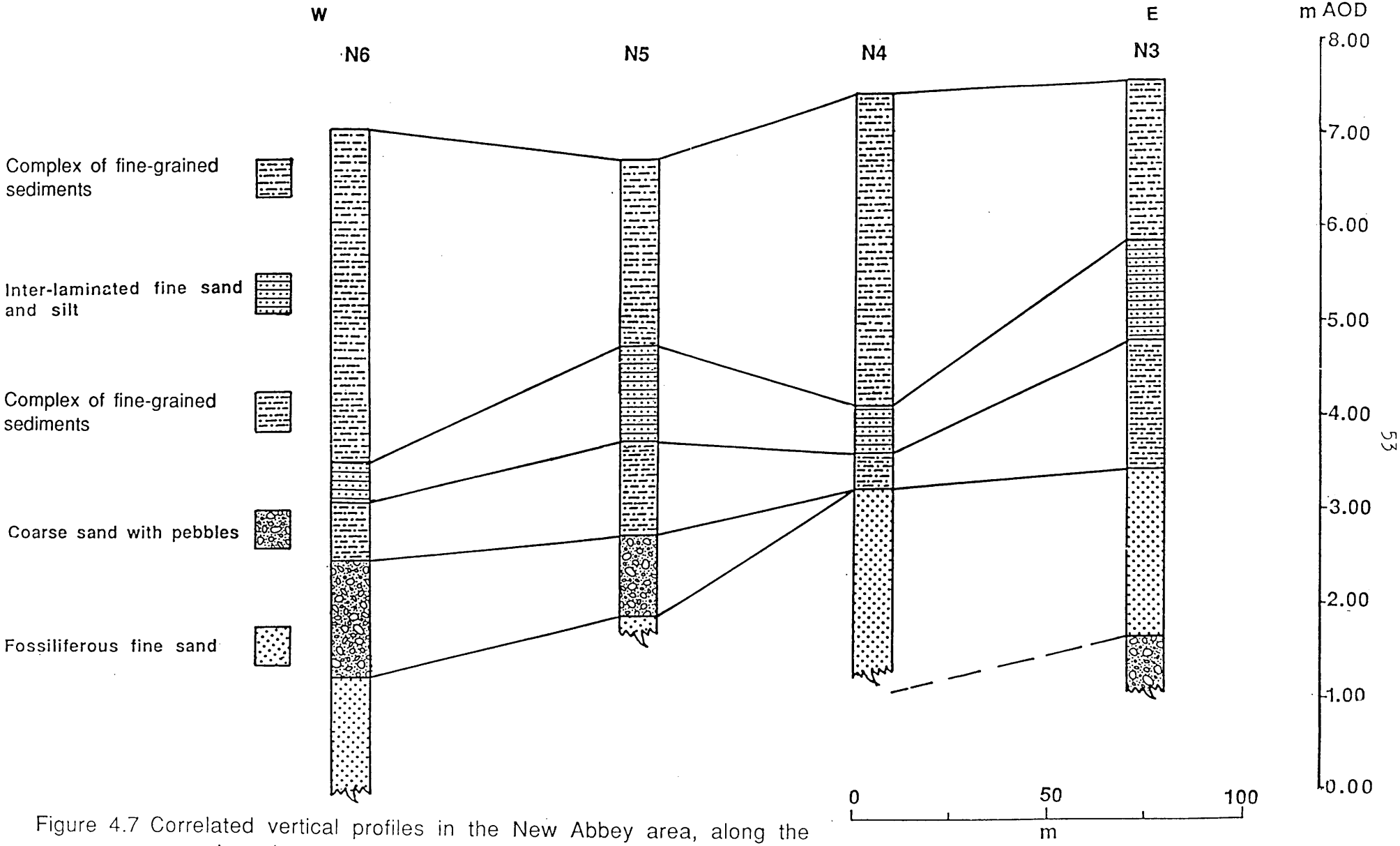

Figure 4.7 Correlated vertical profiles in the New Abbey area, along the approximately East-West line shown in Figure 4.6.

CHAPTER 5

DESCRIPTION OF SEDIMENTARY FACIES

5.1 Introduction

5.1.1 The concept of sedimentary facies

It is useful to consider briefly the concept of sedimentary facies and some of the uses that have been made of the term 'facies' before applying the concept and the term to the coastal sediments that were studied in the course of this project.

The modern concept of facies was introduced into geology by Amand Gressly in 1838 as a result of Gressly's studies of Jurassic rocks in Switzerland (Middleton 1978, 323). Since then the term facies, as applied to sediments and sedimentary rocks, has been expanded, defined and explained by several authors. A recent discussion of the concept and term explains that, 'A *facies* is a body of rock with specified characteristics. Where sedimentary rocks can be handled at outcrop or from boreholes, it is defined on the basis of colour, bedding, composition, texture, fossils and sedimentary structures. A *biofacies* is one for which prime consideration is given to the biological content. If fossils are absent or of little consequence and emphasis is on physical and chemical characteristics of the rock, then the term *lithofacies* is appropriate' (Reading 1986, 4). Further, the term facies may be used in different senses, e.g. 'in a genetic sense for the products of a *process* by which a rock is thought to have formed' or 'in an environmental sense for the environment in which a rock or suite of mixed rocks is thought to have formed' (Reading 1986, 4).

The several facies of Holocene coastal sediments that were recognised in the course of this project (Chapter 4) and are discussed in greater detail in this chapter were distinguished from each other on the basis of processes by which and the environments in which they are thought to have formed. Thus, the term facies is used

in relation to these sediments in the genetic and environmental senses. Also, since these sedimentary facies have been distinguished for the most part on the basis of physical and chemical characteristics and with only minor reference to their fossil content, they appear to be largely lithofacies rather than biofacies on the basis of the criteria given above. Middleton (1978, 324), however, pointed out that the presence or absence of fossils (including trace fossils and fragmental fossil material) constitutes an essential part of the lithology of many sedimentary rocks, so that distinction between lithofacies and biofacies may not always be clear.

5.1.2 Previous recognition of sedimentary facies in Holocene deposits of south-western Scotland

Attempts to define facies of the Holocene coastal sediments of Dumfriesshire and Galloway were made prior to commencement of this research project. In a preliminary study, Jardine (1967) distinguished four facies, which he termed beach, open-bay, estuarine and lagoonal, on the basis of six criteria: shape of the sedimentary body, location of the sedimentary body in relation to the contemporaneous shoreline, texture (grain size), degree of sorting, degree of stratification, and organic content.

In a later publication, Jardine (1975, 174) stated that the coastal deposits are the products of at least seven different sedimentary environments: beach, gulf or open-bay, estuarine (including tidal-flat), lagoonal, coastal-bar, coastal-dune and coastal marsh. Using the six criteria given above, the characteristics of each of the facies representing seven sedimentary environments were described by Jardine & Morrison (1976, 177-179).

Recently, Griffiths (1988, 25) suggested that Jardine's (1967) six criteria are not adequate to allow a definite environmental interpretation and the assignment of a particular facies to a depositional environment to be made. In the area studied by Griffiths (Wigtown Bay, west of the areas considered in this project) the reasons for

the inadequacy of the criteria were partly a lack, or limited evidence, of the criteria as a result of changing sedimentological conditions through time, and partly because of an uneven distribution of suitable sections within the field area. Both of these reasons apply also in the areas studied in the present project, but they do not completely negate attempts to distinguish sedimentary facies and environments of deposition in the areas studied by Griffiths and in this project; they only present a greater challenge.

Griffiths (1988, 29) showed how the challenge may be met when she wrote, 'To resolve these problems, detailed attention must be paid to lateral changes in facies and to juxtaposition of environments'. Her remarks lead to consideration of the lateral and vertical relationships between sedimentary facies and environments, and the criteria by which sedimentary facies were recognised in the course of the project discussed in this thesis.

5.1.3 Sedimentary facies recognised in this study

In the four coastal areas studied, several different sedimentary facies were formed during Holocene times, and others are forming at present.

The relationships between the individual present-day facies are those that exist between two or more laterally-adjacent depositional units. The relationships between the Holocene sedimentary facies are more complex; there are both laterally-adjacent and vertically-adjacent facies. As remarked by Reading (1986, 4-5), the importance of relationships between facies has been recognised at least since Walther's **Law of Facies** was expounded in 1894. In essence, Walther noted that facies occurring in a conformable vertical sequence were formed in laterally-adjacent environments, and facies in vertical contact must be products of geographically neighbouring environments. This principle has long been used to explain how a prograding delta yields a coarsening-upwards sequence (Reading 1986, 5). Equally, it may be used to explain the facies sequences that were encountered in stream-bank exposures and

vertical boreholes through the Holocene sediments of the four areas studied in the course of this project. In the latter case, however, the sequences have resulted from shifts in sub-environment brought about by marine transgression and regression within a generally estuarine environment.

The present-day (four) and Holocene (seven) sedimentary facies recognised in the Dalbeattie, Kirkcudbright, New Abbey and Lochar Gulf areas are listed in Table 5.1. The criteria used for their distinction, and the characteristics considered in their descriptions below were: shape of the sedimentary body, location of the sedimentary body in relation to contemporaneous deposits, texture (grain size), degree of sorting, sedimentary structures (where observed) and faunal content (where faunal remains were found). Grain size was determined initially on the basis of field observation (cf. Chapter 1.6.2 above). In certain cases, later laboratory analyses led to amendment of the size grade recorded in the field. In such cases, the size grade recorded in the description is that determined in the laboratory.

5.2 Present-day sedimentary facies

Four present-day sedimentary facies were recognised: tidal-flat, tidal-channel, salt-marsh and sand-barrier.

5.2.1 Tidal-flat facies

Present-day tidal-flats consist of sediments that are being deposited between MHW and MLW in certain circumstances (Fig. 5.1). Weimer et al. (1982, 191) indicated that tidal-flats occur on open coasts of low relief and relatively low energy and in protected areas of high-energy coasts associated with estuaries, lagoons, bays and other areas behind barrier islands. These authors subdivided tidal-flats into intertidal and subtidal environments and noted that these environments control facies distribution. They also noted that, although the intertidal zone makes up the major

extent of the tidal-flat, the subtidal zone represents that part of the tidal-flat most likely to be preserved.

Reineck (1975) proposed the terms **sand-flats, mixed-flats** and **mud-flats** to denote respectively the lower, middle and upper parts of the area between low tide and high tide on intertidal flats. Weimer et al. (1982, 197), however, pointed out that these descriptive size-grade terms are relative and 'mud', for example, does not mean that only silt and/or clay is present; minor amounts of sand may also be present.

The following data are relevant in relation to defining (a) the tidal-flat environment of the Dalbeattie, Kirkcudbright and New Abbey areas and, (b) the characteristics of the tidal-flat facies of these areas. Tidal-flats were not studied in detail in the Lochar Gulf area.

The areal extent of the tidal-flats is wide at the heads of Auchencairn Bay and Rough Firth (in the Dalbeattie area) and Kirkcudbright Bay, and at the mouth of New Abbey Pow (Figs 2.3, 2.4 and 2.5). In places, where there is low relief on the adjacent seaboard, the intertidal flat is more than 2km in width. The tidal range within the area of the Solway Firth varies greatly, in general being greater in the east than in the west (Fig. 5.2). On the basis of tidal data from localities on the shores of the Solway Firth, spring tidal range is 6.7m at Kirkcudbright Bay, mean high water level being 3.77m A.O.D. and mean low water level 2.93m B.O.D. Spring tidal range at Hestan Island, offshore from Auchencairn Bay, is 7.40m, mean high water level being 4.20m A.O.D. and mean low water level 3.20m B.O.D. (Table 5.2). These are macrotidal ranges (cf. Davies 1973; Hayes 1975; Nichols & Biggs 1985).

The size grade of the tidal-flat deposits differs slightly between one area and another. The sediments of the Kirkcudbright area are composed mainly of medium to fine sand with rare silt and clay, whereas the tidal-flat sediments of the Dalbeattie and New Abbey areas consist mostly of fine sand with silt and clay. Sedimentary

structures within the deposits, e.g. current ripples and interlaminations of sand and silt, were identified occasionally. The presence of molluscs (frequent to abundant) was noted, although genera and species were not identified. The limited presence of sedimentary structures is almost certainly due to disturbance by molluscs and other fauna (cf. the activity of the gastropod *Hydrobia ulvae,* the amphipod *Corophium volutator* and the polychaete *Nereis diversicolor,* Bridges & Leeder 1976, 544-545; see also Wilson 1967). A further factor in the disturbance of the sediments may be the migration of the numerous tidal creeks which cut the tidal flats of the Dalbeattie, Kirkcudbright and New Abbey areas.

Because there is marked disturbance, it is difficult to subdivide the tidal-flat sediments into high, medium and low sub-facies on the basis of their sedimentary characteristics. However, a distinction can be made between the high-tidal sediments on the one hand and the medium-tidal and low-tidal sediments on the other as the grain size becomes progressively finer from lower to higher positions on the tidal flats. The sediments of the low- and medium-tidal zones are mainly of medium- to fine-sand grade and are rich in macro- and micro-fauna. In contrast, the sediments of the high-tidal zone are mainly silt and clay with fine sand, and fauna is rare in these sediments.

5.2.2 Tidal-creek facies

As pointed out by Weimer et al. (1982, 193), the deposits that accumulate in the creeks that traverse tidal flats are, from a geological standpoint, the most important tidal facies. This is illustrated by the fact that, although examination of a tidal-flat surface at any instant in time usually shows tidal creeks occupying less than 50 percent of the total surface area, the tidal creeks and major tidal channels are dynamic features that continually shift position. This certainly appeared to be the case in the present-day intertidal zone of the Dalbeattie, Kirkcudbright and New Abbey

areas, where shifting of the positions of the creeks was noted between one period of fieldwork and another.

In these areas, the tidal creeks are wide. Generally they are about 1-2m in depth. The courses are sinuous, and constantly changing position, thus leading to erosion and deposition, as shown especially in the Dalbeattie area (Plate 5.1). Deposition is taking place mostly on the margins of the larger creeks (where current ripples may be present, Plate 5.2) and on point bars. The sediments on the floors of the creeks are characterised by the presence of pebble-sized clasts of mud and sand. Where observed, the tidal-creek deposits were well-laminated.

5.2.3 Salt marsh facies

Sediments of the salt marsh facies form vegetation-covered areas adjacent to and landwards of MHWS (Fig. 1.2). They are flooded occasionally by spring tidal waters (Jardine 1980, 4-5), being separated from the more seaward unvegetated intertidal zone by 'cliffs' that commonly are less than 1m in height. Landwards, these deposits extend over variable distances up to several tens of, occasionally more than one hundred, metres and in places they form barriers that separate small ponds from the open sea, e.g. in the Dalbeattie area (Fig. 5.1).

Characteristically, the salt marsh deposits are traversed by ramifying systems of narrow creeks or gullies, which essentially are extensions of the gullies that transect the adjacent tidal-flats (Plate 5.3). The depth of the gullies is variable, decreasing landwards, but frequently exceeds one metre throughout much of the salt marsh area. In size grade and depositional arrangement, the salt marsh sediments generally comprise laminated silt and clay (Plate 5.4).

5.2.4 Sand-barrier facies

The sand-barrier facies is limited to one locality, in the Dalbeattie area. At NX

813 527, on the western side of Orchardton Bay, peaty black-grey clay and other Holocene deposits are separated from salt marsh deposits and the marine waters of Craigrow Bay by a sand barrier c.150-200m in width (Fig. 5.3). Since the eastern marginal part of the barrier rests on present-day salt marsh deposits and the maximum elevation of the barrier is at approximately the same level as the maximum elevation reached by exceptional present-day spring tides in this area, the barrier is thought to be a product of recent coastal (storm) processes. The deposits of the barrier are brown to red coarse sand, well-sorted but apparently devoid of stratification.

5.3 Holocene sedimentary facies

As concluded in Chapter 4, in the four areas studied, many of the Holocene raised coastal depositional bodies comprise several facies, arranged adjacent to each other either in vertical sequence or in lateral juxtaposition or in a combined vertical and lateral relationship. Collectively the facies represent a sedimentary complex that was deposited in a variety of environments or sub-environments. The various sedimentary facies that have been distinguished are listed in Table 5.1 and their characteristics are given in Chapter 5.3.1 below.

5.3.1 Description of Holocene sedimentary facies

Seven Holocene sedimentary facies were recognised: complex of fine-grained sediments (A); inter-laminated fine sand and silt (B); coarse sand with pebbles (C); fine sand, rich in microfaunal remains (D); clay, rich in plant debris (E); coastal gravel and sand (F); peat (G) (Table 5.1).

The recognition of four of these facies (A-D) was based on the record of numerous natural (vertical) sections and artificial (vertical) boreholes through the Holocene deposits of the Dalbeattie, Kirkcudbright and New Abbey areas and, to a lesser

extent, the area of the former Lochar Gulf. The characteristics of these four facies are presented in tabular form in Tables 5.3, 5.4 and 5.5. The fact that these tables show representative rather than actual sections in three of the areas studied is a reminder that, not only do the sedimentary facies concerned occur in more than one area, but they extend laterally for a considerable distance within any one of the areas and therefore would be misrepresented by data from a single location.

The three other facies (E-G) are more restricted in their distribution. This reflects the fact that they are products of more specialised environments than the supratidal or intertidal environments in which facies A-D were deposited.

5.3.1.1 Complex of fine-grained sediments (facies A)

This facies constitutes the total thickness (c. 1.90m - 4.10m) of the raised Holocene sediments over most of the Dalbeattie area and the uppermost part in the Kirkcudbright (0.91m - 2.30m) and New Abbey (1.65m - 3.70m) areas. In the New Abbey area, it also is present as a c. 0.35m - 1.30m thick sub-surface unit, below facies B (Table 5.5). It has also been recognised in the Lochar Gulf area.

The appearance of the sediments of this facies varies from one exposure to another, being massive in places (mainly in the upper part) and laminated in others. In size grade the facies consists mainly of silt with clay, or silt with clay and very fine sand. Occasional plant debris is present, especially in the upper part. There are rare occurrences of echinoid spines and sponge spicules, especially in the lower layers of the unit. The colour changes from grey to brown upwards through the profile. Mainly on the basis of observations in the Dalbeattie area, there appear to be three sub-facies, Aa, Ab and Ac, arranged one above the other, and discussed in detail in Chapter 10.

5.3.1.2 Inter-laminated fine sand and silt (facies B)

This facies is missing in the Dalbeattie area, but is present in the three other areas studied. In the Kirkcudbright and New Abbey areas it comprises a c. 0.40m - 0.97m thick layer of interstratified fine sand laminae and silt laminae within which plant debris and rare to occasional foraminiferal tests, echinoid spines and sponge spicules occur (Tables 5.4 and 5.5).

5.3.1.3 Coarse sand with pebbles (facies C)

This facies is present mainly in the New Abbey area. In the Dalbeattie and Kirkcudbright areas it forms a minor facies, up to 0.35m thick, composed of pebbly sand rich in plant debris. It is developed only locally, and may have been deposited from reworked adjacent Pleistocene glaciofluvial sediments.

In the New Abbey area, layers of this facies, lenticular in shape, are exposed in the banks of New Abbey Pow upstream from its mouth. In these exposures it was observed that the size grade is mainly pebbly coarse sand, occasionally interstratified with thin layers of clay. Small quantities of plant debris, mainly leaves and pieces of wood, are present. There appears to be an erosional surface between this facies and the underlying facies D.

5.3.1.4 Fine sand, rich in microfaunal remains (facies D)

This facies was detected at the base of one borehole (D9) in the Dalbeattie area but occurs much more extensively in the three other areas studied. It is developed most fully in the area of the former Lochar Gulf. In size-grade the sediments consist mainly of fine sand but they also contain small amounts of medium sand and silt. Quartz is the main mineral present, especially in the deposits within the Lochar Gulf area. The sediments, predominantly grey in colour, are rich in small faunal remains; molluscan shell fragments, foraminiferal tests, ostracod valves, fragments of echinoid

spines and sponge spicules are present. In places, abundant remains of plant debris are present. Small fragments of (?) charcoal have been recorded in the Lochar Gulf area (Jardine 1980, 29).

5.3.1.5 Clays, rich in plant debris (facies E)

This facies is present in the Dalbeattie area. Approximately 2km SSW of the town of Dalbeattie and immediately south of Broomisle, there is a low flat area that is bounded in the east by mounds of Pleistocene glaciofluvial deposits and Holocene sediments of facies A, and in the west by solid rocks (Fig. 5.3). This area is covered by a layer of surface peat of variable thickness (facies G, see 5.3.2.7, below). The Holocene succession, represented by borehole D5 at location NX 8224 5897, is shown in Table 5.6.

The grey to black clay facies of this area obviously differs greatly in character from the adjacent Holocene sediments (of facies A) to the east of it. Clearly, in the case of the grey to black clay facies there was very little sand and silt input but a very high organic (plant) input during deposition. The sediments of this facies (E) were probably deposited in a lake, separated from the sea by barriers of Pleistocene glaciofluvial gravels and areas of Holocene coastal sediments.

This facies is probably present in the Lochar Gulf area, but was not studied in the course of the present work.

5.3.1.6 Coastal gravel and sand (facies F)

The coastal gravel and sand facies (F) occurs in the Dalbeattie, New Abbey and Lochar Gulf areas. In the southern part of the Dalbeattie area (Fig. 5.3) the sediments of this facies form elongate, sheet-like bodies of pebbles and cobbles, occasionally interstratified with coarse pebbly sand sheets or lenses of sand, arranged

approximately parallel to the present shoreline. In detail, two sheets of gravel form ridges, with gently sloping sides, that rest on the surface of finer-grained deposits (of facies A). The two ridges occur at different altitudes above O.D. and the thickness of the gravel varies from place to place, up to c. 1.0m. In a few exposures, the gravel is seen to be imbricate, with long axes of the clasts dipping towards the present position of the sea. The gravel ridges are thought to have formed baymouth bars at two different times during Holocene progradation by the sea (cf. Chapter 6).

In the New Abbey area, the most obvious development of this facies, mapped by Jardine (1980, 34-36), consists of horizontally-bedded interstratified gravels and sands that form a broad, low ridge extending southwards from near the mouth of New Abbey Pow for a distance of more than 1km. The gravels and sands overlie deposits of facies D (5.3.1.4, above), a relationship that led Jardine (1980, 35) to suggest that the gravel ridge formed a baymouth bar between Aird's Hill and a headland located east of Ingleston Hill (Fig. 2.5) about the time of the maximum of the Holocene marine transgression. The sediments of this facies consist of pebbles and cobbles, occasionally showing imbricate structure in exposures in small cliffs oriented parallel to the present shoreline.

In the Lochar Gulf area at least three Holocene gravel and sand spit-like ridges, one c. 600m in length, the others 150-200m in length, occur near the south-western edge of the gulf (Fig. 5.4). A larger ridge of gravel and sand, occurring at the south-eastern edge of the gulf, may represent Pleistocene sand and gravel debris re-distributed only in minor degree by the sea in Holocene times (Jardine 1980, 29). The deposits of the ridges were not investigated in the course of the research project discussed here, but Jardine (1980, 29) established that the largest of the three ridges located at the western edge of the mouth of the Lochar Gulf is c. 2.5m in thickness and

the gravel rests on Holocene marine deposits that probably are equivalent to facies D as defined in this Chapter above.

5.3.1.7 Peat (facies G)

Thin covers of peat are present in many small hollows within the four areas studied. Larger and thicker expanses of peat, of greater interest in relation to the research project although they were not studied in detail, occur in the vicinity of Broomisle (Dalbeattie area) and in the Lochar Gulf area.

At Broomisle, the peat, variable in thickness up to c. 1.5 m, covers clays, rich in plant debris, of facies E (Chapter 5.3.1.5, above). The peat appears to have accumulated in a hollow bounded in the east by mounds of Pleistocene glaciofluvial deposits and Holocene sediments of facies A, and bounded in the west by solid rocks (Fig. 5.3)

In the Lochar Gulf area, much of the large tract of Holocene raised coastal deposits that occupy the former gulf is covered by peat, up to at least 3.5m in thickness in places. According to Jardine (1980, 33-34 and fig. 7), the main area of the Lochar Gulf was cut off from the sea around 6645 ± 120 years B. P. Thereafter, peat formation commenced in the abandoned embayment.

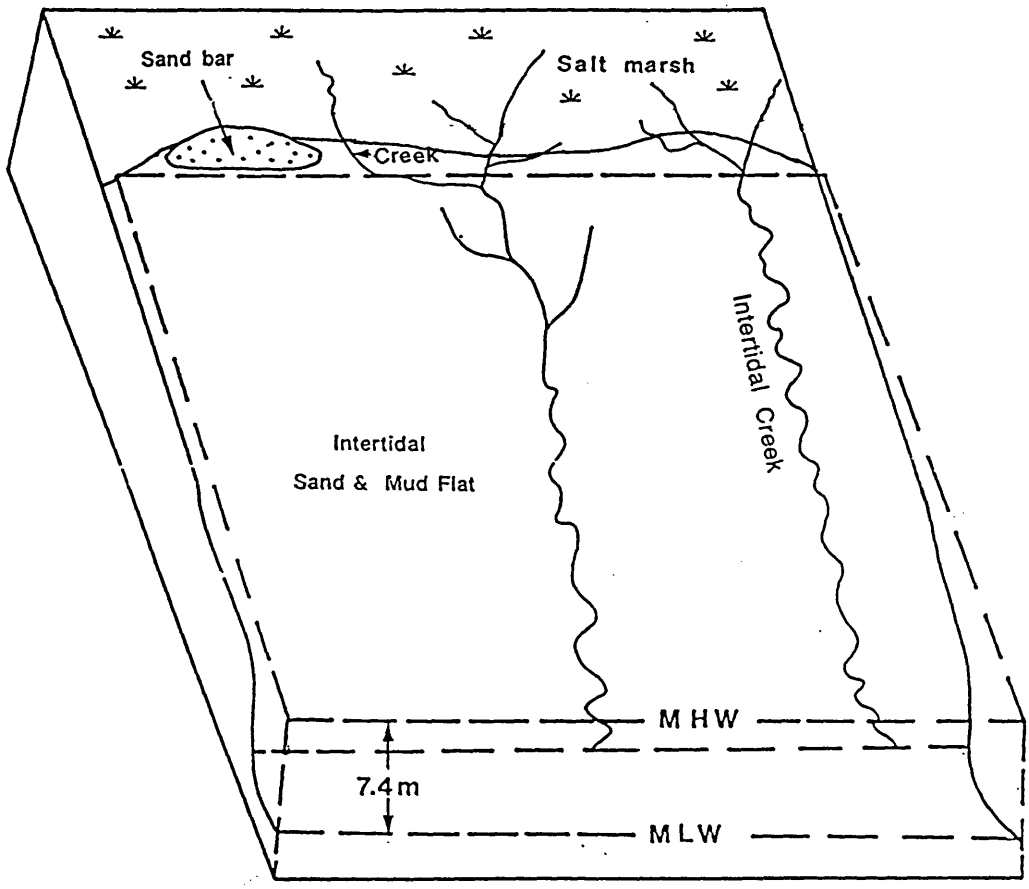

Figure 5.1 Block diagram of the intertidal zone between MHW and MLW, showing the sedimentary facies that develop in this zone.

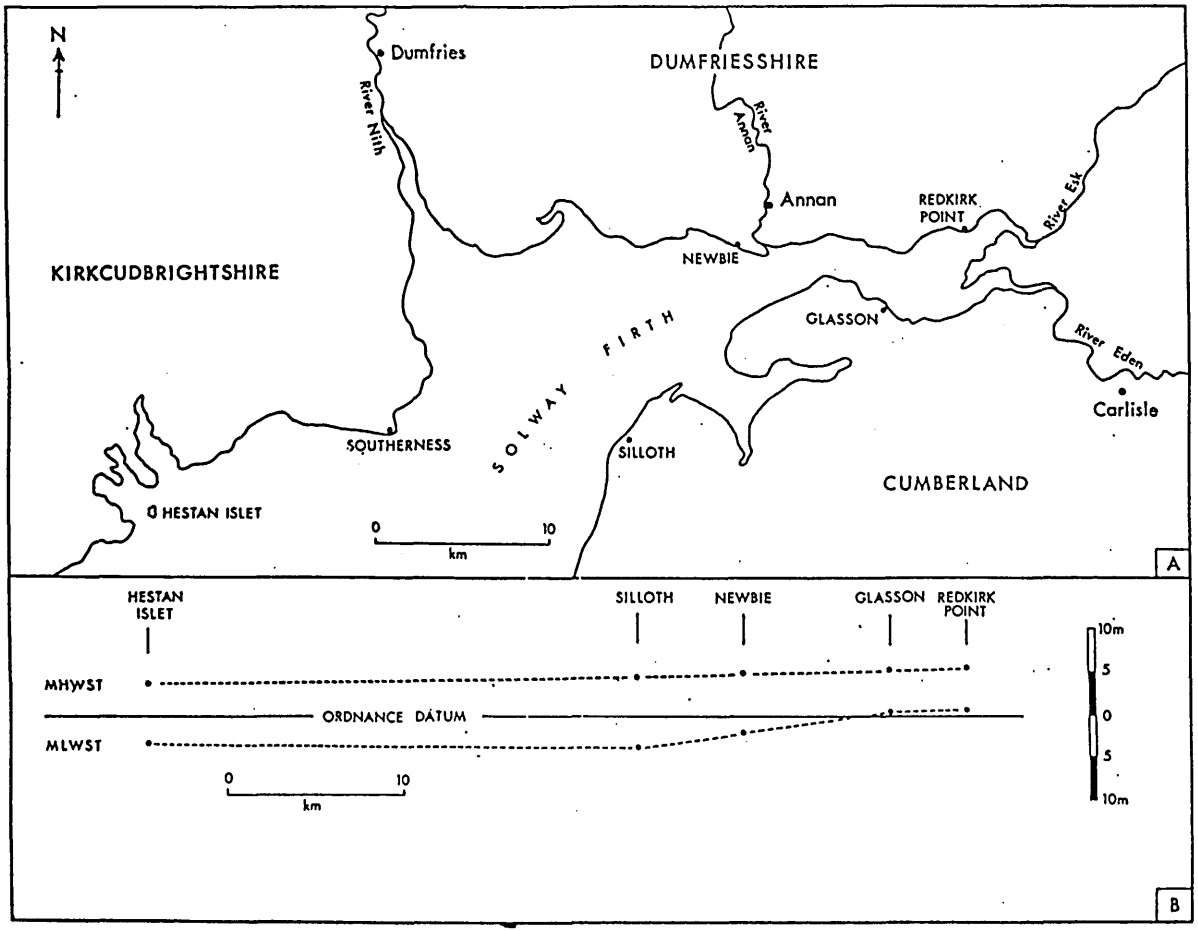

Figure 5.2 A. Map of the eastern part of the Solway Firth, showing coastal locations for which tidal data are given in Table 5.2.

B. Idealised west-east section of the eastern part of the Solway Firth. The heights of present mean high water spring tides (MHWST) and present mean low water spring tides (MLWST) at locations shown in Fig. 5.2A are projected on to the section. The tidal data used are from Table 5.2.

(Jardine 1975, fig. 12).

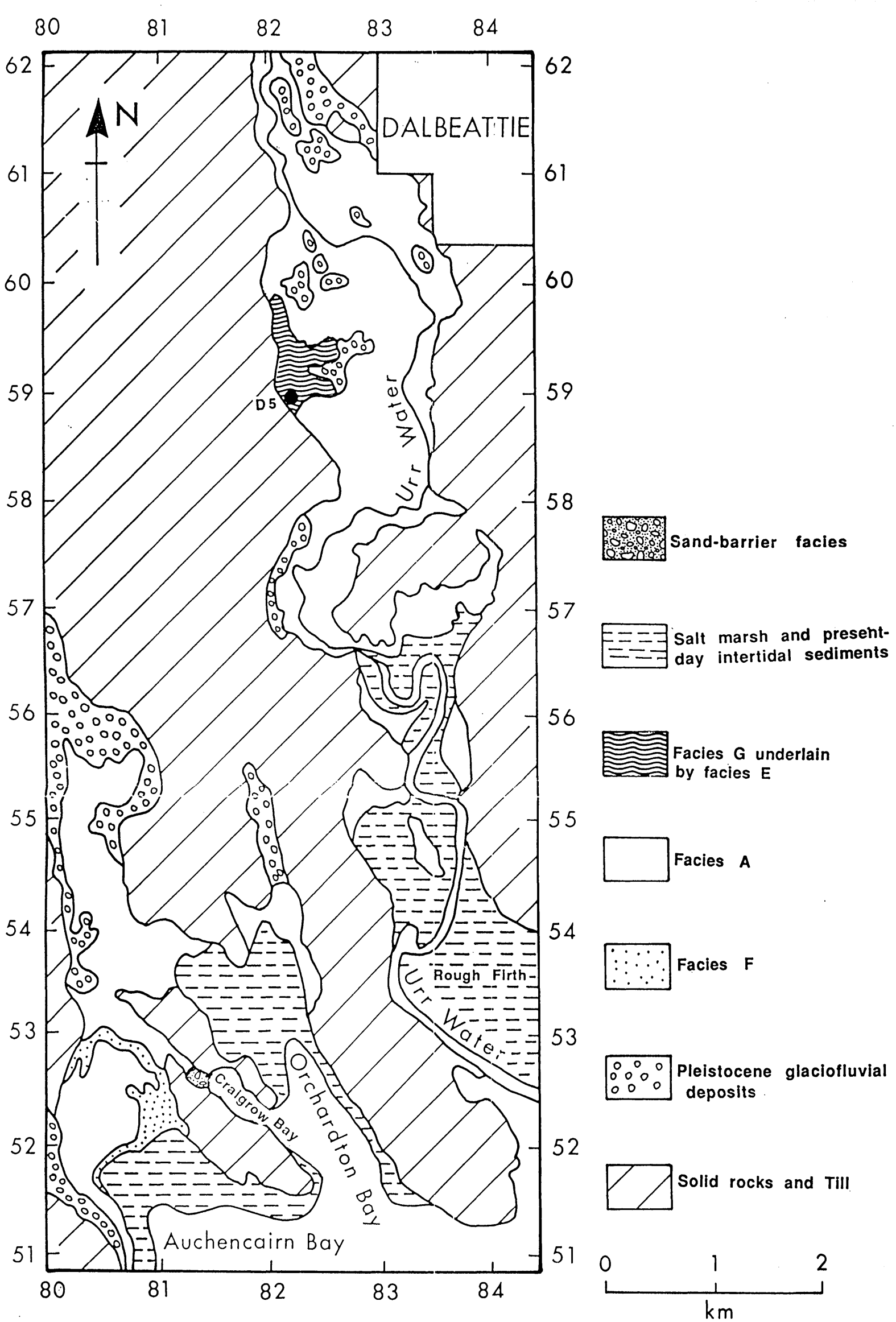

Figure 5.3 Map of the Dalbeattie area showing the surface distribution of sedimentary facies recognised in the field. The position of borehole D5 is also shown.

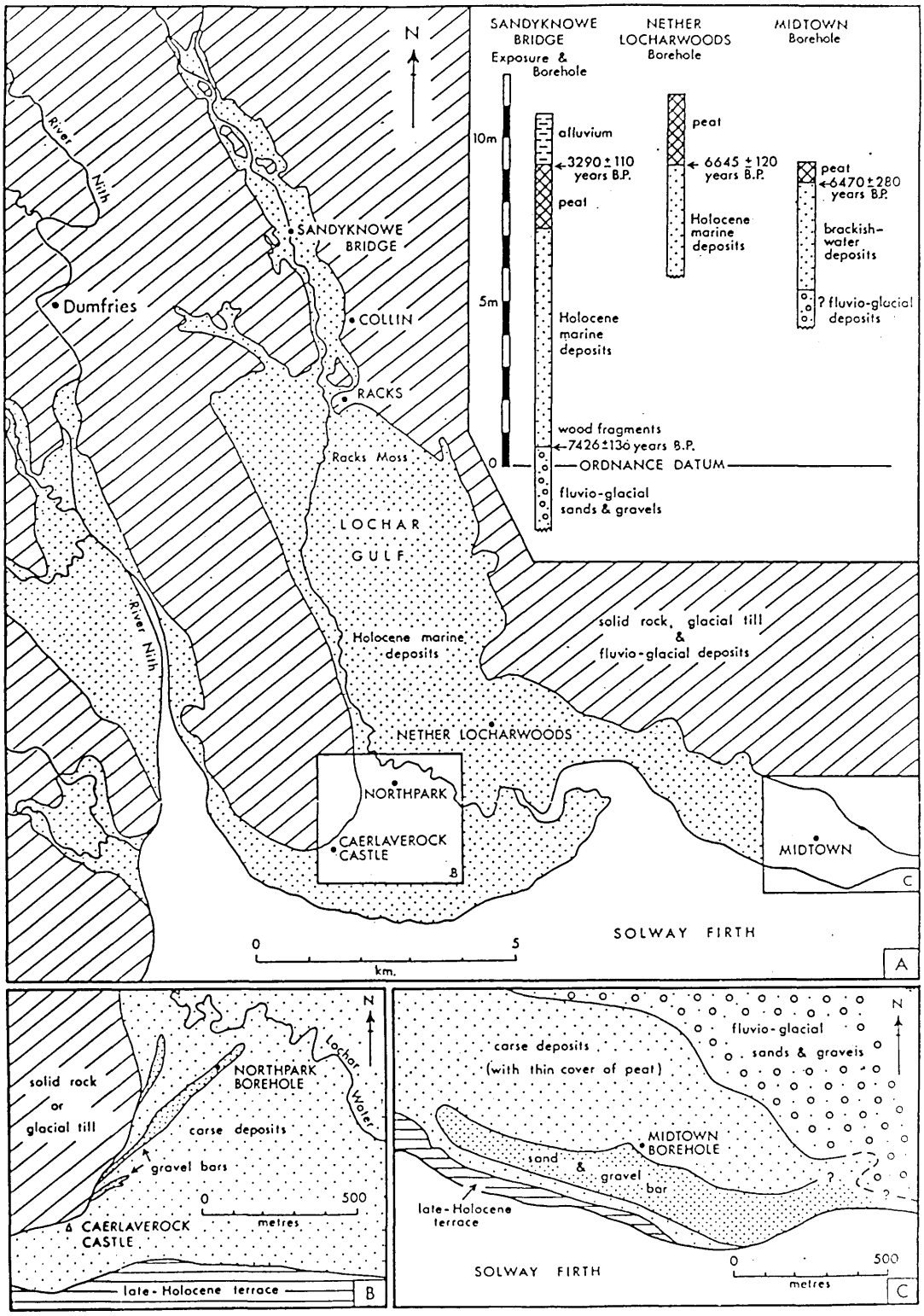

Figure 5.4 A. Map of the former Lochar Gulf and surrounding area south east of Dumfries, showing the maximum extent of the sea during the Holocene epoch (indicated by the boundary between Holocene marine deposits and other rocks). Inset: summaries of sedimentary sequences in boreholes at Sandyknowe Bridge, Nether Locharwoods and Midtown.

B. Map of south-western part of the Lochar Gulf, showing the distribution of gravel bars between Caerlaverock Castle and Lochar water, and the location of the borehole at Northpark.

C. Map of the area in the vicinity of the borehole at Midtown.
(Jardine 1975, fig. 6).

Table 5.1 Sedimentary facies identified in the course of the research project, and their occurrence in the four geographical areas of study.

X = facies present, --- = facies absent.

a) Present-day intertidal sediments

Facies	Dalbeattie	Kirkcudbright	New Abbey
Tidal-flat	X	X	X
Tidal-creek	X	X	X
Salt marsh	X	X	X
Sand-barrier	X	- - -	- - -

b) Holocene raised coastal sediments

Facies		Dalbeattie	Kirkcudbright	New Abbey	Lochar Gulf
A	Complex of fine-grained sediments	X	X	X	X
B	Inter-laminated fine sand and silt	- - -	X	X	(X)
C	Coarse sand with pebbles	(X)	(X)	X	- - -
D	Fine sand, rich in microfaunal remains	(X)	X	X	X
E	Clay, rich in plant debris	X	- - -	- - -	?
F	Coastal gravel and sand	X	- - -	X	X
G	Peat	X	- - -	- - -	X

Table 5.2 Tidal data for locations on the shore of the Solway Firth (after Jardine 1975, Table 2). The locations listed are shown in Fig. 5.6

Location	Spring tidal range	MHW level (Spring Tides)	MLW level (Spring Tides)
Portpatrick	3.50m	+2.00m	-1.50m
Drummore	5.20m	+2.70m	-2.50m
Isle of Whithorn	6.40m		
Kirkcudbright Bay	6.70m	+3.77m	-2.93m
Hestan Islet	7.40m	+4.20m	-3.20m
Silloth	8.40m	+4.80m	-3.60m
Newbie		+5.00m	-2.00m
Glasson		+5.44m	+0.24m
Redkirk Point		+5.51m	+1.71m

Table 5. 3 Representative section through the Holocene raised coastal sediments in the Dalbeattie area, showing the lithology and other characteristics of the sediments and the facies to which each sedimentary unit was assigned.

Lithology, etc.	Thickness	Facies
Topsoil		
Brown silt, with clay and very fine sand, becoming grey clayey silt at depth; little evidence of disturbance by organisms; occasional plant debris	0.40m to 1.10m	Ac
Grey silt, with very fine sand and clay; rare echinoid spines and sponge spicules	0.80m to 1.40m	Ab
Grey to dark grey clayey silt with fine sand; occasional plant remains and rare echinoid spines and sponge spicules	0.70m to 1.60m	Aa
Fine sand, rich in microfaunal remains	> 0.20m	D
Black plant debris intermixed with pebble-sized clasts	0.05m to 0.10m	

Table 5.4 Representative section through the Holocene raised coastal sediments in the Kirkcudbright area, showing the lithology and other characteristics of the sediments and the facies to which each sedimentary unit was assigned.

Lithology, etc.	Thickness	Facies
Topsoil		
Brown silt with clay and very fine sand, becoming grey clayey silt with plant debris at depth; rare echinoid spines and sponge spicules	0.91m to 2.30m	A
Inter-laminated fine sand, silt and clay, with rare sponge spicules, echinoid spines and foraminifers	0.40m to 0.95m	B
Grey pebbly sand rich in plant debris	0.35m	C
Fine sand, rich in mica flakes, ostracods and foraminifers; echinoid spines and sponge spicules are also present	> 1.30m.	D
Black plant debris intermixed with angular pebble-sized clasts	c. 0.10m	

Table 5.5 Representative section through the Holocene raised coastal sediments in the New Abbey area, showing the lithology and other characteristics of the sediments and the facies to which each sedimentary unit was assigned.

Lithology, etc.	**Thickness**	Facies
Topsoil		
Brown silt with clay and very fine sand, becoming grey clayey silt with depth; occasional plant debris, very rare echinoid spines and sponge spicules	**1.65m to 3.70m**	A
Inter-laminated fine sand, silt and clay, with rare sponge spicules, echinoid spines and foraminifers	**0.45m to 0.97m**	B
Grey clayey silt with lenses of fine sand; rare echinoid spines and sponge spicules	**0.35m to 1.30m**	A
Pebbly very coarse to coarse sand containing plant debris, mainly leaves and pieces of wood; laterally lenticular in shape	**0.58m to 1.11m**	C
Fine sand, rich in mica flakes, ostracods and foraminifers; echinoid spines and sponge spicules are also present	> 1.80m.	D

Table 5.6 Succession of Holocene coastal sediments in borehole D5 (NX 822 589), Dalbeattie area. The top of the borehole is at 9.005m AOD.

Lithology, etc.	Thickness
Peat; at the base mixed with black clays	0.55m
Grey to black, uniform sticky clay, rich in plant debris	1.85m
Plant debris, containing patches of brown sand with pebbles	0.02m
Angular pebbles and brown patches of sand, with plant debris and seeds	0.35m
Pleistocene sediments	

Plate 5.1 Tidal creeks in the intertidal zone of the Urr Water, near the village of Palnackie, Dalbeattie area

Plate 5.2 Tidal creeks and current ripples in the intertidal zone of the Urr Water, near the village of Palnackie, Dalbeattie area

Plate 5.3 Creeks or gullies in salt marsh deposits at the head of Auchencairn Bay, Dalbeattie area.

Plate 5.4 Small cliffs in salt marsh deposits, showing sedimentary laminae, south of Pow Foot, New Abbey area

PART III

SEDIMENTOLOGICAL, MINERALOGICAL AND GEOCHEMICAL ANALYSES

CHAPTER 6

SEDIMENTOLOGICAL STUDIES OF THE PLEISTOCENE AND HOLOCENE GRAVEL DEPOSITS

6.1 Introduction

In the course of mapping the Holocene raised coastal sediments in the Dalbeattie area, two ridges composed of gravel and sand, overlying fine-grained sediments and forming a distinct sedimentary unit (facies F of Chapter 5.3.1.6, above), were recognised in the area between Torr House and Torr Hill, NW of Auchencairn Bay. Also, in the New Abbey area, Jardine (1980, 34-36) noted that a low ridge of gravel and sand extends southwards from near the mouth of New Abbey Pow for a distance of more than 1km (see also Chapter 5.3.1.6, above). It is thought that each of these deposits was thrown above the contemporaneous normal high water mark by the action of occasional storms, to form a semi-permanent upstanding feature of the coastal landscape.

The two ridges of gravel and sand in the Dalbeattie area occur at different altitudes from each other. The higher ridge extends in an east-west direction as a narrow strip approximately parallel to the present shoreline at the head of Auchencairn Bay, whilst the lower ridge, exposed in a few low cliffs, forms a barrier that separates present-day supratidal (salt marsh) deposits from a more landward complex of Holocene fine-grained sediments. The higher ridge is about 1km in length and the lower ridge about 800m in length. Widths are variable, reaching a maximum of c.250m in the lower ridge (Fig. 6.1).

Samples of gravel-sized clasts were collected from exposures or by digging small pits in the higher ridge (at locations between NX 804 531 and NX 808 529) and in the lower ridge (at locations between NX 808 521 and NX 810 522) at Torr in the Dalbeattie area. Dip-direction readings were taken of the long axes of imbricated pebbles *in situ* at the same locations in these ridges and also at NX 985 657 in the main gravel ridge in the New Abbey area, and at NX 986 653 in a smaller gravel ridge in the New Abbey area (Fig. 6.2).

Pleistocene glaciofluvial deposits of gravel and sand occur adjacent to, and underlie, the Holocene raised coastal deposits in parts of all four geographical areas studied. In the Dalbeattie area, samples of gravel-sized clasts were collected from two abandoned gravel pits, at Chapelcroft (NX 804 550) and at Broomisle (NX 823 592). Dip-direction readings were taken of the orientation of long axes of pebbles in a gravel deposit exposed below Holocene fine-grained estuarine-marine deposits in the banks of Potterland Lane at (approximately) NX 803 553 (Fig. 6.1).

The samples of Pleistocene and Holocene gravels were collected and dip-direction readings were taken with the following main aims in view:

1) Determination of the shape, sphericity, degree of roundness and lithological composition of the clasts comprising the gravels.

2) Determination of the flow directions of the wave-fronts or currents that deposited the Pleistocene and Holocene gravels.

Subsidiary aims were:

3) Relationships between the Pleistocene and Holocene gravels on the basis of pebble shape, sphericity, roundness and lithological composition.

4) Determination of the provenances of the Pleistocene glaciofluvial gravels and the Holocene beach gravels.

6.2 Shapes of gravel clasts

Three aspects of sedimentary grain or clast morphology are shape, sphericity and roundness (Tucker 1981, 17). The shape or form is generally defined by plotting two axial ratios, intermediate axial dimension / longest axial dimension and shortest axial dimension / intermediate axial dimension, against each other, as suggested by Zingg (1935) and used by many workers (e.g. Krumbein 1953; Bluck 1967; Rose 1975; Nemec & Steel 1984; see also Lindholm 1987, 107). Four shape classes are recognised by this method: equant (more commonly called spheroid), blade, disc and rod.

In the present project, shapes of Pleistocene pebbles (71 from Chapelcroft pit, 34 from Broomisle pit) and of Holocene pebbles (48 from the higher ridge at Torr, 86 from the lower ridge at Torr) in the Dalbeattie area were determined by measuring the lengths of the short, intermediate and long axes and then plotting the ratios intermediate / long and short / intermediate against each other (Tables 6.1 and 6.2 and Figs. 6.3 and 6.4).

In summary, the predominant shapes of Pleistocene pebbles are:
at Chapelcroft, discs (33.80%); at Broomisle, spheroids (38.23%). The predominant shapes of pebbles in the Holocene gravel ridges at Torr are: higher ridge, blades and discs (each 29.16%); lower ridge, discs (41.86%).

6.3 Sphericity of gravel clasts

Sphericity is a measure of how closely a clast shape approaches that of a

sphere. A perfect sphere has a sphericity of 1.0 and, according to Folk (1980), most sedimentary grains have sphericities of between 0.6 and 0.7. It should also be noted that, for any numerical value of sphericity, there are several possible shapes. For example, a clast with a sphericity of 0.5 may be bladed, discoidal or rod-shaped (Lindholm 1987, 107).

Sphericities determined in the present project are shown diagrammatically in Figures 6.3 and 6.4. The results may be expressed as follows:

1) Sphericity of 71 pebbles from the Pleistocene gravels at Chapelcroft: mainly 0.5 to 0.9; seven pebbles 0.3 to 0.5.

2) Sphericity of 34 pebbles from the Pleistocene gravels at Broomisle: mainly 0.5 to 0.9; four pebbles 0.3 to 0.5; one pebble >0.9.

3) Sphericity of 48 pebbles from the higher ridge of Holocene gravels at Torr: mainly 0.5 to 0.9; six pebbles 0.3 to 0.5; two pebbles > 0.9.

4) Sphericity of 86 pebbles from the lower ridge of Holocene gravels at Torr: mainly 0.5 to 0.9; one pebble <0.3; ten pebbles 0.3 to 0.5; one pebble >0.9.

6.4 Roundness of gravel clasts

Roundness is geometrically independent of sphericity and shape, although this fact is sometimes not appreciated because of careless usage (Lindholm 1987, 107). Roundness is concerned with the curvature of the corners and edges of a grain or clast, and usually six classes, from very angular to well rounded, are distinguished (Tucker 1981, 17). Tucker also noted that, for environmental interpretation, the roundness measures are more significant than shape or sphericity. He also emphasised (Tucker

1981, 18) that care must be exercised in interpreting roundness values since the roundness characteristics of a clast may be inherited and, in addition, intense abrasion may lead to fracturing and angularity in clasts.

Roundness may be measured by a series of difficult and tedious operations or calculated by the use of complex formulae. More commonly, however, roundness is determined by the use of visual comparison charts. The latter method, using the roundness and sphericity chart of Powers (1953), was adopted in the present project. The results obtained are shown in detail in Table 6.1 and summarised in Table 6.3.

In brief, angular pebbles (52.11%) are most abundant in the Pleistocene gravels at Chapelcroft, whereas sub-rounded pebbles (38.23%) are most abundant in the Pleistocene gravels at Broomisle.

In the higher ridge of Holocene gravels at Torr, sub-rounded pebbles (56.25%) are by far the most abundant, whereas in the lower ridge rounded (32.56%) and sub-rounded pebbles (31.39%) are approximately equal in abundance. When the results for the two Holocene gravel ridges are compared it is seen that, taken together, rounded and sub-rounded pebbles make up the bulk of these deposits (higher ridge 72.91%, lower ridge 63.95%).

6.5 Lithological composition of gravel clasts

The lithological compositions of the rock clasts collected from the Pleistocene gravel pits at Chapelcroft and Broomisle and from the higher and lower ridges of Holocene gravel at Torr were identified. Three categories were recognised: arenaceous rocks (mainly greywackes); granite/granodiorite; argillaceous rocks (shales). The

results are given in Table 6.1 and are summarised in Table 6.4.

The results show that the vast majority (c. 70%) of the Pleistocene gravels in both pits consist of greywackes, presumably derived from local or not too distant outcrops of Upper Ordovician and Silurian rocks (see Chapter 2.1 above and Figs. 2.1 and 2.2). In contrast, the majority (c. 60%) of the rock clasts in the higher ridge of Holocene gravels at Torr consist of granite/granodiorite, whilst the majority (c. 58%) of the rock clasts in the lower ridge consist of greywackes.

6.6 Relationship between shape and lithological composition of gravel clasts

The relationship between shape and lithological composition of clasts in the two Pleistocene and two Holocene gravel ridges studied in the course of the research project is shown in Table 6.5. The data indicate that the shapes of the gravel clasts do not depend on the lithological composition of the clasts either in the case of the Pleistocene or the Holocene deposits.

In the case of the Holocene beach gravels, it may be noted that the disc shape is the most abundant in both greywacke clasts (higher ridge 33.33%, lower ridge 34.00%) and granite/granodiorite clasts (higher ridge 31.03%, lower ridge 51.45%).

In the Pleistocene gravels at Chapelcroft, the disc shape is the most abundant in greywacke clasts (34.00%) and granite/granodiorite clasts (33.33%). In contrast, in the Pleistocene gravels at Broomisle, the spheroid shape is the most abundant in greywacke clasts (30.43%) and granite/granodiorite clasts (62.50%).

6.7 Relationship between roundness and lithological composition of gravel clasts

The relationship between roundness and lithological composition of clasts in the two Pleistocene and two Holocene gravel ridges studied in the course of the research project is shown in Table 6.6. The data indicate that the majority of the clasts in the higher ridge of Holocene gravels are sub-rounded in both greywacke pebbles (66.67%) and granite/granodiorite pebbles (51.72%), whilst in the lower ridge the majority of clasts are either rounded or sub-rounded in both greywacke pebbles (rounded 36.00%, sub-rounded 34.00%) and granite/granodiorite pebbles (rounded 27.71%, sub-rounded 28.57%).

In the Pleistocene gravels, greywacke clasts are relatively more rounded than granite/granodiorite clasts. This is especially notable in the Chapelcroft pit where greywacke pebbles range from rounded (22%) through sub-rounded (16%) and sub-angular (24%) to angular (38%), whereas granite/granodiorite clasts in the same pit are mainly angular (80.95%). This may indicate that the greywacke pebbles have been transported a greater distance than the granite/granodiorite pebbles, which most probably were derived from the nearby Criffell-Dalbeattie granite/granodiorite pluton. The same trend, though less marked, is to be seen in the relationship between roundness and lithological composition in the case of the Pleistocene gravels of the Broomisle pit. There, greywacke pebbles range from sub-rounded (47.87%) through sub-angular (34.78%) to angular (17.39%), whereas granite/granodiorite clasts are mainly angular (62.50%); sub-rounded (25.00%) and sub-angular (12.50%) specimens make up the remainder of the sampled clasts.

6.8 Palaeocurrent flow directions

6.8.1 Pleistocene gravels

As noted above (Chapter 6.1), dip-direction readings were taken of the orientation of long axes of clasts in gravel deposits exposed in the banks of Potterland Lane at (approximately) NX 803 553 (Fig. 6.1). The oriented gravels are situated about 500m south of a sheet of Pleistocene gravel deposits the surface of which slopes gently to the south. The oriented gravels are also situated about 300m to the NW of a ridge of Pleistocene gravels the summit of which stands several metres above the flatter area where the oriented gravels now occur. Fine-grained sediments, which are thought to have been deposited in the course of the Holocene marine transgression, overlie the oriented gravels.

The rose diagram constructed from the clast-orientation data (Fig. 6.1) suggests that the final alignment of the clasts was produced by flow from the SE. At least two possible explanations of such a flow orientation are these:

1) The oriented gravels were derived from an ice mass located to the SE of their present position, the gravels being transported to that position by water flowing down a SE-NW oriented slope at the time of ice melting. Thus, the oriented gravels may be part of an outwash mass associated with the ridge of (? ice-contact) glaciofluvial gravels that is now located SE of their position.

2) The oriented gravels may originally have been part of the sheet of Pleistocene gravels that lies a short distance to the north of the location where orientation directions were measured in the banks of Potterland Lane. In the early phases of the Holocene marine transgression, as the sea penetrated into the shallow hollow now

occupied by Potterland Lane, the sheet of Pleistocene gravels may have been eroded by marine action and the clasts re-oriented so that their present alignment is indicative of SE-NW onshore flow action.

6.8.2 Holocene gravels

As also noted in Chapter 6.1 above, dip-direction readings were recorded for the orientation of long axes of clasts in the two Holocene gravel ridges at Torr, Dalbeattie area, and two Holocene gravel ridges in the New Abbey area. In all four cases, the rose diagrams constructed from the clast-orientation data indicate that the waves that deposited the beach gravel ridges, presumably in storm conditions, moved in a SE to NW direction (Figs.6.1 and 6.2). The results are consistent with the shapes and geographical positions of the gravel ridges in relation to contemporaneous major coastal features (headlands and embayments) in the vicinity of Auchencairn Bay (Dalbeattie area, Fig. 6.1) and the mouth of New Abbey Pow (New Abbey area, Fig. 6.2).

6.9 Relationships between Pleistocene and Holocene gravels of the Dalbeattie area

In this section, the relationships between the Pleistocene and Holocene gravel deposits of the Dalbeattie area are considered, mainly on the basis of pebble shape, roundness and lithological composition, to a lesser extent on the basis of sphericity.

1) Shape: In both the Pleistocene and Holocene gravels, the disc is the commonest clast shape (Pleistocene 30.48%, Holocene 37.31%; Table 6.7). Spheroids are next in abundance in both cases. Blades are slightly more abundant in the

Pleistocene than in the Holocene deposits, whereas rods are slightly commoner in the Holocene than in the Pleistocene deposits. The higher percentage of blades in the Pleistocene deposits suggests that the Holocene deposits are more mature than the Pleistocene deposits, as a result of marine wave and current action in transport and deposition of the Holocene sediments, compared with glaciofluvial current action in the case of the Pleistocene deposits. It may be noted (Table 6.1) that the disc- and blade-shaped clasts are mostly larger than the spheroid- and rod-shaped clasts if the intermediate axis of the clasts is used to describe the size attributes (cf. Bluck 1967).

2) Sphericity: The sphericity of the Holocene pebbles is concentrated mainly between values of 0.5 and 0.7 (Fig. 6.4), whereas the sphericity of the Pleistocene pebbles is scattered between values of 0.3 and 0.9 (Fig. 6.3). This indicates better sorting in the Holocene than in the Pleistocene gravels.

3) Roundness: As shown clearly in Table 6.8, the estimated roundness categories of the two major groups of gravel deposits show that (as would be expected) the Holocene beach gravels are more rounded than the Pleistocene glaciofluvial gravels. This is probably due to Holocene marine wave and current action causing abrasion of the corners and edges of clasts during coastal transport and deposition.

4) Lithological composition: As shown in Table 6.9, the Holocene gravels consist of nearly equal proportions of greywacke clasts (50.74%) and granite/granodiorite clasts (47.76%), whilst the Pleistocene gravels consist mainly of greywacke clasts (68.57%) and a much smaller proportion of granite/granodiorite clasts (28.57%). The differences in lithological

composition are almost certainly a reflection of provenance of the two groups of gravels. The Pleistocene gravels, being glaciofluvial deposits, were derived dominantly from the NW and west, where greywackes are the major bedrock, although some granite/granodiorite clasts were derived locally from the western part of the Criffell-Dalbeattie pluton. In contrast, the Holocene beach gravels may have been derived partly from Pleistocene glaciofluvial gravels that were being eroded by marine action within the Dalbeattie area during the Holocene marine transgression and regression, and from outcrops of granite/granodiorite of the Criffell-Dalbeattie pluton that were exposed simultaneously to the south and SE of the area of Holocene marine deposition.

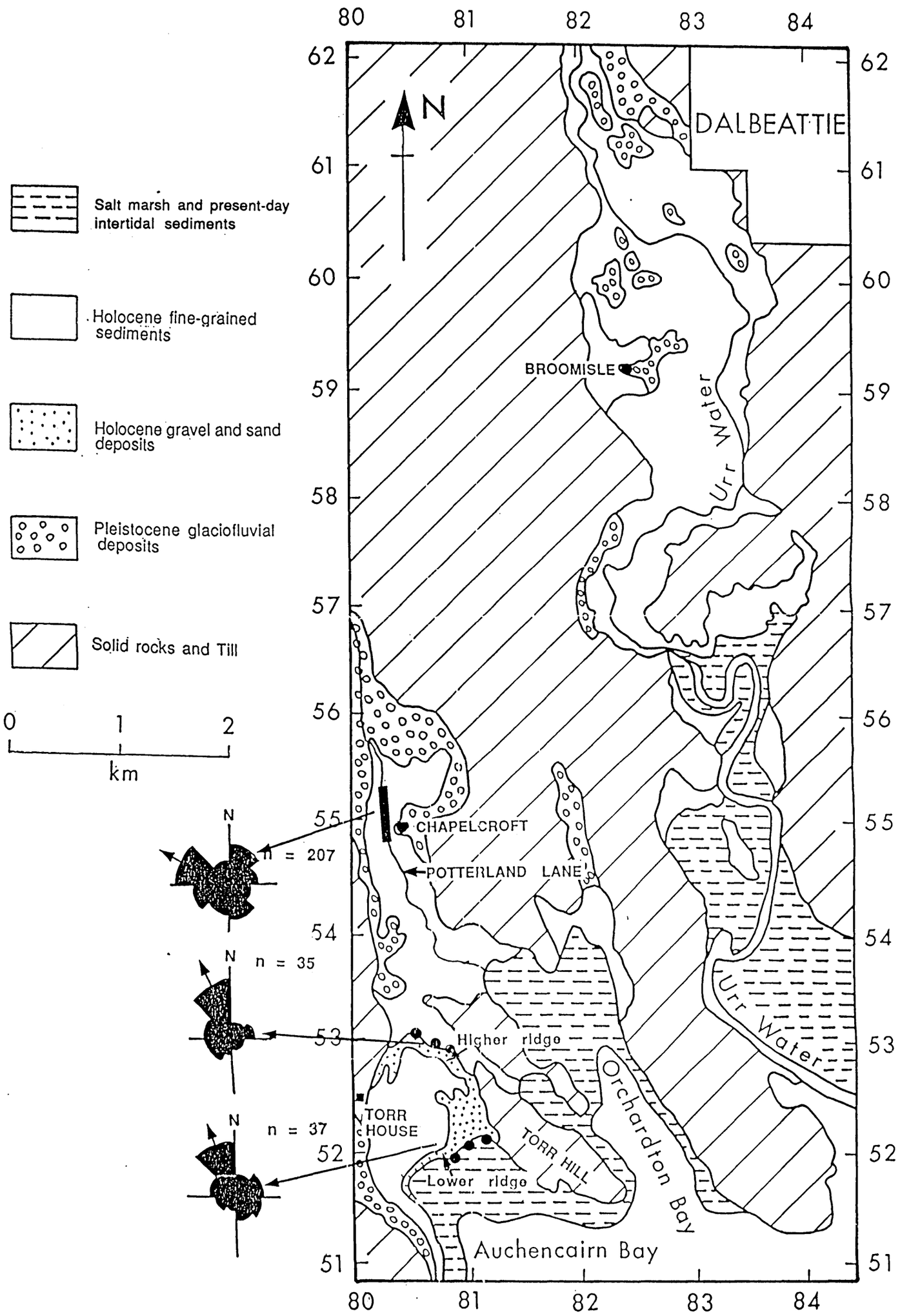

Figure 6.1 Map of the Dalbeattie area, showing the positions of the Pleistocene gravel ridges at Chapelcroft and Broomisle and the higher and lower Holocene gravel ridges at Torr. The position of Potterland Lane, where the orientation of gravel clasts was measured, is also shown. Rose diagrams, showing clast orientations, are included.

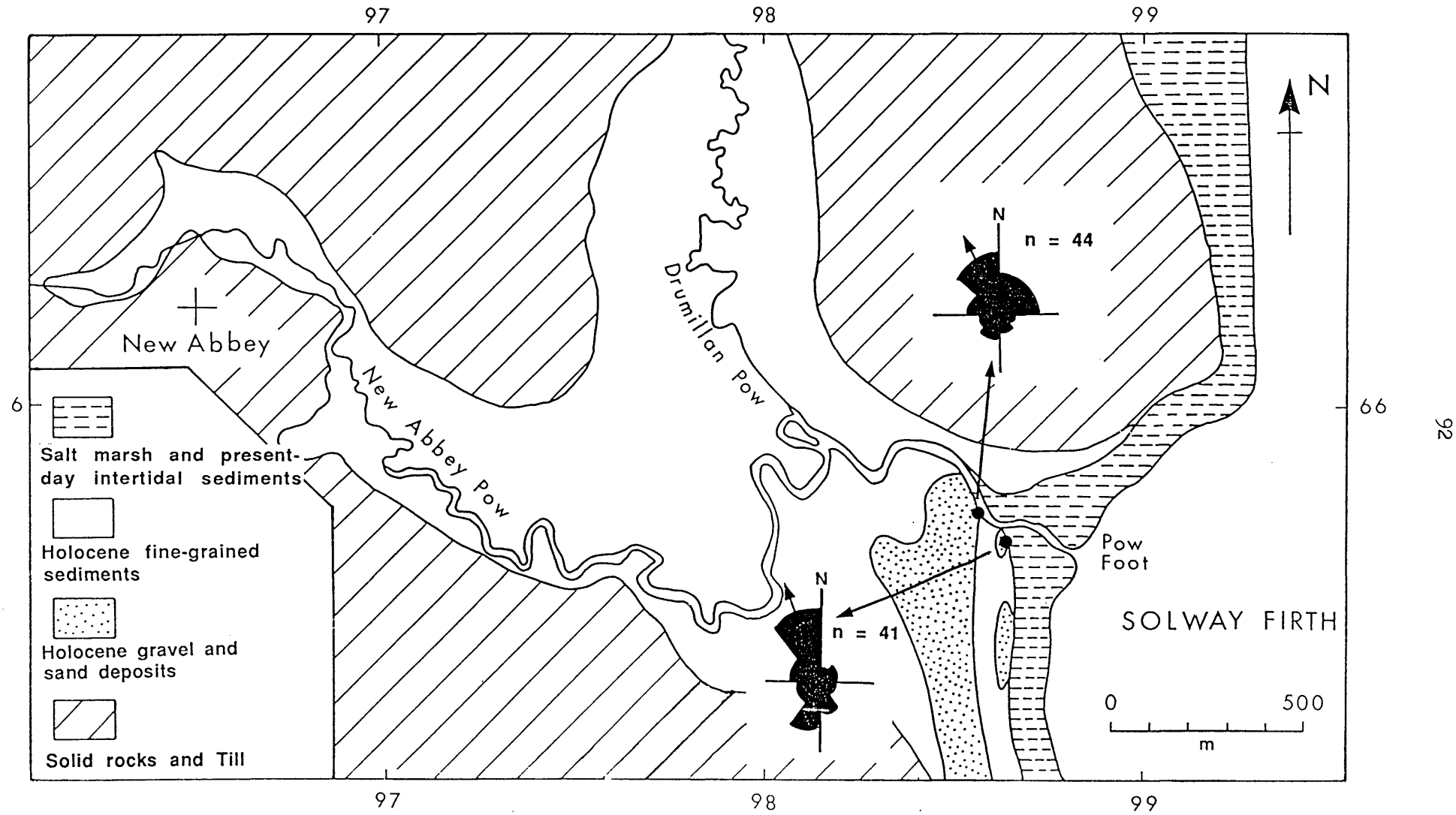

Figure 6.2 Map of the New Abbey area, showing the positions of two sites where the orientation of Holocene gravel clasts was measured. Rose diagrams, showing clast orientations, are also included.

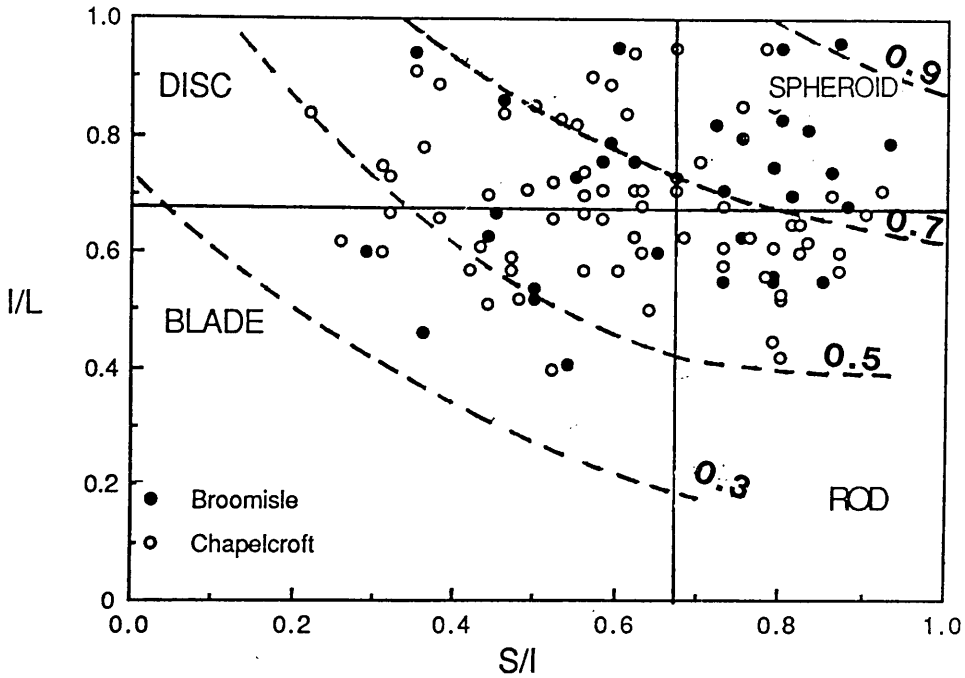

Figure 6.3 Shape classes and sphericity values for Pleistocene gravel clasts, Dalbeattie area

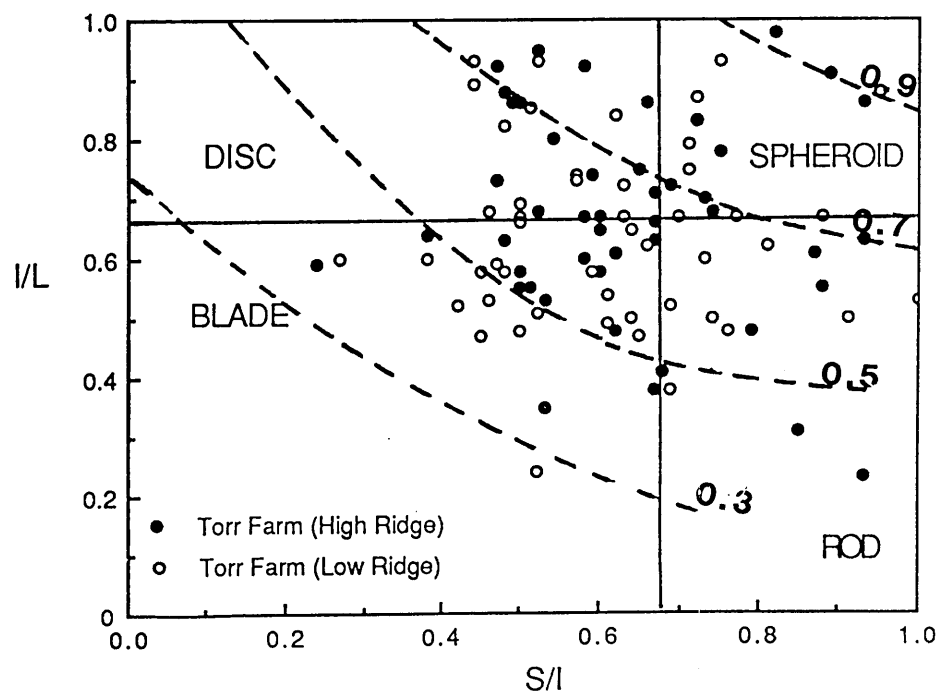

Figure 6.4 Shape classes and sphericity values for Holocene gravel clasts, Dalbeattie area

Table 6.1 Lengths (in cm) of the three axes (S = short, I = intermediate, L = long), calculated shapes according to Zingg's diagram (1935), estimated roundness according to Power's chart (1953) and lithological compositions of the Pleistocene and Holocene gravel deposits studied in the Dalbeattie area.

Table 6.1a Pleistocene gravel, Chapelcroft (NX 804 550)

S	I	L	I / L	S / I	Shape	Roundness	Lithology
3.50	8.30	14.60	0.57	0.42	Blade	Subang.	Greywacke
2.40	6.30	7.10	0.89	0.38	Disc	Ang.	Greywacke
4.20	5.20	5.80	0.90	0.80	Sphd.	Ang.	Greywacke
2.40	4.90	6.90	0.71	0.49	Disc	Ang.	Granite
2.60	4.20	6.60	0.63	0.62	Blade	Subr.	Greywacke
1.40	3.90	5.00	0.78	0.36	Disc	Ang.	Granite
2.20	3.60	4.30	0.84	0.61	Disc	Rd.	Greywacke
1.50	2.90	4.00	0.72	0.52	Disc	Ang.	Granite
1.30	4.00	5.30	0.75	0.31	Disc	Ang.	Greywacke
2.30	4.20	5.10	0.82	0.55	Disc	Rd.	Greywacke
0.90	2.80	4.20	0.67	0.32	Disc	Ang.	Greywacke
2.00	3.20	4.46	0.71	0.63	Disc	Ang.	Granite
1.20	3.70	5.10	0.73	0.32	Disc	Ang.	Greywacke
1.15	2.60	5.10	0.51	0.44	Blade	Ang.	Greywacke
1.00	3.20	5.30	0.60	0.31	Blade	Ang.	Greywacke
1.90	2.55	3.00	0.85	0.75	Sphd.	Rd.	Greywacke
1.60	2.80	3.10	0.90	0.57	Disc	Rd.	Greywacke
1.40	2.70	6.80	0.40	0.52	Blade	Ang.	Greywacke
1.90	2.60	3.80	0.68	0.73	Sphd.	Ang.	Granite
1.50	1.80	2.90	0.62	0.83	Rod	Ang.	Granodiorite
1.15	1.95	3.40	0.57	0.60	Blade	Ang.	Greywacke
1.75	2.20	3.70	0.59	0.47	Blade	Ang.	Greywacke
0.70	2.00	2.20	0.91	0.35	Disc	Ang.	Greywacke
1.50	2.20	3.50	0.63	0.68	Rod	Ang.	Granodiorite
1.10	2.30	4.46	0.52	0.48	Blade	Subr.	Granite
0.60	1.40	2.30	0.61	0.43	Blade	Ang.	Granite
0.80	1.10	1.90	0.58	0.73	Rod	Ang.	Granodiorite
0.90	1.30	1.70	0.76	0.70	Sphd.	Ang.	Granodiorite
0.70	1.20	1.70	0.71	0.58	Disc	Ang.	Granite
1.10	1.90	2.90	0.66	0.58	Blade	Subang.	Greywacke
1.40	2.70	4.10	0.66	0.52	Blade	Rd.	Granite
1.20	2.60	3.10	0.84	0.46	Disc	Rd.	Greywacke
1.40	1.80	1.90	0.95	0.78	Sphd.	Ang.	Greywacke
1.00	1.90	2.30	0.83	0.53	Sphd.	Subr.	Greywacke
1.00	1.70	1.90	0.89	0.59	Sphd.	Ang.	Greywacke
0.70	1.60	2.30	0.70	0.44	Disc	Ang.	Greywacke
1.40	2.10	2.20	0.95	0.67	Sphd.	Subang.	Greywacke
0.90	1.60	2.30	0.70	0.56	Disc	Rd.	Greywacke
0.95	1.50	2.20	0.68	0.63	Disc	Subr.	Granodiorite
1.45	1.60	2.40	0.67	0.90	Rod	Subr.	Granodiorite
0.95	1.40	1.90	0.73	0.67	Sphd.	Subr.	Greywacke
0.80	1.20	1.70	0.71	0.67	Sphd.	Ang.	Greywacke
0.80	1.10	1.80	0.61	0.73	Rod	Subang.	Greywacke

(continued)

Table 6.1a continued

8.00	10.0	24.0	0.42	0.80	Rod	Ang.	Greywacke
4.50	7.00	14.0	0.50	0.64	Blade	Subr.	Greywacke
2.00	3.20	4.50	0.71	0.62	Disc	Rd.	Greywacke
2.40	3.00	5.80	0.52	0.80	Rod	Subr.	Greywacke
2.30	2.90	3.40	0.85	0.79	Sphd.	Subr.	Greywacke
0.80	3.00	4.80	0.62	0.26	Blade	Ang.	Greywacke
0.60	2.70	4.20	0.84	0.22	Disc	Ang.	Greywacke
1.50	1.90	3.10	0.61	0.79	Rod	Ang.	Greywacke
0.80	2.10	3.20	0.66	0.38	Blade	Subr.	Greywacke
2.00	3.20	3.40	0.94	0.62	Disc	Subr.	Greywacke
0.80	1.70	3.00	0.57	0.47	Blade	Ang.	Granodiorite
1.40	1.50	2.50	0.60	0.82	Rod	Subang.	Greywacke
1.40	1.70	2.60	0.65	0.82	Rod	Subang.	Greywacke
1.35	1.65	2.55	0.65	0.81	Rod	Subang.	Greywacke
1.40	1.60	2.80	0.57	0.87	Rod	Subang.	Greywacke
1.10	1.40	2.50	0.56	0.78	Rod	Rd.	Greywacke
1.30	1.70	2.70	0.63	0.76	Rod	Rd.	Greywacke
1.00	1.60	2.65	0.60	0.63	Blade	Rd.	Greywacke
1.30	1.50	2.50	0.60	0.87	Rod	Rd.	Greywacke
0.90	1.80	2.10	0.85	0.50	Disc	Ang.	Granite
1.10	1.20	1.70	0.71	0.92	Sphd.	Ang.	Granodiorite
1.20	1.40	2.00	0.70	0.86	Sphd.	Ang.	Granodiorite
0.90	1.60	2.40	0.67	0.56	Disc	Ang.	Granite
0.90	1.60	2.80	0.57	0.56	Blade	Ang.	Granodiorite
1.10	1.40	3.10	0.45	0.79	Rod	Ang.	Granodiorite
0.65	2.00	2.70	0.74	0.56	Disc	Subang.	Greywacke
0.90	1.80	2.10	0.85	0.50	Disc	Subang.	Greywacke
0.80	1.00	1.90	0.53	0.80	Rod	Subang.	Greywacke

Table 6.1b Pleistocene gravel, Broomisle (NX 823 592)

S	I	L	I/L	S/I	Shape	Roundness	Lithology
4.10	4.80	8.80	0.55	0.85	Rod	Subr.	Greywacke
0.90	3.10	5.20	0.60	0.29	Blade	Ang.	Shale
3.10	3.80	5.40	0.70	0.81	Sphd.	Ang.	Greywacke
2.00	2.30	2.40	0.96	0.87	Sphd.	Ang.	Granite
1.60	2.00	2.10	0.95	0.80	Sphd.	Ang.	Granite
2.30	2.60	3.80	0.68	0.88	Sphd.	Ang.	Granite
1.20	3.40	3.60	0.94	0.35	Disc	Ang.	Shale
1.75	3.20	4.40	0.73	0.55	Disc	Subr.	Greywacke
1.10	2.20	4.20	0.52	0.50	Blade	Subr.	Greywacke
1.70	2.95	3.90	0.76	0.58	Disc	Subr.	Greywacke
3.00	3.60	4.40	0.81	0.83	Sphd.	Subr.	Greywacke
2.20	3.00	4.20	0.71	0.73	Sphd.	Subang.	Greywacke
2.00	3.40	4.30	0.79	0.59	Disc	Subang.	Greywacke
1.10	2.40	2.80	0.86	0.46	Disc	Subr.	Granite
1.90	2.35	3.35	0.70	0.81	Sphd.	Subr.	Greywacke
1.90	2.40	4.40	0.55	0.79	Rod	Ang.	Greywacke
1.20	2.00	2.10	0.95	0.60	Disc	Subr.	Greywacke

(continued)

Table 6.1b continued

0.90	1.20	1.90	0.63	0.75	Rod	Subr.	Greywacke
1.20	1.50	1.80	0.83	0.80	Sphd.	Subr.	Greywacke
1.20	1.40	1.90	0.74	0.86	Sphd.	Subr.	Greywacke
0.95	1.20	1.60	0.75	0.79	Sphd.	Subr.	Granite
0.60	1.10	2.70	0.41	0.54	Blade	Subang.	Granite
0.90	1.80	3.30	0.54	0.50	Blade	Ang.	Greywacke
0.90	2.00	3.00	0.67	0.45	Disc	Ang.	Granodiorite
1.30	1.80	2.20	0.82	0.72	Sphd.	Ang.	Granite
0.70	1.60	2.55	0.63	0.44	Blade	Subang.	Greywacke
0.60	1.40	2.30	0.61	0.43	Blade	Subang.	Greywacke
0.80	1.30	1.70	0.76	0.62	Disc	Subang.	Greywacke
1.40	1.50	1.90	0.79	0.93	Sphd.	Subang.	Greywacke
1.00	1.55	2.60	0.60	0.65	Blade	Subang.	Greywacke
1.10	1.40	2.50	0.56	0.79	Rod	Subang.	Greywacke
0.40	1.10	2.40	0.46	0.36	Blade	Rd.	Greywacke
0.90	1.20	1.50	0.80	0.75	Sphd.	Rd.	Shale
0.80	1.10	2.00	0.55	0.73	Rod	Subr.	Greywacke

Table 6.1c Holocene beach gravel, higher ridge, at Torr (NX 804 531 to NX 808 529)

S	I	L	I / L	S / I	Shape	Roundness	Lithology
2.05	4.20	6.65	0.63	0.48	Blade	Subr.	Greywacke
1.85	3.65	4.55	0.80	0.59	Disc	Subr.	Granodiorite
1.85	3.15	4.80	0.60	0.58	Blade	Rd.	Granite
5.85	6.15	10.25	0.63	0.93	Rod	Subr.	Granite
2.80	4.20	6.60	0.63	0.67	Rod	Subr.	Greywacke
1.15	1.85	3.85	0.48	0.62	Blade	W.Rd.	Granite
2.20	3.55	5.75	0.61	0.62	Blade	Subr.	Greywacke
3.25	5.55	7.45	0.74	0.59	Disc	Rd.	Granite
2.75	5.65	6.50	0.86	0.49	Disc	Subr.	Greywacke
2.40	2.60	4.70	0.55	0.51	Blade	Rd.	Granite
2.80	6.00	6.55	0.92	0.47	Disc	Subr.	Granite
2.50	4.15	6.15	0.67	0.60	Disc	Ang.	Granite
2.00	3.50	7.80	0.64	0.38	Blade	W.Rd.	Granite
2.60	4.90	9.20	0.53	0.53	Blade	Ang.	Greywacke
2.30	4.05	6.05	0.67	0.58	Disc	Subr.	Granite
2.90	4.00	4.90	0.83	0.72	Sphd.	Subr.	Granite
2.20	4.65	6.35	0.73	0.47	Disc	Rd.	Granite
2.40	3.25	4.80	0.68	0.74	Sphd.	Rd.	Greywacke
2.70	3.20	4.20	0.76	0.84	Sphd.	Rd.	Greywacke
1.45	3.60	6.10	0.59	0.24	Blade	Subr.	Granite
2.80	3.20	5.20	0.61	0.87	Rod	Rd.	Shale
2.45	4.75	5.00	0.95	0.52	Disc	Rd.	Granite
2.00	2.90	4.00	0.72	0.69	Sphd.	Subang.	Greywacke
2.90	3.50	4.25	0.98	0.82	Sphd.	Subang.	Granodiorite
2.90	3.25	3.55	0.91	0.89	Sphd.	Subr.	Granite
2.25	3.90	4.20	0.92	0.58	Disc	Subr.	Granite
1.25	1.35	5.95	0.23	0.93	Rod	Subr.	Greywacke
1.80	3.00	5.15	0.58	0.60	Blade	Subr.	Granodiorite
2.50	3.40	4.80	0.70	0.73	Sphd.	Subr.	Granite
1.70	2.15	4.50	0.48	0.79	Rod	Subr.	Greywacke
2.50	3.35	4.30	0.78	0.75	Sphd.	Su	Granite

(continued)

Table 6.1c continued

1.10	2.20	3.80	0.58	0.50	Blade	W.Rd.	Greywacke
1.65	2.75	4.20	0.65	0.60	Blade	Ang.	Granite
1.50	2.25	3.40	0.66	0.67	Rod	W.Rd.	Granite
1.80	2.70	3.80	0.71	0.67	Sphd.	Subr.	Granite
2.50	3.70	4.30	0.86	0.93	Sphd.	Ang.	Granite
1.40	2.70	4.00	0.68	0.52	Disc	Ang.	Greywacke
1.20	1.80	4.40	0.41	0.67	Rod	Subr.	Granodiorite
2.80	2.70	3.80	0.71	0.67	Sphd.	Ang.	Granodiorite
0.90	1.70	4.80	0.35	0.53	Blade	Ang.	Granodiorite
1.60	3.20	3.70	0.86	0.50	Disc	Subr.	Greywacke
1.45	2.25	3.05	0.75	0.65	Disc	Subr.	Greywacke
1.00	1.50	3.90	0.38	0.67	Rod	Subr.	Greywacke
1.50	1.70	3.10	0.55	0.88	Rod	Subr.	Greywacke
1.35	2.80	3.20	0.88	0.48	Disc	Subr.	Greywacke
0.90	1.80	3.30	0.55	0.50	Blade	Subr.	Granodiorite
0.90	1.05	3.35	0.31	0.85	Rod	Subr.	Granodiorite
1.65	2.50	2.90	0.86	0.66	Disc	Subr.	Greywacke

Table 6.1d Holocene beach gravel, lower ridge, at Torr (NX 808 521 to NX 810 to 522)

S	I	L	I / L	S / I	Shape	Roundness	Lithology
1.80	3.60	4.10	0.88	0.50	Disc	Subr.	Granodiorite
1.10	1.80	2.20	0.81	0.61	Disc	Subr.	Granite
1.10	2.30	2.40	0.96	0.48	Disc	Rd.	Granite
1.25	2.40	3.50	0.69	0.52	Disc	Rd.	Granite
1.55	2.20	4.25	0.51	0.70	Rod	Rd.	Granodiorite
1.05	1.60	5.20	0.30	0.66	Rod	Subr.	Granite
2.60	3.20	4.90	0.31	0.81	Rod	Subr.	Greywacke
1.10	2.35	2.80	0.84	0.47	Disc	Subr.	Greywacke
1.40	2.30	3.05	0.77	0.61	Disc	W.Rd.	Greywacke
1.20	2.30	4.10	0.56	0.52	Blade	Rd.	Greywacke
1.90	2.90	4.20	0.69	0.65	Disc	Subr.	Greywacke
1.00	2.60	3.20	0.81	0.38	Disc	W.Rd.	Granite
1.55	2.30	2.80	0.82	0.69	Sphd.	W.Rd.	Greywacke
0.85	1.85	3.25	0.57	0.46	Blade	W.Rd.	Greywacke
0.90	2.00	2.40	0.83	0.45	Disc	Subr.	Greywacke
1.00	1.60	3.50	0.46	0.63	Blade	Subr.	Greywacke
1.00	2.20	2.40	0.92	0.45	Disc	Subr.	Granodiorite
1.30	2.30	2.80	0.82	0.57	Disc	Rd.	Granite
1.40	2.25	2.90	0.77	0.62	Disc	Rd.	Greywacke
1.40	2.70	2.95	0.91	0.52	Disc	Rd.	Greywacke
1.60	2.10	2.60	0.81	0.72	Sphd.	Rd.	Greywacke
1.10	1.60	2.10	0.76	0.69	Sphd.	Rd.	Greywacke
1.05	2.10	2.20	0.95	0.50	Disc	Rd.	Granite
1.00	2.10	3.00	0.70	0.48	Disc	Subr.	Greywacke
0.70	1.60	2.25	0.71	0.44	Disc	Rd.	Greywacke
1.20	1.70	2.40	0.71	0.71	Sphd.	Subr.	Greywacke

(continued)

Table 6.1d continued

0.80	1.10	2.00	0.55	0.73	Rod	Rd.	Granite
0.85	1.20	1.50	0.80	0.71	Sphd.	Rd.	Greywacke
1.30	2.20	2.70	0.82	0.59	Disc	Rd.	Greywacke
1.00	2.25	2.70	0.81	0.44	Disc	Subr.	Granite
0.50	1.80	3.00	0.60	0.27	Blade	Subr.	Greywacke
1.25	2.20	2.45	0.89	0.57	Disc	Subr.	Shale
0.90	1.40	1.60	0.87	0.64	Sphd.	Subr.	Greywacke
0.70	1.40	1.50	0.93	0.50	Disc	Rd.	Granodiorite
1.10	1.75	2.40	0.73	0.63	Disc	Subang.	Granodiorite
1.20	1.60	2.10	0.76	0.75	Sphd.	Subang.	Granodiorite
0.80	1.90	2.30	0.83	0.42	Disc	Rd.	Granite
1.00	1.30	1.85	0.70	0.77	Sphd.	Subang.	Granite
1.20	1.20	1.80	0.67	1.00	Sphd.	W.Rd.	Greywacke
1.00	1.10	2.05	0.54	0.91	Rod	Subang.	Greywacke
0.90	1.40	2.10	0.67	0.64	Disc	W.Rd.	Greywacke
1.40	1.60	2.10	0.76	0.88	Sphd.	Subang.	Greywacke
1.00	1.05	1.90	0.55	0.95	Rod	Rd.	Greywacke
0.80	1.05	1.90	0.55	0.76	Rod	Rd.	Greywacke
0.70	0.95	1.80	0.53	0.74	Rod	Subr.	Granite
2.20	4.30	9.20	0.47	0.51	Blade	Ang.	Greywacke
1.00	2.00	3.70	0.54	0.50	Blade	Ang.	Granodiorite
1.90	3.50	3.80	0.92	0.54	Disc	Subr.	Greywacke
1.20	1.80	1.80	1.00	0.67	Sphd.	Rd.	Greywacke
1.00	2.50	3.90	0.64	0.40	Blade	Subr.	Granite
1.60	1.95	3.00	0.65	0.82	Rod	Rd.	Granite
1.10	1.40	2.40	0.58	0.79	Rod	Rd.	Greywacke
1.30	1.70	1.80	0.94	0.76	Sphd.	Subr.	Granite
0.90	2.40	2.70	0.88	0.38	Disc	Rd.	Greywacke
1.50	1.80	2.70	0.67	0.83	Sphd.	Rd.	Greywacke
1.00	1.50	2.80	0.54	0.67	Rod	Rd.	Greywacke
1.00	2.05	2.50	0.82	0.49	Disc	Subang.	Granite
1.40	1.80	1.90	0.95	0.78	Sphd.	Subang.	Granodiorite
1.00	2.00	2.60	0.77	0.50	Disc	Subr.	Greywacke
2.80	3.20	5.50	0.58	0.88	Rod	Subang	Granite
1.05	1.50	2.05	0.73	0.70	Sphd.	Subang.	Granite
2.50	3.10	8.30	0.37	0.81	Rod	Subr.	Granodiorite
1.05	1.20	1.60	0.75	0.87	Sphd.	Subr.	Greywacke
0.70	0.80	1.30	0.61	0.87	Rod	W.Rd.	Greywacke
3.50	4.80	7.10	0.68	0.73	Sphd.	W.Rd.	Greywacke
2.00	3.55	5.50	0.65	0.56	Blade	Ang.	Granite
2.00	3.45	4.00	0.86	0.56	Disc	Ang.	Granite
1.60	3.00	4.40	0.68	0.53	Disc	Ang.	Greywacke
3.10	3.80	4.60	0.83	0.82	Sphd.	Subr.	Greywacke
2.10	3.90	4.30	0.91	0.54	Disc	Subr.	Greywacke
2.60	2.80	3.40	0.82	0.93	Sphd.	W.Rd.	Granite
1.40	3.00	5.00	0.60	0.47	Blade	Subr.	Greywacke
1.50	2.40	2.90	0.83	0.63	Disc	W.Rd.	Granodiorite
0.80	2.40	3.50	0.83	0.33	Disc	Ang.	Granite
0.60	1.90	2.40	0.79	0.32	Disc	Ang.	Granite
1.20	1.60	2.40	0.67	0.75	Sphd.	Subr.	Greywacke
1.50	2.00	2.60	0.77	0.75	Sphd.	Subr.	Greywacke

(continued)

Table 6.1d continued

1.00	1.80	2.60	0.70	0.56	Disc	Rd.	Greywacke
1.30	2.00	2.70	0.74	0.65	Disc	Rd.	Greywacke
1.45	2.70	3.50	0.77	0.54	Disc	Ang.	Granodiorite
1.45	1.70	4.40	0.39	0.85	Rod	Subr.	Greywacke
1.40	1.85	2.45	0.75	0.76	Sphd.	W.Rd.	Greywacke
1.20	1.50	2.35	0.64	0.80	Rod.	W.Rd.	Greywacke
1.60	1.70	2.40	0.71	0.94	Sphd.	Rd.	Greywacke
1.25	2.10	2.90	0.72	0.60	Disc	Rd.	Greywacke

Table 6.2 Shape distribution of the gravel clasts studied in the Dalbeattie area

Shape	Pleistocene		Holocene	
	Chapelcroft n=71	Broomisle n=34	Higher ridge n=48	Lower ridge n=86
Blade	23.94%	23.54%	29.16%	12.79%
Disc	33.80%	23.54%	29.16%	41.86%
Rod	23.94%	14.70%	20.83%	18.60%
Spheroid	18.31%	38.23%	20.83%	26.74%

Table 6.3 Degree of roundness of the gravel clasts in the Dalbeattie area

Roundness	Pleistocene		Holocene	
	Chapelcroft n=71	Broomisle n=34	Higher ridge n=48	Lower ridge n=86
W. Rd.	0.00	0.00	6.25%	17.44%
Rounded	15.49%	5.88%	16.66%	32.56%
Sub.Rd.	15.49%	38.23%	56.25%	31.39%
Subang.	16.90%	26.47%	4.16%	10.46%
Angular	52.11%	29.41%	10.41%	9.30%

Table 6.4 Lithological compositions of the gravel clasts studied in the Dalbeattie area

Lithological composition	Pleistocene		Holocene	
	Chapelcroft n=71	Broomisle n=34	Higher ridge n=48	Lower ridge n=86
Greywacke	70.42%	67.64%	37.50%	58.14%
Granite/ Granodiorite	29.58%	23.53%	60.42%	40.70%
Shale	0.00%	8.82%	2.08%	1.16%

Table 6.5 Relationship between shape and lithological composition of gravel clasts studied in the Dalbeattie area

	Blade	Disc	Rod	Spheroid
Pleistocene gravels				
Chapelcroft				
Greywacke (n=50)	24.00%	34.00%	24.00%	18.00%
Granite/Granodiorite (n=21)	23.81%	33.33%	28.57%	19.05%
Broomisle				
Greywacke (n=23)	21.74%	26.09%	21.74%	30.43%
Granite/Granodiorite (n=8)	12.50%	25.00%	0.00%	62.50%
Shale (n=3)	33.33%	33.33%	0.00%	33.33%
Holocene gravels				
Higher ridge				
Greywacke (n=18)	22.22%	33.33%	27.77%	16.66%
Granite/Granodiorite (n=29)	27.59%	31.03%	13.79%	27.59%
Lower ridge				
Greywacke (n=50)	12.00%	34.00%	20.00%	34.00%
Granite/Granodiorite (n=35)	11.43%	51.45%	20.00%	17.14%

Table 6.6 Relationship between degree of roundness and lithological composition of gravel clasts studied in the Dalbeattie area

	W.Rd.	Round	Subrd.	Subang.	Angular
Pleistocene gravels					
Chapelcroft					
Greywacke(n=50)	0.00%	22.00%	16.00%	24.00%	38.00%
Granite/Granodiorite (n=21)	0.00%	0.00%	14.28%	4.76%	80.95%
Broomisle					
Greywacke (n=23)	0.00%	4.34%	47.87%	34.78%	17.39%
Granite/Granodiorite (n=8)	0.00%	00.00%	25.00%	12.50%	62.50%
Shale (n=3)	0.00%	33.33%	0.00%	0.00%	33.33%
Holocene gravels					
Higher ridge					
Greywacke (n=18)	5.55%	11.10%	66.67%	5.55%	11.10%
Granite/Granodiorite (n=29)	10.34%	17.24%	51.72%	3.45%	17.24%
Lower ridge					
Greywacke (n=50)	22.00%	36.00%	34.00%	4.00%	4.00%
Granite/Granodiorite (n=35)	8.57%	27.71%	28.57%	20.00%	17.14%

Table 6.7 Average shape distribution of gravel clasts studied in the Dalbeattie area

	Blade	Disc	Rod	Spheroid
Pleistocene gravels (n=105)	23.81%	30.48%	20.95%	24.76%
Holocene gravels (n=134)	17.92%	37.31%	19.40%	25.37%

Table 6.8 Average degree of roundness of gravel clasts studied in the Dalbeattie area

	W.Rd.	Round	Subrd.	Subang.	Angular
Pleistocene gravels (n=105)	0.00%	10.47%	22.85%	21.90%	44.74%
Holocene gravels (n=134)	10.94%	25.54%	40.14%	8.95%	11.94%

Table 6.9 Average lithological compositions of gravel clasts studied in the Dalbeattie area

	Greywacke	Granite/ Granodiorite	Shale
Pleistocene gravels (n=105)	68.57%	28.57%	2.86%
Holocene gravels (n=134)	50.74%	47.76%	1.49%

Chapter 7

GRAIN-SIZE ANALYSIS

7.1 Introduction

Grain-size analysis is a fundamental descriptive measure of sediments and sedimentary rocks. It is also important in determining the distance of sediment transport, and in understanding the processes involved during transportation and depositon (cf. Passega 1957; Sahu 1964; Sly et. al. 1983; Lindholm 1987, 154). In addition, grain-size analysis can be used to help to distinguish between sediments of different environments and facies (Tucker 1981, 16).

The Holocene raised coastal sediments and present-day intertidal sediments that are the subject of this research project represent a complex of environments. As stated in Chapter 1.4 above, the main aims of this part of the project were to determine:

(a) The textural characteristics of the Holocene sediments and present-day intertidal sediments in the four geographical areas of study.

(b) Grain-size variation within the Holocene sediments from one area to another.

(c) Vertical variation in grain size within the Holocene sediments.

(d) Criteria for distinction between the present-day intertidal sediments and the Holocene sediments.

(e) Modes of transportation and deposition of the Holocene sediments in the various environments and sub-environments of deposition.

It was noted, however, that deductions about environments of deposition should be based on a combination of several approaches, e.g. facies, palaeocurrent, basin

geometry and grain-size analyses, rather than on one type of analysis on its own (Leeder 1982b, 40).

Several methods have been used to discriminate between and interpret depositional environments on the basis of grain-size distribution, such as plotting skewness against sorting (Friedman 1961), comparing the coarsest fraction with the median-size fraction (Passega 1964), analysing cumulative curve shape (Visher 1969) and comparing mean, standard deviation, skewness and kurtosis variables and variables related to the tails of the distribution curves (Abu el-ella & Coleman 1985). Also, since grain-size distribution is dependent partly on the effect of the transporting fluid on the sediment grains, it provides a basis for interpreting the hydraulic conditions during transportation and deposition of the sediments (cf. Middleton 1976; Sagoe & Visher 1977; Brown 1985). In relation to this, Lambiase (1980) pointed out that in the present Avon River estuary (Nova Scotia) the hydraulic environment certainly does control sediment distribution, and grain-size distribution reflects this control. Other relevant studies of grain-size distribution are those of Quaternary sediments around Lake Gardsjon, SW Sweden (Melkerud 1983), of variations in floodplain deposits of the River Severn, England (Brown 1985), and of recent estuarine environments in the Tigris-Euphrates delta, Arabian Gulf (Darmoian & Lindqvist 1988).

7.2 Methods of study

In the present study, grain-size analysis was carried out by sieving and sedimentation methods. The method used depended on the grade of sediment being analysed. When sand grade was dominant, sieving was used. Sediment composed of silt

and clay was analysed by the pipette method.

The samples studied were analysed by standard techniques, modified from those described by Carver (1971) and Folk (1974), and were as follows:

1) Bulk samples were examined by the naked eye and binocular microscope to determine their lithology and grain-size, after which about 40g of each sample from fine sediments (silt and clay) and about 60g from each sample from the coarser sediments (sand) were obtained by mixing and quartering after drying at room temperature.

2) 30ml of 6% hydrogen peroxide (H_2O_2) was added to samples that were rich in organic matter, and the samples then left overnight . About 20ml of distilled water was added to the resultant suspension, which was then heated on a sand bath for about ten minutes to remove excess hydrogen peroxide, and finally washed with distilled water and left to dry.

3) The dry samples were weighed. They were then suspended in a 0.01M solution of Calgon (Sodium hexametaphosphate, $Na_4P_2O_7.10H_2O$) and left overnight.

4) Distilled water was added, and the suspension was stirred for about 30 minutes, to produce complete dispersion.

5) Using a wash bottle, the dispersed samples were washed on a 62 μm sieve over a long funnel. The silt and clay passing through the sieve were collected in a one litre graduated cylinder.

6) The sand fraction was dried, prior to being analysed by the sieving method.

7) The sieving of the sand fraction was carried out according to the method

described by Folk (1974, 33-34).

8) The grain-size distribution of the clay + silt fraction (< 62 μm) in suspension was calculated according to Stokes's Law, using the pipette method.

7.3 Grain-size parameters

The grain-size terminology used here is that proposed by Folk (1974). The measures used most commonly in calculating graphic statistical grain-size parameters are given by the following formulae (after Folk & Ward 1957; Folk 1974). The terminology used is that of Folk (1974).

1) Median (Md)

The grain-size corresponding to the 50% point on the cumulative curve is the median.

2) Graphic mean (Mz)

The graphic mean is the standard graphic measure for determining overall grain size. It takes into account the total grain-distribution curves, the tails of which are considered especially significant in sedimentary processes. The graphic mean is given by the formula:

$$Mz = \frac{\phi 16 + \phi 50 + \phi 84}{3}$$

Folk & Ward (1957) suggested the following scale for graphic mean size, in ϕ units based on the Wentworth (1922) size scale:

Mz -1ϕ to 0ϕ very coarse sand 0ϕ to 1ϕ coarse sand

1ϕ	to	2ϕ	medium sand	2ϕ	to	3ϕ	fine sand
3ϕ	to	4ϕ	very fine sand	4ϕ	to	5ϕ	coarse silt
5ϕ	to	6ϕ	medium silt	6ϕ	to	7ϕ	fine silt
7ϕ	to	8ϕ	very fine silt		> 8ϕ	clay	

3) Inclusive graphic standard deviation (σ_I)

This measure of sorting is given by the formula:

$$\sigma I = \frac{(\phi 84 - \phi 16)}{4} + \frac{(\phi 95 - \phi 5)}{6.6}$$

This includes about 90% of the distribution and is the best overall measure of sorting. The following verbal classification scale for sorting was suggested by Folk (1974):

σ_I				
		<	0.35ϕ	very well sorted
	0.35ϕ	to	0.50ϕ	well sorted
	0.50ϕ	to	0.71ϕ	moderately well sorted
	0.71ϕ	to	1.00ϕ	moderately sorted
	1.00ϕ	to	2.00ϕ	poorly sorted
	2.00ϕ	to	4.00ϕ	very poorly sorted
		>	4.00ϕ	extremely poorly sorted

4) Inclusive graphic skewness (Sk_I)

This parameter is used to describe the symmetry of the grain-size distribution.

$$Sk_I = \frac{(\phi 16 + \phi 84 - 2\phi 50)}{2(\phi 84 - \phi 16)} + \frac{(\phi 5 + \phi 95 - 2\phi 50)}{2(\phi 95 - \phi 5)}$$

This formula incorporates 90% of the distribution and it determines the skewness of the tails and the central portion of the cumulative curve. When the curve is symmetrical, $Sk_I = 0.0$. If the value is positive, it indicates an excess of fine sediment and if negative it indicates an excess of coarse material. The following verbal limits of skewness were suggested by Folk (1974):

Sk_I		
	+1.00 to +0.30	strongly fine skewed
	+0.30 to +0.10	fine skewed
	+0.10 to -0.10	near symmetrical
	-0.10 to -0.30	coarse skewed
	-0.30 to -1.00	strongly coarse skewed

5) Graphic kurtosis (K_G)

This is the parameter used to measure the ratio between the sorting in the extremes of the grain-size distribution curve and the sorting in the central portion of the curve.

$$K_G = \frac{\phi 95 - \phi 5}{2.44\ (\phi 75 - \phi 25)}$$

The descriptive terms of the graphic kurtosis suggested by Folk (1974) are as

follows:

K_G		<	0.67	very platykurtic
	0.67	to	0.90	platykurtic
	0.90	to	1.11	mesokurtic
	1.11	to	1.50	leptokurtic
	1.50	to	3.00	very leptokurtic
		>	3.00	extremely leptokurtic

When the tails of the curve are better sorted than the central portion, the curve is platykurtic and when the central portion is better sorted than the tails the curve is peaked or leptokurtic.

7.4 Textural characteristics of the sediments

7.4.1 Sediments of the Dalbeattie area

Grain-size analysis was carried out for 44 samples of Holocene raised coastal sediments. The samples are representative of the vertical and lateral sedimentary distribution at nine sites (D2 to D10, Fig. 3.1) and also representative of the various sedimentary facies and sub-facies of the Dalbeattie area described and discussed in Chapter 5.3.2 above (see also Table 5.1). In addition, 12 selected surface samples from the present-day intertidal zone were analysed.

Percentage weights of sand, silt and clay grades were calculated (Table 7.1A & 7.1B), and the results plotted on a triangular diagram (Fig. 7.1B ; after Lindholm 1987, 156, modified from Folk 1974, 27-29). The diagram shows that the Holocene raised coastal sediments in the Dalbeattie area are composed of silt (18 samples), mud (18 samples), fine sandy silt (5 samples), sandy mud (3 samples) and silty sand (1 sample). The percentage of clay in the present-day intertidal sediments is much

lower; the analysed samples comprised fine sandy silt (7 samples) and coarse silty sand (5 samples).

7.4.2 Sediments of the Kirkcudbright area

Grain-size analysis was carried out for 16 samples of Holocene raised coastal sediments. The samples are representative of the vertical and lateral sedimentary distribution at four sites (Fig. 3.2) and are also representative of the various sedimentary facies of the Kirkcudbright area described and discussed in Chapter 5.3.2 above (see also Table 5.1). In addition, eight surface samples from the present-day intertidal zone of the Dee estuary were analysed.

Percentage weights of sand, silt and clay grades were calculated (Tables 7.2A & 7.2B), and the results plotted on a triangular diagram (Fig. 7.1C). From the diagram, it is concluded that the Holocene sediments comprise a variety of size grades; silt (8 samples), sandy silt (4 samples), silty sand (3 samples) and mud (1 sample). The present-day intertidal sediments do not differ greatly in grain-size composition from that of the Holocene sediments; the analysed present-day samples comprised silt (3 samples), sandy silt (2 samples) and silty sand (3 samples).

7.4.3 Sediments of the New Abbey area

Grain-size analysis was carried out for 15 samples of Holocene raised coastal sediments. The samples are representative of the vertical sedimentary distribution at two sites (N5 and N6, Fig. 3.3) and also representative of the various sedimentary facies of the New Abbey area described and discussed in Chapter 5.3.2 above (see also Table 5.1). In addition, four surface samples from the present-day intertidal sediments at the mouth of New Abbey Pow were analysed.

Percentage weights of sand, silt and clay grades were calculated (Table 7.3A & 7.3B) and the results plotted on a triangular diagram (Fig. 7.1D). The diagram shows that the Holocene raised coastal sediments in the New Abbey area are composed of silt (5 samples), sandy silt (5 samples), sand (2 samples), mud (2 samples) and silty sand (1 sample). Except that they contain no mud, the present-day intertidal sediments do not differ greatly in grain-size composition from that of the Holocene sediments; the analysed present-day samples comprised sandy silt (3 samples) and silty sand (1 sample).

7.4.4 Sediments of the Lochar Gulf area

Grain-size analysis was carried out for 35 samples of Holocene sediments from eight sites with the area of the former Lochar Gulf. The samples are representative of part of the vertical sedimentary distribution at these sites (Fig. 3.4). However, since the area of the former Lochar Gulf is very much larger than each of the other three areas, the eight sites probably are not truly representative of the sediments within the gulf as a whole.

Percentage weights of sand, silt and clay grades were calculated (Table 7.4), and the results plotted on a triangular diagram (Fig. 7.1E). The diagram shows that, at the sites sampled within the former gulf, the Holocene sediments consist mainly of silty sand (28 samples), there being minor amounts of silt (2 samples), sandy silt (2 samples), muddy sand (2 samples), and clayey sand (1 sample).

7.5 Graphical presentation of grain-size data

7.5.1 Histograms

Using the Wentworth (1922) scale, representative histograms were drawn

from the grain-size data obtained from both the Holocene raised coastal sediments and the present-day intertidal sediments of the Dalbeattie, Kirkcudbright, New Abbey and Lochar Gulf areas (Figs. 7.2 to 7.11)

The histograms show that most of the Holocene sediments of the Dalbeattie area are bimodal or polymodal in nature. The dominant modal class is coarse silt, there being secondary modes in the fine silt and clay grades (Figs. 7.2 to 7.4). The present-day intertidal sediments in the same area are largely unimodal in nature, the modal class being fine sand (Fig. 7.5).

The Holocene raised coastal sediments of the Kirkcudbright and New Abbey areas are bimodal or polymodal in the upper part of the vertical sections or profiles that were studied. The dominant size class (modal class) is coarse silt. In the lower part of the same sections or profiles, the sediments are unimodal in nature, the dominant size grade being fine sand (Figs.7.6 & 7.7 and 7.9). The present-day intertidal sediments of the Kirkcudbright and New Abbey areas are mostly unimodal in nature, the dominant size grades being fine sand and coarse silt (Figs. 7.8 and 7.10).

Most of the Holocene sediments within the former Lochar Gulf are unimodal in nature, fine sand being the dominant size grade (Fig.7.11).

7.5.2 Analysis of cumulative curves

Several authors have suggested that the shape of a cumulative curve is a function of the relative proportions of the distribution of the grain populations (Tanner 1959 &1964; Spencer 1963; Visher 1969). Also, the idea has been advanced that each grain population is related to a specific sediment-transport mechanism (Fuller 1961; Moss 1962, 1963 & 1972; Spencer 1963; Visher 1969; Middleton 1976; Sagoe & Visher 1977). Cumulative curve shape has also been attributed to the

grain-size distribution of the source material (Shea 1974). As mentioned in Chapter 7.1 above, the relation between the characteristics of a cumulative curve and the hydraulic conditions of transportation and deposition of sediment were discussed by Lambiase (1977 & 1980).

Cumulative curves were constructed for all the samples of Holocene raised coastal sediments and present-day intertidal sediments that were analysed. Selected curves are shown in Figures 7.12 to 7.20. On the basis of comparison of the shapes of these cumulative curves with those of previous studies (Visher 1969; Middelton 1977; Sagoe & Visher 1977; Darmoian & Lindqvist 1988) the following conclusions may be drawn:

1) The majority of the samples from the Holocene raised coastal sediments in the Dalbeattie area and the upper part of the sections in the Kirkcudbright and New Abbey areas are similar to those for sediments of tidal-flat areas described in previous studies. They reflect the occurrence of large suspension populations that include mainly the sizes finer than very fine sand.

2) The Holocene sediments of the lower part of the sections studied in the Kirkcudbright and New Abbey areas are represented by cumulative curves similar to those for beach sediments in previous studies, the majority of the grain-size populations being fine sand and very fine sand.

3) The majority of the samples from the former Lochar Gulf are similar to beach sediments, the grain-size population being in the medium to fine sand and very fine sand grades.

4) The present-day intertidal sediments of the Dalbeattie, Kirkcudbright

and New Abbey areas, mainly of fine sand grade, have cumulative curves similar to those of beach sediments (Visher1969).

7.6 Statistical grain-size parameters in relation to Holocene sedimentary facies

The statistical parameters, median, mean, standard deviation, skewness and kurtosis, were calculated for the results of the grain-size analysis, using the equations given by Folk & Ward (1957; see also Chapter 7.3 above). The calculated parameters and their means and ranges are presented in Tables 7.5 to 7.8.

The relationships between each of the four main parameters (Mz, σ_I, Sk_I and K_G) and the Holocene sedimentary facies present in each of the four geographical areas studied were examined by plotting the values of these parameters against depth below ground level in appropriate sections through the Holocene sediments (Figs. 7.21 to 7.28). The diagrams suggested the following relationships:

7.6.1 Dalbeattie area

A complex of fine-grained sediments (facies A, Chapter 5.3.1.1 above) constitutes the total thickness of the Holocene sediments over most of the Dalbeattie area. In detail three sub-facies, arranged one above the other, are present. These are (see also Figs 7.21, 7.22, and 7.23):

Clayey silt sub-facies of facies A

Clayey coarse silt with fine sand sub-facies of facies A

Clayey silt sub-facies of facies A

Graphic mean size (Mz) changes from fine silt or clay grade in the lowermost sub-facies to medium to fine silt grade in the middle sub-facies, and back again to fine silt or clay grade in the uppermost sub-facies.

Graphic standard deviation (σ_I) changes slightly through the vertical sections, but sorting is always poor or extremely poor. It may be noted that the sorting is relatively better in the middle sub-facies than in the lowermost and uppermost sub-facies.

Graphic skewness (Sk_I) varies throughout the vertical sections plotted in Figures 7.21, 7.22 and 7.23 from strongly coarse skewed, through near symmetrical to strongly fine skewed. There does not appear to be a clear relationship between skewness and the sedimentary sub-facies represented by the plots.

Graphic kurtosis (K_G) varies throughout the vertical sections plotted, and there is no clear relationship between kurtosis and the sedimentary sub-facies represented by the plots.

7.6.2 Kirkcudbright area

The vertical section (K1) represented in the plots for the Kirkcudbright area (Fig. 7.24) includes three of the sedimentary facies described in Chapter 5.3.1 above. These are, in descending order:

Complex of estuarine fine-grained sediments (facies A)

Inter-laminated fine sand and silt (facies B)

Fine sand, rich in microfaunal remains (facies D)

Graphic mean size (Mz) changes from fine sand grade in facies D to coarse silt grade in facies B. The change in mean size between facies B and facies A is not clear.

Graphic standard deviation (σ_I)plots show that facies B is better sorted than facies A.

Graphic skewness (Sk_I) changes from near symmetrical in facies B to mainly fine skewed in facies A.

Graphic kurtosis (K_G) changes from mainly platykurtic and very platykurtic in facies B to leptokurtic and very leptokurtic in facies A.

7.6.3 New Abbey area

The two vertical sections (N5 and N6) represented in the plots for the New Abbey area (Figs. 7.25 and 7.26) include four of the sedimentary facies described in Chapter 5.3.1 above. In descending order, these facies are:

Complex of fine-grained sediments (facies A)

Inter-laminated fine sand and silt (facies B)

Clayey silt sub-facies of facies A

Coarse sand with pebbles (facies C)

Fine sand, rich in microfaunal remains (facies D)

In Figures 7.25 and 7.26, the four main grain-size parameters show a distinction between the four lowermost facies or sub-facies in the list above and the uppermost facies in the list above, as follows.

Graphic mean size (Mz) in the lower part of the sedimentary sequence is in the coarse silt and fine sand grade, whereas in the upper part it is in the fine to medium silt grade.

Graphic standard deviation (σ_I) distinguishes between the two major parts of

the sedimentary sequence, showing the lower part to be poorly sorted and the upper part to be very poorly sorted.

Graphic skewness (Sk_I) does not show a clear distinction between the major sedimentary facies. Most of the sediments are fine to very fine skewed.

Graphic kurtosis (K_G) plots show that much of the lower part of the sequence is very leptokurtic, whereas the sediments of the uppermost facies are leptokurtic to platykurtic.

7.6.4 Lochar Gulf area

As noted in Chapter 7.4.4 above, the sites within the former gulf from which samples were obtained probably are not truly representative of the sediments in the gulf as a whole. Plots of grain-size parameters against depths below ground level were made for analysed samples from sites at South Kirkblain (NY 0269 6956) and Horseholm (NY 0313 7062). It should be noted, in Figures 7.27 and 7.28, that the samples from the South Kirkblain section represent the sedimentary sequence from ground level down to c. 3m below ground level, whereas the samples from the Horseholm section represent the sedimentary sequence between c. 3m and 8m below ground level. No direct comparisons therefore can be made for the results obtained from these sections. Figures 7.27 and 7.28 show that:

Graphic mean size (Mz) is mainly in the fine to medium sand grade at Horseholm. Mz varies from medium silt to medium sand grade in the South Kirkblain section.

Graphic standard deviation (σ_I) determinations show that the Horseholm sediments are well to moderately well sorted. The sediments in the section at South

Kirkblain are poorly to very poorly sorted.

Graphic skewness (Sk_I) in the Horseholm sediments is mainly near symmetrical or fine skewed except at c. 6m below ground level, where it is coarse skewed. In the South Kirkblain section, Sk_I changes from coarse skewed to strongly fine skewed up the section.

Graphic kurtosis (K_G) in the Horseholm section is mainly mesokurtic to leptokurtic except at c. 6m below ground level, where it is very leptokurtic. In the South Kirkblain section, K_G changes from very leptokurtic to mesokurtic up the section.

7.6.5 Inferences

1) The statistical parameters assist in the distinction between the three sub-facies within facies A in the Dalbeattie area.

2) In the Kirkcudbright area, Mz distinguishes between facies D and the overlying facies B and A, but not between facies B and A. In contrast, σ_I, Sk_I, and K_G distinguish between facies B (below) and facies A (above).

3) In the New Abbey area, Mz, σ_I, Sk_I and K_G assist in the distinction between a unit comprising the four lower facies or sub-facies (facies D, facies C, sub-facies Aa and facies B in ascending order) and the uppermost sedimentary facies (facies A).

4) In the Lochar Gulf area, facies distinction is less clear than in the other three areas studied, but the parameters suggest that the sediments sampled in the Horseholm borehole belong to a different facies from the sediments sampled in the South Kirkblain section.

7.7 Inter-relationships of the statistical grain-size parameters

The inter-relationships between the four statistical grain-size parameters, Mz, σ_I, Sk_I, and K_G, for the Holocene sediments that were sampled and analysed were determined by constructing scatter diagrams for all six mutual relationships between the four parameters, (a) in relation to the four areas of study (Figs. 7.29 to 7.36), and (b) in relation to five of the sedimentary facies (Figs. 7.37 and 7.38).

7.7.1 Relationships within the four areas of study

1) Mean size (Mz) versus standard deviation (σ_I)

In all four areas there is a poor linear relationship between these parameters. The relevant regression equations and correlation coefficients are these:

$y = 2.672 - 4.533 - 2x$; $r = -0.01$, for the Holocene sediments, Dalbeattie area

$y = 1.889 + 0.143x$; $r = 0.03$, for the present-day sediments, Dalbeattie area

$y = 1.173 - 0.132x$; $r = -0.18$, for the Holocene sediments, Kirkcudbright area

$y = 0.298 - 0.015x$; $r = -0.0$, for the present-day sediments, Kirkcudbright area

$y = 1.537 + 7.301x$; $r = 0.12$, for the Holocene sediments, New Abbey area

$y = - 0.247 + 0.337x$; $r = 0.36$, for the present-day sediments, New Abbey area

$y = 0.854 + 0.199x$; $r = 0.04$, for the Holocene sediments, Lochar Gulf area.

The diagrams do not assist in distinction between the various facies present in the Holocene sediments in these areas.

2) Mean size (Mz) versus skewness (Sk_I)

In all four areas there is a poor linear relationship between these parameters. The relevant regression equations and correlation coefficicents are these:

$y = 1.173 - 0.132x$; $r = -0.18$, for the Holocene sediments, Dalbeattie area

$y = 0.298 - 0.006x$; $r = -0.01$, for the present-day sediments, Dalbeattie area

$y = 0.163 - 0.004x$; $r = 0.15$, for the Holocene sediments, Kirkcudbright area

$y = 0.665 + 0.155x$; $r = 0.22$, for the present-day sediments, Kirkcudbright area

$y = 0.324 + 0.013$; $r = 0.02$, for the Holocene sediments, New Abbey area

$y = - 0.545 + 0.135x$; $r = 0.10$ for the present-day sediments, New Abbey area

$y = 0.232 - 0.025x$; $r = -0.01$, for the Holocene sediments, Lochar Gulf area.

In general, the finer-grained sedimentary sub-facies (clayey silt, and clayey coarse silt with fine sand) are fine skewed, whilst the coarser-grained sedimentary facies (inter-laminated fine sand and silt, and fine sand) are coarser skewed.

3) Mean size (Mz) versus kurtosis (K_G)

In the Dalbeattie and Kirkcudbright areas there is a fairly good inverse relationship between these parameters, whereas in the New Abbey and Lochar Gulf areas the relationship between these parameters is very poor. The relevant regression equations and correlation coefficients are these:

$y = 2.41 - 0.213x$; $r = 0.25$, for the Holocene sediments, Dalbeattie area

$y = 4.64 - 0.636x$; $r = 0.48$, for the present-day sediments, Dalbeattie area

$y = 2.118 - 0.18x$; $r = -0.20$, for the Holocene sediments, Kirkcudbright area

$y = 1.733 + 0.049x$; $r = 0.01$, for the present-day sediments, Kirkcudbright area

$y = 1.511 - 0.048x$; $r = -0.02$, for the Holocene sediments, New Abbey area

$y = 0.384 + 0.163x$; $r = 0.30$, for the present-day sediments, New Abbey area

$y = 1.446 - 0.045x$; $r = -0.01$, for the Holocene sediments, Lochar Gulf area.

4) Standard deviation (σ_I) versus skewness (Sk_I).

In all four areas there is a poor linear relationships between these parameters. The relevant regression equations and correlation coefficients are these:

$y = 0.505 - 0.106x$; $r = -0.01$, for the Holocene sediments, Dalbeattie area

$y = 0.195 + 0.012x$; $r = 0.01$, for the present-day sediments, Dalbeattie area

$y = 0.234 + 0.07x$; $r = 0.03$, for the Holocene sediments, Kirkcudbright area

$y = -0.662 + 0.407x$; $r = 0.33$, for the present-day sediments, Kirkcudbright area

$y = 0.175 + 0.114x$; $r = 0.07$, for the Holocene sediments, New Abbey area

$y = 0.521 - 0.399x$; $r = -0.29$, for the present-day sediments, New Abbey area

$y = 0.009 + 0.081x$; $r = 0.10$, for the Holocene sediments, Lochar Gulf area.

5) Standard deviation (σ_I) versus kurtosis (K_G)

In the Dalbeattie, Kirkcudbright and New Abbey areas there is a poor linear relationship between these parameters. In contrast, there is a good positive relationship between these parameters in the Lochar Gulf area. Relevant regression equations and correlation coefficients are these:

$y = 0.553 + 0.169x$; $r = 0.05$, for the Holocene sediments, Dalbeattie area

$y = 3.193 - 0.563x$; $r = -0.26$, for the present-day sediments, Dalbeattie area

$y = -0.943 + 0.861x$; $r = 0.33$, for the Holocene sediments, Kirkcudbright area

$y = 3.202 - 0.669x$; $r = -0.44$, for the present-day sediments, Kirkcudbright area

$y = 2.465 - 0.626x$; $r = 0.15$, for the Holocene sediments, New Abbey area

$y = 0.852 + 0.198x$; $r = 0.14$, for the present-day sediments, New Abbey area

$y = 1.460 - 0.114x$; $r = -0.05$, for the Holocene sediments, Lochar Gulf area.

6) Skewness (Sk_I) versus kurtosis (K_G)

In all areas there is a very poor linear relationship between these two parameters. Relevant regression equations and correlation coefficients are these:

$y = 0.892 + 0.199x$; $r = 0.02$, for the Holocene sediments, Dalbeattie area

$y = 1.406 + 1.57x$; $r = 0.06$, for the present-day sediments, Dalbeattie area

$y = 1.169 - 0.272x$; $r = 0.00$, for the Holocene sediments, Kirkcudbright area

$y = 2.043 - 0.852x$; $r = -0.37$, for the present-day sediments, Kirkcudbright area

$y = 0.750 + 1.277x$; $r = 0.11$, for the Holocene sediments, New Abbey area

$y = 1.083 + 0.242x$; $r = 0.12$, for the present-day sediments, New Abbey area

$y = 1.394 - 0.835x$; $r = -0.17$, for the Holocene sediments, Lochar Gulf area.

As a general comment it may be said that, as shown by the regression equations and correlation coefficients, the scatter diagrams do not show good relationships between the various statistical grain-size parameters. This may be due to the fine-grained nature of the sediments, which are mainly of silt grade in the areas studied in the course of the research project. Other studies, e.g. those of Friedman (1967), which showed good relationships between the statistical grain-size parameters, were concerned with coarser-grained sediments, mainly of sand grade.

7.7.2 Relationships within facies

Figures 7.37 and 7.38 show the relationships between the statistical grain-size parameters, Mz, σ_I, Sk_I and K_G, for analysed samples of five of the Holocene sedimentary facies. The Figures show that the grain-size parameters differentiate between facies D and facies A (which are the two facies that occur most widely throughout the areas studied). The Figures also show that the plots for facies B

fall generally betweeen the clusters for facies D and facies A. Plots of Mz versus σ_I, Sk_I and K_G differentiate facies C from the other facies. The similarities between facies E and facies A are shown by the overlapping of their plots.

7.8 Grain-size image (CM diagram)

Passega (1957) proposed a combination, on a bi-logarithmic diagram, of two grain-size parameters, the coarest, one percentile, value (C) and the median value (M) given by the grain-size cumulative curve. He argued that the texture of a clastic sediment represented in this way is characteristic of the depositional agents that caused accumulation of the sediment. After analysis of many samples, he confirmed (Passega 1964) the usefulness of CM patterns as indicative of the relationship between sediment texture and the transporting mechanism that built up the deposit.

Passega & Byramjee (1969) extended the graphic method proposed by Passega (1957) and represented the textures of clastic deposits by 'grain-size images' that comprised CM, FM, LM and AM diagrams, F, L and A being the percentage by weight in a sample of the fractions finer than 125, 31 and 4 microns, respectively. The CM diagram has also used by other workers, e.g. Royse (1968), Vandenberghe (1975) and Brown (1985).

For practical purposes, Passega & Byramjee (1969) subdivided the CM diagram into nine classes, designated I to IX (Fig. 7.37). The distribution, within these nine classes, of the analysed samples of the Holocene raised coastal sediments from the four areas of study, is shown in Table 7.9 .

The majority of the analysed samples from the Dalbeattie, Kirkcudbright and New Abbey areas fall into classes VII and VIII. According to Passega & Byramjee (1969), samples within class VIII represent sediments transported by uniform

suspension, in a situation where the bottom currents have low turbulence but the turbulence nevertheless is sufficient to prevent the particles from forming a pelagic suspension. Class VII represents sediments transported, as a uniform suspension, by currents that are not in contact with the water-substrate interface. The sediments of class VII are mainly coarser grade than those of class VIII.

The analysed samples from the former Lochar Gulf are distributed mainly in classes III and VII and therefore represent sediments transported, as a uniform suspension, by currents not in contact with the water-substrate interface (VII) and sediments transported by graded suspension (III).

From the above inferences, in combination with the distribution of the samples of the Holocene sediments in the CM diagram of Figure 7.37, it may be concluded that the majority of the fine sediments in the sampled sections at Dalbeattie and in the upper part of the sampled sections at Kirkcudbright and New Abbey were transported by currents with uniform suspension. The sediments in the lower part of the sampled sections at Kirkcudbright and New Abbey were transported by currents not in contact with the water-substrate interface. The sampled sediments in the Lochar Gulf sections show variability, but generally they were transported by currents not in contact with the water-substrate interface, by uniform suspension in some cases and by graded suspension in others.

7.9 Conclusions from grain-size analyses

The grain-size analyses carried out on selected samples of the Holocene raised coastal sediments and present-day intertidal sediments from the four geographical areas of study lead, directly or indirectly, to the following conclusions:

1) Most of the samples from the Holocene raised coastal sediments in the

Dalbeattie, Kirkcudbright and New Abbey areas are of silt grade; fine sand and clay is present in minor amounts. The majority of the Lochar Gulf samples consist of sand grade sediments.

2) Generally, the percentages of fine silt and clay increase upwards in the Holocene sediments of the Dalbeattie area and in the upper facies of the Holocene sediments of the Kirkcudbright and New Abbey areas, whilst coarse silt and fine sand form the major part of the lower facies in the latter two areas.

3) The present-day intertidal sediments are generally coarser grained and sandier than the upper facies of the Holocene raised coastal sediments in the Dalbeattie, Kirkcudbright and New Abbey areas but they resemble the sediments of the lower facies (fine sand) in the same areas.

4) Representative histograms indicate that the majority of the Holocene raised coastal sediments are bimodal or polymodal in nature in the Dalbeattie area, and in the upper part of the succession in the Kirkcudbright and New Abbey areas, whilst most of the studied samples of the Lochar Gulf area and in the lower part of the successions in the Kirkcudbright and New Abbey areas are unimodal. The present-day intertidal sediments in the Dalbeattie, Kirkcudbright and New Abbey areas are mainly unimodal.

5) Cumulative curves show that the Holocene raised coastal sediments were deposited under a variety of environmental conditions. There are resemblances between the curves for sediments of the Dalbeattie area and the curves for the upper part of the sedimentary successions in the Kirkcudbright and New Abbey areas. These curves resemble those for estuarine sediments. Cumulative curves for the lower part of the Kirkcudbright and New Abbey successions resemble each other and those for beach sediments. Cumulative

curves for the Lochar Gulf are variable, depending on the nature of the sediments, but the majority of the analysed samples gave curves similar to those for beach sediments.

6) Variations in the values of the statistical grain-size parameters (Mz, σ_I, Sk_I and K_G) through vertical profiles of the Holocene raised coastal sediments in the various areas studied assist in distinction between some of the sedimentary facies present in these areas.

7) The majority of the fine-grained sediments in the areas studied are poorly to very poorly sorted, whereas the coarser-grained sediments are medium to poorly sorted.

8) Plots of the inter-relationships between the statistical grain-size parameters, Mz, σ_I, Sk_I and K_G, differentiate between facies A, B, C and D, and show the similarities between facies E and facies A.

9) The CM diagram shows that most of the Holocene raised coastal sediments in the Dalbeattie, Kirkcudbright and New Abbey areas were transported in uniform suspension conditions whereas the sandier sediments of the Lochar Gulf were mostly transported by either uniform suspension or graded suspension.

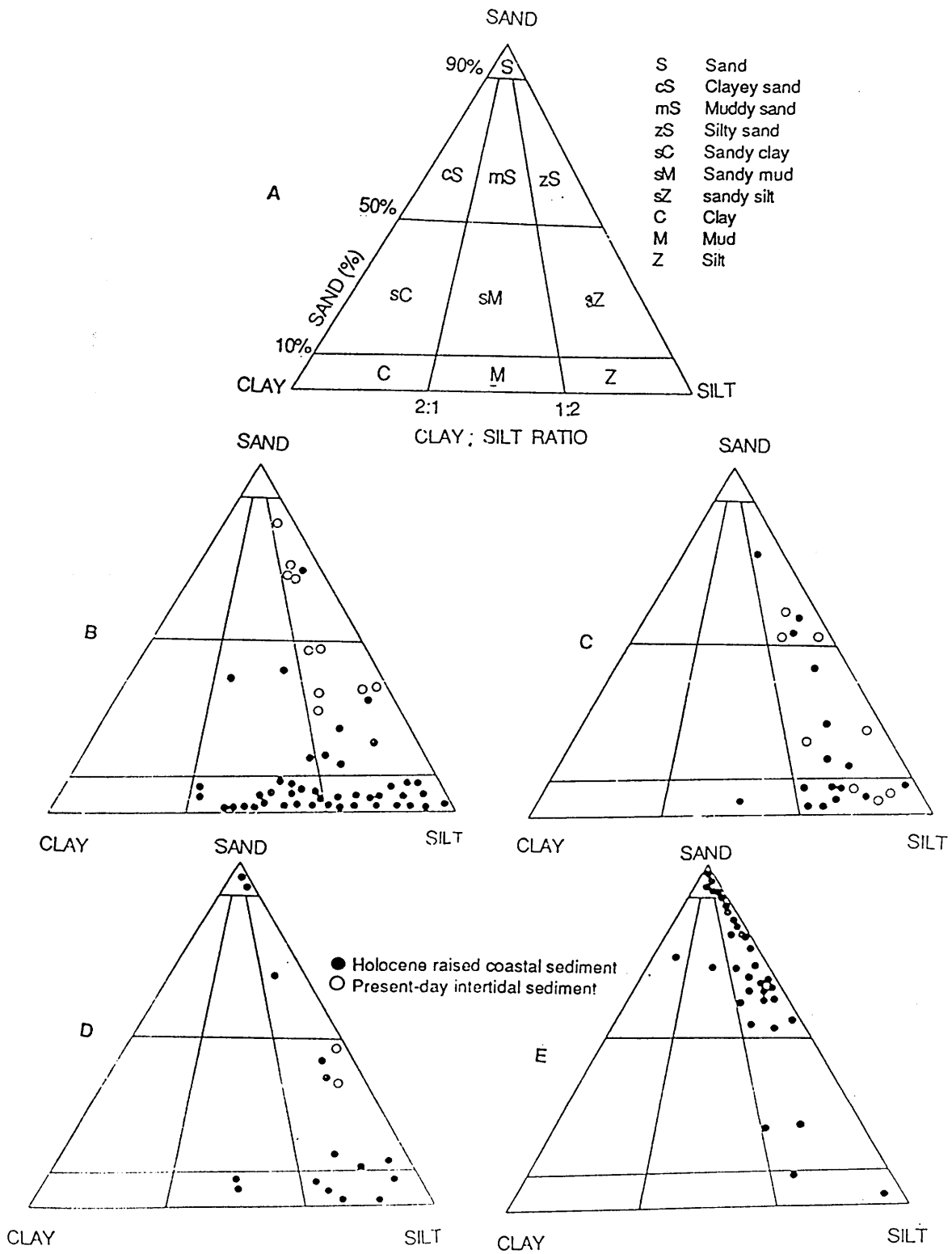

Figure 7.1 Percentage weights of sand, silt and clay grades, plotted on triangular diagrams; A, terminology, after Lindholm 1987, 156; B, samples from Dalbeattie area; C, samples from Kirkcudbright area; D, samples from New Abbey area; E, samples from Lochar Gulf area.

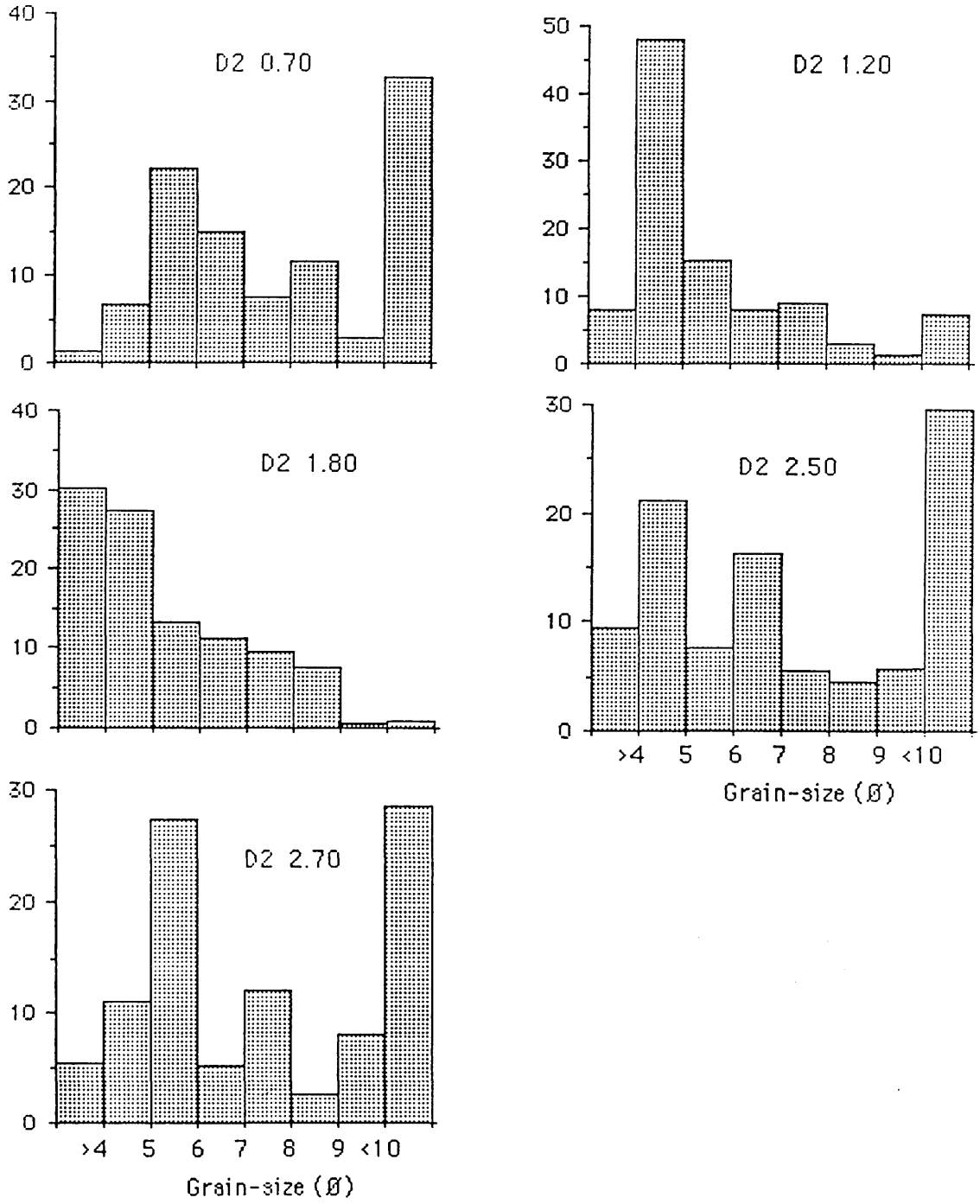

Figure 7.2 Histograms showing grain-size distribution in five samples from section D2, Holocene sediments, Dalbeattie area.
Vertical scale = weight percentage

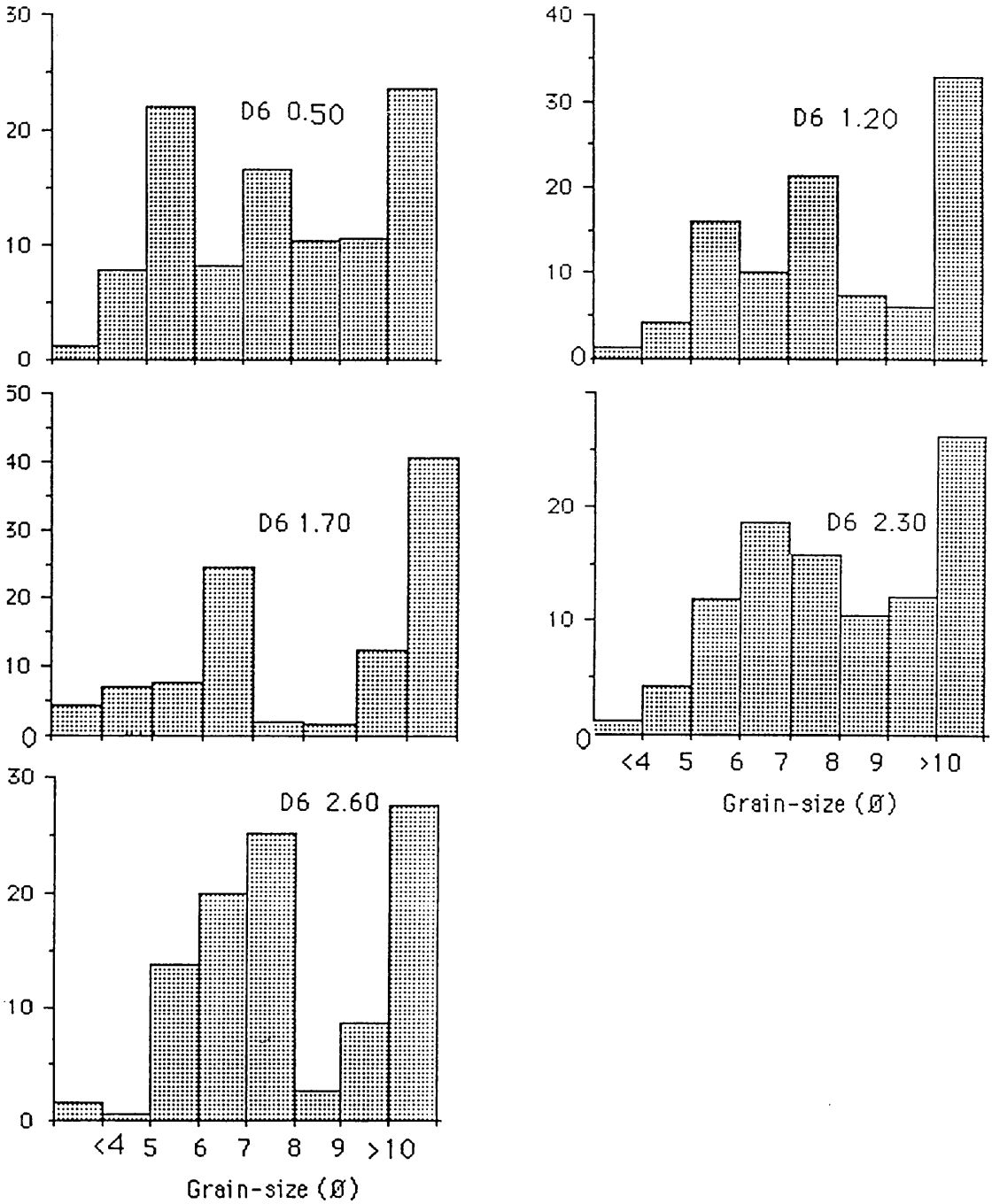

Figure 7.3 Histograms showing grain-size distribution in five samples from section D6, Holocene sediments, Dalbeattie area.
Vertical scale = weight percentage

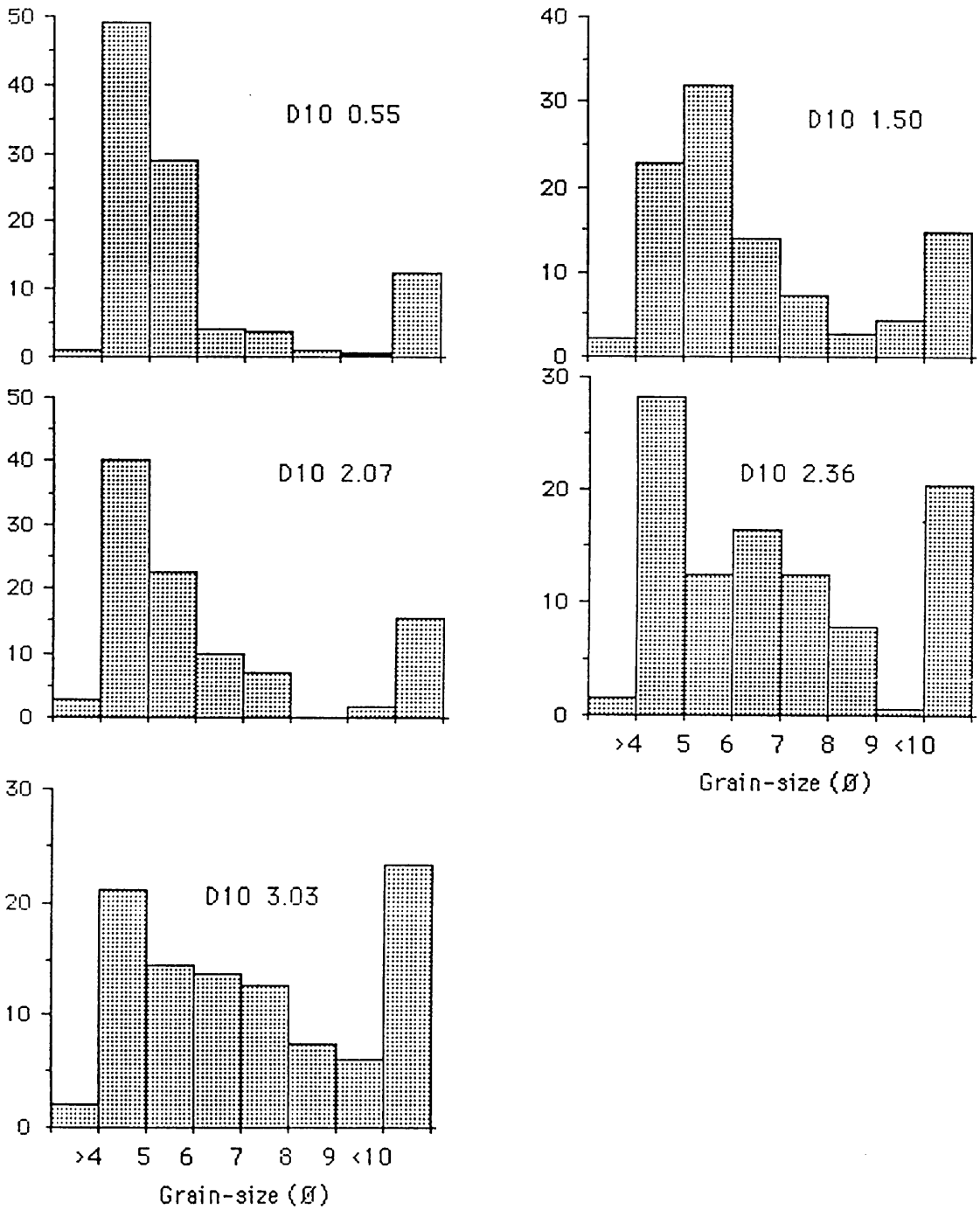

Figure 7.4 Histograms showing grain-size distribution in five samples from section D10, Holocene sediments, Dalbeattie area.
Vertical scale = weight percentage

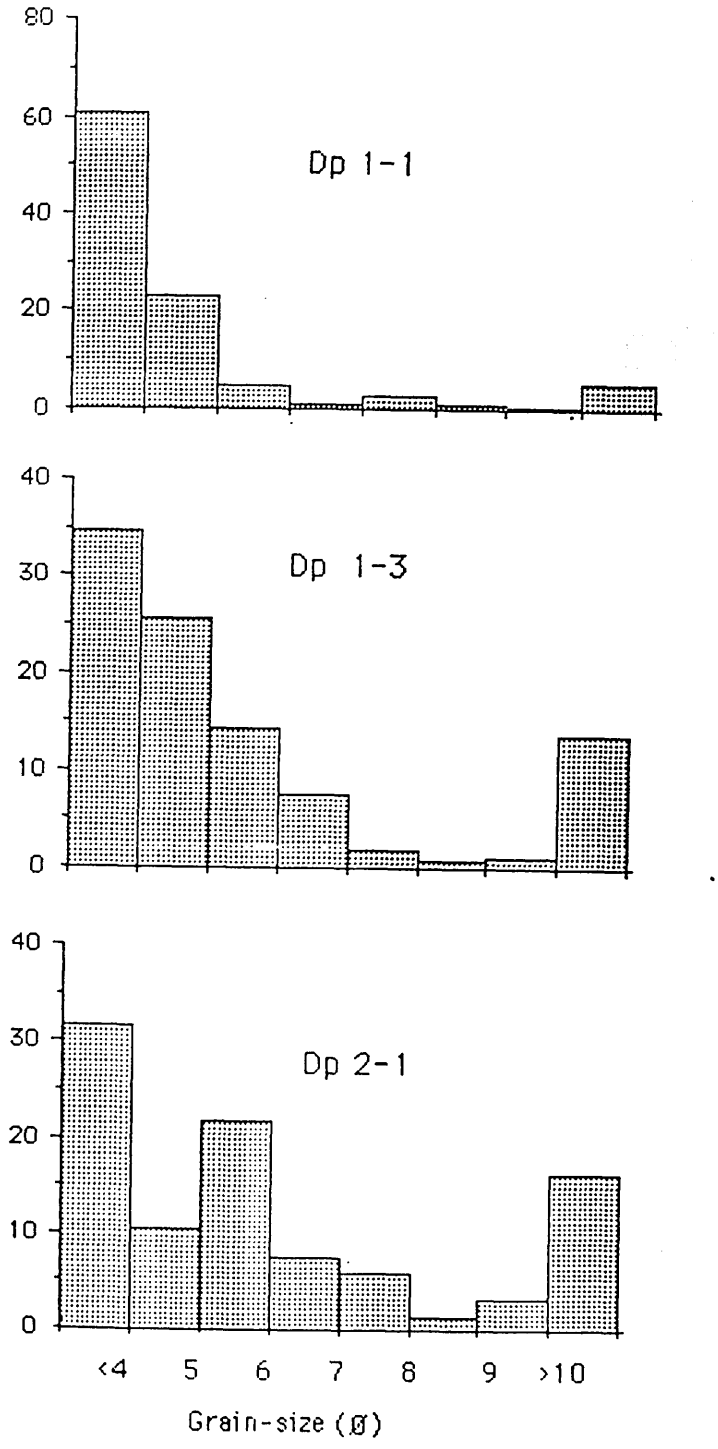

Figure 7.5 Representative histograms showing grain-size distribution in present-day intertidal sediments of the Dalbeattie area. Vertical scale = weight percentage.

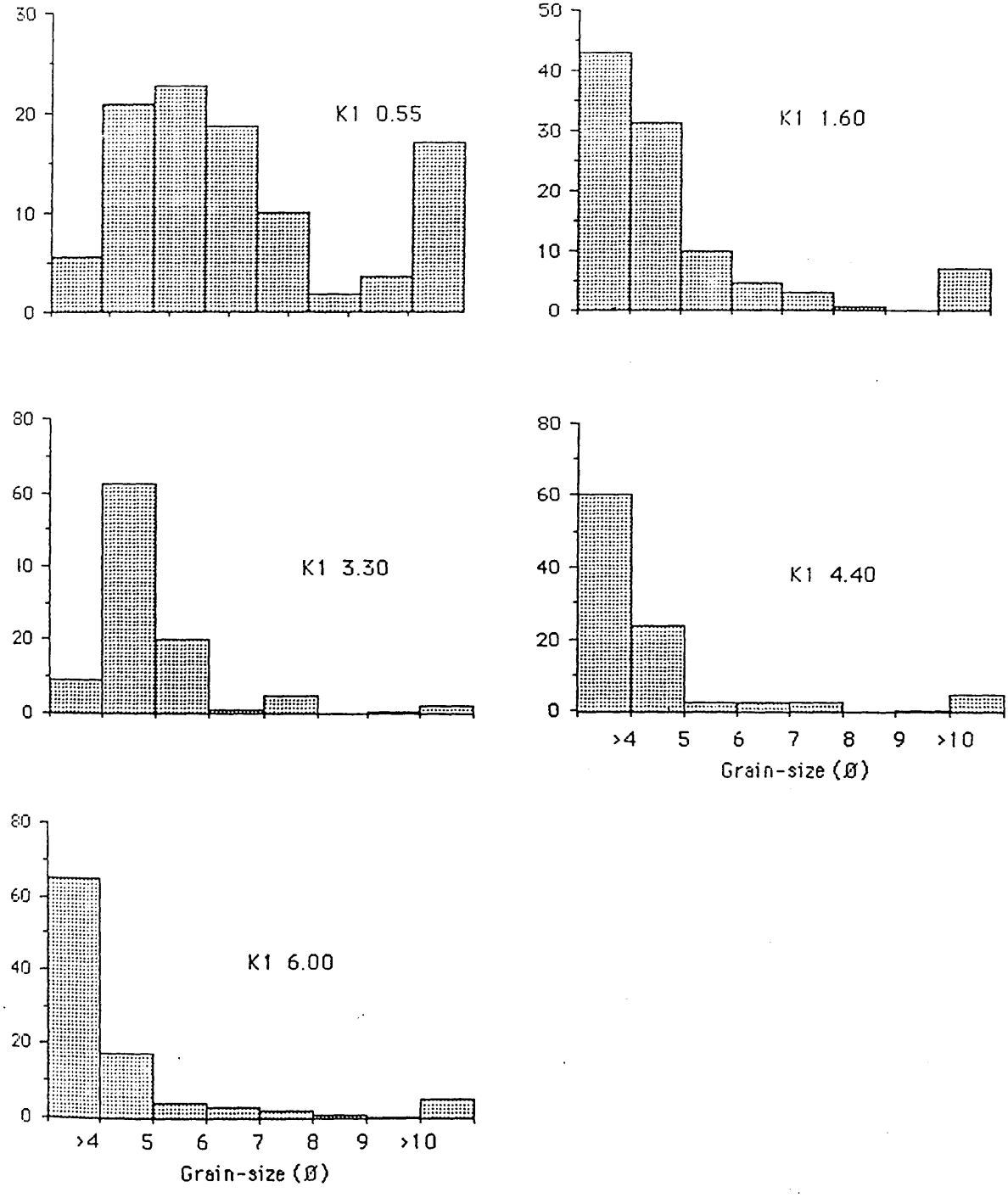

Figure 7.6 Histograms showing grain-size distribution in five samples from section K1, Holocene sediments, Kirkcudbright area. Vertical scale = weight percentage.

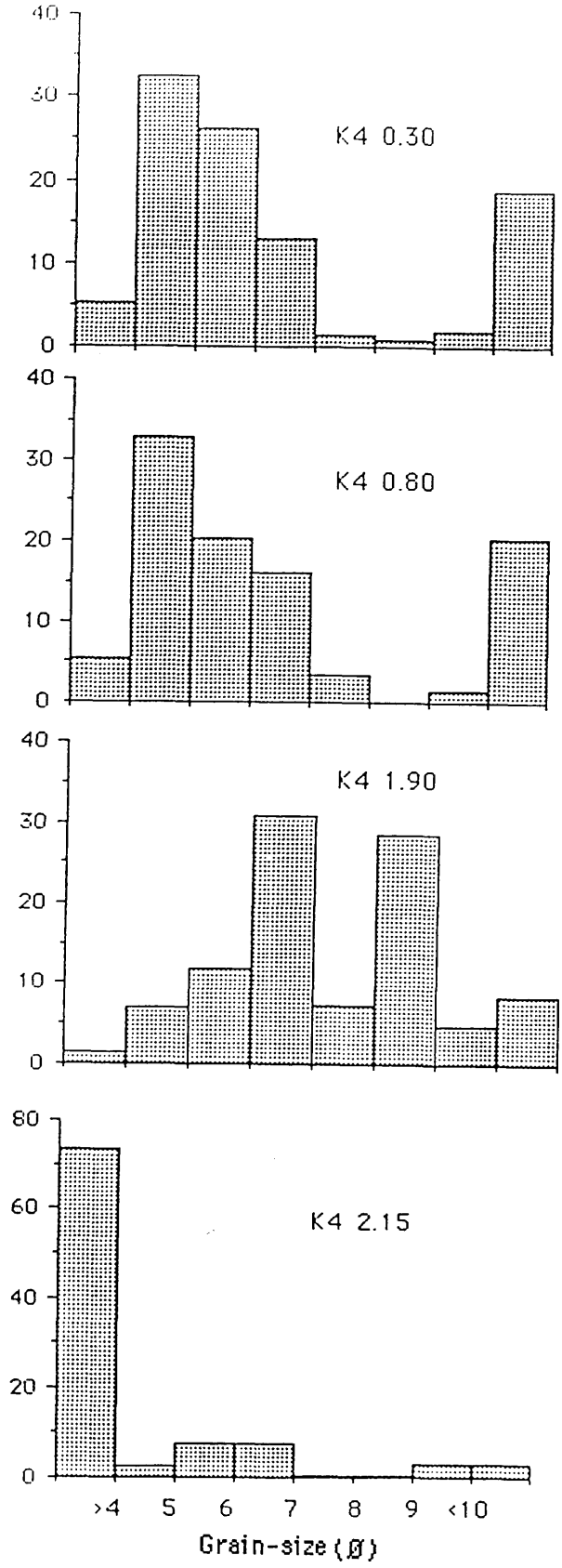

Figure 7.7 Histograms showing grain-size distribution in four samples from section K4, Holocene sediments, Kirkcudbright area. Vertical scale = weight percentage.

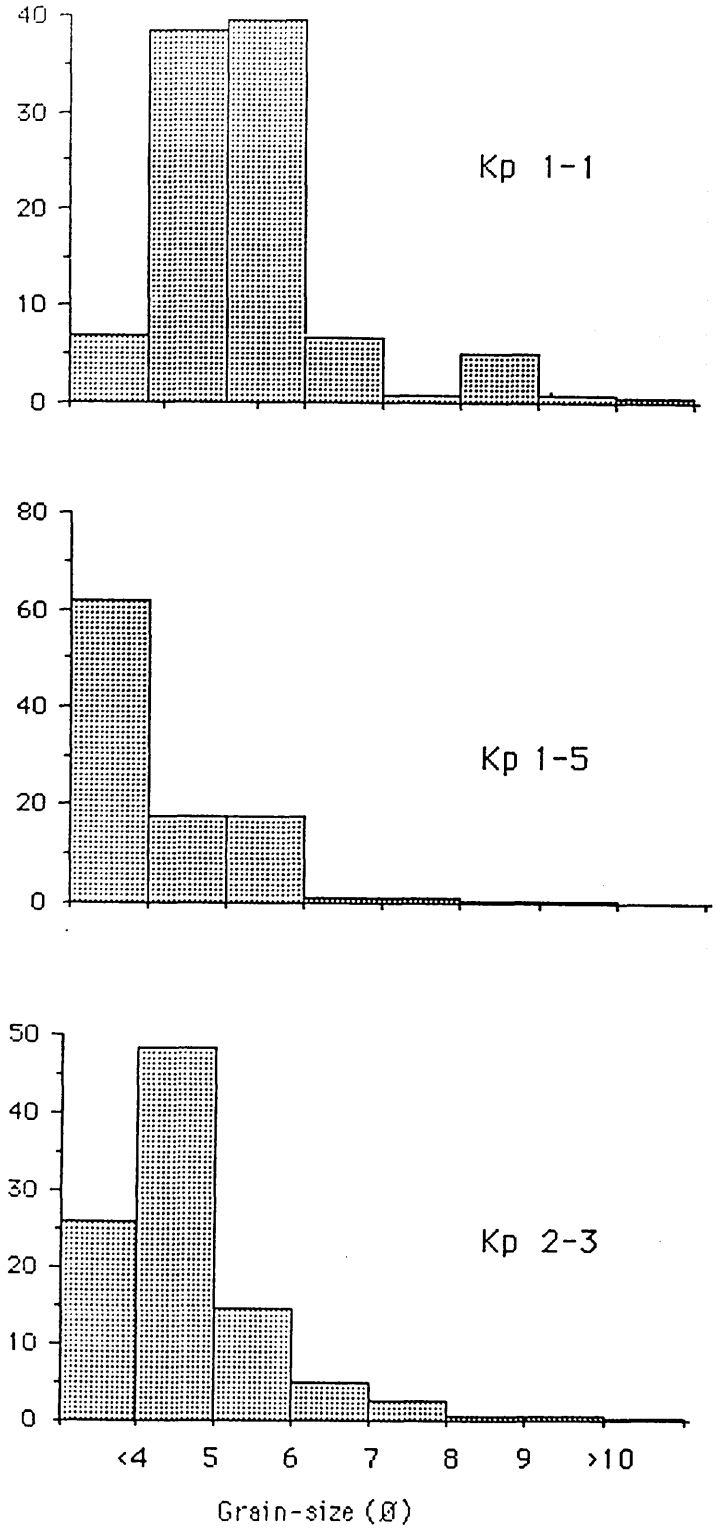

Figure 7.8 Representative histograms showing grain-size distribution in present-day intertidal sediments of the Kirkcudbright area. Vertical scale = weight percentage.

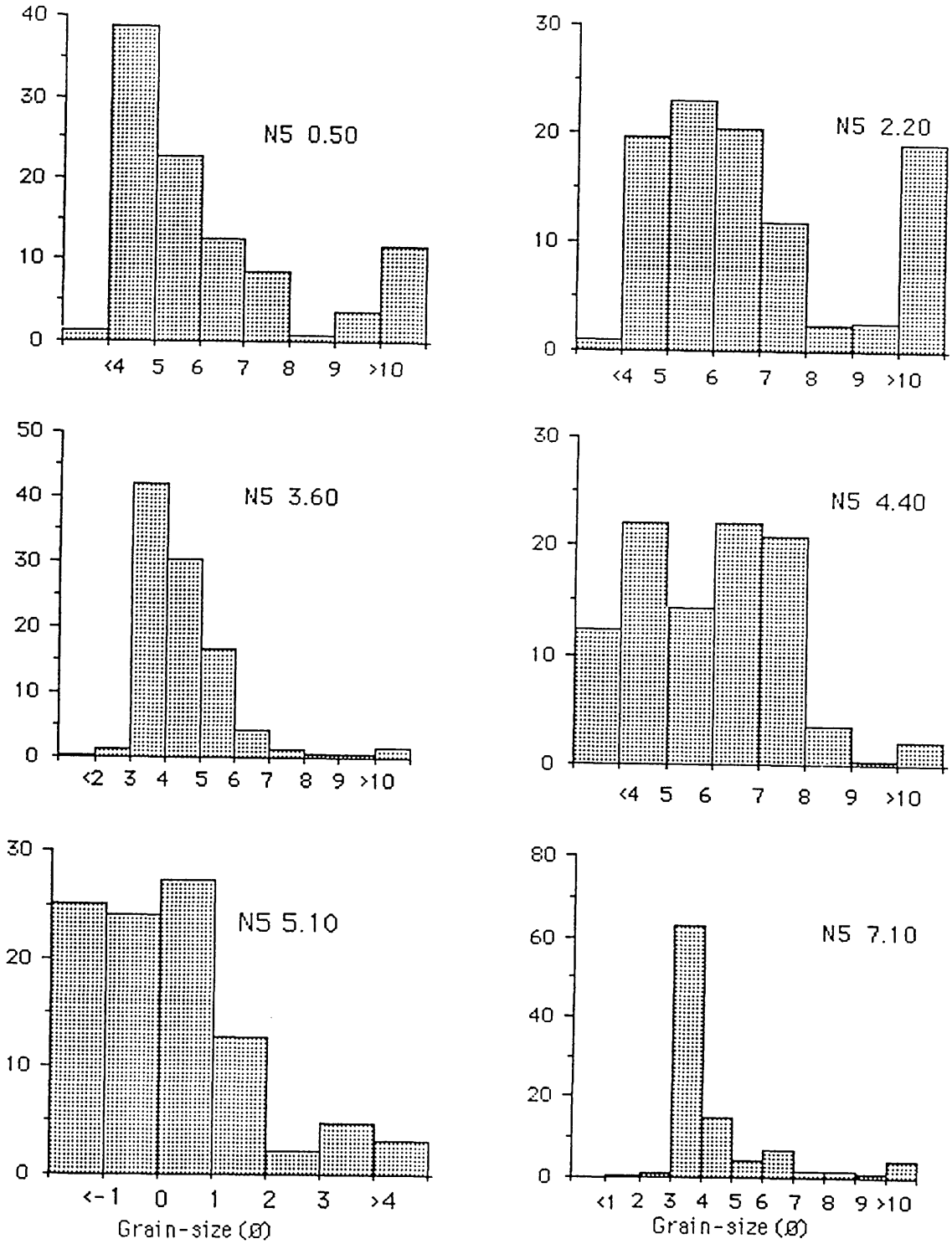

Figure 7.9 Histograms showing grain-size distribution in six samples from section N5, Holocene sediments, New Abbey area.
Vertical scale = weight percentage.

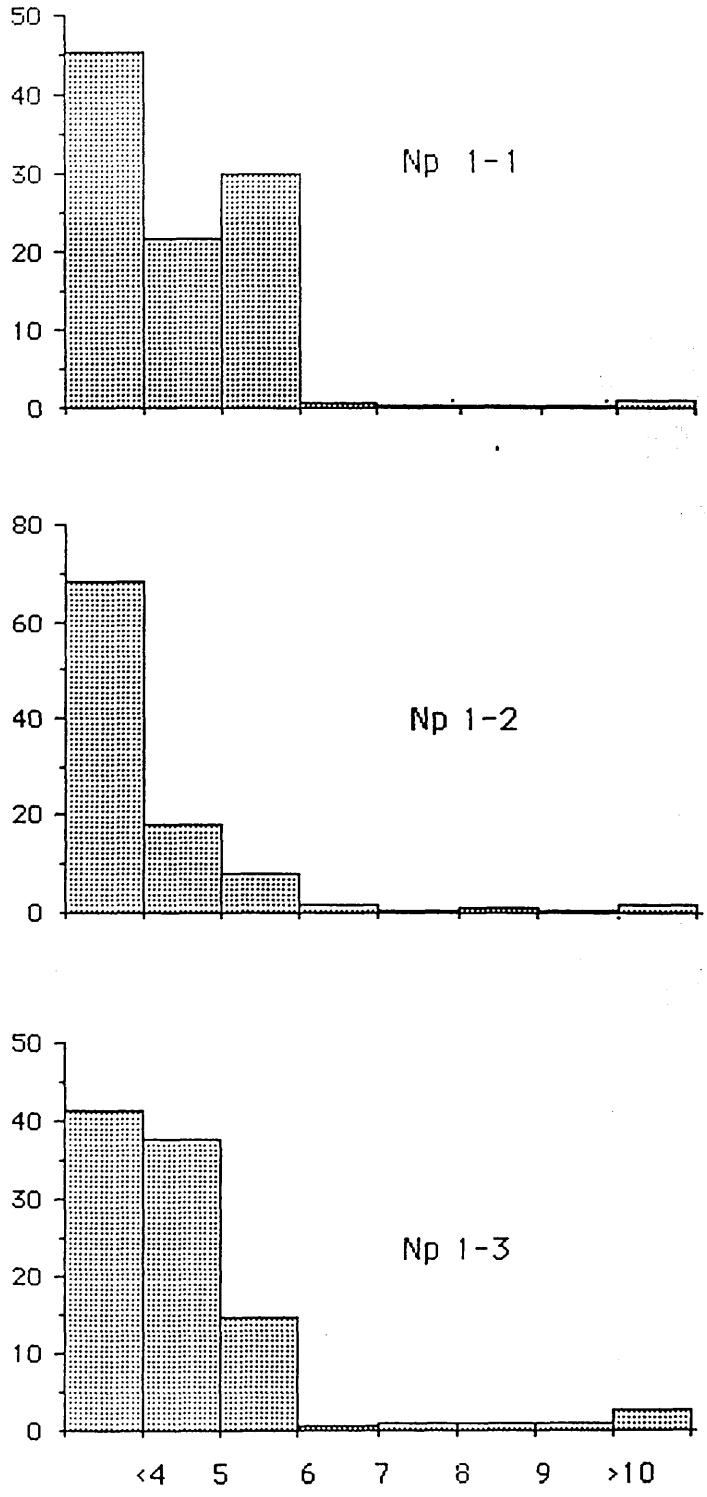

Figure 7.10 Representative histograms showing grain-size distribution in present-day intertidal sediments of the New Abbey area. Vertical scale = weight percentage.

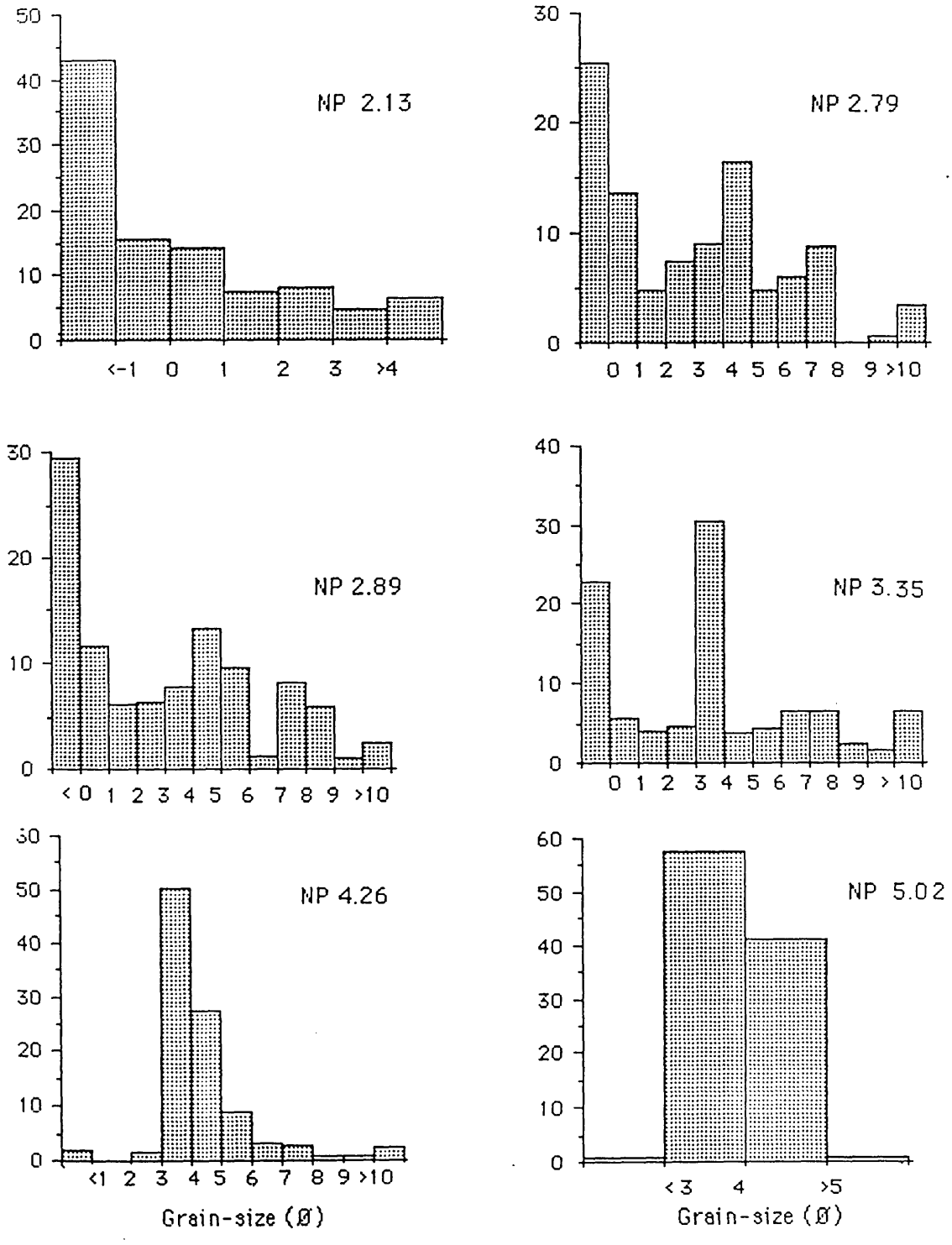

Figure 7.11 Histograms showing grain-size distribution in six samples from Northpark section, Holocene sediments, Lochar Gulf area. Vertical scale = weight percentage.

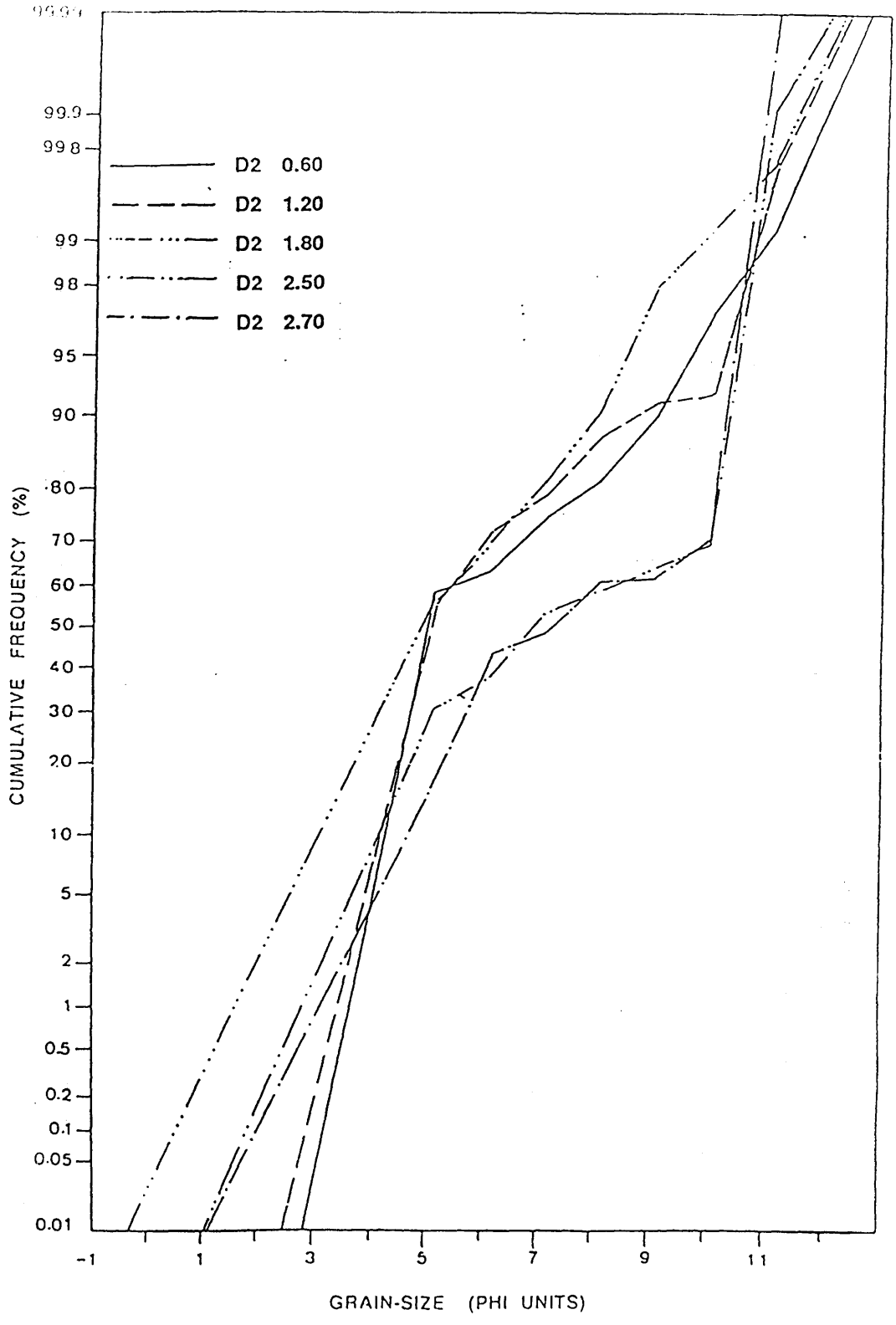

Figure 7.12 Cumulative curves showing grain-size distribution in five samples from section D2, Holocene sediments, Dalbeattie area.

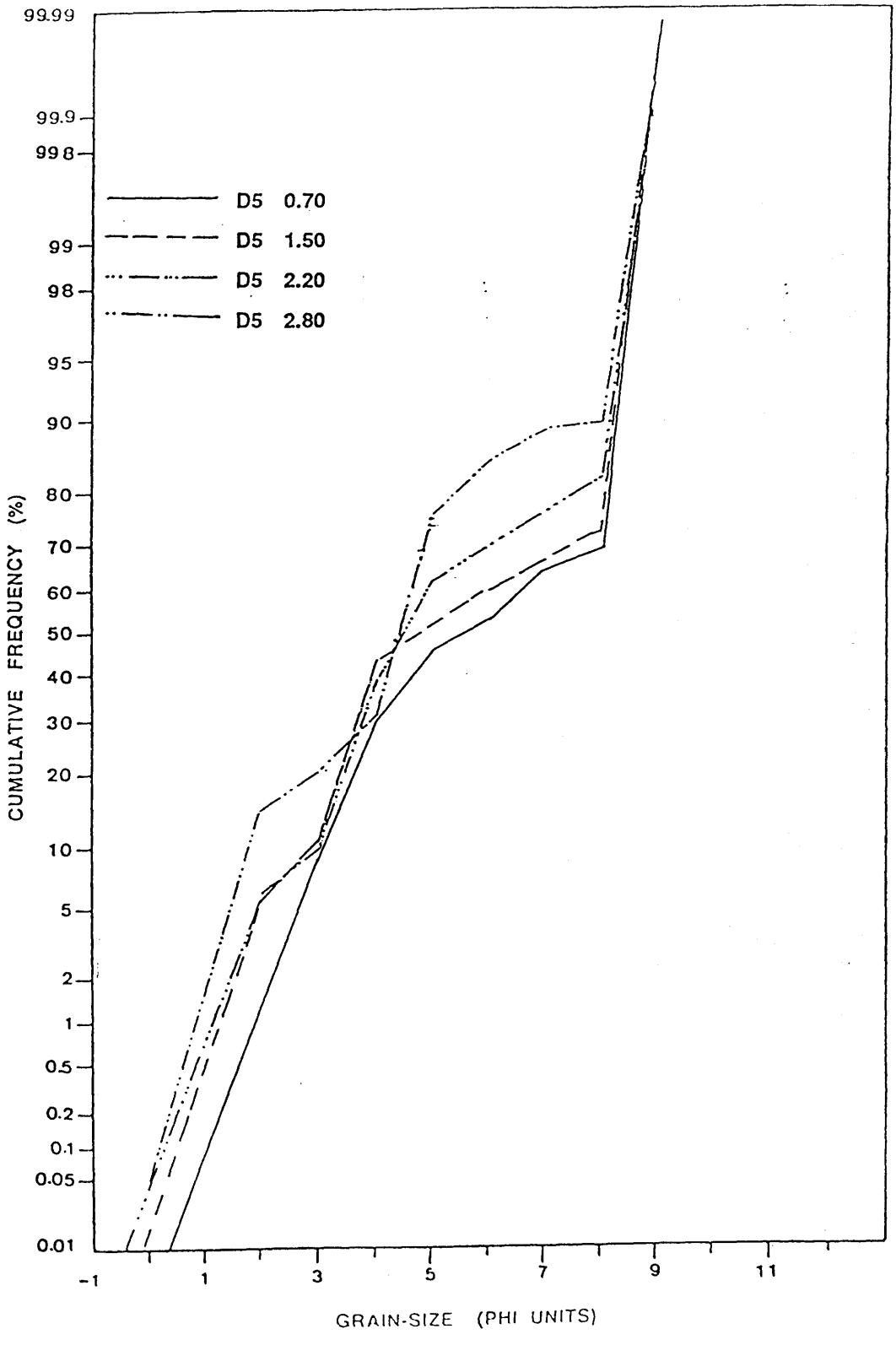

Figure 7.13 Cumulative curves showing grain-size distribution in four samples from section D5, Holocene sediments, Dalbeattie area.

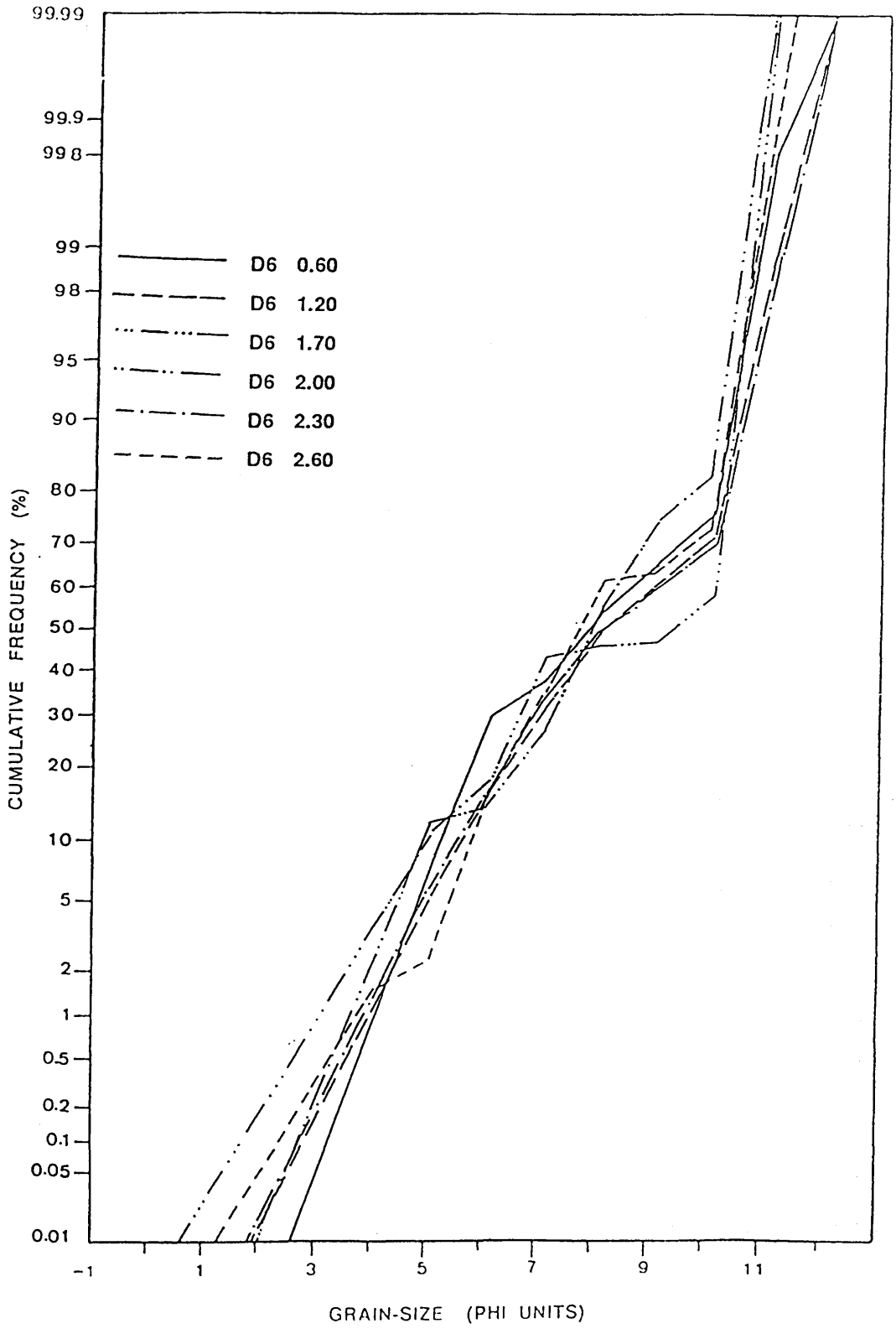

Figure 7.14 Cumulative curves showing grain-size distribution in six samples from section D6, Holocene sediments, Dalbeattie area.

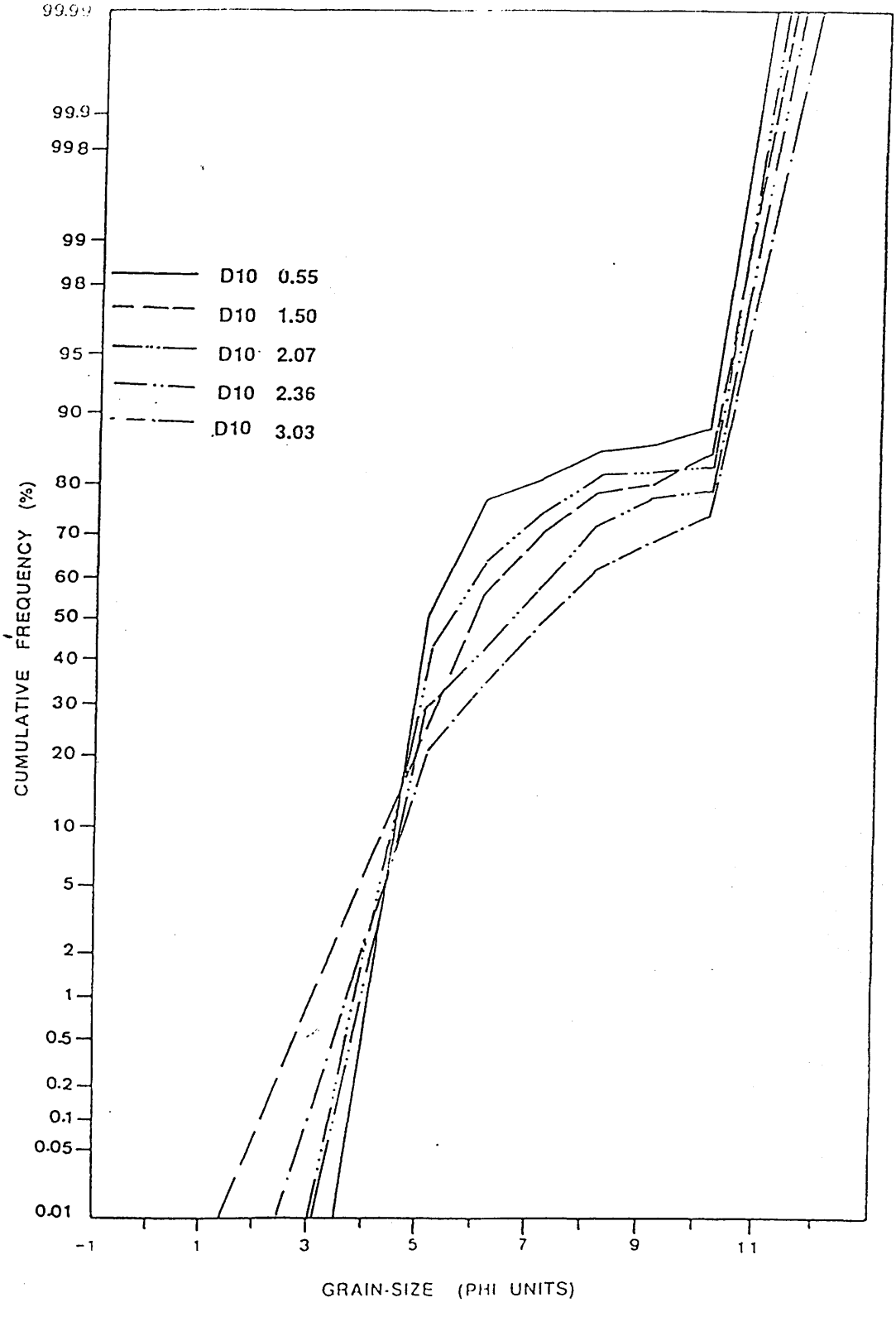

Figure 7.15 Cumulative curves showing grain-size distribution in five samples from section D10, Holocene sediments, Dalbeattie area.

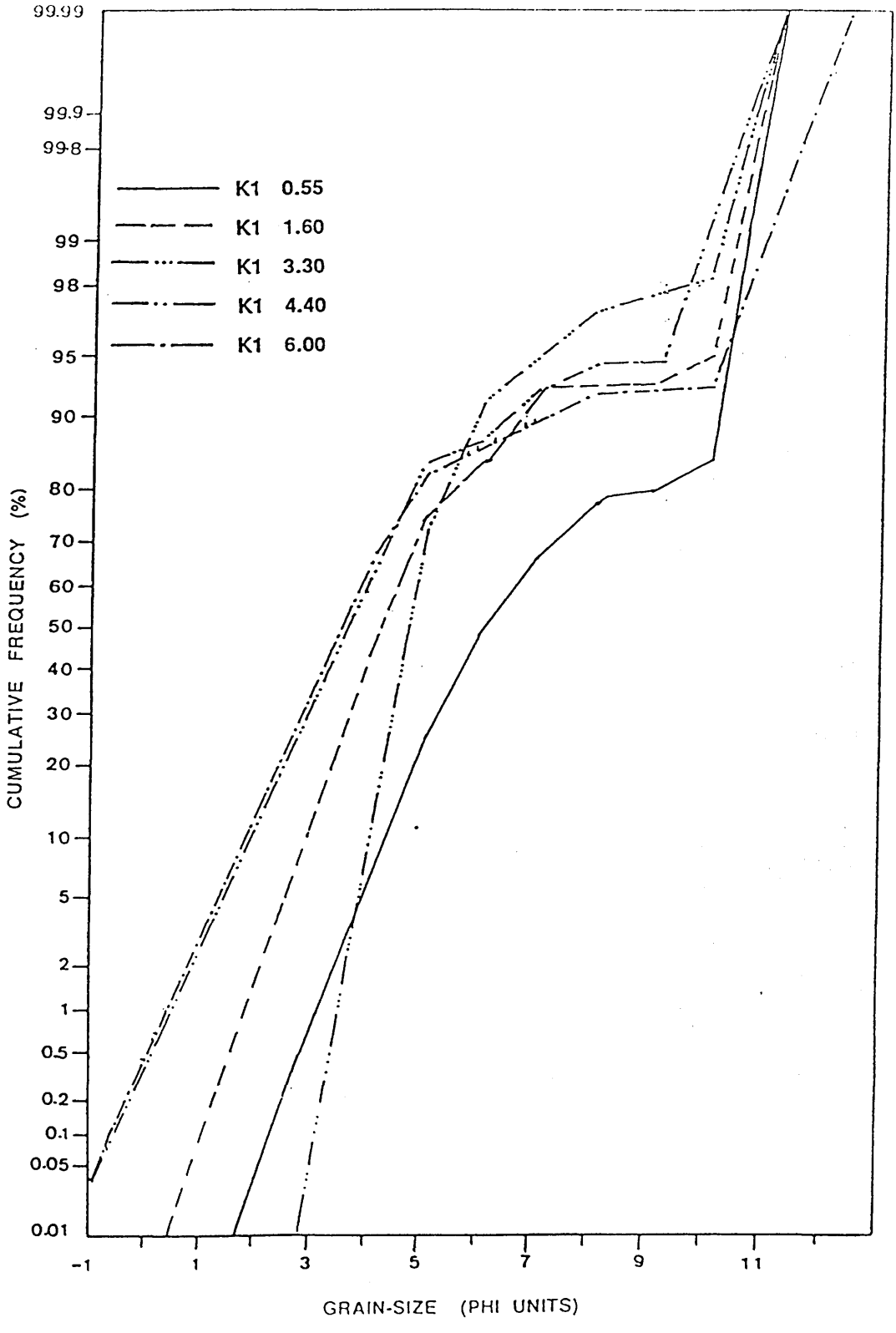

Figure 7.16 Cumulative curves showing grain-size distribution in five samples from section K1, Holocene sediments, Kirkcudbright area.

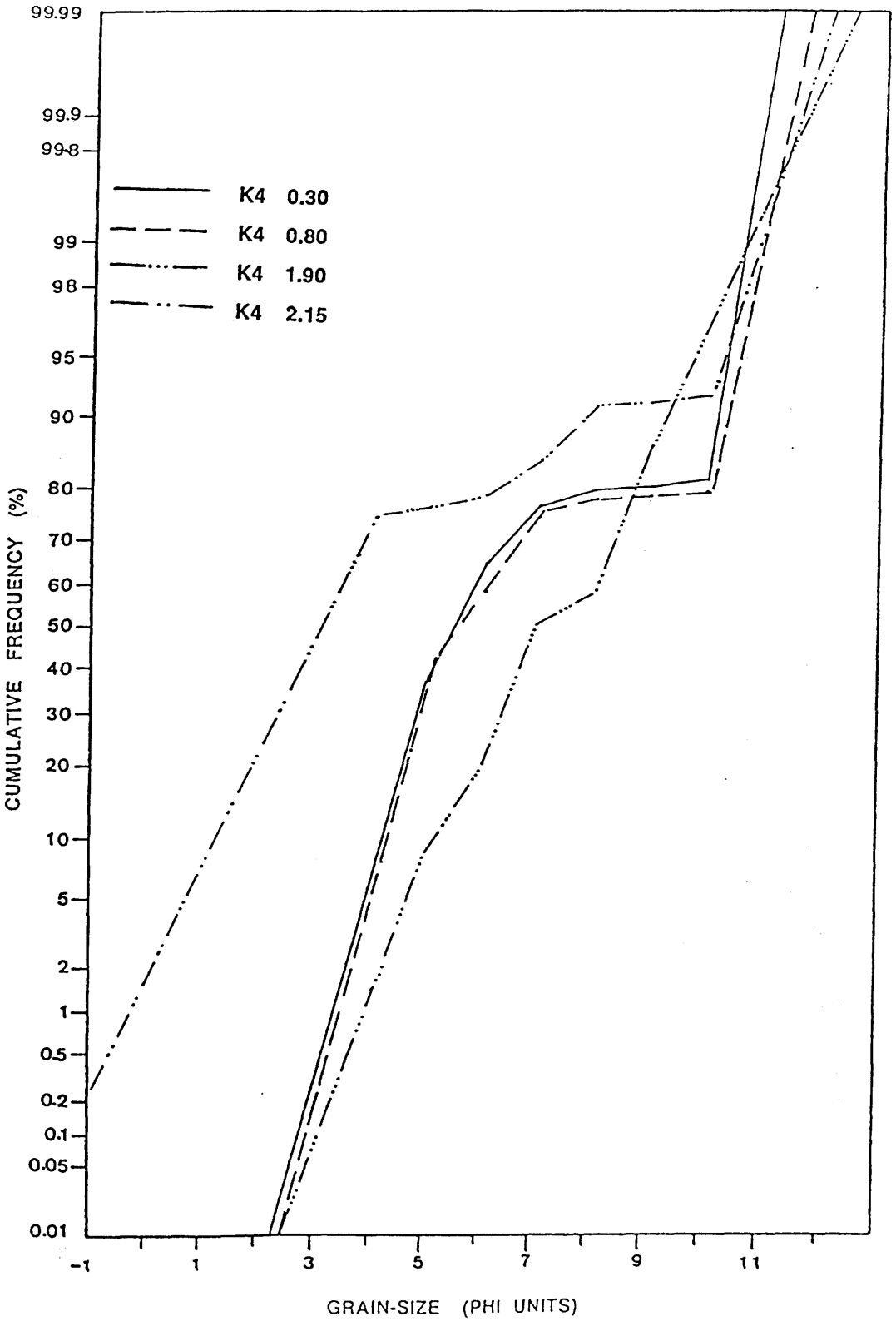

Figure 7.17 Cumulative curves showing grain-size distribution in four samples from section K4, Holocene sediments, Kirkcudbright area.

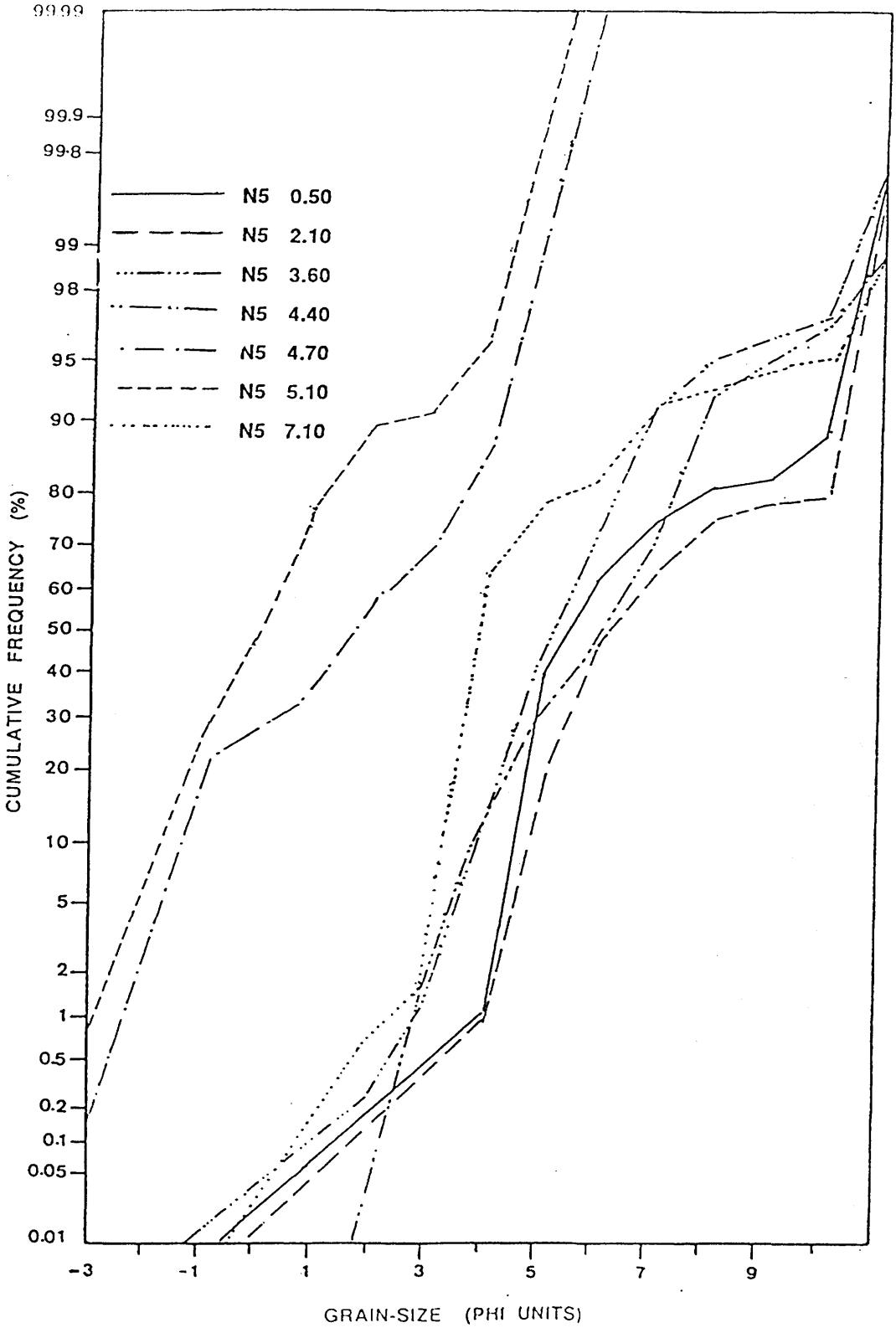

Figure 7.18 Cumulative curves showing grain-size distribution in seven samples from section N5, Holocene sediments, New Abbey area.

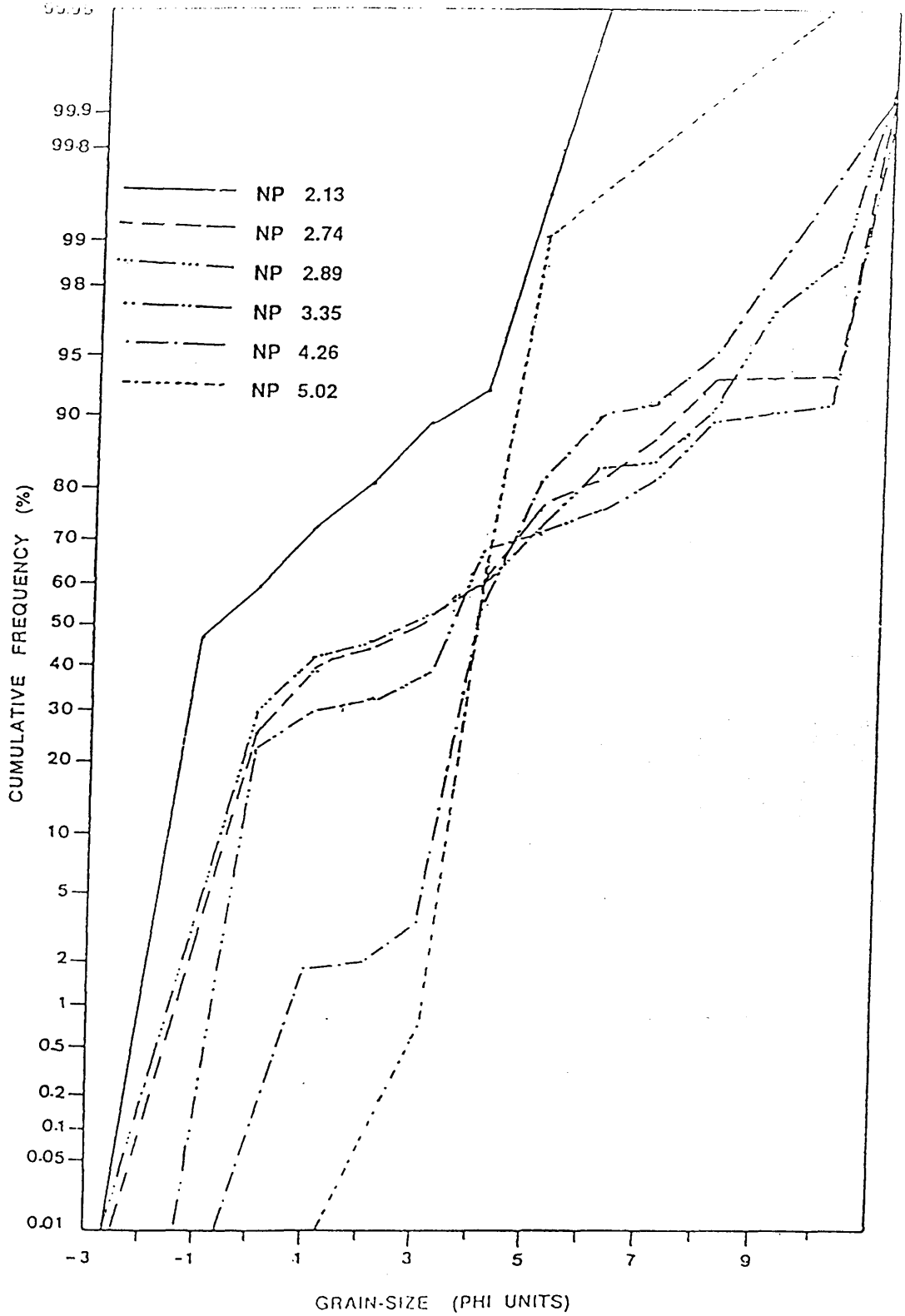

Figure 7.19 Cumulative curves showing grain-size distribution in six samples from Northpark section, Holocene sediments, Lochar Gulf area.

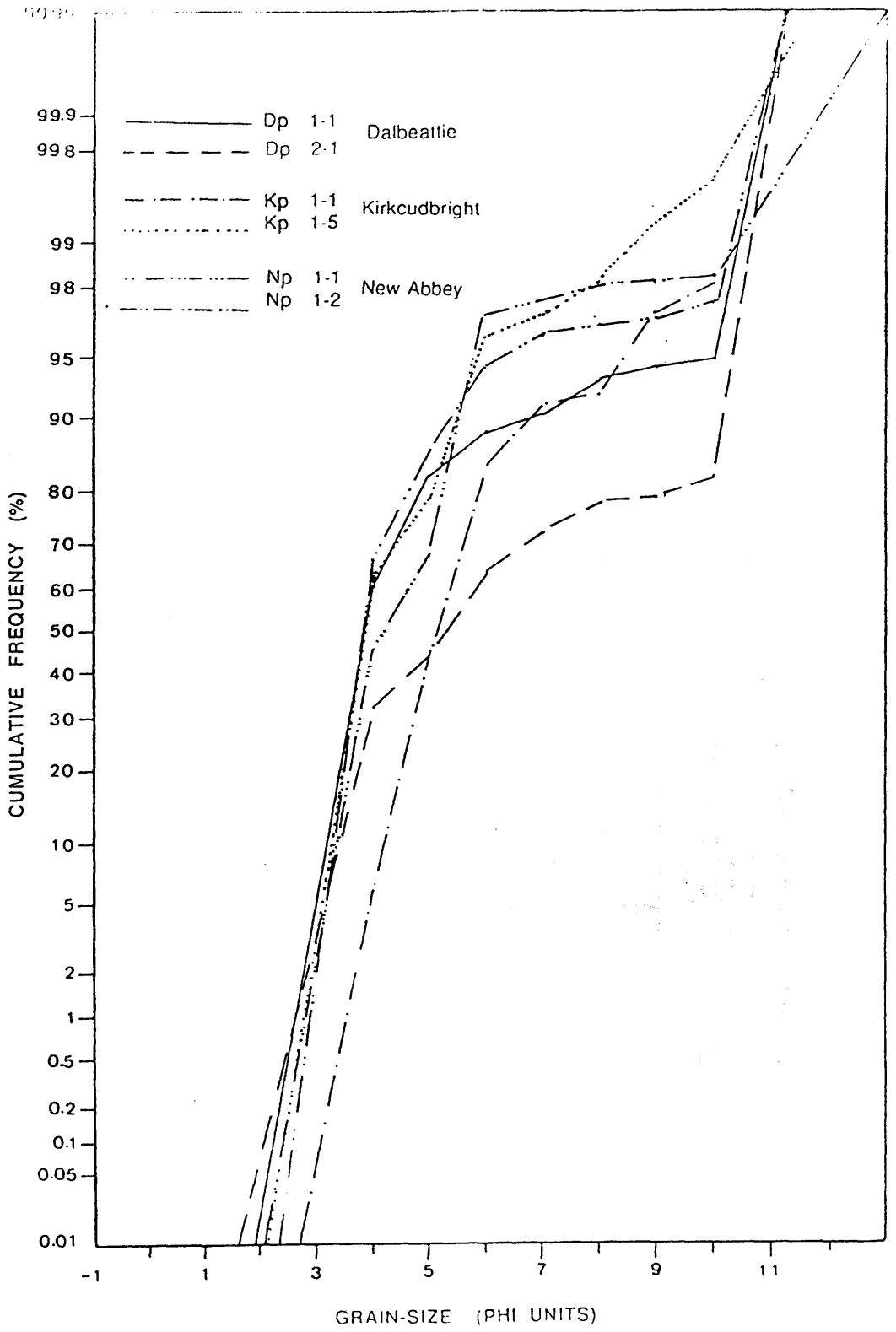

Figure 7.20 Representative cumulative curves showing grain-size distribution in present-day intertidal sediments of the Dalbeattie, Kirkcudbright and New Abbey areas.

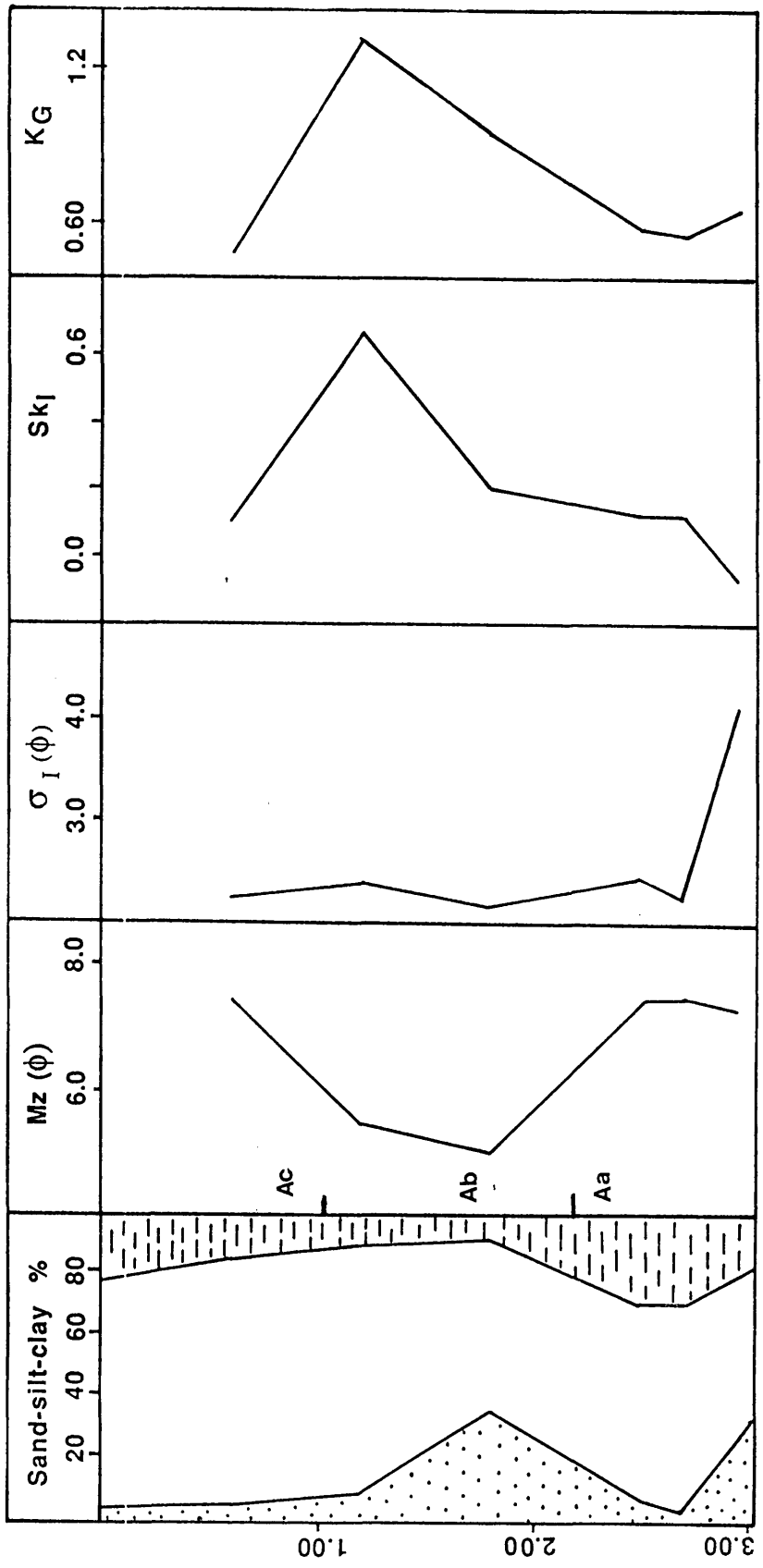

Figure 7.21 Sand-silt-clay percentages and grain-size parameters, Mz, σ_I, Sk_I, K_G, in relation to depth (in metres) below ground surface, section D2, Dalbeattie area. Ac, Ab, Aa = Sub-facies

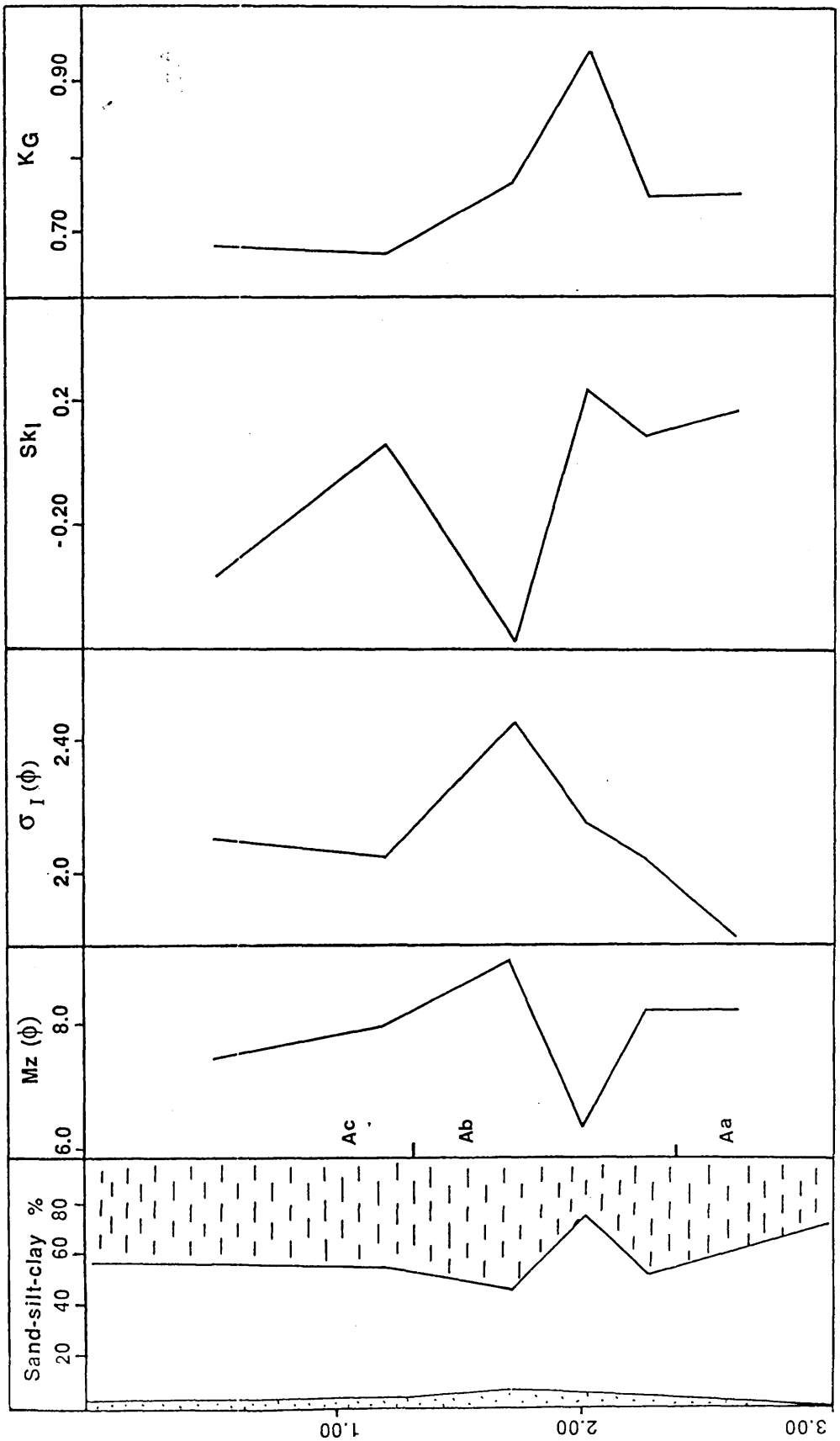

Figure 7.22 Sand-silt-clay percentages and grain-size parameters, Mz, σ_I, Sk_I, K_G, in relation to depth (in metres) below ground surface, section D6, Dalbeattie area. Ac, Ab, Aa = Sub-facies

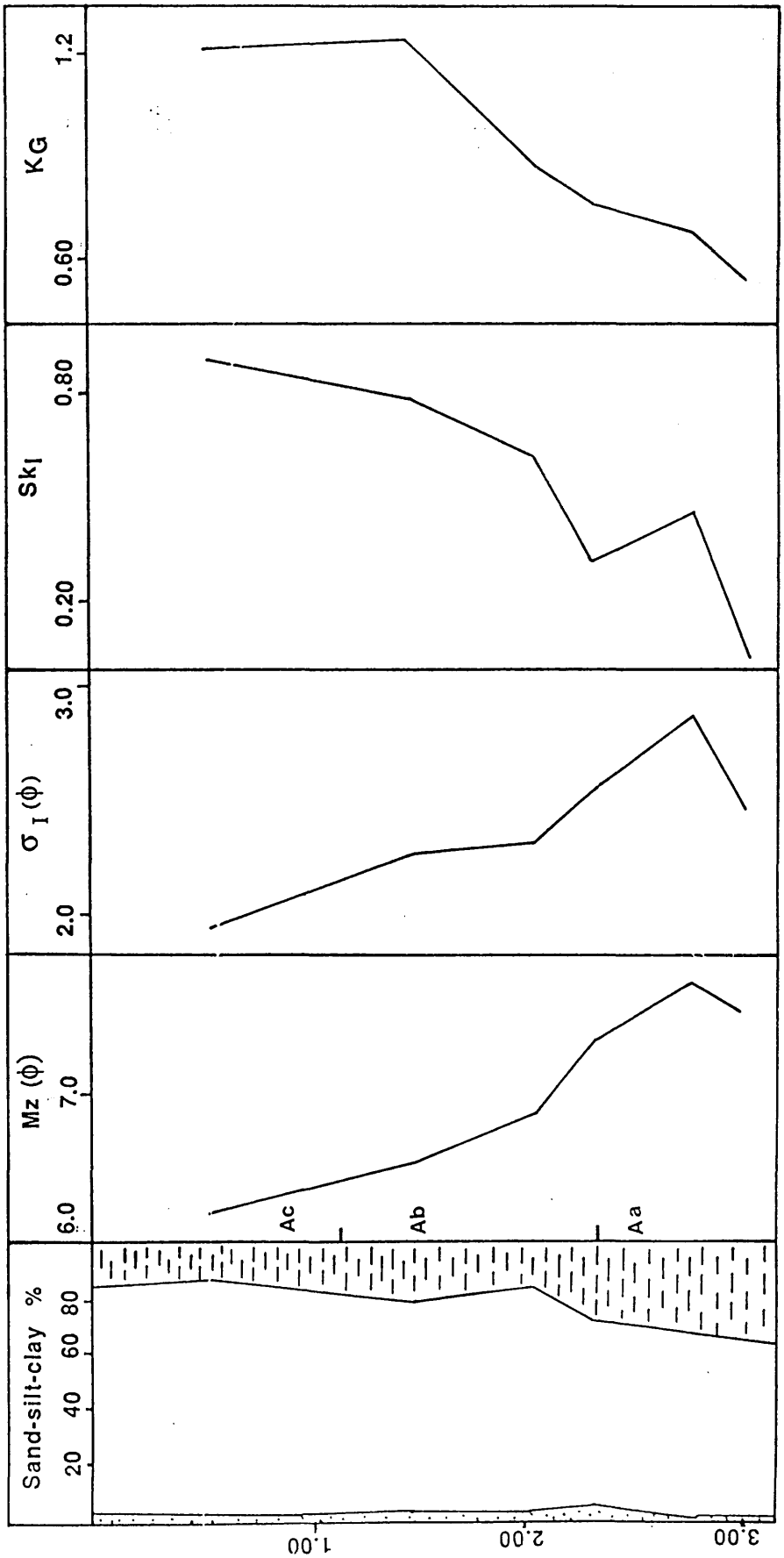

Figure 7.23 Sand-silt-clay percentages and grain-size parameters, Mz, σ_I, Sk_I, K_G, in relation to depth (in metres) below ground surface, section D10, Dalbeattie area. Ac, Ab, Aa = Sub-facies

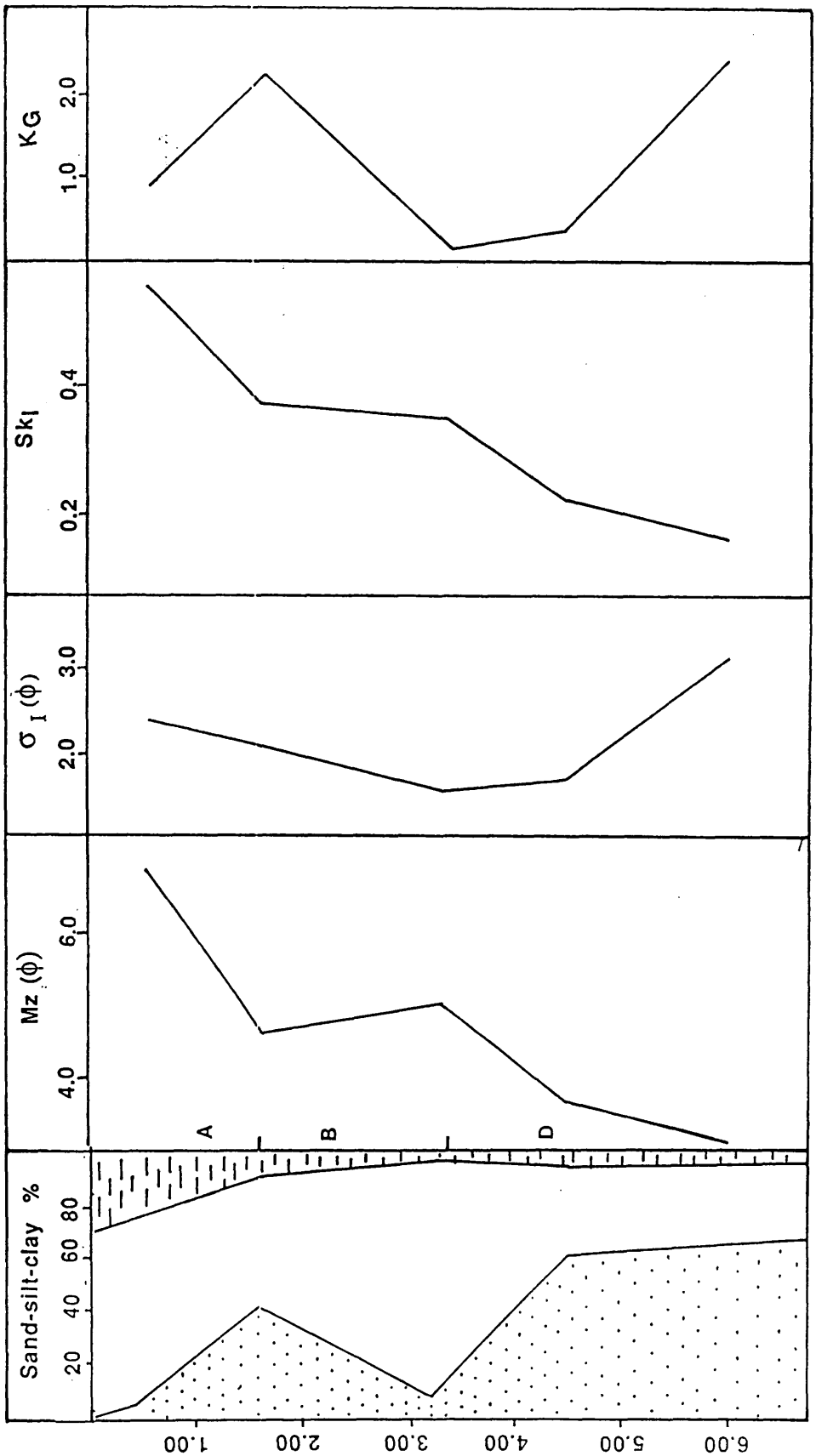

Figure 7.24 Sand-silt-clay percentages and grain-size parameters, Mz, σ_I, Sk_I, K_G, in relation to depth (in metres) below ground surface, section K1, Kirkcudbright area. A, B, D = Facies

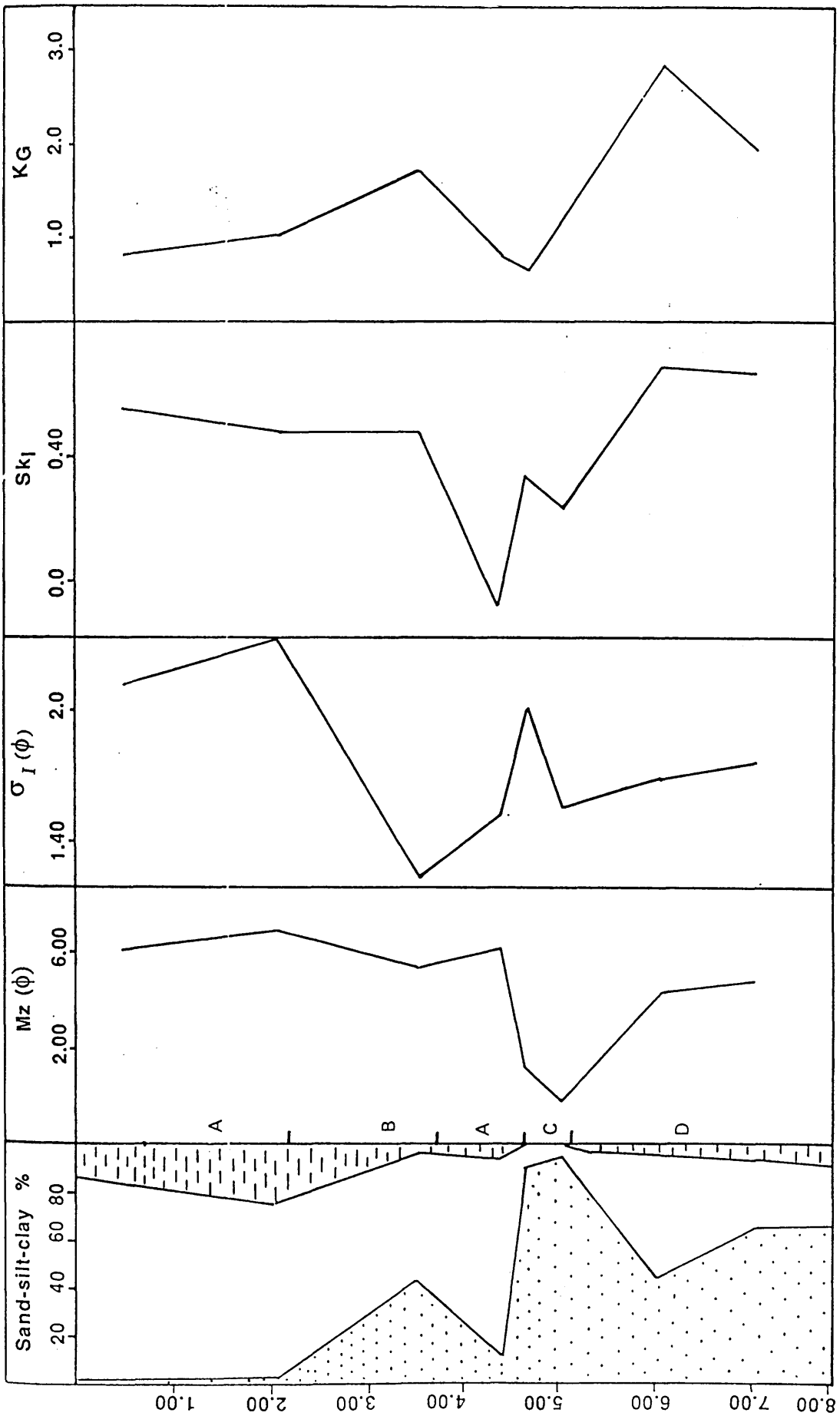

Figure 7.25 Sand-silt-clay percentages and grain-size parameters, Mz, σ_I, Sk_I, K_G, in relation to depth (in metres) below ground surface, section N5, New Abbey area. A, B, C, D = Facies

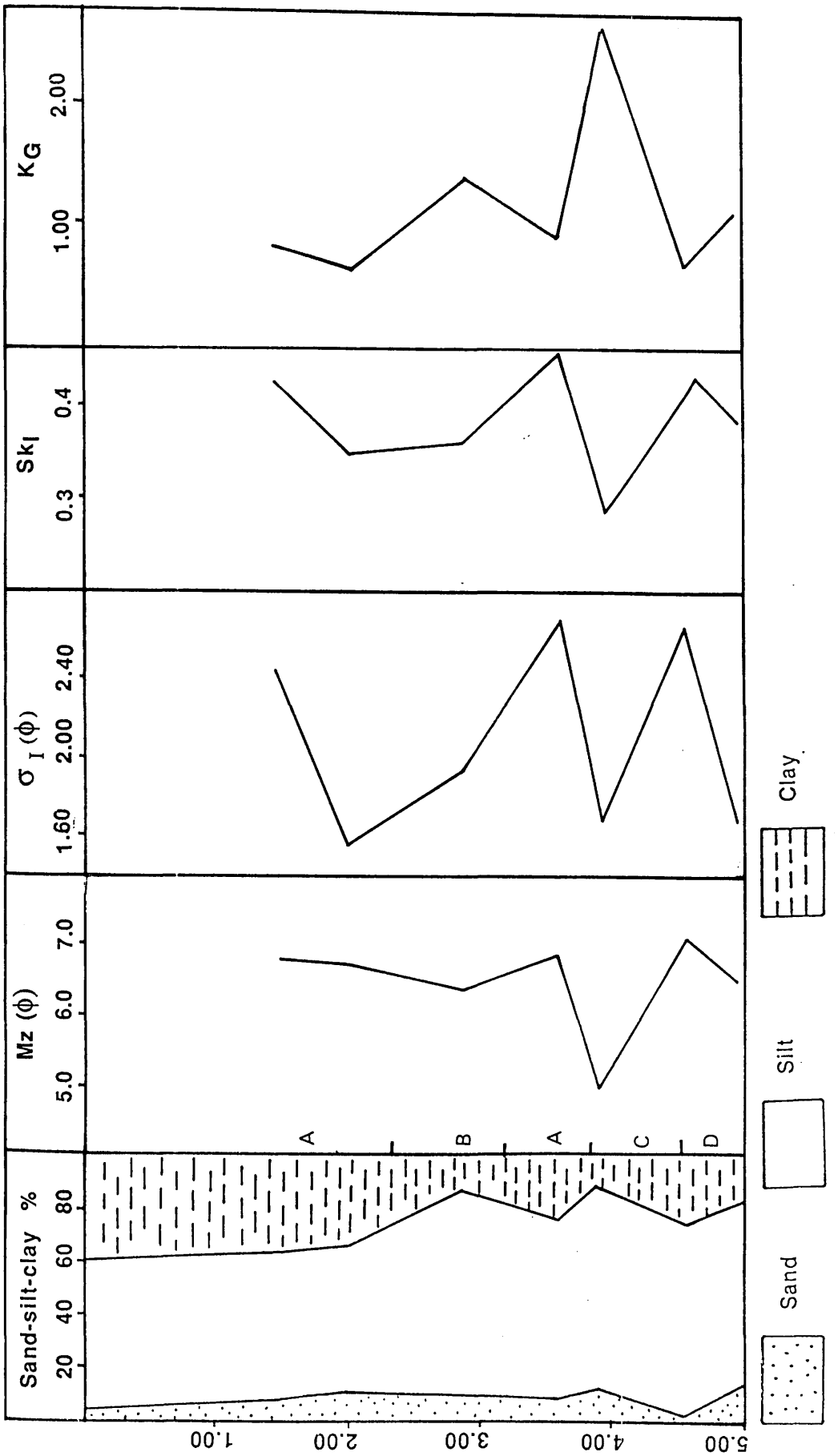

Figure 7.26 Sand-silt-clay percentages and grain-size parameters, Mz, σ_I, Sk_I, K_G, in relation to depth (in metres) below ground surface, section N6, New Abbey area. A, B, C, D = Facies

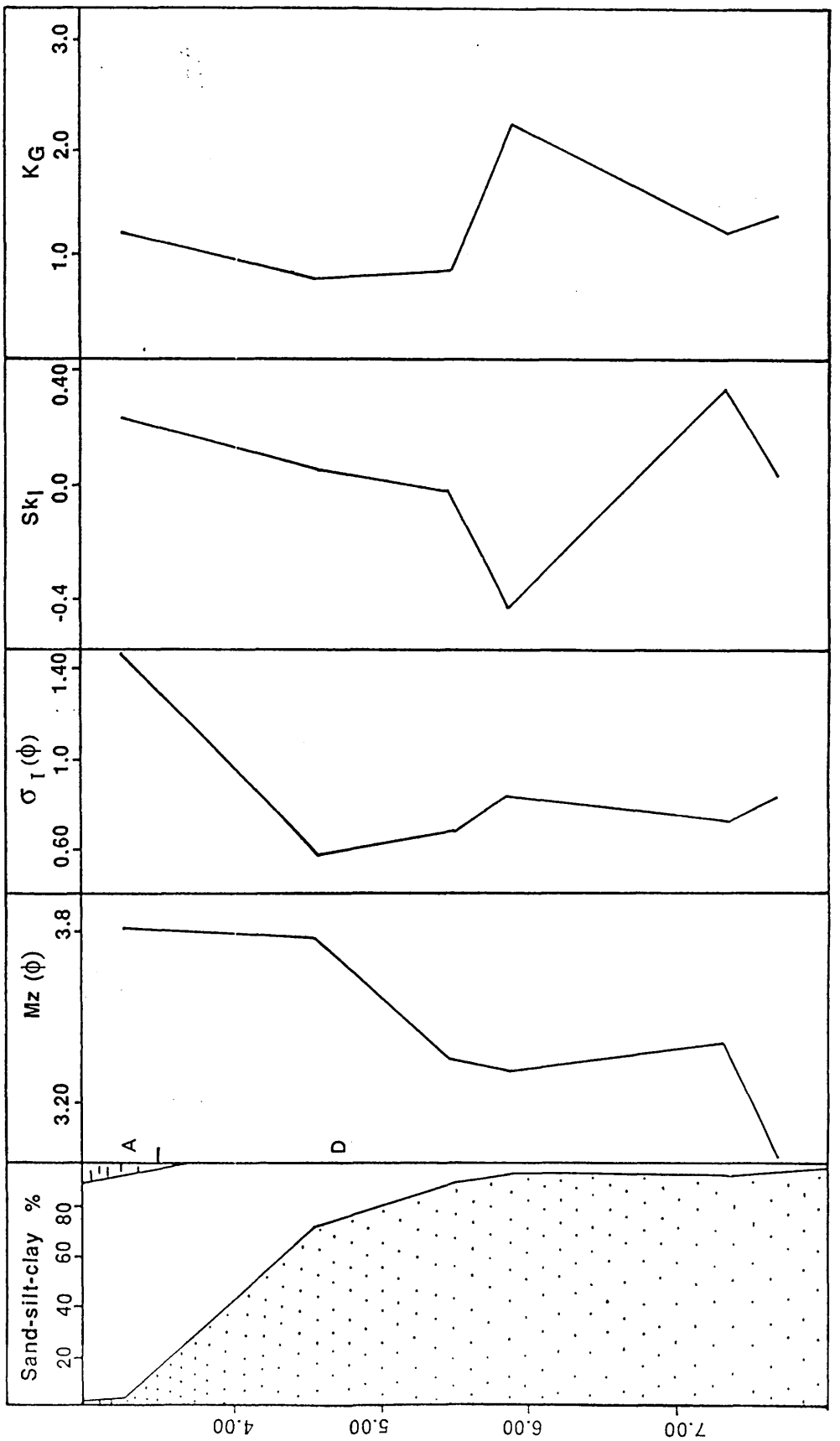

Figure 7.27 Sand-silt-clay percentages and grain-size parameters, Mz, σ_I, Sk_I, K_G, in relation to depth (in metres) below ground surface, Horseholm section , Lochar Gulf area. A, D = Facies

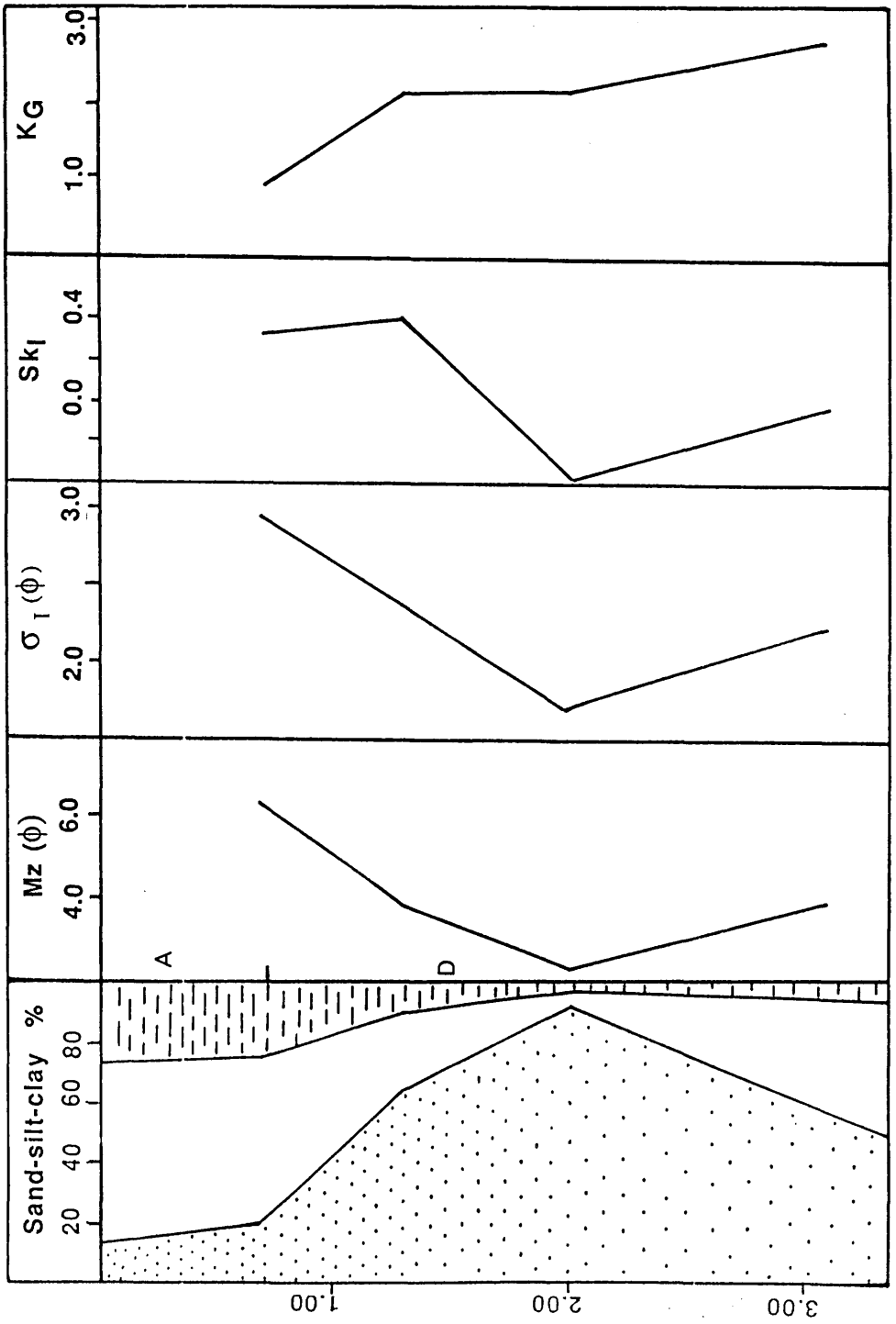

Figure 7.28 Sand-silt-clay percentages and grain-size parameters, Mz, σ_I, Sk_I, K_G, in relation to depth (in metres) below ground surface, Bankend Bridge section, Lochar Gulf area. A, D = Facies

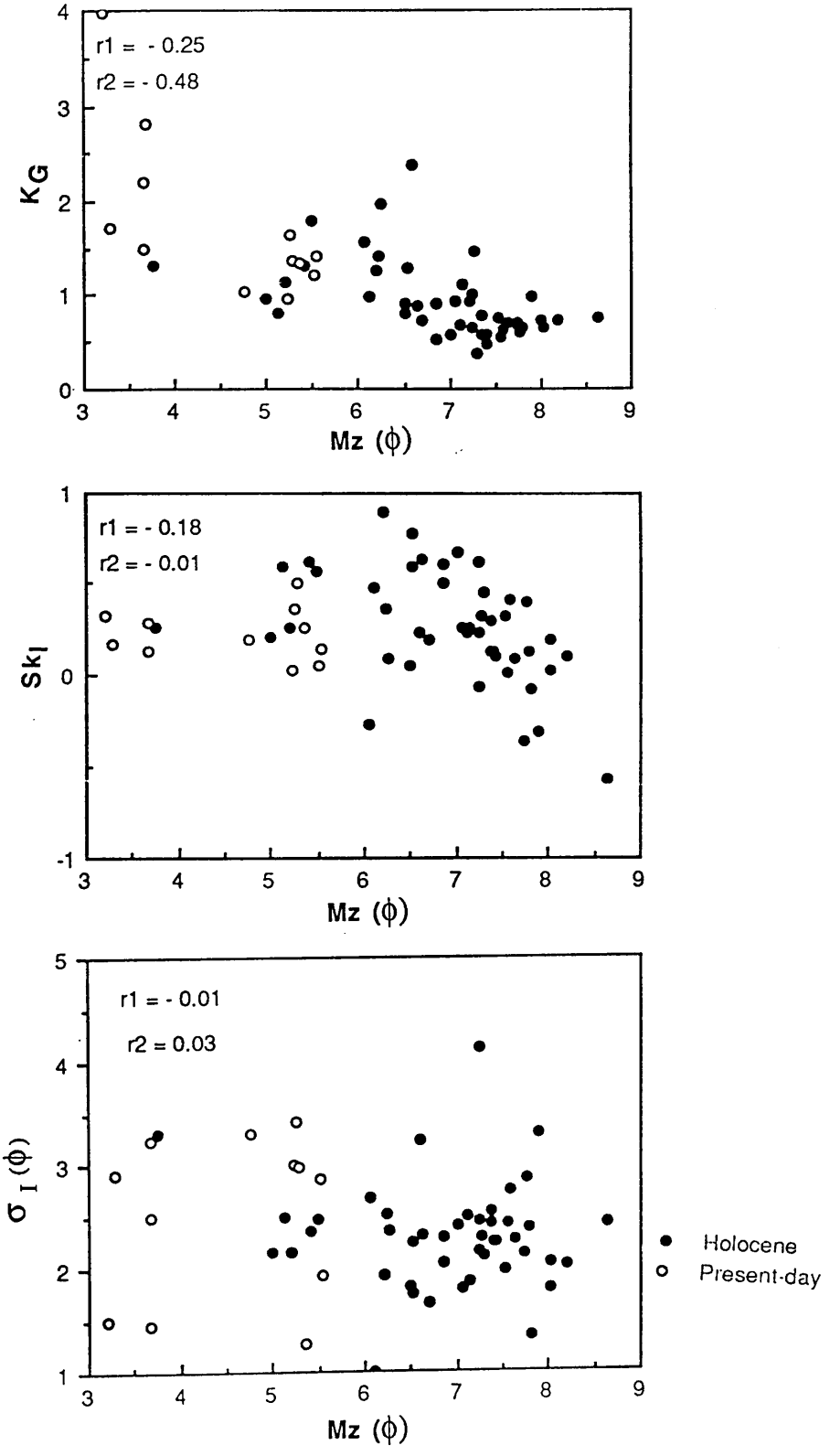

Figure 7.29 Scatter plots of Mz against σ_I, Sk_I and K_G for analysed samples of Holocene and present-day sediments, Dalbeattie area.

r1 = Correlation coefficient, Holocene sediments
r2 = Correlation coefficient, present-day sediments

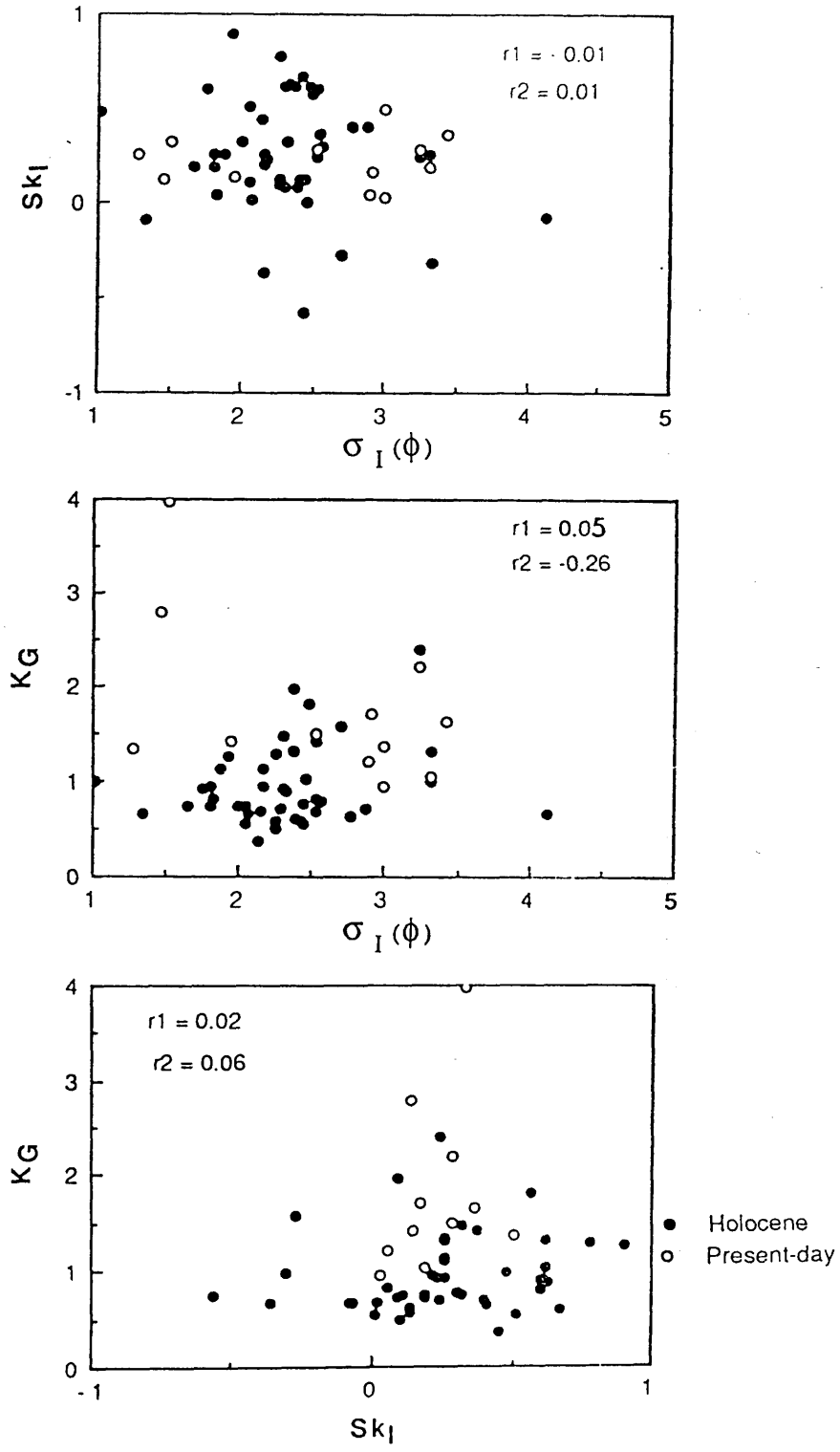

Figure 7.30 Scatter plots of σ_I against Sk_I and K_G and of Sk_I against K_G for analysed samples of Holocene and present-day sediments, Dalbeattie area.

r1 = Correlation coefficient, Holocene sediments

r2 = Correlation coefficient, present-day sediments

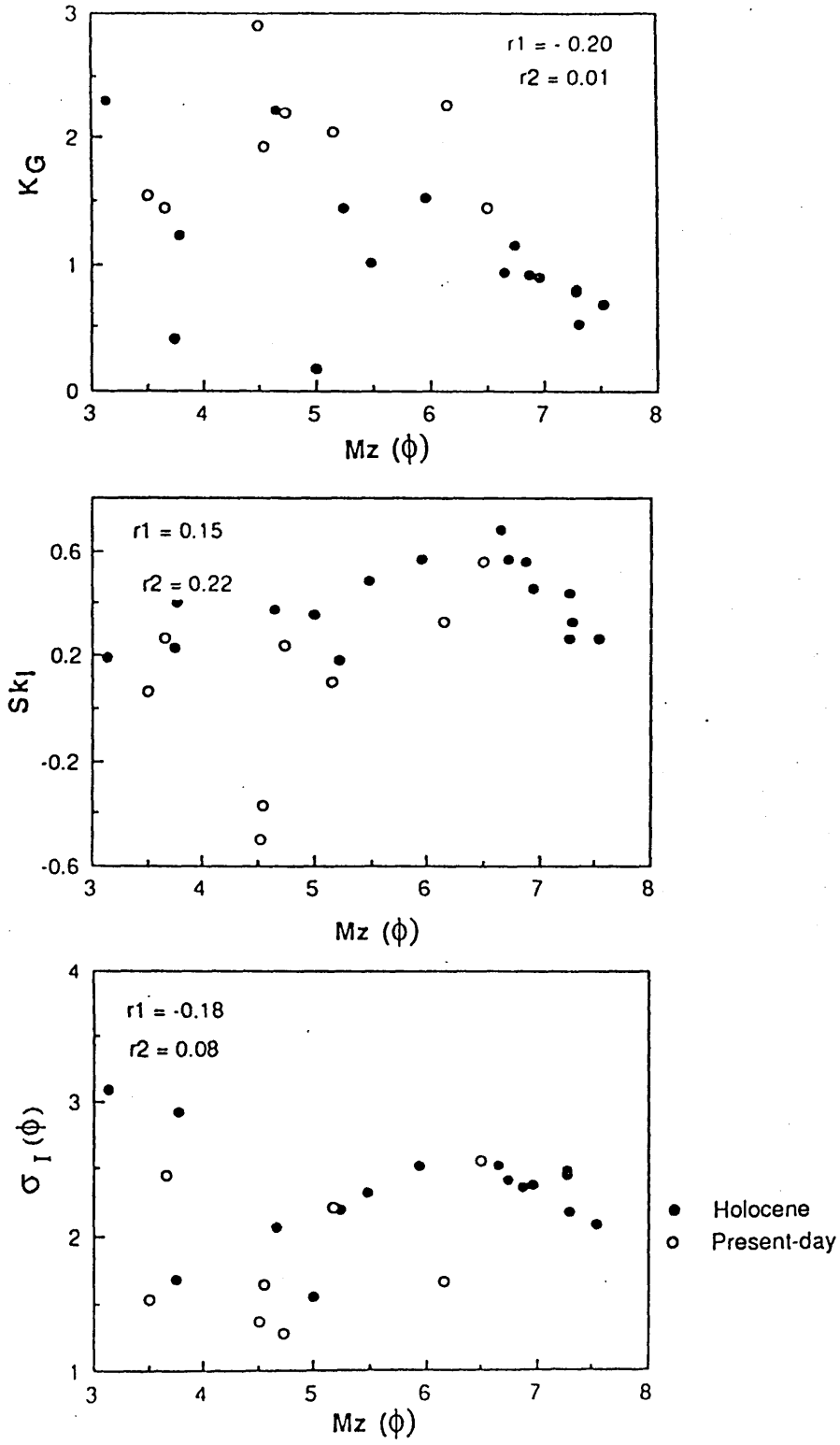

Figure 7.31 Scatter plots of Mz against σ_I, Sk_I and K_G for analysed samples of Holocene and present-day sediments, Kirkcudbright area.

r1 = Correlation coefficient, Holocene sediments

r2 = Correlation coefficient, present-day sediments

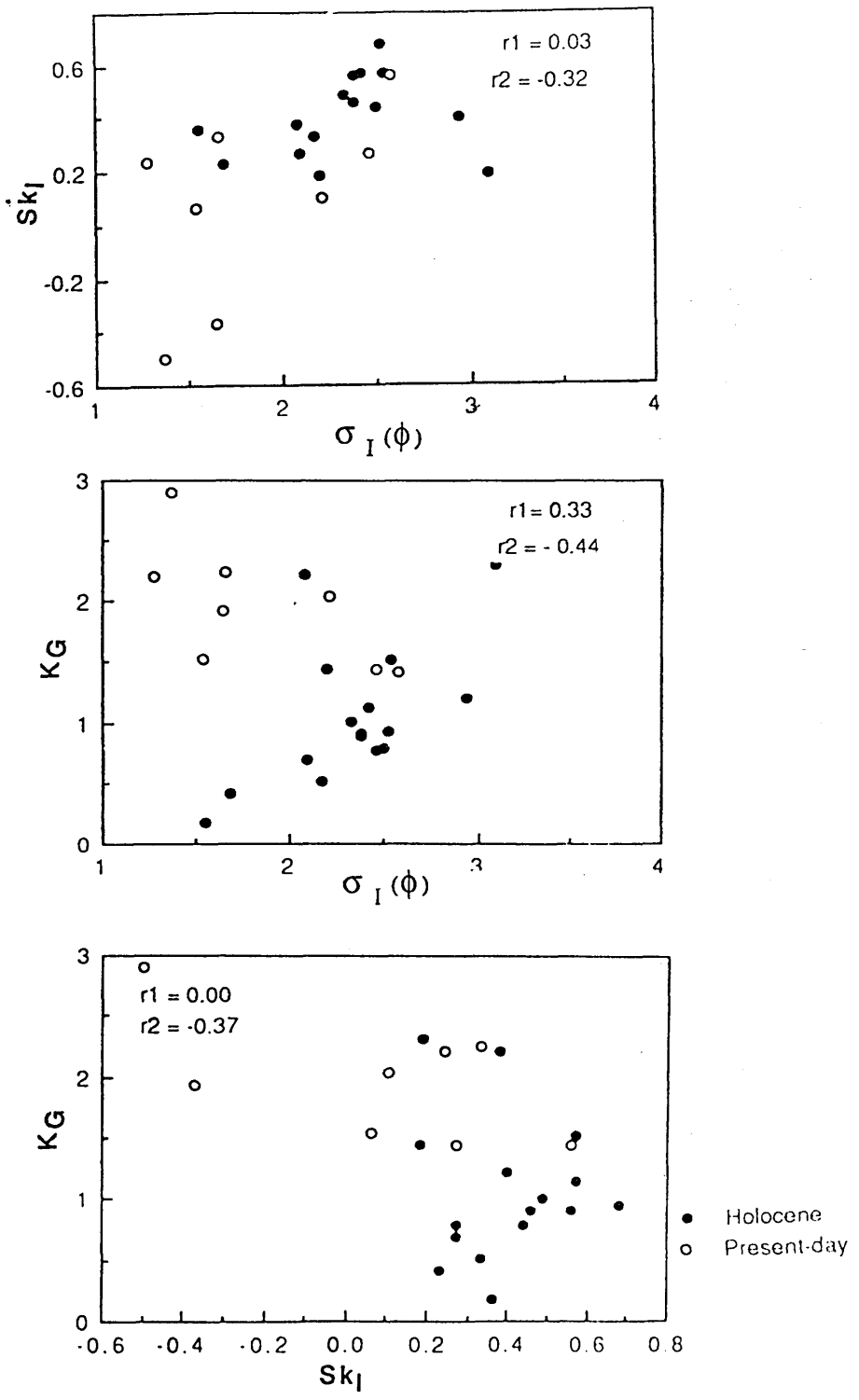

Figure 7.32 Scatter plots of σ_I against Sk_I and K_G and of Sk_I against K_G for analysed samples of Holocene and present-day sediments, Kirkcudbright area.

r1 = Correlation coefficient, Holocene sediments

r2 = Correlation coefficient, present-day sediments

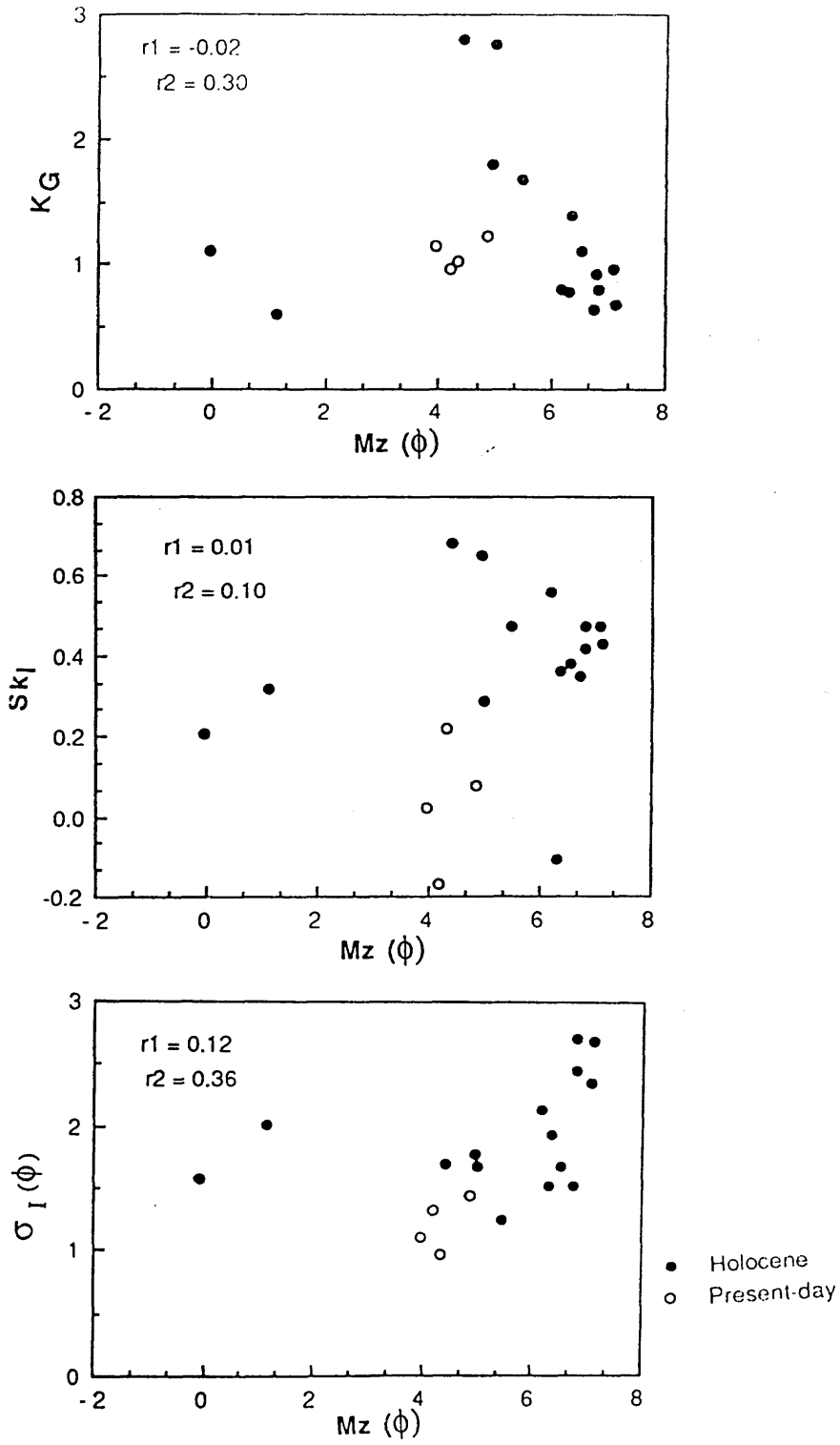

Figure 7.33 Scatter plots of Mz against σ_I, Sk_I and K_G for analysed samples of Holocene and present-day sediments, New Abbey area.

r1 = Correlation coefficient, Holocene sediments

r2 = Correlation coefficient, present-day sediments

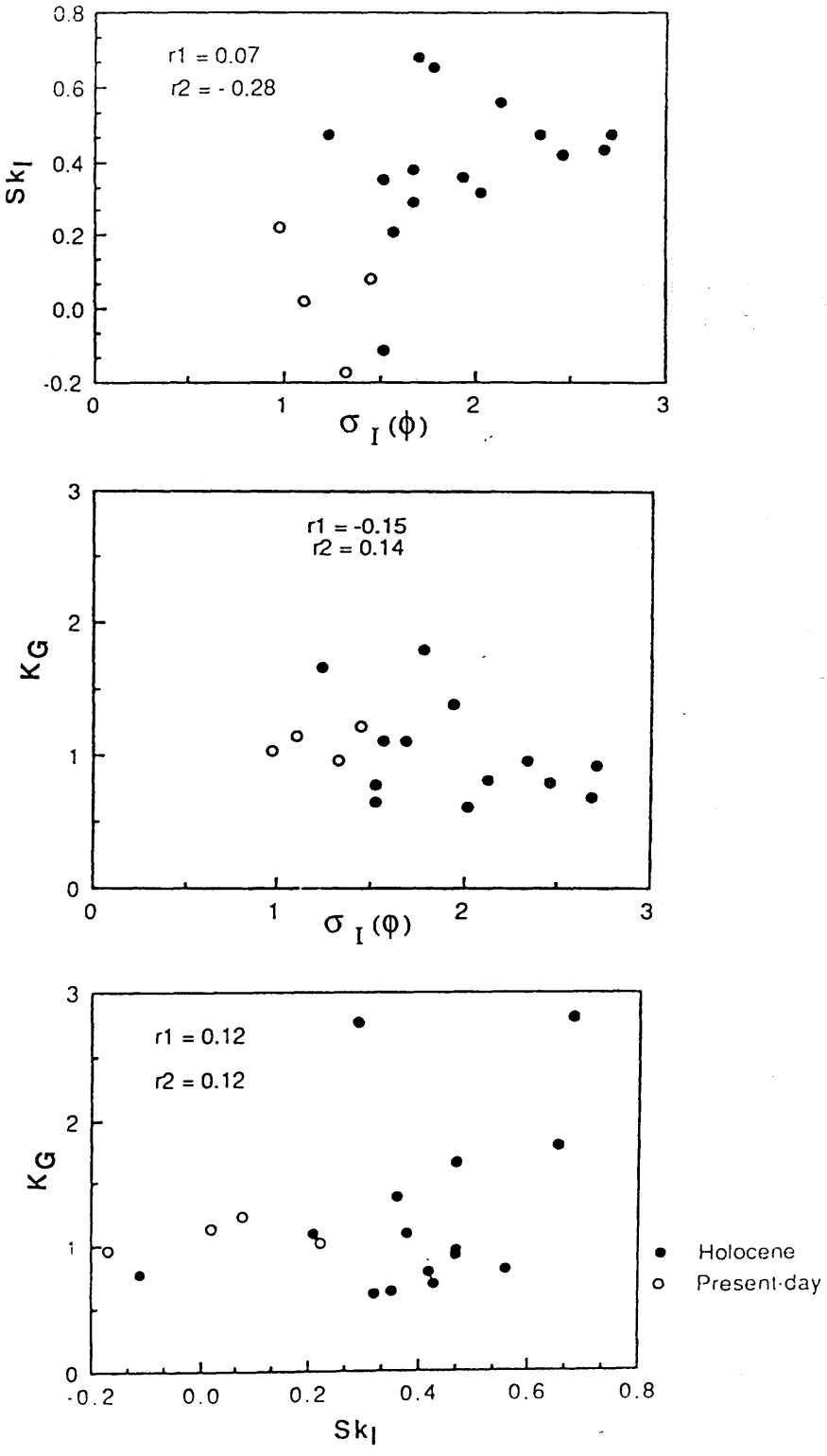

Figure 7.34 Scatter plots of σ_I against Sk_I and K_G and of Sk_I against K_G for analysed samples of Holocene and present-day sediments, New Abbey area.

r1 = Correlation coefficient, Holocene sediments

r2 = Correlation coefficient, present-day sediments

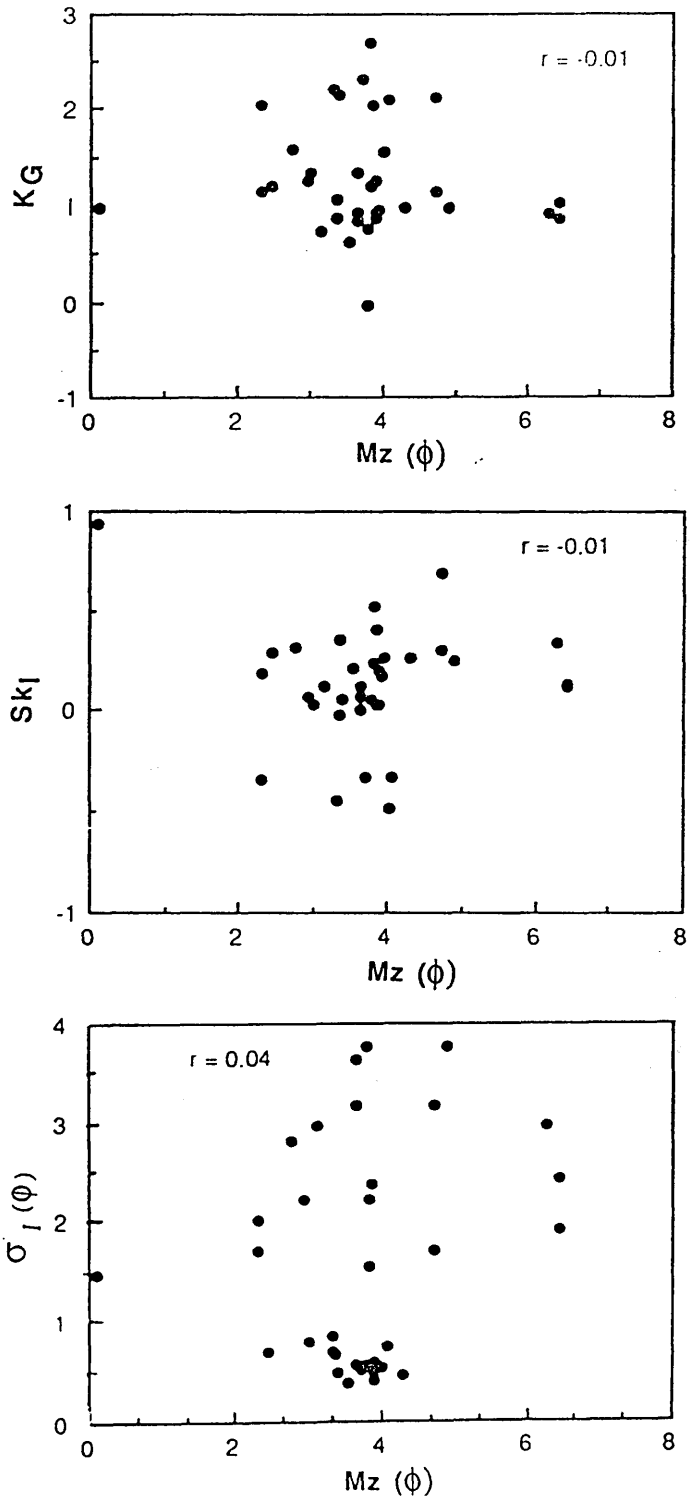

Figure 7.35 Scatter plots of Mz against σ_I, Sk_I and K_G for analysed samples of Holocene sediments, Lochar Gulf area.

r1 = Correlation coefficient, Holocene sediments

r2 = Correlation coefficient, present-day sediments

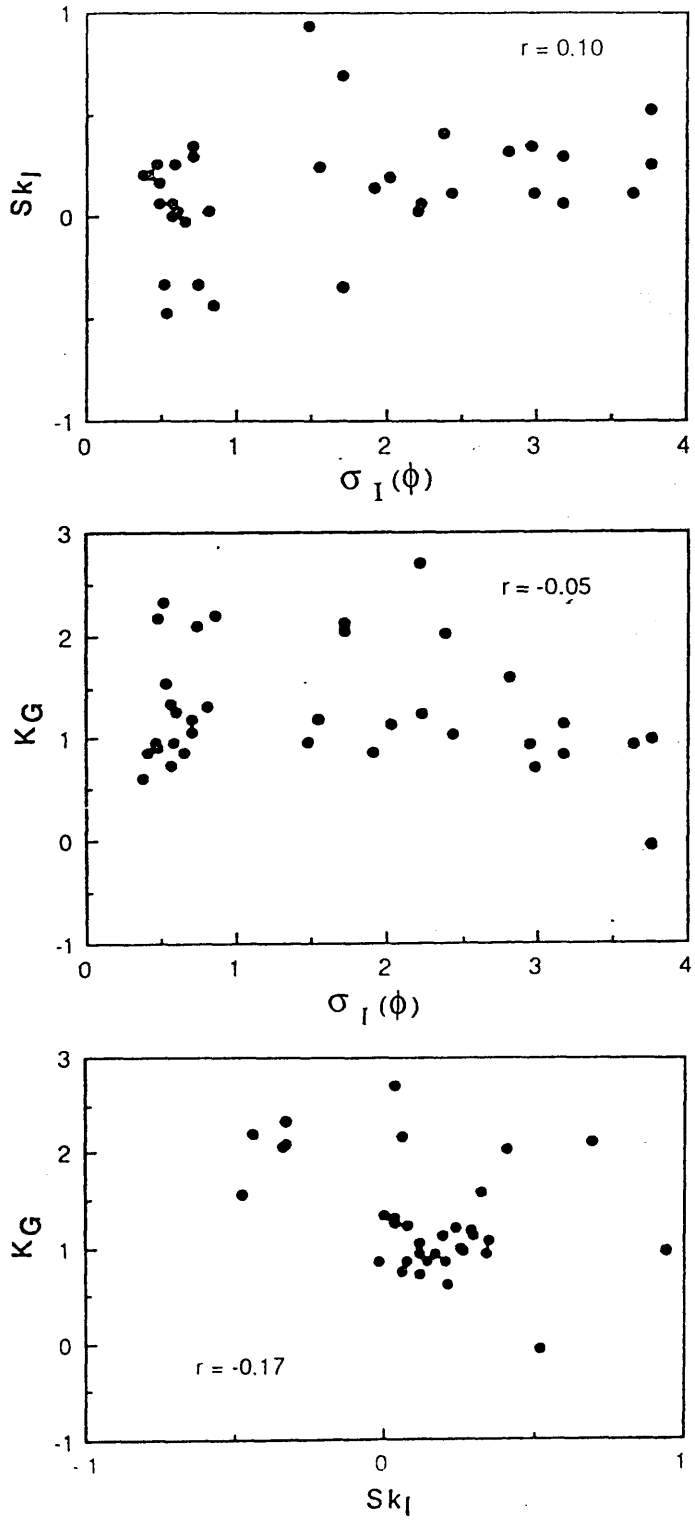

Figure 7.36 Scatter plots of σ_I against Sk_I and K_G and of Sk_I against K_G for analysed samples of Holocene, Lochar Gulf area.

r = Correlation coefficient

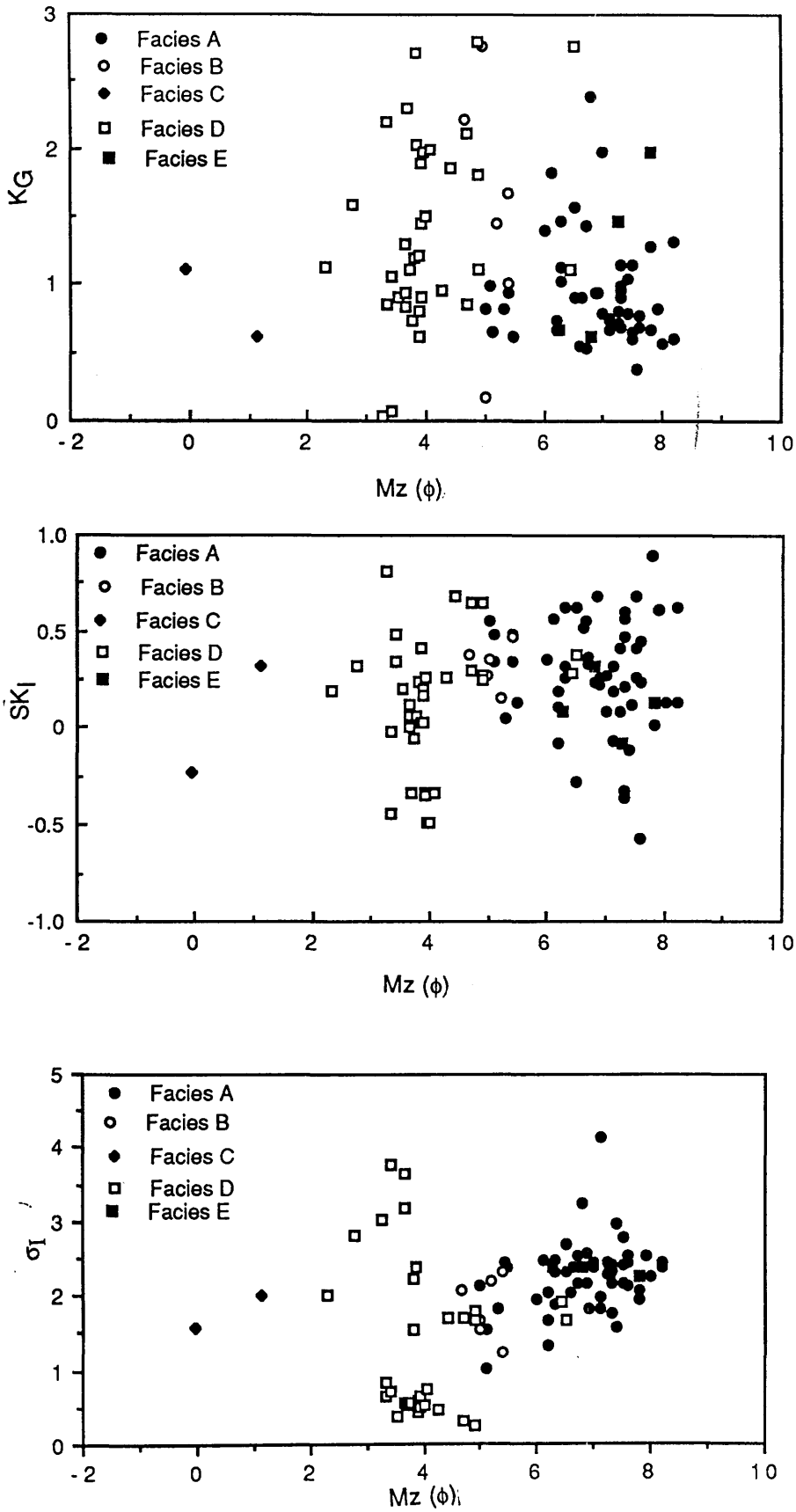

Figure 7.37 Scatter plots of Mz (ϕ) against σ_I, SK_I and K_G for analysed samples of the various sedimentary facies of the Holocene sediments from the four areas studied.

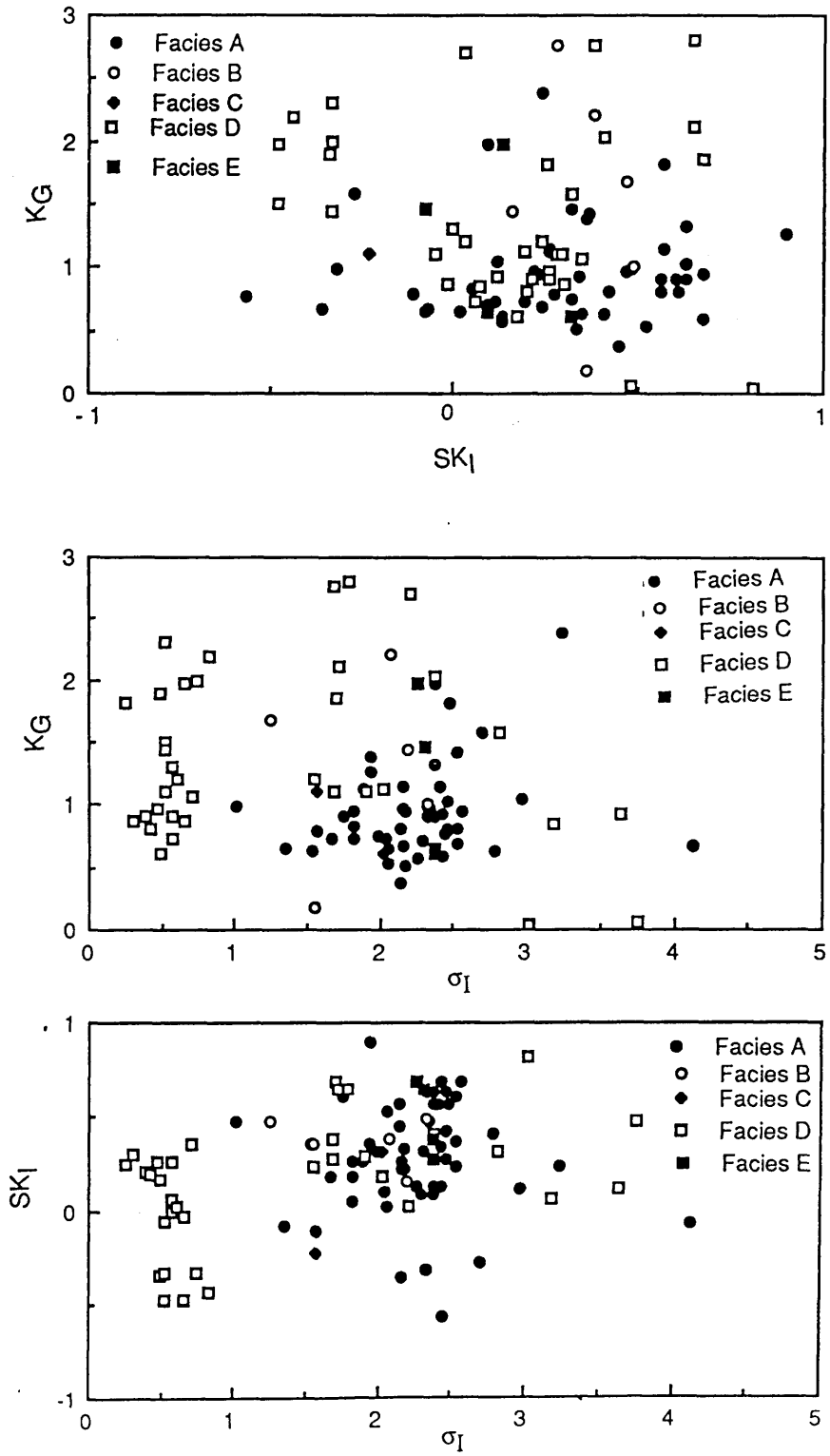

Figure 7.38 Scatter plots of σ_I against SK_I and K_G and of SK_I against K_G for analysed samples of the various sedimentary facies of the Holocene sediments from the four areas studied.

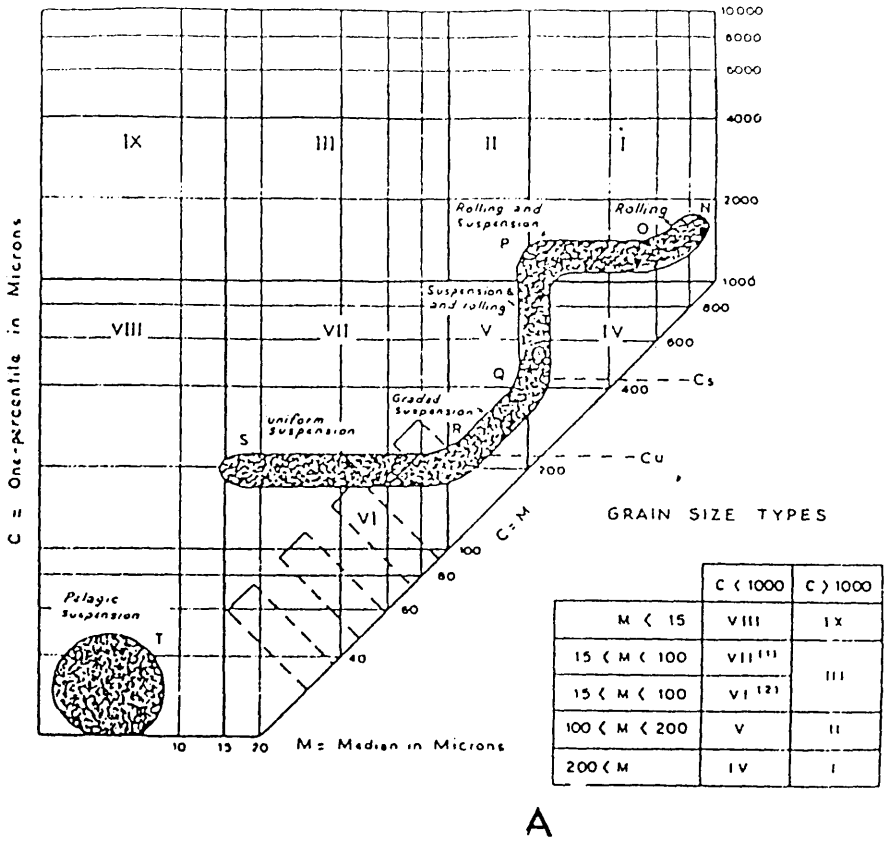

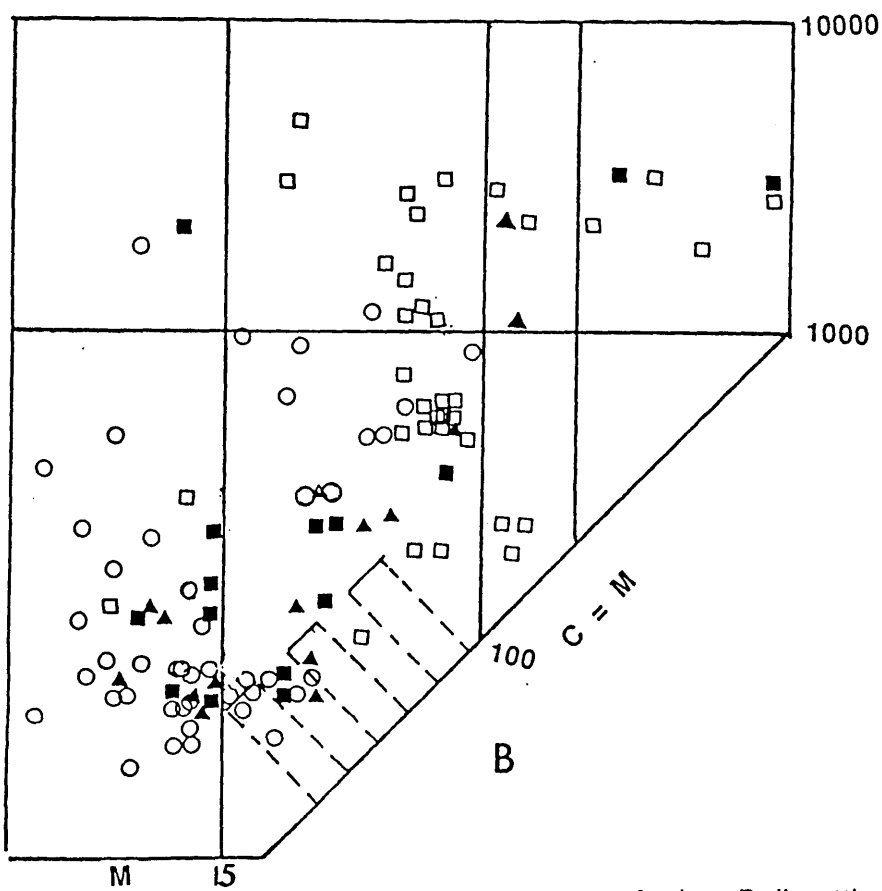

Figure 7.39 CM diagram for Holocene sediments of the Dalbeattie, Kirkcudbright, New Abbey and Lochar Gulf areas: A, Passega & Byramjee's (1969) diagram, showing the nine classes these authors distinguished; B, distribution of analysed sediments within these nine classes

Table 7. 1A Weight percentages of the sand, silt and clay fractions in the Holocene raised coastal sediments, Dalbeattie area

Sample	Sand%	Silt%	Clay%
D2 0.60	6.38	76.61	16.17
D2 1.20	8.07	80.40	11.50
D2 1.80	30.05	59.59	8.82
D2 2.50	9.52	50.55	39.92
D2 2.70	5.34	55.64	39.02
D2 2.95	35.38	39.16	24.65
D3 1.00	35.50	27.21	36.66
D3 1.40	5.59	67.52	26.84
D3 1.90	2.00	69.09	33.74
D3 2.20	0.98	73.56	25.10
D3 2.95	1.22	66.76	31.86
D4 0.50	3.92	66.30	30.09
D4 1.20	4.55	56.35	39.10
D4 2.10	0.60	67.86	31.52
D4 2.90	1.15	96.99	1.93
D5 0.70	1.40	51.57	47.15
D5 1.50	5.66	54.20	40.11
D5 2.20	6.62	62.56	37.49
D5 2.80	15.60	67.28	32.71
D6 0.50	1.17	54.37	44.44
D6 1.20	1.40	52.08	47.80
D6 1.70	4.43	41.24	55.41
D6 2.00	2.60	72.15	25.24
D6 2.30	1.26	49.10	48.89
D6 2.60	1.66	59.38	38.84
D7 0.40	2.47	73.96	24.16
D7 1.10	5.93	32.83	60.00
D7 1.60	2.67	73.95	23.46
D7 2.25	3.96	76.04	20.80
D7 3.70	0.60	77.60	20.74
D8 0.40	11.36	71.90	16.71
D8 1.60	13.52	64.68	20.81
D8 2.00	1.83	61.34	37.70
D8 2.70	1.83	69.41	28.39
D9 0.40	4.13	55.26	39.23
D9 1.06	22.83	72.20	5.93
D9 1.56	5.57	85.79	9.35
D9 2.92	63.13	26.09	9.09

Continued

Table 7.1A continued

D10 0.55	1.17	85.27	14.00
D10 1.50	2.23	75.77	21.88
D10 2.07	2.89	79.76	17.33
D10 2.36	1.66	68.38	28.43
D10 2.80	6.30	60.07	33.61
D10 3.03	2.02	60.16	36.78

Table 7. 1B Weight percentages of the sand, silt and clay fractions in the present-day intertidal sediments, Dalbeattie area

Sample	Sand%	Silt%	Clay%
Dp 1-1	60.69	32.44	6.84
Dp 1-2	45.00	39.52	15.35
Dp 1-3	34.50	50.15	14.89
Dp 1-4	13.73	71.76	14.51
Dp 1-5	64.40	26.66	8.94
Dp 1-6	64.80	23.56	11.56
Dp 1-7	81.40	13.45	5.12
Dp 1-8	67.50	25.41	7.42
Dp 2-1	31.80	45.39	20.94
Dp 2-2	28.75	52.31	19.94
Dp 2-3	46.00	37.52	16.47
Dp 2-4	30.60	63.25	5.85

Table 7. 2A Weight percentages of the sand, silt and clay fractions in the Holocene raised coastal sediments, Kirkcudbright area

Sample	Sand%	Silt%	Clay%
K1 0.55	5.66	71.97	22.23
K1 1.60	43.16	48.08	8.71
K1 3.30	8.95	88.87	2.23
K1 4.40	61.08	33.24	5.64
K1 6.00	65.30	36.75	6.85
K2 0.50	3.47	66.87	29.66
K2 1.60	0.60	73.08	26.04
K2 4.20	28.90	59.21	11.95
K3 0.60	3.19	68.07	28.71
K3 1.80	27.85	57.93	13.85
K3 3.50	5.64	78.63	15.68
K3 5.10	13.38	68.60	15.91
K4 0.30	5.25	73.05	21.63
K4 0.80	5.37	72.62	21.00
K4 1.90	1.40	56.79	41.75
K4 2.15	73.14	19.22	6.56

Table 7. 2B Weight percentages of the sand, silt and clay fractions in the present-day intertidal sediments, Kirkcudbright area

Sample	Sand%	Silt%	Clay%
Kp 1-1	6.82	84.32	6.59
Kp 1-5	61.70	36.99	1.18
Kp 2-1	8.28	75.08	16.00
Kp 2-2	1.50	86.33	12.23
Kp 2-3	26.09	70.50	1.54
Kp 2-4	21.50	63.98	13.40
Kp 3-4	62.00	32.18	5.63
Kp 4-3	59.70	39.56	0.77

Table 7. 3A Weight percentages of the sand, silt and clay fractions in the Holocene raised coastal sediments, New Abbey area

Sample	Sand%	Silt%	Clay%
N5 0.50	1.34	82.42	17.45
N5 2.10	1.03	74.88	24.08
N5 3.60	43.94	52.74	3.27
N5 4.40	12.24	80.50	6.25
N5 4.70	91.63	7.55	0.00
N5 5.10	96.65	3.28	0.00
N5 6.20	44.71	50.32	3.95
N5 7.10	64.73	28.71	6.48
N6 1.40	8.34	53.29	37.96
N6 2.00	10.58	52.48	36.91
N6 2.90	6.73	79.38	13.86
N6 3.70	9.54	67.22	23.08
N6 3.90	13.41	75.83	10.47
N6 4.60	3.68	70.43	25.85
N6 5.00	14.54	65.78	17.89

Table 7. 3B Weight percentages of the sand, silt and clay fractions in the present-day intertidal sediments, New Abbey area

Sample	Sand%	Silt%	Clay%
Np 1-1	45.30	52.95	1.27
Np 1-2	68.47	28.47	3.01
Np 1-3	41.49	53.83	4.64
Np 1-4	26.00	68.80	5.20

Table 7. 4 Weight percentages of the sand, silt and clay fractions in the Holocene raised coastal sediments, Lochar Gulf area

Sample	Sand%	Silt%	Clay%
NP 2.13	92.94	6.56	0.00
NP 2.74	60.10	36.10	3.65
NP 2.89	59.26	23.96	16.14
NP 3.35	67.91	20.31	10.54
NP 4.26	50.61	42.25	4.10
NP 5.02	58.09	41.89	0.00
SK 0.60	8.20	67.05	24.75
SK 1.20	63.62	30.34	4.70
SK 2.10	82.94	16.99	0.29
SK 2.90	73.54	18.06	26.42
BB 070	20.93	53.10	25.29
BB 1.30	63.66	25.59	10.80
BB 2.00	92.01	5.14	2.61
BB 3.10	58.27	37.09	4.50
HH 3.22	2.35	89.85	7.75
HH 4.57	72.66	27.32	0.00
HH 5.48	90.95	9.03	0.00
HH 5.79	94.64	5.33	0.00
HH 7.31	94.15	4.54	0.00
HH 7.62	95.87	4.11	0.00
NM 3.88	94.55	5.42	0.00
NM 4.19	64.61	33.36	0.00
NM 5.33	89.33	10.23	0.00
NM 6.93	83.80	16.27	0.00
NM 7.46	96.49	3.47	0.00
PH 2.13	60.66	39.32	0.00
PH 3.20	86.34	13.65	0.00
PH 3.50	80.14	19.82	0.00
PH 4.82	89.63	10.35	0.00
PH 5.30	86.52	40.72	0.00
PH 6.37	59.28	40.72	0.00
MT 3.14	64.01	36.00	0.00
MT 4.06	65.05	15.61	15.41
MT 4.16	54.42	34.96	10.47
MT 4.31	85.08	11.92	0.00
HM 0.71	18.55	60.77	20.68
HM 1.93	88.61	11.38	0.00
HM 3.56	85.97	14.03	0.00

Table 7.5A Statistical parameter values for the Holocene samples from the Dalbeattie area; Median = Md(ϕ), Mean = Mz(ϕ), Standard deviation = $\sigma_I(\phi)$, Skewness = Sk_I, Kurtosis = K_G.

Parameter sample		Md (ϕ)	Mz (ϕ)	$\sigma_I(\phi)$	Sk_I	K_G
D2	0.60	7.06	7.41	2.25	0.11	0.49
D2	1.20	4.65	5.41	2.37	0.63	1.32
D2	1.80	4.60	5.00	2.16	0.22	0.96
D2	2.25	6.90	7.36	2.43	0.13	0.59
D2	2.70	7.00	7.40	2.25	0.13	0.57
D2	2.95	6.05	7.25	4.13	- 0.07	0.67
D3	0.60	3.95	5.11	2.52	0.61	0.81
D3	1.00	6.60	6.06	2.70	- 0.27	1.57
D3	1.40	5.40	6.63	2.33	0.63	0.90
D3	1.90	5.60	7.01	2.42	0.68	0.60
D3	2.20	6.60	6.70	1.66	0.19	0.74
D3	2.95	5.95	6.85	2.05	0.52	0.54
D4	0.50	6.20	7.30	2.13	0.45	0.37
D4	1.20	7.30	7.63	2.29	0.09	0.72
D4	2.10	7.00	7.53	1.99	0.32	0.75
D4	2.90	5.90	6.11	1.01	0.48	0.99
D5	0.70	7.55	7.78	2.38	0.13	0.61
D5	1.50	7.90	7.80	1.34	- 0.08	0.66
D5	2.20	6.50	7.26	2.31	0.32	1.47
D5	2.80	6.00	6.25	2.38	0.09	1.97
D6	0.50	7.80	7.73	2.15	- 0.36	0.68
D6	1.20	7.90	8.03	2.06	0.02	0.66
D6	1.70	9,85	8.63	2.44	- 0.57	0.76
D6	2.00	6.90	7.23	2.17	0.23	0.94
D6	2.30	8.15	8.20	2.04	0.11	0.74
D6	2.60	7.80	8.01	1.81	0.19	0.73
D7	0.40	6.60	7.13	1.88	0.26	1.12
D7	1.10	8.50	7.90	2.32	- 0.32	0.99
D7	1.60	6.00	6.51	1.75	0.60	0.91
D7	2.25	6.55	6.50	1.82	0.05	0.82
D7	3.70	6.60	7.05	1.81	0.26	0.94
D8	0.40	5.90	6.23	2.53	0.37	1.43
D8	1.60	5.80	6.60	3.23	0.24	2.39
D8	2.00	7.00	7.58	2.77	0.41	0.64
D8	2.70	6.20	7.25	2.46	0.63	1.02

Continued

Table 7.5A continued

D9	0.40	6.65	7.11	2.52	0.24	0.69
D9	1.06	5.00	5.16	2.16	0.26	1.14
D9	1.56	5.10	5.48	2.48	0.57	1.82
D9	2.92	3.30	3.76	3.31	0.26	1.31
D10	0.55	5.00	6.20	1.93	0.90	1.27
D10	1.50	5.10	6.53	2.25	0.78	1.30
D10	2.07	5.80	6.86	2.30	0.61	0.91
D10	2.36	6.85	7.36	2.56	0.30	0.78
D10	2.80	6.60	7.75	2.87	0.43	0.70
D10	3.03	7.60	7.56	2.45	0.01	0.55

Table 7.5B Statistical parameter values for the present-day intertidal samples from the Dalbeattie area (Median = Md(ϕ), Mean = Mz(ϕ), Standard deviation = $\sigma_I(\phi)$, Skewness = Sk_I, Kurtosis = K_G).

Parameter / Sample	Md (ϕ)	Mz (ϕ)	σ_I (ϕ)	Sk_I	K_G
Dp 1-1	3.20	3.28	2.91	0.17	1.71
Dp 1-2	4.15	5.25	3.42	0.36	1.64
Dp 1-3	4.50	5.28	2.99	0.50	1.37
Dp 1-4	5.90	5.53	1.94	0.14	1.41
Dp 1-5	3.45	3.66	2.52	0.28	1.49
Dp 1-6	3.20	3.66	3.23	0.28	2.20
Dp 1-7	3.25	3.20	1.51	0.33	3.98
Dp 1-8	3.80	3.68	1.46	0.13	2.80
Dp 2-1	5.20	5.32	3.02	0.03	0.96
Dp 2-2	5.35	5.51	2.88	0.05	1.22
Dp 2-3	4.40	4.75	3.31	0.19	1.04
Dp 2-4	5.15	5.35	1.28	0.26	1.34

Table 7.6A Statistical parameter values for the Holocene samples from the Kirkcudbright area; Median = Md(ϕ), Mean = Mz(ϕ), Standard deviation = $\sigma_I(\phi)$, Skewness = Sk_I, Kurtosis = K_G.

Parameter	Md (ϕ)	Mz (ϕ)	$\sigma_I(\phi)$	Sk_I	K_G
Sample					
K1 0.55	5.80	6.88	2.37	0.56	0.91
K1 1.60	4.35	4.65	2.07	0.38	2.22
K1 3.30	4.80	5.00	1.55	0.36	0.17
K1 4.40	3.60	3.75	1.68	0.23	0.41
K1 6.00	3.00	3.13	3.09	0.19	2.30
K2 0.60	6.45	7.28	2.45	0.27	0.78
K2 1.60	6.40	7.29	2.49	0.44	0.79
K2 4.20	5.00	5.48	2.32	0.49	1.01
K3 0.60	6.60	7.30	2.17	0.33	0.52
K3 1.80	5.28	5.23	2.19	0.18	1.45
K3 3.50	5.90	6.95	2.38	0.46	0.90
K3 5.50	5.00	5.95	2.53	0.57	1.52
K4 0.30	5.35	6.66	2.52	0.68	0.94
K4 0.80	5.60	6.73	2.41	0.57	1.14
K4 1.90	7.00	7.53	2.09	0.27	0.69
K4 2.15	2.95	3.78	2.94	0.40	1.22

Table 7.6B Statistical parameter values for the present-day samples from the Kirkcudbright area (Median = Md(ϕ), Mean = Mz(ϕ), Standard deviation = $\sigma_I(\phi)$, Skewness = Sk_I, Kurtosis = K_G

Parameter	Md (ϕ)	Mz (ϕ)	$\sigma_I(\phi)$	Sk_I	K_G
Sample					
Kp 1-1	5.00	4.51	1.37	- 0.50	2.91
Kp 1-5	4.00	4.55	1.64	- 0.37	1.93
Kp 2-1	5.30	6.50	2.57	0.56	1.44
Kp 2-2	6.00	6.16	1.66	0.33	2.25
Kp 2-3	4.60	4.73	1.28	0.24	2.21
Kp 2-4	5.30	5.16	2.21	0.10	2.04
Kp 3-4	3.50	3.66	2.45	0.27	1.45
Kp 4-3	3.50	3.55	1.54	0.06	1.53

Table 7.7A Statistical parameter values for the Holocene samples from the New Abbey area; Median = Md(ϕ), Mean = Mz(ϕ), Standard deviation = $\sigma_I(\phi)$, Skewness = Sk_I, Kurtosis = K_G.

Parameter	Md (ϕ)	Mz (ϕ)	$\sigma_I(\phi)$	Sk_I	K_G
Sample					
N5 0.50	5.30	6.18	2.13	0.56	0.81
N5 2.10	6.20	7.08	2.34	0.47	0.96
N5 3.60	5.20	5.45	1.24	0.47	1.67
N5 4.40	6.20	6.30	1.57	-0.11	0.78
N5 4.70	0.60	1.13	2.02	0.32	0.61
N5 5.10	0.00	-0.05	1.57	-0.23	1.11
N5 6.20	3.95	4.41	1.70	0.68	2.80
N5 7.10	4.80	4.93	1.78	0.65	1.86
N6 1.40	5.85	6.81	2.45	0.42	0.80
N6 2.00	5.90	6.75	1.53	0.35	0.64
N6 2.90	5.90	6.35	1.94	0.36	1.39
N6 3.70	5.80	6.78	2.71	0.47	0.92
N6 3.90	5.00	4.98	1.68	0.28	2.76
N6 4.60	6.20	7.11	2.68	0.43	0.69
N6 5.00	5.60	6.53	1.68	0.38	1.11

Table 7.7B Statistical parameter values for the present-day samples from the New Abbey area Median = Md(ϕ), Mean = Mz(ϕ), Standard deviation = $\sigma_I(\phi)$, Skewness = Sk_I, Kurtosis = K_G

Parameter	Md (ϕ)	Mz (ϕ)	$\sigma_I(\phi)$	Sk_I	K_G
Sample					
Np 1-1	4.35	4.18	1.33	-0.17	0.97
Np 1-2	4.00	3.95	1.10	0.02	1.14
Np 1-3	4.15	4.33	0.97	0.22	1.03
Np 1-4	4.85	4.86	1.45	0.08	1.23

Table 7.8 Statistical parameter values for the Holocene samples from the Lochar Gulf area (Median = Md(ϕ), Mean = Mz(ϕ), Standard deviation = σ_I(ϕ), Skewness = Sk_I, Kurtosis = K_G

Parameter	Md (ϕ)	Mz (ϕ)	σ_I (ϕ)	Sk_I	K_G
Sample					
NP 2.13	-0.85	0.10	1.48	0.94	0.97
NP 2.74	3.00	3.13	2.98	0.12	0.72
NP 2.89	4.00	3.63	3.18	0.07	0.84
NP 3.35	4.00	3.65	3.64	0.12	0.93
NP 4.26	4.10	4.70	1.71	0.69	2.11
NP 5.02	4.20	4.28	0.47	0.26	0.96
SK 0.60	6.35	6.45	2.43	0.12	1.04
SK 1.20	3.30	2.95	2.23	0.07	1.24
SK 2.10	2.20	2.31	2.02	0.19	1.13
SK 2.90	2.50	2.76	2.81	0.32	1.58
BB 0.70	5.25	6.28	2.96	0.34	0.93
BB 1.30	3.65	3.86	2.38	0.41	2.03
BB 2.00	2.65	2.31	1.71	-0.34	2.05
BB 3.10	3.85	3.83	2.21	0.03	2.71
HH 3.22	3.60	3.81	1.55	0.24	1.20
HH 4.57	3.75	3.78	0.57	0.06	0.74
HH 5.48	3.35	3.35	0.66	-0.02	0.86
HH 5.79	3.55	3.33	0.83	-0.44	2.20
HH 7.31	3.35	3.43	0.70	0.35	1.06
HH 7.62	4.05	3.25	3.01	0.81	0.03
NM 3.88	3.40	3.40	3.75	0.48	0.06
NM 4.19	3.70	3.65	0.57	0.00	1.30
NM 5.33	3.95	3.88	0.60	0.03	1.21
NM 6.93	4.00	3.94	0.58	0.26	0.91
NM 7.46	3.90	3.88	0.42	0.20	0.80
PH 2.13	4.20	4.01	0.53	-0.48	1.50
PH 3.20	3.85	3.70	0.52	-0.33	2.30
PH 3.50	4.20	4.06	0.74	-0.33	2.00
PH 4.82	3.78	3.94	0.48	-0.34	1.89
PH 5.30	4.18	3.95	0.65	-0.33	1.98
PH 6.37	4.03	3.91	0.53	-0.48	1.45
MT 3.14	3.95	3.90	0.48	0.17	0.90
MT 4.06	4.00	4.90	3.76	0.25	0.90
MT 4.16	4.30	4.71	3.18	0.30	1.10
MT 4.31	2.30	2.46	0.70	0.29	1.10
HM 0.71	5.80	6.43	1.91	0.14	0.86
HM 1.93	3.80	3.76	0.52	-0.05	1.80
HM 3.56	3.50	3.53	0.38	0.21	0.61

Table 7.9 Distribution of analysed Holocene samples in the various areas studied among the nine classes of the CM diagram of Passega & Byramjee(1969).

		Number of samples in each class						
Area	**Samples**	**I**	**II**	**III**	**V**	**VII**	**VIII**	**IX**
Dalbeattie	45	0	0	1	0	17	26	1
Kirkcudbright	15	0	2	0	0	7	6	0
New Abbey	15	2	0	0	0	6	6	1
Lochar Gulf	35	4	2	10	3	14	2	0

CHAPTER 8

CLAY MINERALOGICAL STUDIES

8.1 Introduction

In this chapter a general account is given of the results of clay mineral analysis of samples of the Holocene raised coastal and present-day intertidal sediments from the four geographical areas of study. Aspects of the results that may throw light on the sources of the sediments and that may indicate differences in clay mineralogy attributable to changes in environmental conditions are discussed more fully in Chapters 10 and 11 below.

The clay minerals were examined and identified by X-ray diffraction (XRD) and Scanning Electron Microscopy (SEM).

8.2 Preparation techniques and methods of separation of clay minerals for analysis

All preparation techniques may modify clay minerals. Even such an apparently mild treatment as standing in water can modify smectites significantlty if they are left immersed for a long enough period. In addition, being silicates, clays are easily damaged by mechanical processes and, being very fine grained, with large surface areas, they may be modified by chemical treatments. All pre-treatments therefore must be as mild as possible, both physically and chemically (Brown & Brindley 1980, 306).

Preparation and pre-treatment of the oriented clay samples for X-ray diffraction were as follows (modified from Folk 1974; Hutchison 1974, 225-228; Thorez 1976, 1; Brown & Brindley 1980, 305-355).

1) Vigorous shaking of samples with distilled water to remove soluble salts that may cause flocculation of the clay particles. This procedure was applied several times, the distilled water being changed between periods of shaking.

2) After vigorous shaking for 10 to 15 minutes, until complete dispersion had occurred, the sand fraction was separated from the clay plus silt fraction by wet sieving through a 63μm sieve.

3) In samples where the silt plus sand fraction was rich in organic matter, 6% H_2O_2 (hydrogen peroxide) was added and the samples left overnight.

4) In a few samples, in which dispersion had not taken place, the dispersion agent sodium hexametaphosphate (Calgon) was added and the samples left overnight.

5) Distilled water was added to the silt plus clay fraction in a one litre cylinder and the solution was then stirred mechanically for 10 to 15 minutes.

6) Separation of the clay particles (< 2μm) from the silt fraction (2μm - 63μm) was achieved by repeated decantation from the water suspension, according to Stokes's Law.

7) Since clay minerals generally have a platy morphology and consequently readily develop a parallel-oriented arrangement, preparations of oriented clay samples were made on glass slides using pipette techniques. The glass slides were left undisturbed until they had dried at room temperature.

8) The thin, oriented air-dried clays were examined, using a Phillips diffractometer with Ni-filtered CU-Kα radiation. The goniometer scanning speed was 1 degree per minute for a few samples and 2 degrees per minute for the majority of the samples. The X-ray tubes were operated at 40 Kv and 20 mA.

9) Various treatments were used in order to identify the clay mineral species within the mixture of clay minerals:

(a) Samples were left as untreated, air-dried samples.

(b) Oriented samples were left overnight in ethylene glycol in an evacuated desiccator.

(c) Oriented samples were heated to 450°C for 3 hours.

(d) Some of the clay samples were heated to 600°C for 3 hours.

The laboratory procedural steps for clay mineral investigation are shown in Figure 8.1.

8.3 Identification of clay minerals by XRD

8.3.1 General points

Identification of clay minerals may be made by observation of their basal reflections produced by X-ray diffraction (cf. Brown 1961; Hutchison 1974, 128; Villumsen & Nielsen 1976; Thorez 1976; Brindley & Brown 1980, 305-359).

1) **Illite**

The term "illite" is used throughout this work as a collective name for all the 10 Å non-expanding clay material (muscovite, illite *sensu stricto*, biotite, phengite) (cf. Gaudette et al. 1966). Illite may be identified by the reflections at 10Å, 5 Å and 3.3 Å in untreated, glycolated and heated samples. Birkeland & Janda (1971) pointed out that illite may be identified by a sharp symmetrical (001) peak between 9.28 Å and 10.5 Å. The illite recorded by peaks between 10.1 Å and 10.5 Å may be slightly hydrated or randomly interstratified with small amounts of vermiculite or chlorite.

The shape of the basal reflection of illite can be used for an evaluation of the crystallinity. When the material is well crystallised, the (001) reflection at 10 Å is relatively narrow and symmetrical, as in muscovite. When the composite layers of illite are progressively and then intensively stripped of their original K^+, the shape of the (001) reflection becomes asymmetrical (Thorez 1976, 12). The intensity

ratio of (002)/(001) is proposed as a first approximation indicative of the Al_2O_3/FeO minus MgO content in the octahedral layer of illites (Esquevin 1969). From the low intensity of the (002) reflection at 5 Å and from a (060) determination it is possible to differentiate between illite and biotite (Stevens et al. 1987).

2) **Chlorite**

Chlorite displays a sharp symmetrical (001) peak between 13.81 Å and 14.2 Å and a peak near 7 Å that is commonly more intense than the (001). These peaks are not affected by ethylene glycol treatment or by heating to 550°C (Birkeland & Janda 1971; Thorez 1976, 31). Also, according to Thorez (1976, 31), degraded chlorite with unstable layer shows various forms of collapse that maintain the (001) reflections between 10 Å and 13 Å, and soil chlorite collapses or is decomposed at 450°C.

The small size and rather irregular crystallinity of the particles in clay-chlorite provoke some diffuseness of the reflections and the absence of some ordinarily weak reflections. Chlorites in which the number of octahedral positions occupied by Fe-ions does not exceed 30% show medium to strong intensities for the first orders of the (001) series (Brown 1961).

3) **Kaolinite**

Kaolinite is one of the dioctahedral layer silicates, which also include dicktite, nacrite and halloysite. This group, called kandites, can be identified by X-ray diffraction techniques, both as oriented aggregates and as random powder preparations. In oriented preparations, kandites are easily recognisable by their (001) sequence of harmonic reflections at 7 Å (001), 3.58 Å (002) and 2.37 Å (003). The (001) reflections are stable after glycolation; between 400°C and 450°C they show a slight decrease of intensity. After having been heated to 500°C, they are

suppressed from the X-ray pattern (Thorez 1976, 4). Almohandis (1984) pointed out that the reflections at 7.15 Å (001), 3.58 Å (002) and 2.37 Å (003) are the most diagnostic for kaolinite. These reflections disappear and collapse upon heating to 550°C. By heating, differentiation between kaolinite and chlorite is possible, although the identification of kaolinite in the presence of chlorite is difficult because of the overlapping of some of the (001) reflections. In the present work, the methods of Bradley (1954) and Biscaye (1965), which depend on the (002) reflection of kaolinite (3.58 Å), and may become resolved from the (004) of chlorite at 3.5 Å, were used. Also, heating to 550°C was used to differentiate between the two minerals. The reflections of kaolinite collapse and disappear upon heating to 550°C, whereas the reflections of chlorite are not affected on heating to 550°C.

4) Vermiculite

Vermiculite is identifiable at 14 Å in untreated and glycolated samples and, after heat treatment, at 10 Å. Thorez (1976, 26) indicated that the identification of vermiculite is often a difficult problem because of the mineral's variable behaviour upon treatment. He pointed out that normal naturally or artificially Mg-saturated vermiculite may be identified by the (001) reflection at 14 Å. Glycolated samples may be identified at 14 Å (001) and samples heated to 500°C at 9.6 Å to 10 Å, while desaturated vermiculite may be identified by (001) reflections at 14 Å. Expansion takes place after glycol treatment to give reflections at 10 Å when heated to 500°C. The vermiculite with hydroxyl interlayered materials, identifiable at 14 Å (001), is variable after glycol treatment and reflections move to between12 Å and 14 Å after heating to 500°C.

Vermiculite is identified by a (001) reflection between 13.5 Å and 14.5 Å that expands to less than 15 Å on glycolation and collapses to about 10 Å after heating

(Birkeland & Janda 1971). According to Walker (1961), true vermiculite can be positively identified only by its lack of expansion with glycol.

5) **Montmorillonite**

Montmorillonite shows one or more peaks between 12.00 Å and 12.80 Å or 13.39 Å and 15.23 Å. The peaks expand to 16 Å to 18 Å after the mineral has been placed in an ethylene glycol atmosphere at 80°C to 90°C for abouit 15 hours. After glycolation, the (001) peak is more clearly defined than the unglycolated (001) peak (Birkeland & Janda 1971). After glycol treatment, montmorillonite exhibits a series of basal X-ray peaks at 17 Å, 8.5 Å, 5.7 Å, 4.2 Å and 2.8 Å.

6) **Mixed-layer clays**

The mixed-layer clays encountered in the present work are mostly irregular (random) mixed-layer vermiculite-montmorillonite and/or montmorillonite-chlorite and rare mixed-layers of illite-chlorite. All the mixed-layer minerals were identified according to the methods described by Thorez (1976).

Table 8.1 shows the values in d(Å) of the characteristics of the series (001) of relevant clay minerals after various treatments.

8.3.2 Semi-quantitative determination of clay mineral composition

Without a scanning electron microscope equipped with chemical analysis facilities, quantitative analysis of a mixture of clay minerals in a complex is not yet possible, although several methods have been used to calculate the percentage of each clay mineral in a mixture (e.g. recently Villumsem & Nielsen 1976; Parker et al. 1983; Gold et al. 1983; Pederstad & Jørgensen 1985).

X-ray diffraction cannot be used directly as a measure of a clay mineral's abundance because of variations between diffractograms, crystallinity of the minerals and chemical composition of different samples of the same mineral. However,

comparisons of clay minerals from sample to sample have been made by examining the ratios of peak areas, and this method has been used to show changes in clay mineral distribution. Correction factors have been given by Bradley (1953), Johns et al. (1954), Weaver (1958), Biscaye (1965), Jørgensen (1965) and Pederstad & Jørgensen (1985).

The relative proportions of the clay mineral species examined in the present project were determined from the peak areas in the X-ray diffractograms. The relative clay mineral contents were determined as follows:

1) The peak area of the 3.3 Å untreated sample was compared with the 3.57 Å peak after heating of the sample to 450°C, to give the relative amounts of illite and kaolinite.

2) In the clays analysed during the project, chlorite and vermiculite were both present in the same sample. The value given by twice the peak area of the 10 Å untreated reflection of illite was compared with the peak area of the 14 Å reflection after heating to 450°C, to give the relative amounts of illite and chlorite. After heating to 450°C, the intensity of the 14 Å reflection decreases because of the disappearance of vermiculite. The difference between the peak areas of the 14 Å reflection before and after heating gives the peak area for vermiculite. This difference may be compared with the value of three times the peak area of the 10 Å untreated reflection, to give the relative amounts of vermiculite and illite (Pederstad & Jørgensen 1985).

3) The glycolated peak area of the mixed-layer minerals (montmorillonite-chlorite or montmorillonite-vermiculite) 15 Å to 17 Å was compared with the value of 3.5 times the peak area of the 10 Å glycolated peak of illite, to give the relative amounts of the mixed-layer minerals and illite.

4) To cover the possibility of the presence of montmorillonite, which is very rare,

the peak area of the 17 Å glycolated montmorillonite was compared with the value of four times the 10 Å peak area of the glycolated illite, to give the relative amounts of illite and montmorillonite (Johns et al. 1954).

In addition to the previously-described method of calculation of the percentage clay mineral composition of the Holocene and present-day intertidal clays studied, the relative abundances of identified clay minerals were estimated semi-quantitatively on the basis of the intensity and width of the deflection peaks (Taggart & Kaiser 1960; Carroll 1970; Carver 1971). The abundance of the clay minerals is expressed in semi-quantitative terms including, in order of decreasing abundance: major, abundant, common, minor, trace and absent (Tables 8.7 to 8.10). This method was used to give an indication of the distribution of the clay minerals both laterally and vertically, and to compare the results so obtained with those obtained by the quantitative percentage method described above.

8.4 Clay mineral distribution

Clay mineral distribution in the four areas studied is shown in Tables 8.2 to 8.5. Maxima, minima, means and standard deviations for the values shown in these tables are given in Table 8.6.

8.4.1 Dalbeattie area

(a) Holocene raised coastal sediments

Eight types of clay minerals were recognised in the Holocene raised coastal sediments in the nine vertical sections studied in this area (Figs. 8.2 and 8.3; Tables 8.2 and 8.7). The distribution of these clay minerals reflects lateral and vertical changes in the clays of the various facies of the Holocene coastal sediments (Chapter 5).

Illite (major to abundant), chlorite (major to common), kaolinite (common to minor) and vermiculite in variable amounts (abundant to trace or absent), montmorillonite (trace or absent) and mixed-layer clays, dominantly of montmorillonite-chlorite or montmorillonite-vermiculite, are present in most of the samples studied. Illite-chlorite mixed-layer clays are present in one sample at the top of section D6. The mixed-layer clay minerals are not found in section D5, which represents sediments deposited in a lagoonal environment separated from the sea by Pleistocene glaciofluvial deposits and Holocene estuarine fine-grained sediments of facies A (Chapter 5.3.2.1). The mixed-layer clays, montmorillonite-chlorite or montmorillonite-vermiculite, are absent in section D9, and the clay minerals in that section are, in order of decreasing abundance, illite, chlorite, vermiculite and kaolinite. The sediments in that section are thought to have been deposited in conditions similar to those that led to deposition of the sediments in section D5.

(b) Present-day intertidal sediments

Four types of clay minerals were recognised in the analysed samples of present-day intertidal sediments of the Dalbeattie area: illite (major to abundant), chlorite (major to common), kaolinite and vermiculite (in variable amounts) (Fig. 8.4; Tables 8.2 and 8.7).

8.4.2 Kirkcudbright area

(a) Holocene raised coastal sediments

Six clay minerals were recognised in the clay fraction of samples collected from the Holocene raised coastal sediments of the Kirkcudbright area (Fig. 8.5). The clay minerals recognised were illite (major to abundant), chlorite (major to trace), kaolinite (common to minor), vermiculite (abundant to absent) and mixed-layer clays represented by montmorillonite-chlorite and/or montmorillonite-vermiculite

(abundant to absent) (Tables 8.3 and 8.8).

(b) Present-day intertidal sediments

Three main clay minerals were recognised in the clay fraction of sediments collected from the surface of the intertidal zone of the River Dee at low water. The clay minerals recognised were: illite (major), chlorite (common to minor) and kaolinite (abundant to common). Vermiculite (minor to trace, in two samples only) and montmorillonite (trace in one sample) were also detected (Fig. 8.6; Tables 8.3 and 8.8).

8.4.3 New Abbey area

(a) Holocene raised coastal sediments

Six clay minerals were recognised in the clay fraction examined from two selected vertical sections, N5 and N6. The dominant clay minerals in section N5 were illite (major to abundant), chlorite (major to common), vermiculite (common to trace) and kaolinite (major to absent). Mixed-layer clays of montmorillonite-chlorite and/or montmorillonite-vermiculite were also recognised. The clay minerals recognised in section N6 were illite (major to abundant), kaolinite (major to common), chlorite (abundant to common) and vermiculite (minor; common in one sample). Montmorillonite-chlorite and/or montmorillonite-vermiculite (common to trace) were also identified (Fig. 8.7).

From Tables 8.4 and 8.9 it may be inferred that there is both vertical variation in clay mineral content in the sections studied (N5 and N6) and lateral variation in the nature and abundance of the clay minerals.

(b) Present-day intertidal sediments

Three clay minerals were recognised in the clay fraction of the present-day

surface sediments of the intertidal zone near the mouth of New Abbey Pow: illite (major), chlorite (abundant) and kaolinite (minor) (Tables 8.4 and 8.9).

8.4.4 Lochar Gulf area

Six clay minerals were recognised in the clay fraction of samples of Holocene raised coastal sediments from part of the Northpark borehole (NY 0372 6685) of the Lochar Gulf area: illite (major), chlorite (abundant to common), kaolinite (common to trace), vermiculite (minor to absent), mixed-layer illite-vermiculite (minor, in one sample) and mixed-layer montmorillonite-vermiculite (minor, in one sample) (Table 8.5 and 8.10).

Four clay minerals were recognised in the sections at South Kirkblain (NY 0269 6956) and Bankend Bridge (NY 0291 0647) (Fig. 8.8): chlorite (major to absent), illite (major to abundant), kaolinite (abundant to common) and vermiculite (major to minor).

Three clay minerals were recognised in the clay fraction of samples from the Midtown borehole (NY 1189 6577), Highlandman's Pool section (NY 0447 6692) and Horseholm borehole (NY 0313 7062): illite (major), chlorite (abundant) and kaolinite (trace). Few of the samples from these locations contained clay minerals because of the sandy nature of the sediments at these sites.

8.5 Scanning Electron Microscopic (SEM) studies of the clay minerals

Scanning of twenty selected samples from the Holocene raised coastal sediments from the four geographical areas studied was carried out. The purposes of the scanning were to:

1) Show the morphological features of the clay minerals under high magnification.

2) Differentiate between authigenic and detrital clay minerals.

3) Examine the clay particles by energy dispersion X-ray spectrum analysis (EDX) to yield characteristic peaks that show the composition of the clay minerals, and thus lead to identification of the clay mineral species and the associated elements within the clays.

Many studies of clay minerals by SEM have been made (e.g. Bohor & Hughes 1977; Welton 1984; McHardy & Birnie 1988). In the present study, the scanning and EDX were carried out using a Cambridge S360 SEM with integrated Link AN 10,000 series EDX analyser. All the analysed samples were coated in gold.

Occasionally, it was found that the features of the clay minerals could not be identified clearly and, therefore, the morphology of the clays could not be determined. This may have been due to the mixing of clay flakes and to the presence of mixed-layer clays, which can cause covering of particles. In such cases, it was concluded that XRD is more helpful than SEM in clay mineral identification.

Most of the clay minerals identified by XRD were recognisable on the bases of their morphology under SEM analysis and peak compositions shown by EDX analysis.

The clay minerals identified by SEM were as follows:

1) Illite

Both detrital and authigenic illite were identified. The detrital illite (Plate 8.1) is characterised by irregular flake platelets oriented parallel to each other. Occasionally, authigenic illite or chlorite is also recognisable within these flakes of illite.

The authigenic illite is mostly filamentous in morphology (Plate 8.2) and occurs in association with kaolinite or chlorite. This may be due to diagenetic transfer of other clay minerals to illite.

Authigenic and detrital illite can readily be differentiated on the basis of morphology.

The EDX spectrum peaks for detrital and authigenic illite are distinctly different from the peaks for other clay minerals. They resemble each other except in the amounts of Fe and Ti that are present. Representative EDX spectrum peaks for illite are shown in Figure 8.9.

2) Chlorite

It was found that both detrital and authigenic chlorite is present. The detrital chlorite mostly formed face to face particles or parallel flakes, and kaolinite was present in association with the chlorite (Plate 8.3).

Authigenic chlorite, which was common, mostly had a rosette morphology (Plate 8.4). Representative EDX spectrum peaks for the chlorite particles (Figs. 8.10 and 8.11) show that most of the chlorites examined are rich in Fe and the amount of Mg is low. Also, Ti was associated with chlorite in variable amounts.

3) Kaolinite

Kaolinite recognised in the clays was mostly detrital in origin, and was without clear morphology. Some authigenic kaolinite was identified, arranged in stacked plates with face to face structure. The kaolinite particles appeared to be intermixed with other clay minerals, especially mixed-layer clays.

The EDX spectrum peaks (Fig. 8.12) show the typical composition peaks for kaolinite, in addition to peaks for Fe, which may be related to mixed-layer clays.

4) Smectite

Smectite, in association with other clay minerals, was detected in the form of mixed-layer clays in most of the samples studied.

8.6 Genesis of the clay minerals

8.6.1 Introduction

Prior to commencement of this project, there were no detailed clay

mineralogical studies of Holocene raised coastal sediments in Scotland; studies of unconsolidated rock material were concerned mainly with clay minerals in the soil. On the basis of analyses carried out over the last 40 years (e.g. Mitchell 1955, MacKenzie 1965; Wilson 1966; 1970; 1971; 1973; 1976), it has been concluded that the types of clay minerals found in Scottish soils are dependant largely on the parent materials and drainage classes of the soils. Thus, significant differences have been noted between soils developed on basic igneous rocks on the one hand and on granitic and certain kinds of metamorphic rocks on the other. Soils of the former group are characterised by a predominance of vermiculite or montmorillonite and soils of the latter group by a predominance of illite (Wilson et al. 1984).

Limited analysis of soils developed on raised estuarine sediments in south-western and other parts of Scotland suggest that the most abundant clay minerals in these soils are smectite-illite interstratified clays, illite and kaolinite, with chlorite occuring widely but in small amounts (Wilson et al. 1984). As shown in Tables 8.2 to 8.5, the main clay minerals recognised in the present study were crystalline to weathered illite, chlorite, kaolinite and vermiculite. There were also minor amounts of montmorillonite and irregular mixed-layers of montmorillonite-chlorite and/or montmorillonite-vermiculite and rare mixed-layers of illite-vermiculite.

The genesis and behaviour of each of the clay minerals recognised in the clay fraction (< 2μm) of the samples studied in the course of the project are discussed below.

8.6.2 Illite

According to Weaver & Pollard (1973), illite is relatively stable, and therefore is presumed to be formed, in an environment where the waters have a high

K/H^+ ratio. In addition, Macchi (1987) noted that illite can be produced by reaction between pyrophyllite and K-feldspar:

$$Al_2(Si_8O_{20})(OH)_4.nH_2O + KAlSi_3O_8 \text{ ----------> } KAl_4(Si_7AlO_{20})$$

pyrophyllite K-feldspar illite

Further, Stevens et al. (1987) suggested that mica minerals may all be represented by the 10 Å reflection in X-ray diffraction but, from determination of the (060) reflection and the intensity of the (002) reflection, it may be possible to differentiate between different types of mica. He suggested that all the minerals of this group are formed in regional crystalline bedrocks and can be derived by simple mechanical weathering. From the observations made by Macchi (1987) and Stevens et al. (1987), it may be suggested that the high percentage of illite in the clays of the areas studied in the course of this project may be related to the high concentration of mica in many of the rock types that form the bedrocks in these areas.

Settling tendencies of illite and other clay minerals in saline waters are discussed by Whitehouse et al. (1960), and the stability of illite in different environments has been discussed by many authors. Powers (1957) suggested that illite alters to chlorite in saline waters, and Karlin (1980) reported that illite and chlorite are abundant components of marine sediments, illite being more abundant in marine than freshwater sediments. In a study of the Pamlico estuarine sediments, Edzwald & O'melia (1975) found that amounts of illite are minor in the upper reaches of the river but increase towards the mouth of the river, where the salinity is high. They claimed that illite can be shown to be a stable clay undergoing particle aggregation. Also in relation to the fluvial-estuarine environment, Nelson (1960) suggested that illite may be expected to aggregate more slowly than kaolinite and be deposited downstream, whilst Griffin & Ingram (1955) found that illite and chlorite

occurred at the lower end of an estuary.

In the present work, illite was found to be the dominant clay mineral in most of the samples studied; both detrital and authigenic illite were present. The crystallinity, diagenesis and weathering of the illite are considered below on the basis of calculation techniques suggested by several authors.

Intensity ratios of the (001) and (002) reflections, i.e. $I_{(001)}/I_{(002)}$, are greater than 3.00 in the majority of the samples (Table 8.11), indicating that most of the illite is dioctahedral and Fe-rich (Grim et al. 1951; White 1962). Also, values obtained for the intensity ratio $I_{(002)}/I_{(001)}$ (Table 8.11) suggest that the 'illite' in the samples studied has the composition of biotite, muscovite and phengite (Esquevin 1969). In addition, since most of the samples show an asymmetry of the (001) reflection towards the low angle side, it may be concluded that there is transition of the illite to the mixed layer systems (Reynolds & Hower 1970; Kodoma et al. 1969).

On calculating the crystallinity of illite according to the method of Donoyer de Segonzac (1970) (Table 8.11), it was found that there is variation in the crystallinity within the deposits studied in vertical sections. In section D6 of the Dalbeattie area, the illite is poorly crystalline in what Donoyer de Segonzac called the sedimentation and diagenetic zones (Fig. 8.13). In section D9, also in the Dalbeattie area, all the illite is well crystallised and is present in the anchizone.

Figure 8.13 shows the characteristics of illite in selected vertical sections within the study areas on the basis of the crystallinity index (or acute index) and the $Al_2O_3/FeO + MgO$ composition of the octahedral layer. Evolution of the crystallinity and of the composition of the illite takes place from the diagenetic or weathering zone towards the epizone. It may be concluded from this diagram that the degree of crystallinity is variable, and the $I_{(002)}/I_{(001)}$ ratio indicates that the Holocene raised coastal sediments have been affected by diagenesis in varying degree. The

majority of the illite minerals have the composition of biotite and muscovite, with lesser amounts of illite (*sensu stricto*) and phengite, suggesting that the source rocks contained illite and mica minerals. The present-day intertidal surface sediments show differences in the crystallinity index of illite from one area to another, but the illite present has octahedral layer composition and is composed of biotite or muscovite mica except in one sample, which is of phengite.

A more general conclusion is that the illite in the present-day intertidal sediments is more crystalline than the illite in the Holocene raised coastal sediments, perhaps because the illite in the present-day sediments has been subjected to less weathering than the Holocene sediments.

8.6.3 Chlorite

Edzwald & O'melia (1975) stated that chlorite minerals are abundant components of marine sediments, whilst Kantorowicz (1984) stated that chlorite and interstratified chlorite-vermiculite occur in non-marine sandstones, either together or in isolation. Chlorite may occur in either saline or fresh depositional pore water or during burial of sediments. Fe-chlorite formation requires reducing conditions. Biscaye (1965) reported that chlorite occurs as a widespread primary constituent of rocks of low-grade metamorphism and in shales as a product of weathering of other clay minerals such as illite (cf. Jackson 1959, 136; Quigley & Martin 1963). Several workers have suggested that chlorite may form by alteration of other land-derived minerals in marine environments (Grim et al. 1949; Grim & Johns 1954; Powers 1954; Griffin & Ingram 1955).

Griffin & Ingram (1955) reported that a chloritic mineral similar to the chlorite in an estuary is present in the lower part of the river entering the estuary. They suggested that this chlorite was formed in an estuarine environment, either in

the present estuary and washed upstream during times of high winds, or in a former enlarged part of the estuary. Downstream within the estuary, chlorite increases relative to kaolinite. According to Griffin & Ingram (1955), the formation of chlorite and illite may be explained in several ways. The two-layered kaolinite being introduced into the estuary may be changed to three-layered chlorite or illite by the addition of a silicon sheet to the kaolinite or by the breakdown of the kaolinite in the marine environment and re-arrangement of the material into chlorite or illite. Much of the material that is amorphous to the X-ray may be degraded soil washed into the river and its estuary. It may form the three-layered structures that are re-arranged in the marine environment.

Donoyer de Segonzac (1970) suggested that chlorites produced from the three-layered clay minerals are unstable under two conditions: 1) in highly leached surficial environments, and 2) under temperatures and pressures higher than those present in the epizone.

Millot (1970, 305) stated that illite and chlorite are common inherited detrital minerals in many soils and sediments. These minerals will be stable during weathering that is mainly physical in character, in poorly drained soils of modest chemical activity, in sediments deposited in alkaline water and in the course of alkaline diagenesis.

During their studies of clays in Scottish soils, Wilson et al. (1984) suggested that chlorite occurs in minor amounts, particularly in granitic soils in eastern Scotland and in the Dalbeattie area. They also suggested that chlorite and vermiculite occur occasionally in soils derived from glaciofluvial deposits and raised beaches..

In the present project, chlorite minerals were found to occur in most of the vertical sections studied, as a mineral second in abundance after illite. Amounts varied from one section to another and there was a clear change in amount from the base to the

top in the same section. From calculated chlorite amounts (Tables 8.2 to 8.5), it is concluded that chlorite is more abundant in samples of Holocene raised coastal sediments and present-day intertidal sediments from the Dalbeattie area than in samples from the other areas. Generally, there is less chlorite in the topmost parts of the sections studied than in the lower parts. The chlorite minerals detected in the present work are mostly detrital in origin. A few are authigenic.

It was noted in most of the sections that, when chlorite decreased, vermiculite increased, an observation that agrees with that of Wilson et al. (1984), who suggested that chlorites in surface horizons (of soils) tend to be altered to vermiculite.

Varieties of chlorite and their recognition from the character of the basal peaks obtained by XRD have been discussed by several authors (e.g. Bayliss 1975; Thorez 1976, 31-32; Brindley & Brown 1980, 340). In the present study, observation of peak intensities and changes produced by various treatments showed that Fe-chlorite is dominant, with Mg-chlorite occasional and swelling chlorite rare.

8.6.4 Kaolinite

The genesis of kaolinite has been discussed by many authors. According to Keller (1958a), Millot (1970) and Donoyer de Segonzac (1970), kaolinite is a product of weathering and soil formation under strong acid leaching conditions (e.g. it is common in granitic soils; Wilson et al. 1984). Weaver (1959), Wilson & Pittman (1977) and Karlson et al. (1979) noted that kaolinite is common in sedimentary rocks and is a typical mineral in the alteration of acidic rocks (cf. Stevens et al. 1987).

Birkeland & Janda (1971) reported that kaolinite is commonly associated with montmorillonite minerals, whilst McMurty & Fan (1974) noted that the percentages of montmorillonite and kaolinite are higher when sedimentary cover is

greater than 50%, and when it is less, the percentage of mica is higher. Montmorillonite and kaolinite are closely associated with Quaternary and older sediments and probably formed from feldspar and non-micaceous ferro-magnesian minerals, although they also form from mica.

As regards the stability of kaolinite, Edzwald & O'melia (1975) claimed that kaolinite is dominant at the upper end of an estuary where salinity is least, and decreases in abundance towards the mouth. Previously Griffin & Ingram (1955)(see also Chapter 8.6.3 above) had suggested that kaolinite is the dominant clay mineral in the freshwater part of an estuary, and they had further suggested that when the two-layered kaolinite is introduced to the estuary it can be changed into three-layered chlorite or illite by the addition of a silica sheet to the kaolinite or by the breakdown of the kaolinite in the marine environment. Donoyer de Segonzac (1970) showed that kaolinite is very sensitive to the geochemical environment; the mineral is stable in acidic conditions and unstable in alkaline conditions. The same author suggested that most of the kaolinite in marine sediments is detrital in origin and may be used as a palaeogeographical indicator of climate and shoreline position. According to Keller (1968), some kaolinite is produced by diagenetic transformation of illitic clays in the presence of acidic waters containing high concentrations of organic material. Grim (1968, 530) reported that kaolinite is present in marine sediments but less abundant than illite. The abundance of kaolinite increases close to the shore.

Kaolinite is one of the dominant clay minerals in the samples analysed from the four areas studied in the course of the research project. In the Dalbeattie area, changes in the abundance and crystallinity of kaolinite are apparent in each of the vertical sections that were sampled (Figs. 8.2 and 8.3). In section D6, the kaolinite has well developed crystallinity and is dominant in the topmost samples, and crystallinity and abundance decrease with depth. In section D9, important changes in

crystallinity and abundance of the kaolinite occur, whilst in section D5, which represents a lagoonal environment, the crystallinity of the kaolinite is moderately to well developed in the top samples and the abundance decreases and the crystallinity becomes moderate to poor in the basal samples.

Kaolinite is also abundant and the crystallinity is moderately to well developed in samples analysed from the present-day intertidal zone in the Dalbeattie area (Fig. 8.4).

In the Kirkcudbright area, kaolinite is common to moderate in abundance in sections K1 and K2 (Fig. 8.5 and Table 8.3); it is most common in samples from near the top of the sections, and decreases in abundance with depth. The crystallinity of the kaolinite is moderate to poor in samples from near the top of the sections, but improves with depth, the crystallinity in samples from the base of the sections being well developed. The amount of kaolinite in section K4 is less than in sections K1 and K2 - minor to common near the top of the section, becoming minor at the base. Crystallinity of the kaolinite is poor to moderate near the top and becomes well developed at the base of section K4 .

Kaolinite is abundant in samples from the present-day intertidal surface zone in the Kirkcudbright area, and the crystallinity is well developed (Fig. 8.6; Table 8.3).

In the New Abbey area, samples from sections N5 and N6 (Fig. 8.7) were examined. The amount of kaolinite varies vertically in each of the sections studied, but in general the mineral is always moderately to poorly crystalline, the crystallinity being better developed in the lower part than in the upper part of the sections. Kaolinite is dominant in the topmost samples in both sections, decreases in abundance at about 2m below ground level, increases around 2.9m below ground level and decreases again in abundance near the base.

Kaolinite is dominant in present-day surface sediments in the New Abbey area, crystallinity being moderately to well developed.

In the area of the former Lochar Gulf, kaolinite is common in samples from near the top of the sections at South Kirkblain (SK) and Bankend Bridge (BB)(Fig. 8.8), becoming minor to trace with depth; crystallinity is moderate. Samples from the Northpark and Midtown boreholes contain minor amounts to traces of kaolinite. It should be noted, however, that all the samples analysed from these two sites were obtained from depths greater than 2m below the ground surface.

8.6.5 Vermiculite

Experimentally, it has been found that biotite, particularly phlogopite, is altered to vermiculite with the interlayer K^+ being substituted by Mg^{++} and *vice versa* (Barshad 1948). In podzol soil profiles, biotite may be completely transformed to hydrous mica and then to vermiculite (Walker 1947; 1949; 1950).

The formation of vermiculite from chlorite has been described by Jørgensen (1965). The process was assumed to be an exchange between Mg from the brucite layer and protons in exchangeable position. Walker (1961) assumed that the vermiculite was always of secondary origin, formed by the alteration of rock-forming mica, pyroxene, amphibole, chlorite and feldspar. Most vermiculites are trioctahedral and form by alteration of trioctahedral micas and chlorites. The original layer charge on the mica or chlorite may be reduced slightly during the alteration to vermiculite by oxidation of octahedral ferrous iron or by hydroxylation of oxygen to OH. Fine-grained vermiculite in soils and sediments may be either trioctahedral or dioctahedral. Dioctahedral vermiculite presumably forms primarily by alteration of dioctahedral illite (Brindley & Brown 1980, 98).

In the present work, the vermiculite generally is abundant to common, but is present in minor amounts or is absent in some samples from the Holocene sediments and present-day intertidal surface sediments of the Dalbeattie area. In the Kirkcudbright and New Abbey areas, vermiculite is common to absent in the Holocene raised coastal sediments, whilst in the present-day intertidal sediments it is very rare or absent. In the Lochar Gulf area, the amount of vermiculite varies from section to section.

From the analyses, it is concluded that the amount of vermiculite present varies inversely with the amount of chlorite present. Vermiculite appears to be a diagenetic product of alteration of chlorite and illite.

8.6.6 Mixed-layer clay minerals

Mixed-layer clay minerals are clay minerals in which different kinds of layers alternate with each other. According to Millot (1970, 15-18), there are various types of mixed-layer structures: regular, irregular or segregation of alternating packets. The same author stated that there are intermediate layers or mixed minerals or structures that are intermediate between the original clay mineral and the new mineral (Millot 1970, 101).

The origin of mixed-layer clays probably is a transitional stage in the transformation of illite or chlorite into mixed-layer clays and then into montmorillonite (Millot 1970, 108):

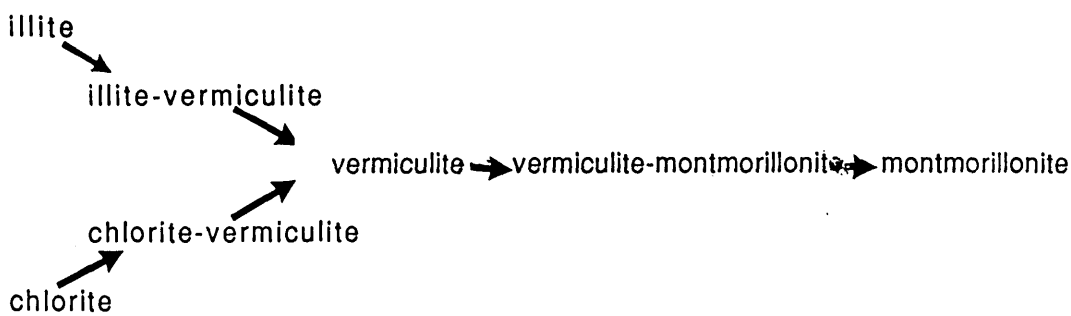

In the present work, mixed-layers of vermiculite-montmorillonite and/or chlorite-montmorillonite were recorded in most of the Holocene raised coastal sediments but were very rare in the Lochar Gulf samples. Mixed-layer clays were identified in the present-day intertidal sediments.

It was also noted that traces of minor mixed-layers of illite-vermiculite or illite-chlorite were present in a few of the samples studied. Most of the mixed-layer minerals present were random or irregular mixed-layer varieties.

8.6.7 Montmorillonite

Montmorillonite is known to be formed by degradation of micas during weathering. Also, subaqueous weathering of acid volcanic ash usually produces montmorillonite.

In the present study, montmorillonite or montmorillonite-like minerals were observed in trace or minor amounts, and with very poor crystallinity, in a few samples from the sections studied in the Dalbeattie area.

8.7 Variation in the vertical distribution of clay minerals

The relative abundance of the various clay minerals in the Holocene sediments of the areas studied leads to recognition of the following points:

1) Dalbeattie area (Figs. 8.14 and 8.15)

Generally, illite is the major clay mineral from the base to the top of the sections studied. There is no clear change in its abundance from base to top. Chlorite increases from the top to the base, whilst vermiculite is more abundant at the top and decreases in abundance with depth. Occasionally, vermiculite is abundant at the contact between the Holocene sediments and the underlying Pleistocene deposits.

Kaolinite increases from the top to the base in some sections (e.g. D5), but shows no trend in others.

2) Kirkcudbright area (Fig. 8.16)

Illite increases in abundance from top to base. Similarly, chlorite is more abundant in the lower part of the sections studied (fine sand facies) than in the upper part (clayey silt facies), whilst vermiculite is abundant near the top and decreases with depth. The amount of kaolinite present is small, but it shows an increase from the top to the base of the sections.

3) New Abbey area (Fig. 8.17)

Chlorite is the main clay mineral in the lower part of the sections, but it decreases in abundance upwards. Illite varies in abundance through the sections, but it is the major clay mineral in the upper part (clay silt facies). Kaolinite varies in abundance, being major to abundant in the uppermost facies, decreases in the middle facies (inter-laminated fine sand and silt), and increases in the lowermost facies (fine sand).

4) Lochar Gulf area (Fig. 8.18)

In the Northpark borehole, illite is the major clay mineral. It decreases slightly in abundance with depth. Chlorite, also decreasing in abundance with depth, is the most dominant clay mineral after illite. Vermiculite and kaolinite, present in small quantities only, increase slightly in abundance with depth.

From the above, it is concluded that the clay mineral species vary in abundance from the base to the top of the sections studied. This variation may be caused by diagenesis of the clays, as chlorite transforms to vermiculite under diagenetic conditions and mixed-layer minerals (also present in the deposits sampled in the vertical sections) represent a mid-stage in the diagenesis of clays. Another reason for the variable abundance of clay mineral species may be changes in environmental

conditions. This is suggested by the correlation that appears to exist between the distribution of the clay minerals and the succession of sedimentary facies present in the sections studied.

8.8 Conclusions from the clay mineral studies

The clay mineral studies suggested the following conclusions concerning the Holocene raised coastal sediments and present-day intertidal sediments:

1) The main clay mineral species present in the Holocene raised coastal sediments are, in descending order of abundance, illite, chlorite, kaolinite, vermiculite and mixed-layers of various clay species. Very small amounts of montmorillonite are also present.

2) Semi-quantitative determination of clay compositions indicated that clay mineral abundance varies from one vertical section to another in the Holocene sediments, there being a noticeable relationship between change in sedimentary facies and change in clay-mineral abundance.

3) The main clay mineral species present in the present-day intertidal sediments are, in descending order of abundance, illite, chlorite, kaolinite and vermiculite. Montmorillonite and mixed-layer clays are rare or absent in these sediments.

4) Illite is more abundant in the Holocene than in the present-day intertidal sediments.

5) Illite is of variable crystallinity in both the Holocene and present-day sediments. This may be due to different sources or the effects of diagenesis and/or it may reflect the presence of both detrital and authigenic illite (detected in SEM and EDX studies).

6) The crystallinity index for illite suggests that the illite present in the analysed

samples has the composition of biotite and muscovite.

7) The fact that illite is the most abundant clay mineral in the sediments may be due to the large amounts of mica in the source rocks and to alteration effects in the environments of deposition.

8) SEM and EDX studies showed that both detrital and authigenic chlorite are present in the sediments studied. This may be due to both the effect of provenance and the environmental conditions of formation of the sediments.

9) SEM and EDX studies showed that most of the chlorites are rich in Fe.

10) Kaolinite is present in all the samples studied. As shown by SEM and EDX studies, it is mainly detrital, but small quantities of authigenic kaolinite are present.

11) The crystallinity of the kaolinite varies from poorly-crystalline to very well developed forms.

12) The kaolinite may have been derived from K-feldspar that was present in the source rocks.

13) Vermiculite is present in most of the samples studied, increasing in amount near the top of most of the Holocene sections. The vermiculite is thought to be mainly an alteration product, derived from other clay minerals in both the Holocene raised coastal sediments and present-day intertidal sediments. The abundance of vermiculite varies inversely with the abundance of chlorite.

14) The mixed-layer clays are common in most of the Holocene sediments, but rare or absent in the present-day intertidal sediments.

15) The montmorillonite, present in only a few samples in the Holocene raised coastal sediments in the Dalbeattie area, may have formed by degradation of micas during weathering.

16) In terms of vertical variation of clay mineral contents in the sections of

Holocene raised coastal sediments studied, the following points were noted: illite is common and shows no clear variation in abundance from the base to the top in most sections; chlorite generally decreases from the base towards the top in most sections studied, especially in the Kirkcudbright and New Abbey areas; vermiculite is generally low in abundance in the lower part of sections and its abundance increases towards the top; kaolinite shows no clear trend in most of the sections studied.

17) From EDX studies it was found that Ti is associated with most of the clay minerals that are present.

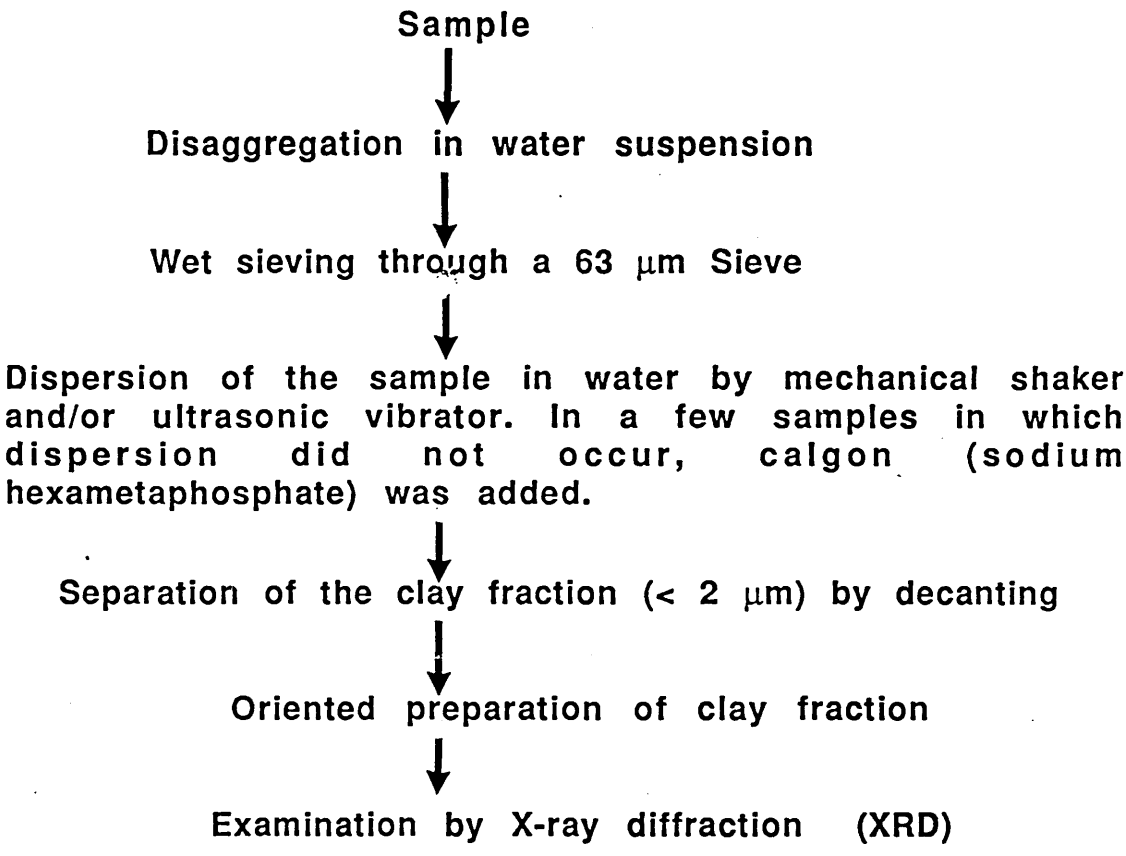

Figure 8.1 Laboratory procedure for clay mineral separation and investigation by X-ray diffraction.

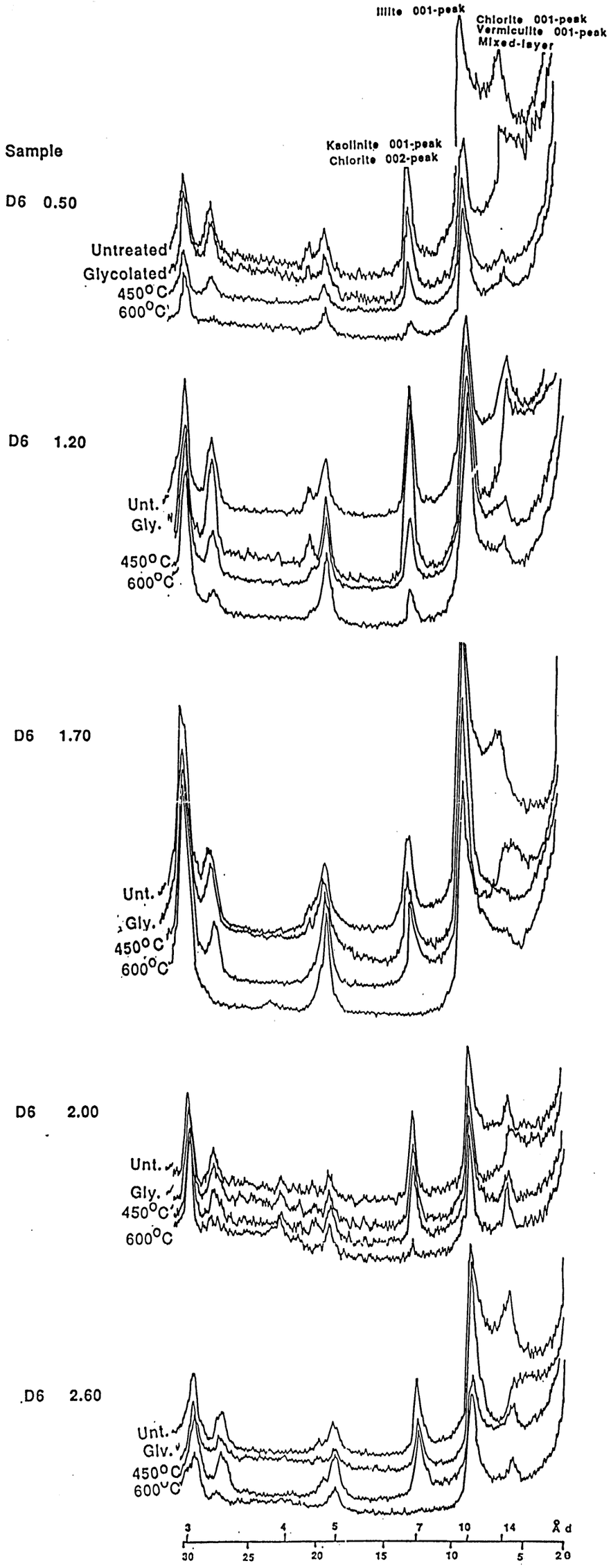

Figure 8.2 XRD diffractograms for oriented samples of the clay fraction (< 2μm) of the Holocene raised coastal sediments in section D6, Dalbeattie area.

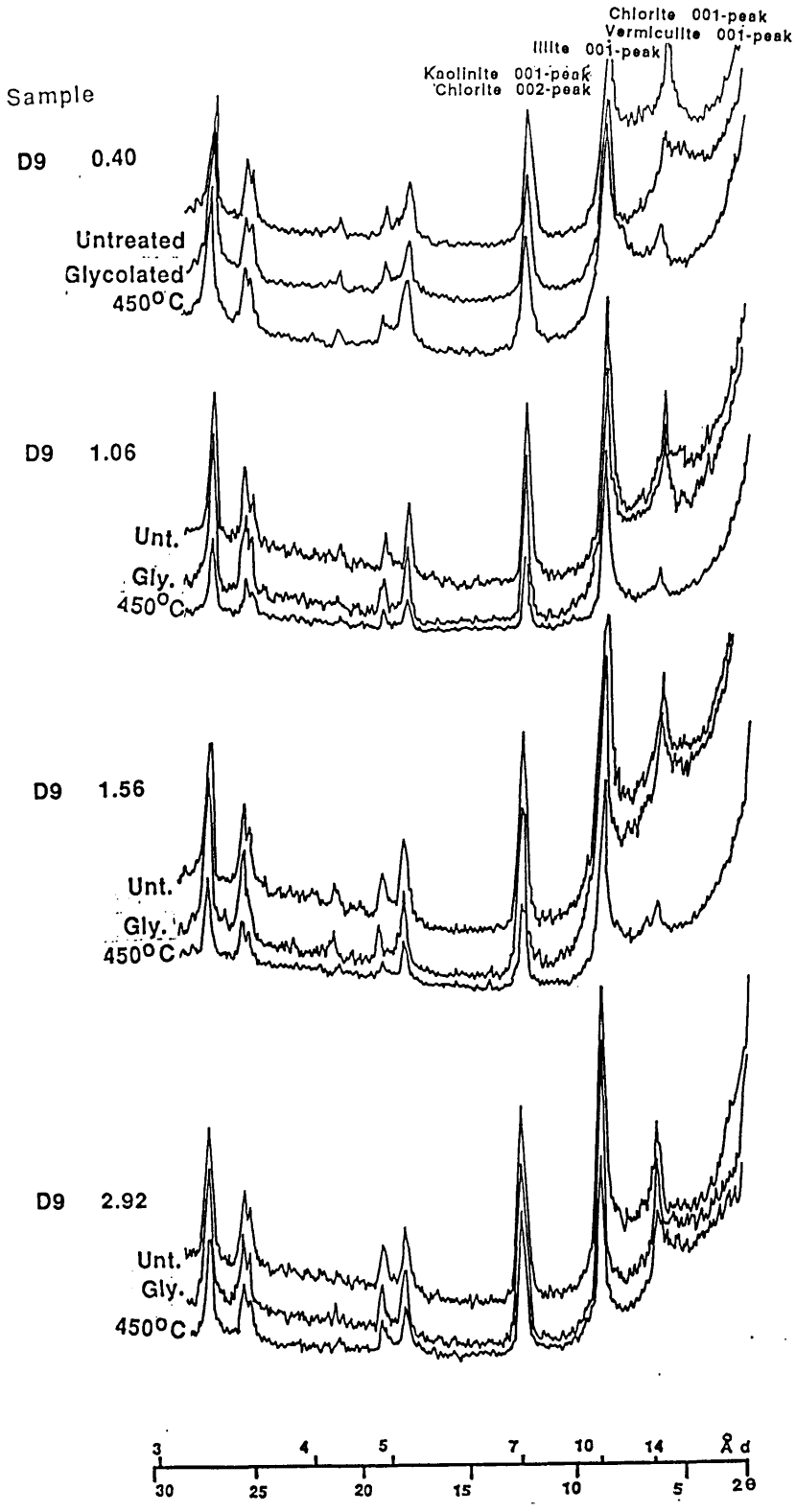

Figure 8.3 XRD diffractograms for oriented samples of the clay fraction (< 2μm) of the Holocene raised coastal sediments in section D9, Dalbeattie area.

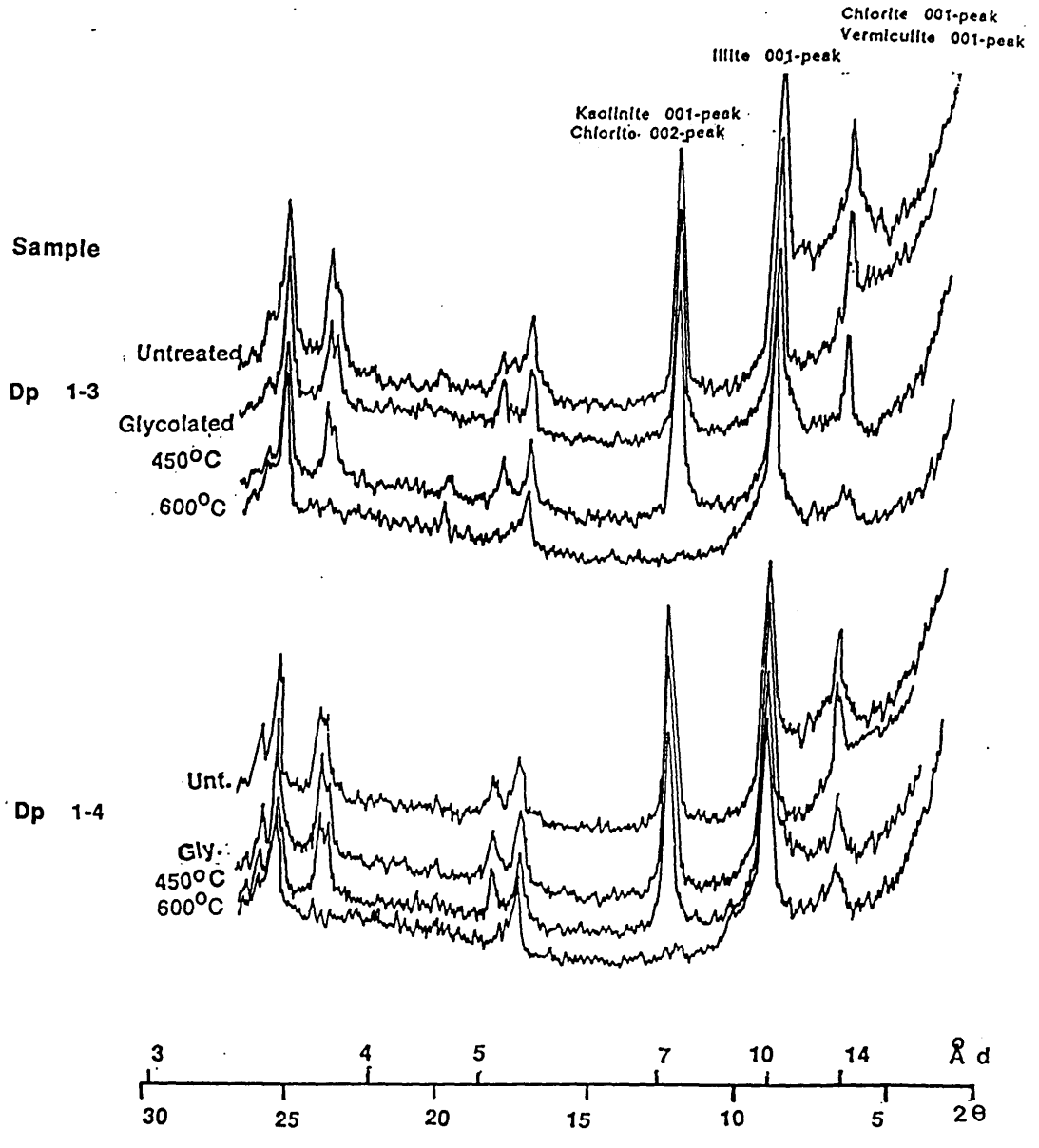

Figure 8.4 XRD diffractograms for oriented samples of the clay fraction (< 2μm) of present-day sediments in the Dalbeattie area.

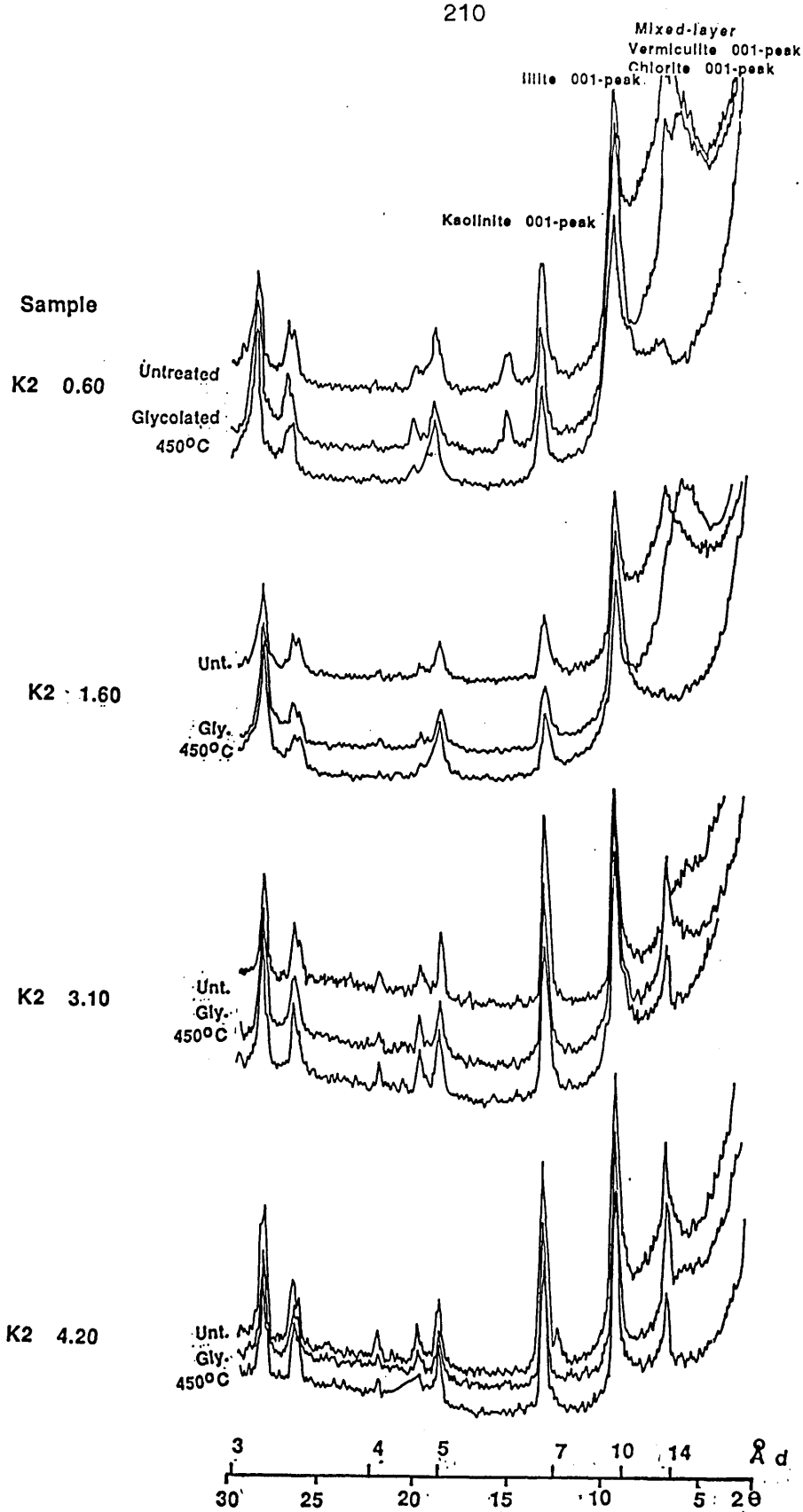

Figure 8.5 XRD diffractograms for oriented samples of the clay fraction (< 2μm) of the Holocene raised coastal sediments in section K2, Kirkcudbright area.

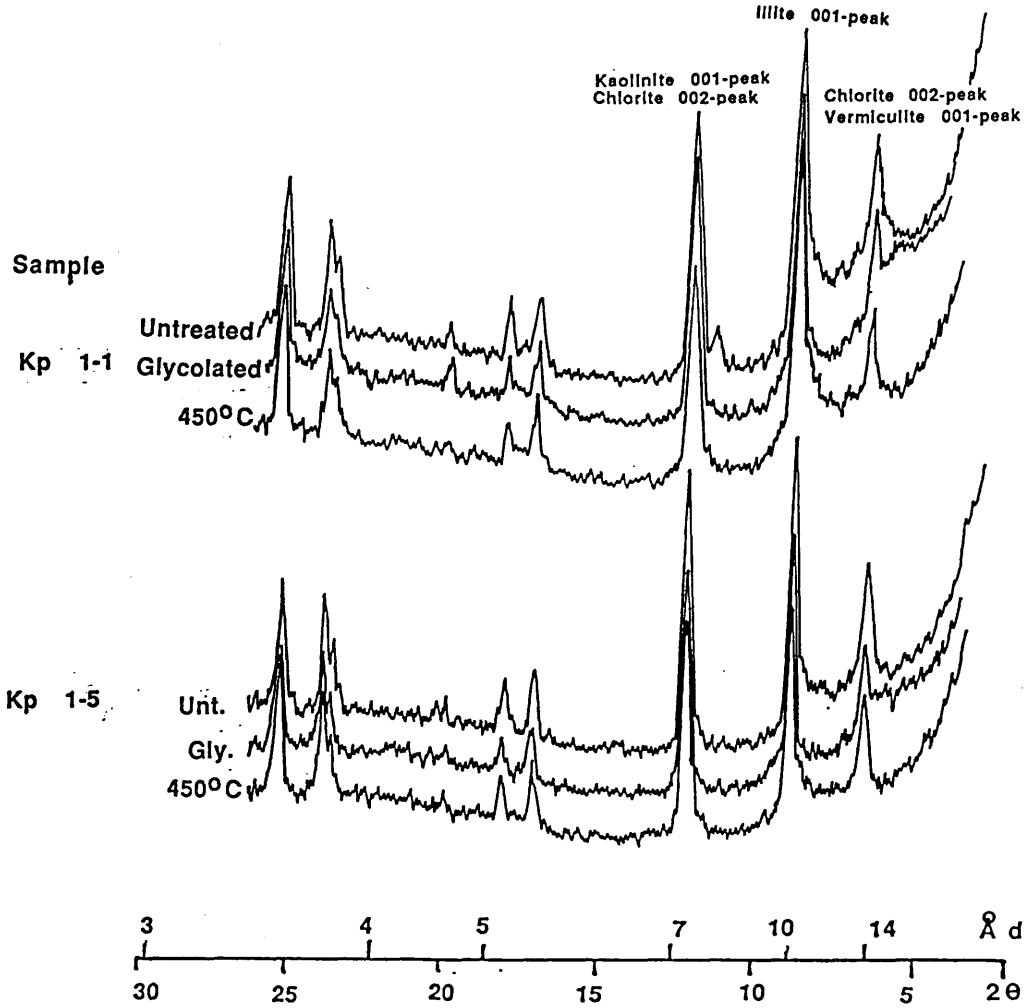

Figure 8.6 XRD diffractograms for oriented samples of the clay fraction (< 2μm) of present-day sediments in the Kirkcudbright area.

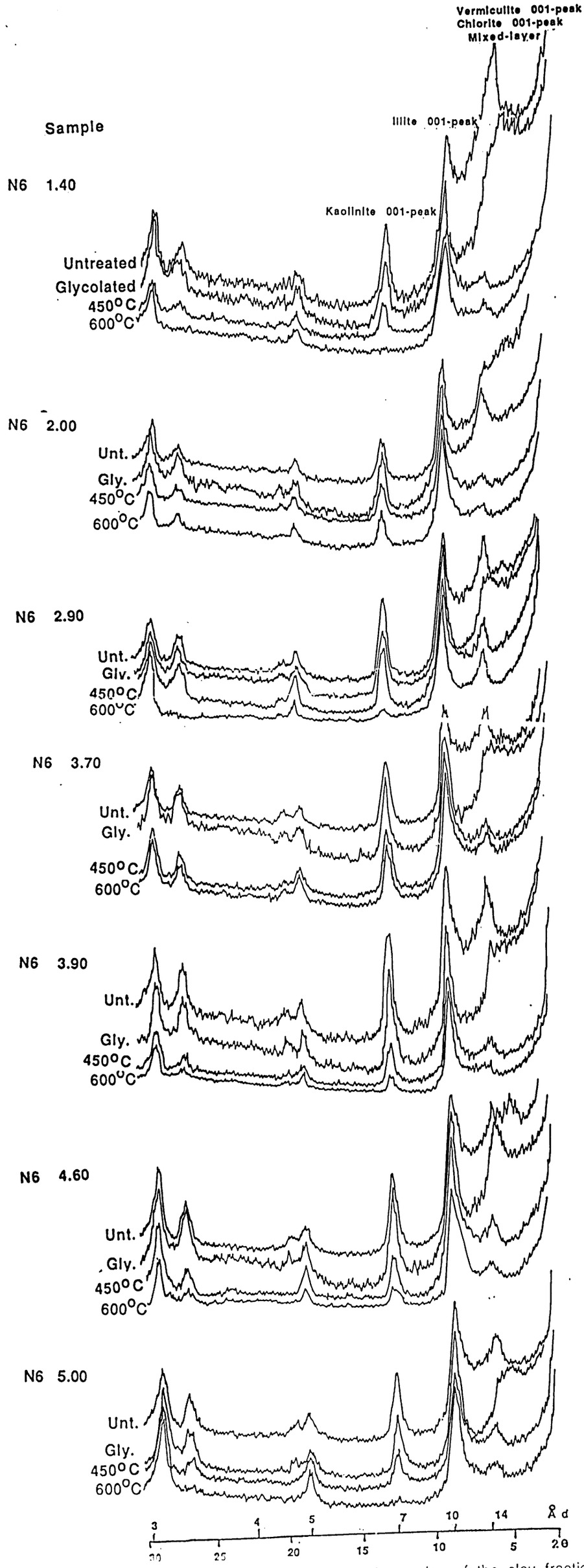

Figure 8.7 XRD diffractograms for oriented samples of the clay fraction (< 2μm) of the Holocene raised coastal sediments in section N5, New Abbey area.

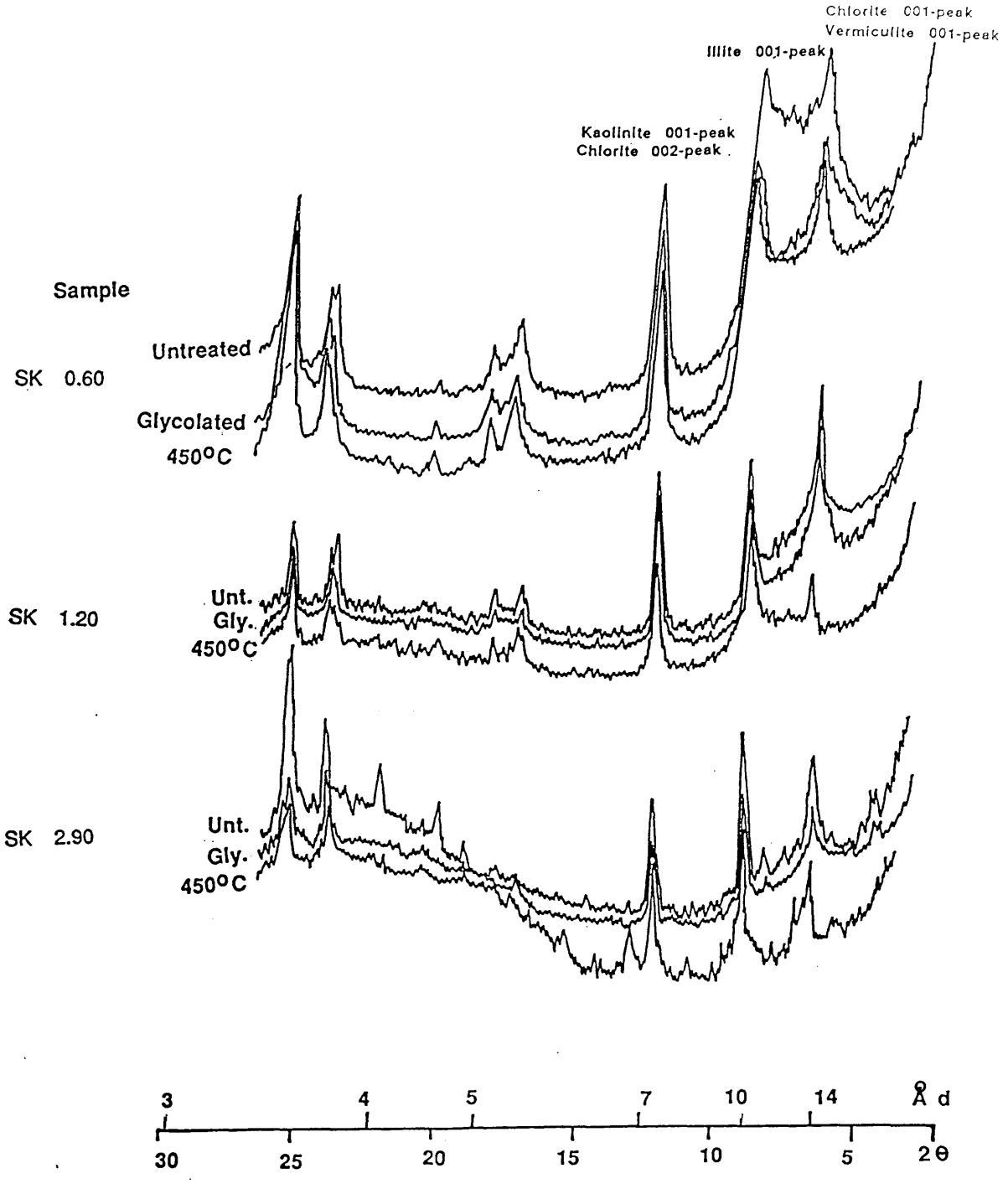

Figure 8.8 XRD diffractograms for oriented samples of the clay fraction (< 2μm) of the Holocene raised coastal sediments in the South Kirkblain section, Lochar Gulf area.

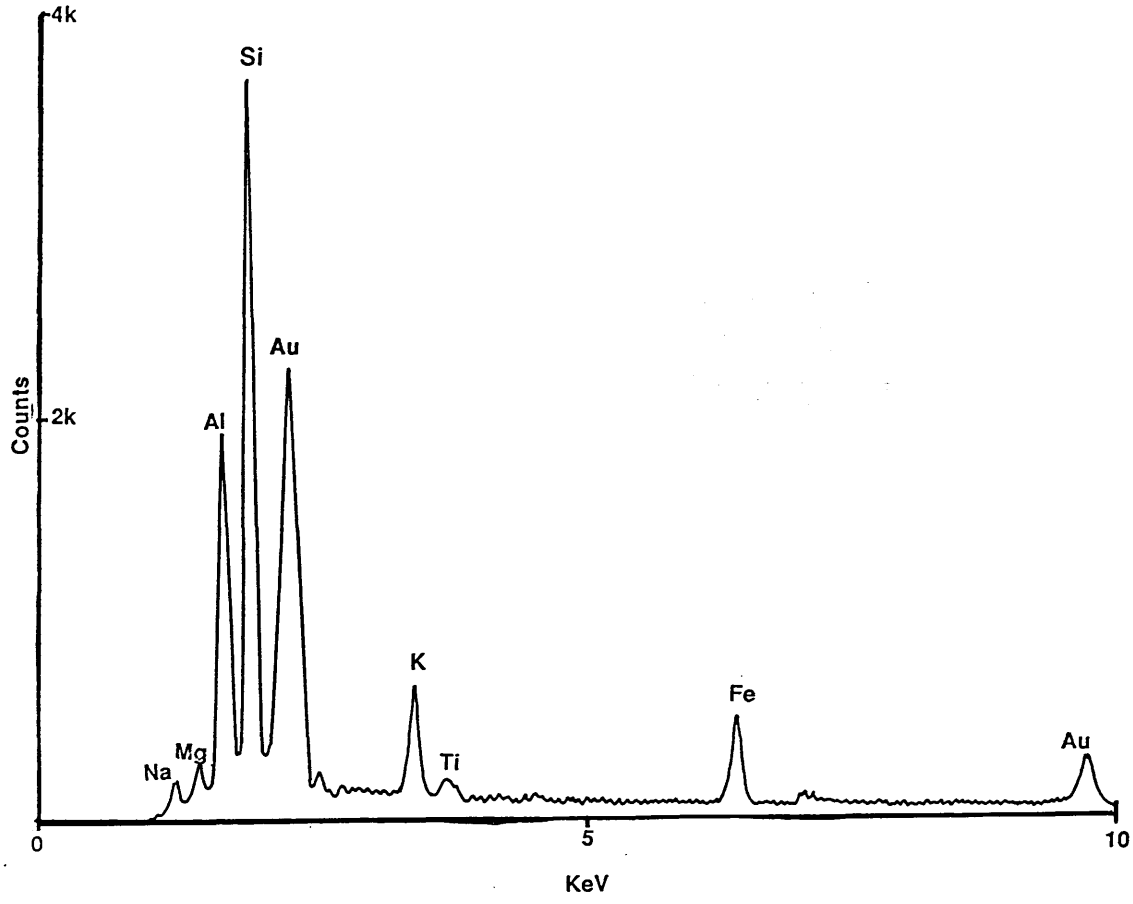

Figure 8.9 EDX peak traces for illite particles, sample D6 1.70, Holocene raised coastal sediments, Dalbeattie area.

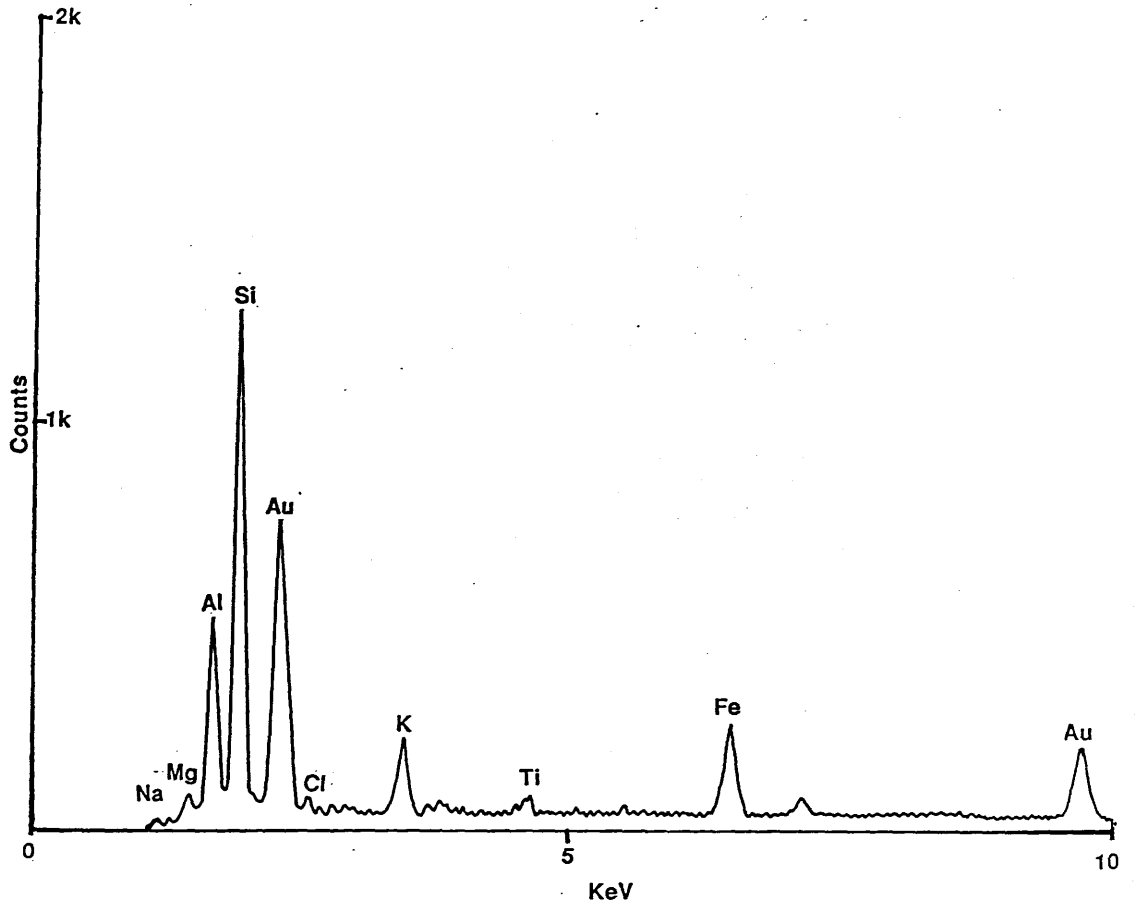

Figure 8.10 EDX peak traces for chlorite particles, sample N6 3.90, Holocene raised coastal sediments, New Abbey area.

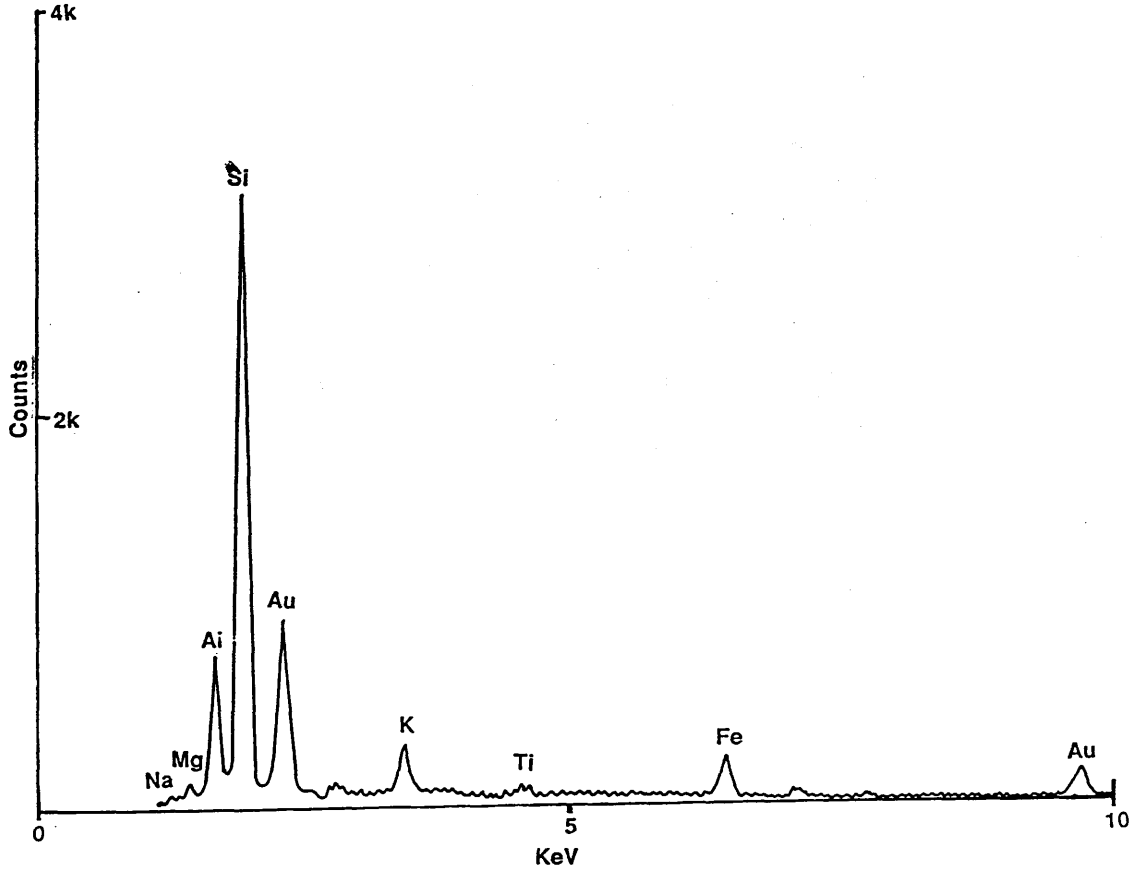

Figure 8.11 EDX peak traces for chlorite particles, sample K2 3.10, Holocene raised coastal sediments, Kirkcudbright area.

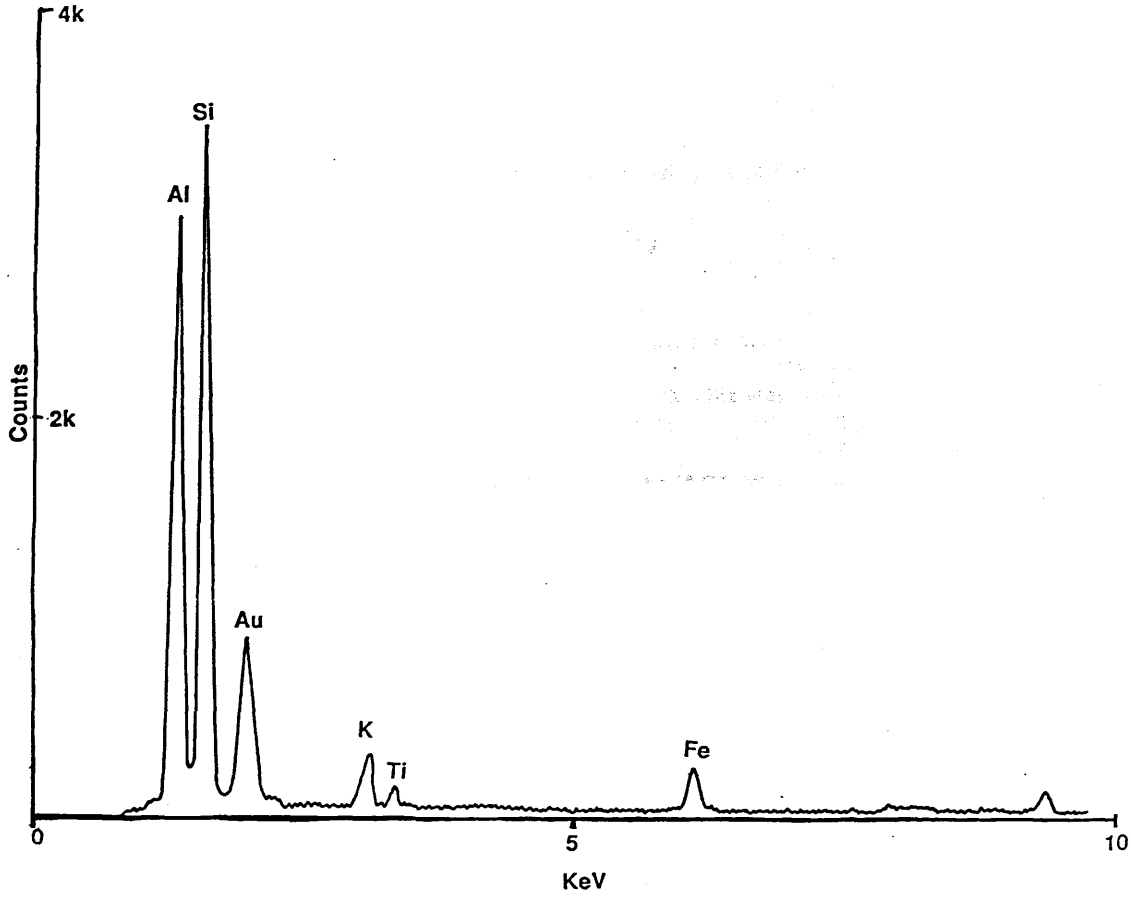

Figure 8.12 EDX peak traces for kaolinite particles, sample D8 0.40, Holocene raised coastal sediments, Dalbeattie area.

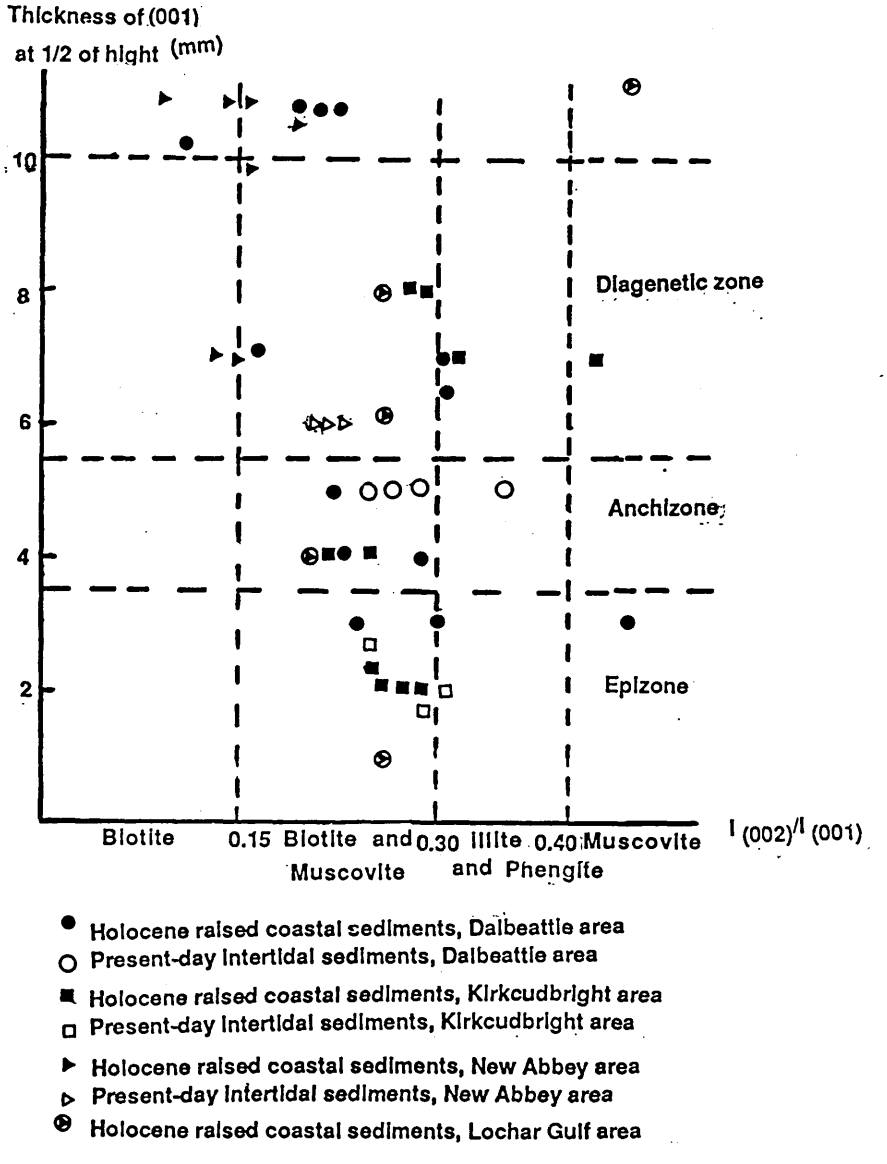

Figure 8.13 Illite crystallinity indices for representative samples from the four areas of study, plotted on Thorez's (1976, fig.8) diagram.

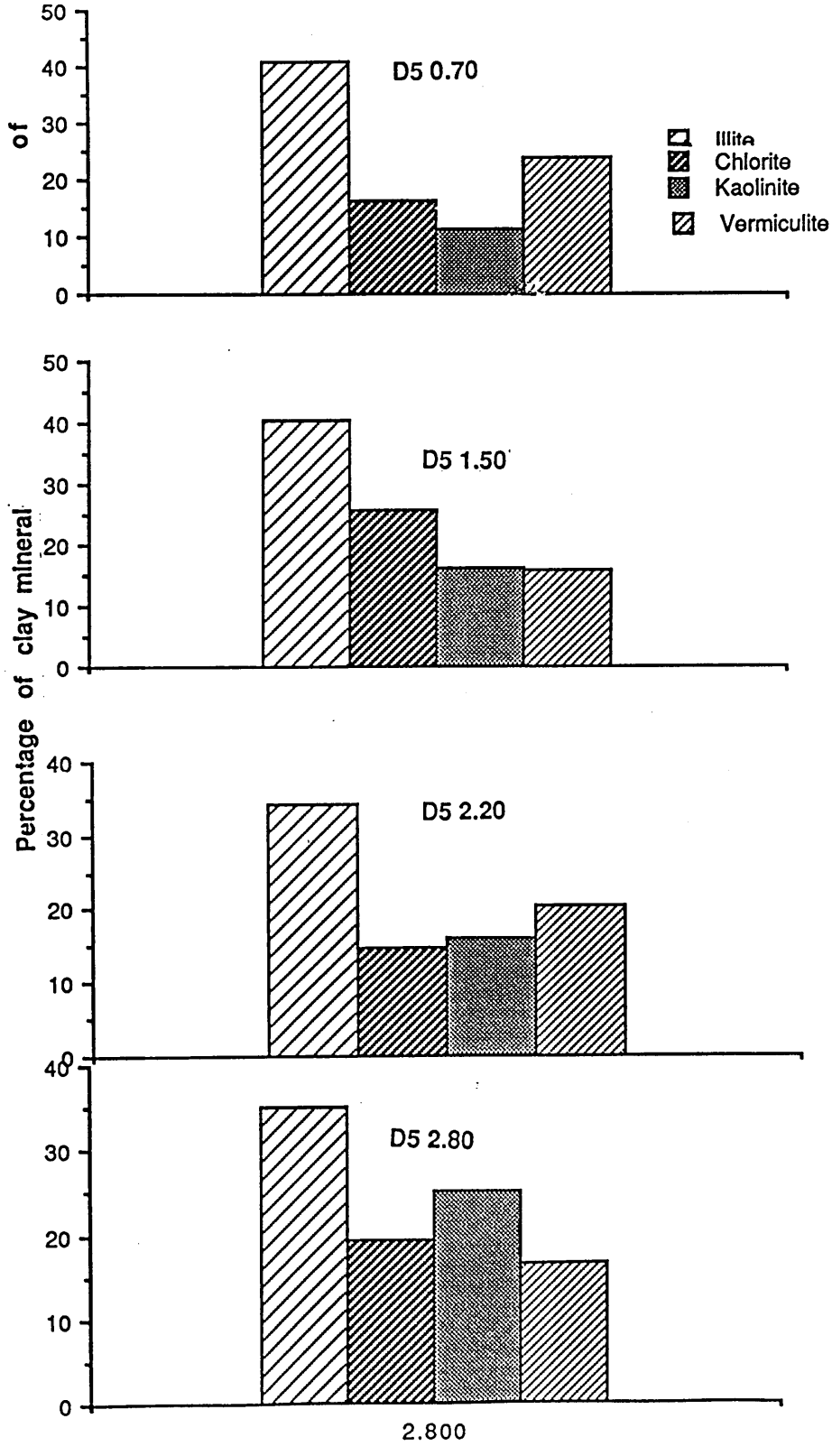

Figure 8.14 Histograms, showing vertical variation in the percentages of illite, chlorite, kaolinite and vermiculite, section D5 of the Holocene raised coastal sediments, Dalbeattie area.

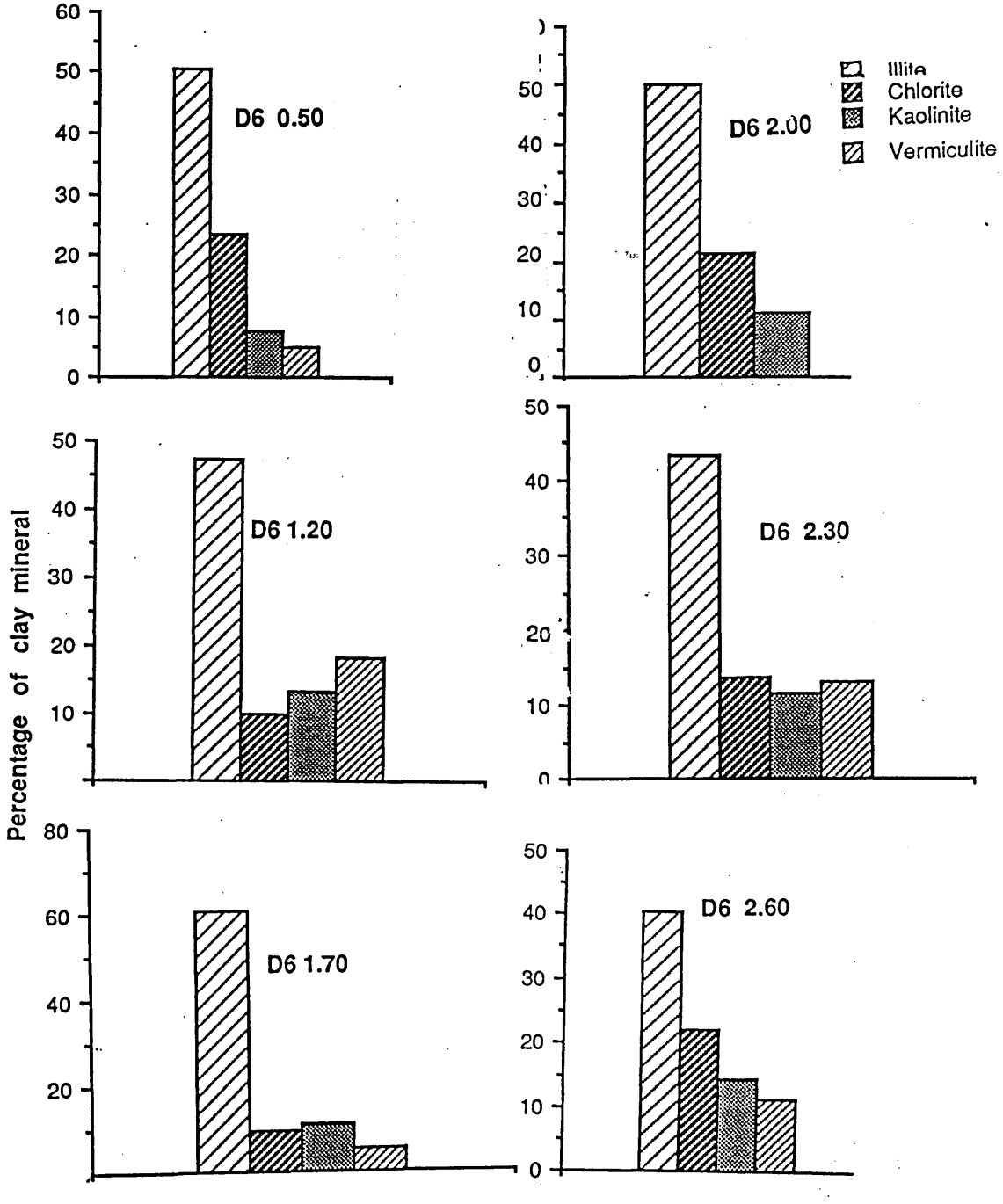

Figure 8.15 Histograms, showing vertical variation in the percentages of illite, chlorite, kaolinite and vermiculite, section D6 of the Holocene raised coastal sediments, Dalbeattie area.

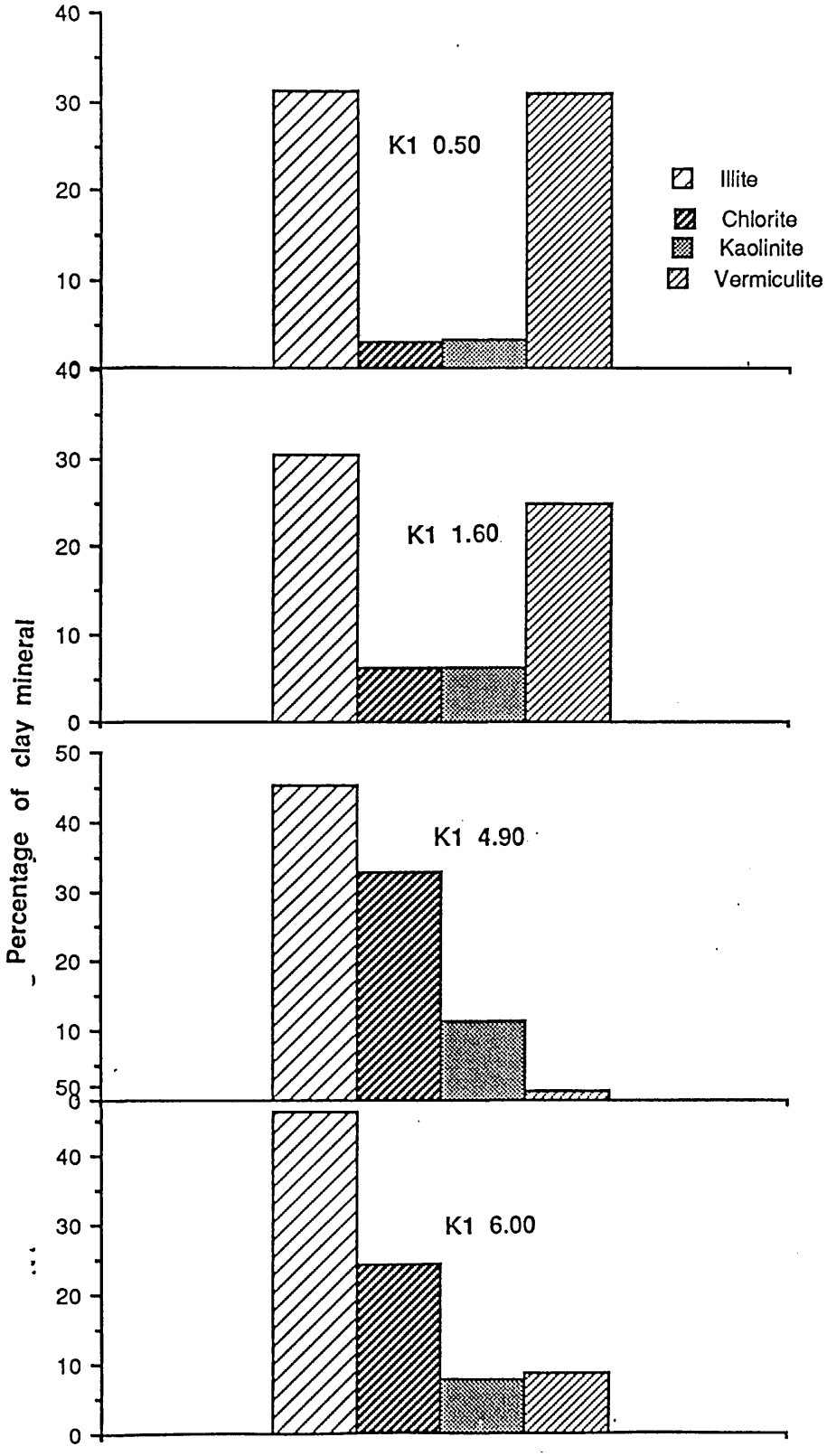

Figure 8.16 Histograms, showing vertical variation in the percentages of illite, chlorite, kaolinite and vermiculite, section K1 of the Holocene raised coastal sediments, Kirkcudbright area.

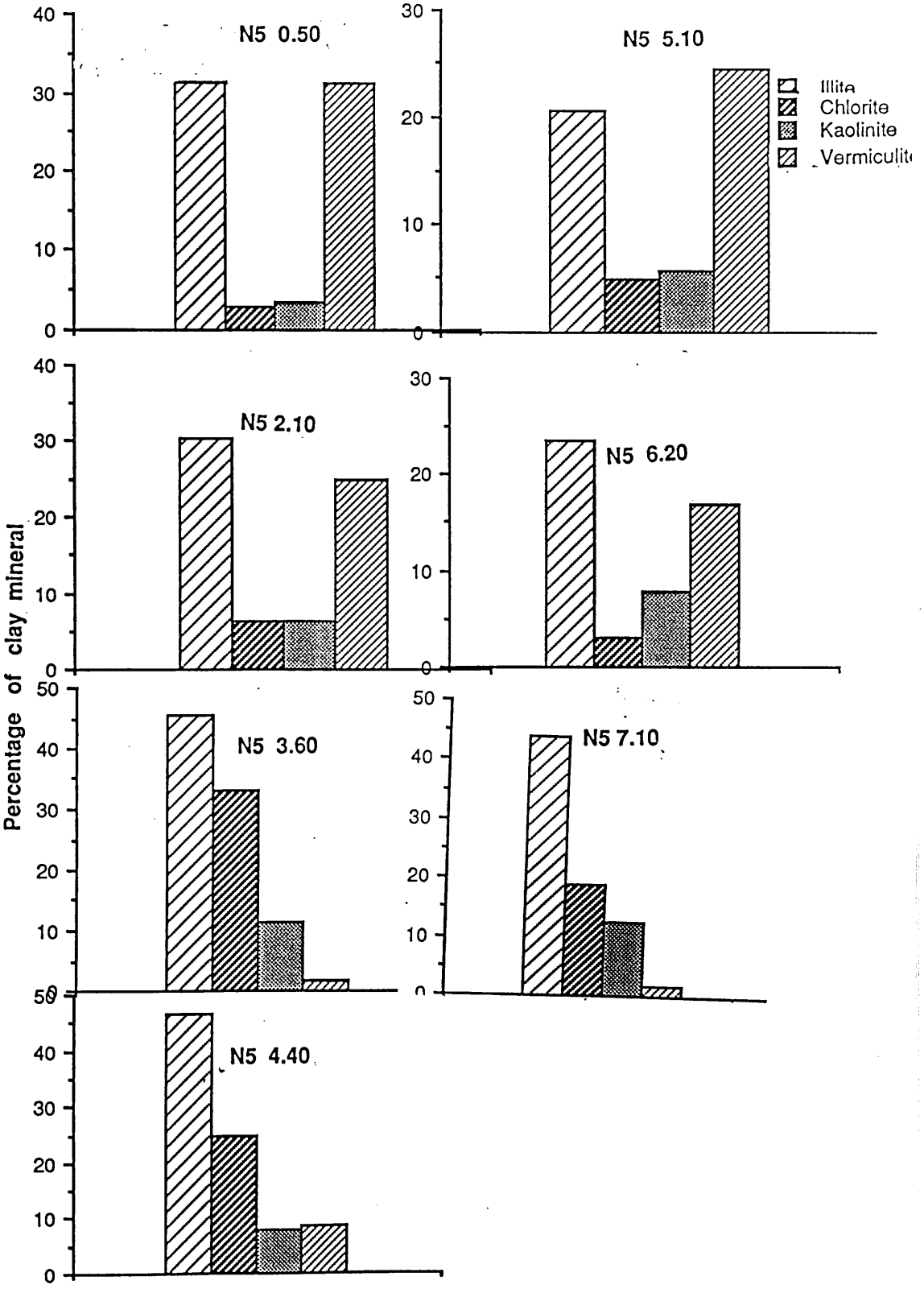

Figure 8.17 Histograms, showing vertical variation in the percentages of illite, chlorite, kaolinite and vermiculite, section N5 of the Holocene raised coastal sediments, New Abbey area.

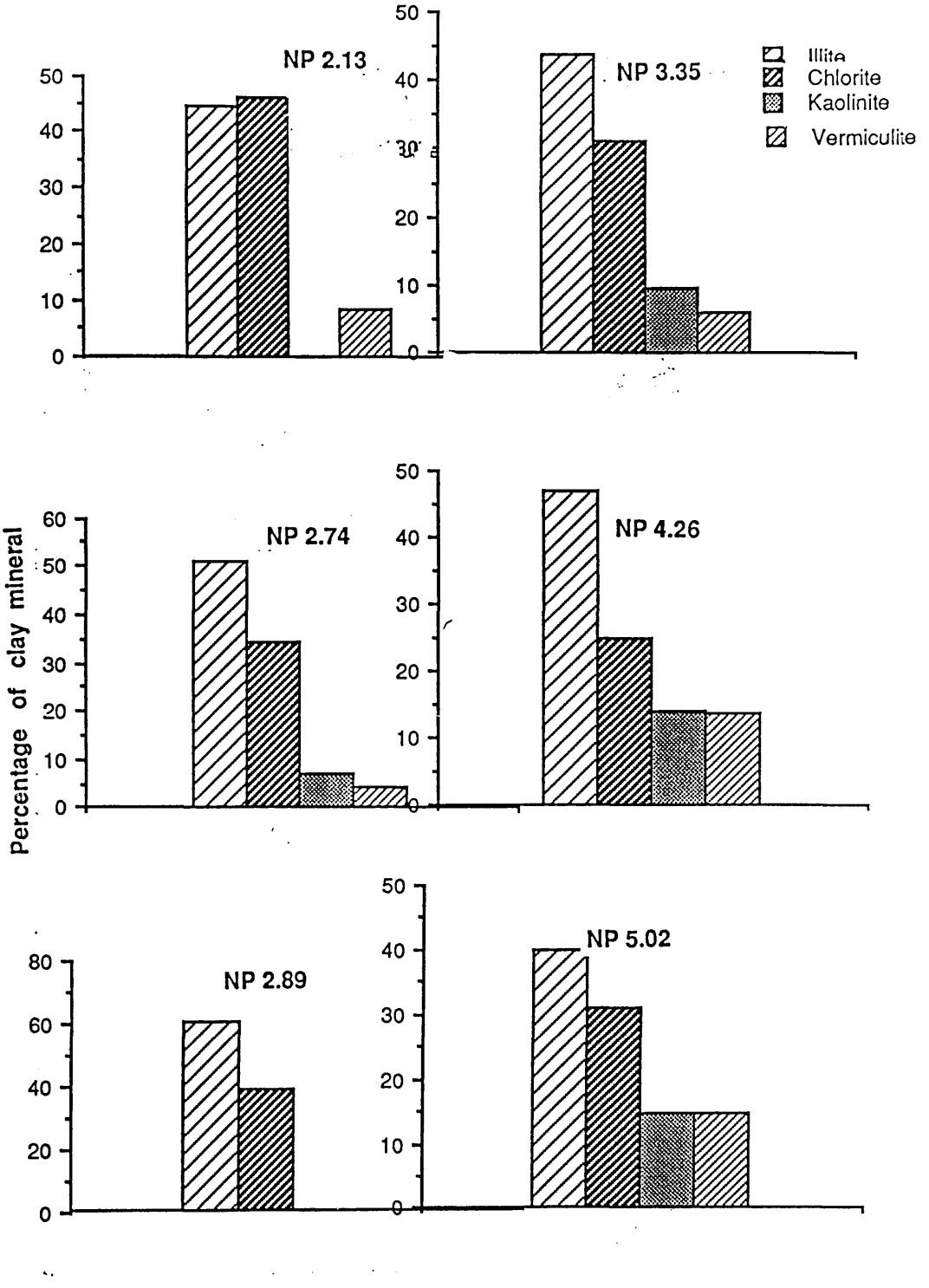

Figure 8.18 Histograms, showing the vertical variation in the percentages of illite, chlorite, kaolinite and vermiculite, Northpark (NP) section of the Holocene raised coastal sediments, Lochar Gulf area.

Table 8.1 Values in d (Å) of the characteristic reflections of relevant clay minerals after various treatments: N = natural, untreated sample; EG=Ethylene glycol treatment; 450°C and 600°C heat treatments (modified from Carrol 1970; Thorez 1976, 39; Hutchison, 1974, 228)

Clay mineral	Treatment	Values of d, in Å, of the characteristic reflections of minerals after treatments			
		(001)	(002)	(003)	(004)
Illite	N	10.00	5.00	3.33	2.50
	EG		No change		
	450°C		No change		
	600°C		No change		
Kaolinite	N	7.10	3.58	2.33	---
	EG	7.10	No change		
	450°C	7.10	No change		
	600°C	Disappearance of all reflections			
Chlorite	N	14.00	7.00	4.72	3.50
	EG		No change		
	450°C	No change or slight change in even orders			
	600°C	No change but disappearance in even orders			
Vermiculite	N	14.00	7.00	4.72	3.50
	EG		No change		
	450°C	10.00	5.00	3.33	2.50
	600°C	10.00	5.00	3.33	2.50
Montmorillonite	N	13.00-15.00	7.00	5.10	- - -
	EG	17.00	8.50	5.70	4.20
	450°C	10.00	5.00	3.30	- - -
	600°C	10.00	5.00	3.30	- - -
Mixed-layer clays	Depends on the kinds of clay mineral present and effects during various treatments				

Table 8.2 Clay mineral contents, as percentages of the clay fraction, in sediments of the Dalbeattie area.

A. Holocene raised coastal sediments

Sample		Illite	Chlorite	Kaolin.	Verm.	Mont.	Mixed-layer
D2	0.60	37.35	15.05	7.03	27.50	0.00	8.05
D2	1.20	39.00	16.00	6.50	23.40	0.00	9.50
D2	1.80	40.60	22.00	6.07	16.00	0.00	12.30
D2	2.50	51.20	27.42	12.00	0.00	0.00	0.00
D2	2.70	48.00	29.32	10.35	0.00	0.00	6.21
D2	2.95	35.20	38.44	9.20	9.06	0.00	5.60
D3	0.60	41.06	13.10	13.30	32.32	0.00	0.00
D3	1.00	36.64	4.73	4.52	33.82	0.00	20.29
D3	1.40	41.14	9.97	15.96	1.00	2.99	29.02
D3	2.20	41.32	14.76	21.40	0.00	0.00	22.14
D3	2.95	40.12	18.30	16.40	0.00	0.00	23.82
D4	0.50	38.21	16.05	11.82	22.30	0.00	6.80
D4	1.20	32.04	37.20	6.50	4.30	3.72	14.09
D4	2.10	30.56	35.20	4.53	16.00	2.50	10.35
D4	2.90	42.60	26.59	9.88	8.45	0.00	0.00
D5	0.70	48.75	16.25	11.25	23.74	0.00	0.00
D5	1.50	40.57	25.79	16.23	15.94	0.00	0.00
D5	2.20	34.47	14.70	16.00	20.58	0.00	0.00
D5	2.80	35.00	19.33	25.00	16.66	0.00	0.00
D6	0.50	50.39	23.62	7.87	5.24	0.00	12.86
D6	1.20	47.57	10.31	13.59	18.44	0.00	5.88
D6	1.70	60.40	9.48	11.11	5.55	0.00	0.00
D6	2.00	50.00	21.38	11.00	0.00	0.00	16.56
D6	2.30	43.31	13.79	11.74	13.20	0.00	13.54
D6	2.60	40.31	22.06	14.60	11.50	0.00	10.45
D7	0.40	44.30	26.22	10.30	7.50	0.00	9.88
D7	1.10	51.00	19.50	13.50	0.00	0.00	14.25
D7	1.60	39.00	21.67	10.33	7.35	0.00	18.00
D7	2.25	48.00	18.75	14.35	5.62	0.00	13.82
D7	3.70	44.36	27.51	9.68	7.98	0.00	8.50
D8	0.40	46.23	16.00	18.32	0.00	8.55	0.00
D8	1.60	28.00	32.15	8.70	3.66	0.00	18.22
D8	2.00	38.00	23.05	10.22	6.83	0.00	17.32
D8	2.70	31.54	35.52	16.00	0.00	0.00	12.50
D9	0.40	36.42	14.28	17.14	18.28	0.00	12.85
D9	1.06	51.42	20.00	11.86	12.00	0.00	6.56
D9	1.56	47.69	13.46	9.39	29.80	0.00	0.00
D9	2.92	56.77	13.20	12.11	17.20	0.00	0.00

Continued

Table 8.2 Continued

D10	0.55	35.34	16.96	6.06	25.45	0.00	16.16
D10	1.50	36.00	16.85	6.20	25.20	0.00	16.00
D10	2.07	43.47	11.04	2.09	33.47	0.00	9.93
D10	2.36	50.41	26.56	8.33	15.62	0.00	0.00
D10	2.80	50.51	25.51	10.26	13.77	0.00	0.00
D10	3.03	54.79	30.60	16.36	7.20	0.00	0.00

B. Present-day sediments

Sample	Illite	Chlorite	Kaolin.	Verm.	Mont.	Mixed-layer
Dp 1-3	47.41	24.55	13.79	11.07	0.00	0.00
Dp 1-4	50.30	22.53	15.09	12.07	0.00	0.00
Dp 1-7	34.33	33.78	10.23	14.33	0.00	0.00
Dp 2-1	32.94	36.82	7.64	13.52	0.00	0.00
Dp 2-2	43.55	21.30	6.38	19.88	0.00	0.00
Dp 2-3	53.24	29.60	5.30	9.23	0.00	0.00
Dp 2-4	35.55	27.77	13.56	6.56	2.22	0.00

Table 8.3 Clay mineral contents, as percentages of the clay fraction, in sediments of the Kirkcudbright area.

A. Holocene raised coastal sediments

Sample		Illite	Chlorite	Kaolin.	Verm.	Mont.	Mixed-layer
K1	0.50	31.40	3.04	3.46	31.11	5.24	34.05
K1	1.60	30.55	6.25	6.25	25.00	16.66	13.88
K1	4.90	45.54	33.12	11.38	1.60	0.00	8.28
K1	6.00	46.47	24.66	7.92	8.81	0.00	12.11
K2	0.60	20.50	4.90	5.70	24.59	0.00	44.26
K2	1.60	23.43	2.92	7.81	16.73	0.00	49.09
K2	3.10	44.09	18.89	12.59	1.75	0.00	22.83
K2	4.20	36.32	17.92	11.20	15.20	0.00	19.25
K3	0.60	31.50	12.35	9.43	23.60	0.00	16.65
K3	1.80	47.22	9.30	13.48	21.50	0.00	0.00
K3	3.50	45.33	7.94	18.69	10.66	0.00	16.25
K3	4.20	55.80	19.60	24.16	0.00	0.00	0.00
K4	0.30	32.45	15.21	14.20	2.05	0.00	37.19
K4	0.80	41.73	22.19	19.42	16.64	0.00	0.00
K4	1.90	51.19	17.49	13.49	17.44	0.00	0.00
K4	2.15	40.00	27.75	15.00	15.00	0.00	0.00

B. Present-day sediments

Sample	Illite	Chlorite	Kaolin.	Verm.	Mont.	Mixed-layer
Kp 1-1	50.45	4.58	20.10	16.51	0.00	8.25
Kp 1-2	52.34	5.30	17.69	14.32	0.00	7.32
Kp 1-5	39.05	16.44	17.18	27.37	0.00	0.00
Kp 2-3	48.12	6.02	13.65	32.12	0.00	0.00
Kp 3-4	50.90	21.03	11.55	11.30	0.00	0.00

Table 8.4 Clay mineral contents, as percentages of the clay fraction, in sediments of the New Abbey area.

A. Holocene raised coastal sediments

Sample	Illite	Chlorite	Kaolin.	Verm.	Mont.	Mixed-layer
N5 0.50	31.40	3.04	3.46	31.11	5.24	34.05
N5 2.10	30.55	6.25	6.25	25.00	16.66	13.88
N5 3.60	45.54	33.12	11.38	1.60	0.00	8.28
N5 4.40	46.47	24.66	7.92	8.81	0.00	12.11
N5 5.10	20.50	4.90	5.70	24.59	0.00	44.26
N5 6.20	23.43	2.92	7.81	16.73	0.00	49.09
N5 7.10	44.09	18.89	12.59	1.75	0.00	22.83
N6 1.40	32.39	12.85	7.19	12.85	10.28	37.27
N6 2.00	39.40	6.27	10.10	21.50	0.00	32.62
N6 2.90	37.00	27.75	0.00	10.66	0.00	23.34
N6 3.70	39.35	31.71	0.00	0.00	6.02	13.65
N6 3.90	36.52	27.82	0.00	2.05	0.00	21.30
N6 4.60	32.56	16.00	0.00	16.64	0.00	41.60
N6 5.00	39.03	29.56	0.00	17.44	16.82	9.23

B. Present-day sediments

Sample	Illite	Chlorite	Kaolin.	Verm.	Mont.	Mixed-layer
Np 1-1	37.00	3.20	17.36	22.88	7.50	6.90
Np 1-3	37.50	9.87	20.83	20.41	0.00	12.50
Np 1-4	45.00	21.00	28.00	0.00	0.00	6.20

Table 8.5 Clay mineral contents, as percentages of the clay fraction, in sediments of the Lochar Gulf area

Sample	Illite	Chlorite	Kaolin.	Verm.	Mont.	Mixed-layer
NP 2.13	44.72	46.58	0.00	8.68	0.00	0.00
NP 2.74	51.06	34.46	7.37	4.24	0.00	2.80
NP 2.89	60.22	39.24	0.00	0.00	0.00	0.00
NP 3.35	43.69	31.02	9.68	6.20	0.00	0.00
NP 4.26	47.14	25.14	14.28	13.71	0.00	14.28
NP 5.02	39.88	30.82	14.66	14.66	0.00	0.00
SK 0.60	46.19	22.82	11.95	11.90	0.00	0.00
SK 1.20	35.80	43.12	19.35	12.90	0.00	0.00
SK 2.90	56.52	39.13	4.30	0.00	0.00	0.00
BB 0.70	22.30	0.00	15.30	58.55	0.00	0.00
BB 1.30	42.50	29.30	8.60	17.56	0.00	0.00
BB 3.10	47.65	28.50	11.30	0.00	0.00	0.00
MT 4.06	39.75	25.30	14.45	20.48	0.00	0.00
MT 4.16	39.77	25.70	10.28	13.22	0.00	0.00
HH 3.22	39.75	51.80	29.50	0.00	0.00	0.00
PH 0.71	56.22	31.60	10.63	0.00	0.00	0.00

Table 8.6 Values of Maximum (Ma), Minimum (Mn), Mean ($\bar{X}$) and Standard Deviation (σ) of clay minerals (< 2 μm) for the analysed samples in the various areas of study.

1. Dalbeattie area

A. Holocene raised coastal sediments

N = 44 Clay Min.	Ma	Mn	$\bar{X}$	σ
Illite	60.40	28.00	42.90	7.30
Chlorite	38.44	4.73	20.90	8.22
Kaolinite	25.00	2.09	11.35	4.56
Vermiculite	33.82	0.00	12.77	10.27

B. Present-day intertidal sediments

N = 8 Clay Min.	Ma	Mn	$\bar{X}$	σ
Illite	53.24	32.94	42.47	8.24
Chlorite	36.82	21.30	28.05	5.78
Kaolinite	15.09	5.30	10.28	3.94
Vermiculite	19.88	6.56	12.38	4.22

2. Kirkcudbright area

A. Holocene raised coastal sediments

N = 16 Clay Min.	Ma	Mn	$\bar{X}$	σ
Illite	55.80	20.50	38.77	9.97
Chlorite	33.12	2.92	15.22	9.10
Kaolinite	24.16	3.46	12.14	5.50
Vermiculite	31.11	0.00	14.48	9.59

Continued

Table 8.6 continued

B. Present-day intertidal sediments

N = 5	Ma	Mn	$\bar{X}$	σ
Clay Min.				
Illite	52.34	39.05	48.17	5.32
Chlorite	21.03	5.30	10.67	7.55
Kaolinite	20.10	11.55	16.03	3.41
Vermiculite	32.12	11.30	20.32	8.96

3. New Abbey area

A. Holocene raised coastal sediments

N = 14	Ma	Mn	$\bar{X}$	σ
Clay Min.				
Illite	39.35	22.35	33.56	5.15
Chlorite	37.09	6.27	24.16	10.01
Kaolinite	20.52	5.54	11.57	6.64
Vermiculite	23.61	0.00	6.50	7.60

B. Present-day intertidal sediments

N = 3	Ma	Mn	$\bar{X}$	σ
Clay Min.				
Illite	45.00	37.00	39.83	4.48
Chlorite	21.00	3.20	11.36	8.99
Kaolinite	28.00	17.36	22.06	5.43
Vermiculite	22.88	0.00	14.43	12.55

Continued

Table 8.6 continued

4. Lochar Gulf area, Holocene raised coastal sediments

N = 16 Clay Min.	Ma	Mn	$\bar{X}$	σ
Illite	60.22	22.30	45.33	9.21
Chlorite	46.58	0.00	30.14	10.51
Kaolinite	19.35	0.00	10.25	5.32
Vermiculite	58.55	0.00	12.23	14.04

Table 8.7 Relative abundances of clay minerals, Dalbeattie area; Ma = Major, Co = Common, Ab = Abundant, Mi = Minor, Tr = Trace

A. Holocene raised coastal sediments

Sample		Illite	Chlorite	Kaolin.	Verm.	Mont.	Mixed-layer
D2	0.60	Ma	Co	Mi	Ab	Tr	Tr
D2	1.20	Ma	Co	Mi	Ab	Tr	Mi
D2	1.80	Ma	Co	Mi	Mi	Tr	Mi
D2	2.50	Ma	Ab	Mi	- -	- -	- -
D2	2.70	Ma	Ab	Tr	Mi	- -	Tr
D2	2.95	Ab	Mi	Mi	- -	- -	Mi
D3	0.60	Ma	Ab	Tr	Mi	Tr	Co
D3	1.00	Ma	Ab	Mi	Mi	Tr	Co
D3	1.40	Ma	Ab	Tr	Mi	Mi	Mi
D3	2.20	Ma	Ab	Co	Mi	- -	Co
D3	2.95	Ma	Ab	Mi	Tr	Mi	- -
D4	0.60	Ma	Ab	Co	Tr	- -	Mi
D4	1.20	Ab	Ma	Mi	Tr	Tr	Co
D4	2.10	Ab	Ma	Tr	Co	Tr	Co
D4	2.90	Ma	Ab	Co	Tr	- -	- -
D5	0.70	Ma	Ab	Mi	Mi	- -	- -
D5	1.50	Ab	Ma	Tr	Co	- -	- -
D5	2.20	Ab	Ma	Mi	Tr		
D5	2.80	Ma	Ab	Mi	- -	- -	- -
D6	0.50	Ma	Ab	Mi	Tr	- -	Mi
D6	1.20	Ma	Ab	Mi	Mi	- -	- -
D6	1.70	Ma	Co	Tr	Mi	- -	Co
D6	2.00	Ma	Co	Co	- -	- -	Co
D6	2.30	Ma	Ab	Mi	Mi	- -	Mi
D6	2.60	Ma	Ab	Mi	Mi	- -	Co
D7	0.40	Ma	Ab	Mi	Mi	- -	Mi
D7	1.10	Ma	Co	Co	- -	- -	Mi
D7	1.60	Ma	Co	Co	- -	- -	Co
D7	2.25	Ma	Co	Co	Tr	- -	Mi
D7	3.70	Ma	Ab	Co	Mi	- -	Co
D8	0.40	Ma	Co	Ab	- -	Mi	- -
D8	1.60	Ab	Ma	Mi	Tr	Mi	Co
D8	2.00	Ma	Ab	Mi	Tr	- -	- -
D8	2.70	Ab	Ma	Ma	- -	- -	Co

Continued

Table 8.7 continued

D9	0.40	Ab	Ma	Mi	Co	- -	- -
D9	1.06	Ma	Ab	Mi	Co	- -	- -
D9	1.56	Ma	Ab	Mi	Mi	- -	- -
D9	2.92	Ma	Ab	Mi	Co	- -	- -
D10	0.55	Ab	Ma	Mi	Mi	- -	Tr
D10	1.50	Ma	Ab	Mi	Mi	- -	- -
D10	2.07	Ma	Ab	Mi	Mi	- -	Tr
D10	2.36	Ab	Ma	Mi	Tr	- -	Tr
D10	2.80	Ab	Ma	Mi	Tr	- -	Tr
D10	3.03	Ma	Ab	Co	- -	- -	- -

B. Present-day intertidal sediments

Sample	Illite	Chlorite	Kaolin.	Verm.	Mont.	Mixed-layer
Dp 1-3	Ma	Co	Ab	Mi	- -	- -
Dp 1-4	Ma	Ab	Ab	Tr	- -	- -
Dp 1-7	Ab	Ma	Tr	Co	- -	- -
Dp 2-1	Ma	Ab	Tr	Co	- -	- -
Dp 2-2	Ma	Co	Mi	Ab	- -	- -
Dp 2-3	Ma	Ab	Tr	Mi	- -	- -
Dp 2-4	Ma	Ab	Tr	Co	- -	- -

Table 8.8 Relative abundances of clay minerals, Kirkcudbright area; Ma = Major, Co = Common, Ab = Abundant, Mi = Minor, Tr = Trace

A. Holocene raised coastal sediments

Sample		Illite	Chlorite	Kaolin.	Verm.	Mont.	Mixed-layer
K1	0.50	Ab	Ma	Co	Co	- -	Mi
K1	1.60	Ma	Co	Ab	Mi	- -	Co
K1	4.90	Ma	Mi	Co	Tr	- -	Mi
K1	6.00	Ma	Co	Mi	Tr	- -	Mi
K2	0.60	Ab	Ma	Mi	Co	- -	Co
K2	1.60	Ma	Tr	Co	Ab	- -	Ab
K2	3.10	Ma	Co	Mi	Tr	- -	Mi
K2	4.20	Ma	Co	Mi	Tr	- -	Co
K3	0.60	Ma	Co	Ab	Tr	- -	Mi
K3	1.80	Ma	Mi	Ab	Tr	- -	Mi
K3	3.50	Ma	Tr	Ab	Tr	- -	- -
K3	4.20	Ma	Mi	Co	- -	- -	- -
K4	0.30	Ma	Co	Mi	Mi	- -	Co
K4	0.80	Ma	Co	Ab	Mi	- -	- -
K4	1.90	Ma	Co	Co	Co	- -	Mi
K4	2.15	Ma	Tr	Ab	- -	- -	- -

B. Present-day sediments

Sample	Illite	Chlorite	Kaolin.	Verm.	Mont.	Mixed-layer
Kp 1-1	Ma	Co	Ab	- -	Tr	Mi
Kp 1-2	Ma	Co	Co	Mi	- -	- -
Kp 1-5	Ma	Mi	Ab	- -	- -	- -
Kp 2-3	Ma	Ma	Ab	Tr	- -	- -
Kp 3-4	Ma	Co	Ab	- -	- -	- -

Table 8.9 Relative abundances of clay minerals, New Abbey area; Ma = Major, Co = Common, Ab = Abundant, Mi = Minor, Tr = Trace

A. Holocene raised coastal sediments

Sample		Illite	Chlorite	Kaolin.	Verm.	Mont.	Mixed-layer
N5	0.50	Ma	Co	Ab	Tr	- -	Mi
N5	2.10	Ma	Co	Ab	Tr	- -	Co
N5	3.60	Ab	Ma	Tr	Mi	- -	Tr
N5	4.40	Ma	Ab	Tr	Tr	- -	Mi
N5	5.10	Ma	Ab	Tr	Tr	- -	Mi
N5	6.20	Ma	Co	Tr	Tr	- -	Co
N5	7.10	Ma	Ab	Tr	- -	- -	Tr
N6	1.40	Ma	Co	Co	Mi	- -	Mi
N6	2.00	Ma	Co	Co	Mi	- -	Mi
N6	2.90	Ab	Ma	Ab	- -	- -	Mi
N6	3.70	Ab	Ab	Ma	- -	- -	Mi
N6	3.90	Ab	Ma	Ab	Mi	- -	Mi
N6	4.60	Ma	Ab	Co	Mi	- -	Co
N6	5.00	Ma	Ab	Co	Mi	- -	Co

B. Present-day sediments

Sample		Illite	Chlorite	Kaolin.	Verm.	Mont.	Mixed-layer
Np	1-1	Ma	Ab	Mi	- -	- -	- -
Np	1-3	Ma	Ab	Mi	- -	- -	- -
Np	1-4	Ma	Ab	Mi	- -	- -	- -

Table 8.10 Relative abundances of clay minerals in the Holocene raised coastal sediments, Lochar Gulf area; Ma = Major, Co = Common, Ab = Abundant, Mi = Minor, Tr = Trace

A.

Sample	Illite	Chlorite	Kaolin.	Verm.	Mont.	Mixed-layer
NP 2.31	Ma	Ab	Tr	- -	- -	Mi
NP 2.74	Ma	Co	Co	Mi	- -	--
NP 2.89	Ma	Co	Co	Tr	- -	- -
NP 3.35	Ma	Ab	Mi	Tr	- -	- -
NP 4.26	Ma	Co	Mi	Mi	- -	Mi
NP 5.02	Ma	Co	Mi	Mi	- -	- -
SK 0.60	Ab	Ma	Co	Mi	- -	- -
SK 1.20	Ab	Ma	Co	Co	- -	- -
SK 2.90	Ab	Ma	Tr	Co	- -	- -
BB 0.70	Co	- -	Ab	Ma	- -	- -
BB 1.30	Ma	Ab	Mi	Co	- -	- -
BB 3.10	Ma	Ab	Mi	Co	- -	- -
MT 4.06	Ma	Ab	Tr	- -	- -	- -
MT 4.16	Ma	Ab	Tr	- -	- -	- -
HH 3.22	Ma	Ab	Tr	- -	- -	- -
PH 0.71	Ma	Ab	Tr	- -	- -	- -

Table 8.11 Ratio of intensity of (001)reflection (5Å) to intensity of (001) reflection (10Å) of illite, thickness of (001) reflection (10Å) at half height and character of this reflection in selected studied sections.

A. Holocene raised coastal sediments

1. Dalbeattie area.

Sample		(002)/(001)	Thickness of (001), in mm, at half height	Character of (001)
D5	0.70	0.218	4.00	Nearly symmetrical
D5	1.50	0.218	4.00	Nearly symmetrical
D5	2.20	0.283	4.00	Asymmetrical
D5	2.80	0.300	7.00	Asymmetrical
D6	0.50	0.230	17.00	Asymmetrical wide
D6	1.20	0.228	15.00	Asymmetrical wide
D6	1.70	0.194	16.00	Nearly symmetrical
D6	2.00	0.159	7.00	Nearly symmetrical
D6	2.30	0.114	11.00	Asymmetrical
D6	2.60	0.147	11.00	Asymmetrical
D9	0.40	0.310	6.50	Asymmetrical
D9	1.06	0.300	3.50	Nearly symmetrical
D9	1.56	0.230	5.00	Nearly symmetrical
D9	2.92	0.240	3.50	Nearly symmetrical

2. Holocene raised coastal sediments in Kirkcudbright area.

Sample		(002)/(001)	Thickness of (001), in mm, at half height	Character of (001)
K1	0.50	0.300	9.00	Nearly symmetrical
K1	1.60	0.250	4.00	Symmetrical
K1	4.90	0.260	3.00	Symmetrical
K1	6.00	0.280	4.00	Symmetrical
K2	0.50	1.120	8.00	Asymmetrical
K2	1.20	0.270	3.00	Nearly symmetrical
K2	1.70	0.280	3.20	Nearly symmetrical
K2	2.00	0.250	4.00	Nearly symmetrical
K4	0.30	0.310	6.50	Nearly symmetrical
K4	0.80	0.300	3.50	Asymmetrical
K4	1.30	0.280	8.00	Asymmetrical
K4	2.15	0.330	6.00	Asymmetrical

Continued

Table 8.11 continued

3. Holocene raised coastal sediments in New Abbey area.

Sample		(002)/(001)	Thickness of (001), in mm, at half height	Character of (001)
N6	1.40	0.130	7.00	Asymmetrical wide
N6	2.00	0.150	7.00	Asymmetrical wide
N6	2.80	0.150	9.00	Asymmetrical wide
N6	3.70	0.090	9.50	Asymmetrical wide
N6	3.90	0.230	9.00	Asymmetrical wide
N6	4.60	0.140	9.00	Asymmetrical wide
N6	5.00	0.150	8.00	Asymmetrical wide

4. Holocene raised coastal sediments in Lochar Gulf area.

Sample		(002)/(001)	Thickness of (001), in mm, at half height	Character of (001)
SK	0.60	0.130	7.00	Asymmetrical wide
SK	1.20	0.150	7.00	Asymmetrical wide
SK	2.90	0.150	9.00	Asymmetrical wide
MT	3.14	0.240	6.50	Nearly symmetrical
MT	4.06	0.240	6.50	Nearly symmetrical

B. Present-day intertidal sediments.

1. Dalbeattie area

Sample		(002)/(001)	Thickness of 001, in mm, at half height	Character of (001)
Dp	1-3	0.350	5.00	Nearly symmetrical
Dp	1-4	0.280	5.00	Nearly symmetrical
Dp	2-1	0.230	5.00	Nearly symmetrical
Dp	2-4	0.250	5.00	Nearly symmetrical

Continued

Table 8.11 Continued

2. Kirkcudbright area

Sample		(002)/(001)	Thickness of (001), in mm, at half height	Character of (001)
Kp	1-1	0.250	3.30	Nearly symmetrical
Kp	1-5	0.300	3.00	Nearly symmetrical
Kp	2-3	0.280	2.80	Nearly symmetrical

3. New Abbey area

Sample		(002)/(001)	Thickness of (001), in mm, at half height	Character of (001)
Np	1-1	0.230	6.00	Nearly symmetrical
Np	1-5	0.230	5.50	Nearly symmetrical
Np	2-3	0.220	6.00	Symmetrical

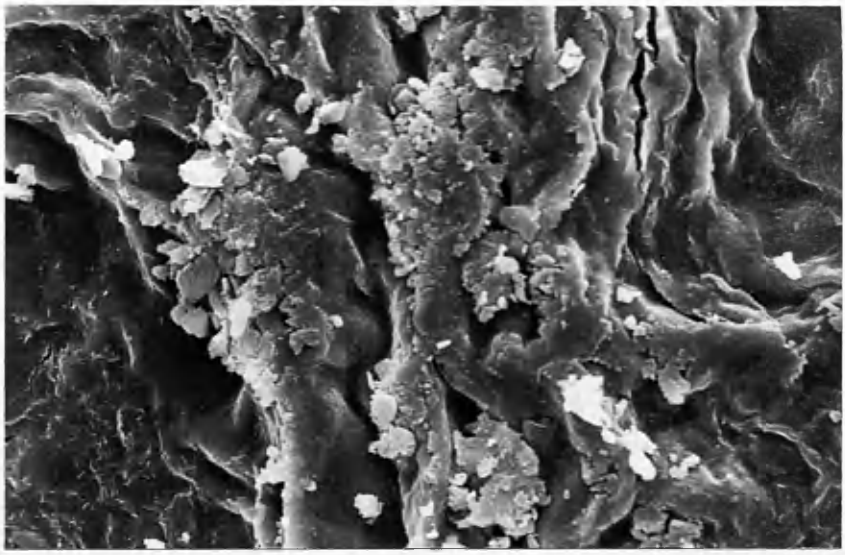

Plate 8.1 SEM photograph of sample D6 1.70, showing detrital illite flakes.

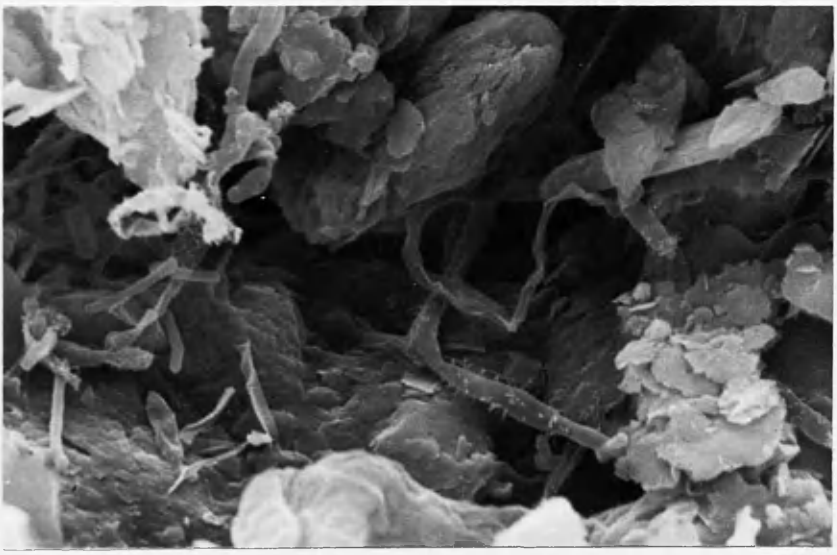

Plate 8.2 SEM photograph of sample D6 2.00, showing filamentous authigenic illite flakes.

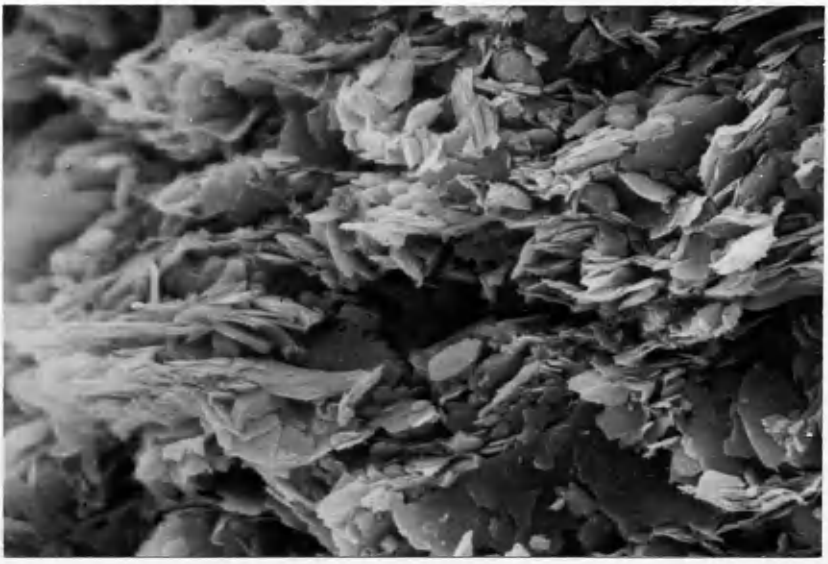

Plate 8.3 SEM photograph of sample N6 3.90, showing detrital chlorite.

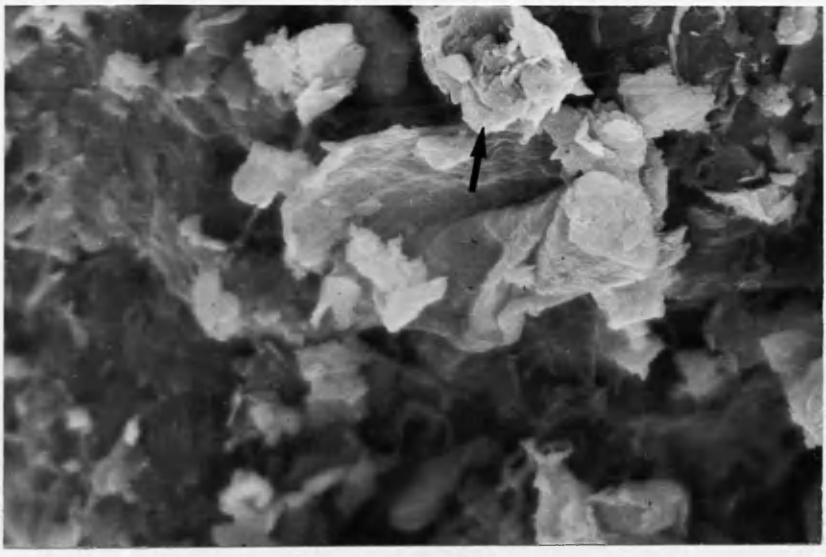

Plate 8.4 SEM photograph of sample N6 3.90, showing rosette morphology of authigenic chlorite.

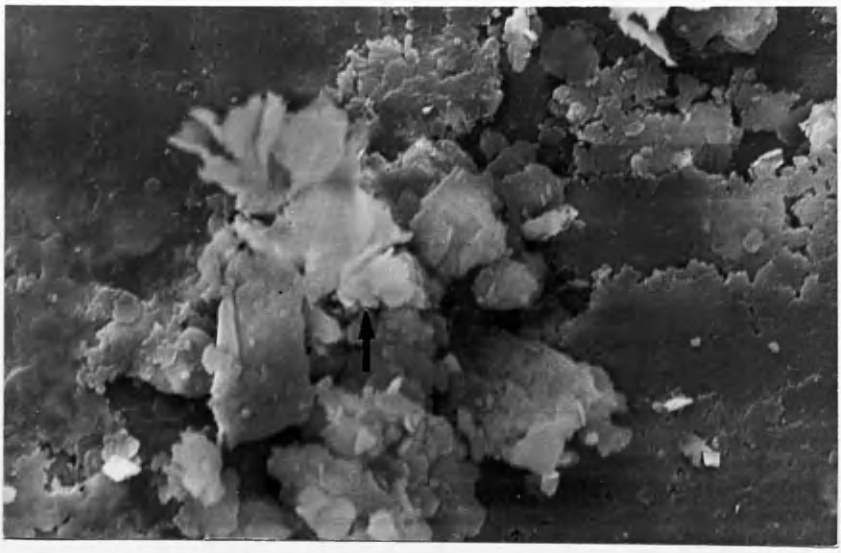

Plate 8.5 SEM photograph of sample D8 0.40, showing stacked plates of kaolinite..

CHAPTER 9

GEOCHEMISTRY OF THE SEDIMENTS

9.1 Introduction

The Holocene raised coastal sediments in the four areas of study consist mainly of clayey silt and variable proportions of clay and fine sand, especially in the upper part of the succession. Detailed X-ray fluorescence and wet chemical analyses were made of the major and trace element contents in bulk samples of the fine sediments and in the clay fraction of selected samples of the Holocene sediments from the four areas. Similar analyses were made of bulk samples of fine sediment and of the clay fraction of selected samples of the present-day intertidal surface sediments from the Dalbeattie, Kirkcudbright and New Abbey areas. In total, 152 samples were analysed for determination of the major elements and 107 samples were analysed for determination of sixteen trace elements. Few samples of the clay fraction were used in determination of trace elements because of difficulties in the separation of a large amount of the clay fraction (more than 5g) from the bulk sediment.

9.2 Aims of the geochemical studies

As far as the writer is aware, few studies of the geochemistry of Holocene raised coastal sediments and present-day intertidal sediments of Scotland have been made. Most of the studies that have been made are concerned with soil chemistry. The purposes of the geochemical studies in the present research project therefore were:

1) To record the chemical composition of the Holocene raised coastal sediments in the four areas of study, and simultaneously substantially increase the available geochemical data on these sediments in Scotland as a whole.

2) To record the chemical composition of the present-day intertidal sediments in

the Dalbeattie, Kirkcudbright and New Abbey areas, and simultaneously substantially increase the available geochemical data on these sediments in Scotland as a whole.

3) To examine qualitatively the mineralogical control on the distribution of the major and trace elements in the Holocene sediments and to determine whether or not the elements change laterally and vertically with change in sedimentary facies and change in grain size.

4) To compare the chemical compositions of the Holocene raised coastal sediments and the present-day intertidal surface sediments in the Dalbeattie, Kirkcudbright and New Abbey areas.

5) In selected samples, to study the composition of the clay fraction in order to throw light on the distribution and concentration of major and trace elements with a view to determining the origins and sources of the clay minerals.

6) To compare the results of the geochemical analyses of the clay fraction with clay species recognised by XRD.

9.3 Laboratory methods and calculation procedures

In this section, the laboratory methods used and calculation procedures adopted are described briefly.

9.3.1 X-ray fluorescence (XRF)

X-ray fluorescence analysis was used to determine ten major oxides (SiO_2, TiO_2, Al_2O_3, Fe oxides total, MnO, MgO, CaO, Na_2O, K_2O and P_2O_5) and 16 trace elements (Zr, Y, Sr, U, Rb, Th, Pb, Ga, Zn, Cu, Ni, Co, Cr, Ba, Ce and La). Major element analyses were performed on fused glass beads (Harvey et al. 1973). The beads were made by fusing 0.375g of 100 mesh rock powder and 2.000g of flux (lithium tetraborate).

Trace element compositions were determined on pressed pellets consisting of 6.000g of 250 mesh rock powder and 1.000g of thermal binder (phenol formaldehyde).

All the major and trace element determinations were carried out by the Phillips PW 1450/20 sequential automatic X-ray spectrometer. The X-ray spectrometer used three different detector tubes (W, Cr & Mo) and five different reflecting crystals [Ge, LiF(220), LiF(200), P.E. (Pentaerythritol) and T.A.P (thallium acid phthalate)] for analysing the major and trace elements. With occasional minor modifications, the combinations of tubes and crystals and details of current, voltage scintillation or flow detection and analysing angles followed those described by Leake et al. (1969).

For precision, all the XRF major element measurements were made in duplicate and averaged.

9.3.2 Wet chemical analysis

Ferrous iron oxide (FeO), water (H_2O) and carbon dioxide (CO_2) contents were determined by a standard procedure of wet chemical analysis. Ferrous iron was determined by titration with standard dichromate solution after the rock had been attacked with sulphuric and hydrofluoric acids.

The FeO% determined by titration was used to calculate the amount of ferric iron (Fe_2O_3) present, according to the following relationship:

$Fe_2O_3 = Fe^*_2O_3$ (XRF value) - 1.112 x FeO (titration result), where $Fe^*_2O_3$ is the total of the iron oxides present, i.e. Fe_2O_3 + FeO.

Water and carbon dioxide contents in a sample were determined simultaneously. The sample was inserted in a combustion tube at 1100^oC to 1200^oC. The water and carbon dioxide produced were removed with a current of nitrogen, absorbed and their quantities determined gravimetrically.

9.3.3 Niggli numbers

Niggli numbers avoid the problems caused by the fact that the largest single constituent of most rock analyses is SiO_2, and increases in SiO_2 are nearly always accompanied by decreases in other constituents because of the constant sum effect caused by all analyses being reported to 100%. Niggli numbers also simplify the number of separate chemical constituents to be considered by limited grouping together of elements that commonly substitute for each other in rock-forming minerals. The numbers are designed to facilitate graphical plotting so that large numbers of analyses can be dealt with and trends of variations deciphered that cannot be readily recognised in tables of numbers. They are also equally usable for studying the mineralogy of igneous, metamorphic, metasomatic or sedimentary rocks with none of the assumptions made in normative calculations. Finally, linking chemical and mineralogical variations is simplified using Niggli numbers. Basically, Niggli numbers are molecular proportions adjusted (Niggli 1954) so that:
al (Al_2O_3) + c (CaO) + fm (MgO + Feo + $2Fe_2O_3$ + MnO) + alk (Na_2O + K_2O) = 100, with si ($Si0_2$), p (P_2O_5) and ti (TiO_2) being calculated on the same basis as that used to reduce al + c + fm + alk to 100. It should be noted that Niggli k, considered below, is a measure of the ratio mol.K_2O/mol.(K_2O + Na_2O).

Most common sediments are dominated by mixtures of quartz, feldspar, sheet minerals and carbonates. Van de Kamp & Leake (1985) pointed out that, since albite and K-feldspars have equimolecular amounts of Na_2O + K_2O and Al_2O_3, Niggli al-alk = 0, whereas sheet minerals (mica, clay minerals and chlorites) normally have a strongly positive al-alk value, which enables their presence to be deduced and the al present in sheet minerals to be distinguished from that in feldspar.

Although anorthite, $CaO.Al_2O_3$ $2SiO_2$, has al-alk of 50, so that increasing calcic plagioclase increases al-alk, this can be distinguished from al-alk increases

due to clay minerals, micas and chlorites by the positive correlation of c and al-alk in plagioclase which is absent in sheet minerals. Similarly, increases in k caused by increased K-feldspar can be distinguished from increased k caused by enhanced mica contents because increase in K-feldspar results in falling al-alk, whereas larger mica contents give larger al-alk values. By judicious choice of such variables plotted, it is possible to use Niggli numbers of sediments to derive a good deal of information about the nature of the constituent minerals in the sediments. For example, since detrital calcic-rich feldspar is comparatively rare, most al-alk values in sediments are relative to the clay mineral content, and if plots of al-alk against trace elements are made it is possible to deduce which trace elements are dominantly in the clay minerals and micas (e.g. Ti, Ni, Cr) and which are antipathetic to the sheet minerals (such as Sr).

9.4 Major elements geochemistry

A large number of studies has been made of the major element geochemistry of sediments, to reflect differences in mineral distribution (e.g. Pearson 1979; Loring 1982; Melkerud 1983; Pederstad & Jørgensen 1985; Van de kamp & Leake 1985). Geochemical criteria, as means of differentiating marine from fresh water sediments on the basis of their mineral contents have also been discussed by many workers (e.g. Dewis et al. 1972; Roaldset 1972; Villumsen & Nielsen 1976).

In the present work a detailed analysis was made of the major elements in the Holocene raised coastal and present-day intertidal sediments with a view to comparing these two groups of sediments, and in an attempt to differentiate between the various sedimentary facies within the Holocene raised coastal sediments. Means and standard deviations were calculated for bulk sediment samples and samples of the clay fraction from each of the four areas studied (Tables 9.1 to 9.4).

The major elements used in the chemical correlation are discussed below and

their distributions shown in Tables 9.6 to 9.8.

The data in Tables 9.6 to 9.8 show that the major element contents of the complete Holocene sedimentary succession in the Dalbeattie area and the upper part of the Holocene successions in the Kirkcudbright and New Abbey areas are very similar. This supports the suggestion that these three groups of deposits belong to the same sedimentary facies (facies A of Chapter 5.3.2.). In contrast, the geochemical data show that the lower part of the Holocene sedimentary succession in the Kirkcudbright and New Abbey areas (facies B and D of Chapter 5.3.2) differs from the upper part of the Holocene succession (facies A) in the same areas. In addition, the major element content of the Holocene sediments of the former Lochar Gulf differs noticeably from that of most of the Holocene sediments in the three other areas studied.

It may also be noted that the major element content of the present-day intertidal surface sediments of the Dalbeattie, Kirkcudbright and New Abbey areas resembles that of Holocene facies B and D (of the Kirkcudbright and New Abbey areas).

In both the Holocene and present-day sediments, the SiO_2 percentages in the bulk samples studied show inverse relationships with the percentages of TiO_2, Al_2O_3, $Fe^*_2O_3$, MgO, and K_2O (Figs. 9.1 to 9.5), poor inverse correlation with the percentages of CaO and CO_2 (Figs. 9.6 to 9.7) and undefined relationships with the percentages of MnO, Na_2O and P_2O_5. In the clay fraction, the SiO_2 content is thought to be contained within the clay minerals, and also in very small amounts of quartz, the latter of which were detected by XRD.

Generally, most alkali rocks are enriched in Ti, and Ti, being relatively resistant, remains during weathering. Its concentration is highest in sedimentary rocks (Mielke 1979,13-37). Also, Wedepohl (1978) suggested that the presence of TiO_2 in sediments is due to terrigenous material consisting of: (1) weathering residues in the form of either chemically unaltered grains such as rutile or partly

decomposed minerals such as mica; (2) products of weathering such as anatase and clay minerals; (3) diagenetic minerals.

In the present work (Tables 9.6 to 9.8), the TiO_2 content in the Holocene raised coastal sediments of the Dalbeattie area and in the upper facies of the Kirkcudbright and New Abbey areas is higher than in the present-day intertidal sediments of all three areas.

Figure 9.8 shows a positive relationship between Niggli al-alk and Niggli ti in the bulk samples of the Holocene raised coastal sediments, confirming that the TiO_2 is associated with the clay minerals, whilst the relationship in the present-day intertidal sediments is poor or shows no correlation. This may be due to the TiO_2 being present in the form of detrital or unaltered grains such as rutile.

Generally, the Al_2O_3 content in a sediment increases as the amount of the clay fraction increases. Schultz (1964) pointed out that montmorillonite, illite and mixed-layer clays are the common aluminous varieties and, therefore, the amount of alumina should bear a fairly consistent relation to the total clay content in each sample.

In both the Holocene and present-day sediments analysed, the abundance of Al_2O_3 may be directly related to the abundance of clay minerals and mica. The strong positive relationship between Al_2O_3 and K_2O (Fig. 9.9) and the positive correlations of Niggli al-alk with K_2O (Fig. 9.10) and Niggli k with Niggli al-alk (Fig. 9.11), together with the relationship of Niggli al-alk versus Niggli k x Niggli alk (Fig. 9.12), are good indications that Al_2O_3 and K_2O are dominantly in the clay minerals and other sheet silicates rather than in feldspars in the various areas of study. This agrees with Argast & Donnelly's (1987) suggestion that concentration of Al_2O_3 correlates well with K_2O concentration and the Al_2O_3-K_2O trend passes near the origin of the Al_2O_3-K_2O graph. The trend has a slope of about 0.3, the ratio of K_2O to Al_2O_3 in illite. K-feldspar does not have K_2O and Al_2O_3 in the necessary ratio to

produce this trend. The slight negative correlation between Niggli al-alk and Na_2O and the undefined relationship between Niggli al-alk and CaO (Figs. 9.13 to 9.14) indicate that the Al_2O_3 is contained mainly in the clay minerals and other sheet silicates rather than in feldspar.

The clay fraction of the samples studied has high Al_2O_3 and K_2O contents and low CaO and Na_2O, all of which confirm the importance of illite.

The relationships between CaO and CO_2, and between CaO and P_2O_5 (Fig 9.15), are slightly positive or undefined. For the most part, CaO is more abundant in the present-day intertidal sediments than in the Holocene raised coastal sediments.

The correlation between Niggli c and Niggli al-alk (Fig. 9.16) shows that the majority of the analysed samples have a low content of CaO when the Niggli al-alk value is high, indicating that CaO is not present or is present in very small amounts in the clay minerals. A few samples show a negative correlation between Niggli al-alk and Niggli c in both the Holocene and present-day intertidal sediments, which indicates that the increases in CaO and Al_2O_3 contents are not due to the presence of anorthite ($CaO.Al_2O_3$ $2SiO_2$). It is suggested that the presence of organic carbonates, fossil shells and apatite is responsible for the abundance of CaO in these samples.

In both the Holocene and present-day sediments, the Na_2O content is variable, with a wide range in most of the samples from the four areas, and there is no significant difference between the Na_2O content in the bulk samples and clay fractions of the sediment studied. The Na_2O may be shared by detrital feldspars and clay minerals (cf. Mielke 1979), and the concentration of Na_2O agrees approximately with the suggestion by Heier & Billings (1969) that the concentration of Na_2O in shales averages 0.80%.

A few samples in both the Holocene raised coastal sediments and the present-day intertidal sediments have relatively high Na_2O content (1% to 3%).

This may be due to the presence of detrital grains of plagioclase feldspars (Fig. 9.13).

Fe_2O_3 is more abundant than FeO in most of the samples studied and the total iron oxide is greater in the clay fraction than in the bulk-sediment samples from both the Holocene and present-day intertidal sediments. Weaver & Beck (1971) confirmed the suggestion that chloritic clays are rich in iron (23.9 % Fe as Fe_2O_3). Roaldset (1972) noted that an increase in illite content leads to an increase in the Fe_2O_3, MgO and K_2O contents and suggests the presence of considerable amounts of trioctahedral illite.

In the present work, the high percentages of FeO and Fe_2O_3 may be due to the high proportion of clay fraction in the sediments studied. This suggestion is confirmed by the high content of iron oxides in samples of the clay fraction. The relationship between Niggli al-alk and $Fe^*_2O_3$ (i.e. total iron oxides) (Fig. 9.17) is positive in both the Holocene and present-day intertidal sediments, which may be an indication that the iron oxides are contained mainly in clay minerals and other sheet silicates.

The MgO content in the sediments analysed in the present work is mainly in the clays such as chlorite and illite, as confirmed by the high content of MgO in the studied samples of the clay fraction. Figure 9.18, showing positive correlation between Niggli al-alk and Niggli fm, confirms that the Mg and Fe are contained in clay minerals and other sheet silicates.

The P_2O_3 content in both the Holocene and present-day sediments is very low in the four areas studied. The undefined relationship between CaO and P_2O_5 (Fig. 9.15) and the positive relationship between al-alk and P_2O_5 (Fig. 9.19) may be due to the P_2O_5 being contained mainly in clay minerals and sheet silicates. This is in agreement with Wedepohl's (1978) suggestion that the absorption of P on clay minerals can be significant.

9.5 Trace elements geochemistry

Trace elements have been used by many workers to determine the provenances of sediments or the environments of deposition. Atherton (1986) used the relationships between Rb, Zn, Ba, V and K to differentiate between fluvial, glaciofluvial and estuarine sediments. Previous work (e.g. Van de Kamp et al. 1976; Senior & Leake 1978; Van de Kamp & Leake 1985) has shown that, typically, many trace elements such as Cr, Ni, Ti, Rb, Y, Zn, La and Ce are contained dominantly in the clay-mineral fraction of a sediment whereas Sr usually is contained in detrital plagioclase or carbonates. Also, Lerman (1966), Couch & Grim (1968), Brockamp (1973) and Villumsen & Nielsen (1976) pointed out that B, Li and Rb are incorporated in the clay fraction in amounts that increase with salinity. Hickman & Wright (1983), during a study of the Appin Group slates, used the relationships between Y + La + Ce, Ni + Cr and Sr to suggest the provenances of the rocks. They also tried to distinguish between and correlate the various rock units within the Appin Group slates on the basis of trace element compositions and they suggested that the most useful trace elements in this respect are P, Cr, Zn, Cu, Pb, Sr, Y, Nb, Ba, La and Ce, the elements which give clearest separation on a triangular plot being Cr, Zn and Y.

In the present project, trace elements study was carried out to determine the distribution of these elements and establish their relationships with the various sedimentary facies in the Holocene raised coastal sediments. Further aims were to compare the concentrations of these elements in the Holocene sediments and in the present-day intertidal sediments in the various areas studied, and to investigate the sources of the trace elements and their relationships with the clay minerals. Using Niggli al-alk, Niggli k and K_2O contents as a measure of the clay-mineral content, plots were made against the trace elements and between the trace elements in an attempt to determine the provenances of the sediments.

Table 9.5 shows the means and standard deviations of trace element concentrations, and Tables 9.6 to 9.8 show the concentrations of trace elements, calculated in ppm, in the various sediments and in selected samples of the clay fraction.

9.5.1 Niggli al-alk versus trace elements

The association of trace elements with clay minerals was studied by Van de Kamp & Leake (1985) using a number of plots of Niggli al-alk versus trace elements. These authors indicated which elements are related to sheet silicates and which elements are not. In addition, the distribution and origin of trace elements and their relationships to clay minerals have been discussed by authors such as Moore(1963), Wedepohl (1978) and Taylor & McLennan(1981).

Plots of trace elements made against Niggli al-alk should show which elements were dominantly added to the sediments in the clay minerals and mica. In the present study, the plots of Niggli al-alk against trace elements show the following relationships:

1) Niggli al-alk shows positive correlations with Y, Sr, Rb, Th, Pb, Ga, Zn, Ni, Co, Ce, Cr, Ba and La in analysed bulk samples of Holocene sediment from the four areas studied (Figs. 9.20 to 9.32). These elements also show slight positive correlations with Niggli al-alk in the present-day intertidal sediments of the Dalbeattie, Kirkcudbright and New Abbey areas (Figs. 9.20 to 9.32).

Generally, the concentration of all the above-named elements is greater in the fine-grained sedimentary facies (clayey silt) than in the coarser-grained facies (fine sand) of the Holocene sediments. Also, the concentrations of these elements are much higher in the clay fractions than in bulk samples. It may be concluded that these elements are contained mainly within clay minerals and other sheet silicates.

It may be noted that the concentration of these elements increases with an

increase in the amount of clay fraction in the bulk sediments and is not related to the clay mineral species present. Accordingly, there is no clear relationship between Niggli al-alk and trace elements in the clay fraction of the samples analysed (Figs. 9.20 to 9.32).

The weak positive correlation of the above-named elements with Niggli al-alk in the present-day intertidal sediments in the Dalbeattie, Kirkcudbright and New Abbey areas may be due to the low amount of clay fraction contained in the bulk samples from the present-day intertidal sediments.

It may be noted that Sr concentrations in the present-day intertidal sediments are higher than in the Holocene raised coastal sediments, possibly due to the abundance of CaO in the present-day intertidal sediments. Because of this possibility, and from the lack of a clear negative correlation between Niggli al-alk and Sr (Fig.9.21), and because of the high concentration of Sr in the clay-fraction samples, it may be concluded that Sr is neither concentrated in K feldspar and clay minerals nor totally absent from these minerals. This is consistent with the results obtained from the CO_2 versus Sr plot (Fig. 9.41) described below.

2) Niggli al-alk shows a poor negative correlation with Zr (Fig. 9.33) that may be due to the association of Zr with detrital minerals such as zircon.

3) In both bulk samples and in the clay fraction of the Holocene raised coastal sediments and present-day intertidal sediments, Cu shows an undefined relationship with Niggli al-alk. Its concentration, however, is greater in the clay fraction than in the bulk sediment (Fig.9.34). Wedepohl (1978) suggested that the accumulation of Cu in sedimentary environments probably is connected with detrital matter such as iron minerals. He also claimed that the organic fraction of shales often is enriched in Cu and he added that most of the Cu is fixed in reducing environments by clays and organic carbon. Accordingly, the enrichment in Cu of samples of the clay fraction (and some bulk samples) in both the Holocene and present-day intertidal sediments

may be due to the presence of organic material and/or to reducing environmental conditions at certain localities. In four samples the concentration of Cu is more than 200 ppm. It is possible that this is due to contamination of the samples in the field. (All four sites concerned were located close to stream banks where there may have been a nearby concentration of metal in the form of overhead electricity wires and/or domestic refuse.)

4) U shows no correlation or very poor positive correlation with Niggli al-alk (Fig. 9.35) in both the Holocene and present-day intertidal sediments. The concentration in samples of the clay fraction is the same as that in the bulk sediments. However, U has a very low concentration in the various facies of the Holocene sediments.

9.5.2 Niggli k versus trace elements

As stated in Chapter 9.3.3 above, Niggli k provides a measure of the ratio mol.K_2O/mol.(K_2O + Na_2O). In the present work it was noted that K_2O increases in the Holocene fine-grained sedimentary facies and in samples of the clay fraction. The relationships between Niggli k and some of the trace elements were plotted (Figs. 9.36 to 9.39). The relationship between Niggli k and Zr is undefined, confirming that Zr is not associated with clay minerals but is associated with detrital minerals, as zircon (Fig. 9.36). There is no clear relationship between Niggli k and Sr (Fig. 9.37), which suggests that Sr is shared by both clay minerals and K feldspar, whilst the relationships between Niggli k and both Rb and Ba are positive (Figs. 9.38 & 9.39), as is usual in crustal materials.

9.5.3 Niggli c versus Sr

The relationships between Niggli c and Sr (Fig. 9.40) and between CO_2 and Sr (Fig. 9.41) were plotted for the Holocene and present-day intertidal sediments to show whether Sr is related to the carbonates and feldspars or to clay minerals. It was noted that samples from the Holocene raised coastal sediments (Fig. 9.40A) had low Niggli c values and Sr probably is not associated with CaO but related to the clay minerals or K feldspar.

Comparison of Figure 9.40B with Figure 9.40A shows that Niggli c and Sr are more highly concentrated in the present-day sediments than in the Holocene sediments. This may be due to the presence of Sr in detrital K feldspars or in carbonate and clay minerals.

9.5.4 CO_2 versus trace elements

Plots of all trace elements against CO_2 were made to show which trace elements are related to carbonate. All the trace elements show undefined relationships except Sr (Fig. 9.41), which shows poor or undefined relationship in the Holocene raised coastal sediments (Fig. 9.41A) and poor relationship in the present-day intertidal sediments (Fig. 9.41B). It is concluded that Sr is weakly related to carbonate in the Holocene raised coastal sediments and more strongly related to carbonate in the present-day intertidal sediments.

9.5.5 Relationships between trace elements

Relationships between Sr and Rb, and between Zn and Ba were plotted (Figs. 9.42 & 9.43) and gave positive relationships between these elements. In Figures 9.42 and 9.43 it is noticeable that there is more than one cluster of the trace element contents due to the presence of several facies of Holocene sediments, each with a different concentration of Sr, Rb, Ba, and Zn. This is especially clear in the

Kirkcudbright and New Abbey sediments, where the upper sedimentary facies (clayey silt) has a greater concentration of these trace elements than the lower facies (silt with fine sand, and fine sand).

Hickman & Wright (1983) pointed out that Ni and Cr indicate basic source regions, whilst Y, La and Ce indicate a granitic source, and Sr is highest where the source contains sedimentary rocks. Accordingly, a triangular plot diagram for Ni +Cr versus Y + La +Ce versus Sr (Fig. 9.44) was constructed to give an indication of the sources of the sediments. The diagram suggests that, in the various areas studied, both the Holocene raised coastal sediments and the present-day intertidal sediments of the same areas were derived from various sources (Fig. 9.44 ; see also Chapter 10, below).

9.6 Vertical variations in the geochemistry of the Holocene sediments

In the four areas studied, the major and trace elements show vertical variation in their distribution within the sampled sections of Holocene raised coastal sediments. Suggested causes of this variation are:

1) Variations in the textural characteristics of the samples studied.

2) Variations in the mechanism of transportation of the sediments, perhaps caused by instability in the position of the shoreline at the time of deposition.

3) Changes, through time, in the physiography or in the environments of deposition.

4) Weathering effects on the various oxides and trace elements. Burek (1985) calculated weathering ratios of some oxides and trace elements (e. g. Ga : Al_2O_3, MgO : Ni, FeO : Co) and showed that vertical variations in these ratios are produced by the effects of weathering.

9.6.1 Dalbeattie area

Figures 9.45 and 9.46 show vertical variations in the distribution of some of the major and trace elements in sections D5 and D10. In section D5, SiO_2 decreases with depth, perhaps because of an increase in the clay mineral content in the lower part of this section. Al_2O_3 and K_2O show slight decrease with depth, whilst $Fe^*_2O_3$ increases slightly to a maximum at the base of the section. Zr is slightly variable and shows a maximum concentration at about 1.2m below ground level. Rb, Zn and Sr are more concentrated near the top and the bottom of the section and are minimal in the middle of the section (c. 1.2m). Ba concentration is greater at the top of the section and decreases with depth. The vertical variation of the major and trace elements in this section is not marked. This may be due to the homogeneity of the sediments, which, it is suggested, were deposited in a lagoonal semi-closed local environment, and to the high content of organic material, including peat.

The vertical variation of the same oxides and elements in the D10 section is such that SiO_2 shows inverse relationship with Al_2O_3 and $Fe^*_2O_3$. SiO_2 reaches a maximum in the clayey silt (facies A) at a depth of c. 0.70 m below the surface, whilst other oxide contents are minimal at this depth. Plots of the concentrations of the trace elements Ba, Zr, Sr, Rb and Zn show slight changes in concentration through the section. It may be noted that the slight change in the content of major and trace elements in both selected sections is difficult to use as a discriminatory tool between the various sedimentary facies, perhaps because these facies vary only slightly in their textural characteristics.

9.6.2 Kirkcudbright area

Al_2O_3, $Fe^*_2O_3$ and K_2O contents are at their maxima near the top of section K1 and have an inverse relationship with SiO_2 (Fig. 9.47). Changes in the contents of these oxides occur at the changes of facies from fine sand to inter-laminated fine

sand and silt in the lower part of this section, and from inter-laminated fine sand and silt to clayey silt in the upper part of the section.

The trace elements show slight changes in their concentrations with the changes in sedimentary facies.

It may be concluded from the above that it is possible to use the change in contents of certain of the major elements and the change in concentration of some of the trace elements to detect changes in the sedimentary facies in this area.

9.6.3 New Abbey area

In section N5 of the New Abbey area (Fig. 9.48), changes in the oxide contents correspond with changes in sedimentary facies. As in the uppermost sub-facies (clayey silt) of the Dalbeattie area and the upper part of the succession in the Kirkcudbright area, the change in contents is slight. There is a clear break in the geochemical contents at a depth of about 3.0m below ground level. At depths of between 3.0m and 5.0m, large variations in the geochemical content reflect sudden changes in sedimentary nature that are indicative of unstable conditions at the time of deposition. Below 5.0m depth, the geochemical content shows stability within the fine sand facies.

There are slight fluctuations in the concentrations of the trace elements Ba, Zr, Sr, Rb and Zn through the vertical sections.

9.6.4 Lochar Gulf

In the Holocene raised coastal sediments of the former Lochar Gulf, major and trace element contents show a wide variation both laterally and vertically (Fig. 9.49). SiO_2 content increases with depth, whilst Al_2O_3, $Fe^*_2O_3$ and K_2O contents decrease. The trace elements Ba, Zr, Sr, Rb and Zn show no clear variation with depth.

A break in the concentration of the major elements at about 1.0m below the ground surface may have been caused by weathering of some elements and concentration of others and by a change in sedimentary facies.

In this area the vertical variation is great and differs from one section to another.

9.7 Element variation in different types of sediments

Generally, it is possible to discriminate between the Holocene coastal sediments and the present-day intertidal sediments by using the trace element concentration. Table 9.5 shows that the concentration of most of the trace elements associated with the clay minerals (e.g. Y, Rb,Th, Ga, Zn, Ni, Co, Cr, Ce, Ba and La) is greater in the Holocene raised coastal sediments than in the present-day intertidal sediments. In contrast, Zr is more concentrated in the present-day intertidal sediments than in the Holocene raised coastal sediments because of the strong relationship between this element and detrital minerals. Also, it may be noted that Sr is more concentrated in the present-day intertidal sediments than in the Holocene raised coastal sediments.

Table 9.5 summarises the concentration of the trace elements in bulk samples and in samples of the clay fraction, and indicates that the majority of the trace elements are more highly concentrated in the clay fraction than in the coarser-grained fractions of the sediments.

9.8 Conclusions

From geochemical studies of bulk samples of the Holocene raised coastal sediments and present-day intertidal sediments, and geochemical analysis of the clay fraction of selected samples, the following may be concluded:

1) The average major element compositions of the majority of the Holocene raised coastal sediments of the Dalbeattie area and of the upper facies (clayey silt) of

the same sediments in the Kirkcudbright and New Abbey areas are generally similar. Similarly, the lower facies (inter-laminated fine sand and silt, and fine sand) of the Kirkcudbright and the New Abbey areas resemble each other in geochemical content.

2) The SiO_2 content in the Holocene raised coastal sediments of the Lochar Gulf area is higher than that in the Holocene sediments of the Dalbeattie, Kirkcudbright and New Abbey areas. The high SiO_2 value is a sign that the sediments were derived either from clastic sedimentary rocks rich in mature quartz or from mature sandstone.

3) Generally, the SiO_2 content shows slight or no clear vertical variation in the Holocene sections studied in the Dalbeattie area, whilst it shows an increase with depth in the Kirkcudbright and New Abbey areas. In the Lochar Gulf area, the vertical distribution of SiO_2 varies from one locality to another.

4) In both the Holocene and present-day sediments of all four areas studied, SiO_2 shows an inverse relationship with Al_2O_3, $Fe^*_2O_3$, TiO_2, MgO and K_2O.

5) The positive relationships between Niggli al-alk and P_2O_5, and Niggli al-alk and Niggli ti indicate that P_2O_5 and TiO_2 are present mainly in clay minerals.

6) The positive relationship of Niggli al-alk with $Fe^*_2O_3$ in the Holocene raised coastal sediments and the greater concentration of the total iron oxides in the clay fraction than in bulk samples indicates the association of these oxides with clay minerals.

7) The major elements content of the present-day surface sediments of the Kirkcudbright and New Abbey areas is similar to that of the lower facies (silty sand or fine sand) of the Holocene sediments of the same areas.

8) The SiO_2 content of the present-day intertidal sediments of the Dalbeattie area is greater than that of the Holocene raised coastal sediments of the same area.

9) The SiO_2 content of the present-day intertidal sediments of the Kirkcudbright area is greater than that of the Holocene sediments in the same area.

10) In the Dalbeattie, Kirkcudbright and New Abbey areas, the CaO content is greater in the present-day intertidal sediments than in the Holocene sediments, perhaps because of a greater content of organic carbonates or shell fossils and/or apatite in the present-day sediments. No clear relationship has been established between CaO and P_2O_5. The relationship between CaO and SiO_2 is undefined in the Holocene raised coastal sediments and there is an inverse relationship between these oxides in the present-day intertidal sediments (Fig. 9.6). The relationship between CaO and CO_2 is very poorly positive or undefined in the Holocene raised coastal sediments and positive in the present-day intertidal sediments. The relationship between Niggli al-alk and Niggli c shows that most of the samples have a very low CaO content and, in this case, the CaO is related to clay minerals.

11) The wide variability and low content of Na_2O in the bulk samples studied, and the presence of Na_2O in samples of the clay fraction may be due to the presence of this oxide in both clay minerals and detrital minerals such as feldspar.

12) The high contents of Al_2O_3 and K_2O in the fine-grade sediments (clayey silt) in all the areas studied, and the strong inverse relationships between these oxides and SiO_2, together with the positive relationships between Niggli al-alk and K_2O and between Niggli al-alk and Niggli k, indicate that Al_2O_3 and K_2O are related mainly to the clay minerals present in the sediments.

13) The variable content of major elements in the present-day intertidal sediments from one locality to another within the same area may be due to the analysed samples having been collected from different physiographic positions or different sedimentary bodies within the present intertidal zone. Some of the

samples were collected from point-bars, others from the sides of gullies or areas between gullies.

14) The positive relationships between Niggli al-alk and Y, Sr, Rb, Th, Pb, Zn, Ni, Co, Ce, Cr, Ba and La in the bulk samples show that these elements are associated with clay minerals. The concentration of these elements is greater in the finer-grade sedimentary facies (clayey silt, and clayey silt with fine sand) than in the coarser facies (inter-laminated fine sand and silt, and fine sand).

15) Niggli al-alk gave undefined relationships with trace elements in samples of the clay fraction, and positive relationships in bulk samples, since concentration of the trace elements depends on the magnitude of the clay fraction and not on the clay mineral type or species.

16) The high concentration of trace elements in the clay fraction confirms that the majority of the elements concerned are associated with clay minerals.

17) The variability in major elements content and in the concentration of the trace elements within the clay fraction of the Holocene and present-day intertidal samples may be due to differences in clay-mineral species and/or the presence of small amounts of other minerals such as quartz and feldspar.

18) In the Holocene raised coastal sediments, major and trace element contents change vertically with changes in sedimentary facies.

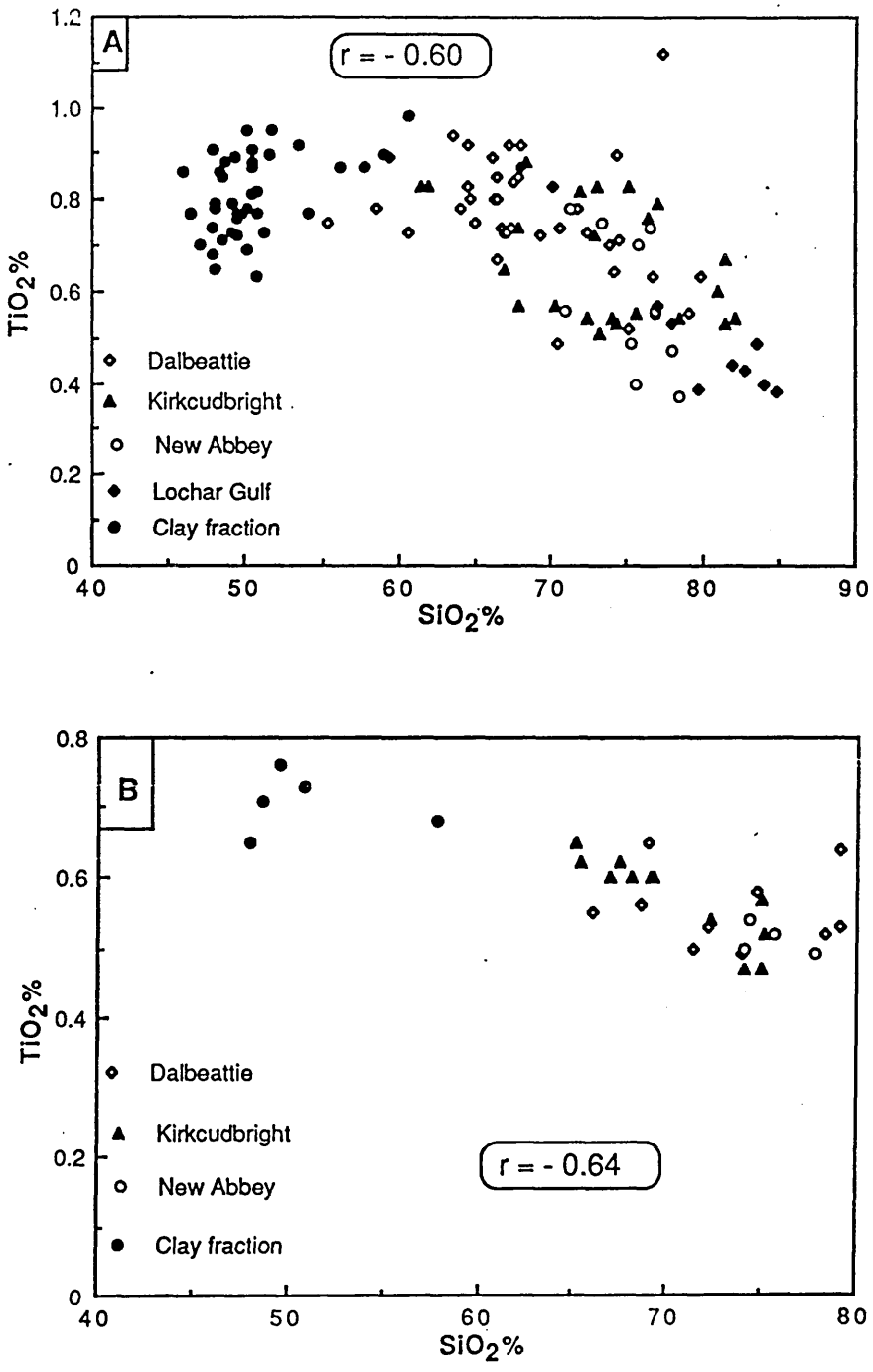

Figure 9.1 Plot of SiO_2% against TiO_2%:
A, Holocene sediments;
B, Present-day intertidal sediments.
Bulk sample values for individual areas are shown separately. Values for samples of the clay fraction from the Dalbeattie, Kirkcudbright and New Abbey areas are grouped together.
r is the correlation coefficient for the distribution of the bulk sample values for all areas.

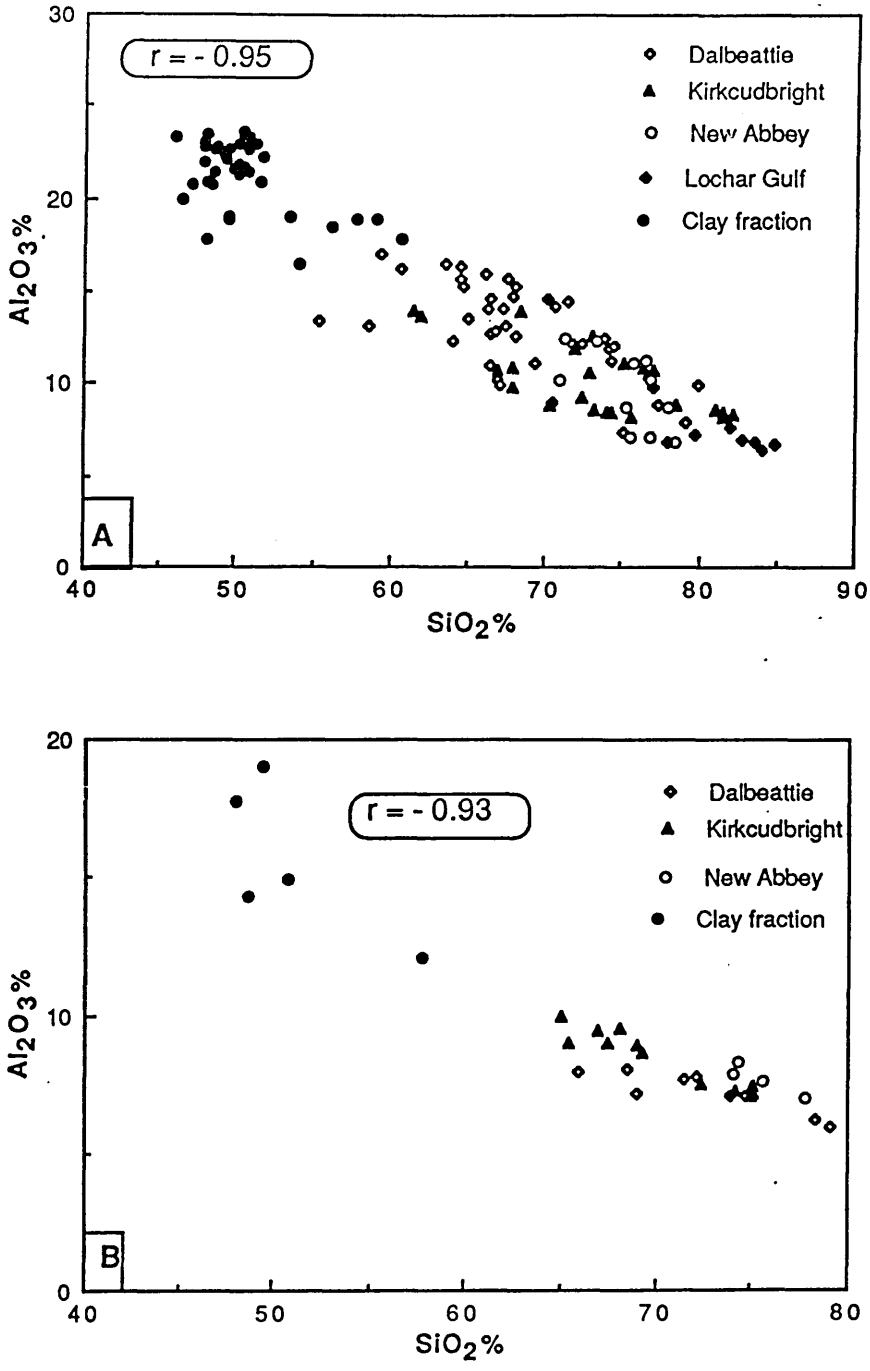

Figure 9.2 Plot of SiO_2% against Al_2O_3%:
A, Holocene sediments;
B, Present-day intertidal sediments.
Bulk sample values for individual areas are shown separately. Values for samples of the clay fraction from the Dalbeattie, Kirkcudbright and New Abbey areas are grouped together.
r *is the correlation coefficient for the distribution of the bulk sample values for all areas.*

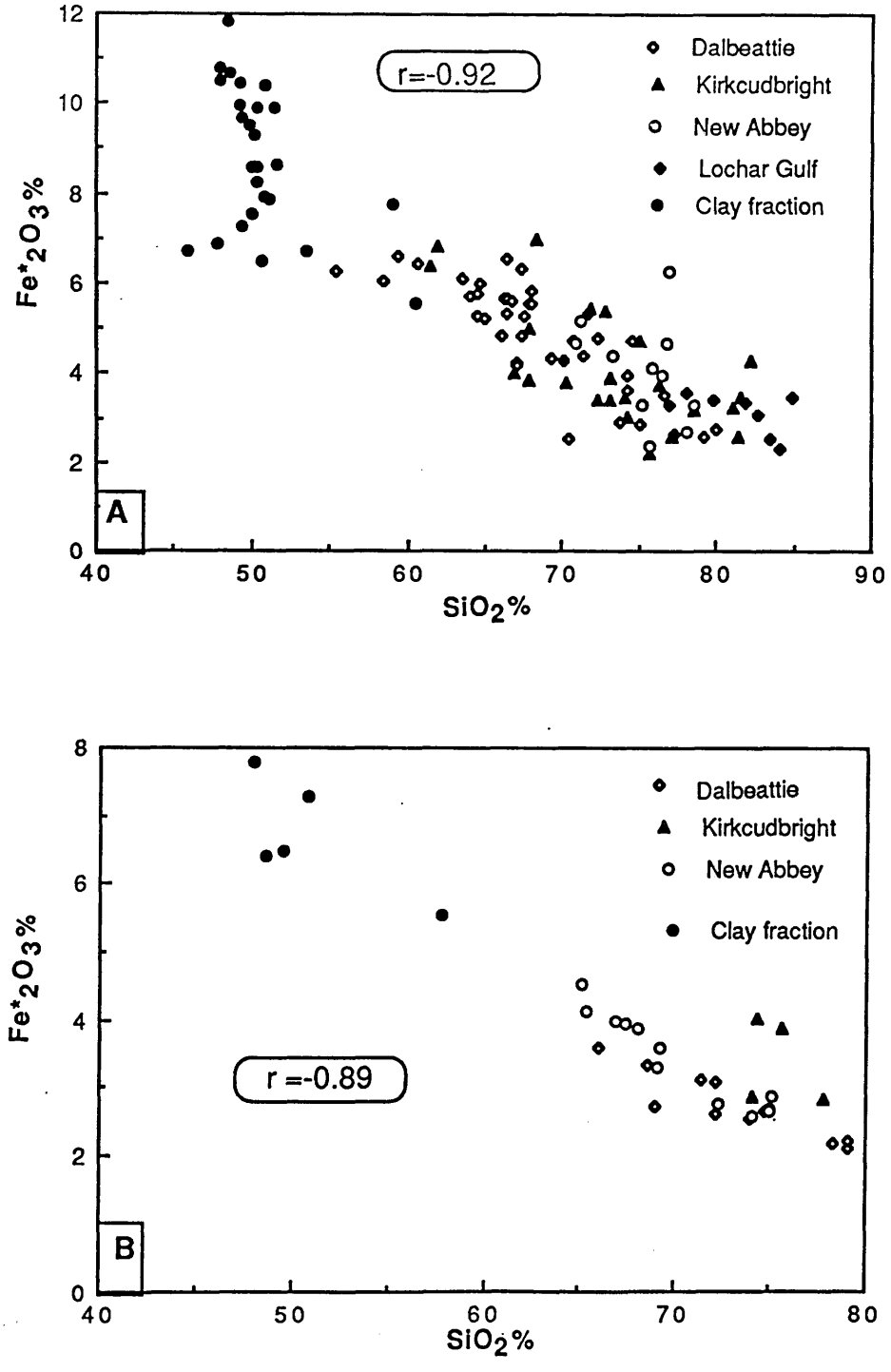

Figure 9.3 Plot of SiO_2% against $Fe^*_2O_3$%:
A, Holocene sediments;
B, Present-day intertidal sediments.
Bulk sample values for individual areas are shown separately. Values for samples of the clay fraction from the Dalbeattie, Kirkcudbright and New Abbey areas are grouped together.
r *is the correlation coefficient for the distribution of the bulk sample values for all areas.*

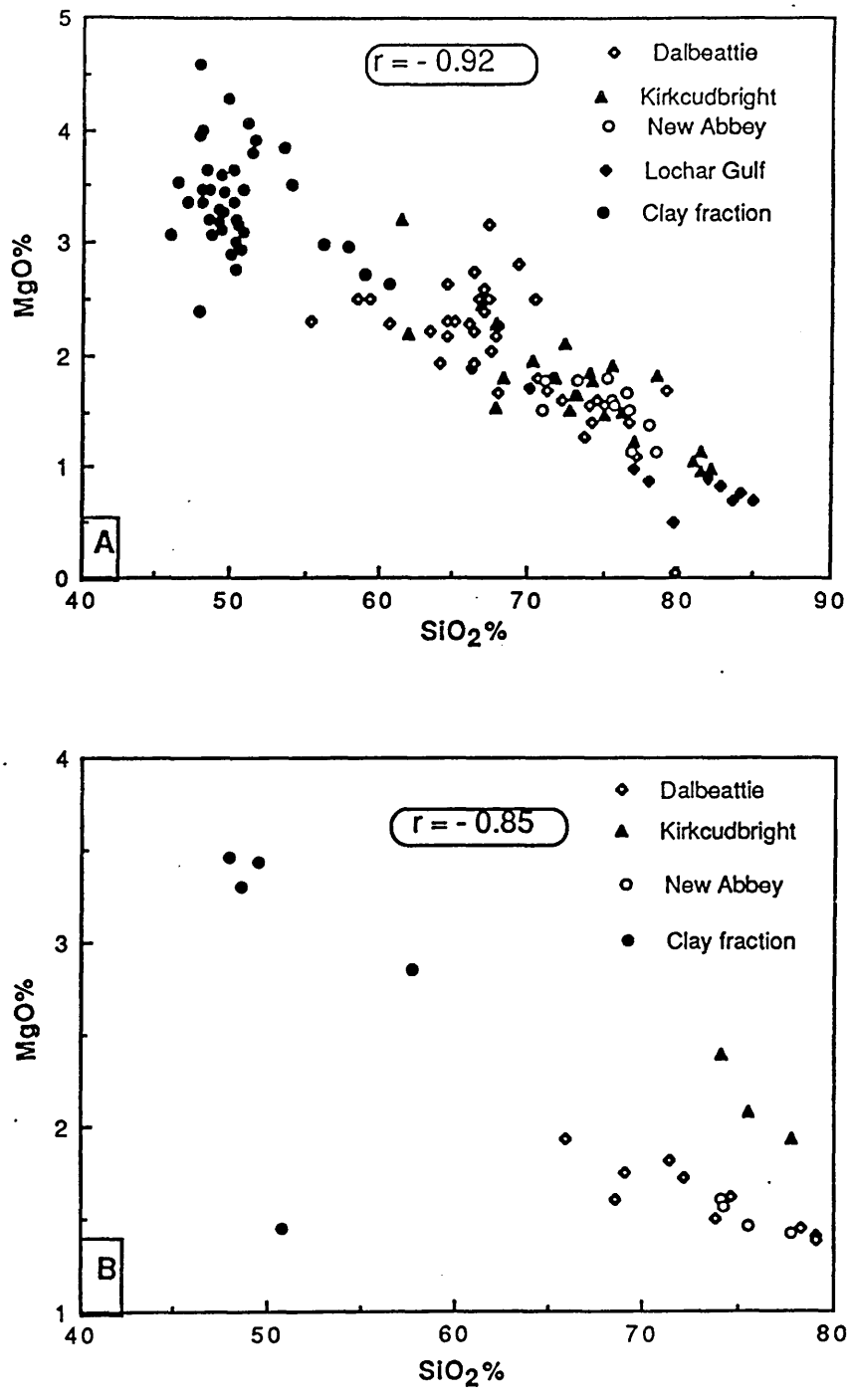

Figure 9.4 Plot of SiO_2% against MgO%:
A, Holocene sediments;
B, Present-day intertidal sediments.
Bulk sample values for individual areas are shown separately. Values for samples of the clay fraction from the Dalbeattie, Kirkcudbright and New Abbey areas are grouped together.
r is the correlation coefficient for the distribution of the bulk sample values for all areas.

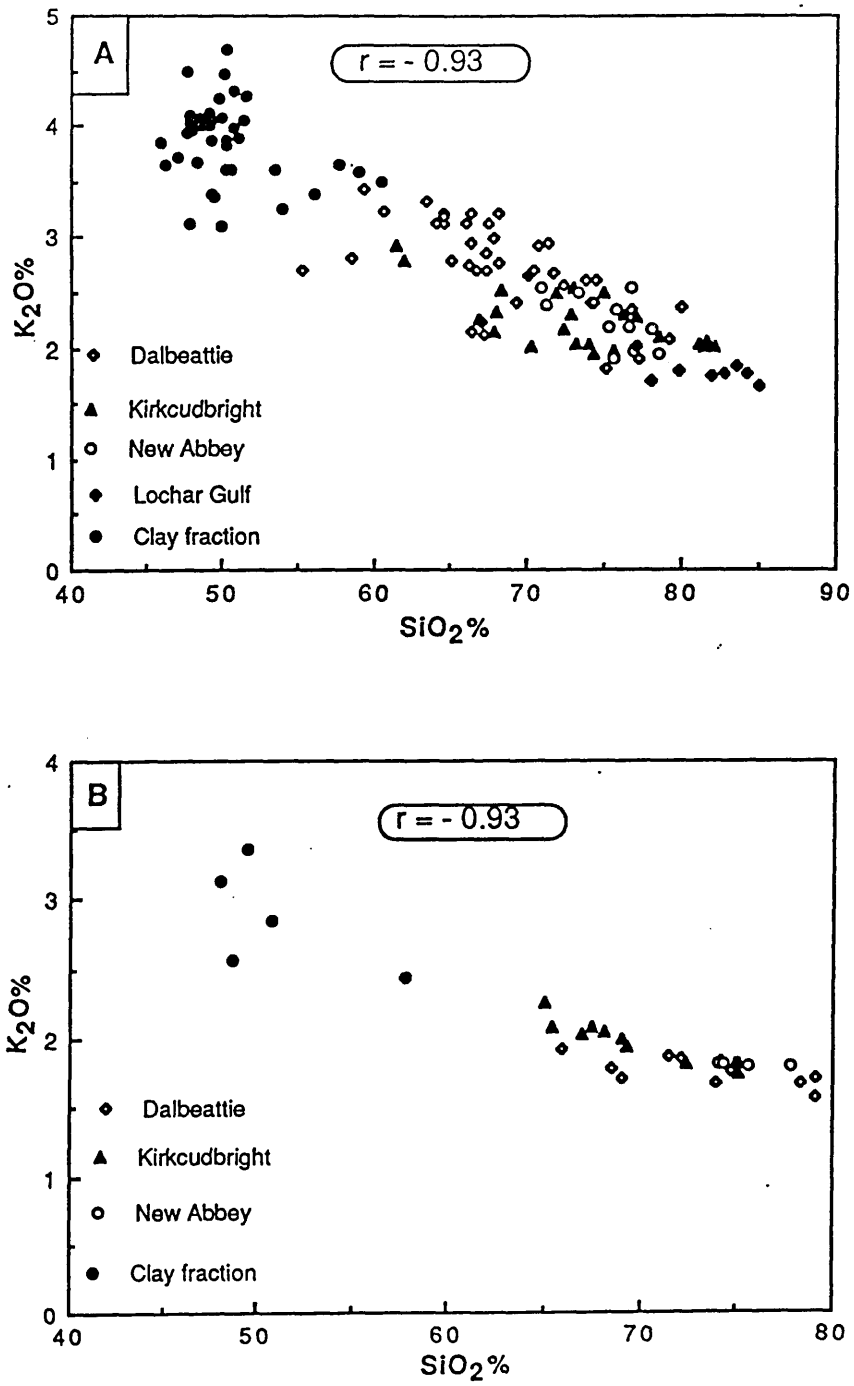

Figure 9.5 Plot of SiO_2% against K_2O%:
A, Holocene sediments;
B, Present-day intertidal sediments.
Bulk sample values for individual areas are shown separately. Values for samples of the clay fraction from the Dalbeattie, Kirkcudbright and New Abbey areas are grouped together.
r *is the correlation coefficient for the distribution of the bulk sample values for all areas.*

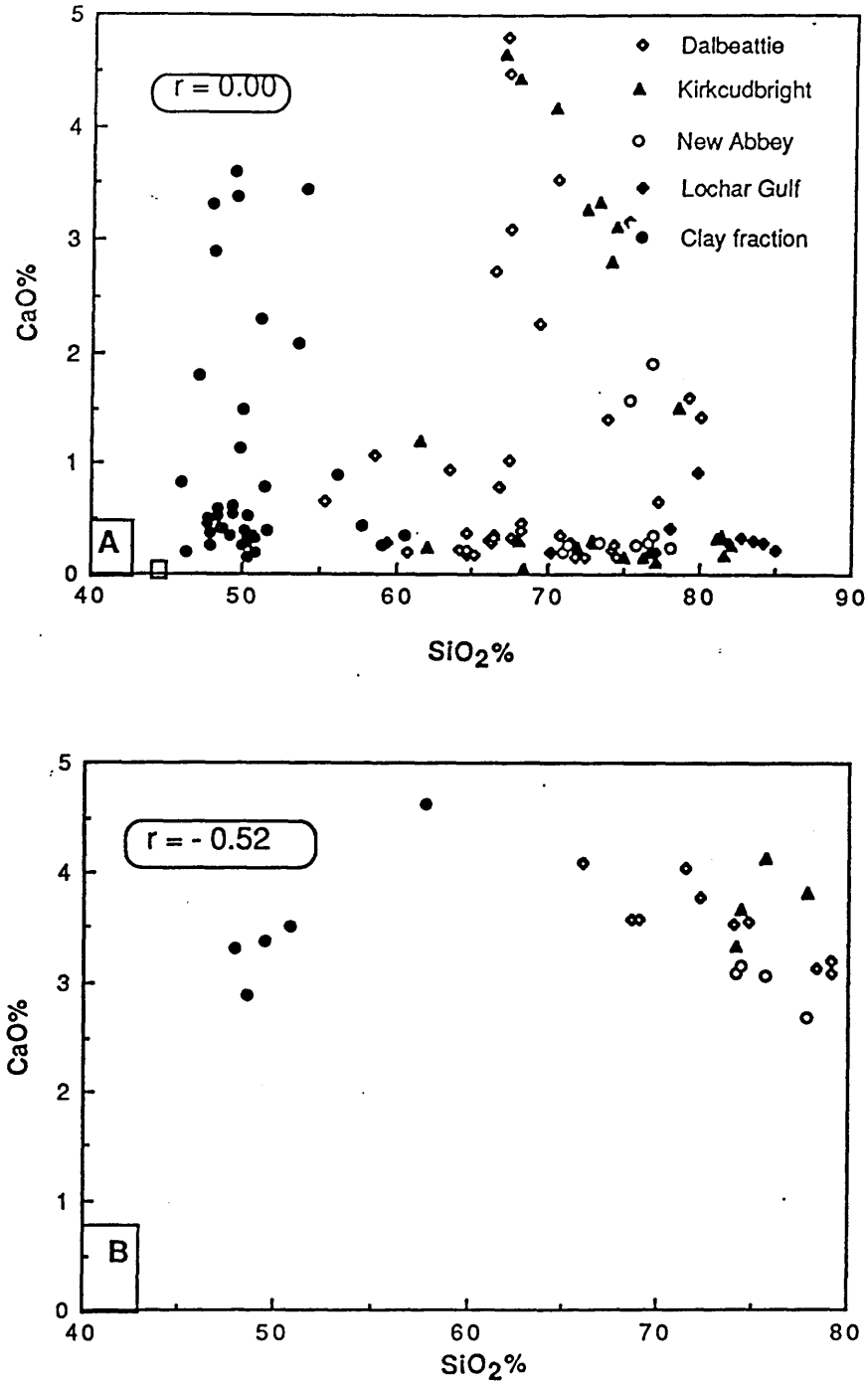

Figure 9.6 Plot of SiO_2% against CaO%:

A, Holocene sediments;

B, Present-day intertidal sediments.

Bulk sample values for individual areas are shown separately. Values for samples of the clay fraction from the Dalbeattie, Kirkcudbright and New Abbey areas are grouped together.

r *is the correlation coefficient for the distribution of the bulk sample values for all areas.*

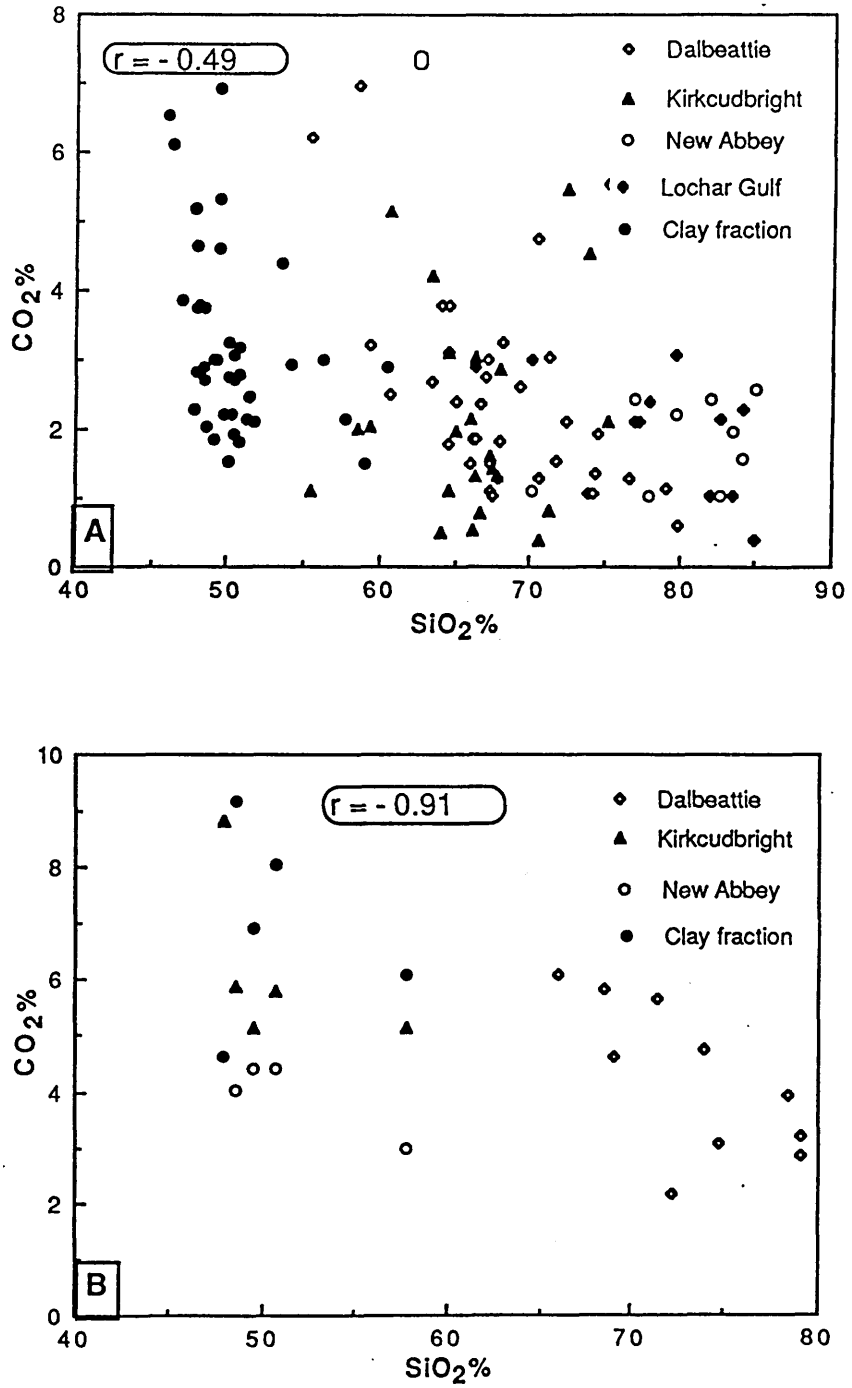

Figure 9.7 Plot of SiO_2% against CO_2%:
A, Holocene sediments;
B, Present-day intertidal sediments.
Bulk sample values for individual areas are shown separately. Values for samples of the clay fraction from the Dalbeattie, Kirkcudbright and New Abbey areas are grouped together.
r is the correlation coefficient for the distribution of the bulk sample values for all areas.

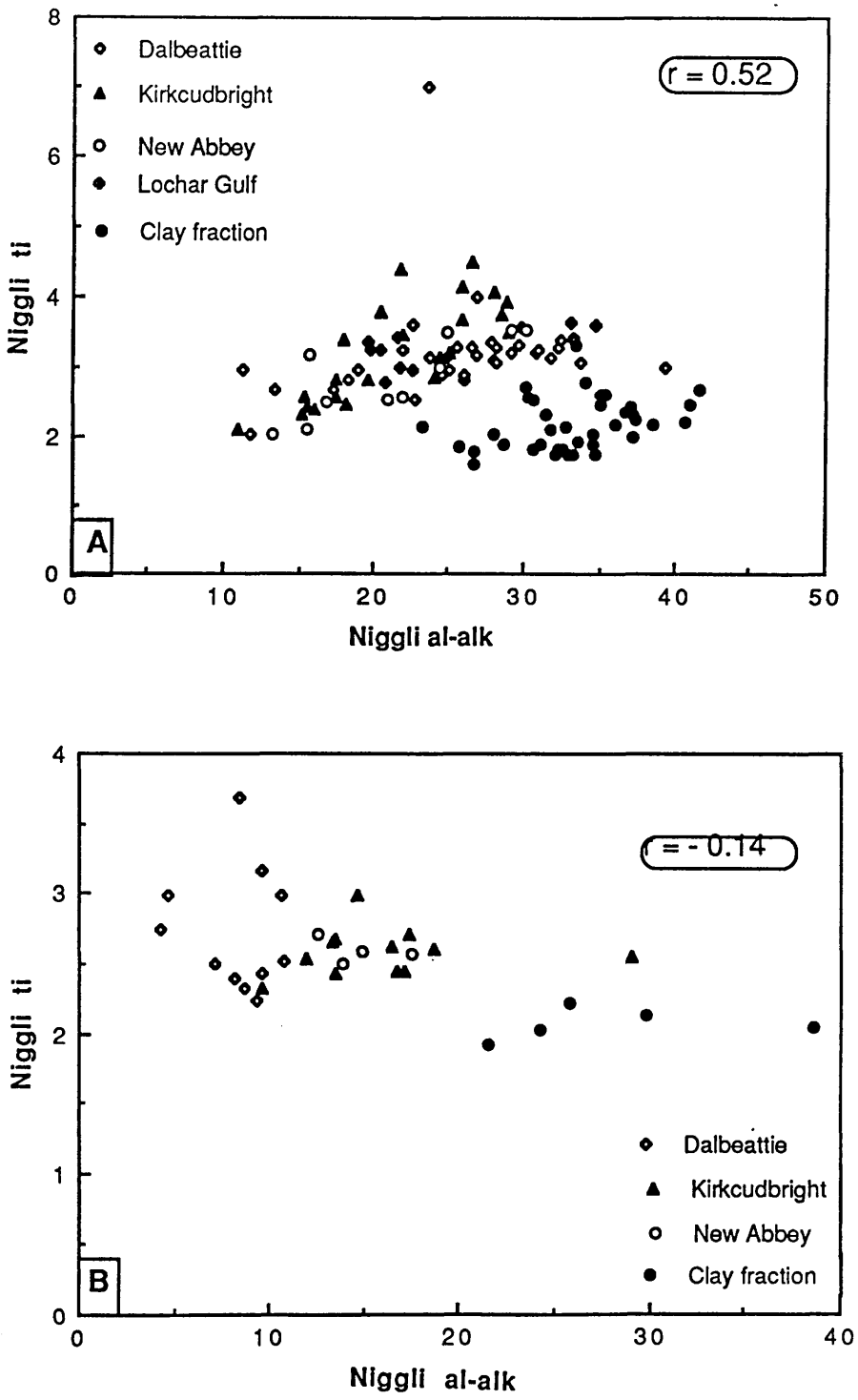

Figure 9.8 Plot of Niggli al-alk against Niggli ti:
A, Holocene sediments;
B, Present-day intertidal sediments.
Bulk sample values for individual areas are shown separately. Values for samples of the clay fraction from the Dalbeattie, Kirkcudbright and New Abbey areas are grouped together.
r *is the correlation coefficient for the distribution of the bulk sample values for all areas.*

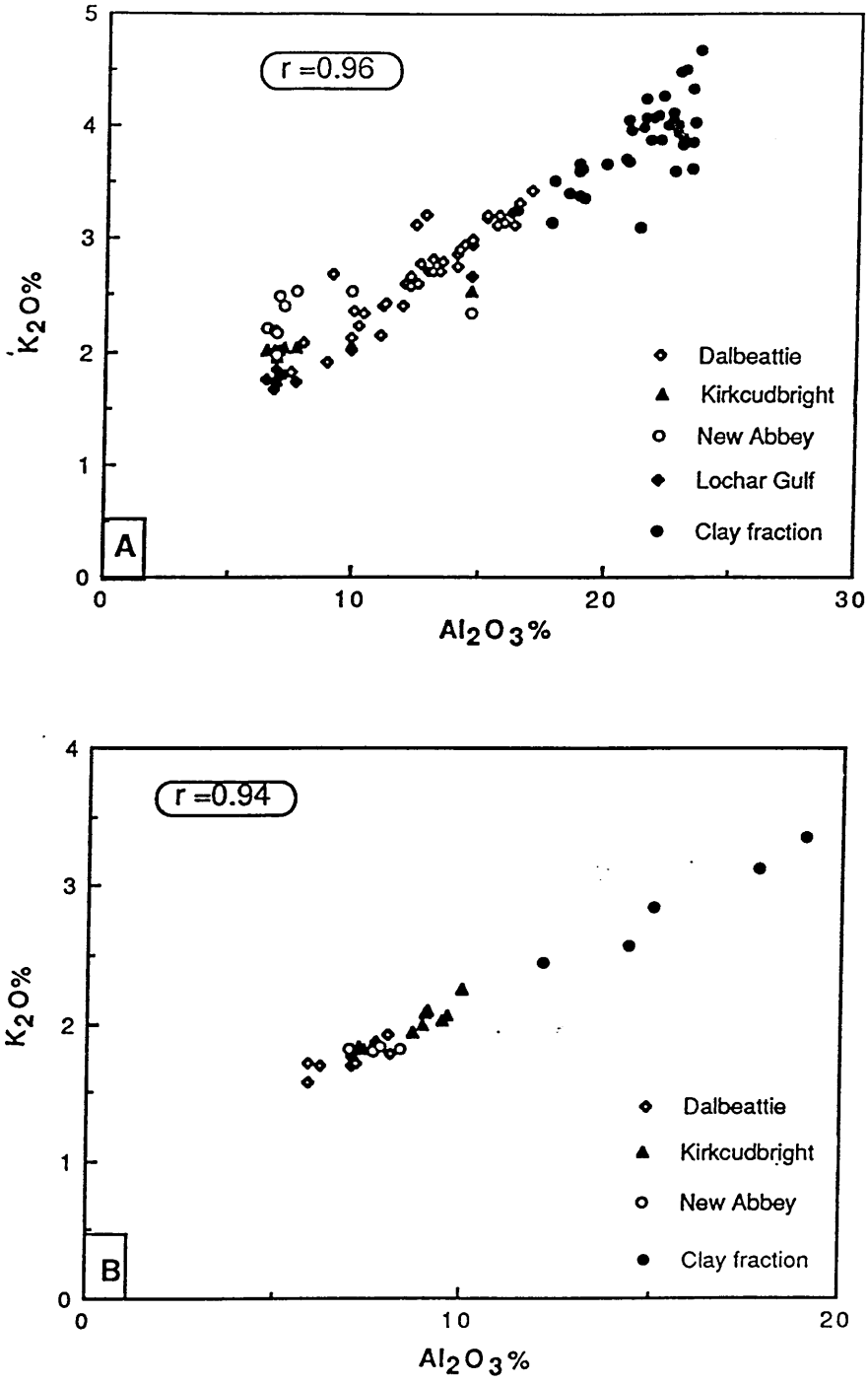

Figure 9.9 Plot of $Al_2O_3\%$ against $K_2O\%$:
A, Holocene sediments;
B, Present-day intertidal sediments.
Bulk sample values for individual areas are shown separately. Values for samples of the clay fraction from the Dalbeattie, Kirkcudbright and New Abbey areas are grouped together.
r *is the correlation coefficient for the distribution of the bulk sample values for all areas.*

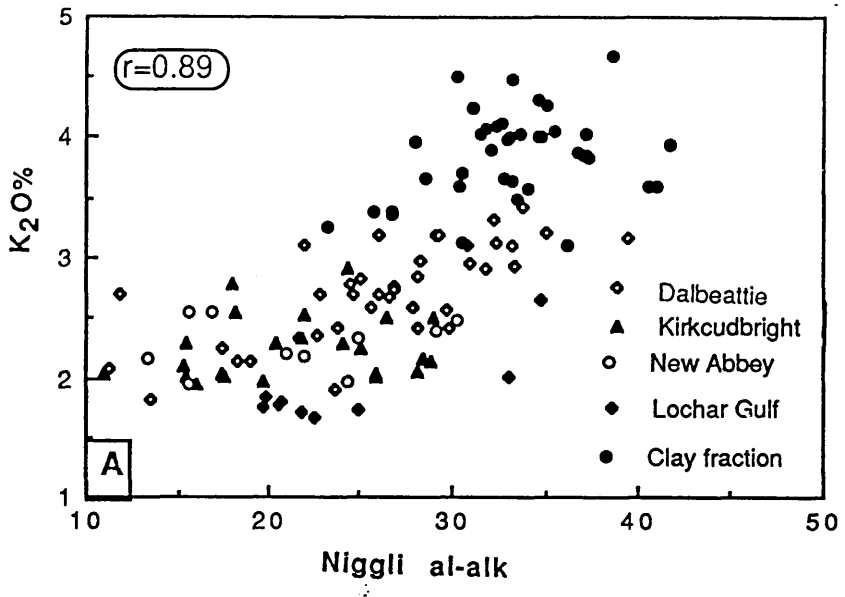

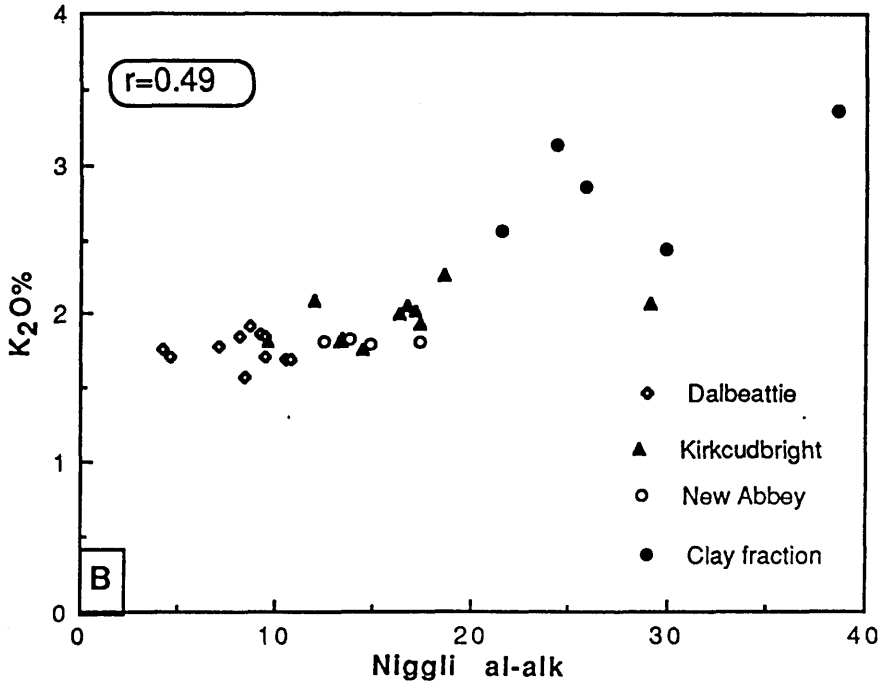

Figure 9.10 Plot of Niggli al-alk against K_2O%:
A, Holocene sediments;
B, Present-day intertidal sediments.
Bulk sample values for individual areas are shown separately. Values for samples of the clay fraction from the Dalbeattie, Kirkcudbright and New Abbey areas are grouped together.
r *is the correlation coefficient for the distribution of the bulk sample values for all areas.*

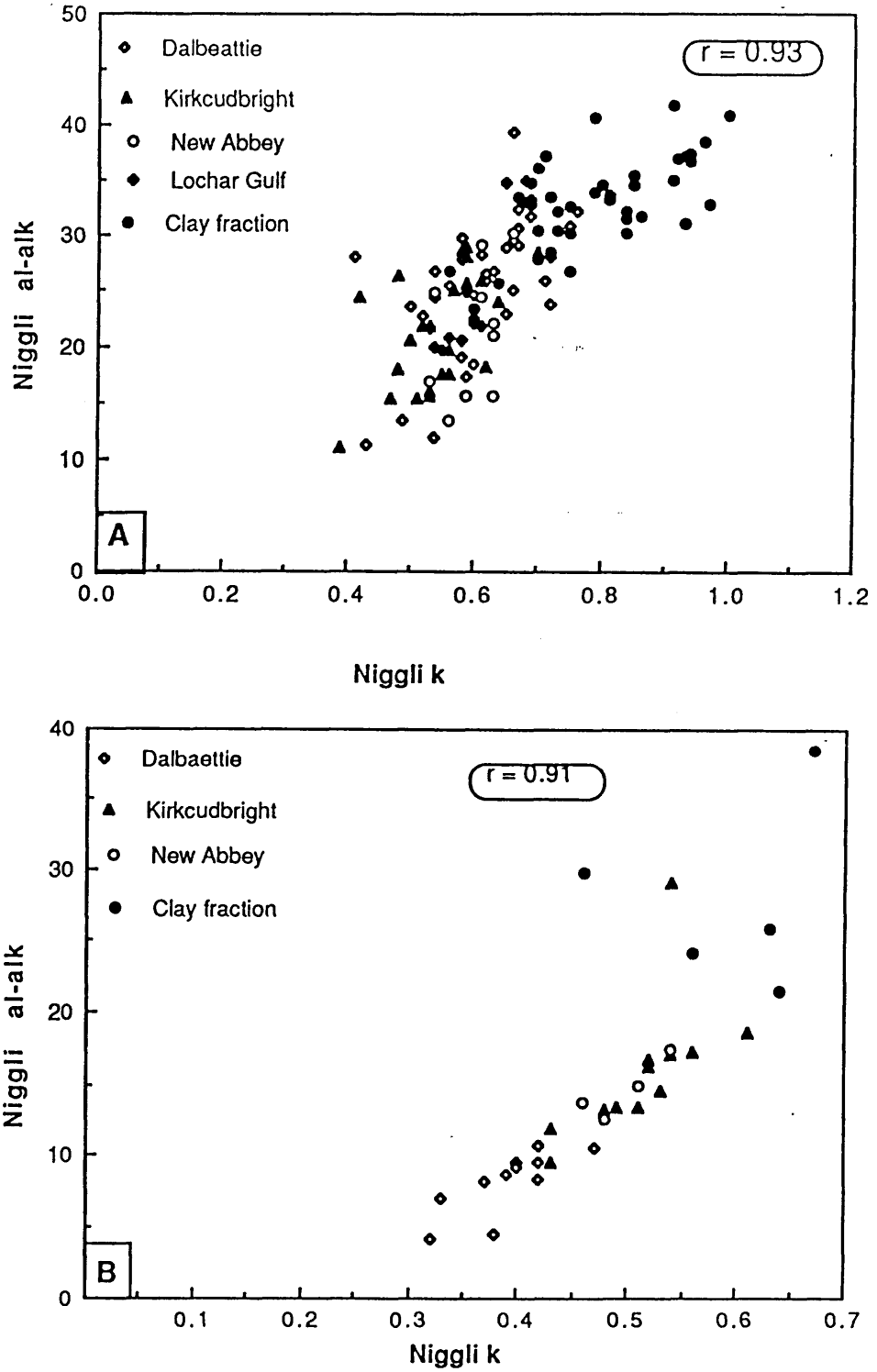

Figure 9.11 Plot of Niggli k against Niggli al-alk:
A, Holocene sediments;
B, Present-day intertidal sediments.
Bulk sample values for individual areas are shown separately. Values for samples of the clay fraction from the Dalbeattie, Kirkcudbright and New Abbey areas are grouped together.
r *is the correlation coefficient for the distribution of the bulk sample values for all areas.*

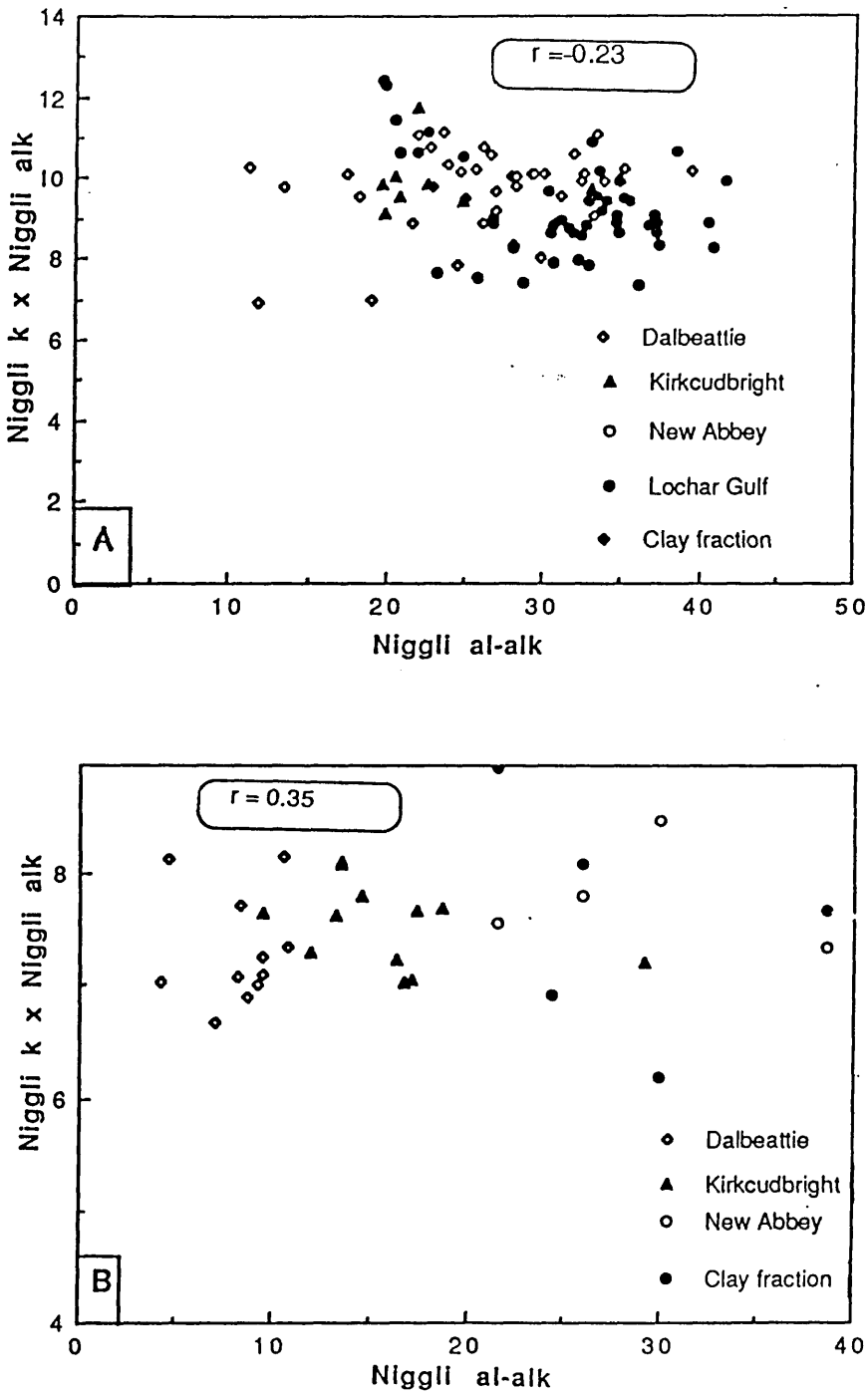

Figure 9.12 Plot of Niggli al-alk against Niggli k x Niggli alk:
A, Holocene sediments;
B, Present-day intertidal sediments.
Bulk sample values for individual areas are shown separately. Values for samples of the clay fraction from the Dalbeattie, Kirkcudbright and New Abbey areas are grouped together.
r *is the correlation coefficient for the distribution of the bulk sample values for all areas.*

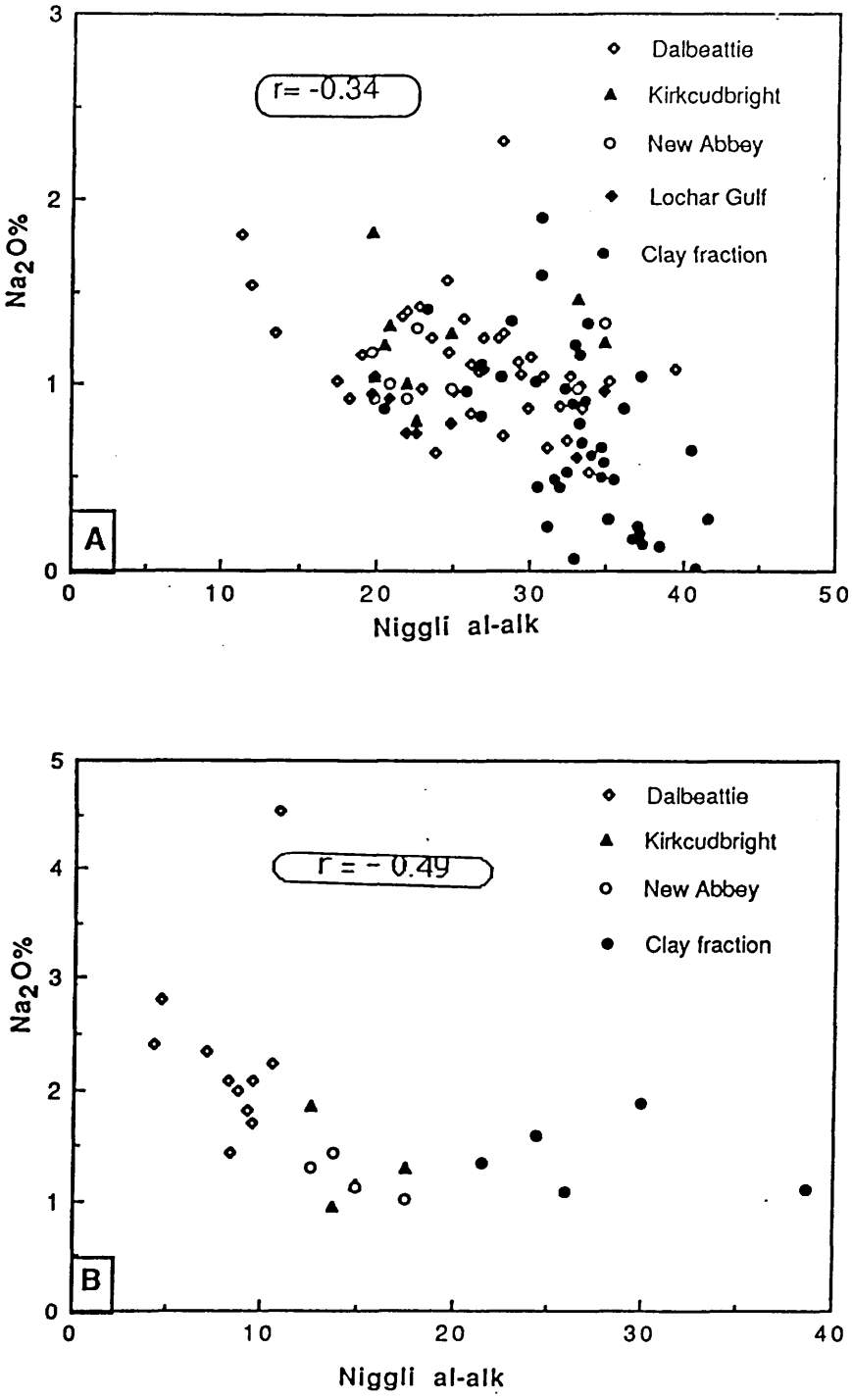

Figure 9.13 Plot of Niggli al-alk against $Na_2O\%$:
A, Holocene sediments;
B, Present-day intertidal sediments.
Bulk sample values for individual areas are shown separately. Values for samples of the clay fraction from the Dalbeattie, Kirkcudbright and New Abbey areas are grouped together.
r *is the correlation coefficient for the distribution of the bulk sample values for all areas.*

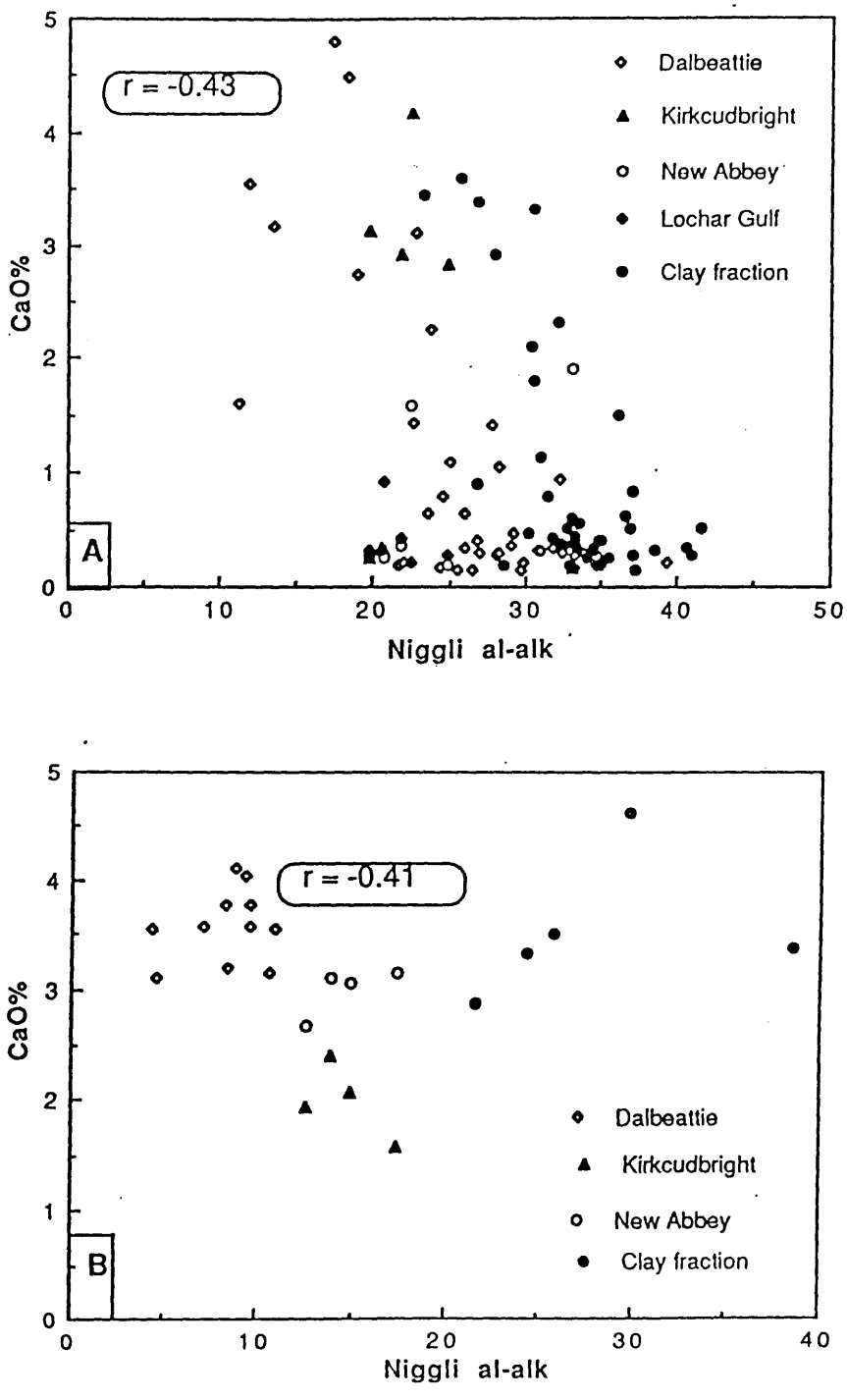

Figure 9.14 Plot of Niggli al-alk against CaO%:
A, Holocene sediments;
B, Present-day intertidal sediments.
Bulk sample values for individual areas are shown separately. Values for samples of the clay fraction from the Dalbeattie, Kirkcudbright and New Abbey areas are grouped together.
r *is the correlation coefficient for the distribution of the bulk sample values for all areas.*

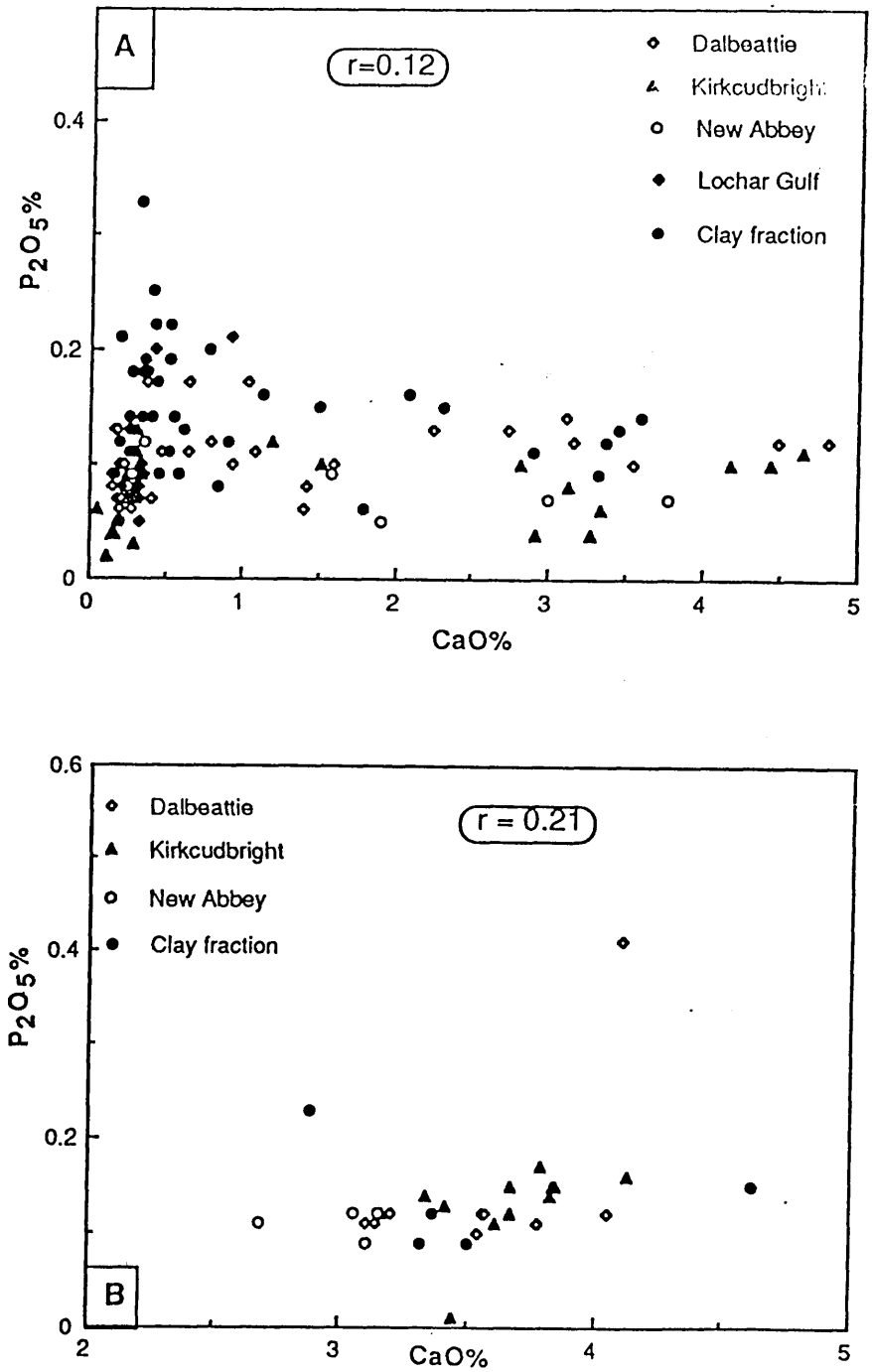

Figure 9.15 Plot of CaO% against P_2O_5%:
A, Holocene sediments;
B, Present-day intertidal sediments.
Bulk sample values for individual areas are shown separately. Values for samples of the clay fraction from the Dalbeattie, Kirkcudbright and New Abbey areas are grouped together.
r *is the correlation coefficient for the distribution of the bulk sample values for all areas.*

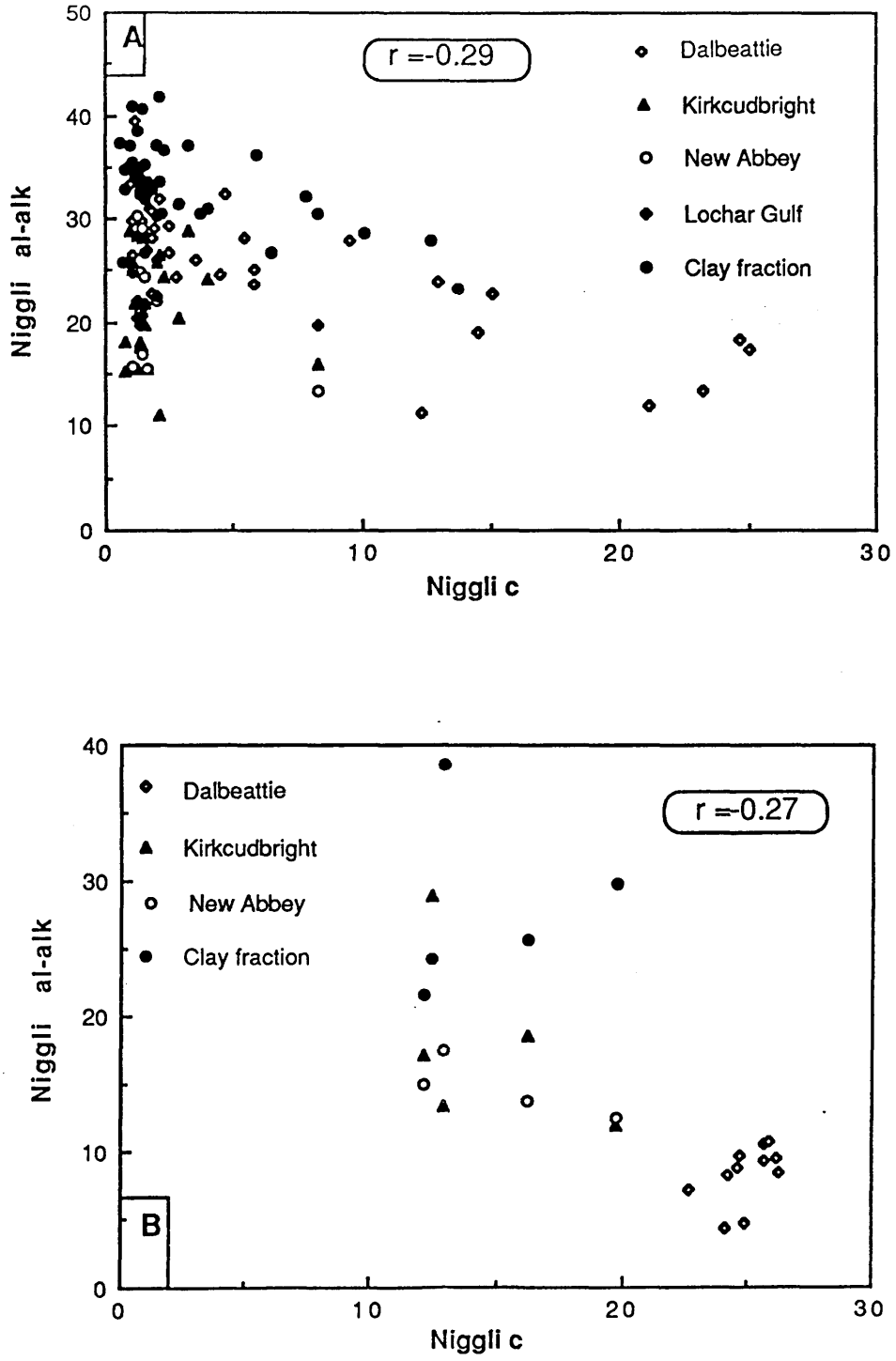

Figure 9.16 Plot of Niggli c against Niggli al-alk:
A, Holocene sediments;
B, Present-day intertidal sediments.
Bulk sample values for individual areas are shown separately. Values for samples of the clay fraction from the Dalbeattie, Kirkcudbright and New Abbey areas are grouped together.
r *is the correlation coefficient for the distribution of the bulk sample values for all areas.*

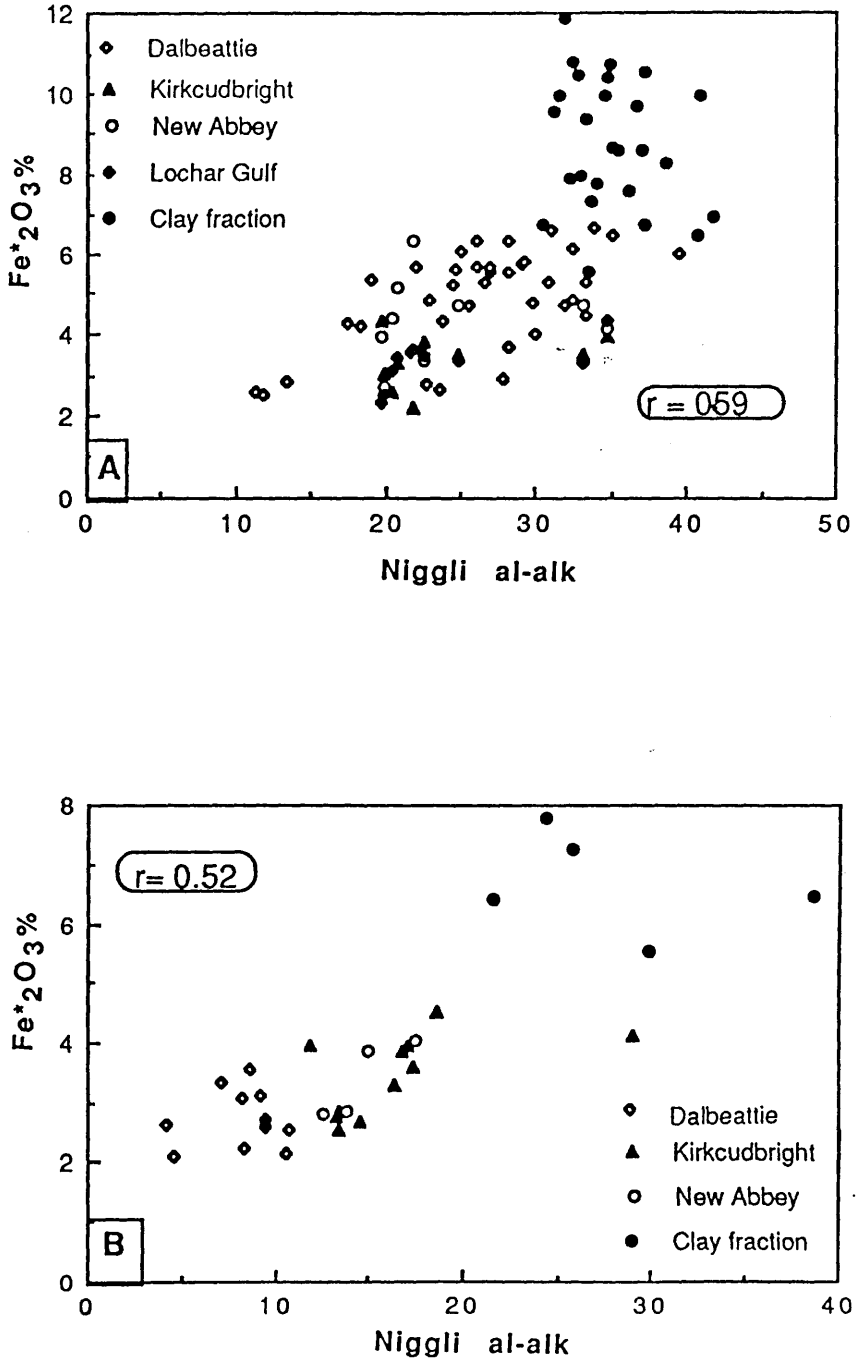

Figure 9.17 Plot of Niggli al-alk against $Fe^*_2O_3$%:
A, Holocene sediments;
B, Present-day intertidal sediments.
Bulk sample values for individual areas are shown separately. Values for samples of the clay fraction from the Dalbeattie, Kirkcudbright and New Abbey areas are grouped together.
r *is the correlation coefficient for the distribution of the bulk sample values for all areas.*

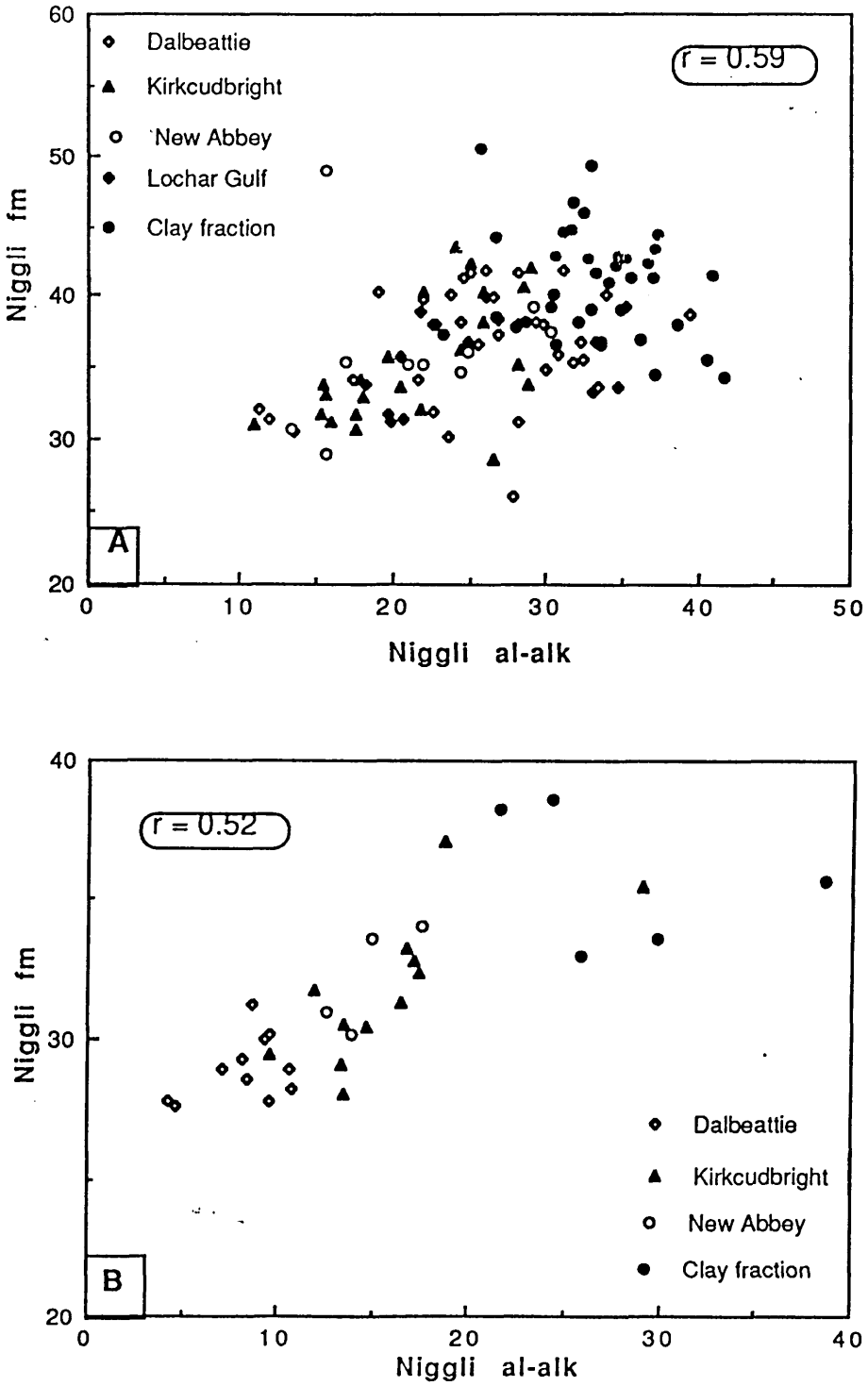

Figure 9.18 Plot of Niggli al-alk against Niggli fm:
A, Holocene sediments;
B, Present-day intertidal sediments.
Bulk sample values for individual areas are shown separately. Values for samples of the clay fraction from the Dalbeattie, Kirkcudbright and New Abbey areas are grouped together.
r *is the correlation coefficient for the distribution of the bulk sample values for all areas.*

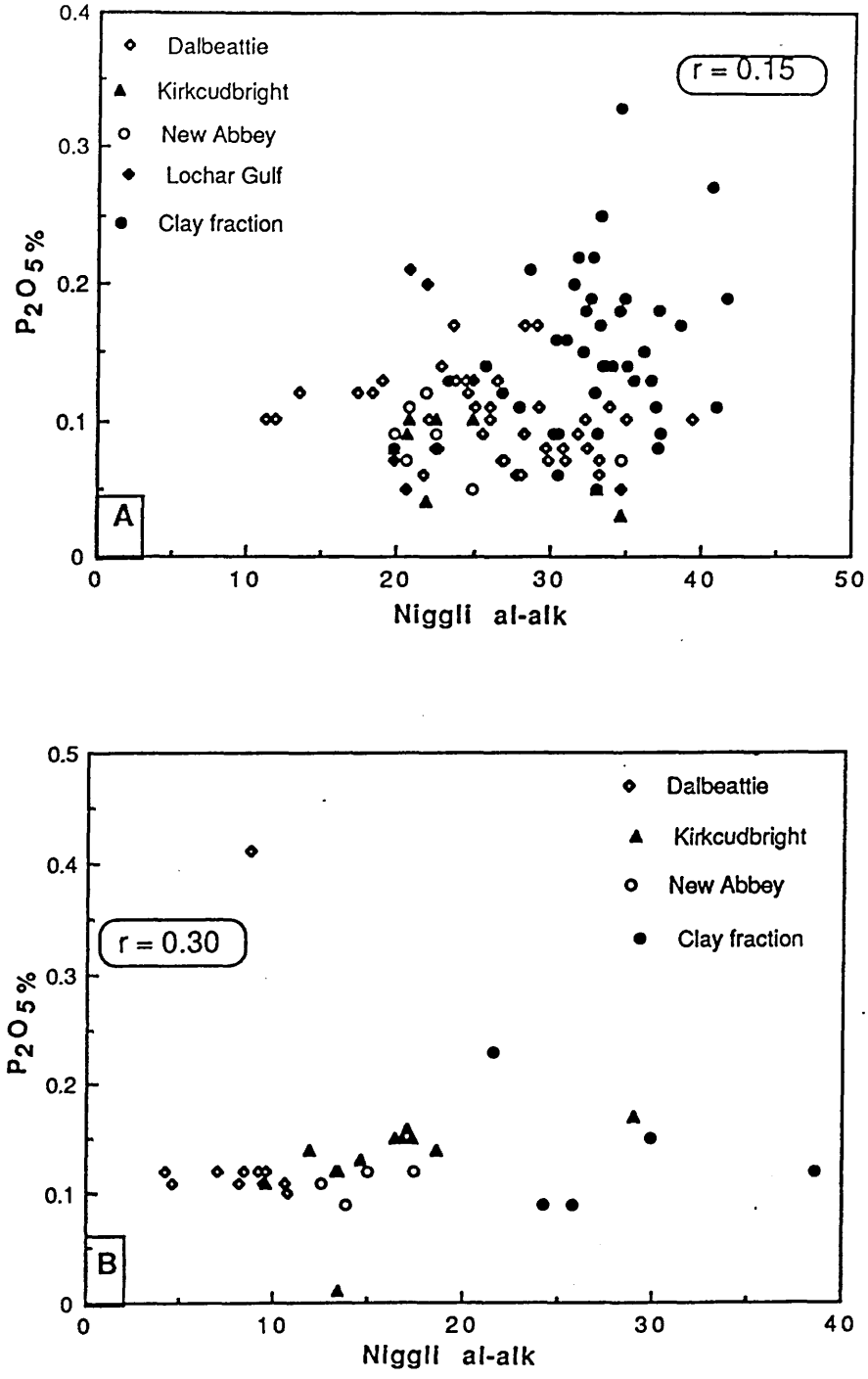

Figure 9.19 Plot of Niggli al-alk against $P_2O_{5\%}$:
A, Holocene sediments;
B, Present-day intertidal sediments.
Bulk sample values for individual areas are shown separately. Values for samples of the clay fraction from the Dalbeattie, Kirkcudbright and New Abbey areas are grouped together.
r is the correlation coefficient for the distribution of the bulk sample values for all areas.

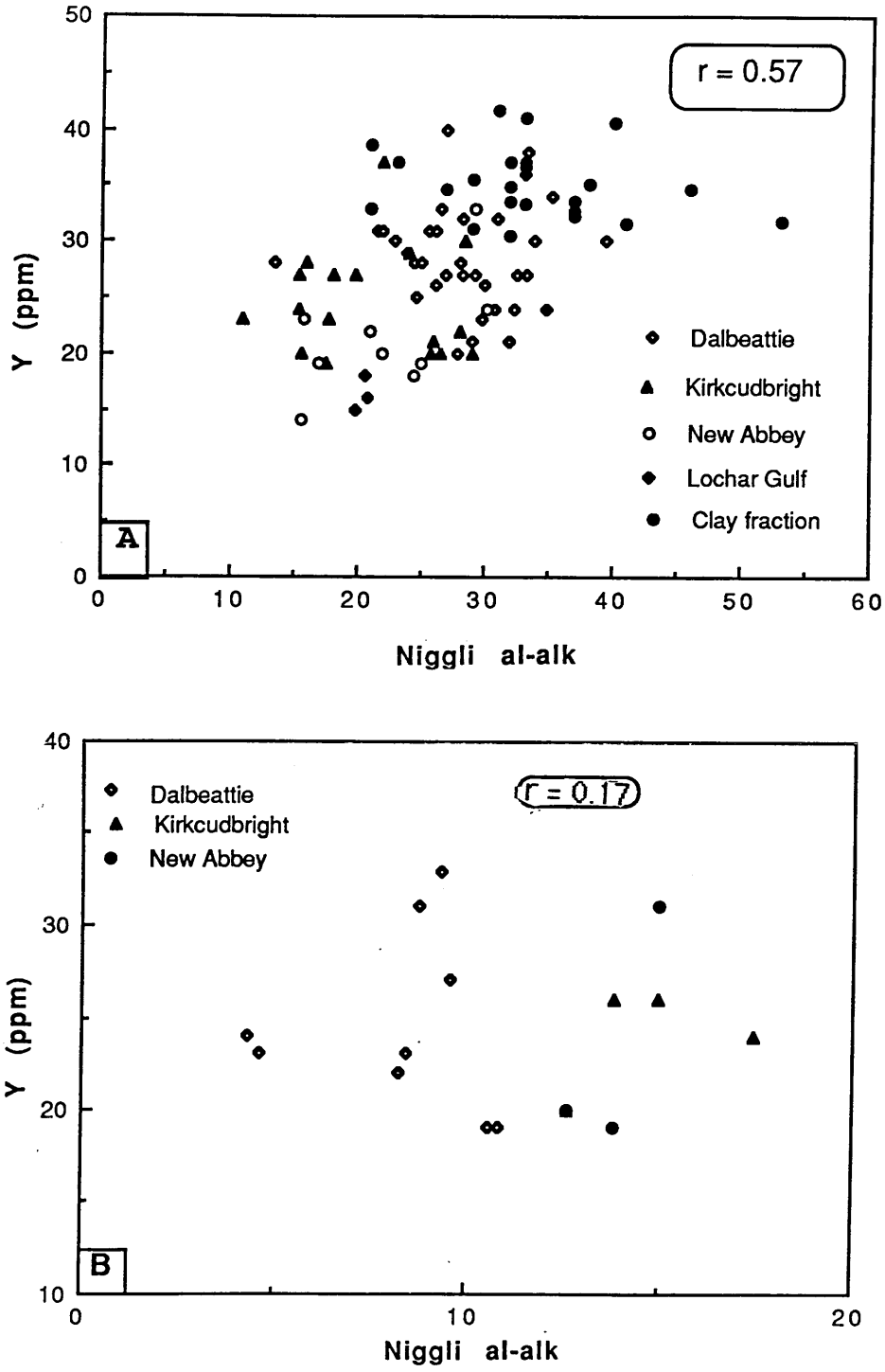

Figure 9.20 Plot of Niggli al-alk against Y (ppm):
A, Holocene sediments;
B, Present-day intertidal sediments.
Bulk sample values for individual areas are shown separately. Values for samples of the clay fraction from the Dalbeattie, Kirkcudbright and New Abbey areas are grouped together.
r *is the correlation coefficient for the distribution of the bulk sample values for all areas.*

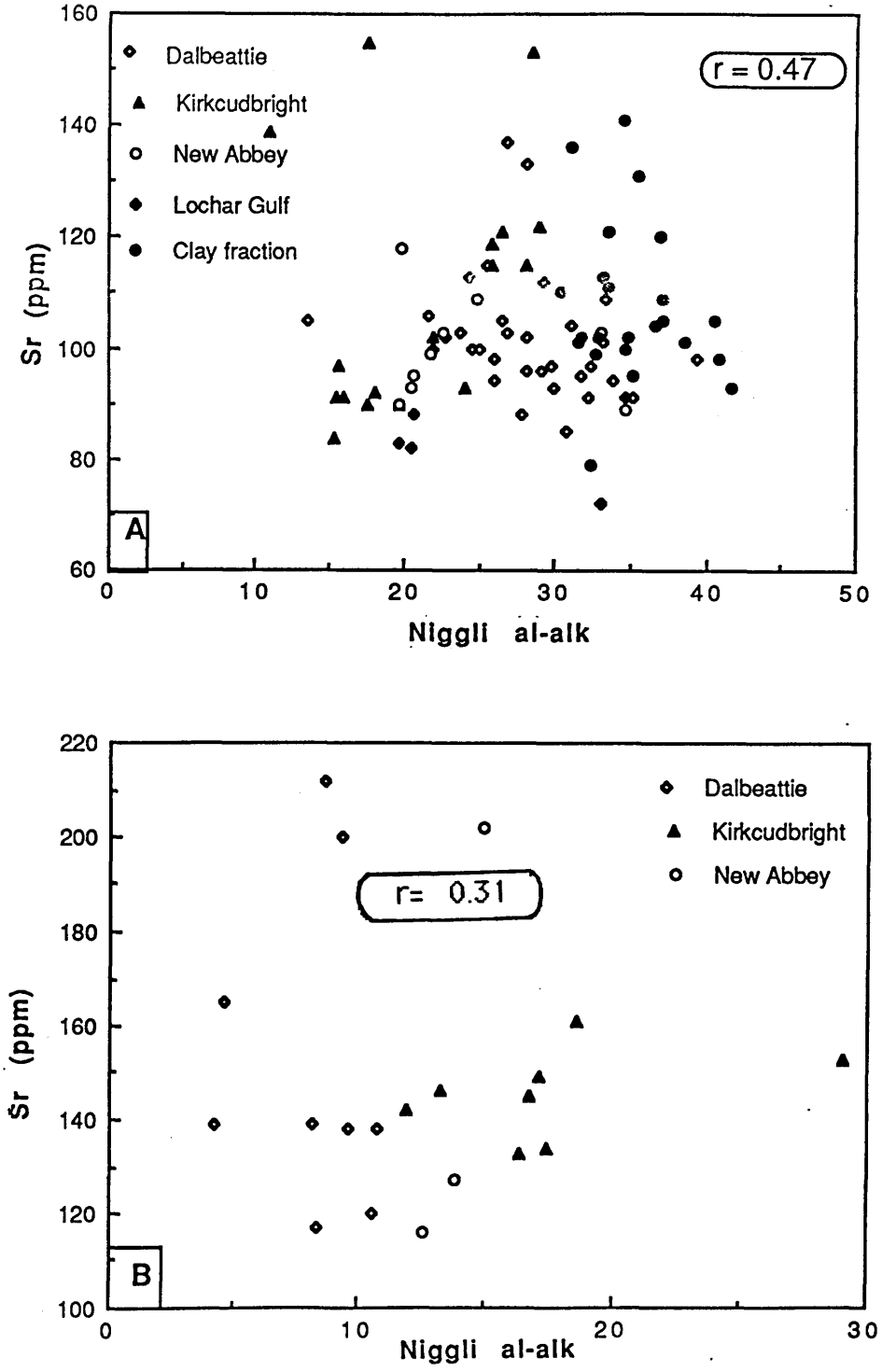

Figure 9.21 Plot of Niggli al-alk against Sr (ppm):
A, Holocene sediments;
B, Present-day intertidal sediments.
Bulk sample values for individual areas are shown separately. Values for samples of the clay fraction from the Dalbeattie, Kirkcudbright and New Abbey areas are grouped together.
r *is the correlation coefficient for the distribution of the bulk sample values for all areas.*

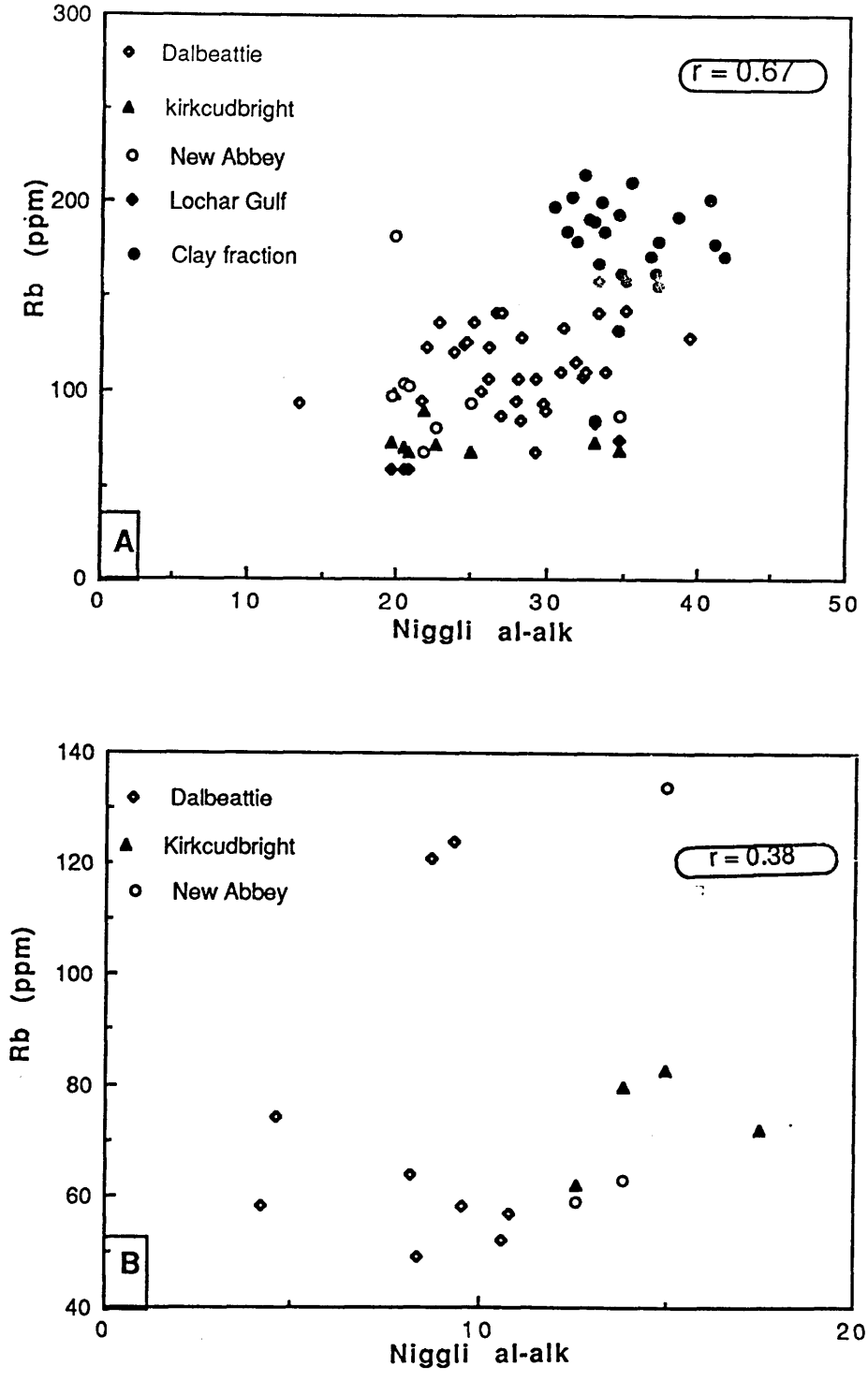

Figure 9.22 Plot of Niggli al-alk against Rb (ppm):
A, Holocene sediments;
B, Present-day intertidal sediments.
Bulk sample values for individual areas are shown separately. Values for samples of the clay fraction from the Dalbeattie, Kirkcudbright and New Abbey areas are grouped together.
r is the correlation coefficient for the distribution of the bulk sample values for all areas.

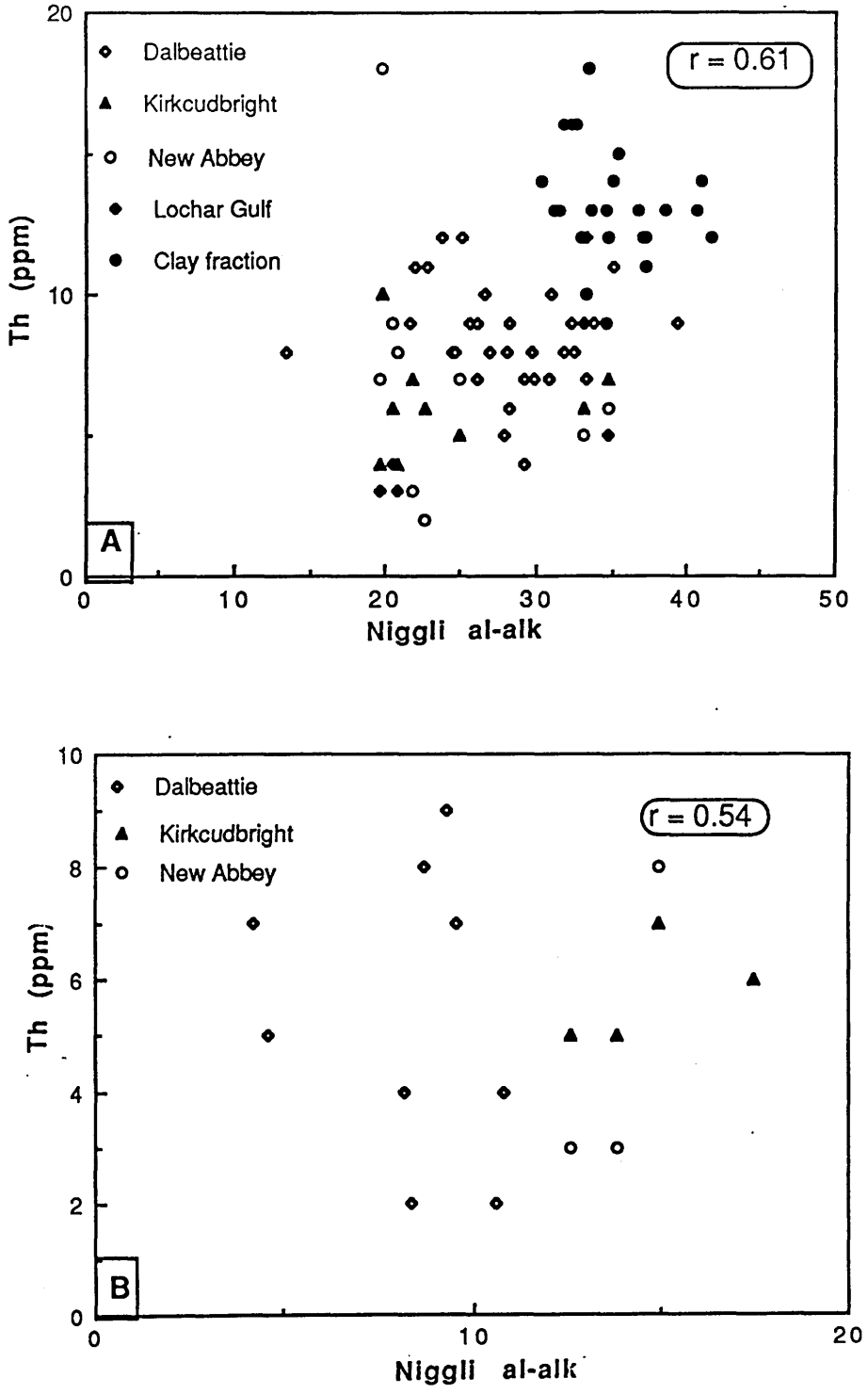

Figure 9.23 Plot of Niggli al-alk against Th (ppm):
A, Holocene sediments;
B, Present-day intertidal sediments.
Bulk sample values for individual areas are shown separately. Values for samples of the clay fraction from the Dalbeattie, Kirkcudbright and New Abbey areas are grouped together.
r is the correlation coefficient for the distribution of the bulk sample values for all areas.

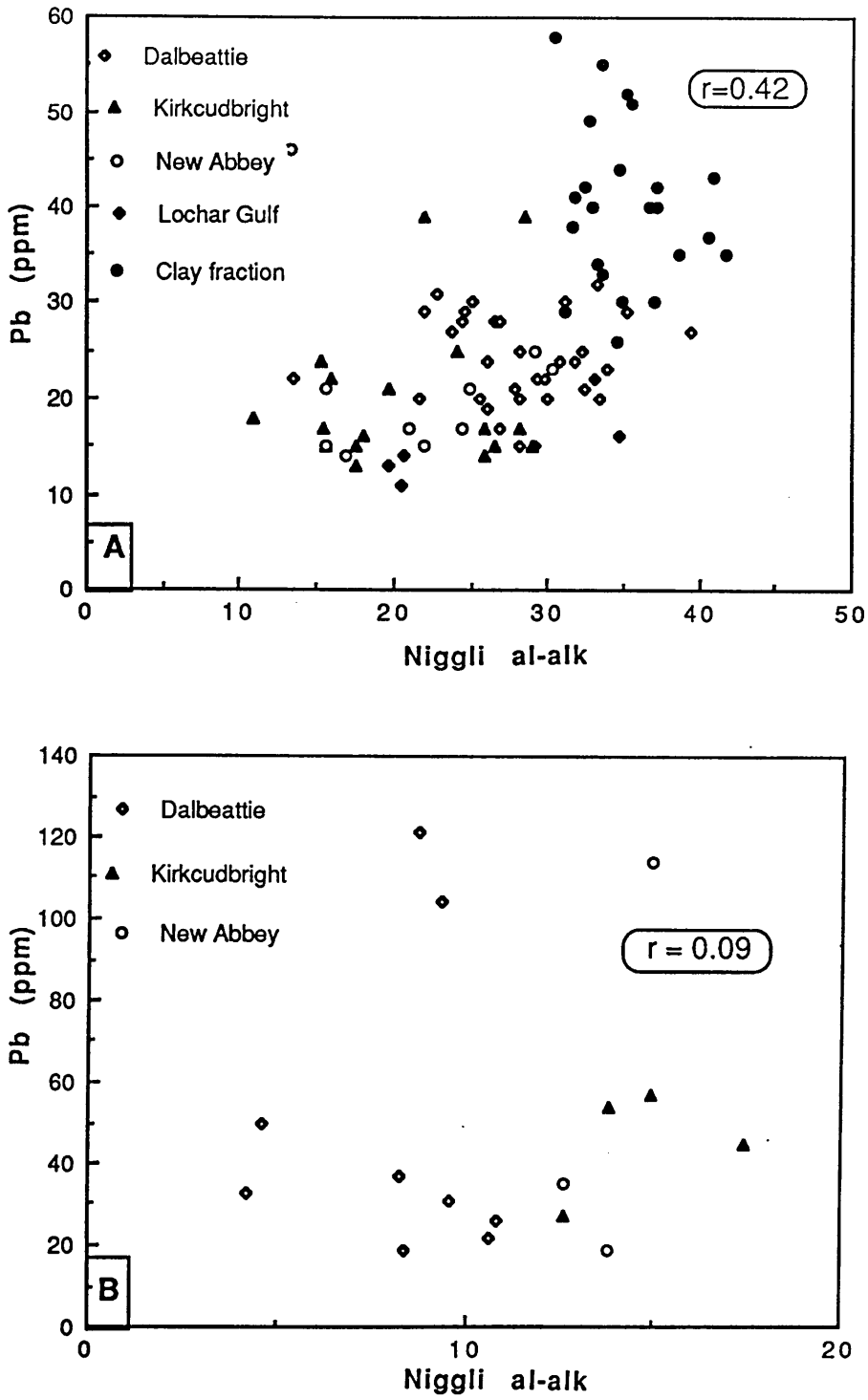

Figure 9.24 Plot of Niggli al-alk against Pb (ppm):
A, Holocene sediments;
B, Present-day intertidal sediments.
Bulk sample values for individual areas are shown separately. Values for samples of the clay fraction from the Dalbeattie, Kirkcudbright and New Abbey areas are grouped together.
r *is the correlation coefficient for the distribution of the bulk sample values for all areas.*

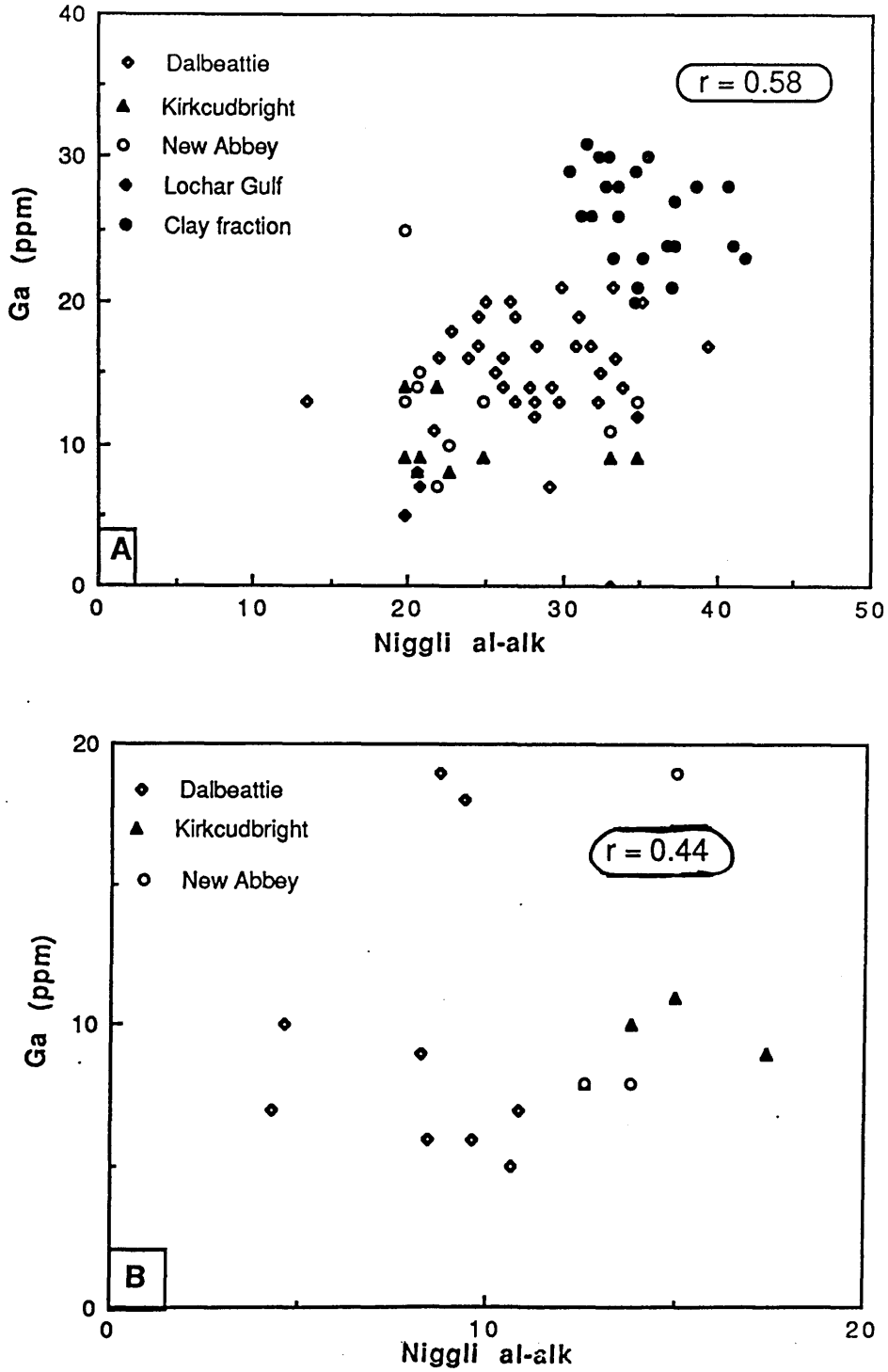

Figure 9.25 Plot of Niggli al-alk against Ga (ppm):
A, Holocene sediments;
B, Present-day intertidal sediments.
Bulk sample values for individual areas are shown separately. Values for samples of the clay fraction from the Dalbeattie, Kirkcudbright and New Abbey areas are grouped together.
r is the correlation coefficient for the distribution of the bulk sample values for all areas.

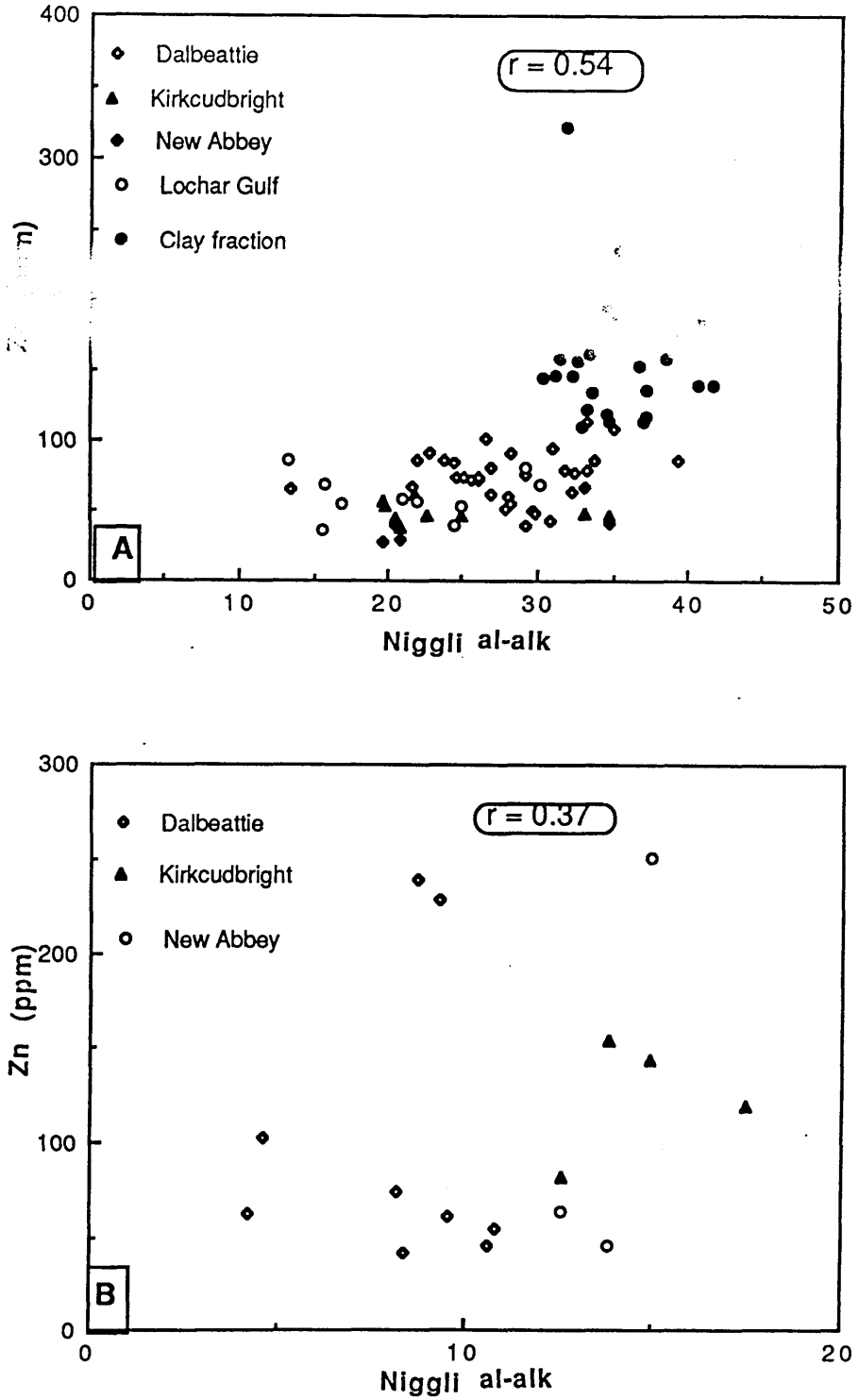

Figure 9.26 Plot of Niggli al-alk against Zn (ppm):
A, Holocene sediments;
B, Present-day intertidal sediments.
Bulk sample values for individual areas are shown separately. Values for samples of the clay fraction from the Dalbeattie, Kirkcudbright and New Abbey areas are grouped together.
r *is the correlation coefficient for the distribution of the bulk sample values for all areas.*

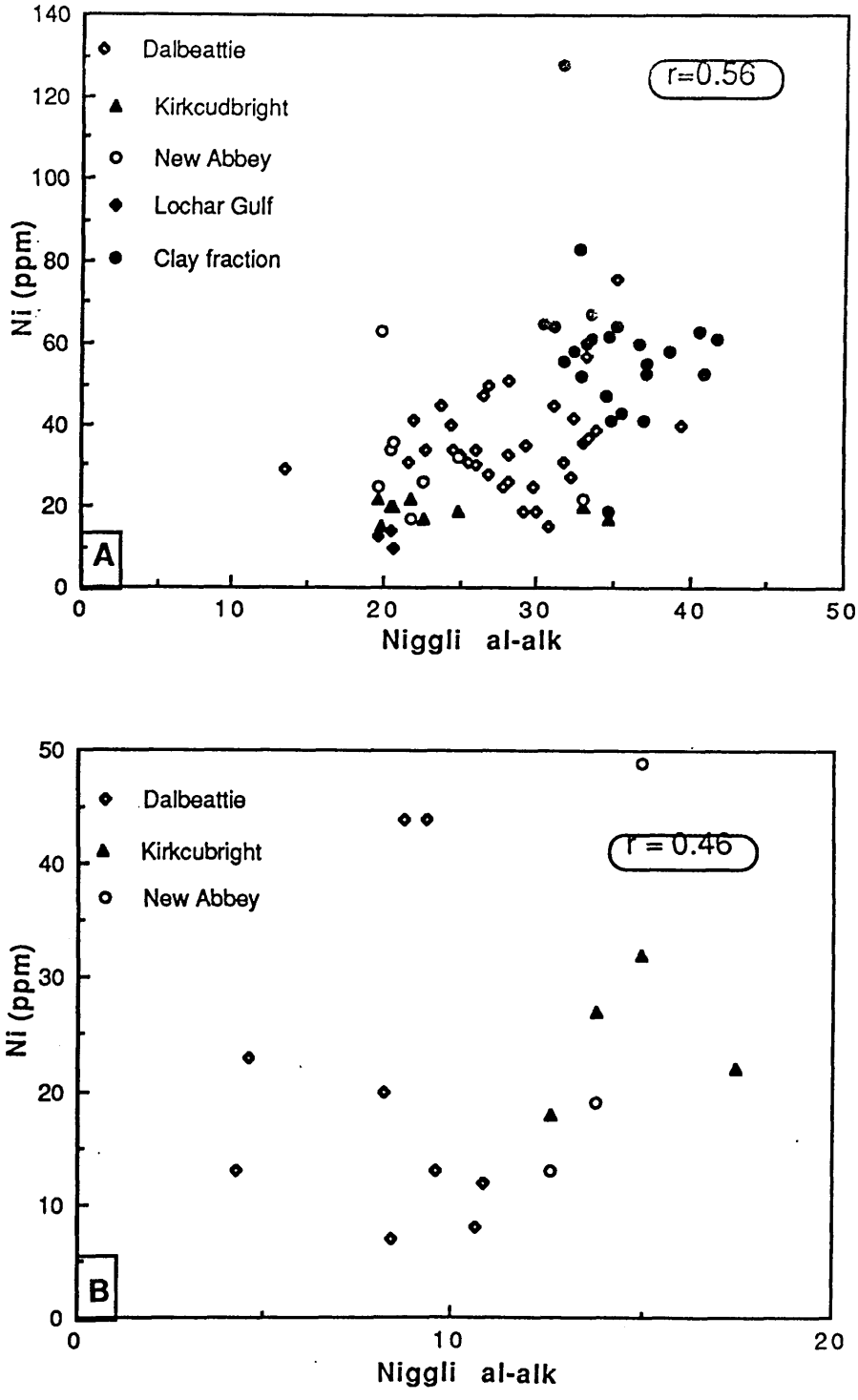

Figure 9.27 Plot of Niggli al-alk against Ni (ppm):
A, Holocene sediments;
B, Present-day intertidal sediments.
Bulk sample values for individual areas are shown separately. Values for samples of the clay fraction from the Dalbeattie, Kirkcudbright and New Abbey areas are grouped together.
r *is the correlation coefficient for the distribution of the bulk sample values for all areas.*

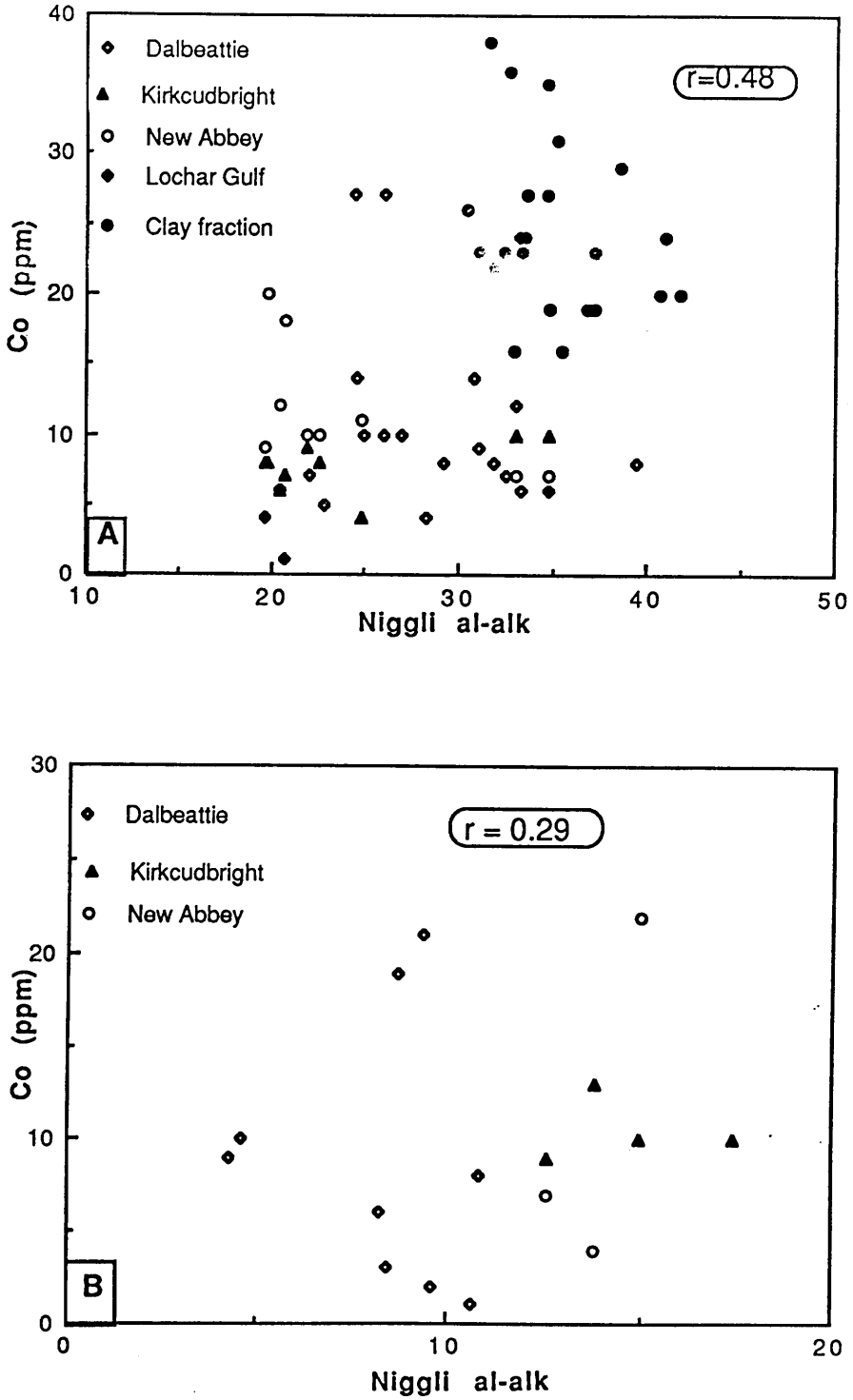

Figure 9.28 Plot of Niggli al-alk against Co (ppm):
A, Holocene sediments;
B, Present-day intertidal sediments.
Bulk sample values for individual areas are shown separately. Values for samples of the clay fraction from the Dalbeattie, Kirkcudbright and New Abbey areas are grouped together.
r *is the correlation coefficient for the distribution of the bulk sample values for all areas.*

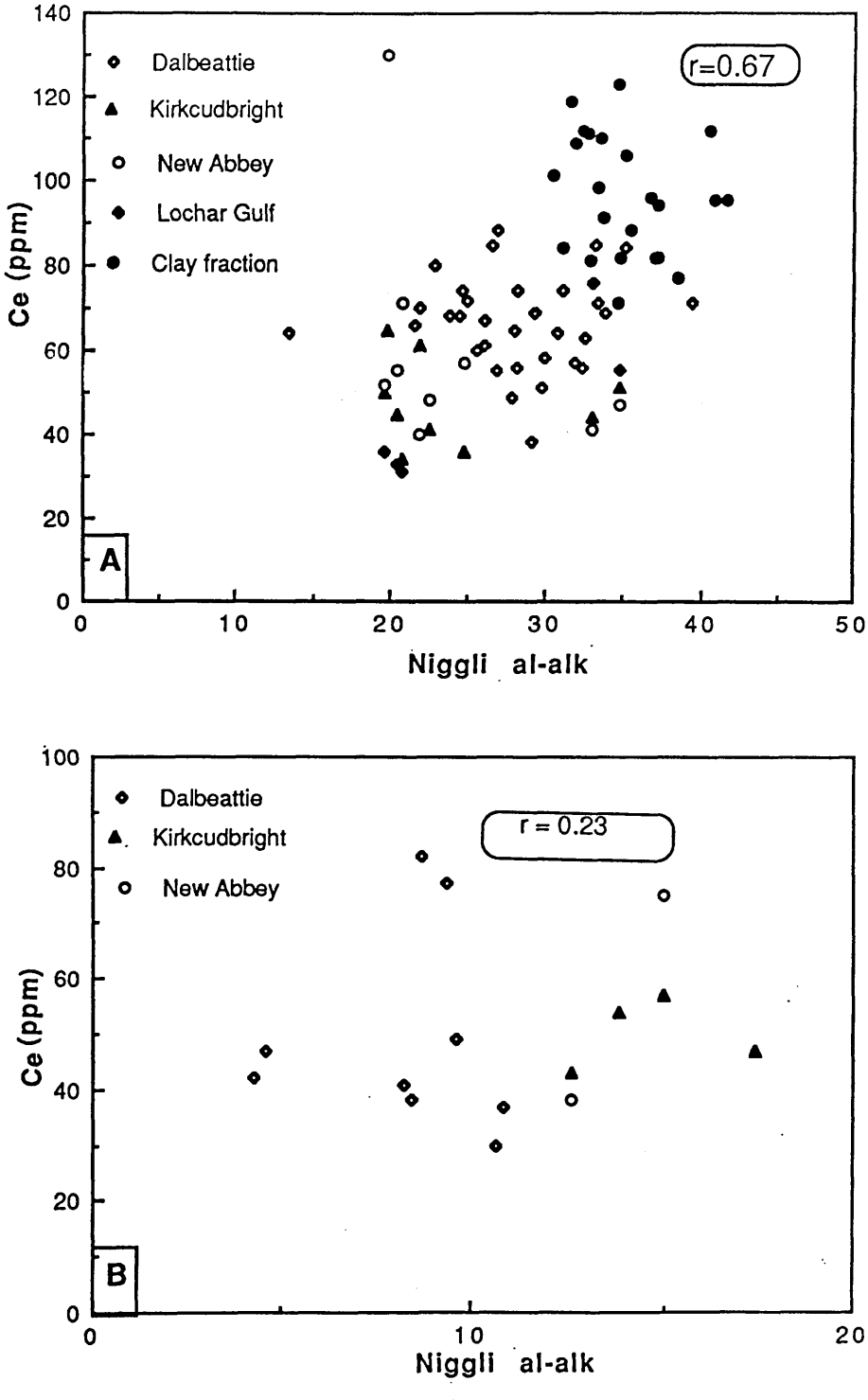

Figure 9.29 Plot of Niggli al-alk against Ce (ppm):
A, Holocene sediments;
B, Present-day intertidal sediments.
Bulk sample values for individual areas are shown separately. Values for samples of the clay fraction from the Dalbeattie, Kirkcudbright and New Abbey areas are grouped together.
r *is the correlation coefficient for the distribution of the bulk sample values for all areas.*

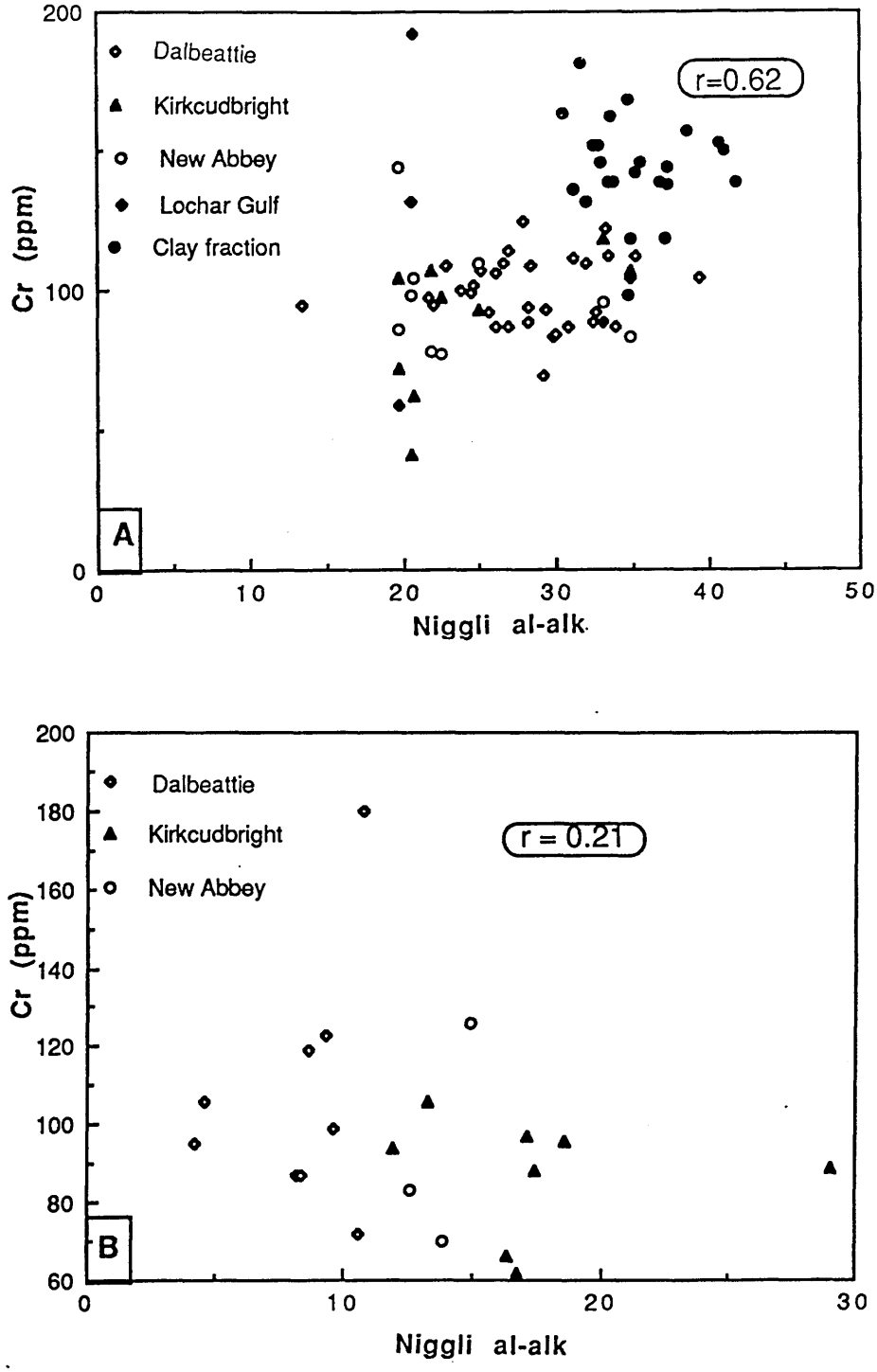

Figure 9.30 Plot of Niggli al-alk against Cr (ppm):
A, Holocene sediments;
B, Present-day intertidal sediments.
Bulk sample values for individual areas are shown separately. Values for samples of the clay fraction from the Dalbeattie, Kirkcudbright and New Abbey areas are grouped together.
r *is the correlation coefficient for the distribution of the bulk sample values for all areas.*

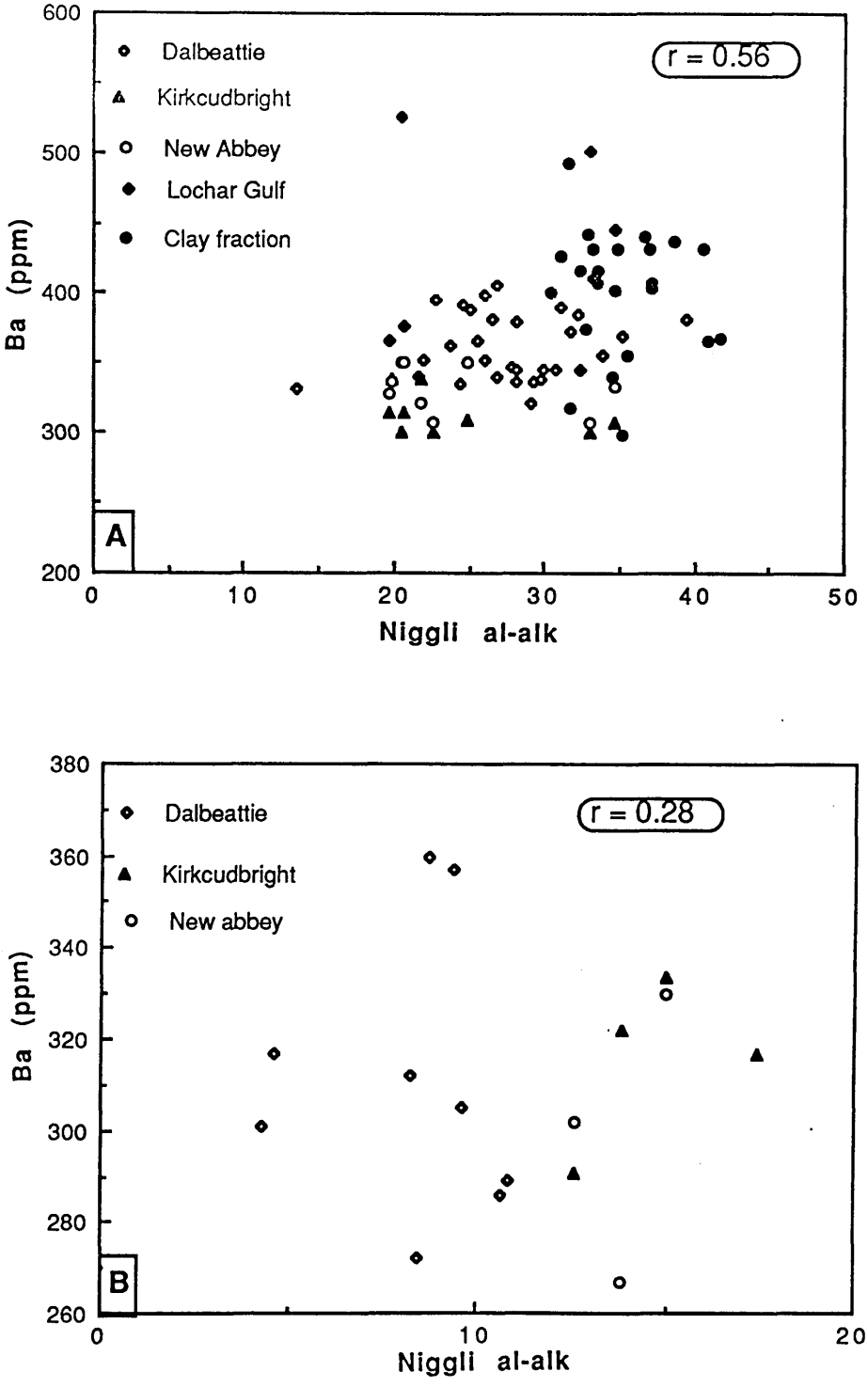

Figure 9.31 Plot of Niggli al-alk against Ba (ppm):
A, Holocene sediments;
B, Present-day intertidal sediments.
Bulk sample values for individual areas are shown separately. Values for samples of the clay fraction from the Dalbeattie, Kirkcudbright and New Abbey areas are grouped together.
r *is the correlation coefficient for the distribution of the bulk sample values for all areas.*

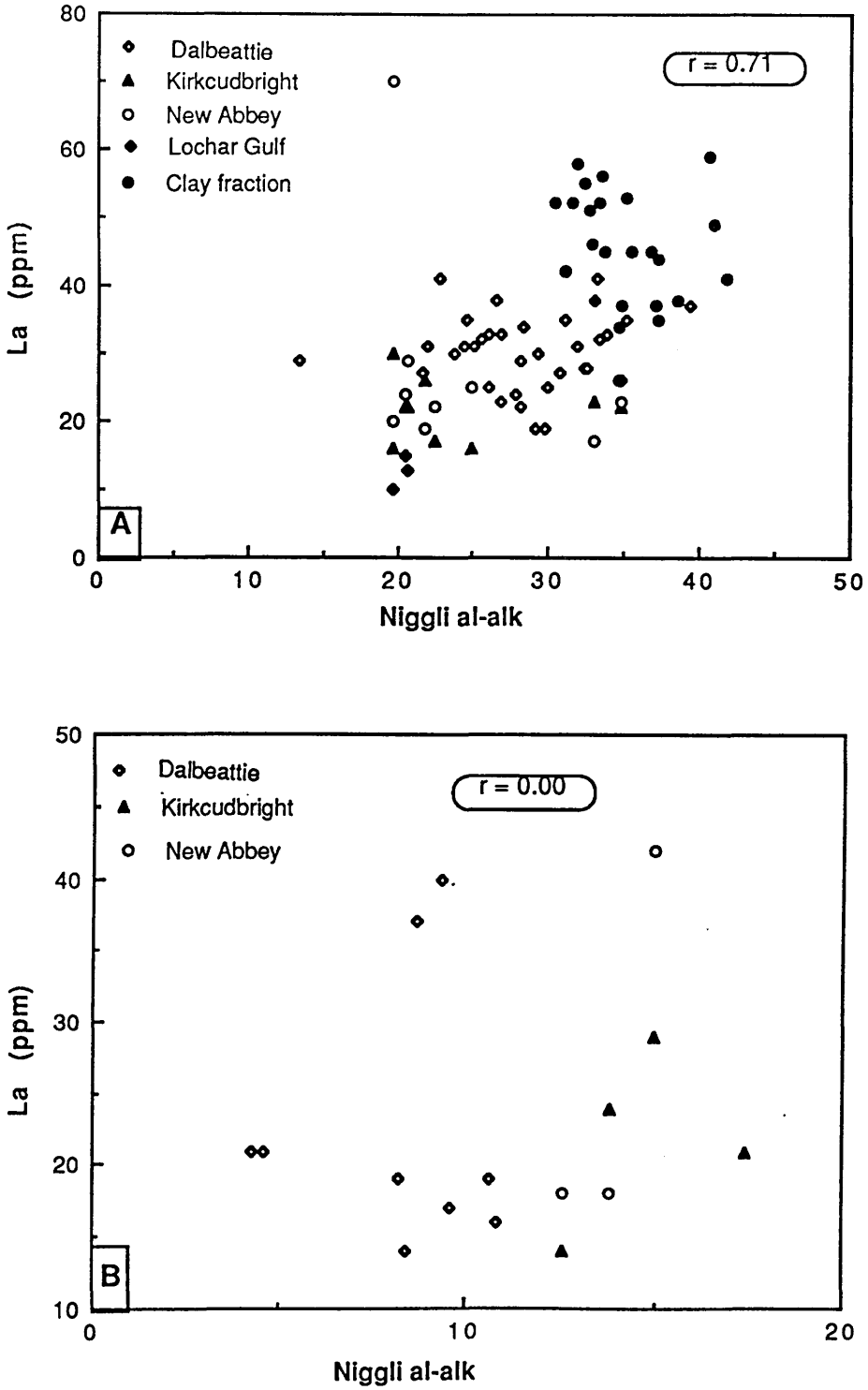

Figure 9.32 Plot of Niggli al-alk against La (ppm):
A, Holocene sediments;
B, Present-day intertidal sediments.
Bulk sample values for individual areas are shown separately. Values for samples of the clay fraction from the Dalbeattie, Kirkcudbright and New Abbey areas are grouped together.
r *is the correlation coefficient for the distribution of the bulk sample values for all areas.*

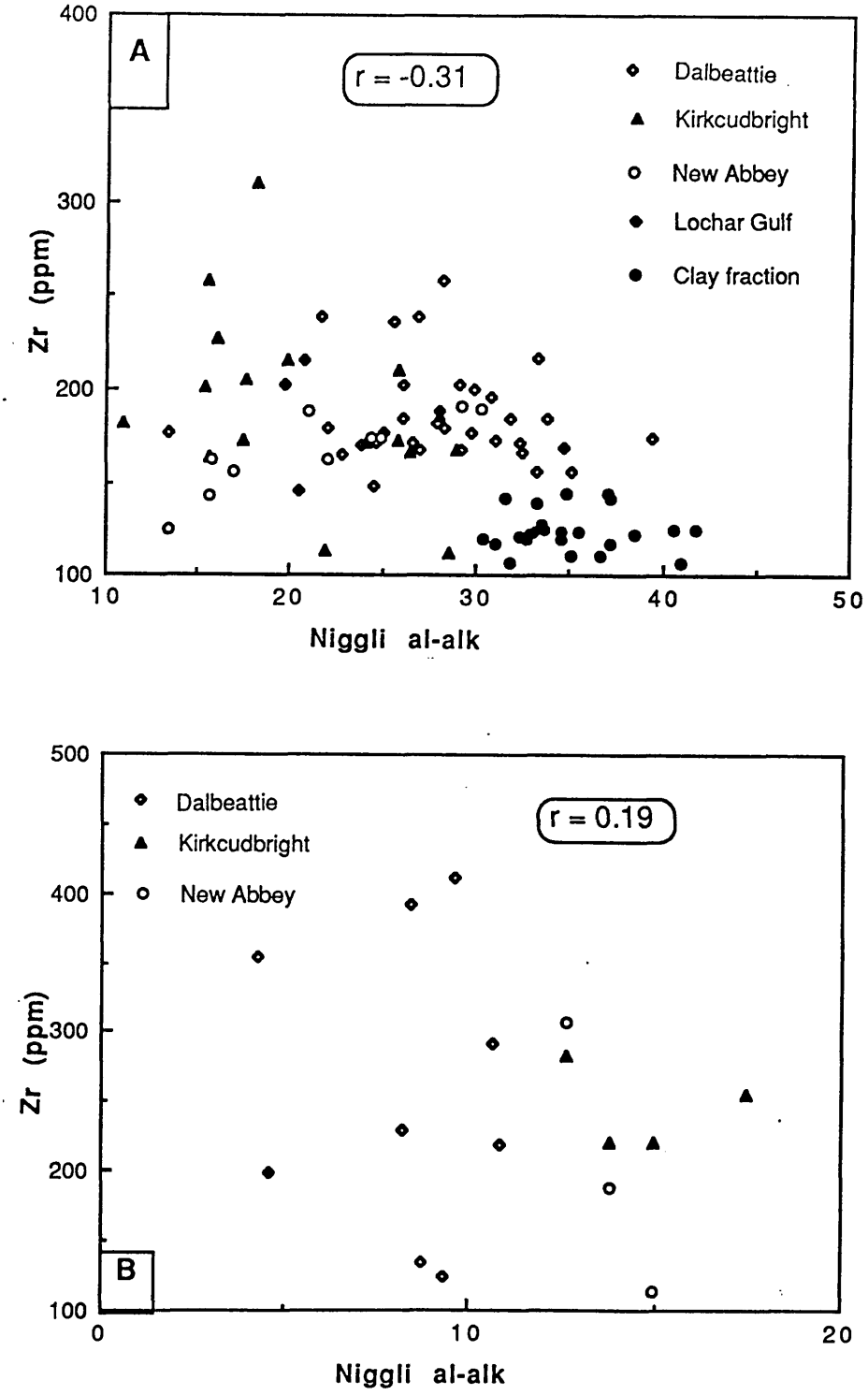

Figure 9.33 Plot of Niggli al-alk against Zr (ppm):
A, Holocene sediments;
B, Present-day intertidal sediments.
Bulk sample values for individual areas are shown separately. Values for samples of the clay fraction from the Dalbeattie, Kirkcudbright and New Abbey areas are grouped together.
r *is the correlation coefficient for the distribution of the bulk sample values for all areas.*

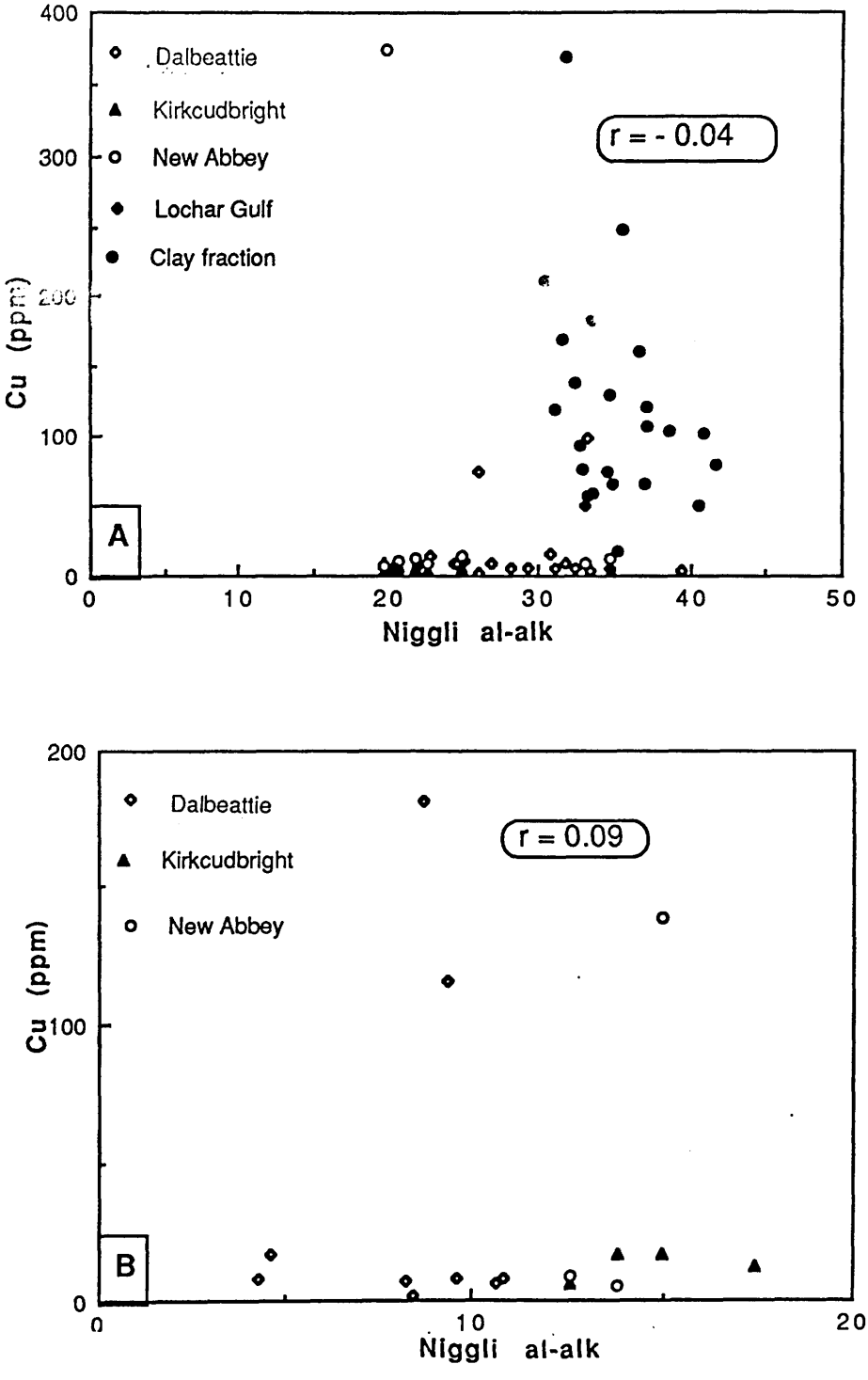

Figure 9.34 Plot of Niggli al-alk against Cu (ppm):
A, Holocene sediments;
B, Present-day intertidal sediments.
Bulk sample values for individual areas are shown separately. Values for samples of the clay fraction from the Dalbeattie, Kirkcudbright and New Abbey areas are grouped together.
r *is the correlation coefficient for the distribution of the bulk sample values for all areas.*

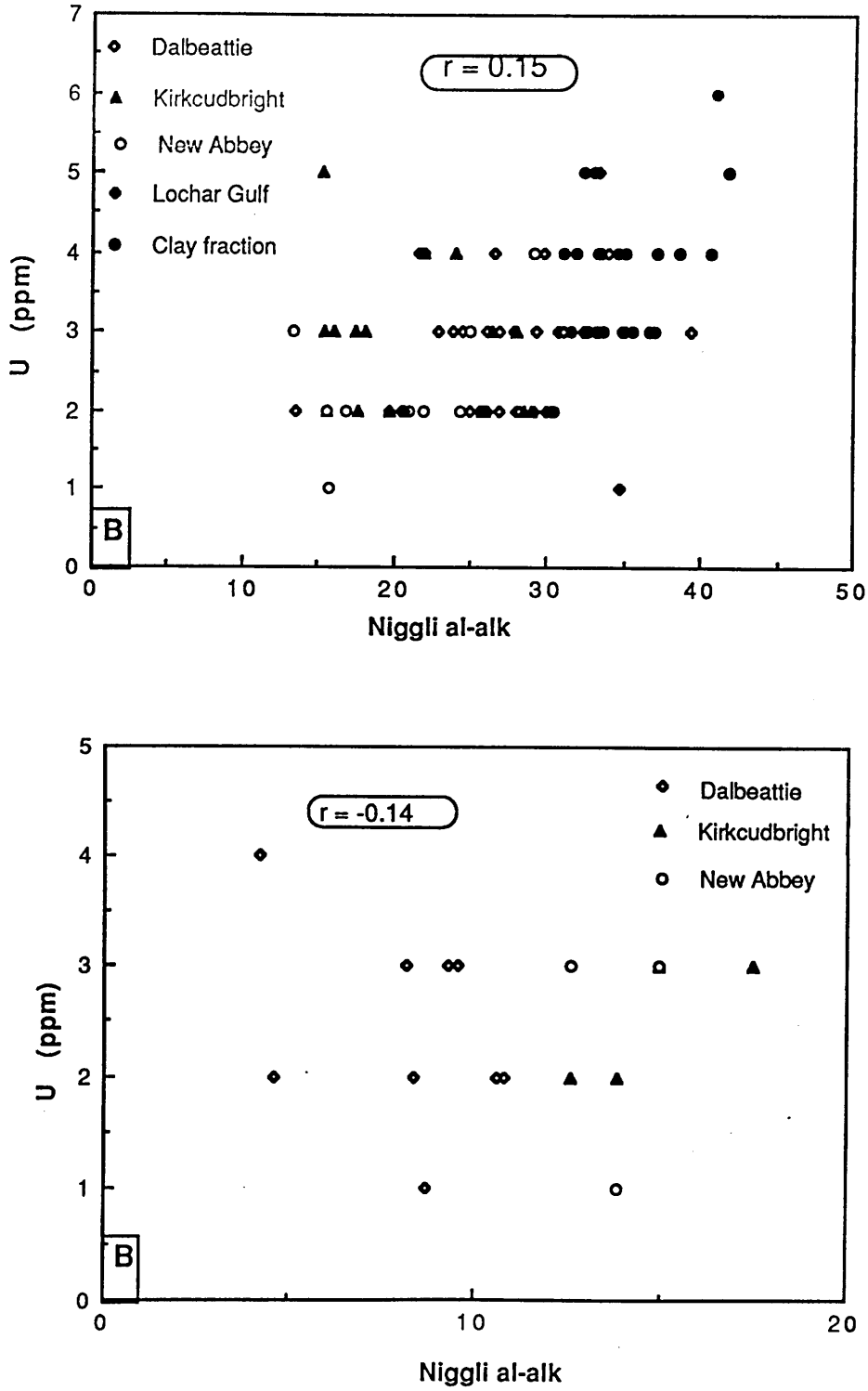

Figure 9.35 Plot of Niggli al-alk against U (ppm):
A, Holocene sediments;
B, Present-day intertidal sediments.
Bulk sample values for individual areas are shown separately. Values for samples of the clay fraction from the Dalbeattie, Kirkcudbright and New Abbey areas are grouped together.
r is the correlation coefficient for the distribution of the bulk sample values for all areas.

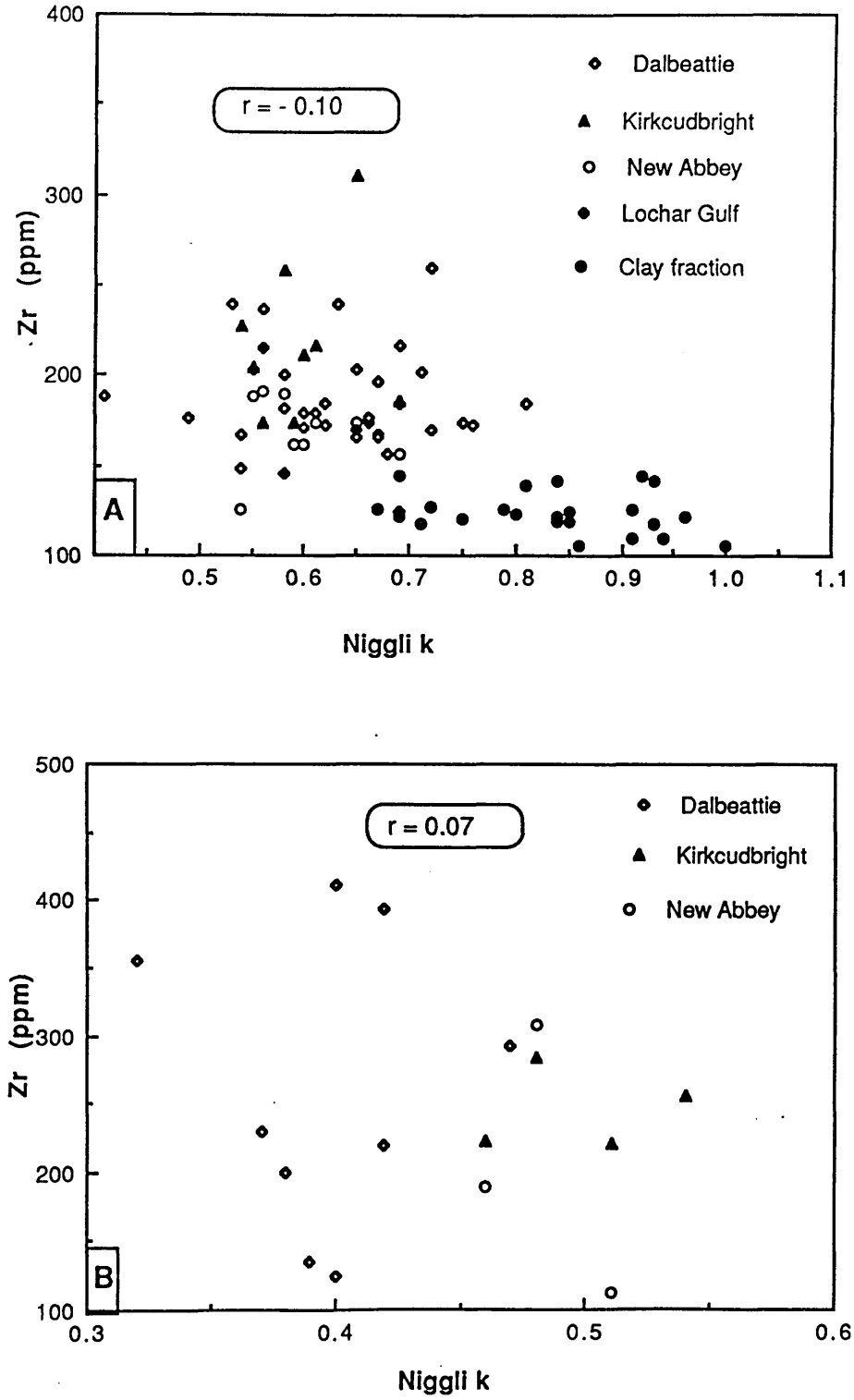

Figure 9.36 Plot of Niggli k against Zr (ppm):
A, Holocene sediments;
B, Present-day intertidal sediments.
Bulk sample values for individual areas are shown separately. Values for samples of the clay fraction from the Dalbeattie, Kirkcudbright and New Abbey areas are grouped together.
r *is the correlation coefficient for the distribution of the bulk sample values for all areas.*

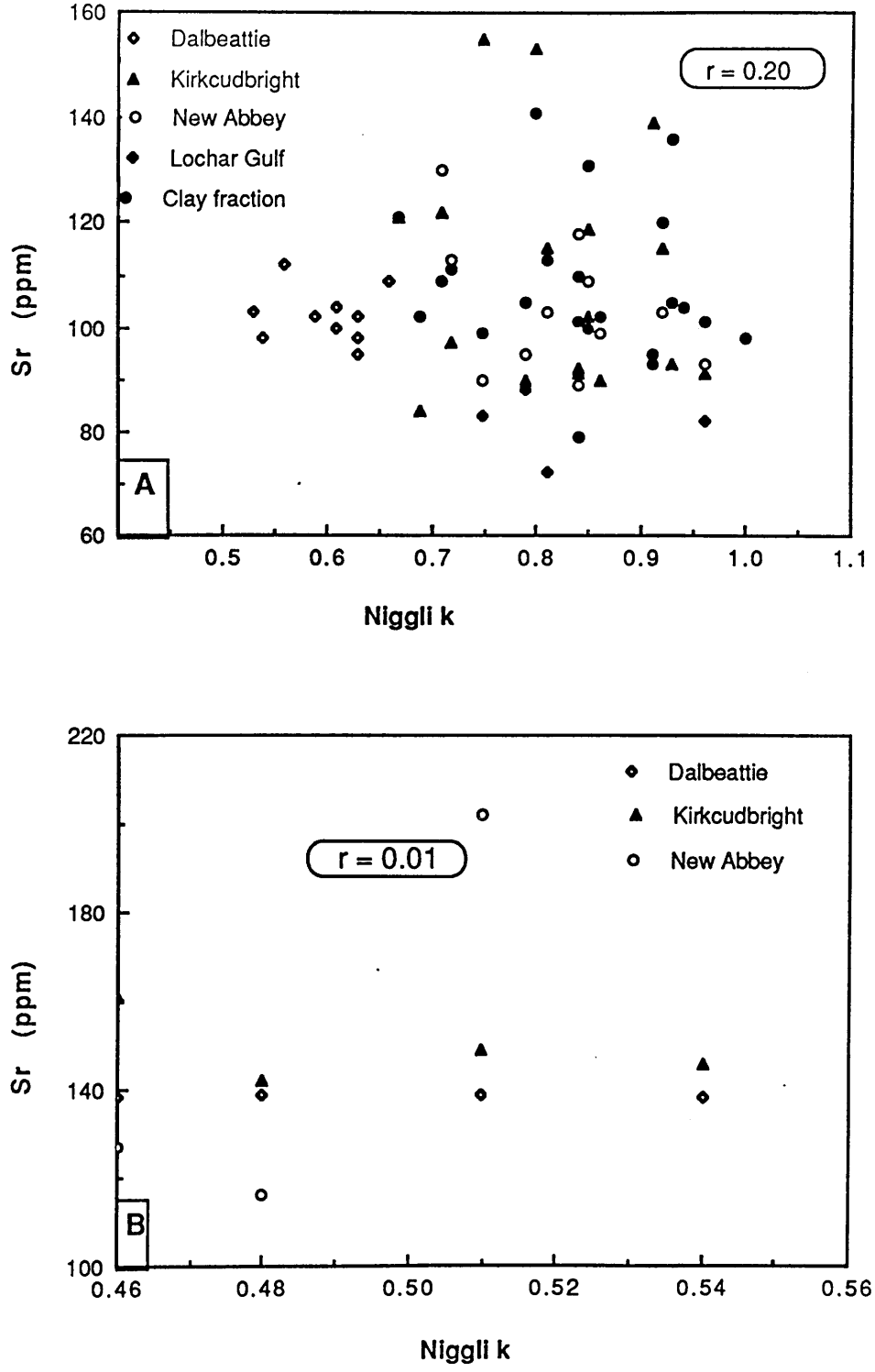

Figure 9.37 Plot of Niggli k against Sr (ppm):
A, Holocene sediments;
B, Present-day intertidal sediments.
Bulk sample values for individual areas are shown separately. Values for samples of the clay fraction from the Dalbeattie, Kirkcudbright and New Abbey areas are grouped together.
r *is the correlation coefficient for the distribution of the bulk sample values for all areas.*

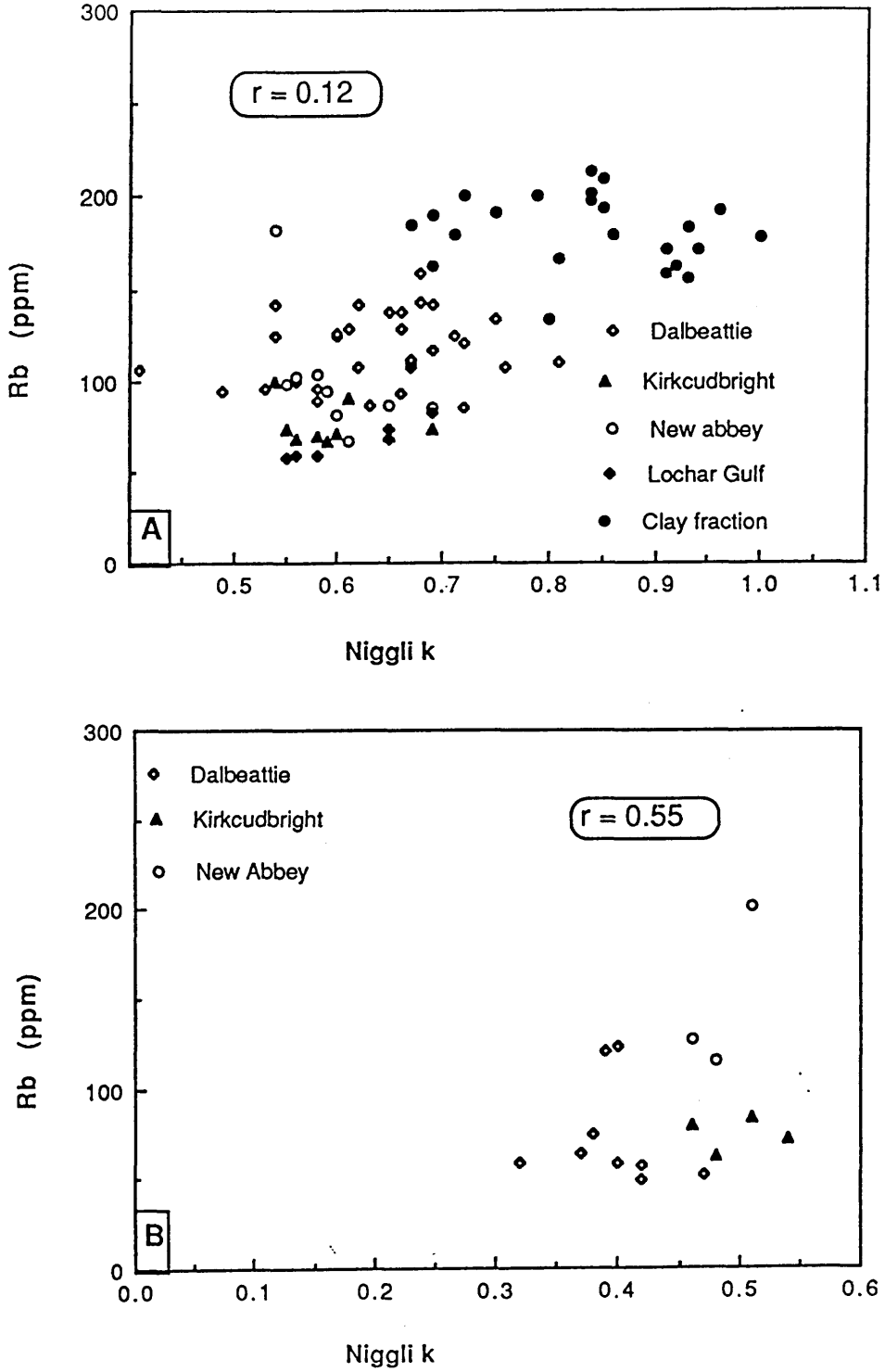

Figure 9.38 Plot of Niggli k against Rb (ppm):
A, Holocene sediments;
B, Present-day intertidal sediments.
Bulk sample values for individual areas are shown separately. Values for samples of the clay fraction from the Dalbeattie, Kirkcudbright and New Abbey areas are grouped together.
r *is the correlation coefficient for the distribution of the bulk sample values for all areas.*

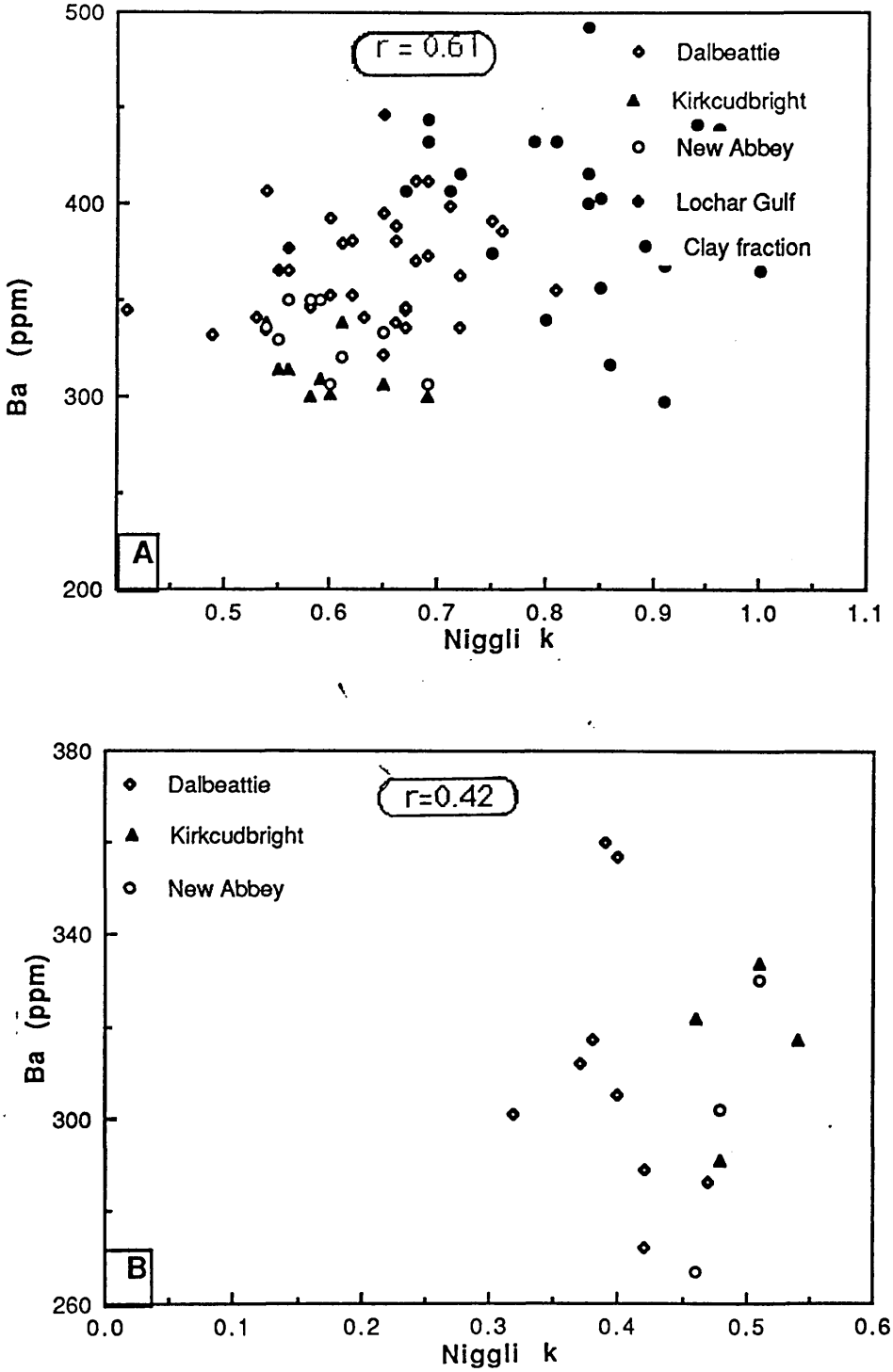

Figure 9.39 Plot of Niggli k against Ba (ppm):
A, Holocene sediments;
B, Present-day intertidal sediments.
Bulk sample values for individual areas are shown separately. Values for samples of the clay fraction from the Dalbeattie, Kirkcudbright and New Abbey areas are grouped together.
r *is the correlation coefficient for the distribution of the bulk sample values for all areas.*

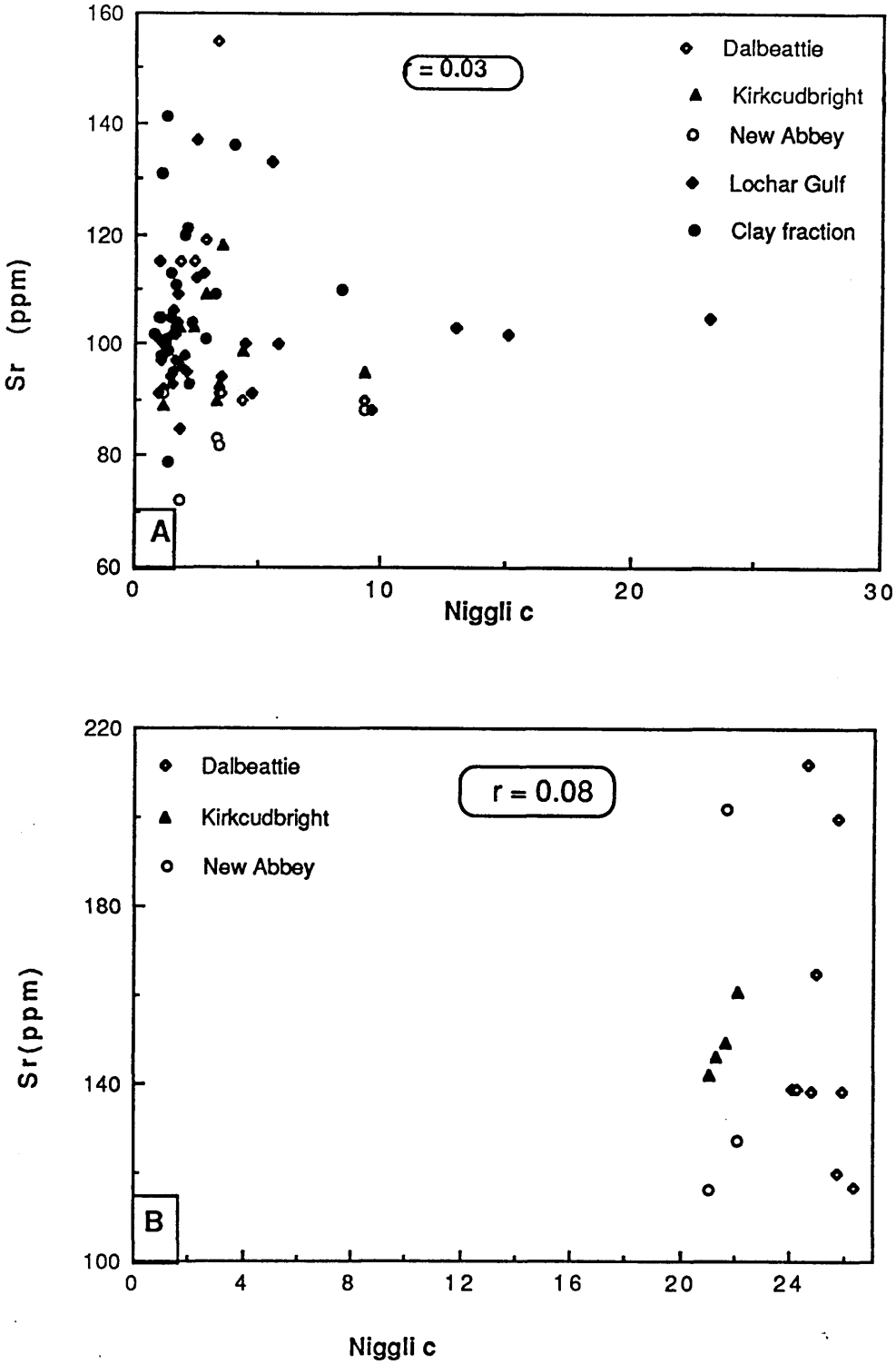

Figure 9.40 Plot of Niggli c against Sr (ppm):
A, Holocene sediments;
B, Present-day intertidal sediments.
Bulk sample values for individual areas are shown separately. Values for samples of the clay fraction from the Dalbeattie, Kirkcudbright and New Abbey areas are grouped together.
r *is the correlation coefficient for the distribution of the bulk sample values for all areas.*

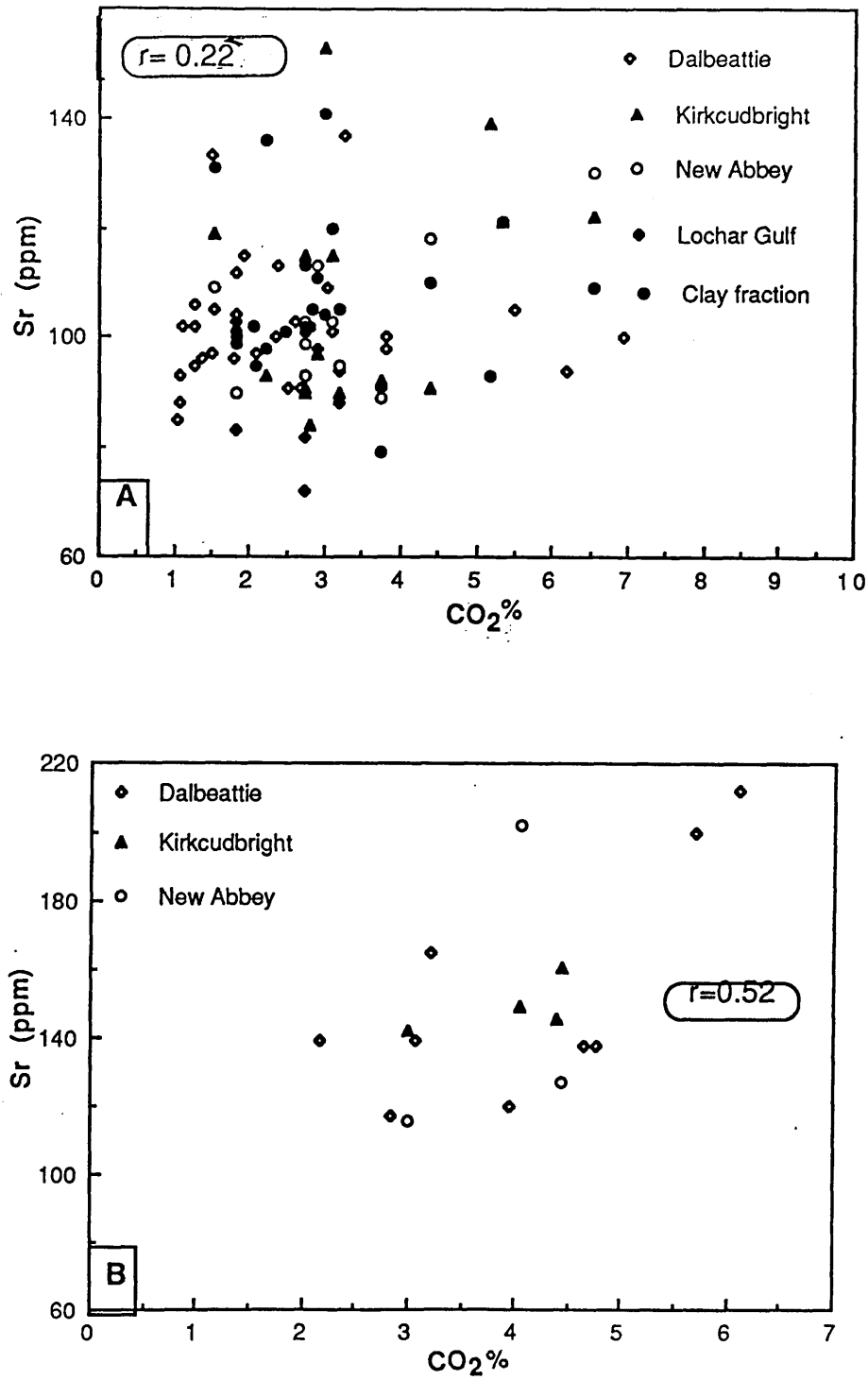

Figure 9.41 Plot of CO_2 against Sr (ppm):
A, Holocene sediments;
B, Present-day intertidal sediments.
Bulk sample values for individual areas are shown separately. Values for samples of the clay fraction from the Dalbeattie, Kirkcudbright and New Abbey areas are grouped together.
r *is the correlation coefficient for the distribution of the bulk sample values for all areas.*

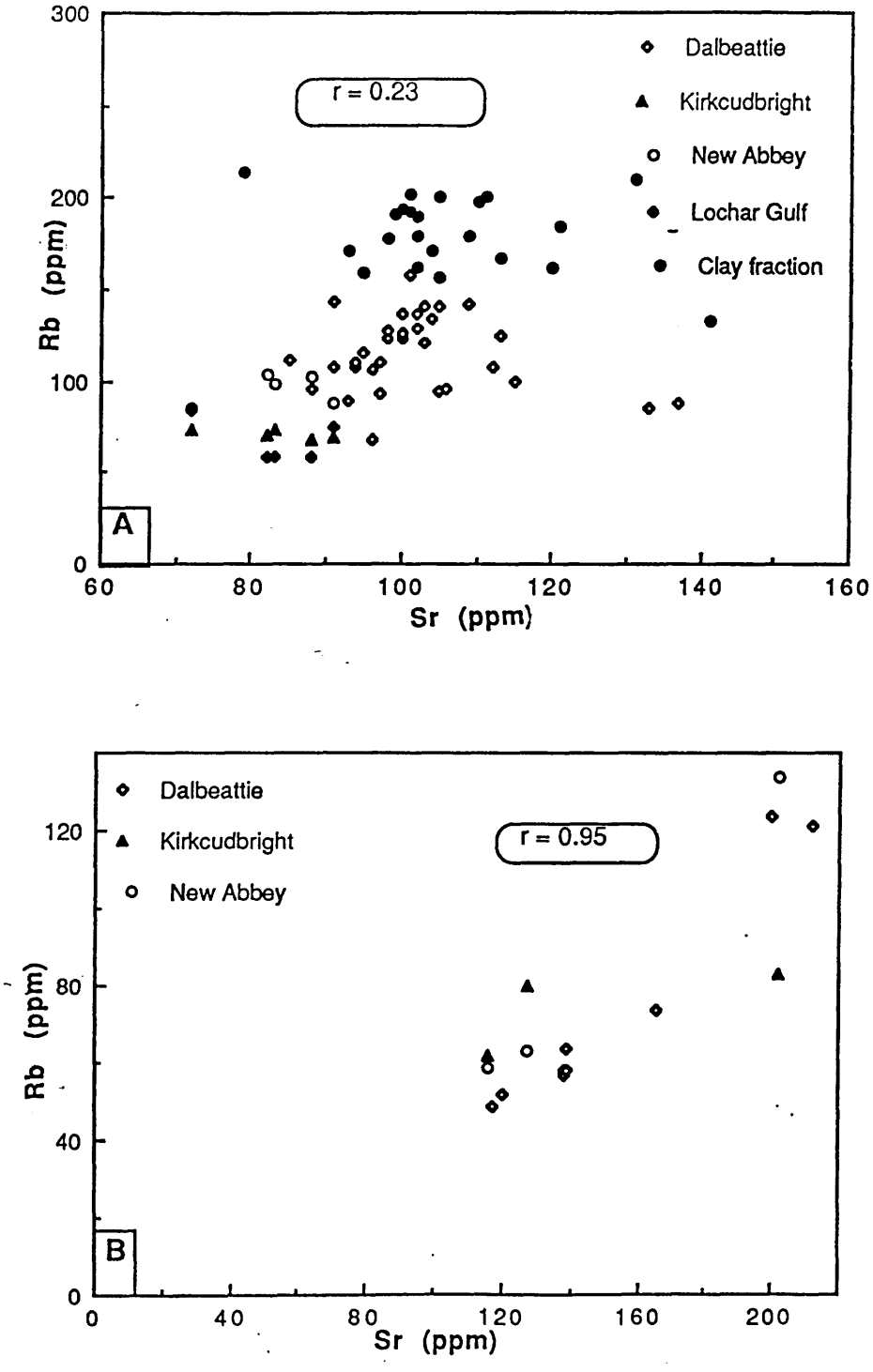

Figure 9.42 Plot of Sr(ppm) against Rb (ppm):
A, Holocene sediments;
B, Present-day intertidal sediments.
Bulk sample values for individual areas are shown separately. Values for samples of the clay fraction from the Dalbeattie, Kirkcudbright and New Abbey areas are grouped together.
r is the correlation coefficient for the distribution of the bulk sample values for all areas.

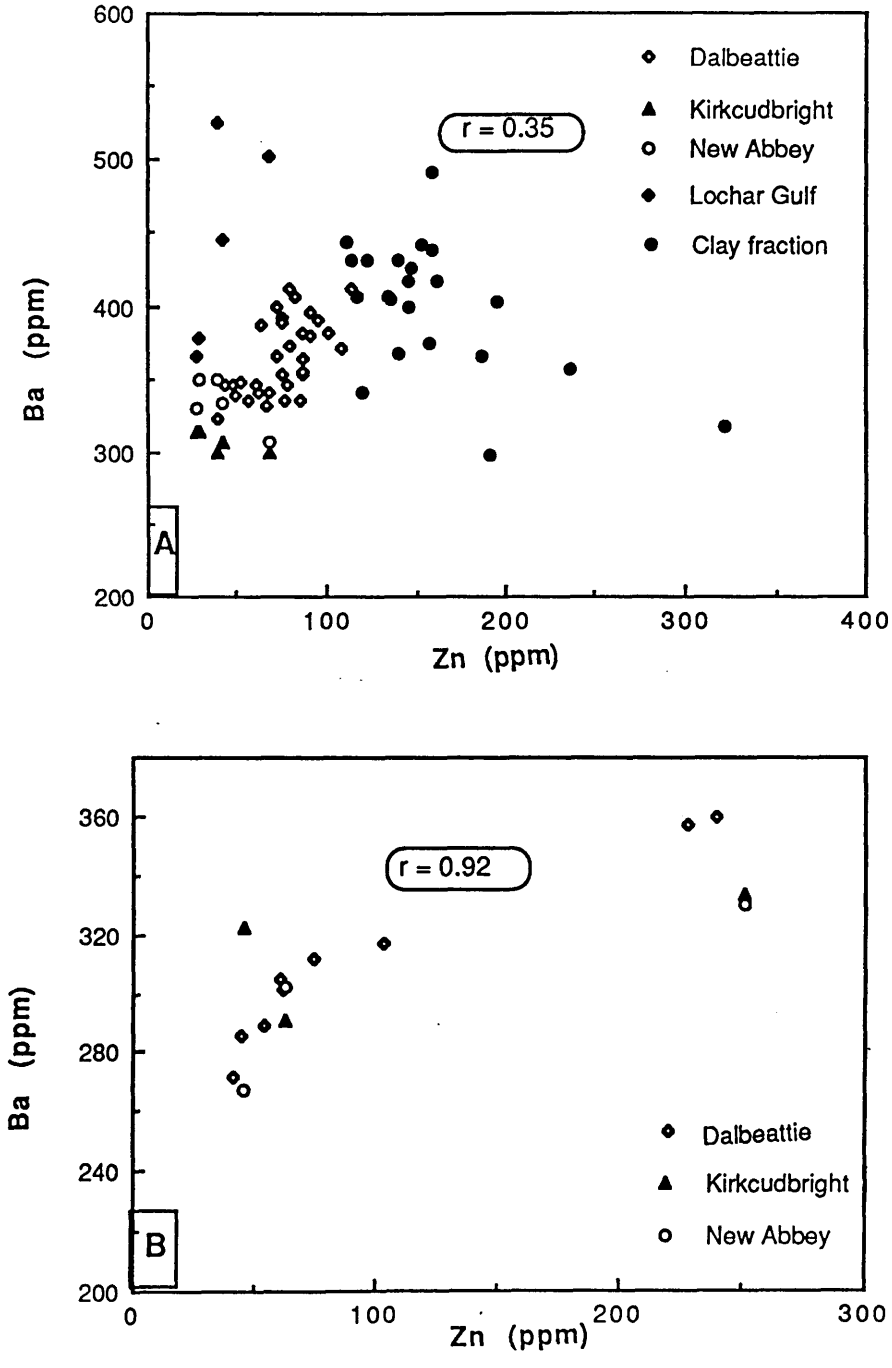

Figure 9.43 Plot of Zn (ppm) against Ba (ppm):
A, Holocene sediments;
B, Present-day intertidal sediments.
Bulk sample values for individual areas are shown separately. Values for samples of the clay fraction from the Dalbeattie, Kirkcudbright and New Abbey areas are grouped together.
r *is the correlation coefficient for the distribution of the bulk sample values for all areas.*

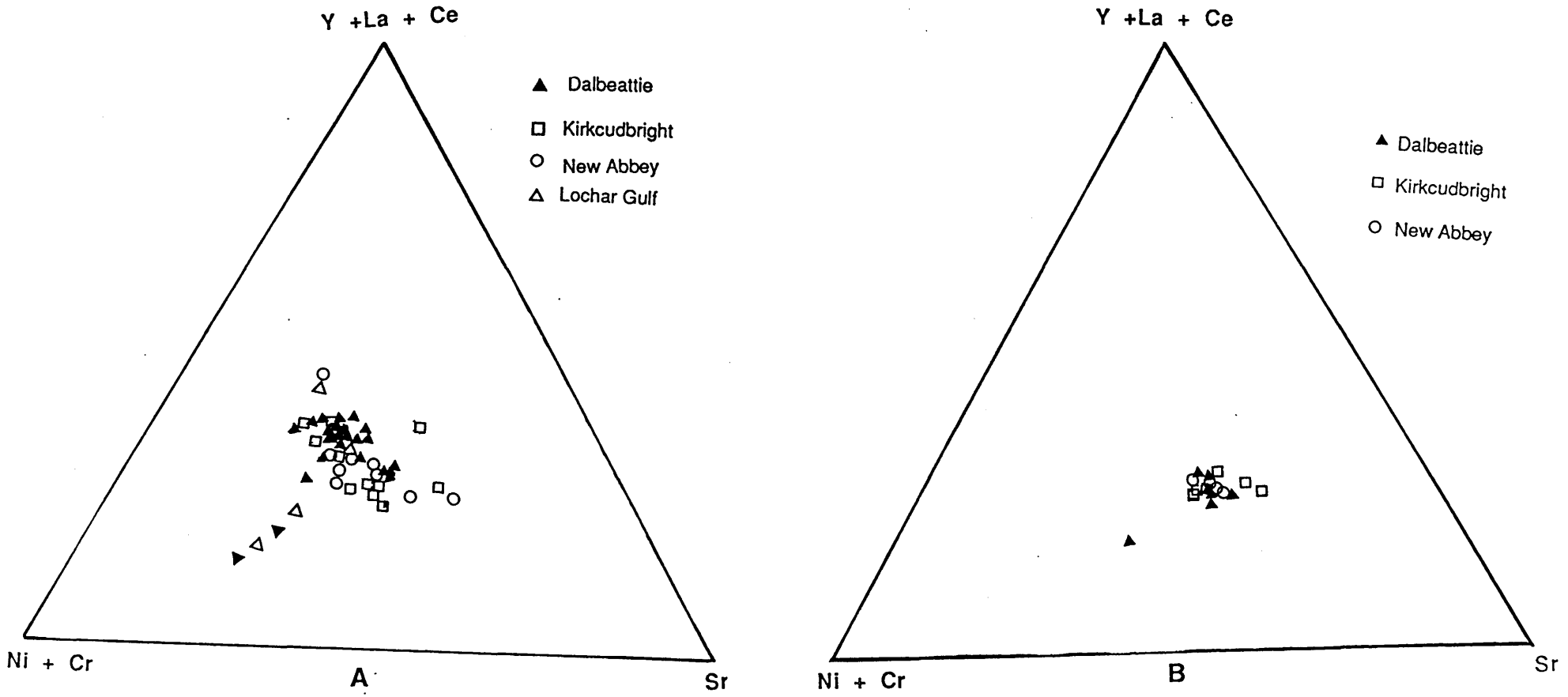

Figure 9.44 Triangular plot diagram of Ni + Cr versus Y + La + Ce versus Sr: A, Holocene sediments, Dalbeattie, Kirkcudbright, New Abbey and Lochar Gulf areas; B, present-day sediments, Dalbeattie, Kirkcudbright and New Abbey areas. Based on Hickman & Wright (1983).

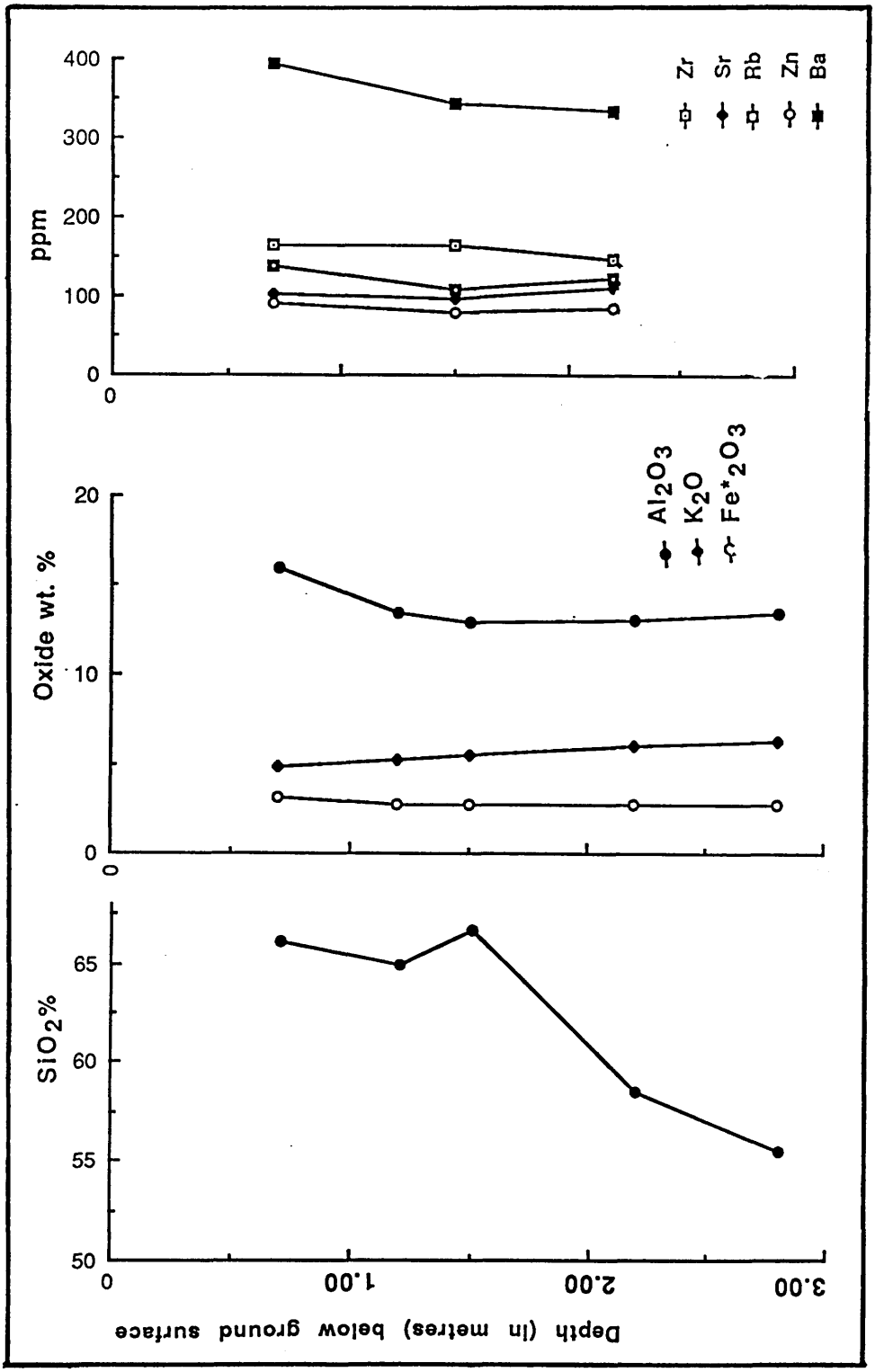

Figure 9.45 Plots of vertical variations in selected major and trace elements distribution in section D5, Dalbeattie area.

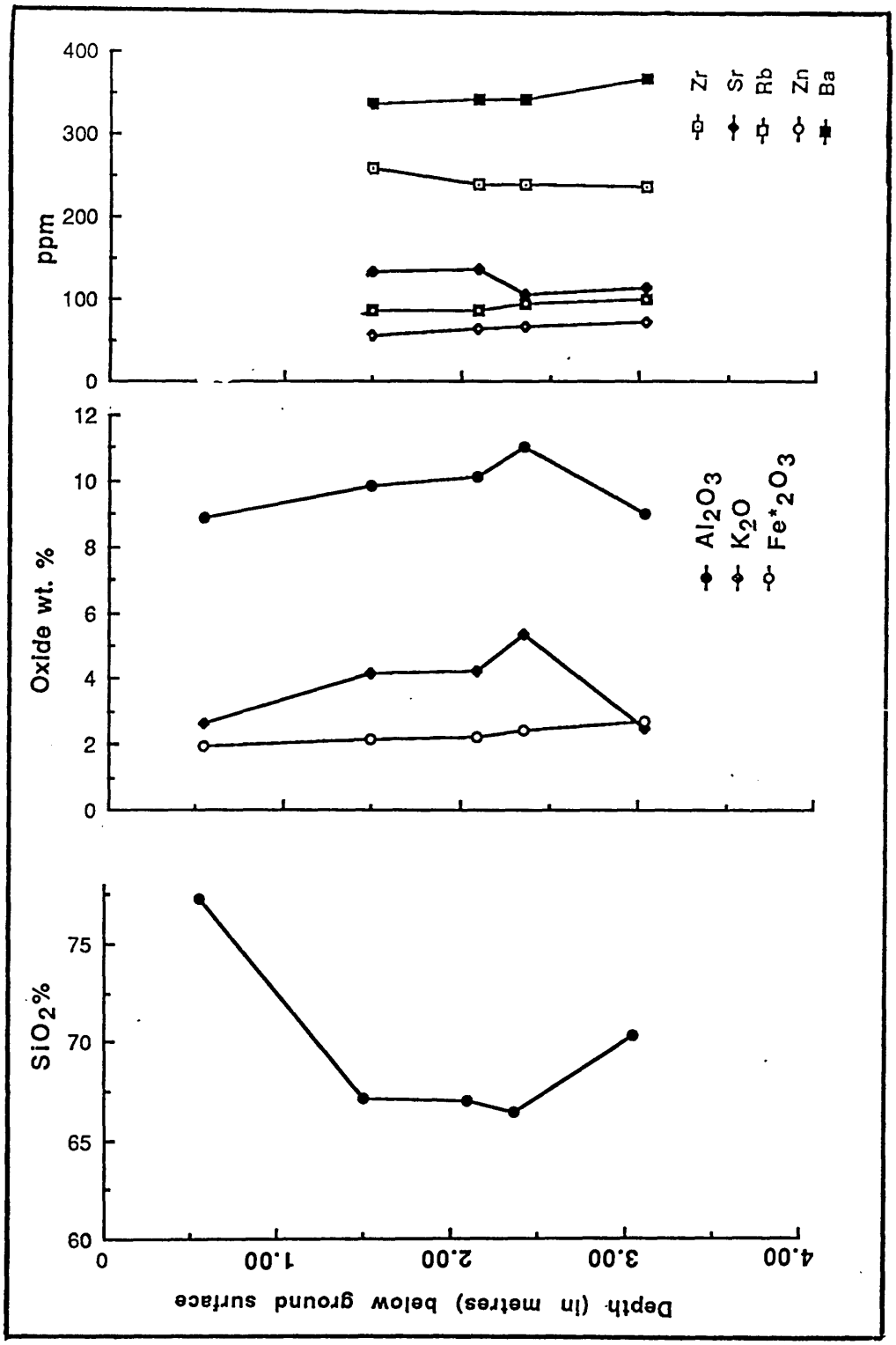

Figure 9.46 Plots of vertical variations in selected major and trace elements distribution in section D10, Dalbeattie area.

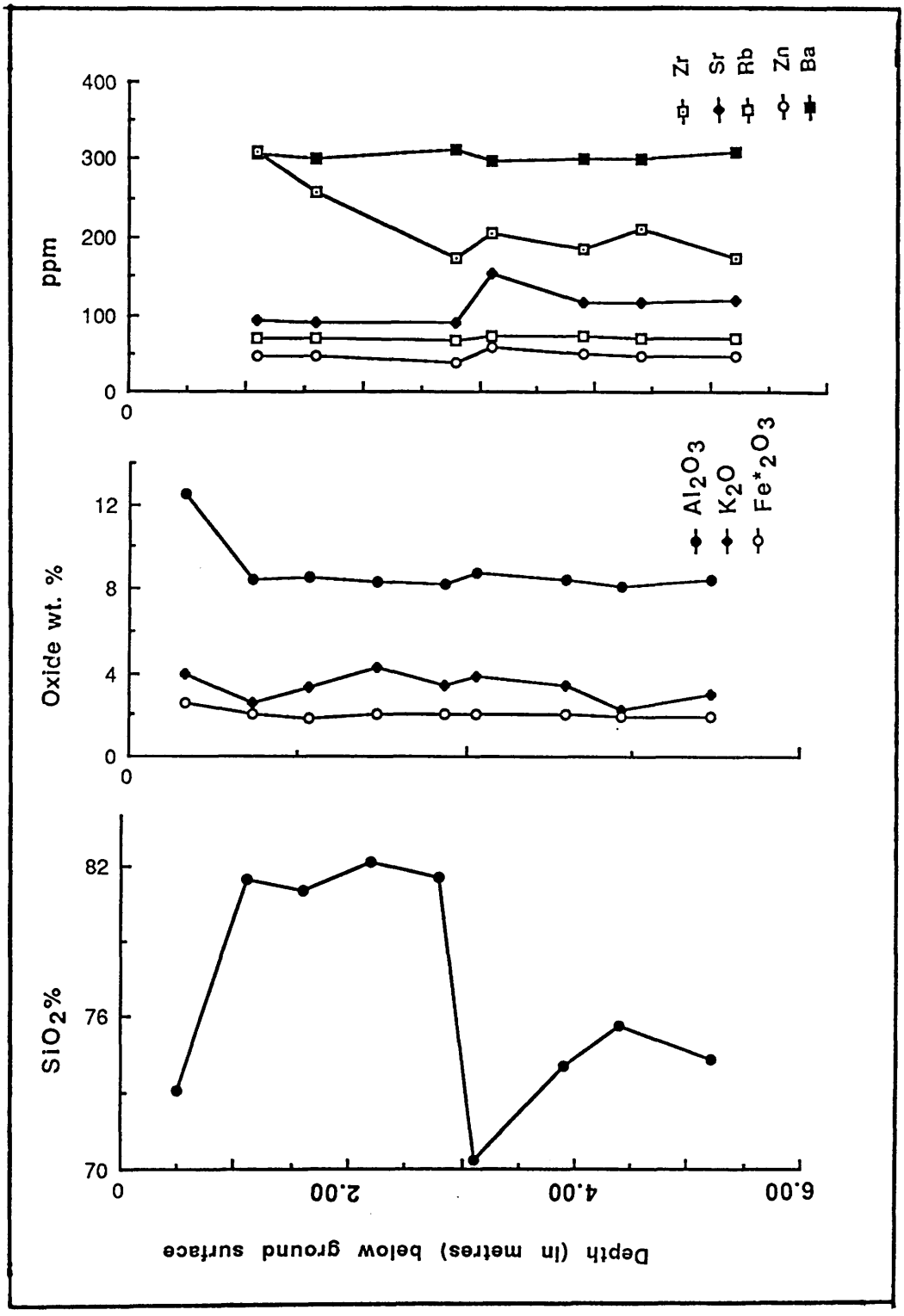

Figure 9.47 Plots of vertical variations in selected major and trace elements distribution in section K1, Kirkcudbright area.

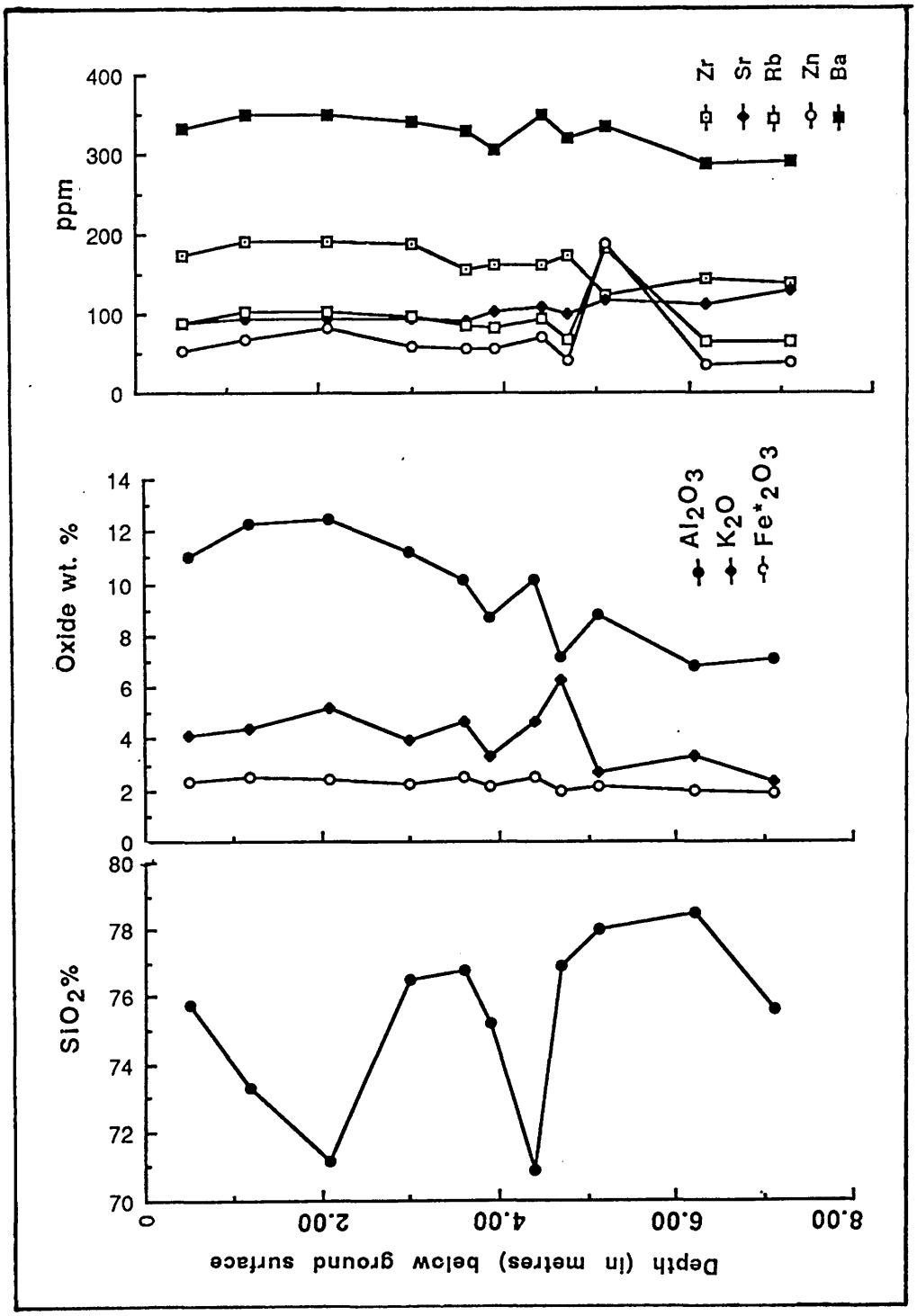

Figure 9.48 Plots of vertical variations in selected major and trace elements distribution in section N5, New Abbey area.

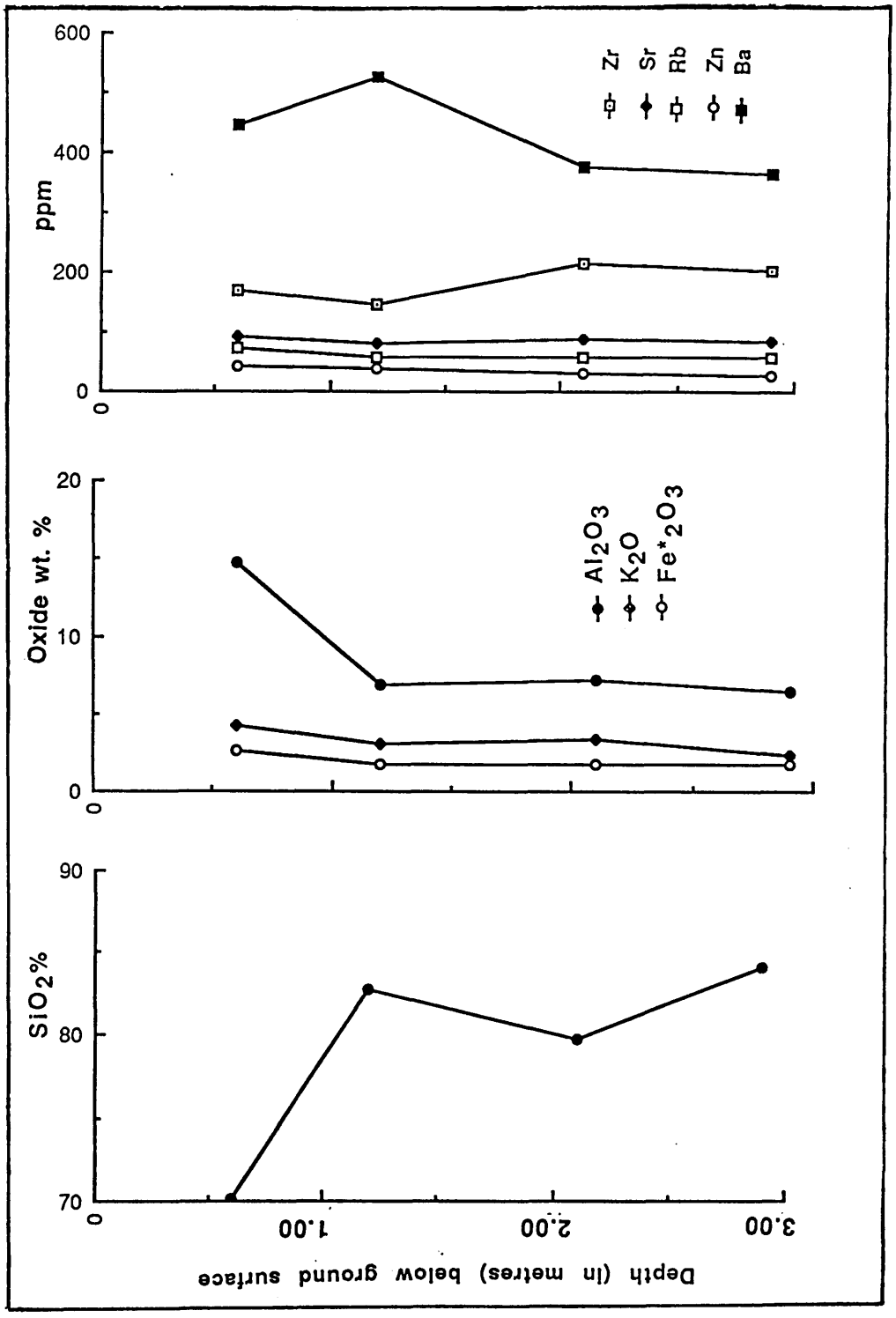

Figure 9.49 Plots of vertical variations in selected major and trace elements distribution in section South Kirkblain (SK), Lochar Gulf area.

Table 9.1 Mean($\bar{X}$) and standard deviation (σ) of major elements data for Holocene and present-day bulk sediment samples and samples of the clay fraction, Dalbeattie area.
(n = number of analysed samples)

	Holocene n = 39		Present-day n = 11		Clay fraction n = 29	
	$\bar{X}$	σ	$\bar{X}$	σ	$\bar{X}$	σ
SiO_2	68.46	5.50	73.75	4.28	50.6	3.03
TiO_2	0.76	0.12	0.55	0.05	0.83	0.04
Al_2O_3	12.85	2.47	7.15	0.82	21.96	1.46
Fe_2O_3	3.25	1.12	1.46	0.50	6.81	1.65
FeO	1.47	0.42	1.14	0.12	1.76	0.32
MnO	0.06	0.06	0.08	0.03	0.07	0.05
MgO	2.06	0.47	1.63	0.18	3.30	0.46
CaO	1.00	1.26	3.60	0.35	0.62	0.55
Na_2O	1.12	0.34	1.82	0.37	0.57	0.34
K_2O	2.73	0.40	1.77	0.10	3.96	0.33
P_2O_5	0.10	0.03	0.14	0.09	0.50	0.26
H_2O	3.89	1.78	2.39	0.96	6.32	1.64
CO_2	2.26	1.57	4.37	0.96	2.97	1.21

Table 9.2 Mean($\bar{X}$) and standard deviation (σ) of major elements data for Holocene and present-day bulk sediment samples and samples of the clay fraction, Kirkcudbright area.
(n = number of analysed samples)

	Holocene n = 23		Present-day n = 12		Clay fraction n = 8	
	$\bar{X}$	σ	$\bar{X}$	σ	$\bar{X}$	σ
SiO_2	73.54	5.67	70.22	4.96	49.42	2.65
TiO_2	0.67	0.13	0.57	1.22	0.80	0.05
Al_2O_3	10.19	1.94	8.43	0.85	19.97	2.19
Fe_2O_3	2.45	1.04	1.83	1.07	7.21	2.93
FeO	1.51	0.42	1.41	0.39	1.58	0.33
MnO	0.07	0.04	0.09	0.05	0.09	0.04
MgO	1.72	0.52	1.87	0.48	3.56	0.27
CaO	1.47	1.64	3.66	1.23	1.77	1.63
Na_2O	1.26	0.33	1.25	0.35	2.35	0.58
K_2O	2.25	0.27	1.96	0.52	3.62	0.27
P_2O_5	0.08	0.03	0.13	0.05	0.15	0.05
H_2O	3.02	1.23	3.14	1.28	6.14	1.15
CO_2	2.15	1.49	5.91	2.09	3.70	1.48

Table 9.3 Mean($\bar{X}$) and standard deviation (σ) of major elements data for Holocene and present-day bulk sediment samples and samples of the clay fraction, New Abbey area. (n = number of analysed samples)

	Holocene n = 11		Present-day n = 4		Clay fraction n = 2	
	$\bar{X}$	σ	$\bar{X}$	σ	$\bar{X}$	σ
SiO_2	75.33	2.53	75.46	1.72	51.63	6.48
TiO_2	0.58	0.14	0.51	0.02	0.78	0.12
Al_2O_3	9.62	2.05	7.71	0.55	19.60	1.54
Fe_2O_3	2.46	1.16	2.03	0.44	6.33	0.43
FeO	1.46	0.40	1.22	0.22	2.19	0.22
MnO	0.08	0.11	0.07	0.01	0.07	0.01
MgO	1.53	0.23	1.51	0.09	3.17	0.25
CaO	1.26	1.26	2.99	0.21	1.35	0.64
Na_2O	1.01	0.18	1.22	0.18	1.30	0.76
K_2O	2.24	0.24	1.81	0.10	3.55	0.23
P_2O_5	0.08	0.02	0.11	0.01	0.9	0.04
H_2O	2.76	0.46	2.16	0.22	6.70	1.95
CO_2	2.06	0.87	3.97	0.67	3.42	0.59

Table 9.4 Mean($\bar{X}$) and standard deviation (σ) of major elements data for Holocene bulk sediment samples and samples of the clay fraction, Lochar Gulf area. (n = number of analysed samples)

	Holocene n = 11		Clay fraction n = 4	
	$\bar{X}$	σ	$\bar{X}$	σ
SiO_2	80.24	4.68	51.35	5.57
TiO_2	0.47	0.14	0.75	0.10
Al_2O_3	8.12	2.64	21.51	2.33
Fe_2O_3	1.82	0.53	5.92	1.46
FeO	1.29	0.32	2.34	1.16
MnO	0.11	0.07	0.05	0.03
MgO	0.89	0.34	3.58	0.87
CaO	0.35	0.23	0.50	0.08
Na_2O	0.84	0.14	0.98	0.18
K_2O	1.88	0.31	4.05	0.43
P_2O_5	0.10	0.06	0.12	0.05
H_2O	2.40	1.36	6.78	1.94
CO_2	1.94	0.92	2.73	0.87

Table 9.5 Mean($\bar{X}$) and standard deviation (σ) of trace element concentrations in Holocene and present-day bulk sediment samples and samples of the clay fraction from the various areas studied. (n = number of analysed samples)

	Holocene n = 65		Present-day n = 20		Clay fraction n = 23	
	$\bar{X}$	σ	$\bar{X}$	σ	$\bar{X}$	σ
Zr	182.38	34.22	252.25	83.66	130.41	22.00
Y	26.24	7.38	23.70	4.29	32.90	7.78
Sr	102.76	16.16	148.80	27.37	107.40	0.97
U	2.72	0.98	2.43	0.87	3.37	1.03
Rb	102.03	30.21	73.20	24.60	177.60	30.00
Th	7.63	3.00	5.00	2.07	12.90	2.47
Pb	21.70	26.89	45.40	29.35	40.63	8.40
Ga	15.21	14.14	9.60	12.21	26.27	3.13
Zn	69.15	29.06	104.90	65.95	159.22	47.15
Cu	19.96	210.56	29.50	51.24	124.50	78.09
Ni	30.86	13.33	21.30	12.21	61.54	17.25
Co	11.77	6.19	9.20	5.82	24.54	6.15
Cr	98.67	22.44	97.25	26.30	145.22	17.23
Ce	60.29	17.71	48.85	14.21	96.82	14.44
Ba	353.83	44.23	308.50	24.43	400.40	45.49
La	27.35	9.47	22.25	8.59	47.36	7.40

Table 9.6 Major and trace elements analyses of the Holocene raised coastal sediments (bulk samples) from the various areas studied (D2 to D10, Dalbeattie area; K1 to K4, Kirkcudbright area; N5, New Abbey area; SK and BB, Lochar Gulf area).

	D2 1.1b	D2 2.5b	D2 2.95b	D3 1.4b	D4 0.5b	D4 1.2b	D4 1.6b	D4 2.1b	D4 2.5b	D4 2.90b
SiO_2	66.67	71.35	64.10	70.68	66.23	64.65	67.88	66.45	68.08	67.36
TiO_2	0.67	0.78	0.78	0.74	0.80	0.80	0.85	0.85	0.87	0.74
Al_2O_3	12.76	14.41	12.38	14.13	14.10	15.22	14.68	14.65	15.27	13.07
Fe_2O_3	4.04	3.00	3.42	3.15	5.62	4.69	4.09	5.00	3.94	2.77
FeO	1.45	1.28	2.05	1.42	0.03	1.19	1.34	1.40	1.68	1.89
MnO	0.03	0.02	0.03	0.04	0.07	0.08	0.10	0.05	0.11	0.08
MgO	1.94	1.69	1.93	1.80	1.88	2.18	2.17	2.22	2.26	3.15
CaO	0.34	0.28	0.21	0.35	0.29	0.22	0.30	0.32	0.47	3.10
Na_2O	0.84	0.86	1.39	0.88	1.52	1.08	1.27	0.65	1.05	0.97
K_2O	3.20	2.94	3.11	2.91	2.74	3.18	2.98	2.95	3.20	2.70
P_2O_5	0.10	0.06	0.10	0.09	0.07	0.10	0.09	0.07	0.11	0.14
H_2O	5.20	4.32	6.74	2.17	5.01	6.74	2.17	5.01	5.86	3.82
CO_2	2.91	3.04	3.80	1.28	1.84	3.80	1.28	1.84	1.83	1.11
Total	99.91	104.03	100.04	99.64	100.20	101.09	100.73	98.98	99.99	100.29
$Fe^*_2O_3$	5.66	4.42	5.70	4.73	5.65	6.01	5.58	6.56	5.81	4.87
Zr	--	202	217	179	184	167	174	179	173	167
Y	--	31	27	31	21	40	30	32	32	27
Sr	--	98	109	100	95	103	98	102	104	112
U	--	3	5	4	4	3	3	2	3	3
Rb	--	124	142	124	116	141	128	129	134	107
Th	--	9	7	11	8	8	9	9	10	7
Pb	--	19	20	29	24	28	27	25	19	14
Ga	--	16	16	16	17	19	17	17	19	14
Zn	--	72	79	87	79	82	87	92	95	77
Cu	--	21	17	17	8	16	15	17	18	18
Ni	--	34	37	41	31	50	40	51	45	35
Co	--	12	13	11	14	20	19	18	19	18
Cr	--	106	112	95	110	114	104	109	111	93
Ce	--	67	71	70	57	88	71	74	74	69
Ba	--	399	411	352	373	406	381	380	391	336
La	--	33	32	31	31	33	37	34	35	30

	D5 0.7b	D5 1.2b	D5 1.5b	D5 2.2b	D5 2.8b	D6 0.5b	D6 1.2b	D6 1.7b	D6 2.00b	D6 2.6b
SiO_2	66.12	65.01	66.77	58.53	55.45	64.56	67.50	63.52	60.73	59.39
TiO_2	0.89	0.75	0.74	0.78	0.75	0.92	0.84	0.94	0.73	0.89
Al_2O_3	15.96	13.46	12.91	13.08	13.40	16.34	15.62	16.50	16.22	17.03
Fe_2O_3	2.81	3.49	3.88	3.90	4.91	3.55	3.21	4.14	4.20	4.00
FeO	1.84	1.57	1.54	1.96	1.25	1.54	1.88	1.77	2.03	2.36
MnO	0.02	0.05	0.07	0.09	0.06	0.04	0.02	0.04	0.04	0.05
MgO	2.27	2.21	2.51	2.50	2.30	2.31	2.04	2.22	2.27	2.49
CaO	0.30	0.49	0.80	1.08	0.65	0.18	0.33	0.94	0.19	0.29
Na_2O	1.03	1.56	1.17	0.96	1.11	0.98	1.03	0.70	1.01	0.52
K_2O	3.13	2.79	2.70	2.82	2.70	3.11	3.11	3.32	3.22	3.42
P_2O_5	0.08	0.13	0.12	0.11	0.11	0.07	0.08	0.10	0.10	0.11
H_2O	4.20	5.32	4.01	6.95	10.45	4.32	3.10	3.24	4.32	6.17
CO_2	1.50	2.38	2.35	8.00	6.20	3.11	1.05	2.67	2.50	3.20
Total	100.15	99.21	99.57	100.76	99.34	101.30	99.81	100.10	97.56	99.92
$Fe^*_2O_3$	4.85	5.23	5.59	6.08	6.30	5.26	5.30	6.11	6.46	6.62
Zr	165	--	166	148	--	171	176	--	185	156
Y	30	--	27	28	--	25	28	--	26	38
Sr	102	--	97	113	--	100	100	--	94	101
U	3	--	3	3	--	3	2	--	2	3
Rb	137	--	110	125	--	126	137	--	107	158
Th	11	--	8	8	--	8	12	--	7	12
Pb	31	--	21	28	--	29	30	--	24	32
Ga	18	--	15	17	--	19	20	--	14	21
Zn	91	--	78	85	--	75	75	--	75	114
Cu	13	--	14	14	--	12	17	--	16	22
Ni	34	--	42	40	--	34	33	--	30	57
Co	14	--	15	16	--	8	11	--	8	18
Cr	109	--	92	99	--	102	107	--	87	122
Ce	80	--	63	68	--	74	72	--	61	85
Ba	395	--	345	335	--	392	388	--	353	411
La	41	--	28	31	--	35	31	--	25	41

Continued

Table 9.6 continued

	D7 0.4b	D7 1.1b	D7 1.6b	D7 2.25b	D7 3.70b	D8 0.40b	D8 1.2b	D8 2.00b	D8 2.70b	D9 0.4b
SiO_2	75.11	73.80	72.35	71.72	69.35	74.18	74.30	64.55	67.31	68.10
TiO_2	0.52	0.70	0.70	0.73	0.78	0.72	0.64	0.90	0.83	0.92
Al_2O_3	7.39	12.30	1221	12.19	11.15	11.95	11.20	15.70	14.04	12.61
Fe_2O_3	1.30	2.02	3.38	3.86	2.50	2.72	1.56	3.72	4.52	3.96
FeO	1.40	0.79	1.28	1.31	1.65	1.14	1.89	1.84	1.64	1.42
MnO	0.07	0.02	0.03	0.07	0.08	0.02	0.05	0.09	0.42	0.03
MgO	1.55	1.28	1.61	1.80	2.80	1.55	1.40	2.64	2.50	1.67
CaO	3.16	1.40	0.15	0.16	2.25	0.21	0.27	0.37	1.04	0.40
Na_2O	1.27	1.25	0.87	1.06	0.63	1.14	2.32	1.12	0.72	1.07
K_2O	1.82	2.60	2.57	2.67	2.41	2.41	2.42	3.20	2.85	2.76
P_2O_5	0.12	0.06	0.08	0.13	0.13	0.07	0.06	0.17	0.17	0.07
H_2O	2.14	2.32	3.12	3.73	4.25	2.19	3.41	2.94	2.34	5.90
CO_2	5.52	1.06	2.09	1.52	2.62	1.08	1.37	1.79	1.50	3.25
Total	101.37	99.60	100.44	100.95	100.60	99.38	100.89	99.03	99.88	102.16
$Fe^*_2O_3$	2.86	2.90	4.80	5.32	4.33	3.99	3.66	5.76	6.34	5.54
Zr	196	172	156	184	176	182	177	172	170	--
Y	24	24	34	30	28	20	23	33	29	--
Sr	85	91	91	94	94	95	93	141	121	--
U	3	3	3	4	2	3	4	4	3	--
Rb	111	108	143	110	94	95	93	141	121	--
Th	7	9	11	9	8	5	8	10	12	--
Pb	24	25	29	23	22	21	22	28	27	--
Ga	17	13	20	14	13	14	13	20	16	--
Zn	43	64	109	87	66	52	50	102	87	--
Cu	11	14	24	19	12	5	12	20	17	--
Ni	15	27	76	39	29	25	25	47	45	--
Co	3	12	30	16	13	6	7	15	19	--
Cr	87	89	112	87	95	125	83	110	100	--
Ce	64	56	84	69	64	49	51	85	68	--
Ba	346	386	370	355	332	348	338	381	363	--
La	27	28	35	33	29	24	19	38	30	--

	D9 1.06b	D9 1.56b	D9 2.00b	D9 2.92b	D10 0.55b	D10 1.50b	D10 2.10b	D10 2.36b	D10 3.03b	K1 0.50b
SiO_2	76.69	74.51	79.90	79.10	77.28	67.13	67.00	66.42	70.42	73.05
TiO_2	0.63	0.71	0.63	0.55	1.12	0.73	0.73	0.80	0.49	0.83
Al_2O_3	10.32	12.06	9.95	7.88	8.85	9.86	10.16	11.00	9.04	12.54
Fe_2O_3	2.52	3.49	1.45	1.22	1.58	2.49	2.15	3.46	1.17	2.54
FeO	0.90	1.10	1.19	1.24	0.97	1.53	1.87	1.69	1.22	1.23
MnO	0.03	0.04	0.05	0.08	0.05	0.11	0.09	0.14	0.09	0.03
MgO	1.40	1.60	1.43	1.68	1.10	2.39	2.59	2.74	2.50	1.64
CaO	0.20	0.15	0.22	1.60	0.65	4.48	4.81	2.73	3.54	0.29
Na_2O	1.36	1.35	1.41	1.81	1.24	0.92	1.01	1.15	1.53	1.22
K_2O	2.34	2.60	2.36	2.08	1.91	2.13	2.24	2.41	2.69	2.54
P_2O_5	0.06	0.09	0.08	0.10	0.17	0.12	0.12	0.13	0.10	0.03
H_2O	2.77	1.92	1.02	2.09	3.36	4.81	3.89	3.95	2.34	2.95
CO_2	1.28	0.70	0.61	1.13	2.09	3.00	2.76	2.96	4.75	1.32
Total	100.50	100.32	100.30	100.56	100.47	99.62	99.42	99.58	98.88	100.21
$Fe^*_2O_3$	3.52	4.71	2.77	2.60	2.66	4.19	4.23	5.34	2.53	3.91
Zr	200	188	--	203	--	269	239	239	237	--
Y	26	28	--	21	--	27	27	31	31	--
Sr	93	96	--	133	--	133	137	106	115	--
U	2	2	--	2	--	2	2	4	2	--
Rb	89	106	--	68	--	85	87	95	100	--
Th	7	8	--	4	--	6	8	9	9	--
Pb	20	20	--	15	--	15	17	20	20	--
Ga	12	13	--	7	--	12	13	11	15	--
Zn	48	61	--	39	--	56	63	68	72	--
Cu	9	13	--	6	--	13	16	17	18	--
Ni	19	33	--	19	--	26	28	31	31	--
Co	8	13	--	7	--	16	11	11	10	--
Cr	84	94	--	69	--	89	87	97	92	--
Ce	58	65	--	38	--	56	55	66	60	--
Ba	346	345	--	322	--	336	341	341	366	--
La	25	29	--	19	--	22	23	27	32	--

Continued

Table 9.6 continued

	K1 1.1b	K1 1.6b	K1 2.2b	K1 2.8b	K1 3.1b	K1 3.9b	K1 4.4b	K1 5.2b	K2 0.6b	K2 1.0b
SiO_2	81.44	81.03	82.15	81.52	70.32	74.05	75.62	74.31	76.30	75.03
TiO_2	0.67	0.60	0.54	0.53	0.57	0.54	0.55	0.53	0.76	0.83
Al_2O_3	8.40	8.51	8.33	8.19	8.81	8.46	8.12	8.42	10.90	11.10
Fe_2O_3	1.48	1.97	2.50	1.99	2.25	1.97	1.13	1.82	2.04	2.96
FeO	1.02	1.16	1.62	1.32	1.41	1.35	0.97	1.07	1.52	1.62
MnO	0.06	0.07	0.14	0.02	0.07	0.09	0.07	0.07	0.03	0.09
MgO	1.14	1.06	0.98	0.98	0.96	1.95	1.85	1.90	1.43	1.47
CaO	0.34	0.33	0.26	0.18	4.17	2.81	2.91	3.12	0.16	0.15
Na_2O	1.20	1.31	1.82	1.45	0.80	1.27	1.00	1.03	1.05	1.07
K_2O	2.02	2.03	2.01	2.05	2.02	2.03	1.97	1.95	2.30	2.50
P_2O_5	0.09	0.10	0.08	0.05	0.10	0.10	0.04	0.08	0.04	0.04
H_2O	2.06	1.82	1.21	1.42	4.32	3.80	4.04	3.75	3.06	2.32
CO_2	0.82	0.50	0.40	0.52	3.11	1.32	3.05	2.84	1.62	2.14
Total	100.74	100.49	102.04	100.20	99.90	99.64	101.37	100.76	101.24	101.32
$Fe^*_2O_3$	2.61	3.26	4.30	3.46	3.82	3.47	2.21	3.01	3.73	4.76
Zr	310	258	173	205	186	211	173	216	227	164
Y	27	24	19	23	22	21	20	27	28	20
Sr	92	91	90	155	115	115	119	90	91	97
U	3	3	3	2	3	2	2	2	3	2
Rb	69	70	68	73	73	71	67	90	99	73
Th	7	6	4	5	6	5	6	7	10	6
Pb	16	17	13	15	17	17	14	21	22	15
Ga	9	8	9	9	9	8	9	14	14	11
Zn	46	45	38	57	49	47	47	62	54	48
Cu	2	4	7	8	8	3	5	6	5	13
Ni	17	20	20	22	20	17	19	22	15	15
Co	10	6	7	8	10	8	4	9	8	5
Cr	107	41	62	72	118	97	93	107	104	80
Ce	51	45	34	50	44	41	36	61	65	38
Ba	307	300	314	298	300	301	309	309	339	338
La	22	22	16	19	23	17	16	26	30	16
	K2 1.6b	K2 2.7b	K2 3.8b	K2 4.2b	K3 0.6b	K3 1.8b	K3 3.5b	K3 4.0b	K4 0.3b	K4 0.80b
SiO_2	71.86	78.51	73.20	72.38	68.33	77.09	66.87	67.87	67.92	72.85
TiO_2	0.82	0.54	0.51	0.54	0.88	0.79	0.65	0.57	0.74	0.72
Al_2O_3	11.95	8.90	8.51	9.22	13.90	10.65	10.65	9.71	10.79	10.57
Fe_2O_3	3.61	1.68	1.81	2.28	5.41	1.15	2.17	2.16	2.10	2.83
FeO	1.64	1.38	1.42	1.04	1.40	1.31	1.67	1.54	2.60	2.30
MnO	0.09	0.10	0.06	0.04	0.05	0.02	0.07	0.10	0.05	0.06
MgO	1.79	1.83	1.64	2.10	1.80	1.22	2.45	2.28	1.53	1.51
CaO	0.24	1.52	3.33	3.27	0.05	0.12	4.64	4.44	0.30	0.30
Na_2O	1.15	1.09	1.18	1.24	1.14	1.63	1.68	2.20	0.66	1.37
K_2O	2.50	2.10	2.04	2.16	2.53	2.28	2.25	2.15	2.33	2.30
P_2O_5	0.09	0.10	0.06	0.04	0.06	0.02	0.11	0.10	0.11	0.13
H_2O	2.54	1.87	4.86	4.86	3.24	3.07	3.66	2.44	2.30	3.20
CO_2	1.96	0.77	1.99	1.09	1.09	1.42	4.23	5.15	2.05	2.12
Total	100.23	100.34	100.63	100.32	99.88	100.77	101.10	100.76	99.70	100.26
$Fe^*_2O_3$	5.43	3.21	3.39	3.44	6.97	2.61	4.03	3.87	4.99	5.39
Zr	--	164	168	166	201	--	182	112	--	113
Y	--	20	20	20	27	--	23	30	--	37
Sr	--	97	122	121	84	--	139	153	--	102
U	--	2	2	3	5	--	4	2	--	4
Rb	--	73	72	77	109	--	90	164	--	184
Th	--	6	4	4	11	--	7	13	--	14
Pb	--	15	15	15	24	--	18	39	--	39
Ga	--	11	10	9	16	--	14	22	--	25
Zn	--	48	51	51	74	--	64	132	--	171
Cu	--	13	6	8	9	--	11	74	--	98
Ni	--	15	19	24	29	--	29	59	--	56
Co	--	5	7	27	14	--	10	27	--	24
Cr	--	80	93	98	114	--	103	121	--	143
Ce	--	38	44	71	61	--	51	81	--	94
Ba	--	313	300	340	359	--	320	392	--	364
La	--	16	17	34	30	--	22	42	--	44

Continued

Table 9.6 continued

	K4 1.6b	K4 2.1b	N5 0.5b	N5 1.2b	N5 2.1b	N5 3.0b	N5 3.6b	N5 3.9b	N5 4.4b	N5 4.7b
SiO_2	61.45	61.99	75.76	73.32	71.19	76.52	76.80	75.20	70.92	76.92
TiO_2	0.72	0.83	0.70	0.75	0.78	0.74	0.55	0.49	0.56	0.56
Al_2O_3	10.57	13.93	11.05	12.28	12.49	11.19	9.08	8.72	10.18	7.15
Fe_2C_3	4.10	4.44	2.65	2.84	3.44	2.68	2.08	1.72	2.28	5.26
FeO	2.04	2.16	1.32	1.40	1.56	1.13	2.17	1.45	2.17	0.94
MnO	0.12	0.21	0.01	0.05	0.07	0.04	0.09	0.07	0.09	0.04
MgO	3.20	2.19	1.56	1.78	1.77	1.67	1.60	1.80	1.51	1.15
CaO	1.20	0.25	0.27	0.29	0.26	0.28	1.51	1.58	1.91	0.36
Na_2O	1.08	1.36	1.32	0.86	0.99	1.16	0.90	1.30	0.97	0.92
K_2O	2.92	2.79	2.34	2.49	2.40	2.20	2.44	2.19	2.54	1.96
P_2O_5	0.12	0.07	0.07	0.07	0.11	0.09	0.07	0.09	0.05	0.12
H_2O	3.92	4.80	2.63	2.88	2.81	2.71	2.91	2.53	3.11	3.62
CO_2	4.55	5.45	1.11	1.05	2.32	1.57	1.73	2.57	2.43	1.04
Total	99.46	100.28	100.79	100.06	100.20	101.98	101.76	99.71	98.72	100.40
$Fe^*_2O_3$	6.37	6.84	4.12	4.40	5.17	3.94	4.49	3.33	4.69	6.30
Zr	--	171	174	190	191	188	156	162	162	174
Y	--	29	19	24	33	22	19	20	23	18
Sr	--	93	89	93	95	90	103	103	109	99
U	--	4	3	2	4	2	2	2	1	2
Rb	--	127	87	104	102	98	85	81	94	67
Th	--	11	6	9	8	7	5	2	7	3
Pb	--	25	21	23	25	17	14	15	21	17
Ga	--	17	13	14	15	13	11	10	13	7
Zn	--	89	54	69	81	59	55	57	70	40
Cu	--	15	12	7	11	7	8	8	14	12
Ni	--	39	19	34	36	25	22	26	32	17
Co	--	14	7	12	18	9	7	10	11	10
Cr	--	116	83	98	104	86	96	77	110	78
Ce	--	75	47	55	71	52	41	48	57	40
Ba	--	355	333	350	350	329	307	307	350	321
La	--	32	23	24	29	20	17	22	25	19

	N5 5.1b	N5 6.2b	N5 7.1b	SK 0.6b	SK 1.2b	SK 2.1b	SK 2.9b	BB 0.7b	BB 1.3b	BB 2.0b
SiO_2	78.02	78.47	75.60	70.12	82.75	79.75	84.15	77.00	84.95	81.95
TiO_2	0.47	0.37	0.40	0.83	0.43	0.39	0.40	0.57	0.38	0.44
Al_2O_3	8.75	6.85	7.07	14.65	6.97	7.17	6.46	9.83	6.71	7.63
Fe_2O_3	1.49	1.48	1.00	2.95	1.91	1.59	1.26	1.29	2.02	2.21
FeO	1.11	1.66	1.21	1.23	1.04	1.62	0.94	1.81	1.31	1.04
MnO	0.04	0.04	0.06	0.06	0.13	0.06	0.13	0.03	0.28	0.07
MgO	1.38	1.13	1.60	1.72	0.84	0.51	0.76	0.98	0.70	0.90
CaO	0.25	3.00	3.77	019	0.32	0.92	0.28	0.20	0.21	0.28
Na_2O	0.92	1.01	0.75	0.96	0.86	0.92	0.94	0.60	0.74	0.79
K_2O	2.17	1.94	1.90	2.66	1.77	1.79	1.76	2.02	1.67	1.74
P_2O_5	0.08	0.07	0.07	0.05	0.05	0.21	0.07	0.05	0.08	0.13
H_2O	2.55	2.74	1.74	2.20	1.30	2.84	1.10	3.94	0.90	1.95
CO_2	1.95	2.26	3.99	3.00	2.14	3.08	2.30	2.10	0.41	1.04
Total	99.18	101.02	99.16	100.62	100.51	100.85	100.55	100.42	100.35	100.35
$Fe^*_2O_3$	2.72	3.32	2.34	4.32	3.07	3.39	2.30	3.30	3.47	3.37
Zr	125	143	139	167	145	215	203	124	--	--
Y	63	14	16	24	18	16	15	36	--	--
Sr	118	113	130	91	82	88	83	72	--	--
U	3	2	1	1	2	2	2	3	--	--
Rb	182	66	66	74	59	59	58	83	--	--
Th	18	4	4	5	4	3	3	9	--	--
Pb	46	15	13	16	11	14	13	22	--	--
Ga	25	8	8	12	8	7	5	0	--	--
Zn	186	36	38	42	39	29	27	68	--	--
Cu	374	19	6	6	6	4	0	51	--	--
Ni	63	19	14	19	14	10	13	36	--	--
Co	20	2	1	6	6	1	4	12	--	--
Cr	144	66	55	104	132	192	59	89	--	--
Ce	130	38	35	55	33	31	36	76	--	--
Ba	336	289	290	446	526	377	366	502	--	--
La	70	15	16	26	15	13	10	38	--	--

Table 9.7 Major and trace elements analyses of the present-day intertidal sediments (bulk samples) from three of the studied areas (Dp, Dalbeattie area; Kp, Kirkcudbright area; Np, New Abbey area)

	Dp 1-2b	Dp 1-3b	Dp 1-4b	Dp 1-5b	Dp 1-6b	Dp 1-7b	Dp 1-8b	Dp 2-1b	Dp 2-2b	Dp 2-3b
SiO_2	75.04	74.71	72.12	73.90	78.37	79.08	79.04	71.40	65.94	68.52
TiO_2	0.65	0.58	0.53	0.49	0.52	0.64	0.53	0.50	0.55	0.56
Al_2O_3	7.17	7.04	7.75	7.04	6.20	5.92	5.89	7.68	8.00	8.07
Fe_2O_3	1.51	1.30	1.85	1.17	0.71	1.04	1.02	1.96	2.41	1.84
FeO	1.10	1.20	1.09	1.22	1.31	1.06	0.96	1.04	1.04	1.33
MnO	0.08	0.08	0.09	0.09	0.07	0.08	0.08	0.12	0.00	0.07
MgO	1.75	1.62	1.73	1.50	1.45	1.38	1.41	1.82	1.94	1.60
CaO	3.57	3.56	3.78	3.54	3.14	3.20	3.10	4.05	4.10	3.57
Na_2O	1.70	2.42	2.07	1.53	2.23	1.43	2.81	1.82	1.99	2.35
K_2O	1.72	1.77	1.86	1.69	1.69	1.58	1.72	1.87	1.93	1.79
P_2O_5	0.12	0.12	0.11	0.10	0.11	0.12	0.11	0.12	0.41	0.12
H_2O	1.77	2.16	2.17	2.34	1.18	1.87	0.80	2.77	3.95	3.51
CO_2	4.65	3.08	2.18	4.75	3.96	2.84	3.22	5.68	6.09	5.84
Total	100.83	99.64	97.33	99.36	99.94	100.23	99.69	100.79	98.49	99.10
$Fe^*_2O_3$	2.73	2.63	3.06	2.53	2.17	2.22	2.09	3.12	3.57	3.32
Zr	411	355	230	219	293	393	199	--	--	124
Y	27	24	22	19	19	23	23	--	--	33
Sr	138	139	139	138	120	117	165	--	--	200
U	3	4	3	2	2	2	2	--	--	3
Rb	58	58	64	57	52	49	74	--	--	124
Th	7	7	4	4	2	2	5	--	--	9
Pb	31	33	37	26	22	19	50	--	--	104
Ga	6	7	9	7	5	6	10	--	--	18
Zn	61	62	74	54	45	41	103	--	--	228
Cu	8	8	7	8	6	2	17	--	--	116
Ni	13	13	20	12	8	7	23	--	--	44
Co	2	9	6	8	1	3	10	--	--	21
Cr	99	95	87	180	72	87	106	--	--	123
Ce	49	42	41	37	30	38	47	--	--	77
Ba	305	301	312	289	286	272	317	--	--	357
La	17	21	19	16	19	14	21	--	--	40

	Dp 2-4b	Kp 1-1b	Kp 1-3b	Kp 1-4b	Kp 1-5b	Kp 2-1b	Kp 2-2b	Kp 2-3b	Kp 2-4b	Kp 3-1b
SiO_2	72.12	65.03	67.42	66.89	72.30	65.35	69.21	69.04	68.09	75.03
TiO_2	0.53	0.65	0.62	0.60	0.54	0.62	0.60	0.60	0.60	0.57
Al_2O_3	7.75	10.00	9.04	9.48	7.55	9.01	8.70	8.93	9.55	7.13
Fe_2O_3	1.85	2.78	2.32	1.69	1.51	1.86	1.79	2.00	2.09	1.43
FeO	1.09	1.56	1.46	2.05	1.12	2.04	1.63	1.15	1.61	1.11
MnO	0.09	0.10	0.11	0.15	0.08	0.13	0.09	0.01	0.09	0.08
MgO	1.73	2.40	1.94	2.08	1.59	2.27	1.81	1.97	2.15	1.58
CaO	3.78	3.34	3.83	4.13	3.67	3.79	3.67	3.85	3.84	3.42
Na_2O	2.07	0.96	1.85	1.16	1.30	1.15	1.02	1.20	1.27	1.02
K_2O	1.86	2.26	2.09	2.03	1.82	2.08	1.94	2.00	2.06	2.64
P_2O_5	0.11	0.14	0.14	0.16	0.12	0.17	0.15	0.15	0.15	0.13
H_2O	2.17	4.37	3.78	4.32	3.73	3.35	3.57	3.06	2.64	2.04
CO_2	2.18	5.82	5.16	5.87	5.14	8.81	8.33	6.23	4.80	5.46
Total	100.24	99.41	99.76	100.61	100.61	100.47	100.51	100.19	98.94	100.76
$Fe^*_2O_3$	2.61	4.51	3.94	3.97	2.75	4.13	3.60	3.28	3.88	2.66
Zr	135	--	--	222	284	221	255	--	246	347
Y	31	--	--	26	20	26	24	--	25	23
Sr	212	--	--	161	142	149	146	--	153	134
U	1	--	--	2	2	3	3	--	2	3
Rb	121	--	--	80	62	83	72	--	74	60
Th	8	--	--	5	5	7	6	--	3	4
Pb	121	--	--	54	27	57	45	--	44	28
Ga	19	--	--	10	8	11	9	--	10	7
Zn	239	--	--	154	82	144	120	--	128	70
Cu	181	--	--	17	6	17	12	--	15	4
Ni	44	--	--	27	18	32	22	--	22	14
Co	19	--	--	13	9	10	10	--	11	6
Cr	119	--	--	96	94	97	106	--	89	88
Ce	82	--	--	54	43	57	47	--	55	45
Ba	360	--	--	322	291	334	317	--	317	301
La	37	--	--	24	14	29	21	--	28	14

Continued

Table 9.7 continued

	Kp 3-2b	Kp 3-4b	Kp 4-3b	Np 1-1b	Np 1-2b	Np 1-3b	Np 1-4b
SiO_2	75.11	75.00	74.13	74.09	77.85	75.58	74.32
TiO_2	0.52	0.47	0.47	0.50	0.49	0.52	0.54
Al_2O_3	7.39	7.08	7.27	7.86	7.01	7.64	8.33
Fe_2O_3	1.30	1.65	1.54	1.76	1.60	2.20	2.59
FeO	1.40	0.94	0.92	1.00	1.09	1.50	1.30
MnO	0.07	0.07	0.08	0.08	0.06	0.08	0.09
MgO	1.55	1.65	1.45	1.60	1.42	1.46	1.56
CaO	3.16	3.61	3.45	3.10	2.68	3.06	3.15
Na_2O	1.27	1.60	1.18	1.43	1.30	1.13	1.02
K_2O	1.82	1.82	1.84	1.83	1.81	1.80	1.82
P_2O_5	0.12	0.11	0.01	0.09	0.11	0.12	0.12
H_2O	2.14	2.45	2.26	2.47	1.95	2.07	2.18
CO_2	5.52	4.11	5.77	4.45	3.00	4.04	4.40
Total	101.37	100.56	100.56	100.26	100.37	101.34	100.83
Fe^*2O_3	2.86	2.69	2.56	2.87	2.81	3.87	4.03
Zr	273	--	223	189	308	--	113
Y	20	--	19	19	20	--	31
Sr	133	--	145	127	116	--	202
U	3	--	3	1	3	--	3
Rb	59	--	61	63	59	--	134
Th	4	--	4	3	3	--	8
Pb	30	--	27	19	35	--	114
Ga	6	--	9	8	8	--	19
Zn	68	--	74	46	63	--	251
Cu	5	--	8	5	9	--	139
Ni	12	--	14	19	13	--	49
Co	6	--	7	4	7	--	22
Cr	66	--	62	70	83	--	126
Ce	41	--	40	39	38	--	75
Ba	291	--	299	267	302	--	330
La	17	--	16	18	18	--	42

Table 9.8 Major and trace elements analyses of clay fraction samples of the Holocene raised coastal sediments from the various areas studied (D2 to D10, Dalbeattie area; K1 to K4, Kirkcudbright area; N5, New Abbey area; SK and BB, Lochar Gulf area) and five selected samples from two areas of the present-day intertidal sediments (Dp, Dalbeattie area; Kp, Kirkcudbright area)

	D2 1.10	D2 2.50	D2 2.70	D3 1.40	D3 1.90	D4 0.50	D4 1.20	D4 2.10	D4 2.90	D5 0.70
SiO_2	47.91	50.40	50.67	49.18	50.17	50.39	50.11	48.50	53.53	60.60
TiO_2	0.74	0.81	0.77	0.73	0.69	0.88	0.95	0.85	0.92	0.98
Al_2O_3	22.00	23.63	22.63	22.53	22.84	21.70	21.80	21.48	18.96	17.85
Fe_2O_3	8.81	6.06	4.87	9.24	7.59	6.80	7.12	10.24	4.16	3.52
FeO	1.76	1.95	1.44	1.12	1.57	1.62	1.30	1.45	2.30	1.82
MnO	0.04	0.03	0.04	0.04	0.06	0.11	0.10	0.18	0.07	0.06
MgO	3.95	3.00	2.92	3.30	3.65	3.21	3.35	3.47	3.83	2.64
CaO	0.38	0.32	0.35	0.36	0.40	0.52	0.26	0.42	2.09	0.34
Na_2O	0.52	0.13	0.64	0.89	0.68	0.23	0.48	0.45	0.44	0.91
K_2O	4.09	4.68	3.60	4.12	4.48	3.87	4.06	4.07	3.61	3.50
P_2O_5	0.18	0.17	0.27	0.19	0.25	0.11	0.13	0.22	0.16	0.14
H_2O	6.32	4.99	8.14	4.26	4.31	7.09	8.61	7.34	6.02	5.15
CO_2	3.74	2.73	3.18	1.84	2.74	3.08	1.52	2.72	4.39	2.90
Total	100.44	98.93	99.63	97.80	99.43	99.61	99.80	101.39	100.48	100.41
$Fe^*_2O_3$	10.77	8.26	6.47	10.48	9.33	8.60	8.56	11.85	6.72	5.54
Zr	--	121	--	--	--	122	125	120	139	144
Y	--	37	--	--	--	21	40	37	33	32
Sr	--	102	--	--	--	110	111	109	121	102
U	--	5	--	--	--	4	4	3	4	3
Rb	--	214	--	--	--	192	201	191	167	162
Th	--	16	--	--	--	13	13	16	10	12
Pb	--	42	--	--	--	35	37	49	34	30
Ga	--	30	--	--	--	28	28	28	23	21
Zn	--	147	--	--	--	160	140	158	123	114
Cu	--	139	--	--	--	104	50	93	57	66
Ni	--	58	--	--	--	58	63	83	60	41
Co	--	23	--	--	--	29	20	36	23	19
Cr	--	152	--	--	--	157	153	152	139	118
Ce	--	112	--	--	--	77	112	111	98	82
Ba	--	416	--	--	--	438	432	375	432	432
La	--	26	--	--	--	38	59	51	52	37

	D6 0.50	D6 1.70	D6 2.60	D7 0.40	D7 1.60	D7 2.25	D7 3.70	D8 0.40	D8 1.40	D8 2.00
SiO_2	45.95	49.45	50.77	47.83	49.17	50.77	49.85	50.34	48.00	51.67
TiO_2	0.86	0.72	0.63	0.91	0.73	0.82	0.77	0.91	0.79	0.95
Al_2O_3	23.36	22.57	21.44	22.75	22.41	23.31	21.54	23.35	23.48	22.22
Fe_2O_3	5.17	5.46	5.47	5.03	8.33	8.61	7.34	7.66	8.34	6.63
FeO	1.38	1.65	2.23	1.67	1.45	1.61	1.96	2.04	1.97	1.79
MnO	0.01	0.05	0.04	0.02	0.02	0.05	0.08	0.04	0.09	0.17
MgO	3.06	3.27	3.10	2.40	3.17	3.47	4.27	2.77	3.35	3.90
CaO	0.84	0.55	0.20	0.51	0.34	0.33	1.14	0.28	0.27	0.40
Na_2O	1.04	1.32	1.20	0.27	0.65	0.50	0.24	0.01	0.20	0.28
K_2O	3.85	4.04	3.98	3.94	4.01	4.32	4.25	3.61	4.03	4.27
P_2O_5	0.08	0.14	0.12	0.19	0.18	0.33	0.16	0.11	0.18	0.14
H_2O	7.94	4.89	6.00	10.42	7.34	4.25	6.30	6.54	6.98	5.16
CO_2	6.55	5.33	2.79	5.18	3.01	1.82	2.20	2.21	2.82	2.09
Total	100.09	99.44	97.97	101.12	100.81	100.19	100.10	99.87	100.50	99.67
$Fe^*_2O_3$	6.70	7.29	7.95	6.89	9.94	10.40	9.52	9.93	10.53	8.62
Zr	--	124	106	119	127	--	--	117	--	--
Y	--	29	53	32	37	--	--	23	--	--
Sr	--	93	79	101	105	--	--	99	--	--
U	--	3	4	2	2	--	--	4	--	--
Rb	--	210	179	198	200	--	--	179	--	--
Th	--	15	16	14	18	--	--	12	--	--
Pb	--	51	41	58	55	--	--	42	--	--
Ga	--	30	26	29	28	--	--	27	--	--
Zn	--	236	322	146	162	--	--	118	--	--
Cu	--	248	869	212	183	--	--	107	--	--
Ni	--	43	56	65	67	--	--	53	--	--
Co	--	16	22	26	24	--	--	19	--	--
Cr	--	146	132	163	162	--	--	144	--	--
Ce	--	88	109	101	110	--	--	82	--	--
Ba	--	356	317	400	416	--	--	407	--	--
La	--	45	58	52	56	--	--	35	--	--

Continued

Table 9.8 continued

	D8	D9	D9	D9	D10	D10	K1	K2	K2	K3
	2.70	0.40	1.06	1.56	0.55	3.03	1.60	3.10	3.80	3.50
SiO_2	51.47	49.35	49.66	59.04	50.05	51.19	48.40	54.11	50.42	48.08
TiO_2	0.90	0.89	0.88	0.90	0.78	0.73	0.86	0.77	0.87	0.77
Al_2O_3	20.85	22.05	22.79	18.88	21.35	22.95	20.78	16.42	22.93	20.90
Fe_2O_3	7.81	7.31	7.99	5.69	5.95	5.82	9.21	4.24	8.52	4.88
FeO	1.89	2.14	2.44	1.86	1.44	1.86	2.89	1.94	2.24	2.50
MnO	0.19	0.06	0.05	0.04	0.03	0.09	0.13	0.07	0.06	0.05
MgO	3.79	3.12	3.06	2.73	2.90	4.05	3.65	3.50	3.15	4.00
CaO	0.78	0.61	0.41	0.26	1.50	2.31	0.52	3.44	0.16	2.90
Na_2O	0.49	0.17	0.58	0.62	0.87	0.97	0.07	1.40	0.15	1.03
K_2O	4.04	3.88	4.01	3.59	3.10	3.90	3.25	3.83	3.96	3.38
P_2O_5	0.20	0.13	1.16	0.14	0.15	0.15	0.22	0.13	0.09	0.11
H_2O	5.34	7.62	6.12	4.72	8.76	3.87	6.42	6.32	6.00	6.76
CO_2	2.48	3.01	2.04	1.50	3.24	2.14	2.88	2.94	1.93	3.78
Total	100.23	100.34	101.19	99.97	100.12	100.03	99.68	98.53	100.35	99.73
$Fe^*_2O_3$	9.91	9.69	10.70	7.76	7.55	7.89	12.42	6.40	11.01	7.66
Zr	125	122	--	--	--	125	--	123	119	117
Y	32	21	--	--	--	31	--	27	46	29
Sr	113	120	--	--	--	131	--	141	100	136
U	3	5	--	--	--	5	--	4	4	4
Rb	185	190	--	--	--	171	--	133	194	184
Ni	13	12	--	--	--	12	--	9	13	13
Th	33	40	--	--	--	35	--	26	44	29
Pb	26	30	--	--	--	23	--	20	29	26
Zn	135	111	--	--	--	141	--	120	195	148
Cu	59	77	--	--	--	80	--	74	130	120
Ni	61	52	--	--	--	61	--	47	62	64
Co	27	16	--	--	--	20	--	27	35	23
Cr	139	146	--	--	--	139	--	98	168	136
Ce	91	81	--	--	--	95	--	71	168	84
Ba	407	443	--	--	--	368	--	340	402	426
La	45	46	--	--	--	41	--	34	56	42

	K3	K4	N5	N5	SK	BB	BB	Dp	Dp	Dp
	4.00	0.30	3.00	4.40	0.60	0.70	1.30	1-1	2-2	2-3
SiO_2	49.42	46.35	47.05	56.22	47.84	48.47	57.80	50.77	57.69	49.64
TiO_2	0.77	0.77	0.70	0.87	0.68	0.71	0.87	0.68	0.71	0.65
Al_2O_3	18.89	19.90	20.70	18.51	22.03	22.68	18.83	14.99	14.10	15.35
Fe_2O_3	4.96	11.45	6.03	6.64	5.77	7.45	4.54	5.02	1.84	2.12
FeO	2.14	2.40	2.34	2.03	3.66	1.48	1.90	2.02	1.84	2.12
MnO	0.15	0.06	0.07	0.06	0.08	0.03	0.05	0.22	0.17	0.15
MgO	3.59	3.52	3.35	2.99	4.58	3.20	2.97	1.45	2.85	3.30
CaO	3.58	0.20	1.80	0.90	0.46	0.59	0.44	3.50	4.62	2.88
Na_2O	0.96	1.33	1.90	0.82	1.01	1.15	0.79	1.09	1.87	1.34
K_2O	3.38	3.66	3.71	3.39	4.50	4.01	3.65	2.85	2.44	3.56
P_2O_5	0.14	0.21	0.06	0.12	0.09	0.09	0.17	0.09	0.15	0.23
H_2O	7.39	4.00	8.06	5.30	6.02	8.98	5.34	8.04	3.15	7.12
CO_2	4.62	6.10	3.84	3.00	2.30	3.74	2.15	8.05	6.10	9.19
Total	99.80	99.95	99.61	102.58	100.02	102.58	99.50	98.77	99.19	99.37
$Fe^*_2O_3$	7.34	14.12	8.63	8.90	9.84	9.09	6.65	5.54	6.40	6.40
Zr	--	106	141	110	145	--	142	144	--	--
Y	--	33	33	38	41	--	33	32	--	--
Sr	--	98	105	95	101	--	104	102	--	--
U	--	6	4	4	3	--	3	3	--	--
Rb	--	178	156	159	202	--	171	162	--	--
Th	--	14	11	14	13	--	13	12	--	--
Pb	--	43	40	52	38	--	40	30	--	--
Ga	--	24	24	23	23	--	24	21	--	--
Zn	--	187	136	191	159	--	154	114	--	--
Cu	--	102	122	17	169	--	161	66	--	--
Ni	--	53	55	64	128	--	60	66	--	--
Co	--	24	23	31	38	--	19	19	--	--
Cr	--	150	138	142	182	--	139	118	--	--
Ce	--	95	94	106	119	--	96	82	--	--
Ba	--	366	405	298	492	--	441	432	--	--
La	--	49	44	53	52	--	45	37	--	--

Continued

Table 9.8 continued

	Kp 1-1	Kp 2-4
SiO_2	49.48	47.99
TiO_2	0.76	0.65
Al_2O_3	19.03	17.78
Fe_2O_3	3.58	4.95
FeO	2.60	2.56
MnO	0.17	0.15
MgO	3.44	3.46
CaO	3.37	3.32
Na_2O	1.10	1.59
K_2O	3.36	3.13
P_2O_5	0.12	0.09
H_2O	4.18	7.23
CO_2	6.94	4.65
Total	98.42	99.96
$Fe^*_2O_3$	6.47	7.79
Zr	--	--
Y	--	--
Sr	--	--
U	--	--
Rb	--	--
Th	--	--
Pb	--	--
Ga	--	--
Zn	--	--
Cu	--	--
Ni	--	--
Co	--	--
Ce	--	--
Ba	--	--
La	--	--

PART IV

PALAEOENVIRONMENTS AND PROVENANCES

CHAPTER 10

SEDIMENTARY ENVIRONMENTS REPRESENTED BY THE HOLOCENE RAISED COASTAL SEDIMENTS

10.1 Introduction

Recognition of the presence of a number of distinct facies within the Holocene sediments of the Dalbeattie, Kirkcudbright and New Abbey areas (Chapter 5) prompts an attempt to identify the environments in which each of these facies was deposited. The relationships between tide-influenced sedimentary environments and facies have been considered by many authors, for example in Britain by Evans (1965), Greensmith & Tucker (1973; 1976) and Griffiths (1988), and elsewhere in a number of papers contained in a publication by de Boer et al. (1988) and in a paper by Frey & Howard (1988).

In this study, identification of the sedimentary environments is based on combinations of the following criteria, characteristics and procedural techniques, all of which may not be present or applicable in the case of any individual sedimentary facies:

1) Sedimentary structures, e.g. cross-stratification, rhythmic interlaminations.

2) Shape and location of the sedimentary body in relation to the position of the contemporaneous shoreline.

3) Lateral and vertical variations in the individual sedimentary units.

4) Correlation of similar sedimentary units, to determine the lateral and vertical continuity of the combined unit.

5) Presence and abundance of plant debris within a sedimentary unit.

6) Comparison of present-day intertidal sediments of known environments with Holocene sediments that possess similar characteristics, on the basis of (a) grain-size analysis, (b) clay-mineralogical analysis and (c) geochemical analysis.

Identification of the environments of deposition represented by the Holocene sediments of the area of the former Lochar Gulf has not been attempted in the course of this project for the following reasons:

1) Much of the surface of the former 'gulf' is covered by a thick layer of peat.

2) Only the upper part of the inorganic sediments is exposed or has been sampled in the course of this project.

3) Only limited data, from widely scattered locations, are available.

10.2 Holocene environments of the Dalbeattie area

As discussed in Chapters 4 and 5, and summarised in Table 5.1, the Holocene inorganic raised coastal deposits of the Dalbeattie area may be subdivided into three main sedimentary facies, those designated A, E and F. Facies E, consisting of grey to black clays, rich in plant debris, is thought to have been deposited in a coastal marsh or lake environment. The sediments of facies F, comprising marine-deposited gravel and sand, are regarded as beach deposits that accumulated on at least two different occasions when storm conditions prevailed.

Facies A, consisting mainly of silt grade clastic material, together with variable proportions of clay and fine sand, is thought to represent a complex of environments which were located close to high water mark. The differentiation of these environments is difficult solely on the basis of the few sedimentary structures that were observed in the deposits and on the geometry of the sedimentary bodies. On the basis of the

dominance of the clay, silt and fine sand fractions and by comparison with the characteristics of the present-day sediments (Chapter 5.2), three sub-facies, Aa, Ab and Ac, may be recognised (Fig. 10.1). The lowermost sub-facies, Aa, is a pale grey-blue clayey silt which, in places (e.g. in an exposure in the western bank of the Urr Water at site D7), shows interlamination of silt and clay. It is suggested that this sub-facies was deposited in a marsh environment, similar to the present-day salt marsh, which was covered by marine waters at times of spring high tides. Sub-facies Ab consists of grey to blue clayey silt with fine sand and rare remains of microfauna, e.g. foraminifers and ostracods. In view of its resemblance to the upper part of the present-day intertidal sediments, it is suggested that the environment of deposition of sub-facies Ab was that of high tidal-flats. The uppermost sub-facies, Ac, comprises brown to grey clayey silt with pieces of plant debris. No traces of lamination were observed in this sub-facies, but in other respects the sediments resemble those of sub-facies Aa. It is therefore tentatively suggested that sub-facies Ac was deposited in the *very* high tidal-flat or supra-tidal environment, similar to that of the present-day salt marsh. Clay mineralogical and geochemical studies (Chapters 8 and 9, above) showed no significant differences in the clay mineral and geochemical content of the three sub-facies of facies A.

At the base of one bore-hole through facies A in the Dalbeattie area (bore-hole D9, cf. Chapter 4.2.1; see also Fig. 10.2) a layer of fine sand with silt, and rich in foraminifers and ostracods, was encountered. As noted in Chapter 4, this deposit resembles the present-day intermediate to low intertidal deposits of the Dalbeattie area. The suggested environment of accumulation of this sediment is therefore the intermediate to low intertidal flat (Chapter 5.2.1). Geochemical analysis of this

deposit showed a high percentage of SiO_2 in comparison with other oxides. The concentration of trace elements was lower than in the (finer-grained) sediments of facies A. It should be noted that this deposit probably is the equivalent of facies D (Table 5.1), which was identified much more extensively in the Kirkcudbright, New Abbey and Lochar Gulf areas.

Geochemical and clay mineralogical analyses of sediments of facies E, represented by samples from bore-hole D5 (Fig. 4.3) gave the following results. The percentage of SiO_2 in these clays is lower than that in the sediments of facies A, the content of other oxides accordingly being higher. The concentration of trace elements is relatively high in the marsh/lake deposits of facies E. Illite is the most abundant clay mineral in this facies.

The mean grain size, clay mineralogy, geochemical content and suggested environments of deposition of the Holocene sedimentary facies identified in the Dalbeattie area are summarised in Table 10.1. The suggested stratigraphical and environmental relationships of the facies are shown in Figure 10.3.

10.3 Holocene environments of the Kirkcudbright area

The Holocene sediments of the Kirkcudbright area represent three main environments of deposition, as follows.

The intertidal mud- and sand-flat environment is represented by facies D (Table 5.1), which is composed of fine sand with coarse silt and a low percentage of clay, and contains a rich microfauna of foraminifers and ostracods together with macrofauna, such as molluscan valves. This sedimentary facies resembles the sediments of the present-day intermediate to low intertidal flats of the Kirkcudbright

area (and Dalbeattie and New Abbey areas) in its textural characteristics, clay mineralogical and geochemical composition and faunal content.

In two of the sections studied in the Kirkcudbright area, facies D sediments were overlain by those of facies B (Table 5.1), which comprises inter-laminated fine sand and silt containing plant debris and occasional to rare remains of foraminifers and ostracods. The sand laminae vary from very fine to fine sand in size grade, are rich in mica flakes and are variable in thickness. Occasionally, very thin laminae are present. When compared with the present-day sediments, facies B resembles both tidal-creek and salt marsh deposits in being laminated (cf. Chapter 5.2.2 and 5.2.3). Because of its faunal content and the size grade of its sediments, this facies probably did not accumulate in a salt marsh environment. It is suggested tentatively, however, that facies B represents intermediate to high tidal-flats.

The major part of the Holocene deposits of the Kirkcudbright area consists of sediments of facies A (Table 5.1). In this area, these sediments are composed mainly of pink grey to dark grey clayey silt with variable proportions of fine sand and clay, and they are rich in mica flakes. Echinoid spines and sponge spicules are present in moderate amounts, but remains of foraminifers and ostracods are rare.

Three superimposed sub-facies of facies A are illustrated diagrammatically in Figure 10.4. The lowermost sub-facies, Aa, is composed mainly of pale to dark grey clayey silt with included fragments of wood, rare echinoid spines and sponge spicules. Mica flakes are uncommon in this sub-facies. As in the case of the Dalbeattie area, it is suggested that this sub-facies accumulated in a salt marsh environment, covered by marine waters at times of spring high tides. The overlying sub-facies, Ab, pink-coloured clayey silt with fine sand, rich in mica flakes and plant debris, and with rare sponge spicules, may have been deposited in the high tidal-flat environment. The

uppermost sub-facies, Ac, is composed of pink to brown to grey clayey silt, and penetrated by root channels. As discussed in relation to the Dalbeattie area, it is tentatively suggested that sub-facies Ac was deposited in the *very* high tidal flat or even supra-tidal environment, similar to that of the present-day salt marsh.

Details of the grain-size, clay mineralogical and geochemical composition of the three major Holocene facies (D, B and A) identified in the Kirkcudbright area are shown in Table 10.2, from which the following conclusions may be drawn. The succession shows a fining-upwards trend. The percentage of illite decreases upwards from the intertidal environment at the base to the supratidal environment at the top, whilst vermiculite and mixed-layer clay minerals show an inverse trend to that of illite. Kaolinite and chlorite show no trend related to inferred changes in environment.

Geochemically, the abundance of Al_2O_3 and of K_2O increases from the intertidal environment (at the base of the succession) to the supratidal environment (at the top). In contrast, the CaO content decreases upwards between facies D and sub-facies Aa. This may be related to the decrease in content of macro- and microfauna upwards through the succession. In general, the content of trace elements increases upwards.

The suggested stratigraphical and environmental relationships of the various Holocene sedimentary facies in the Kirkcudbright area are shown in Figure 10.5.

10.4 Holocene environments of the New Abbey area

Using comparison of the properties of the Holocene sediments and present-day sediments as a basis for environmental interpretation, and adopting the same degree of caution in cases of uncertainty as was adopted in 10.2 above, the Holocene sediments of

the New Abbey area appear to represent several environments of deposition, as follows.

The intermediate to low tidal-flat environment probably is represented by facies D (Table 5.1), which is composed of micaceous fine and very fine sand, coarse to fine silt and a low percentage of clay, and contains (unidentified) molluscan shell fragments, tests of foraminifers and ostracod valves. This sedimentary unit resembles the present-day intermediate to low intertidal surface sediments of the New Abbey area in textural characteristics and faunal content. Sedimentary structures appear to be few, but occasional laminae and ripples were observed. The microfaunal remains suggest a fully marine environment of deposition of this facies, and the broken nature of the macrofaunal remains indicates relatively strong current and wave action.

In vertical section N3 (Fig. 4.7) the sediments of facies D were underlain by lenses of pebbly coarse sand which, in the field, were interpreted as resulting from local deposition in intertidal creeks. Examination of the pebbly coarse sand in the laboratory showed that this deposit contains molluscan shell fragments and remains of foraminifers and ostracods, confirming that this sediment was deposited under marine conditions.

In two of the sections studied (N5 and N6, Fig. 4.7; see also Fig. 10.6), lenses of a brown coarse sand containing pebbles and cobbles, together with layers of alternating silt and clay, occurred near the base of the sections. The lenses cut into the underlying sediments of facies D (see Fig. 10.7). The pebbly sand contained no remains of marine fauna, but was rich in remains of land plants, including leaves and pieces of wood. This unit (facies C, Table 5.1), therefore, is interpreted as having been deposited in completely terrestrial conditions, perhaps as a fluvial channel-filling sediment.

In all the sections studied in the New Abbey area, a layer of inter-laminated fine

sand and silt, occasionally with thin laminae of clay, was observed. This sediment resembles the sediments of facies B of the Kirkcudbright area (Chapter 10.3, above) in composition and colour. It is tentatively interpreted, therefore, as having been deposited in the intermediate to high tidal-flat environment.

The uppermost part of the sedimentary succession in most parts of the New Abbey area is composed of clayey silt with fine sand (facies A, Table 5.1). This unit contains organic remains, the nature of which changes upwards, as does the colour from pale grey at the base, through grey, to brown at the top. The unit as a whole appears to lack traces of sedimentary structures, but a few laminae were seen to be present in the lowermost part of this facies.

As in the Dalbeattie and Kirkcudbright areas, three sub-facies of facies A are recognisable. The lowermost sub-facies, Aa, comprises dark grey clayey silt which may have been deposited in salt marsh conditions affected by marine waters during occasional high tides. Sub-facies Ab, of grey clayey silt with fine sand rich in mica flakes and with rare foraminifers and ostracods, may have been deposited as high tidal-flats. The topmost sub-facies, Ac, mostly brown in colour, and containing pieces of wood and other plant remains, rare sponge spicules and abundant mica flakes, may have been deposited in the *very* high tidal-flat or even the supratidal environment.

As discussed in Chapters 5 and 6, facies A is overlain in parts of the New Abbey area by ridges of coastal gravel and sand (facies F), which were deposited in conditions of exceptional storms and, therefore, represent the storm-beach environment.

Mineralogical and geochemical data for the various sedimentary facies and sub-facies and, accordingly, the various environments of deposition, are shown in Table 10.3.

The most abundant clay mineral is illite. It is more abundant in the

intermediate to low tidal-flat than in the intermediate to high tidal-flat and salt-marsh/supratidal sediments.

The geochemical data show greater contents of Al_2O_3 and $Fe^*_2O_3$ in the intermediate to high tidal-flat and salt-marsh/supratidal sediments than in the intermediate to low tidal-flat sediments. The CaO content is higher in the fossiliferous fine sand of facies D (intermediate to low tidal-flat) than in the overlying sediments of facies B and A, which may have been deposited in the intermediate to high tidal-flat and supratidal environments. Trace elements show a greater concentration in the intermediate to high tidal-flat and supratidal (finer-grained) sediments than in the intermediate to low intertidal (fossiliferous fine sand) sediments.

The suggested stratigraphical and environmental relationships of the facies are shown in Figure 10.7.

10.5 Succession of environments

Figures 10.2, 10.4 and 10.6 together with Figures 10.3, 10.5 and 10.7 show successions of environments in the Dalbeattie, Kirkcudbright and New Abbey areas based on the conclusions reached in Chapter 10.2, 10.3 and 10.4 above. In the Dalbeattie area, the sequence appears to begin with the intermediate to low tidal-flat environment (facies D) and is followed by the salt marsh (sub-facies Aa), high tidal-flat (sub-facies Ab) and *very* high intertidal to supratidal, i.e salt marsh, environments (sub-facies Ac). Surprisingly, the high tidal-flat environment appears to be missing between the intermediate to low and salt marsh environments.

In the Kirkcudbright area, the sequence is similar to that in the Dalbeattie area except that here the transition between intermediate to low tidal-flat environment

(facies D) and salt-marsh environment (sub-facies Aa) is represented by the intermediate to high tidal-flat sediments of facies B.

In the New Abbey area, the sequence appears to be similar to that in the Dalbeattie area except that in the former area the period of salt marsh formation (represented by sub-facies Aa) appears to have been interrupted by a local transgressive event during which facies B was deposited in intermediate to high tidal-flat conditions. The fluvial channel environment (facies C) identified in the New Abbey area (Fig. 10.6) is regarded as a local interruption between the intermediate to low tidal-flat (facies D) and salt-marsh (sub-facies Aa) environments.

The broad sequence present in all three areas may represent transgressive conditions (D) followed by minor regressive (Aa) and transgressive (Ab) conditions. A final regression may be represented by sub-facies Ac. Possible interpretations of the omission of the high intertidal environment between the intermediate to low and salt marsh environments in the Dalbeattie and New Abbey areas are either that transgression in these areas was rapid or that sediments originally deposited there were removed by erosion.

Facies	Lithological description	Environment of deposition
Ac	Brown to grey clayey silt with plant debris and oxidised root channels	? Supra-tidal (Salt marsh) or *very* high tidal-flat
Ab	Grey clayey silt with fine sand, rich in mica flakes, and with rare microfauna	High tidal-flat
Aa	Pale grey-blue clayey silt with mica flakes and plant	? Salt marsh

Figure 10.1 Sedimentary facies, lithological description and suggested environments of deposition, Holocene raised coastal sediments, section D2, Dalbeattie area.

Facies	Lithological description	Environment of deposition
Ac	Brown to grey clayey silt with plant debris and oxidised root channels	? Supra-tidal (Salt marsh) or *very* high tidal-flat
Ab	Grey clayey silt with fine sand, rich in mica flakes, and with rare microfauna	High tidal-flat
Aa	Pale grey-blue clayey silt with mica flakes and plant debris	? Salt marsh
D	Fossiliferous fine sand and silt with low percentage of clay	Intermediate to low tidal-flat

Figure 10.2 Sedimentary facies, lithological description and suggested environments of deposition, Holocene raised coastal sediments, section D9, Dalbeattie area.

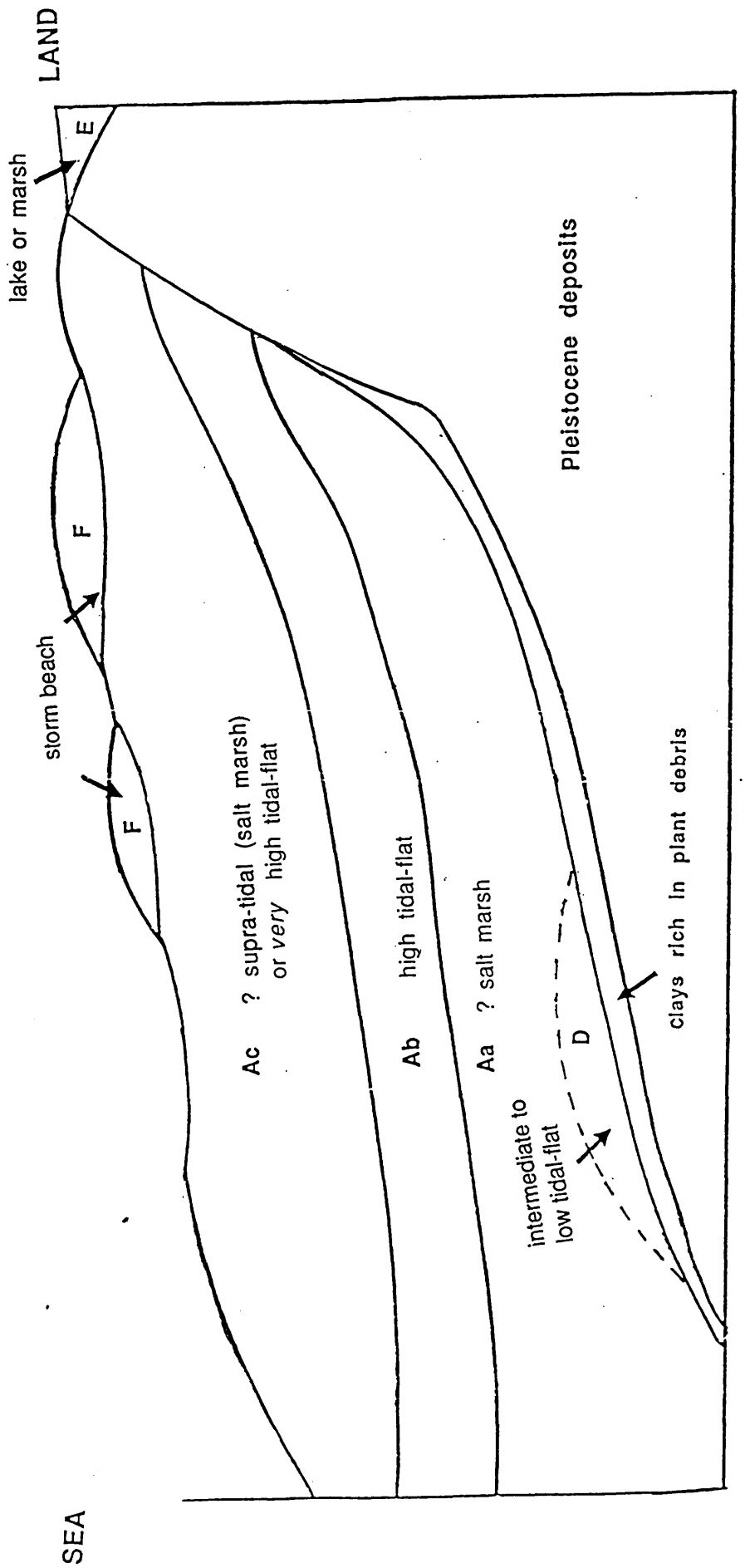

Figure 10.3 Diagrammatic representation of suggested stratigraphical and environmental relationships of the Holocene sedimentary facies (A, B, C, etc.) identified in the Dalbeattie area.

Ac, brown clayey silt
Ab, clayey silt with fine sand
Aa, grey clayey silt

D, fine sand, rich in microfauna
E, clays rich in plant debris
F, coastal gravel and sand

Facies	Lithological description	Environment of deposition
A c	Brown clayey silt, penetrated by root channels	? Supra-tidal (Salt marsh) or *very* high tidal-flat
A b	Pale pink clayey silt with fine sand, rich in mica flakes and plant debris, and with rare sponge spicules	High tidal-flat
A a	Pale to dark grey clayey silt rich in plant debris and with rare microfauna	? Salt marsh
B	Inter-laminated fine sand and silt, with occasional to rare microfauna	? Intermediate to high tidal-flat
D	Fossiliferous fine sand and silt with low percentage of clay	Intermediate to low tidal-flat

Figure10.4 Sedimentary facies, lithological description and suggested environments of deposition, Holocene raised coastal sediments, section K1, Kirkcudbright area.

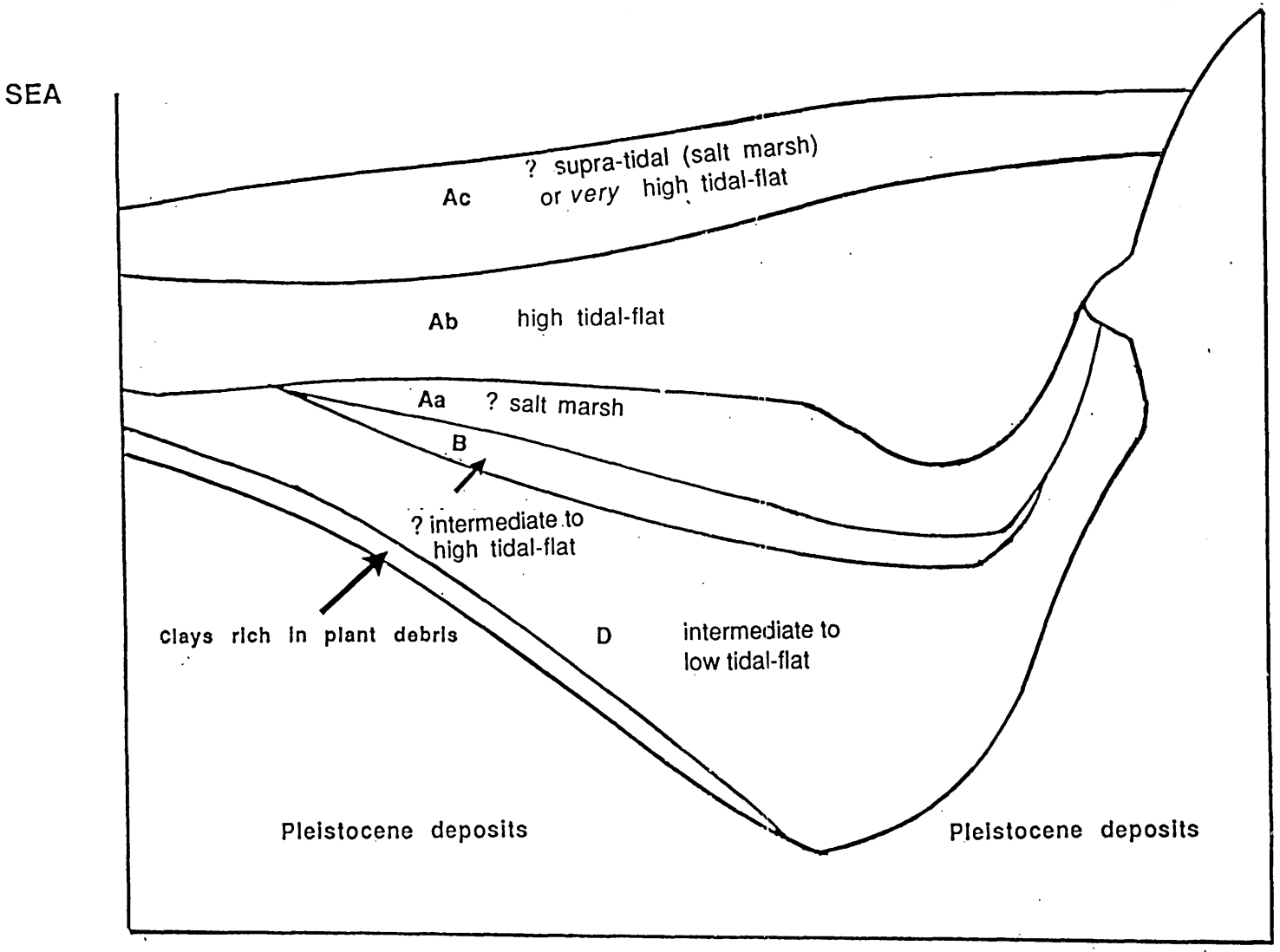

Figure 10.5 Diagrammatic representation of suggested stratigraphical and environmental relationships of the Holocene sedimentary facies (A, B, C, etc.) identified in the Kirkcudbright area.

Ac, brown clayey silt
Ab, clayey silt with fine sand
Aa, grey clayey silt
B, inter-laminated fine sand and silt
D, fine sand, rich in microfauna

Facies	Lithological description	Environment of deposition
Ac	Brown clayey silt with plant debris, and rare sponge spicules	? Supra-tidal (Salt marsh) or *very* high tidal-flat
A b	Grey clayey silt with fine sand, rich in mica and with rare sponge spicules	High tidal-flat
A a	Dark grey clayey silt rich in plant debris, and with rare sponge spicules	? Salt marsh
B	Inter-laminated fine sand and silt, with occasional to rare microfauna	? Intermediate to high tidal-flat
A a	Dark grey clayey silt rich in plant debris and with rare sponge spicules	? Salt marsh
C	Lenses of gravel and sand, rich in plant debris	Fluvial channel-filling
D	Fossiliferous fine sand and silt with low percentage of clay	Intermediate to low tidal-flat

Figure 10.6 Sedimentary facies, lithological description and suggested environments of deposition, Holocene raised coastal sediments, section N6, New Abbey area.

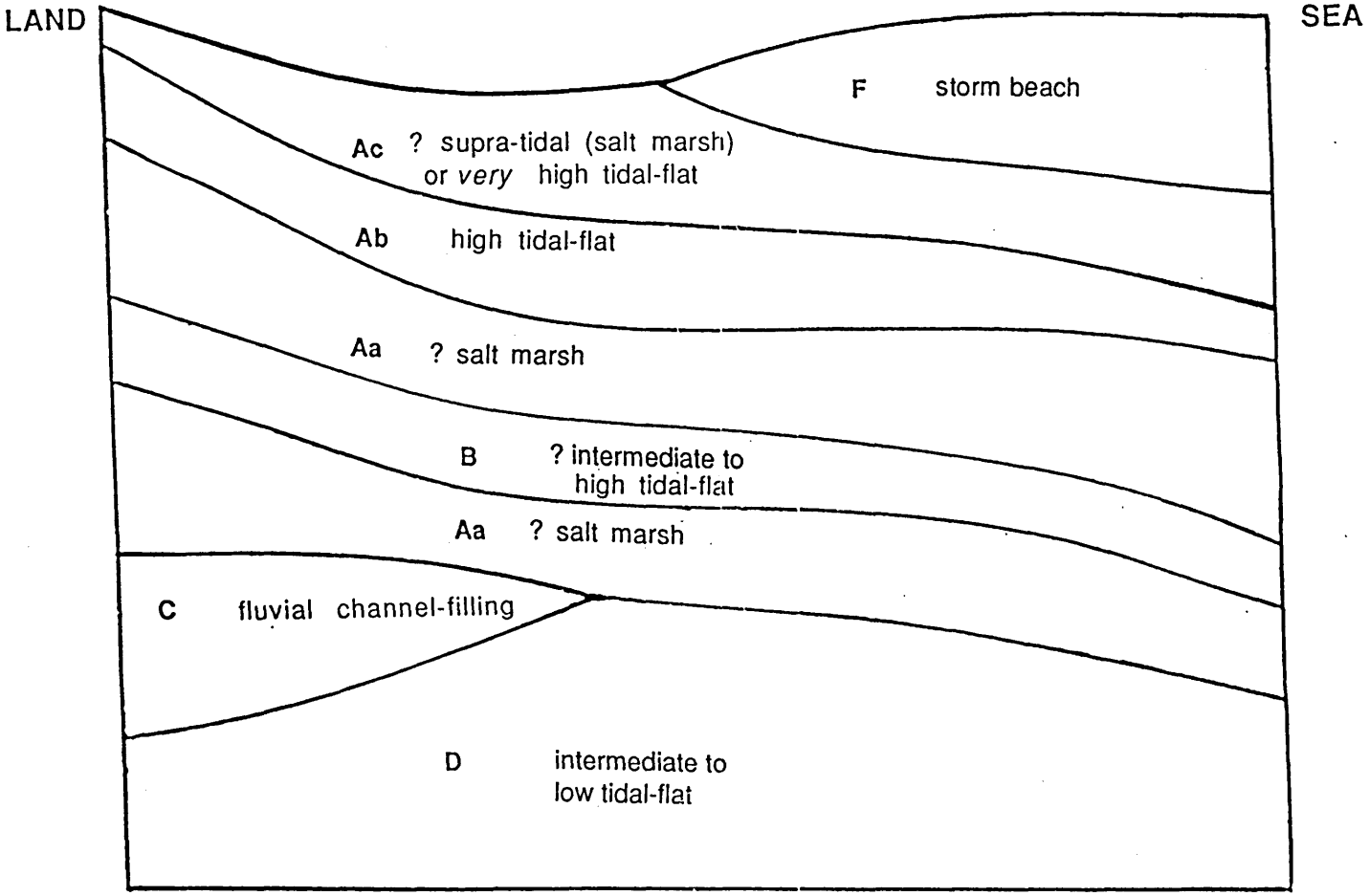

Figure 10.7 Diagrammatic representation of suggested stratigraphical and environmental relationships of the Holocene sedimentary facies (A, B, C, etc.) identified in the New Abbey area.

Ac, brown clayey silt
Ab, clayey silt with fine sand
Aa, grey clayey silt
B, inter-laminated fine sand and silt
C, coarse sand with pebbles
D, fine sand, rich in microfauna
F, coastal gravel and sand

Table 10.1 Environments of deposition in the Dalbeattie area, and their sedimentary mean grain sizes, clay mineral compositions and geochemical contents.

Environment	Intermed. to low tidal-flat	? Salt marsh	High tidal-flat	? Supra-tidal or *very* high tidal-flat	Lake or marsh
Facies	**(D)**	**(Aa)**	**(Ab)**	**(Ac)**	**(E)**
Parameters					
Grain size	**n =1**	**n =15**	**n = 10**	**n =15**	**n = 4**
Mean size(ϕ)	3.76	6.77	7.51	6.75	7.25
Clay Minerals (%)	**n = 1**	**n = 8**	**n = 5**	**n = 8**	**n = 4**
Illite	56.77	41.25	48.85	41.86	41.25
Chlorite	13.20	21.61	11.69	13.71	19.23
Kaolinite	12.11	14.38	10.42	10.02	17.12
Vermiculite	17.80	7.66	16.81	18.28	19.02
Mixed-layers	0.00	10.84	11.06	11.33	0.00
Geochemistry					
Major (%)	**n =1**	**n = 9**	**n = 10**	**n =13**	**n = 5**
SiO_2	79.10	70.16	68.18	68.80	62.38
TiO_2	0.55	0.77	0.79	0.74	0.78
Al_2O_3	7.88	11.19	13.79	12.19	13.76
$Fe^*{}_2O_3$	2.69	4.42	5.33	4.79	5.61
MnO	0.08	0.05	0.06	0.11	0.06
MgO	1.68	1.79	2.07	2.38	2.30
CaO	1.60	0.81	0.57	1.77	0.66
Na_2O	1.81	1.21	1.03	1.04	1.16
K_2O	2.08	2.46	2.86	2.72	2.83
P_2O_5	0.10	0.09	0.10	0.13	0.11
H_2O	2.09	3.82	3.29	3.20	6.19
CO_2	1.13	2.33	2.04	2.14	4.08
Trace (ppm)	**n =1**	**n = 4**	**n = 4**	**n = 11**	**n = 3**
Zr	203	184	184	184	160
Y	21	30	30	30	28
Sr	133	106	106	106	104
U	2	3	3	3	3
Rb	68	123	123	123	124
Th	4	9	9	9	9
Pb	15	25	25	25	17
Ga	7	26	26	16	8
Zn	39	66	66	85	85
Cu	6	12	12	17	14
Ni	19	30	30	41	39
Co	7	11	11	16	15
Cr	69	99	99	104	100
Ce	38	63	63	71	70
Ba	313	363	363	373	358
La	19	28	28	33	33

Table 10.2 Environments of deposition in the Kirkcudbright area, and their sedimentary mean sizes, clay mineral compositions and geochemical contents.

Environment	Intermed. to low tidal-flat	? Intermed. to high tidal-flat	? Salt marsh	High tidal-flat	? Supra-tidal or *very* high tidal-flat
Facies	**(D)**	**(B)**	**(Aa)**	**(Ab)**	**(Ac)**
Parameters					
Grain size	n = 4	n = 2	n = 1	n = 2	n = 6
Mean size (ϕ)	4.58	5.98	7.30	5.80	7.01
Clay Minerals (%)	n = 3	n = 1	n = 1	n = 3	n = 4
Illite	42.78	44.09	40.00	35.05	27.02
Chlorite	25.23	22.35	27.75	8.88	11.33
Kaolinite	10.16	12.59	15.00	9.18	10.70
Vermiculite	8.54	1.75	15.00	19.73	18.59
Mixed-layers	13.43	22.83	0.00	20.97	31.37
Geochemistry					
Major (%)	n = 11	n = 10	n = 4	n = 2	n = 6
SiO_2	71.76	72.86	75.39	72.02	73.29
TiO_2	0.54	0.55	0.57	0.76	0.73
Al_2O_3	8.66	8.79	9.15	11.79	11.63
$Fe^*_2O_3$	3.60	3.20	3.77	4.52	4.96
MnO	0.08	0.08	0.08	0.09	0.05
MgO	1.80	1.98	1.70	1.77	1.56
CaO	3.75	3.31	2.21	0.41	0.21
Na_2O	0.99	1.35	1.65	1.29	1.08
K_2O	2.03	2.05	2.11	2.42	2.42
P_2O_5	0.08	0.07	0.09	0.08	0.09
H_2O	4.59	3.78	2.12	3.03	2.51
CO_2	2.55	2.69	2.24	2.45	1.73
Trace (ppm)	n=5	n=2	n=3	n=1	n=3
Zr	176	177	183	247	176
Y	24	21	21	27	28
Sr	120	117	144	92	94
U	2	3	4	3	4
Rb	94	73	34	89	116
Th	7	5	7	8	10
Pb	21	16	14	20	25
Ga	12	10	9	9	15
Zn	68	50	48	60	87
Cu	20	7	9	7	36
Ni	28	20	30	26	29
Co	15	9	6	10	13
Cr	105	106	71	88	110
Ce	55	44	41	58	65
Ba	330	300	308	322	350
La	26	20	17	25	40

Table 10.3 Environments of deposition in the New Abbey area, and their sedimentary mean grain sizes, clay mineral compositions and geochemical contents.

Facies	Intermed. to low tidal-flat (D)	? Salt marsh (Aa)	? Intermed. to high tidal-flat (B)	? Salt marsh (Aa)	High tidal-flat (Ab)	? Supra-tidal or *very* high tidal-flat (Ac)
Parameters						
Grain size	n = 5	n = 1	n = 1	n = 1	n = 2	n = 2
Mean size (ϕ)	5.98	6.78	5.45	6.35	6.35	6.50
Clay Minerals	n =3	n =1	n =1	n = 2	n=1	n = 2
Illite	38.20	32.59	39.35	33.36	39.40	31.98
Chlorite	33.72	16.00	31.71	21.75	6.27	11.35
Kaolinite	12.03	7.06	12.04	10.02	10.50	18.85
Vermiculite	0.93	0.00	0.00	11.80	10.10	11.60
Mixed-layers	16.00	45.11	13.65	18.44	32.62	32.40
Geochemistry						
Major (%)	n = 4	n =2	n =1	n =1	n = 1	n = 1
SiO_2	77.25	76.65	73.03	71.19	73.32	75.76
TiO_2	0.45	0.65	0.53	0.78	0.70	0.75
Al_2O_3	7.45	10.68	9.45	12.49	12.28	11.05
$Fe^*{}_2O_3$	3.67	4.30	4.10	5.17	4.40	4.12
MnO	0.13	0.06	0.08	0.07	0.05	0.01
MgO	1.31	1.65	1.65	1.78	1.56	1.78
CaO	1.84	1.78	1.73	0.26	0.27	0.29
Na_2O	0.90	1.09	1.13	0.99	1.32	0.86
K_2O	1.99	2.36	2.36	2.40	2.34	2.49
P_2O_5	0.08	0.07	0.07	0.11	0.07	0.07
H_2O	2.66	2.91	2.81	2.80	2.88	2.63
CO_2	2.31	2.00	2.50	2.32	1.05	1.11
Trace(ppm)	n = 2	n = 2	n = 2	n =1	n = 2	n =1
Zr	141	168	159	188	192	174
Y	15	21	20	22	29	19
Sr	122	104	103	90	94	89
U	2	2	2	2	3	3
Rb	66	94	83	89	103	87
Th	4	7	4	7	9	6
Pb	14	21	15	17	24	21
Ga	8	13	11	13	15	13
Zn	37	70	56	59	75	54
Cu	6	14	8	7	9	12
Ni	17	32	24	25	35	19
Co	2	11	9	9	15	7
Cr	61	110	87	86	101	83
Ce	37	57	45	52	64	47
Ba	290	350	307	329	350	333
La	16	25	20	20	27	23

CHAPTER 11

PROVENANCES OF THE HOLOCENE RAISED COASTAL SEDIMENTS

11.1 Introduction

As seen above, especially in Chapter 5, the Holocene raised coastal sediments of the four geographical areas studied in the course of the project comprise several distinct lithological facies. These facies are the products of a number of different sedimentary environments (Chapter 10), but their variation in characteristics may also be due partly to their having been derived from several different provenances.

Many studies of the provenances of Holocene and present-day sediments in various parts of the globe have been made (e.g. recently, Kraft 1971; Pye 1980; Carson & Arcaro 1983; Jelgersma 1983; Van de Kamp & Leake 1985; Roser & Korsh 1988). The most profitable studies have used the clay-mineral and geochemical content of the sediments being studied as indicators of provenance. Here the same methods are used principally, although it may be noted that (for example) the provenances of Holocene beach gravel and sand deposits in the Dalbeattie area (Chapter 6.9, paragraph 4) and of a fluvial pebbly coarse sand unit in the New Abbey area (Chapter 10.4) have been deduced on more general evidence.

11.2 Determination of provenance on the basis of clay-mineral content

Keller (1970) reported that clay minerals may be used as indicators of provenance or diagenesis or both. He noted that montmorillonite may form by alteration of volcanic ash and, in the marine environment, it may be changed to chlorite, whereas illite is mainly stable in the marine environment. McMurty & Fan

(1974) suggested that mica represents a residual concentration from crystalline rocks and that montmorillonite and kaolinite are closely associated with Quaternary and older sedimentary rocks; montmorillonite and kaolinite are probably formed from feldspar and non-micaceous ferromagnesian minerals, although they also may be derived from silica. Stevens et al. (1987) noted that kaolinite is formed by the weathering of granitic bedrocks. Biotite, which is relatively unstable in weathering conditions, was considered by these authors to be the probable parent mineral in the formation of vermiculite and mixed-layer biotite-vermiculite, minerals which often form in soil developed on granitic terrains in cold temperate climates.

The majority of the Holocene raised coastal sediments studied in the present project are of fine grade and were deposited during the Flandrian marine transgression and regression in environments that were broadly estuarine in character. As noted in Chapter 8, the most abundant clay minerals in all facies of the Holocene fine-grained sediments are illite, chlorite, kaolinite and vermiculite, there being subordinate amounts of mixed-layer clays, and a low content of montmorillonite in a few samples. Song et al. (1983) suggested that the relative influence of off-shore and land sources in determining the clay-mineral content of a coastal sediment appears to be reflected in the ratio of illite + montmorillonite (smectite) to kaolinite + chlorite. In the present work, it was found that illite is dominant in all the samples studied, whilst chlorite and kaolinite are less abundant. The amount of vermiculite varies from sample to sample.

With regard to the provenances of the illite, chlorite and kaolinite in the Holocene sediments, the illite may have been partially derived from the fine flakes of mica that are abundant in the fine sand and silt fractions of the sediments, the mica previously having been derived from the granitic rocks and greywackes that outcrop within the areas studied. In contrast, the kaolinite and chlorite may have had their

provenances in the Pleistocene tills that cover large parts of the solid rock within and around the areas studied. This conclusion is in accord with Pye's (1980) study of recent sublittoral fine-grade sediments on the floor of Kilbrannan Sound, Firth of Clyde. Pye suggested that the dominant clay minerals, illite, chlorite and kaolinite, and subordinate montmorillonite and mixed-layer clays in Kilbrannan Sound were derived principally from local glacial till deposits.

11.3 Determination of provenance on the basis of geochemical composition

In their study of the petrography and geochemistry of feldspathic and mafic sediments of the northeastern Pacific margin, Van de Kamp & Leake (1985) suggested that the high Al_2O_3 and K_2O contents of these sediments indicate a high felsic component. They added that a decrease of $Fe^*_2O_3$, TiO_2 and MgO and corresponding increase of K_2O reflects a decrease of mafic-rock and increase of felsic-rock components. An increase of Ba, Rb, La, Ce and Nb and decrease of Co and Y may be attributable to the same change in rock components.

Bhatia & Crook (1986) claimed that La, Ce, Y, Th, Zr, Hf, Nb, Ti and Se are the trace elements most suited for determination of provenance and tectonic setting because of their relatively low mobility during sedimentation processes and their low residence time in sea water. These elements are transported quantitatively into clastic sedimentary rocks during weathering and transportation and their proportional content in the new rock therefore will reflect the signature of the parent rocks. Hickman & Wright (1983) pointed out that P and Zr are associated chiefly with apatite and zircon respectively, two minerals which are concentrated in near-shore sediments. The

elements Y, La and Ce are indicative of a granitic provenance, whereas Ni and Cr indicate basic source areas, and Sr possibly is highest where the source contains sedimentary rocks. The same authors added that the trace elements are influenced by water depth and salinity. Elements such as Cr, Nb and Sr are generally high in concentration in shallow-marine or fresh-water sediments, whereas relatively high concentrations of Ni, Cu, Ce and Pb are indicative of deeper marine water.

The relationships between geochemistry and provenance, outlined above, together with the results of a study of arenaceous rocks made by Pettijohn et al. (1972), are applied now to the Holocene sediments analysed in the course of the project.

The geochemical data presented in Chapter 9 indicate that the SiO_2 content in the finer-grade Holocene sediments (clayey silt, clayey silt with fine sand) is that of the average for shale. In the sandier Holocene sediments (fine sand with silt), the SiO_2 content corresponds with the average for a combination of greywacke and shale. The percentages of Al_2O_3 and K_2O are relatively high in the fine-grained sediments and vary inversely with the SiO_2 content, suggesting that the fine-grained sediments are most probably derived from felsic rocks. The K_2O may have been added from sea water during diagenetic processes. Similarly, the presence of MgO may be related to addition of Mg from sea water, and the high $Fe^*_2O_3$ content may be due to the oxidation conditions at the time of deposition. Other possible sources of the $Fe^*_2O_3$ and MgO are mafic rocks contained within the greywackes. All the above-mentioned oxides correlate positively with the clay-mineral content of the Holocene sediments, perhaps indicating that the oxides were added during clay-mineral formation in the parent rocks and

during diagenesis of the Holocene sediments.

The concentration of CaO is highest in samples of the Holocene fossiliferous fine sand sediments, suggesting that the CaO was derived from mollusc shells and other calcareous skeletal material present within the depositional environment. The high concentration of micaceous material in these sediments may be attributable to the close proximity of the granitic and granodioritic rocks of the Criffell-Dalbeattie pluton, the most probable provenance of the mica.

Pettijohn et al. (1972, 60) suggested that the chemical composition of a sandstone, expressed as log (SiO_2 / Al_2O_3) against log (Na_2O / K_2O), may be used to identify the rock type (e.g. greywacke, arkose, etc.). Most of the sediments analysed in the course of this project are of finer grade than sand. However, applying the diagram used by Pettijohn et al. to the Holocene sediments in the four areas studied (Fig. 11.1), it is found that most of these sediments fall into the categories of arkose and subarkose; a few samples appear to have the composition of lithic arenites. The sediments in the first two categories may have been derived from acidic rocks (e.g. the Criffell-Dalbeattie pluton) and the sediments of the last category from rocks with a high argillaceous content (e.g. the Lower Palaeozoic shales or, to as lesser extent, the greywackes).

Trace element data presented in Chapter 9 show higher concentrations of these elements in the fine-grade sediments (clayey silt) than in the coarser-grade sediments. Also, it may be noted that most of the trace elements are associated with the clay fraction in the Holocene sediments, and have a positive relationship with al-alk (Figs. 9.20 to 9.32). However, plotting of data from the analysed sediments on Hickman & Wright's (1983) triangular diagram of Ni + Cr versus Y + La + Ce versus Sr (Fig.

9.44) does not assist greatly in distinguishing the provenances of the various sedimentary facies. Zr may have been derived from detrital heavy minerals, which are thought to have been come from greywackes.

11.4 Provenance of Holocene coastal gravel deposits

As noted in Chapter 6.5 and 6.9, the Holocene coastal gravels at Torr, in the Dalbeattie area, may have been derived partly from Pleistocene glaciofluvial gravels (themselves composed mainly of Lower Palaeozoic greywacke clasts, to a lesser extent of granite/granodiorite clasts) and partly from outcrops of the granite/granodiorite of the Criffell-Dalbeattie pluton.

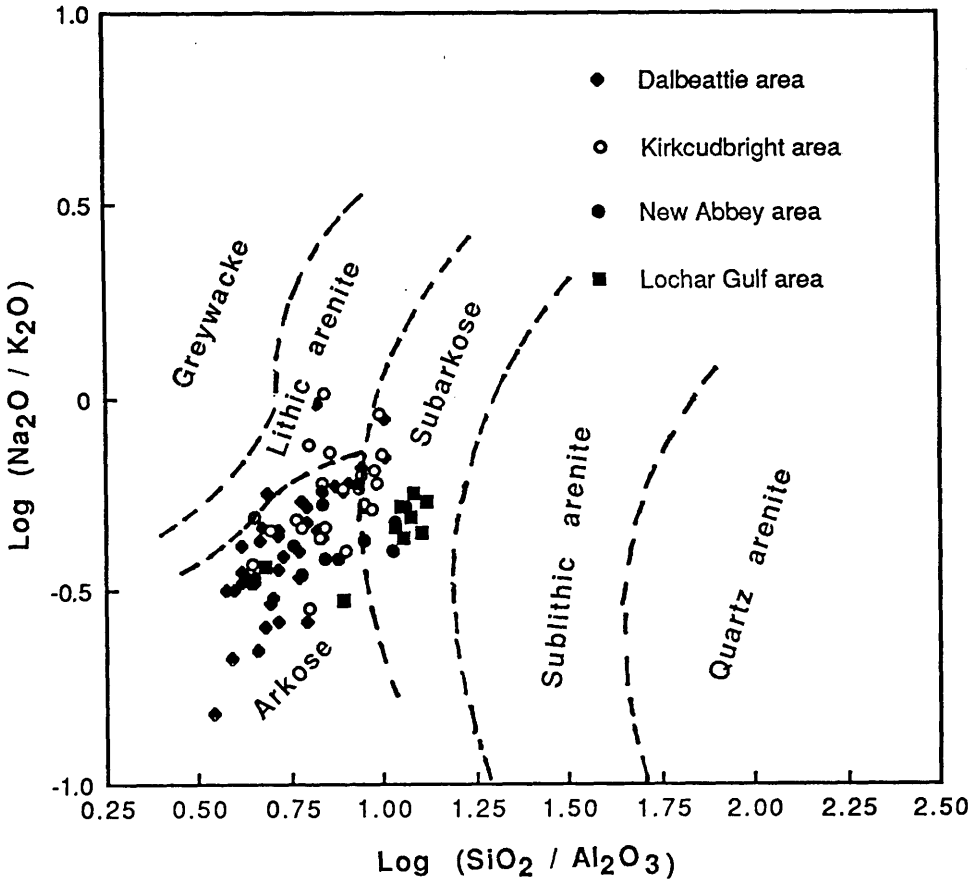

Figure 11.1 Distribution of analysed Holocene samples within the sandstone rock types distinguished by Pettijohn et al. (1972, fig. 2.11).

CHAPTER 12

CONCLUSIONS

12.1 Introduction

Some general conclusions concerning the characteristics of the present-day intertidal sediments and Holocene raised coastal sediments of the Dalbeattie, Kirkcudbright, New Abbey and Lochar Gulf areas are recorded in this final chapter. The extent to which the six major aims of the research project, listed in Chapter 1.4, have been fulfilled is also considered. In addition, a few suggestions are made for further work that might extend aspects of the project that it was possible to investigate only briefly or inadequately in the limited time available.

12.2 Former Holocene shoreline positions in the Dalbeattie and Kirkcudbright areas

The position of the shoreline at the maximum of the Holocene marine transgression in the Dalbeattie and Kirkcudbright areas (Chapter 1.4, Aim 1a) was successfully mapped in the field on the scale 1 : 10,560 by the recognition of small cliffs and breaks in slope, and changes in lithology at the boundaries between Holocene coastal sediments and outcrops of either Pleistocene deposits or older, solid rocks (Chapter 3.1.1).

Aim 1b, determination of the nature and, if possible, successive positions of the shoreline during the post-transgressive period of Holocene marine influence, was more difficult to achieve. However, suggestions made regarding successive environments of deposition in the Dalbeattie and Kirkcudbright areas (Chapter 10.2 and 10.3), in combination with the evidence provided in vertical profiles through the

Holocene sediments (Figs. 4.2, 4.3 and 4.5), allow at least movements of the shoreline to be proposed as follows, although the precise positions of the shoreline have not been established:

1) The commonest (generalised) succession of sedimentary facies and sub-facies in the two relevant areas is, from top to base:

Brown to grey clayey silt (sub-facies Ac)

Grey to blue clayey silt with fine sand (sub-facies Ab)

Grey-blue clayey silt (sub-facies Aa)

Fine sand, rich in microfaunal remains (facies D).

As discussed in Chapter 10.2, 10.3 and 10.4, facies D is interpreted as a deposit that accumulated as an intermediate to low intertidal sand-flat sediment. The sediments of sub-facies Aa are tentatively regarded as salt marsh deposits, whilst sub-facies Ab is taken to represent deposits of the high tidal-flat environment. The uppermost of the Holocene sub-facies, Ac, may have accumulated in the *very* high tidal-flat or supra-tidal (salt marsh) environment. Facies B, inter-laminated fine sand and silt, and regarded tentatively as a deposit of the intermediate to high tidal-flat, interrupts the succession listed above at different 'horizons' in the Kirkcudbright and New Abbey areas. As discussed in Chapter 10.3 and 10.4, in the Kirkcudbright area this facies may represent a transition between the intermediate to low tidal flat regime of facies D and the salt marsh regime of sub-facies Aa. In the New Abbey area, facies B may represent a local fluctuation in the position of the shoreline during a phase of *very* high tidal-flat or salt marsh accumulation, represented by sub-facies Aa.

2) If these environmental interpretations are correct, the sedimentary succession

suggests a slight seaward movement of the shoreline position between deposition of facies D and Aa (recorded in the Kirkcudbright area by the deposition of facies B), followed by a landward movement between deposition of sub-facies Aa and Ab (but interrupted in the New Abbey area during the deposition of sub-facies Aa by a minor landward and then seaward movement of the shoreline). Between deposition of sub-facies Ab and Ac there appears to have been a further seaward movement of the shoreline.

12.3 Present-day and Holocene sedimentary facies

Detailed field study of the lateral and vertical distribution of the present-day intertidal and Holocene raised coastal sediments in the Dalbeattie, Kirkcudbright and New Abbey areas, and of the Holocene sediments in the area of the former Lochar Gulf, led to the recognition of four present-day and seven Holocene sedimentary facies in these areas (Chapter 1.4, Aim 2). The facies were distinguished mainly on the basis of the following criteria (cf. Aim 3a): shapes of the various sedimentary bodies and the locations of these bodies in relation to contemporaneous deposits; textures (grain sizes) of the sediments; degree of sorting of the sediments; nature of the sedimentary structures (where observed) in, and faunal content of, the deposits. The facies recognised in the present-day sediments, and their characteristics, in brief, were:

1) Tidal-flat: identified within the intertidal zone in the Dalbeattie, Kirkcudbright and New Abbey areas; composed of fine sand and mud; occasionally seen to contain sedimentary structures, e.g. current ripples andinterlamination of sand and silt; molluscs and microfauna (foraminifers and ostracods) frequent to abundant; divisible with difficulty into medium-to-low and high tidal flats.

2) Tidal-creek: identified within the intertidal zone in the Dalbeattie, Kirkcudbright and New Abbey areas; creek-floor deposits characterised by pebble-sized clasts of mud and sand; where observed, deposits on creek sides were well-laminated.

3) Salt marsh: adjacent to and landward of present-day MHWS in the Dalbeattie, Kirkcudbright and New Abbey areas; generally composed of laminated silt and clay; traversed by ramifying systems of narrow creeks or gullies.

4) Sand-barrier: limited to one locality, in the Dalbeattie area; composed mainly of well-sorted but apparently unstratified coarse sand.

The facies recognised in the Holocene sediments, and their characteristics, in brief, were:

A) Complex of fine-grained sediments: forms the uppermost part of the Holocene raised coastal sediments throughout much of the Dalbeattie, Kirkcudbright and New Abbey areas; on the basis of colour, textural characteristics, clay mineralogy, geochemistry and organic content, divisible into three sub-facies, Aa, grey clayey silt with mica flakes, plant debris and occasional traces of lamination, Ab, clayey silt with fine sand rich in mica flakes and with rare microfauna, Ac, brown clayey silt with plant remains and penetrated by oxidised root channels.

B) Inter-laminated fine sand and silt: present in the Kirkcudbright, New Abbey and Lochar Gulf areas; interstratified fine sand and silt laminae, with plant debris and rare to occasional microfaunal remains.

C) Coarse sand with pebbles: present mainly in the New Abbey area (a minor facies in the Dalbeattie and Kirkcudbright areas); local lenses of pebbly sand which include plant debris.

D) Fine sand, rich in microfaunal remains: occurs in the Kirkcudbright and New Abbey areas, probably extensively in the area of the former Lochar Gulf and perhaps at depth in the Dalbeattie area; composed mainly of fine sand and coarse silt, with a low percentage of clay; rich in molluscan shell fragments, foraminiferal tests, ostracod valves, echinoid spines and sponge spicules; resembles the present-day intermediate to low tidal-flat sediments in its grain-size, clay mineralogical and geochemical characteristics.

E) Clays, rich in plant debris: identified in the Dalbeattie area; composed mainly of dark-coloured sticky clay, rich in plant debris, and covered by a layer of peat (facies G).

F) Coastal gravel and sand: occurs in the Dalbeattie, New Abbey and Lochar Gulf areas; mostly forms sheet-like ridges oriented approximately parallel to the present shoreline; in places, the gravel clasts exhibit imbricate structure; the two ridges present in the Dalbeattie area occur at different altitudes.

G) Peat: covers the Holocene inorganic sediments thinly in limited parts of the Dalbeattie area and thickly (up to c. 3.5m) and extensively in the Lochar Gulf area.

12.4 Sedimentary characteristics of the Pleistocene and Holocene gravel deposits

Samples of gravel-sized clasts collected from Pleistocene glaciofluvial deposits at Chapelcroft (NX 804 550) and Broomisle (NX 823 592) in the Dalbeattie area and from a Holocene higher gravel ridge (NX 804 531 to NX 808 529) and lower gravel ridge (NX 808 521 to NX 810 522) at Torr in the Dalbeattie area gave the following

sedimentological data (Chapter 1.4, Aim 3b):

1) Shapes : Pleistocene clasts are predominantly discs at Chapelcroft and spheroids at Broomisle; Holocene clasts are predominantly blades and discs in the higher ridge and discs in the lower ridge.

2) Sphericity : sphericity values are mainly between 0.5 and 0.9 in both the Pleistocene and Holocene clasts.

3) Roundness: angular pebbles are most abundant in the Pleistocene gravel at Chapelcroft, whereas sub-rounded pebbles are most abundant in the Pleistocene gravel at Broomisle. Sub-rounded clasts predominate in the Holocene higher ridge at Torr, whereas rounded and sub-rounded clasts are equally dominant in the lower ridge. The Holocene gravel clasts are more rounded than the Pleistocene gravel clasts.

4) Lithological composition: about 70% of the Pleistocene clasts consist of greywacke, whereas about 60% of the clasts in the Holocene higher ridge are of granite/granodiorite and in the lower ridge are of greywacke.

5) The shapes of the clasts in both the Pleistocene and Holocene gravels of the Dalbeattie area do not depend on the lithological composition of the clasts.

6) The Pleistocene greywacke gravel clasts, especially at Chapelcroft, are more rounded than the Pleistocene granite/granodiorite gravel clasts. The Holocene greywacke gravel clasts are more rounded than the Holocene granite/granodiorite gravel clasts.

7) The lithological data show that the Holocene gravels consist of nearly equal proportions of greywacke and granite/granodiorite clasts, whilst the Pleistocene gravels consist predominantly of greywacke clasts. This may indicate that the Pleistocene gravels were derived mainly from the NW and

west, whilst the Holocene gravels were derived partly from the Criffell-Dalbeattie pluton and partly from Pleistocene glaciofluvial deposits.

Dip direction readings taken of the long axes of imbricated pebbles in the higher and lower Holocene gravel ridges at Torr, Dalbeattie area, in Holocene gravel ridges at NX 985 657 and NX 986 653 in the New Abbey area and of clasts in gravel deposits exposed in the banks of Potterland Lane (NX 803 553) in the Dalbeattie area gave the following results:

1) The Holocene gravel ridges at Torr in the Dalbeattie area, and near the mouth of New Abbey Pow in the New Abbey area, were deposited by wave action that came from a SE direction.

2) The gravels exposed in Potterland Lane were deposited by water that flowed from the SE. This may indicate either that the gravel clasts were derived (in Pleistocene times) from an ice mass located to the SE of their present position or that the gravel clasts were eroded from a pre-existing Pleistocene gravel mass in the course of the Holocene marine transgression and re-aligned by SE-NW onshore water action.

12.5 Grain-size characteristics of the Holocene raised coastal sediments and present-day intertidal sediments

Detailed grain-size analysis of samples from both the Holocene and present-day sediments leads to the following conclusions (Chapter 1.4, Aim 4):

1) The majority of the Holocene samples from the Dalbeattie, Kirkcudbright and New Abbey areas are of silt grade, whilst the samples from the Lochar Gulf area are mainly of sand grade. The present-day intertidal sediments in the Dalbeattie, Kirkcudbright and New Abbey areas are mainly of coarser grade and

are sandier than the majority of the Holocene sediments of the same areas.

2) Within vertical sections through facies A of the Holocene sediments, the percentage content of fine silt and clay generally increases upwards.

3) The textural characteristics of the sediments in the lower part of the Holocene succession (facies D) in the Kirkcudbright and New Abbey areas resemble those of the present-day intertidal sediments in the same areas.

4) The upper parts of the sedimentary succession in the Kirkcudbright and New Abbey areas, together with the complete sequence of Holocene sediments over much of the Dalbeattie area, i.e. the sediments of facies A, are mostly bimodal or polymodal in their grain-size distribution. In contrast, the sediments of facies D in these areas, and in the area of the former Lochar Gulf, are unimodal in their grain-size distribution. The present-day intertidal sediments of the Dalbeattie, Kirkcudbright and New Abbey areas are mainly unimodal in their grain-size distribution.

5) Cumulative curves showing grain-size distribution in the sediments of facies A resemble those for sediments of tidal-flat areas. In contrast, cumulative curves showing grain-size distribution in the sediments of facies D resemble those for beach sediments.

6) The majority of the fine-grained (silt-grade) sediments are poorly to very poorly sorted, whereas the coarser-grained (sand-grade) sediments are moderately to poorly sorted.

7) Plots of the inter-relationships between the statistical grain-size parameters, Mz, σ_I, Sk_I and K_G, differentiate between facies A, B, C and D, and show the similarities between facies E and facies A.

8) The CM diagram shows that most of the Holocene sediments of the Dalbeattie, Kirkcudbright and New Abbey areas were transported by uniform suspension, whereas the (sandier) sediments of the Lochar Gulf area were transported mainly by either uniform suspension or graded suspension.

12.6 Clay-mineral content of the Holocene and present-day sediments

Clay mineral analysis of samples from both the Holocene and present-day sediments suggested the following conclusions (Chapter 1.4, Aim 5):

1) The main clay mineral species present in both the Holocene raised coastal sediments and in the present-day intertidal sediments, in descending order of abundance, are illite, chlorite, kaolinite and vermiculite. In Holocene vertical sections or boreholes, there is a noticeable relationship between change in sedimentary facies and change in clay mineral abundance.

2) The crystallinity of illite is variable within both the Holocene and present-day clays. The crystallinity index suggests that the illite mainly has the composition of biotite and muscovite.

3) Both detrital and authigenic illite, chlorite and kaolinite are present. Detrital material greatly predominates over authigenic material in the cases of chlorite and kaolinite.

4) The chlorite is mostly Fe-chlorite.

5) Vermiculite is present in most of the analysed samples. It is more abundant in the uppermost facies (facies A) of the Holocene sediments than in the underlying facies.

6) Mixed-layer clay minerals, present in most of the samples of the Holocene

sediments, may represent stages in the transformation of one clay mineral to another or incomplete weathering.

7) Montmorillonite, present in only a few of the samples of Holocene sediments, may have been produced by degradation of micas during weathering.

8) Titanium is found in association with most of the clay minerals present in the Holocene sediments, perhaps being absorbed on to the surfaces of these minerals.

12.7 Geochemistry of the Holocene and present-day sediments

Geochemical studies of bulk samples and samples of the clay fraction from both the Holocene and present-day sediments suggest the following conclusions (Chapter 1.4, Aim 6):

1) As might be expected, the Holocene sediments in the Dalbeattie, Kirkcudbright and New Abbey areas identified as comprising facies A on the basis of field evidence have similar major-element and trace-element compositions. Similarly, the sediments of facies D, identified in the lower part of the Holocene succession in the Kirkcudbright and New Abbey areas, resemble each other in their geochemical content.

2) The SiO_2 content in the Holocene sediments of the Lochar Gulf area (mainly sand grade) is higher than that in the Holocene sediments of the three other areas studied (mainly fine sand, silt and clay).

3) In both the Holocene and present-day sediments of all the areas studied, the SiO_2 content is inversely related to the content of Al_2O_3, $Fe^*_2O_3$ (i.e. total iron oxide), TiO_2, MgO and K_2O.

4) TiO_2 and P_2O_5 are present mainly in clay minerals.

5) The CaO content in the Holocene sediments of facies D of the Kirkcudbright and New Abbey areas is approximately equal to that in the present-day sediments of the same areas and higher than that in the other Holocene sedimentary facies of these areas. This may indicate that the CaO was derived from fossil shell and other organic carbonate fragments in the sediments of facies D. In the remainder of the Holocene sediments, in which the CaO content is low, the CaO appears to be related to clay minerals.

6) The Al_2O_3 and K_2O present in the sediments are related mainly to clay minerals.

7) The wide variability and low content of Na_2O in the analysed bulk samples, together with the presence of Na_2O in samples of the clay fraction, suggest that the Na_2O is associated with both clay minerals and detrital minerals such as feldspar.

8) Most of the trace elements (Y, Sr, Rb, Th, Pb, Zn, Ni, Co, Ce, Cr, Ba and La) present in the bulk samples are associated with clay minerals.

9) The trace element concentration depends on the magnitude of the clay fraction rather than the clay mineral species.

10) The high concentration of trace elements in the clay fraction, together with the higher concentration of trace elements in the fine-grained sediments than in the coarser-grained sediments, suggests that these elements are associated mainly with clay minerals.

11) In the Holocene sediments, both the major and trace element contents change vertically with changes in sedimentary facies.

12.8 Environments of deposition of the Holocene sediments

Field study of the Holocene raised coastal sediments in the Dalbeattie, Kirkcudbright and New Abbey areas, and to a lesser extent in the area of the former Lochar Gulf, led to recognition of seven sedimentary facies in these areas. The field studies, in combination with laboratory analysis of the grain-size, clay mineralogical and geochemical characteristics of the various Holocene facies, and comparison with the known environments of deposition of the present-day sediments of the same areas, enabled identification of Holocene environments to be made (Chapter 1.4, Aim 2, cf. Aims 4 and 5). In summary, the environments identified were as follows:

1) Dalbeattie area. The three sub-facies of facies A are thought to have accumulated successively in salt marsh (sub-facies Aa), high tidal-flat (sub-facies Ab) and *very* high tidal-flat or even supra-tidal/salt marsh (sub-facies Ac) environments. Other environments of deposition identified in this area were lake or marsh (facies E) and storm beach (facies F).

2) Kirkcudbright area. In this area, five successive environments of deposition were recognised, these being, intermediate to low tidal-flat (facies D), intermediate to high tidal-flat (facies B), salt marsh (sub-facies Aa), high tidal-flat (sub-facies Ab) and *very* high tidal-flat or even supra-tidal/salt marsh (sub-facies Ac).

3) New Abbey area. The five environments of deposition identified in the Kirkcudbright area were also recognised in this area. In addition, however,

two more localised environments (fluvial channel-fill and storm beach) were identified. The full sequence recognised, from earliest to youngest, was as follows: intermediate to low tidal-flat (facies D), fluvial channel-fill (facies C), salt marsh (sub-facies Aa), intermediate to high high tidal-flat (facies B), salt marsh (sub-facies Aa), high tidal-flat (sub-facies Ab), *very* high tidal-flat or even supra-tidal/salt marsh (sub-facies Ac) and storm-beach (facies F).

From the lateral and vertical distribution of the sediments, their fossil content and their conjectural environment of accumulation, it is suggested that the sediments of facies D were deposited under transgressive marine conditions. In contrast, the sediments of facies A and facies B probably were deposited slightly later, at a time when the position of the shoreline fluctuated slightly. In the absence of radiocarbon age-dating of the sediments of the Dalbeattie, Kirkcudbright and New Abbey areas the exact times of these events are not certain. The Holocene sediments that were studied in these three areas, however, together with the Holocene sediments of the Lochar Gulf area, appear to the equivalents of Holocene sediments at Newbie Cottages, further to the east in the Solway Firth area, which Jardine (1975) showed ranged in age from c. 7,400 to 5,500 years B.P. Broadly, the lower part of the relevant Holocene sediments in the Newbie Cottages resemble the sediments of facies D of this study, whilst the sediments of the upper part of the Holocene sediments at Newbie Cottages resemble the sediments of facies A of this study.

12.9 Provenances of the Holocene sediments

Although clay mineralogical and geochemical studies proved rather inconclusive with regard to indicating the provenances of the Holocene sediments (Chapter 1.4, Aim

6), the following possibilities were suggested by these studies.

The illite may have been partially derived from fine flakes of mica, the mica previously having been derived from the granitic rocks and greywackes that outcrop within or close to the areas studied.

The geochemical studies suggest that the fine-grained Holocene sediments may have been derived mainly from felsic rocks. When the compositions of these sediments are represented on the diagram of Pettijohn et al. (1972) for the chemical composition of sandstones, it is found that most of the Holocene sediments fall into the categories of arkose and subarkose, although a few appear to be lithic arenites. Surprisingly, none appear to be of greywacke composition. It is suggested that the arkoses and subarkoses may have been derived from acidic rocks (e.g. the Criffell-Dalbeattie pluton) and the lithic arenites from rocks with a high argillaceous content (e.g. the Lower Palaeozoic shales or, to a lesser extent, the greywackes). Most of the trace elements present in the sediments are contained within the clays.

The Holocene coastal gravels of the Dalbeattie area may have been derived partly from Pleistocene glaciofluvial gravels and partly from outcrops of the granite/granodiorite of the Criffell-Dalbeattie pluton.

12.10 Suggestions for further work

The work carried out in the course of the project has added substantially to the grain-size, clay mineralogical and geochemical data available regarding the Holocene raised coastal sediments and present-day intertidal sediments of the Dalbeattie, Kirkcudbright, New Abbey and Lochar Gulf areas. The following additional studies of the Holocene sediments, it is suggested, would of particular use in furthering the interpretation of the nature of these sediments, the environments in which they

accumulated and the chronology of their deposition:

1) Detailed faunal studies, especially of the foraminifers and ostracods present in facies D.

2) Detailed SEM studies of the clay minerals, to add information concerning the authigenic or detrital nature of the clays, and to suggest the origins of the clays.

3) Heavy mineral studies (of the Holocene sediments and representative solid rocks and Pleistocene deposits that are present in the four areas studied), to provide much more reliable indications of provenance than were given by the clay mineralogical and geochemical studies carried out in the course of the project.

4) Chemical analysis of the organic and $CaCO_3$ content of the fine-grained Holocene sediments to improve the geochemical data available regarding these sediments, and to assist in the interpretation of their environments of deposition.

5) Radiocarbon dating of the organic detritus that underlies parts of the Holocene succession and of the peat that overlies parts of the succession, to provide a time scale for the beginning and end of the Flandrian marine transgression, especially in the Dalbeattie, Kirkcudbright and New Abbey areas. This would supplement or improve the chronology of Flandrian marine transgression and regression on the northern side of the Solway Firth, established to the east of the New Abbey area and to the west of the Kirkcudbright area by Jardine (1975).

REFERENCES

ABU EL-ELLA, R. & COLEMAN, J. M. 1985. Discrimination between depositional environments using grain-size analyses. *Sedimentology*, **32**, 743-748.

ADESANYA, O. 1982. *Seismic velocities of the upper crust of the Southern Uplands.* Ph.D. Thesis, University of Glasgow.

ALMOHANDIS, A. A. 1984. Mineralogy of the Qarain clay deposits, Saudi Arabia. *Arab Gulf Journal of Scientific Research*, **2**, 123-133.

ANDREWS, J. T. 1985. Grain size characteristics of Quaternary sediments, Baffin Island region. *In* Andrews, J. T. (ed) *Quaternary Environments: Eastern Canadian Arctic, Baffin Bay and Western Greenland,* 124-152. Allen and Unwin, Boston.

ARGAST, S. & DONNELLY, T. W. 1987. The chemical discrimination of clastic sedimentary components. *Journal of Sedimentary Petrology*, **57**, 813-823.

ATHERTON, J. K. 1986. Geochemical provenance of recent tidal sediments (abstract). British Sedimentological Reseach Group, Annual Meeting, Nottingham.

BARSHAD, L. 1948. Vermiculite and its relation to biotite as revealed by phase exchange reactions, X-ray analyses, differential thermal curves and water content. *American Mineralogist*, **33**, 655-678.

BAYLISS, P. 1975. Nomenclature of the trioctahehral chlorites. *Canadian Mineralogist*, **13**, 178-180.

BHATIA, M. R. & CROOK, K. A. W. 1986. Trace element characteristics of graywackes and tectonic setting discrimination of sedimentary basins. *Contributions to*

Mineralogy and Petrology, **92**, 181-193.

BIRKELAND, P. W. & JANDA, R. J. 1971. Clay mineralogy of soils developed from Quaternary deposits of the Eastern Sierra Nevada, California. *Geological Society of America Bulletin*, **82**, 2495-2514.

BISCAYE, P. E. 1965. Mineralogy and sedimentation of recent deep sea clay in the Atlantic Ocean and adjacent seas and oceans. *Geological Society of America Bulletin*, **76**, 803-832.

BISHOP, W. W. & COOPE, G. R. 1977. Stratigraphical and faunal evidence for Lateglacial and early Flandrian environments in south-west Scotland. *In* Gray, J. M. & Lowe, J. J. (eds) *Studies in the Scottish Lateglacial environment*, 61-88. Pergamon Press, Oxford.

BLUCK, B. J. 1967. Sedimentation of beach gravels: examples from South Wales. *Journal of Sedimentary Petrology*, **37**, 128-156.

_____ 1980. Evolution of a strike-slip fault controlled basin, Upper Old Red Sandstone, Scotland. *In* Ballance, P. F. & Reading, H. G. (eds) *Sedimentation in oblique-slip mobile zone*.s. Special Publication of the International Association of Sedimentologists, **4**, 63-78.

_____ 1985. The Scottish paratectonic Caledonides. *Scottish Journal of Geology*, **21**, 437-464.

de BOER, P. L., van GELDER, A. & Nio, S. D. (eds). 1988. *Tide-Influenced Sedimentary Environments and Facies*. D. Reidel Publishing Company, Dordrecht.

BOHOR, B. F. & HUGHES, R. E. 1971. Scanning electron microscopy of clays and clay minerals. *Clays and Clay Minerals*, **19**, 49-54.

BOSENCE, D. W. J. 1973. Facies relationships in a tidally influenced environment: A

study from the Eocene of the London basin. *Geologie en Mijnbouw,* **52**, 63-67.

BOYD, W. E. 1982. *The stratigraphy and chronology of late Quaternary raised coastal deposits in Renfrewshire and Ayrshire, western Scotland.* Ph.D. Thesis, University of Glasgow.

BOWEN, D. Q. 1978. *Quaternary Geology.* Pergamon Press, Oxford.

BRADLEY, W. F. 1953. Analysis of mixed-layer clay mineral structure. *Analytical Chemistry,* **25**, 727-730.

_____ 1954. X-ray diffraction criteria for the characterization of chloritic material in sediments. *Clays and Clay Minerals*, **2**, 524-534.

BRIDGES, P. H. & LEEDER, M. R. 1976. Sedimentary model for intertidal mudflat channels, with examples from the Solway Firth, Scotland. *Sedimentology,* **23**, 533-552.

BRINDLEY, G. W. & BROWN, G. 1980. *Crystal structures of clay minerals and their X-ray identification.* Mineralogical Society, London.

BROCKAMP, O. 1973. Borfixierung in authigenen und detritischen Tonen. *Geochimica et Cosmochimica Acta*, **37**, 1339-1351.

BROWN, A. G. 1985. Traditional and multivariate techniques in the interpretation of floodplain sediment grain size variations. *Earth Surface Processes and Landforms,* **10**, 281-291.

BROWN, G. 1961. *X-ray identification and crystal structures of clay minerals.* Mineralogical Society, London.

_____ & BRINDLEY, G. W. 1980. X-ray diffraction procedures for clay mineral identification. *In* BRINDLEY, G. W. & BROWN, G. *Crystal structures of clay minerals and their X-ray identification,* 305-359. Mineralogical Society, London.

BROWN, G. M. 1980. *Scotland Sheet 5 (W), Kirkcudbright. 1: 50 000 geological map of Scotland.* Institute of Geological Sciences.

_____ 1981. *Scotland Sheet 5 (E), Dalbeattie. 1: 50 000 geological map of Scotland.* Institute of Geological Sciences.

_____ 1983a. *Scotland Sheet 6, Annan. 1: 50 000 geological map of Scotland.* Institute of Geological Sciences.

_____ 1983b. *Scotland Sheet 10 (W), Lochmaben. 1: 50 000 geological map of Scotland.* Institute of Geological Sciences.

BROWNE, M. A. E. 1980. Late-Devensian marine limits and the pattern of deglaciation of the Strathearn area, Tayside. *Scottish Journal of Geology*, **16**, 221-230.

_____ & GRAHAM, D. K. 1981. Glaciomarine deposits of the Loch Lomond Stade glacier in the Vale of Leven between Dumbarton and Balloch, west-central Scotland. *Quaternary Newsletter*, **34**, 1-7.

BUREK, C. V. 1985. The use of trace element weathering ratios in Pleistocene geology. *Quaternary Newsletter,* **47**, 4-18.

CARROLL, D. 1970. Clay minerals: A guide to their X-ray identification. *Geological Society of America Special Paper 126.*

CARSON, B. & ARCARO, N. P. 1983. Control of clay-mineral stratigraphy by selective transport in Late Pleistocene-Holocene sediments of Northern Cascadia Basin - Juan de Fuca Abyssal Plain: implications for studies of clay-mineral provenance. *Journal of Sedimentary Petrology*, **53**, 395-406.

CARVER, R. E., 1971. *Procedures in sedimentary petrology.* Wiley, New York.

CHARLESWORTH, J. K. 1926a. The glacial geology of the Southern Uplands of Scotland, west of Annandale and Upper Clydesdale. *Transactions of the Royal*

Society of Edinburgh, **55**, 1-23.

_____ 1926b. The readvance, marginal kame-moraine of the south of Scotland, and some later stages of retreat. *Transactions of the Royal Society of Edinburgh,* **55**, 25-50.

CLIFTON, H. E., 1982. Estuarine deposits. *In* Scholle, P. A. & Spearing, D. (eds) *Sandstone depositional environments*, 179-188. American Association of Petroleum Geologists Memoir 31.

_____ 1983. Discrimination between subtidal and intertidal facies in Pleistocene deposits, Willapa Bay, Washington. *Journal of Sedimentary Petrology*, **53**, 353-369.

COOK, D. R. 1976. *The geology of the Cairnsmore of Fleet granite and its environs, Southwest Scotland.* Ph. D. Thesis, University of St. Andrews.

_____ & WEIR, J. A. 1979. Structure of the Lower Palaeozoic rocks around Cairnsmore of Fleet, Galloway. *Scottish Journal of Geology,* **15**, 187-202.

COOPE, G. R. & PENNINGTON, W. 1977. The Windermere Interstadial of the Late Devensian. *Philosophical Transactions of the Royal Society of London,* **B280**, 337-339.

CORNISH, R. 1981. Glaciers of the Loch Lomond Stadial in the western Southern Uplands of Scotland. *Proceedings of the Geologists' Association*, **92**, 105-114.

COUCH, E. L. & GRIM, R. E. 1968. Boron fixation by illites. *Clays and Clay Minerals*, **16**, 249-256.

DARMOIAN, S. A. & LINDQVIST, K. 1988. Sediments in the estuarine environment of the Tigris/Euphrates delta, Iraq, Arabian Gulf. *Geological Journal,* **23**, 15-37.

DAVIES, J. L. 1972. *Geographical Variation in Coastal Development.* Oliver and Boyd, Edinburgh.

DEWEY, J. F. 1971. A model for the Lower Palaeozoic evolution of the southern margin of the early Caledonides of Scotland and Ireland. *Scottish Journal of Geology*, **7**, 219-240.

_____ 1982. Plate tectonics and the evolution of the British Isles. *Journal of the Geological Society, London*, **139**, 371-412.

DEWIS, F. J., LEVINSON, A. A. & BAYLISS, P. 1972. Hydrogeochemistry of the surface waters of the Mackenzie River drainage basin, Canada - IV. Boron - salinity - clay mineralogy relationships in modern deltas. *Geochimica et Cosmochimica Acta*, **36**, 1359-1375.

DONNER, J. J. 1959. The Late- and Post-glacial raised beaches in Scotland. *Annales Academiae Scientiarum Fennicae*, Series AIII, **53**, 1-25.

_____ 1963. The Late- and Post-glacial raised beaches in Scotland II. *Annales Academiae Scientiarum Fennicae*, Series AIII, **68**, 1-13.

DONOYER de SEGONZAC, G. 1970. The transformation of clay minerals during diagenesis and low grade metamorphism. *Sedimentology*, **15**, 281-346.

_____, FERRERO, J. & KUBLER, B. 1968. Sur la cristallinite de l'illite dans la diagenese et l'anchimetamorphisme. *Sedimentology*, **10**, 137-143.

EDZWALD, J. K. & O'MELIA, C. R. 1975. Clay distributions in recent estuarine sediments. *Clays and Clay Minerals*, **23**, 39-44.

ERDTMAN, G. 1928. Studies in the postarctic history of the forest of north-western Europe. I. Investigations in the British Isles. *Geologiska Föreningens i Stockholm Förhandlingar*, **50**, 123-192.

ESQUEVIN, J. 1969. Influence de la composition chimique des illites sur la cristallinite. *Bulletin de Centre de Recherches de Pau, Societe Nationale des Petroles Aquitaine* , **3**, 147-155.

EVANS, G. 1965. Intertidal flat sediments and their environments of deposition in the Wash. *Quarterly Journal of the Geological Society, London*, **121**, 209-245.

_____ 1979. Quaternary transgressions and regressions. *Journal of the Geological Society, London*, **136**, 125-132.

FOLK, R. L. 1966. A review of grain-size parameters. *Sedimentology*, **6**, 73-93.

_____ 1974. *Petrology of sedimentary rocks.* Hemphill, Austin.

_____ & Ward, W. C. 1957. Brazos River bar: a study in the significance of grain-size parameters. *Journal of Sedimentary Petrology*, **27**, 3-26.

FOSTER, M. D. 1963. Interpretation of the composition of vermiculites and hydrobiotites. *Clays and Clay Minerals*, **10**, 70-89.

FREY, R. W. & HOWARD, J. D. 1988. Beaches and beach-related facies, Holocene barrier islands of Georgia. *Geological Magazine*, **125**, 621-640.

FRIEDMAN, G. M. 1961. Distinction between dune, beach and river sands from their textural characteristics. *Journal of Sedimentary Petrology,* **31**, 514-529.

_____ 1967. Dynamic processes and statistical parameters compared for size frequency distribution of beach and river sands. *Journal of Sedimentary Petrology,* **37**, 327-354.

FULLER, A. O. 1961. Size distribution characterisitics of shallow marine sands from the Cape of Good Hope, South Africa. *Journal of Sedimentary Petrology*, **31**, 256-261.

GARDINER, C. I. & REYNOLDS, S. H. 1932. The Loch Doon 'granite' area, Galloway. *Quarterly Journal of the Geological Society, London,* **88**, 1-34.

_____ 1937. The Cairnsmore of Fleet granite and its metamorphic aureole, *Geological Magazine*, **74**, 289-300.

GAUDETTE, H. E., EADES, J. L. & GRIM, R. E. 1966. The nature of illite. *Clays and*

Clay Minerals, ***13****, 33-48.*

GODWIN, H. 1943. Coastal peat beds of the British Isles and North Sea. *Journal of Ecology,* **31**, 199-247.

_____ & WILLIS, E. H. 1962. Cambridge University Natural Radiocarbon Measurements V, *Radiocarbon*, **4**, 57-70.

GOLD, C. M., CAVELL, P. A. & SMITH, D. G. W., 1983. Clay minerals in mixtures: Sample preparation analysis, and statistical interpretation. *Clays and Clay Minerals,* **31**, 191-199.

GREENSMITH, J. T. & TUCKER, E. V. 1973. Holocene transgressions and regressions on the Essex coast Outer Thames Estuary. *Geologie en Mijnbouw*, **52**,193-202.

_____ 1976. Major Flandrian transgressive cycles, sedimentation and palaeogeography in the coastal zone of Essex, England. *Geologie en Mijnbouw*, **55**, 131-146.

GREENWOOD, B. 1969. Sediment parameters and environment discrimination: an application of multivariate statistics. *Canadian Journal of Earth Sciences,* **6**, 1347-1358.

GREIG, D. C. 1971. *British Regional Geology. The South of Scotland* (3rd edition). Edinburgh, Her Majesty's Stationery Office.

GRIFFIN, G. M. & INGRAM, R. L. 1955. Clay minerals of the Neuse River estuary. *Journal of Sedimentary Petrology*, **25**, 194-200.

GRIFFITHS, A. H. 1988. *A stratigraphical, sedimentological and palaeo-environmental analysis of Holocene and present-day coastal sedimentation: Wigtown Bay, S.W. Scotland,* Ph.D. Thesis, University of Glasgow.

GRIM, R. E. 1968. *Clay Mineralogy* (2nd edition). McGraw-Hill, New York.

_____, BRADLEY, W. F. & BROWN, G. 1951. The mica clay minerals. *In*

Brindley, G. W. (ed) *X-ray identification and structures of clay minerals*, 138-172. Mineralogical Society London, Monograph.

_____, DIETZ, R. S. & BRADLEY, W. F. 1949. Clay mineral composition of some sediments from the Pacific Ocean off the California coast and the Gulf of California. *Geological Society of America Bulletin*, **60**, 1785-1808.

_____ & JOHNS, W. D. 1954. Clay mineral investigation of sediments in the northern Gulf of Mexico. *Clays and Clay Minerals*, **2**, 81-103.

HALL, J. 1970. The correlation of seismic velocities with formations in the south-west of Scotland. *Geophysical Prospecting*, **18**, 134-148.

_____, BREWER, J. A., MATTHEWS, D. H. & WARNER, M. R., 1984. Crustal structure across the Caledonides from the 'WINCH' seismic reflection profile: influences on the evolution of the Midland Valley of Scotland. *Transactions of the Royal Society of Edinburgh : Earth Sciences*, **75**, 97-109.

HARVEY, P. K., TAYLOR, D. M., HENDRY, R. D. & BANCROFT, F. 1973. An accurate fusion method for the analysis of rocks and chemically related minerals by X-ray fluorescence spectrometry. *X-ray Spectrometry*, **2**, 33-44.

HAYES, M. O. 1967. Hurricanes as geological agents: case studies of Hurricanes Carla, 1961, and Cindy, 1963, *Report of the Investigative Bureau of Economic Geologists*, **61**.

_____ 1975. Morphology of sand accumulation in estuaries: an introduction to the symposium. *In* Cronin, L. E. (ed) *Estuarine Research, II, Geology and Engineering*, 3-22. Academic Press, London.

HEIER, K. S. & BILLINGS, G. K. 1969. Rubidium: *In* Wedepohl, K. H. (ed) *Handbook of Geochemistry* Vol. II, Chap. 37. Springer-Verlag, Berlin.

HICKMAN, A. H. & WRIGHT, A. E. 1983. Geochemistry and chemostratigraphical

correlation of slates, marbles and quartzites of the Appin Group, Argyll, Scotland. *Transactions of the Royal Society of Edinburgh : Earth Sciences,* **73**, 251-278.

HOLDEN, W. G. 1977. *The glaciation of central Ayrshire.* Ph.D. Thesis, University of Glasgow.

HORNE, J., PEACH, B. N., & TEALL, J. J. H. 1896. *Explanation of Sheet 5. Kirkcudbrightshire.* Memoir of the Geological Survey, U.K.

HOWARD, J. D. 1975. Estuaries of the Georgia coast, USA: sedimentology and biology. IX. Conclusions. *Senckenbergiana maritima*, **7**, 297-305.

HUTCHISON, C. S. 1974. *Laboratory Handbook of Petrographic Techniques.* Wiley, New York.

JACKSON, M. L. 1959. Frequency distribution of clay minerals in major great soil groups as related to the factors of soil formation. *Clays and Clay Minerals,* **6**, 133-143.

JARDINE, W. G. 1956. *Some aspects of the geomorphology of south west Scotland.* Ph.D. Thesis, University of Cambridge.

_____ 1964. Post-glacial sea levels in south-west Scotland. *Scottish Geographical Magazine*, **80**, 5-11.

_____ 1967. Sediments of the Flandrian transgression in south-west Scotland: terminology and criteria for facies distinction. *Scottish Journal of Geology*, **3**, 221-226.

_____ 1971. Form and age of late-Quaternary shore-lines and coastal deposits of south-west Scotland: critical data. *Quaternaria*, **14**, 103-114.

_____ 1975. Chronology of Holocene marine transgression and regression in south-western Scotland. *Boreas,* **4**, 173-196.

._____ 1977. The Quaternary marine record in southwest Scotland and the Scottish Hebrides. *In* Kidson, C. & Tooley, M. J. (eds) *The Quaternary History of the Irish Sea,* 99-118. Geological Journal Special Issue No. 7. Seel House Press, Liverpool.

_____ 1980. Holocene raised coastal sediments and former shorelines of Dumfriesshire and eastern Galloway. *Transactions and Journal of Proceedings of the Dumfriesshire and Galloway Natural History and Antiquarian Society*, **55**, 1-59.

_____ 1981a. Holocene shorelines in Britain: recent studies. *In* van Loon, A.J. (ed); Quaternary geology: a farewell to A. J. Wiggers. *Geologie en Mijnbouw*, **60**, 297-304.

_____ 1981b. Status and relationships of the Loch Lomond Readvance and its stratigraphical correlatives. *In* Neale, J. & Flenley, J. (eds) *The Quaternary in Britain*, 168-173. Pergamon Press, Oxford.

_____ 1982. Sea-level changes in Scotland during the last 18,000 years. *Proceedings of the Geologists' Association*, **93**, 25-41.

_____ & MORRISON, A. 1976. The archaeological significance of Holocene coastal deposits in south-western Scotland. *In* Davidson, D. A. & Shackley, M. L. (eds) *Geoarchaeology: Earth Science and the Past,* 175-195. Duckworth, London.

_____ & PEACOCK J. D. 1973. Scotland. *In* Mitchell, G. F., Penny, L. F., Shotton, F. W. & West, R. G. (eds); A correlation of Quaternary deposits in the British Isles, 53-59. *Geological Society, London,* Special Report No. **4**.

JELGERSMA, S. 1983. The Bergen inlet, transgressive and regressive Holocene shoreline deposits in the northwestern Netherlands. *Geologie en Mijinbouw,*

62, 471-486.

JOHNS, W. D., GRIM, R. E. & BRADLEY, W. F. 1954. Quantitative estimations of clay minerals by diffraction methods. *Journal of Sedimentary Petrology,* **24**, 242-251.

JOHNSON, H. D. 1975. Tide- and wave-dominated inshore and shoreline sequences from the late Precambrian, Finnmark, North Norway. *Sedimentology*, **22**, 45-74.

JONES, B. F. & WEIR, A. H. 1983. Clay minerals of Lake Albert, an alkaline, saline lake. *Clay and Clay Minerals*, **31**, 161-172.

JØRGENSEN, P. 1965. Mineralogical composition and weathering of some Late Pleistocene marine clays from the Kongsvinger area, southern Norway. *Geologiska Föreningens i Stockholm Förhandlingar*, **87**, 62-83.

KANTOROWICZ, J. 1984. The nature, origin and distribution of authigenic clay minerals from Middle Jurassic Ravenscar and Brent Group Sandstones. *Clay Minerals*, **19**, 359-375.

KARLIN, R. 1980. Sediment sources and clay mineral distributions off the Oregon Coast. *Journal of Sedimentary Petrology*, **50**, 543-560.

KARLSON, W., VOLLSET, J., BIORLVKKE, K. & JØRGENSEN, P. 1979. Changes in mineralogical composition of Tertiary sediments from North Sea wells. *Developments in Sedimentology,* **27**, 281-289. Elsevier, Amsterdam.

KELLER, W. D. 1958a. Argillation and direct bauxitization in terms of concentrations of hydrogen and metal cations at the surface of hyrolyzing aluminum silicates. *American Association of Petroleum Geologists Bulletin*, **42**, 233-245.

_____ 1958b. Glauconitic mica in the Morrison formation in Colorado. *Clays and Clay Minerals*, **5**, 120-128.

_____ 1968. Flint clay and flint clay facies. *Clays and Clay Minerals,* **16**, 113-128.

_____ 1970. Environmental aspects of clay minerals. *Journal of Sedimentary Petrology*, **40**, 788-854.

KLEIN, G. de V. 1977. *Clastic Tidal Facies.* Continuing Education Publication Company, Champaign, Illinois.

KODAMA, H., SHIMODA, S. & SUDO, T. 1969. Hydrous mica complexes: their structure and chemical composition. *Proceedings of the International Clay Conference, Tokyo, 1969*, **1**, 185-196.

KRAFT, J.C. 1971. Sedimentary facies patterns and geologic history of a Holocene marine transgression. *Geological Society of America Bulletin,* **82**, 2131-2158.

KRUMBEIN, W. C. 1941. Measurement and geological significance of shape and roundness of sedimentary particles. *Journal of Sedimentary Petrology*, **11**, 64-72.

LAMBIASE, J. J. 1977. *Sediment dynamics in the macrotidal Avon River Estuary, Nova Scotia.* Ph.D. Thesis, McMaster University.

_____ 1980. Hydraulic control of grain-size distributions in a macrotidal estuary. *Sedimentology*, **27**, 433-446

LEAKE, B. E. et al. (10 authors). 1969. The chemical analysis of rock powders by automatic X-ray fluorescence. *Chemical Geology*, **5**, 7-86.

LERMAN, A. 1966. Boron in clays and estimation of paleosalinities. *Sedimentology*, **6**, 267-280.

LEEDER, M. R. 1971. Aspects of the geology of the south-eastern part of the Criffell intrusion and its associated dykes. *Transactions and Journal of*

Proceedings of the Dumfriesshire and Galloway Natural History and Antiquarian Society, **48**, 1-11.

_____ 1976. Sedimentary facies and the origins of basin subsidence along the northern margin of the supposed Hercynian Ocean. *Tectonophysics*, **36**, 167-179.

_____ 1982a. Upper Palaeozoic basins of the British Isles - Caledonide inheritance versus Hercynian plate margin processes. *Journal of the Geological Society, London,* **139**, 479-491.

_____ 1982b. *Sedimentology: process and product.* George Allen & Unwin, London.

LINDHOLM, R. 1987. *A Practical Approach to Sedimentology*. Allen & Unwin, London.

LORING, D. H. 1982. Geochemical factors controlling the accumulation and dispersal of heavy metals in the Bay of Fundy sediments. *Canadian Journal of Earth Sciences*, **19**, 930-944.

LOWE, J. J. & GRAY, J. M. 1980. The stratigraphic subdivision of the Lateglacial of North-west Europe. *In* Lowe J. J., Gray, J. M. & Robinson, J. E. (eds) *Studies in the Lateglacial of North-west Europe,* 157-175. Pergamon Press, Oxford.

LOWE J. J. & WALKER, M. J. C. 1984. *Reconstructing Quaternary Environments.* Longman, London.

MACGREGOR, M. 1937. The western part of the Criffell-Dalbeattie igneous complex. *Quarterly Journal of the Geological Society, London,* **93**, 457-486.

_____ 1938. The evolution of the Criffell-Dalbeattie Quartz-diorite: a study of granitisation. *Geological Magazine*, **75**, 481-496.

McHARDY, W. J. & BIRNIE, A. C. 1988. Scanning electron microscopy. *In* Wilson,

M. J. (ed) *A Handbook of Determinative Methods in Clay Mineralogy*, 174-208. Blackie, Glasgow.

MACKENZIE, R. C. 1965. Clay minerals of Scottish soils. *Soviet Soil Science*, **4**, 396-406.

McKERROW, W. S., LEGGETT, J. K. & EALES, M. H. 1977. Imbricate thrust model for the Southern Uplands of Scotland. *Nature*, **267**, 237-239.

McLENNAN, S. M. & TAYLOR, S. R. 1983. Geochemical evolution of Archean shales from South Africa. I. The Swaziland and Pongola Supergroups. *Precambrian Research*, **22**, 93-124.

McMURTY, G. M. & FAN, P-F. 1974. Clays and clay minerals of the Santa Ana River drainage basin, California. *Journal of Sedimentary Petrology*, **44**, 1072-1078.

MACCHI, L. 1987. A review of sandstone illite cements and aspects of their significance to hydrocarbon exploration and development. *Geological Journal*, **22**, 333-345.

MAJOU, T. V. & HOWARD, J. D. 1975. Estuaries of the Georgia Coast, USA: Sedimentology and Biology. VI. Animal-sediment relationships of a salt-marsh estuary - Doboy Sound. *Senckenbergiana maritima*, **7**, 205-236.

MANGERUD, J., ANDERSEN, S. T., BERGLUND, B. E. & DONNER, J. J. 1974. Quaternary stratigraphy of Norden, a proposal for terminology and classification. *Boreas*, **3**, 109-126.

MARSHALL, J. R. 1962a. The morphology of the upper Solway salt marshes. *Scottish Geographical Magazine*, **78**, 81-99.

_____ 1962b. The physiographic development of Caerlaverock Merse. *Transactions and Journal of Proceedings of the Dumfriesshire and Galloway*

Natural History and Antiquarian Society, **39**, 102-123.

MASON, C. C. & FOLK, R.L. 1958. Differentiation of beach, dune, and aeolian flat environments by size analysis, Mustang Island, Texas. *Journal of Sedimentary Petrology*, **28**, 211-226.

MAY, J. 1981. *The glaciation and deglaciation of Upper Nithsdale and Annandale.* Ph.D Thesis, University of Glasgow.

MELKERUD, P.-A. 1983. Quaternary deposits and bedrock outcrops in an area around Lake Gardsjön, southwestern Sweden, with physical, mineralogical and geochemical investigations. *Swedish University of Agricultural Sciences, Uppsala. Reports in Forest Ecology and Forest Soils*, **44**, 1-87.

_____ 1986. Clay mineralogical comparisons of weathering profiles associated with spruce and birch stands. *Geologiska Föreningens i Stockholm Förhandlingar*, **107**, 301-309.

MIDDLETON, G. V. 1976. Hydraulic interpretation of sand size distributions. *Journal of Geology*, **84**, 405-426.

_____ 1978. Facies. *In* Fairbridge R. W. & Bourgeois, J. (eds) *The Encylopedia of Sedimentology*, 323-325. Dowden, Hutchinson & Ross. Stroudsburg, Pennsylvania.

MIELKE, J. E. 1979. Composition of the Earth's crust and distribution of the elements. *In* Siegel, F. R. (ed) *Review of research on modern problems in geochemistry,* 13-37. UNESCO, Paris.

MILLOT, G. 1964. *Geologie des Argiles.* Masson, Paris.

_____ 1970. *Geology of Clays.* Chapman & Hall, London.

MITCHELL, W. A. 1955. A review of the mineralogy of Scottish soil clays. *Journal of Soil Science*, **6**, 94-98.

MOORE, J. R. 1963. Bottom sediment studies, Buzzards Bay, Massachusetts. *Journal of Sedimentry Petrology*, **33**, 511-558.

MOSS, A. J. 1962. The physical nature of common sandy and pebbly deposits, Part 1. *American Journal of Science*, **260**, 337-373.

_____ 1963. The physical nature of common sandy and pebbly deposits, Part 2. *American Journal of Science*, **261**, 297-343.

_____ 1972. Bed-load sediments. *Sedimentology*, **18**, 159-219.

NEIHEISEL, J. & WEAVER, C. E. 1967. Transport and deposition of clay minerals southeastern United States. *Journal of Sedimentary Petrology*, **37**, 1084-1116.

NELSON, B. W. 1960. Clay mineralogy of the bottom sediments, Rappahannock River, Virginia. *Clays and Clay Minerals*, **7**, 135-147.

NEMEC, W. & STEEL, R. J. 1984. Alluvial and coastal conglomerates: their significant features and some comments on gravelly mass-flow deposits. *In* Koster, E. H. & Steel, R. J. (eds) *Sedimentology of Gravels and Conglomerates.* Canadian Society of Petroleum Geologists, Memoir 10, 1-31.

NICHOLS, H. 1967. Vegetational change, shoreline displacement and the human factor in the late Quaternary history of south-west Scotland. *Transactions of the Royal Society of Edinburgh*, **67**, 145-187.

NICHOLS, M. M. & BIGGS, R. B. 1985. Estuaries. *In* Davis, R. A. (ed) *Coastal Sedimentary Environments* (2nd edition), 77-186. Springer-Verlag, New York.

NIGGLI, P. 1954. *Rocks and Mineral Deposits.* Freeman, San Francisco.

ORD, D. M., CLEMMEY, H. & LEEDER, M. R. 1988. Interaction between faulting and sedimentation during Dinantian extension of the Solway basin, SW Scotland.

Journal of the Geological Society, London, **145**, 249-259.

PARKER, A., ALLEN, J. R. L. & WILLAMS, B. P. J. 1983. Clay mineral assemblages of the Townsend Tuff Bed (Lower Old Red Sandstone), South Wales and the Welsh Borders. *Journal of the Geological Society, London*, **140**, 769-779.

PARSLOW, G. R. 1964. *The Cairnsmore of Fleet granite and its aureole.* Ph.D. Thesis, University of Newcastle upon Tyne.

_____ 1968. The physical and structural features of the Cairnsmore of Fleet granite and its aureole. *Scottish Journal of Geology*, **4**, 91-108.

_____ 1971. Variations in mineralogy and major elements in the Cairnsmore of Fleet Granite, S.W. Scotland. *Lithos*, **4**, 43-55.

PASSEGA, R. 1957. Texture as characteristic of clastic deposition. *American Association of Petroleum Geologists Bulletin*, **41**, 1952-1984.

_____ 1964. Grain size representation by CM patterns as a geological tool. *Journal of Sedimentary Petrology*, **34**, 830-847.

_____ 1972. Sediment sorting related to basin mobility and environment. *American Association of Petrolum Geologists Bulletin*, **56**, 2440-2450.

_____ & BYRAMJEE, R. 1969. Grain-size image of clastic deposits. *Sedimentology*, **13**, 233-252.

PEARSON, M. J. 1979. Geochemistry of the Hepworth Carboniferous sediment sequence and origin of the diagenetic iron minerals and concretions. *Geochimica et Cosmochimica Acta*, **43**, 927-941.

PEDERSTAD, K. & JØRGENSEN, P. 1985. Weathering in a marine clay during postglacial time. *Clay Minerals*, **20**, 477-491.

PETTIJOHN, F. J., POTTER, P. E. and SIEVER, R. 1972. *Sand and sandstone.* Springer, New York.

PHILLIPS, W. J. 1956. The Criffell-Dalbeattie granodiorite complex. *Quarterly Journal of the Geological Society, London*, **112**, 221-240.

POSTMA, H. 1961. Transport and accumulation of suspended matter in the Dutch Wadden Sea. *Netherlands Journal of Sea Research*, **1**, 148-190.

POWERS, M. C. 1953. A new roundness scale for sedimentary particles. *Journal of Sedimentary Petrology*, **23**, 117-119.

_____ 1954. Clay diagenesis in the Chesapeake Bay area. *Clays and Clay Minerals*, **2**, 68-80.

_____ 1957. Adjustment of land derived clays to the marine environment. *Journal of Sedimentary Petrology*, **27**, 355-372.

PRICE, R. J. 1983. *Scotland's environment during the last 30,000 years.* Scottish Academic Press, Edinburgh.

PROUST, D. 1982. Supergene alteration of metamorphic chlorite in an amphibolite from the Massif Central, France. *Developments in Sedimentology*, **40**, 357-364. Elsevier, Amsterdam.

_____ & Velde, B 1978. Beidellite crystallization from plagioclase and amphibole precursors: local and long-range equilibrium during weathering. *Clay Minerals*, **13**, 199-209.

PYE, M. I. A. 1980. *Studies of burrows in recent sublittoral fine sediments off the west coast of Scotland.* Ph.D Thesis, University of Glasgow.

QUIGLEY, R. M. & MARTIN, R. T. 1963. Chloritized weathering products of a New England glacial till. *Clays and Clay Minerals*, **10**, 107-116.

READING, H. G. 1986. Facies. *In* Reading, H. G. (ed) *Sedimentary environments and facies* (2nd edition), 4-14. Blackwell, Oxford.

REINECK, H. E. 1975. German North Sea tidal flats. *In* Ginsburg, R. N. (ed) *Tidal*

deposits: A casebook of recent examples and fossil counterparts, 5-12. Springer-Verlag, New York.

_____ & SINGH, I. B. 1972. Genesis of laminated sand and graded rhythmites in storm-sand layers of shelf mud. *Sedimentology*, **18**, 123-128.

_____ 1980. *Depositional Sedimentary Environments* (2nd edition). Springer-Verlag, New York.

REYNOLDS, R. C. & HOWER, J. 1970. The nature of interlayering in mixed-layer illite-montmorillonites. *Clays and Clay Minerals*, **18**, 25-36.

RICH, C. I. 1958. Muscovite weathering in a soil developed in the Virgina piedmont. *Clays and Clay Minerals*, **5**, 203-212.

ROALDSET, E. 1972. Mineralogy and geochemistry of Quaternary clays in the Numedal area, southern Norway. *Norsk Geologisk Tidsskrift*, **52**, 335-369.

ROSE, J. 1975. Raised beach gravels and ice wedge casts at Old Kilpatrick, near Glasgow. *Scottish Journal of Geology*, **11**, 15-21.

ROSER, B. P. & KORSCH, R. J. 1988. Provenance signatures of sandstone-mudstone suites determined using discriminant function analysis of major-element data. *Chemical Geology*, **67**, 119-139.

ROYSE, C. F. 1968. Recognition of fluvial environments by particle-size characteristics. *Journal of Sedimentary Petrology*, **38**, 1171-1178.

SAGOE, K. O. & VISHER, G. S. 1977. Population breaks in grain size distribution of sand - a theoretical model. *Journal of Sedimentary Petrology*, **47**, 285-310.

SAHU, B. K. 1964. Depositional mechanisms from the size analysis of clastic sediments. *Journal of Sedimentary Petrology*, **34**, 73-83.

SCHUBEL, J. R. & HIRSCHBERG, D. J. 1978. Estuarine graveyard and climatic change. *In* Wiley, M. (ed) *Estuarine Processes*, Vol.1, 285-303.

SCHULTZ, L. G. 1964. Quantitative interpretation of mineralogical composition from X-ray and chemical data for the Pierre Shale. *U.S. Geological Survey Professional Paper*, 391-C, C1-C31.

SENIOR, A. & Leake B. E. 1978. Regional metasomatism and the geochemistry of the Dalradian metasediments of Connemara, western Ireland. *Journal of Petrology*, **19**, 585-625.

SHEA, J. H., 1974. Deficiencies of clastic particles of certain sizes. *Journal of Sedimentry Petrology*, **44**, 985-1003.

SHOTTON, F. W. 1973. General principles governing the subdivision of the Quaternary System. *In* Mitchell, G. F., Penny, L. F., Shotton, F. W. & West, R. G. *A correlation of Quaternary deposits in the British Isles,* 1-7. Geological Society of London, Special Report No. 4.

SIEMERS, C. T. 1976. Sedimentology of the Rocktown channel sandstone, upper part of the Dakota Formation (Cretaceous), Central Kansas. *Journal of Sedimentary Petrology,* **46**, 97-123.

SLY, P. G., THOMAS, R. L. & PELLETIER, B. R. 1983. Interpretation of moment measures derived from water-lain sediments. *Sedimentology*, **30**, 219-233.

SONG, W., YOO, D. & DYER, K. R. 1983. Sediment distribution, circulation and provenance in a macrotidal bay, Garolim Bay, Korea. *Marine Geology,* **52**, 121-140.

SPENCER, D. W. 1963. The interpretation of grain size distribution curves of clastic sediments. *Journal of Sedimentary Petrology*, **33**, 180-190.

STEVENS, R. L., APRIL, R. H. & WEDEL, P. O. 1987. Sediment color and weathered periglacial sources of Quaternary clays in southwestern Sweden. *Geologiska Föreningens i Stockholm Förhandlingar,* **109**, 241-253.

STEWART, H. B. 1958. Sedimentary reflections of depositional environment in San Miguel Lagoon, Baja California, Mexico. *American Association of Petroleum Geologists Bulletin*, **42**, 2567-2618.

SUQUET, H., IIYAMA, J. T., KODAMA, H., & PEZERAT, H. 1977. Synthesis and swelling properties of saponites with increasing layer charge. *Clays and Clay Minerals*, **25**, 231-242.

TAGGART, M. S. & KAISER, A. D. 1960. Clay mineralogy of Mississippi River deltaic sediments. *Geological Society of America Bulletin*, **71**, 521-530.

TANNER, W. F. 1959. Sample components obtained by the method of differences. *Journal of Sedimentary Petrology*, **29**, 408-411.

_____ 1964. Modification of sediment size distributions. *Journal of Sedimentary Petrology*, **34**, 156-164.

TAYLOR, S. R. & McLENNAN, S. M. 1981. The composition and evolution of the continental crust: rare earth element evidence from sedimentary rocks. *Philosophical Transactions of the Royal Society of London*, **Ser A3**, 318-339.

THOM, B. G. & ROY, P. S. 1985. Relative sea levels and coastal sedimentation in southeast Australia in the Holocene. *Journal of Sedimentary Petrology*, **55**, 257-264.

THOREZ, J. 1975. *Phyllosilicate clay minerals.* G. Lelotte, Dison.

_____ 1976. *Practical identification of clay minerals* . G. Lelotte, Dison.

TUCKER, M. E. 1981. *Sedimentary Petrology : An Introduction.* Blackwell, Oxford.

Van de KAMP, P. C. & LEAKE, B. E. 1985. Petrography and geochemistry of feldspathic and mafic sediments of the northeastern Pacific margin. *Transactions of the Royal Society of Edinburgh: Earth Sciences*, **76**, 411-449.

Van de KAMP, P. C., LEAKE, B. E. & SENIOR, A. 1976. The petrography and

geochemistry of some Californian arkoses with application to identifying gneisses of metasedimentary origin. *Journal of Geology*, **84**, 195-212.

VANDENBERGHE, N. 1975. An evalution of CM patterns for grain-size studies of fine grained sediments. *Sedimentology*, **22**, 615-622.

Van STRAATEN, L. M. J. U. 1961. Sedimentation in tidal flat areas. *Journal of the Alberta Society of Petroleum Geologists,* **9**, 203-226.

_____ & Kuenen, P.H. 1957. Accumulation of fine grained sediments in the Dutch Wadden sea. *Geologie en Mijnbouw*, **19**, 329-354.

VELDE, B. 1985. Clay minerals: A Physico-Chemical Explanation of their Occurrence. *Developments in Sedimentology*, **40**, Elsevier, Amsterdam.

VILLUMSEN, A. & NIELSEN, O. B. 1976. The influence of palaeosalinity, grain size distribution and clay minerals on the content of B, Li and Rb in Quaternary sediments from Eastern Jutland, Denmark. *Sedimentology* , **23**, 845-855.

VISHER, G. S. 1969. Grain size distributions and depositional processes. *Journal of Sedimentary Petrology*, **39**, 1074-1106.

VORREN, T. O. 1976. Grain-size distribution and grain-size parameters of different till types on Hardangervidda, south Norway. *Boreas*, **6**, 219-227.

WALKER, G. F. 1947. The mineralogy of some Aberdeenshire soil clays. *Clay Minerals Bulletin*, **1**, 5-8

_____ 1949. Water layers in vermiculite. *Nature*, **163**, 726-727.

_____ 1950. Trioctahedral minerals in the soil clays of north-east Scotland. *Mineralogical Magazine*, **29**, 72-84.

_____ 1961. Vermiculite minerals. *In* Brown, G. (ed) *X-ray identification and crystal structures of clay minerals*, 297-324. Mineralogical Society, London.

WALLACE, R. 1918. The lower Nith in its relation to flooding and navigation. *Transactions and Journal of Proceedings of the Dumfriesshire and Galloway Natural History and Antiquarian Society,* **5**, 128-136.

WALTON, E. K. 1963. Sedimentation and structure in the Southern Uplands. *In* Johnson, M. R. W. & Stewart, F. H. (eds) *The British Caledonides*, 71-97. Oliver & Boyd, Edinburgh.

WEAVER, C. E. 1958. Geological interpretation of argillaceous sediments. Part I. Origin and significance of clay minerals in sedimentary rocks. *American Association of Petroleum Geologists Bulletin,* **42**, 254-275.

_____ 1959. The clay petrology of sediments. *Clays and Clay Minerals,* **6**, 154-187.

_____ & BECK, K. C. 1971. Clay-water diagenesis during burial: how mud becomes gneiss. *Geological Society of America Special Paper 134.*

_____ & POLLARD, L. D. 1973. The chemistry of clay minerals. *Developments in Sedimentology,* **15.** Elsevier, Amsterdam.

WEDEPOHL, K. H. (ed) 1978. *Handbook of Geochemistry,* II. Springer-Verlag, Berlin.

WEIL, C. B. 1977. *Sediment, structural framework, and evolution of Delaware Bay; a transgressive estuarine delta*. University of Delaware Sea Grant Technical Report No. DEL-SG-4-77.

WEIMER, R. J., HOWARD, J. D. & LINDSAY, D. R. 1982. Tidal flats and associated tidal channels. *In* Scholle, P. A. & Spearing, D. (eds) *Sandstone depositional environments,* 191-245. American Association of Petroleum Geologists, Tulsa, Oklahoma.

WEIR, A. H., ORMEROD E. C. & El MANSEY I. M. I. 1975. Clay mineralogy of the

western Nile Delta. *Clay Minerals*, **10**, 369-386.

WEIR, J. A. 1974. The sedimentology and diagenesis of the Silurian rocks on the coast west of Gatehouse, Kirkcudbrightshire. *Scottish Journal of Geology*, **10**, 165-186.

WELTON, J. E. 1984. *SEM Petrology Atlas*. American Association of Petroleum Geologists, Tulsa, Oklahoma.

WENTWORTH, C. K. 1922. A scale of grade and class terms for clastic sediments. *Journal of Geology*, **30**, 377-392.

WHITE, J. L. 1962. X-ray diffraction studies on weathering of muscovite. *Soil Science*, **93**, 16-21.

WHITEHOUSE, U. G., JEFFREY, L. M. & DEBBRECHT, J. D. 1960. Differential settling tendencies of clay minerals in saline waters. *Clays and Clay Minerals*, **7**, 1-79.

WILSON, J. B. 1967. Palaeoecological studies on shell-beds and associated sediments in the Solway Firth. *Scottish Journal of Geology*, **3**, 329-371.

WILSON, M. D. & PITTMAN, E. D. 1977. Authigenic clays in sandstones: recognition and influence on reservoir properties and palaeoenvironmental analysis. *Journal of Sedimentary Petrology*, **47**, 3-31.

WILSON, M. J. 1966. The weathering of biotite in some Aberdeenshire soils. *Mineralogical Magazine*, **35**, 1080-1093.

_____ 1970. A study of weathering in a soil derived from a biotite-hornblende rock. *Clay Minerals*, **8**, 291-303.

_____ 1971. Clay mineralogy of the Old Red Sandstone (Devonian) of Scotland. *Journal of Sedimentary Petrology*, **41**, 995-1007.

_____ 1973. Clay minerals in soils derived from Lower Old Red Sandstone till: effects of inheritance and pedogenesis. *Journal of Soil Science*, **24**, 26-41.

_____ 1976. Exchange properties and mineralogy of some soils derived from lavas of Lower Old Red Sandstone (Devonian) age. II. Mineralogy. *Geoderma*, **15**, 289-304.:

_____, BAIN, D. C. & DUTHIE D. M. L. 1984. The soil clays of Great Britain: II. Scotland. *Clay Minerals*, **19**, 709-735.

_____, RUSSELL, J. D., TAIT, J. M., CLARK, D. R., FRASER, A. R. & STEPHEN, I. 1981. Swelling hematite/layer silicate complex in weathered granite. *Clay Minerals*, **16**, 261-277.

WUNDERLICH, F. 1969. Studien zur Sedimentbewegung. 1. Transportformen und Schuchtbildung im Gebeit der Jade. *Senckenbergiana maritima*, **1**, 107-146.

ZINGG, T. 1935. Beitrag zur Schotteranalyse. *Schweizerische mineralogische und petrographische Mitteilungen*, **15**, 39-140.